SCAPHITES OF THE "*NODOSUS* GROUP" FROM THE UPPER CRETACEOUS (CAMPANIAN) OF THE WESTERN INTERIOR OF NORTH AMERICA

NEIL H. LANDMAN

Division of Paleontology (Invertebrates)
American Museum of Natural History
New York, New York 10024
(landman@amnh.org)

W. JAMES KENNEDY

Oxford University Museum of Natural History
Parks Road, Oxford, OX1 3PW, United Kingdom
(jim.kennedy@oum.ox.ac.uk)

WILLIAM A. COBBAN

Division of Paleontology (Invertebrates)
American Museum of Natural History
New York, New York 10024

NEAL L. LARSON

Black Hills Museum of Natural History
P.O. Box 614, Hill City, South Dakota 57745
(ammoniteguy@bhigr.com)

BULLETIN OF THE AMERICAN MUSEUM OF NATURAL HISTORY
Number 342, 242 pp., 116 figures, 10 tables
Issued September 21, 2010

Copyright © American Museum of Natural History ISSN 0003-0090

Breaks along Sage Creek, AMNH loc. 3207, Badlands National Park, Pennington County, South Dakota, exposing the *Baculites compressus–B. cuneatus* zones of the Pierre Shale. This is the type locality of *Hoploscaphites nodosus* (Owen, 1852). Fossiliferous concretions wash down from the cutbank above (approximately 25 m high) and litter the creek bottom. Note the American bison on top of the cliff for scale. Photo by Susan M. Klofak (AMNH).

CONTENTS

Abstract 4
Introduction 6
Historical Background 8
Zonation 17
Correlation 21
Mode of Occurrence 26
Repositories 33
Terms and Methods 33
Shell Morphology 37
Jaws 55
Variation Within and Between Species 62
Pathologic Specimens 73
Mode of Life 81
Habitat 86
Methane Seeps 90
Systematic Paleontology 93
Hoploscaphites Nowak, 1911 93
Hoploscaphites nodosus (Owen, 1852) 98
Hoploscaphites brevis (Meek, 1876) 155
Acknowledgments 218
References 219
Appendix 1: List of Localities 234
Appendix 2: Ontogenetic Measurements 241

ABSTRACT

Scaphitid ammonites (scaphites) are common in the Upper Cretaceous Pierre Shale and Bearpaw Shale of the Western Interior of North America. We redescribe *Hoploscaphites nodosus* (Owen, 1852) and *H. brevis* (Meek, 1876) from the *Baculites compressus–B. cuneatus* zones of the upper Campanian. The types of both of these species were collected in the mid-19th century in what was then called Nebraska Territory, and included parts of present-day South Dakota, North Dakota, and Montana. Based on our present knowledge of the distribution of these species, the type material was probably collected from the *B. compressus–B. cuneatus* zones in the Pierre Shale at Sage Creek, a tributary of the Cheyenne River, Pennington County, South Dakota.

Traditionally, the more robust, more coarsely ornamented scaphites (comprising the "*nodosus* group") from the Pierre Shale and Bearpaw Shale were assigned to *Jeletzkytes* Riccardi, 1983, and the more slender, more finely ornamented scaphites were assigned to *Hoploscaphites* Nowak, 1911. However, our large collections of these scaphites from the *Baculites compressus–B. cuneatus* zones reveal a complete intergradation between the two morphological extremes, and for many specimens, the choice of genus is arbitrary. In addition, our studies of other biostratigraphic zones in the Pierre Shale and Bearpaw Shale reveal that cooccurring species of these two "genera" share more in common with each other than they do with congeneric species from other horizons. Furthermore, contrary to earlier assumptions, *Jeletkytes* is not endemic to the Western Interior Basin of North America and occurs, for example, in the U.S. Atlantic Coastal Plain and Europe. We thus provisionally treat *Jeletzkytes* as a junior subjective synonym of *Hoploscaphites*. This expanded definition of *Hoploscaphites* is consistent with present-day concepts of other scaphitid genera such as *Discoscaphites* Meek, 1876, and *Trachyscaphites* Cobban and Scott, 1964.

In *Hoploscaphites nodosus* and *H. brevis*, the juvenile shell is planispirally coiled with a small umbilicus. The whorl section is initially depressed and becomes more compressed through ontogeny. The angle of the body chamber in juveniles is approximately two-thirds of a whorl. At the approach of maturity, the shell uncoils, forming a relatively long shaft and recurved hook. The ratio of whorl width to whorl height reaches a minimum value at midshaft. The apertural margin at maturity is constricted and terminates in a flared lip. Commonly, the last two or three septa, corresponding to the formation of the hook, are more closely spaced (approximated). These features indicate that the rate of growth decreased and eventually stopped at maturity ("morphogenetic countdown" associated with determinate growth). Both species of scaphites occur as dimorphs, which are referred to as macroconchs (presumably females) and microconchs (presumably males). In samples of specimens of the same species within a single concretion, macroconchs are approximately 20% larger than microconchs. In addition to size, dimorphs are distinguished by differences in shape, including the presence or absence of an umbilical bulge, the size of the umbilical diameter, the outline of the umbilical shoulder relative to that of the venter in side view, and the relative change in whorl height in passing from the mature phragmocone to the shaft of the body chamber.

The holotype of *Hoploscaphites nodosus*, by monotypy, is UC 6381, the original of *Scaphites nodosus* Owen (1852: 581, pl. 8, fig. 4). Adults exhibit a range of variation in size, degree of compression, and coarseness of ornament. The exposed phragmocone occupies most of the coiled portion of the shell, and is approximately two-thirds of a whorl in angular length. Adults are large (LMAX averages 91.8 mm in macroconchs and 78.0 mm in microconchs) and ellipsoidal in side view, with a strongly recurved hook (apertural angle averages 73° in macroconchs). The ratio of whorl width to whorl height at midshaft averages 0.99 in macroconchs and 1.02 in microconchs. The whorl section is subquadrate/ovoid to reniform, with broadly rounded to flat flanks, and a broadly rounded venter. Ribs are straight to slightly flexuous and cross the venter with a weak adoral projection. There are 5–7.25 ribs/cm on the venter at midshaft in macroconchs and 6–8 ribs/cm on the venter at midshaft in microconchs. Umbilicolateral tubercles usually appear midway on the exposed phragmocone, but may already be present near the point of exposure. At midshaft, they occur at one-third to one-half whorl height and are relatively widely and evenly spaced, and usually extend to the aperture. Ventrolateral tubercles are generally present at the point of exposure. They are unevenly spaced on the exposed phragmocone, becoming more evenly spaced on the shaft. They attain their

maximum size at midshaft, sometimes forming large, subspinose clavi that project out to the side. They become smaller and more closely spaced on the hook, and usually extend to the aperture. The suture is characterized by a broad, asymmetrically bifid first lateral saddle and narrow, symmetrically to asymmetrically bifid first lateral lobe.

The holotype of *Hoploscaphites brevis*, by original designation and monotypy, is USNM 367, the original of *Scaphites nodosus* var. *brevis* Meek (1876: 428, pl. 25, fig. 1). Adults exhibit a wide range of variation in size, degree of compression, and coarseness of ornament. Adults are small to large (LMAX ranges from 29.5 to 101.5 mm in macroconchs and from 26.7 to 81.2 mm in microconchs), and rounded to ellipsoidal in lateral view. The body chamber consists of a relatively short shaft and a weakly recurved hook (apertural angle averages 59° in macroconchs). The ratio of whorl width to whorl height averages 0.73 at midshaft in both macroconchs and microconchs. The whorl section is subquadrate/ovoid, with fairly flat flanks, and a broadly rounded venter. Ribs are fine and flexuous and cross the venter with a weak adoral projection. There are 6–14 ribs/cm on the venter at midshaft in macroconchs and 8–18 ribs/cm on the venter at midshaft in microconchs. In most small specimens, umbilicolateral tubercles are absent on the phragmocone and, instead, the primary ribs are strong and adorally concave in this area. In large specimens, umbilicolateral tubercles usually appear midway or near the adoral end of the exposed phragmocone. They are small and relatively evenly spaced. In almost all specimens, umbilicolateral tubercles are present on the body chamber, and occur at one-fourth to one-third whorl height. They are more or less uniformly spaced with, occasionally, some approximation near the point of recurvature. In specimens that are rounded in lateral view, the umbilicolateral tubercles are arranged in a broad arc, which is one of the hallmarks of this species. Ventrolateral tubercles are stronger than umbilicolateral tubercles, and are usually present on the phragmocone starting anywhere from the point of exposure to the adoral end of the phragmocone. In general, they are unevenly spaced on the phragmocone, commonly occurring in pairs or clusters, becoming more evenly spaced on the shaft. As in *H. nodosus*, they attain their maximum size at midshaft. The ventrolateral tubercles usually die out near the point of recurvature, but if not, they become smaller, more bullate, and more closely spaced toward the aperture. The suture is the same as that in *H. nodosus*.

Hoploscaphites landesi Riccardi, 1983, is a junior subjective synonym of *H. brevis*. The holotype is a small, compressed, finely ornamented microconch of *H. brevis*. It grades into larger, more robust specimens, with coarser ornament. We thereby expand the definition of *H. brevis* to include a wide range of variation in adult size, and argue that such variation reflects variation in the age (and size) at which individuals reach maturity. Establishment of separate species for different size specimens, given that all other aspects of their morphology (shell shape, whorl cross section, pattern of ribs, distribution of umbilicolateral and ventrolateral tubercles, and suture) are the same, seems unwarrented.

Hoploscaphites nodosus and *H. brevis* are widespread in the *Baculites compressus–B. cuneatus* zones in the Western Interior of North America, which represent a time interval of approximately 580 ky (Cobban et al., 2006). They are also present in parts of the underlying *Didymoceras cheyennense* Zone and the overlying *B. reesidei* Zone, but their exact distribution in these zones is not yet known. *Hoploscaphites nodosus* and *H. brevis* occur in the Bearpaw Shale in Alberta and Saskatchewan, the Bearpaw Shale and Pierre Shale in Montana, and the Pierre Shale in North Dakota, South Dakota, Wyoming, Colorado, and Kansas. They occur in nearshore deposits such as the unnamed shale member of the Pierre Shale in Grand County, Colorado, in offshore deposits such as the DeGrey Member of the Pierre Shale in Buffalo County, South Dakota, and in cold methane seeps in the Pierre Shale in Custer County, South Dakota. They are absent in the U.S. Gulf and Atlantic Coastal plains and northern Europe, although similar forms are present in both these areas in strata above and below the biostratigraphic interval containing the ranges of *H. nodosus* and *H. brevis*. Thus, although *H. nodosus* and *H. brevis* are endemic to the Western Interior of North America, they are part of a more broadly distributed clade that is also present in the U.S. Gulf and Atlantic Coastal plains and northern Europe.

As adults, these scaphites probably lived just above the sea bottom. They preferred oxygenated water, as indicated by the fact that they are generally associated with a diverse molluscan community. Habitat depths are estimated at less than 100 m, based on studies of the mechanical properties of the septa and siphuncle (Tsujita and Westermann, 1998). The high

angle of orientation of the aperture at maturity is incompatible with a nektobenthic mode of life, involving scavenging or searching for food on the bottom. The apertural margin is also constricted and ends in a thin lip, which would have prevented unimpeded movement of the soft body outside of the aperture. Instead, scaphites may have consumed small prey in the water column, which is consistent with the presence of an aptychus-type lower jaw. Adults were probably poor swimmers, based on a comparison of their musculature with that of nautilus (assuming that such a comparison is valid). The uncoiling of the body chamber at maturity also increased the coefficient of drag and decreased hydrodynamic efficiency. The large ventrolateral tubercles on the shaft served as an antipredatory defense against attacks from behind. Healed injuries, as well as lethal injuries, are common on adult shells, especially on the adapical end of the body chamber. As with modern cephalopods, these scaphites were probably preyed upon by fish, reptiles, crustaceans, and other cephalopods.

INTRODUCTION

Studies of the stratigraphy of the Western Interior Basin of North America reveal that during the Late Cretaceous, a broad seaway extended from Mexico to the western Canadian Arctic (fig. 1) (Cobban and Reeside, 1952; Gill and Cobban, 1966; Jeletzky, 1971; Kauffman and Caldwell, 1993). The western shore of this seaway was bordered by a north-south trending unstable cordillera, whereas the eastern margin was formed by the low-lying stable platform of the eastern part of the conterminous United States and Canada (Cobban et al., 1994; Shurr et al., 1994). The sedimentatary record of this interval contains a rich molluscan fauna (Reeside, 1957; Cobban, 1951a, 1951b, 1969; Cobban and Scott, 1964; Cobban and Jeletzky, 1965; Sohl, 1967; Kennedy and Cobban, 1976; Kauffman, 1984; Kauffman et al., 1993; Landman and Waage, 1993; Larson et al., 1997). This fauna is renowned for its cephalopods, of which the most common are baculites and scaphites. Many of these ammonites are extremely well preserved, retaining their original shell material. They are also widely distributed and locally abundant, making them ideal index fossils. As a result, they have been extensively used to subdivide the Upper Cretaceous strata of the Western Interior into fine biostratigraphic zones (fig. 2) (Cobban et al., 2006). These fossils also constitute an extraordinary record of the evolutionary diversification of ammonites over approximately 25 million years.

This monograph is the first in a series treating the Campanian and Maastrichtian scaphites from the Bearpaw Shale and Pierre Shale of North America. It redescribes the species from the upper Campanian *Baculites compressus–B. cuneatus* range zones, comprising *Hoploscaphites nodosus* (Owen, 1852) and *Hoploscaphites brevis* (Meek, 1876). As first articulated by Meek (1876), these scaphites are part of what is known as the "*nodosus* group." They are among the best-known Cretaceous ammonites from North America, having been illustrated in many geology textbooks and guides to invertebrate fossils (Dunbar, 1960; Case, 1992; Monks and Palmer, 2002). They have also been the subject of many studies on the phylogeny of scaphites and the biostratigraphic zonation of the Upper Cretaceous of North America (Whitfield, 1880; Smith, 1905; Frech, 1915; Reeside, 1927a; Elias, 1933; Coryell and Salmon, 1934; Brown, 1943; Cobban and Jeletzky, 1965; Cobban et al., 1992; Jeletzky, 1960, 1962, 1971; Riccardi, 1983; Landman and Waage, 1993; Cooper, 1994; Monks, 2000). *Hoploscaphites nodosus* and *H. brevis*, as well as closely related forms, disappear in the middle of the *Baculites eliasi* Zone and are replaced by another subclade of the "*nodosus* group" including *H. plenus* (Meek, 1876) and *H. criptonodosus* (Riccardi, 1983).

In redescribing these two species, we examine their geographic distribution, biostratigraphy, mode of occurrence, morphology, life history, habitat, and systematics. We also treat the question of intra- and interspecific variation, based on the large number of specimens available to us. These specimens come from Saskatchewan, Alberta, Montana, North Dakota, South Dakota, Wyoming, Colorado, and Kansas. We showcase some of the exquisitely preserved specimens

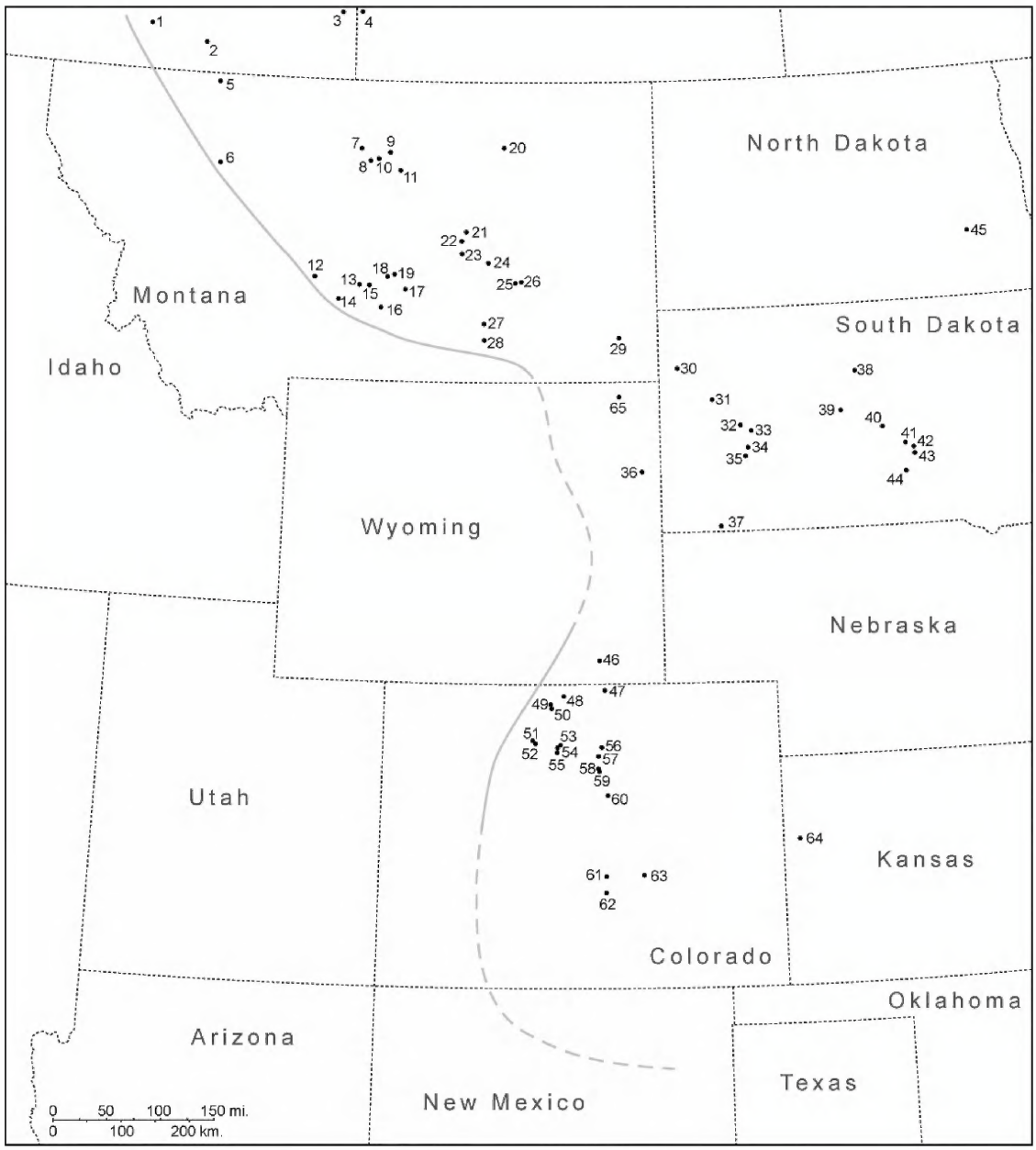

Fig. 1. Map of the upper Campanian *Baculites compressus* Zone showing the shoreline along the western margin of the Western Interior Seaway. The shoreline is dashed, for example, in eastern Wyoming, because of a lack of data. The dots indicate localities of *B. compressus*. Numbers refer to USGS Mesozoic localities, as listed below, except for locality 1 (Geological Survey of Canada). See appendix 1 for a description of localities. **1.** GSC C-186877 (Jerzykiewicz, 1996); **2.** D4129–32; **3.** D4125–27; **4.** D4120; **5.** 7325, D2553, D3634; **6.** 9866; **7.** 23990; **8.** 24178; **9.** D3819, D3820; **10.** D3827; **11.** D6854; **12.** 4710, 6037; **13.** D3624; **14.** D3083; **15.** D490; **16.** D4138; **17.** D764; **18.** D76; **19.** D3595, D3599; **20.** D4209; **21.** 21577, D5659; **22.** D782; **23.** D780; **24.** D2632, D2633; **25.** D3575; **26.** D3578; **27.** 21224; **28.** D3443; **29.** 23057; **30.** D1055; **31.** D4994; **32.** D1598, D2393; **33.** D3074; **34.** D1594, 23072; **35.** D13708; **36.** D2618; **37.** D213; **38.** D1661; **39.** D1657; **40.** D13791; **41.** D4968; **42.** D13507; **43.** D13508; **44.** D4965; **45.** D4101; **46.** D8782; **47.** D5037; **48.** D8378; **49.** D9637, D9640; **50.** D9677; **51.** D5991; **52.** D1351; **53.** D8089; **54.** D4497; **55.** D8068; **56.** D2723; **57.** D2941; **58.** D337; **59.** D40; **60.** D271, D280; **61.** D8004; **62.** D8874; **63.** D1080; **64.** D615; **65.** D440.

Stage		U.S. Western Interior Ammonite Zones	Age (Ma)
Campanian	Upper	*Baculites eliasi*	71.98 ± 0.31
		Baculites jenseni	
		Baculites reesidei	72.94 ± 0.45[a]
		Baculites cuneatus	
		Baculites compressus	73.52 ± 0.39[b]
		Didymoceras cheyennense	74.67 ± 0.15
		Exiteloceras jenneyi	75.08 ± 0.11[b]
		Didymoceras stevensoni	
		Didymoceras nebrascense	75.19 ± 0.28
	Middle	*Baculites scotti*	75.56 ± 0.11[c] 75.84 ± 0.26
		Baculites reduncus	
		Baculites gregoryensis	
		Baculites perplexus	
		Baculites sp. (smooth)	
		Baculites asperiformis	
		Baculites maclearni	
		Baculites obtusus	80.58 ± 0.55[b]
	Lower	*Baculites* sp. (weak flank ribs)	
		Baculites sp. (smooth)	
		Scaphites hippocrepis III	
		Scaphites hippocrepis II	81.86 ± 0.36
		Scaphites hippocrepis I	
		Scaphites leei III	

[a] $^{40}Ar/^{39}Ar$ on sanidine as corrected by Baadsgaard (1993).
[b] Low in zone.
[c] Izett et al. (1998).

Fig. 2. Upper Cretaceous (Campanian and Maastrichtian) ammonite biostratigraphy of the U.S. Western Interior showing the zones of *Baculites compressus* and *B. cuneatus* (Cobban et al., 2006). The absolute ages are derived from $^{40}Ar/^{39}Ar$ analyses of bentonites containing sanidines. In North America, the Campanian is divided into three parts. The Campanian/Maastrichtian boundary is currently placed in the middle of the *B. eliasi* Zone, based on recent work in Tercis, France, and the Vistula River Valley, Poland (Remin, 2009).

from South Dakota. Our material is mostly drawn from collections in the American Museum of Natural History, New York, New York; the Black Hills Museum of Natural History, Hill City, South Dakota; the U.S. Geological Survey, Denver, Colorado; the U. S. National Museum, Washington, D.C.; and the Yale Peabody Museum, New Haven, Connecticut.

HISTORICAL BACKGROUND

The two scaphite species redescribed in this paper are based on material that was originally collected in the mid-19th century during field expeditions to South Dakota and Montana, in what was then called the Nebraska Territory (fig. 3). These expeditions resulted in impressive monographs that covered all aspects of the natural history of the area, including paleontology and stratigraphy. The history of these expeditions, spanning more than 50 years, has been described in detail by Goetzmann (1966), Waage (1968), Hartman (1984, 1999), Foster (1994), and Martin et al. (2007). We are interested in determining the localities where the original ammonite specimens were collected, inasmuch as these sites represent the type localities for the two species.

The description of *Scaphites nodosus* (= *Hoploscaphites nodosus*) was published by David Dale Owen in 1852 in the "Report of a geological survey of Wisconsin, Iowa, and Minnesota; and incidentally of a portion of Nebraska Territory made under instructions from the United States Treasury Deparment" (fig. 4). In 1849, Owen employed one of his "subagents," John Evans, to explore the Upper Missouri River. Evans accompanied a party from the American Fur Company, who facilitated his travel, and eventually reached the White River Badlands east of the Black Hills in Nebraska Territory, now western South Dakota.

Owen (1852: 195) published the "substance" of Evan's report. According to his report, he noted the presence of *Hoploscaphites nodosus* "in the Fox Hills, which form the dividing ridge between the Cheyenne and Moreau River." However, in the description of this species and the figure caption accompanying the illustration of *Scaphites nodosus*, Owen (1852: 581, pl. 8, fig. 4) listed the locality of this species as "Sage Creek, a southern tributary of the Cheyenne," not the dividing ridge between the Cheyenne and Moreau rivers (fig. 3). According to Owen (1852: 195), Evans did, indeed, visit Sage Creek, noting the presence of *Inoceramus* and *Baculites* at the site, and added that

> at most of these localities, and especially on Sage Creek, the Ammonites and other fossils form the nucleus of argillaceous and ferruginous septaria, which lie strewn on the surface, or scattered in the beds of the streams; the soft, argillo-calcareous matrix having been washed

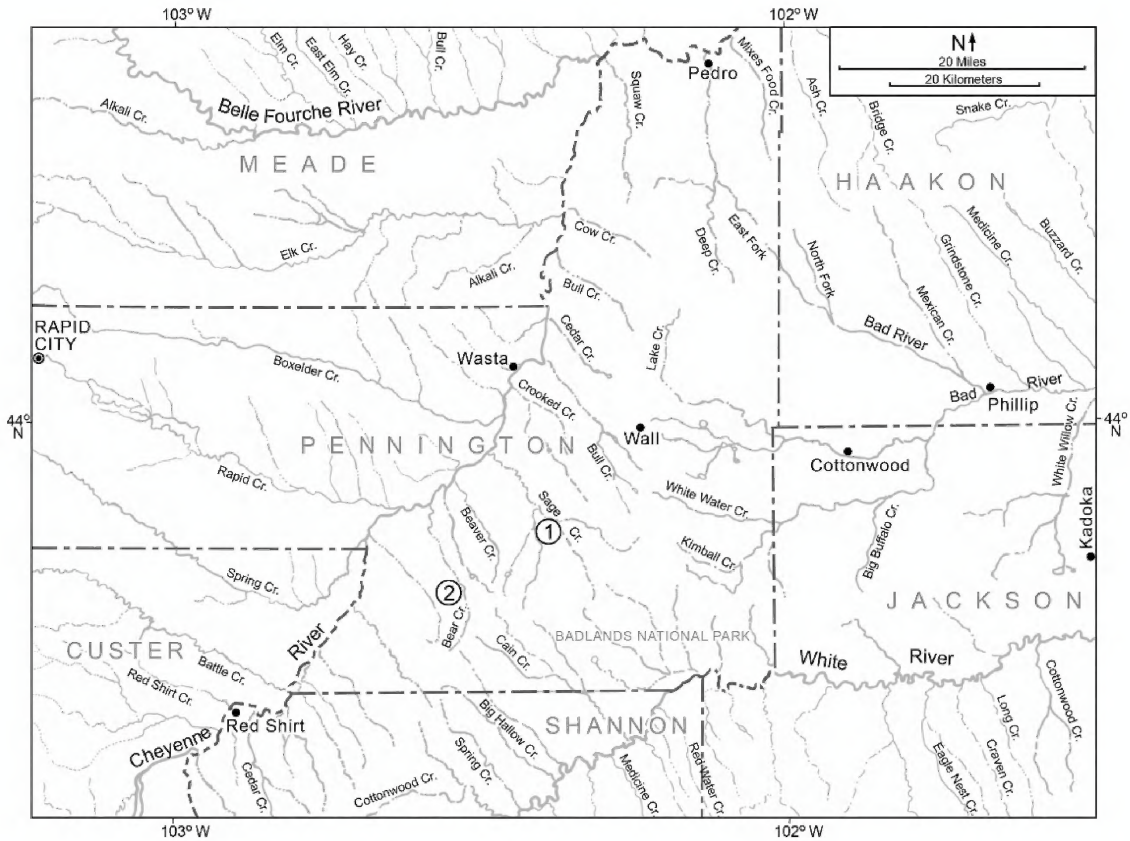

Fig. 3. Drainage map of southwest South Dakota showing the rivers and creeks mentioned in early accounts of western exploration of part of what was then known as the Nebraska Territory. The numbers 1 and 2 indicate Sage Creek and Bear Creek, respectively, two of the collecting localities of Meek and Hayden in 1853.

> from around them. Some of these possess the character of ironstones, others have the property of hydraulic cement. The fossils are mostly procured by breaking up these septaria, which are of very irregular fracture; and it is therefore difficult to obtain them entire.

Of the two localities mentioned by Owen, it is much more likely that the holotype of *Hoploscaphites nodosus* came from the vicinity of Sage Creek rather than the dividing ridge between the Cheyenne and Moreau rivers. The Pierre Shale crops out extensively in the Sage Creek area and contains many specimens of this species. It is less likely that the specimen was collected to the north (the dividing ridge between the Cheyenne and Moreau rivers) because most of the exposures in this area are stratigraphically higher.

The holotype of *Hoploscaphites nodosus* is covered with patches of orange-red material, especially on the body chamber. Similarly colored fossils are sometimes found in medicine bags of Indians from the Northern Great Plains (Landman, 1983). Such fossils were rubbed with a red substance and adorned with pieces of hide and strands of beads. These "sacred stones" or "rock medicine" were used in ceremonies by tribal medicine men to cure the sick. Many of these objects were brought back by explorers during expeditions to the American West in the 19th century. If the holotype of *H. nodosus* were such an amulet, then Evans would have acquired it by trade rather than collection, and its provenance would be even more difficult to establish. (As a curiosity, a

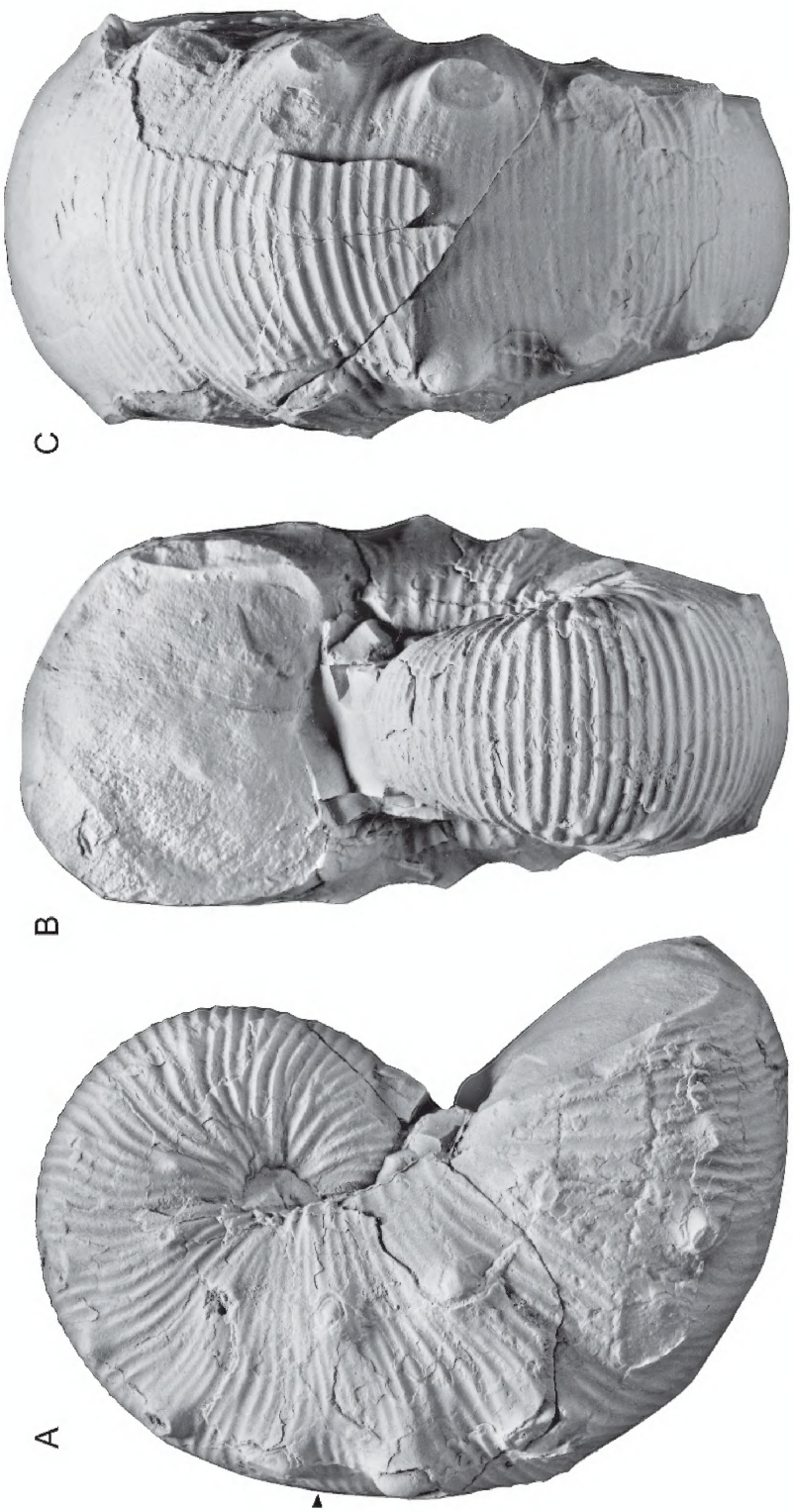

Fig. 4. *Hoploscaphites nodosus* (Owen, 1852), macroconch with part of the hook missing, holotype, UC 6381, Pierre Shale, probably from the Sage Creek area, Pennington County, South Dakota. **A.** Right lateral; **B.** apertural; **C.** ventral. Specimen is illustrated natural size.

specimen of *H. brevis* has been documented in the Hopewell Mounds, Ross County, Ohio, in deposits dating from 100 BCE to 300 CE; J Murphy, personal commun.)

The mineralogy of the red material on the holotype of *Hoploscaphites nodosus* was determined using X-ray diffraction analysis. For comparison, we analyzed similar red material on a specimen (YPM 11169) of *Clioscaphites vermiformis* (Meek and Hayden, 1862) purported to be from a medicine bag, according to the label (fide Landman, 1983: 23, top figure). The results indicate that the red material on the specimen of *C. vermiformis* is a mixture of hematite and quartz grains whereas the red material on the holotype of *H. nodosus* is cinnabar. The cinnabar granules are suspended in a clear resin, possibly lacquer or glue. Unlike hematite, cinnabar does not occur naturally in the Northern Great Plains. It is possible that cinnabar was a pigment in commercial paint in the 19th century. Such paint may have been applied to the specimen after it was brought back east to protect it or prepare it for museum display. In any event, the fact that the red material on the holotype of *H. nodosus* is cinnabar indicates that the specimen probably did not originate in a medicine bag, but was collected by Evans in the field.

Owen did not cite the repository of the holotype of *Hoploscaphites nodosus* nor any of the other specimens he described. The holotype is presently in the Field Museum and is listed as coming from the William F.E. Gurley Collection. Gurley was State Geologist of Illinois from 1893–1897 and his collection was acquired by the University of Chicago (Winchell, 1900). In 1900, Gurley became Associate Curator at the Walker Museum of Paleontology at the University of Chicago and continued there until his death in 1943. The fossil collection of the Walker Museum was transferred to the Field Museum in 1965.

Additional specimens of *Hoploscaphites nodosus* and what was later called *Scaphites nodosus* var. *brevis* (= *Hoploscaphites brevis*) (fig. 5) and *Scaphites nodosus* var. *quadrangularis* (= *H. brevis* and *H. plenus*, microconchs) (fig. 6) were collected by Fielding B. Meek and Ferdinand V. Hayden. This dynamic duo first visited what is now western South Dakota in the summer of 1853, while still assistants of James Hall, then State Geologist of New York. They explored Sage Creek and Bear Creek, both of which are tributaries of the Cheyenne River (fig. 3). Their experience in Sage Creek was recorded by Meek in his journal entry for Monday, June 27, 1853 (housed in the Meek archives of the Smithsonian Institution):

> Along in the bed of [the] creek we found by breaking open nodules fine specimens of Ammonite, Baculite, Scaphite, Inoceramus, Nautilus, Dentatum [sic], etc., together with some small univalves—all these fossils are found in the lower clay beds but they are generally crushed, and fall to fragments when the crumbling clay is touched. Some of the Ammonites are very large, in nodules, not less than 3 ft. in diam.... This is certainly a very fine locality—two or three men could almost load a cart with fossils in two days.

According to a biography of Hayden, the two men amassed 13 boxes of mostly Cretaceous fossils (Foster, 1994).

The material was sent home to James Hall who later sold a portion of the collection to compensate for his expenses (Foster, 1994). A part of this collection was purchased by the American Museum of Natural History in 1875 for 65,000 (Landman and Winston, 1999). The reason for this purchase is stated in *The Seventh Annual Report of the American Museum of Natural History* (1875: 6): "As this work was done from the basis of the New York geological formations, and large collections were made from the Western States for the fuller and more complete illustration and the fixing of the New York geological nomenclature, it became a matter of just pride with us to secure... the interesting and authentic examples of a work so extensive and important." The AMNH collection contains several specimens of *Hoploscaphites nodosus* and *H. brevis* from the Hall collection. For example, AMNH 9520/1, a macroconch of *H. nodosus*, is recorded as having come from the Hall collection and as having been collected at Sage Creek (unpublished Catalogue of the Palaeontological Collection, vol. 3; not listed in Whitfield and Hovey, 1898). It is possible that this specimen was part of Meek and Hayden's original haul.

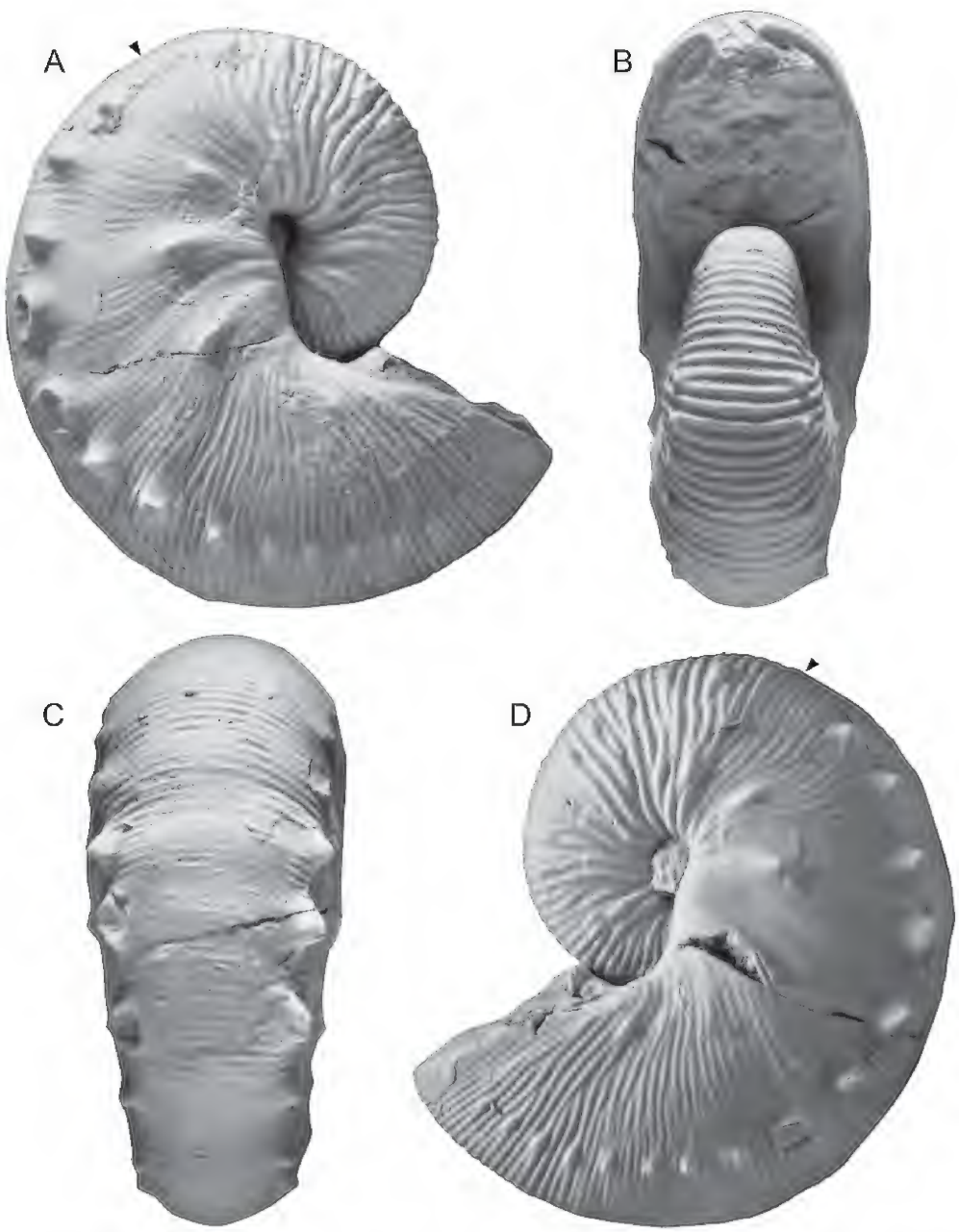

Fig. 5. *Hoploscaphites brevis* (Meek, 1876), macroconch, holotype, USNM 367, Pierre Shale, probably from the Sage Creek area, Pennington County, South Dakota. **A.** Right lateral; **B.** apertural; **C.** ventral; **D.** left lateral. Specimen is illustrated natural size.

After the joint expedition of Meek and Hayden in 1853, Hayden made many more excursions into the field. In the summer of 1854, he explored the region around Fort Union, collecting fossils along the Yellowstone River and at the mouths of the Powder, Tongue, and Bighorn rivers. He revisited Sage Creek in February 1855. His experience was described by Foster (1994: 64): "Despite storms that dumped two feet of snow and dropped the thermometer twenty below zero, they reached Sage Creek where Hayden spent

nearly a week. He also collected around Pineas Spring, on the north fork of what is now called the Bad River." [Pineas Spring, variously spelled Poeno Spring or Pino's Spring, was a popular camp site on the Fort Pierre–Fort Laramie trail located at the head of present day Poeno Creek, a small tributary of the North Fork of the Bad River (fide Waage, 1968)]. Hayden spent another five days at Sage Creek and Bear Creek in May 1855, and filled two carts with fossils. Hayden was also invited by Alexander Culbertson, the agent in charge of all the forts on the upper Missouri and Yellowstone rivers to spend the summer of 1855 around Fort Benton, where he collected fossils along the Missouri River and its tributaries.

Hayden returned to St. Louis in January 1856 with the collections from 1854–1855. According to Foster (1994: 66), "he brought an extraordinary harvest: six tons of specimens accumulated over two years, including more than a thousand pounds of fossils he wanted to work up with Meek, which he expected would occupy them for five years." Meek saw some of the collection in early February 1856 and wrote "They are grand—magnificent. All of them as perfect as recent shells. There are not less than 50 species most of which are new" (quoted in Foster, 1994: 67). In the Meek archives of the Smithsonian Institution, there is a newspaper clipping attached to a letter from Hayden to Meek dated February 6, 1856. The clipping, from a St. Louis newspaper, describes Hayden's collections and is entitled "Remarkable Cabinet of Natural Curiosities":

> We passed an hour very pleasantly on Saturday in examining a collection of Natural curiosities made by Dr. HAYDEN, and in receiving from him an account of his explorations of the country on the Upper Missouri and its tributaries. Two years ago, Dr. HAYDEN, led by a love of adventure and a desire to examine the Geological structure and to become familiar with the Natural History of that far-off and almost unknown region, left this city. He had no experience of the hardships or dangers of such an enterprise, but started out on "his own hook." He soon found friends ready and willing to assist him in his wanderings, and among them Col. A. J. VAUGHAN, U.S. Indian Agent, and the members of the Fur Company on the Upper Missouri. To them he is indebted for many facilities in accomplishing his objects, although at times his explorations led him far from their forts, and frequently among hostile tribes of Indians, who watched his movements with great curiosity, and formed very absurd notions of his sanity in seeking for and collecting the curious specimens in Natural History that now forms his valuable cabinet.
>
> During his absence, he explored the Missouri river from Council Bluffs to Fort Benton, and the Yellow Stone for four hundred miles above its mouth. He also explored the celebrated region of the *Manvaisse Terre* [sic], or Bad Sand [sic], of White river, and made a most valuable collection of the Fossils of that wild and inhospitable section. In this time, his collections in Natural History were very numerous, embracing Fossils, Plants, Insects [indistinct], Shells, Reptiles, Fishes, and Skins of Manduallas [sic] and Birds. Many of these specimens are entirely new to Scientific men, and are in a remarkable state of preservation.
>
> Through the kindness and liberality of Mr. CHAS. P. CHOUTEAU of this city, the most valuable part of the collection—the Fossils—were conveyed from Fort Pierre to this city, and are now arranged at his residence. This collection is well worthy of the attention of our scientific men. We do not know Dr. HAYDEN's intention, but it ought not to be allowed to leave this city, if he should be willing to dispose of it. We have heretofore earnestly advocated the purchase of Mr. WYMAN's collection of Birds, &, and we should be glad to see Dr. HAYDEN's collection purchased in the same way, to be made the foundation of a Cabinet of Natural Curiosities in this city. Will not some of our wealthy men take hte [sic] matter in hand?

The description of the scaphites collected by Meek and Hayden was published in installments starting in 1856. Some of the material was described by Hall and Meek (communicated 1854; imprinted 1855; published 1856) who listed *Scaphites nodosus* and analyzed the ontogenetic development of its suture, but did not illustrate any specimens. In 1856, Meek and Hayden published five articles in *Proceedings of the Academy of Natural Sciences of Philadelphia* (designated as Meek and Hayden, 1856a–e, in the References). In one of the papers (1856e), they listed *Scaphites nodosus* as coming from Formation 4 (= Pierre Shale). Meek and Hayden (1860) included *S. nodosus*, *S.*

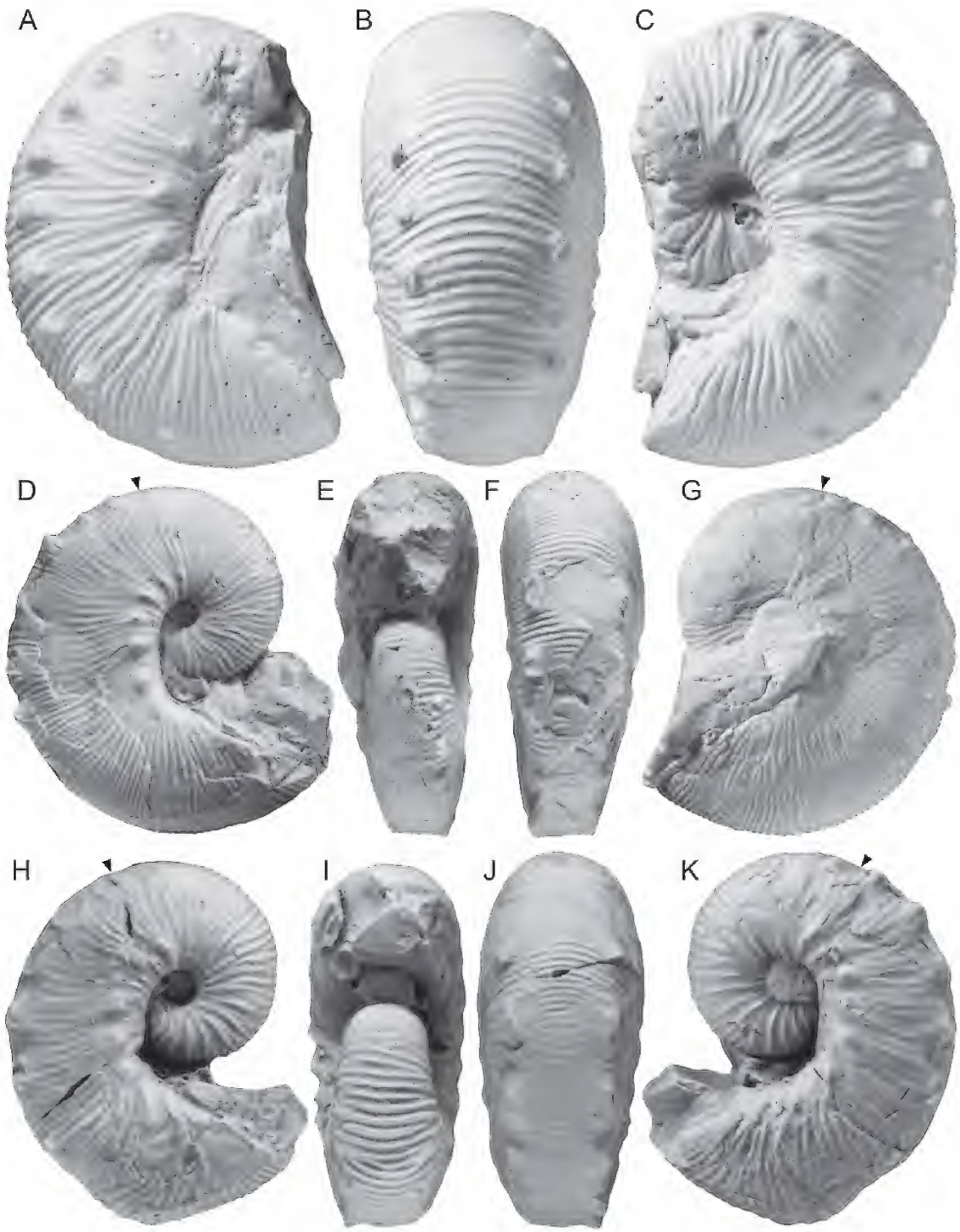

Fig. 6. **A–C.** *Hoploscaphites plenus* (Meek, 1876), microconch, USNM 365 (= *Scaphites nodosus* var. *quadrangularis*, paratype, cast), illustrated in Meek (1876: pl. 25, fig. 4), said to be from the Pierre Shale on the "Yellowstone River, Montana, 150 miles above its mouth," and probably, more specifically, from the Cedar Creek Anticline, Dawson County, Montana. **A.** Right lateral; **B.** ventral; **C.** left lateral. **D–G.**

nodosus var. *brevis*, and *S. nodosus* var. *quadrangularis* in their systematic catalog of fossils collected in the Nebraska Territory by the exploring expeditions under the direction of Lieutenant G.K. Warren. Meek (1864) included these same species in his checklist of the invertebrate fossils of North America.

Meek's full description of *Scaphites nodosus* var. *brevis* and *S. nodosus* var. *quadrangularis* did not appear until 1876. Although Hayden made additional field trips to western South Dakota in 1856, 1857, and 1866, Meek's descriptions were based on material collected in 1854–1855. Hayden (in Meek, 1876: iii, iv) commented that "The accumulation of the materials which compose this volume was commenced in the spring of 1854, and the greater number of the new species of fossils were discovered by the writer of this letter during that and the succeeding year."

Meek (1876) provided the following information about the locality of the holotype of *Scaphites nodosus* var. *brevis* (USNM 367) (fig. 5): "Dr. Owen's type-specimen came from near Cheyenne River, Dakota, where it was found in the upper part of the Fort Pierre group. Ours is from the same horizon on the Yellowstone River, Montana, 150 miles above its mouth." The same locality appears on the label for this specimen. In the *Catalogue of the Type Specimens of Fossil Invertebrates in the Department of Geology, U.S. National Museum* (Schuchert, 1905: 588), the locality is further restricted to the Yellowstone River, near Miles City, Montana, although this was probably added later on (in fact, a distance of 150 miles above the river mouth, as measured along the river, is midway between Miles City and Glendive, Montana). In contrast, the entry for this specimen in the handwritten catalog of the Department of Paleobiology, U.S. National Museum, states that the specimen was collected from the south fork of the Cheyenne River, that is, in western South Dakota. Of these two localities, the latter is much more in agreement with the source of most of our specimens and that of the holotype of *Hoploscaphites nodosus*. In contrast, the exposures of the Pierre Shale near Glendive, Montana, in the Cedar Creek Anticline, while richly fossiliferous, are higher up in the section and yield specimens of *H. plenus* rather than *H. brevis*.

Meek (1876: 429) cited the same Yellowstone River locality for *Scaphites nodosus* var. *quadrangularis*. In the *Catalogue of the Type Specimens of Fossil Invertebrates in the Department of Geology, U.S. National Museum* (Schuchert, 1905: 588), the locality is given as both "Fort Pierre (Cret.). Yellowstone River, near Miles City, Montana, and Cheyenne River, South Dakota." The illustrated specimens are a mixture of microconchs of two species: *Hoploscaphites brevis* (Meek, 1876: pl. 25, fig. 2a–c = USNM 386690) (fig. 6D–G) and *H. plenus* (Meek, 1876: pl. 25, fig. 3a–c = USNM 366; fig. 4 = USNM 365) (fig. 6H–K and 6A–C, respectively). In the handwritten catalog of the Department of Paleobiology, U. S. National Museum, a note states that these three specimens were renumbered. We suspect that the two microconchs of *H. plenus* are from the vicinity of the Yellowstone River, Montana, and the microconch of *H. brevis* is from the vicinity of the Cheyenne River, South Dakota.

Other specimens labeled as *Scaphites nodosus* var. *quadrangularis* in the USNM collections also represent a mixture of spe-

←

Hoploscaphites brevis (Meek, 1876), microconch, USNM 386690 (= *Scaphites nodosus* var. *quadrangularis*, paratype) illustrated in Meek (1876: pl. 25, fig. 2a–c), said to be from the Pierre Shale on the "Yellowstone River, Montana, 150 miles above its mouth," but probably from the Sage Creek area, Pennington County, South Dakota. The aperture is restored in Meek's illustration. **D.** Right lateral; **E.** apertural; **F.** ventral; **G.** left lateral. **H–K.** *Hoploscaphites plenus* (Meek, 1876), microconch, USNM 366 (= *Scaphites nodosus* var. *quadrangularis*, holotype), illustrated in Meek (1876: pl. 25, fig. 3a–c), said to be from the Pierre Shale on the "Yellowstone River, Montana, 150 miles above its mouth," and probably, more specifically, from the Cedar Creek Anticline, Dawson County, Montana. It exhibits a repaired injury just adapical of the point of recurvature. **H.** Right lateral; **I.** apertural; **J.** ventral; **K.** left lateral. Specimens are illustrated natural size. The position of the base of the body chamber in D, G, H, and K is estimated due to poor preservation.

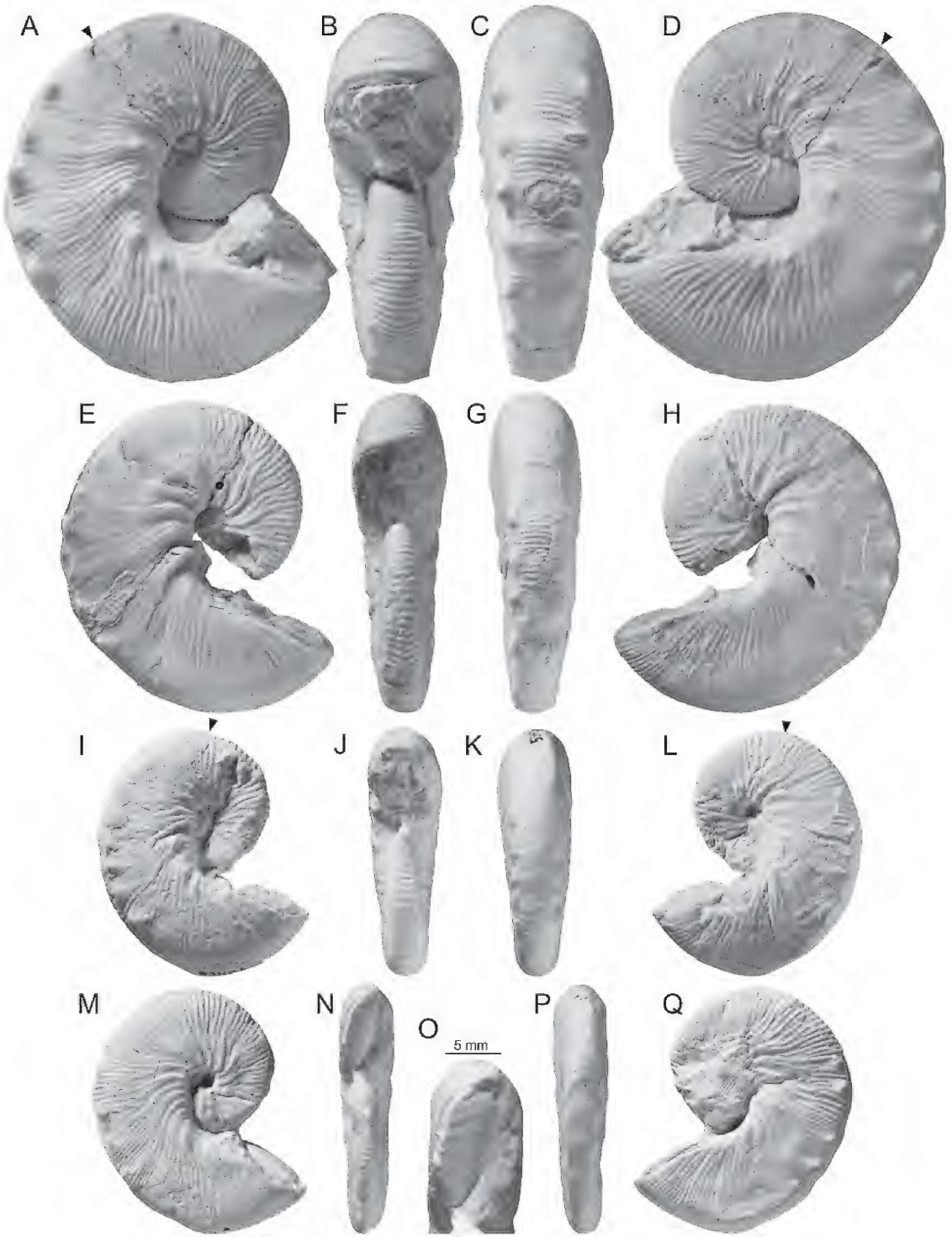

Fig. 7. *Hoploscaphites brevis* (Meek, 1876), microconchs. **A–D.** USNM 12291 (= *Scaphites nodosus* var. *quadrangularis*), illustrated in Whitfield (1880: pl. 13, figs. 10, 11), said to be from the Pierre Shale "on the Cheyenne River, near Rapid and French Creeks, and also from beds which contain a mingling of the

cies. One tray contains six specimens with the number 366 (the number "370" is crossed out) and the locality "Upper Yellowstone 150 mi from mouth." The specimens are all *Hoploscaphites plenus* and, as such, the stated locality is probably correct. However, another specimen (USNM 315704) labeled as a paratype of *Scaphites nodosus* var. *quadrangularis* is actually a macroconch of *H. nodosus*, although it is also labeled as coming from the Yellowstone River, Montana. The specimen (USNM 12291) illustrated by Whitfield (1880: pl. 13, figs. 10, 11) (fig. 7A–D) as *Scaphites nodosus* var. *quadrangularis* is a microconch of *H. brevis*. It is said to be from the Pierre Shale "on the Cheyenne River, near Rapid and French Creeks, and also from beds which contain a mingling of the fossils of this and the succeeding group on Old Woman Fork, Black Hills."

The confusion regarding localities can be traced to several sources. Hayden's explorations in 1854–1855 included both the Pierre Shale along the Cheyenne River, South Dakota, and the Pierre Shale along the Yellowstone River, Montana. Therefore, the specimens may have become mixed up in the field, on the trip back, or at the museum. Indeed, as noted, the suite of specimens was renumbered at some point, presumably at the museum. In addition, Meek considered the two sites as representing the same stratigraphic horizon. He also considered all of the loosely uncoiled specimens (= microconchs) as representing the same species (which he named *Scaphites nodosus* var. *quadrangularis*). As a consequence, he may not have realized that the specimens were mixed up at all, and, in effect, perpetuated the confusion. To further complicate matters, Meek (1876: xxi) wrote most of his massive monograph while wintering in Florida, "away from many desired facilities."

The scaphite collections at the Academy of Natural Sciences of Philadelphia (ANSP) contain the same errors with respect to these species and localities. The academy purchased these collections in 1857 from the Smithsonian Institution. According to Foster (1994: 75), the academy paid Hayden $1,200 for an assortment of vertebrate and invertebrate fossils collected in 1854–1855. One tray in the ANSP collections contains an unnumbered specimen of *Hoploscaphites brevis* and a fragmentary, unidentifiable specimen with the number 366 (one of the same numbers as in the Smithsonian collections). There are three labels in the tray, all of which cite the Smithsonian and list the locality as the Yellowstone River, Montana. In addition, there are two other trays, one of which contains fragmentary specimens from the Pierre Shale of Montana, with the number 366, and the other one of which contains a partial specimen of *H. brevis* with the label "Ft. Pierre Gp., Montana."

ZONATION

Hoploscaphites nodosus and *H. brevis* are present in the Pierre Shale in Montana, North Dakota, South Dakota, Wyoming, Colorado, and Kansas, and in the Bearpaw Shale (referred to as the Bearpaw Formation by the Geological Survey of Canada) in Saskatchewan, Alberta, and Montana. Both of these formations are subdivided into finer lithostratigraphic units, which vary from region to region. Recently, Martin et al. (2007) elevated the Pierre Shale in South Dakota and eastern Wyoming from formational to group status and, concomitantly,

←

fossils of this and the succeeding group on Old Woman Fork, Black Hills." The aperture is restored in Whitfield's illustration. **A.** Right lateral; **B.** apertural; **C.** ventral; **D.** left lateral. **E–H.** GSC 5342a (= holotype, *Hoploscaphites landesi* Riccardi, 1983, pl. 1, figs. 13, 14), "? Demaine Sandstone, Bearpaw Formation, and South Saskatchewan River opposite mouth of Swift Current River, Saskatchewan." **E.** Right lateral; **F.** apertural; **G.** ventral; **H.** left lateral. **I–L.** GSC 5342b (= paratype, *Hoploscaphites landesi* Riccardi, 1983, pl. 1, figs. 15–17), same locality as E–H. **I.** Right lateral; **J.** apertural; **K.** ventral; **L.** left lateral. **M–Q.** GSC 5342c (= paratype, *Hoploscaphites landesi* Riccardi, 1983, pl. 1, figs. 20–22), same locality as E–H. **M.** Right lateral; **N.** apertural; **O.** close-up of the aperture with part of the lower jaw exposed; **P.** ventral; **Q.** left lateral. Specimens are illustrated natural size.

elevated the members of the Pierre Shale to formational status. To maintain consistency with previously published reports, we retain the original nomenclature of the Pierre Shale as used, for example, by Crandell (1958) and Gill and Cobban (1966).

The ammonite zonation of the Upper Cretaceous of the Western Interior of North America was first summarized by Cobban and Reeside (1952). Since then, it has undergone many revisions (e.g., Robinson et al., 1959; Scott and Cobban, 1965, 1975, 1986a, 1986b; Gill and Cobban, 1966; Cobban 1951a, 1958a, 1958b, 1969; Cobban and Hook, 1979; Kennedy and Cobban, 1991; Kennedy et al., 2001; Landman and Waage, 1993), culminating in one of the most refined zonal schemes of any system in the geological record (Cobban et al., 2006). It consists of 66 zones, which are stacked one on top of another. However, it is important to note that the strata themselves are seldom continuously fossiliferous. In particular, the ammonites in the Pierre Shale and Bearpaw Shale tend to occur in concretionary horizons that are separated by intervals that are either nonfossiliferous or contain fossils that are too fragmentary to identify with any certainty. Thus, a zone ususally includes an interval in which the zonal fossils are missing. This is a common and practical approach in establishing a zonation. For example, in defining the ammonite zones of the Pierre Shale at Red Bird, Wyoming, Gill and Cobban (1966: A28) stated "an attempt will be made to estimate the vertical range of certain ammonites at Red Bird including strata that do not contain fossils. . . ." As an illustration, in establishing the top of the *Baculites eliasi* Range Zone and the base of the overlying *Baculites baculus* Range Zone, Gill and Cobban (1966: A33) noted that "Unit 87, 15 feet above the highest collection of *B. eliasi* (D1969), contains abundant *Inoceramus typicus*, a pelecypod characteristic of the Range Zone of *Baculites baculus*. This 15-foot interval is arbitrarily divided between the two zones... ." Thus, the top of the *B. eliasi* Range Zone and the base of the overlying *B. baculus* Range Zone are defined at a horizon that does not contain either fossil. Although this approach is unavoidable, it nevertheless introduces a certain amount of error into the zonal scheme, which affects the limits of resolution in correlating strata from one geographic region to another.

Recognition of a biostratigraphic zone also depends upon the proper identification of the fossil taxon on which the zone is based. As a result of taxonomic revisions over time, the upper and lower boundaries of a zone can change and new zones and subzones can be added, leading to a more refined zonation. For example, in the early version of the ammonite zonation of the Upper Cretaceous of the Western Interior (Cobban and Reeside, 1952), the *Baculites compressus* Zone occupies a thick stratigraphic interval. *Baculites compressus* (Say, 1820) is characterized by an elliptical cross section, smooth to weakly ribbed venter, and lack of ornament on the flanks, except in large specimens. Subsequently, *Baculites cuneatus* Cobban, 1962a, was described. This form was previously included in *B. compressus*, but differs from it in having a trigonal cross section with a very narrow venter, and moderately strong ribbing on the venter and flanks in both small and large specimens. In addition, *B. compressus* var. *robinsoni* Cobban, 1962a, was described from central Montana and southern Canada. It differs from *B. cuneatus* in having a broader venter, stronger ornament, and less deeply incised suture. According to Cobban (1962a), this variety is either a geographic subspecies of *B. compressus* or transitional to *B. cuneatus*. As a consequence of these taxonomic revisions, later versions of the ammonite zonation of the Upper Cretaceous (e.g., Gill and Cobban, 1966; Scott and Cobban, 1986a) include a thinner *B. compressus* Zone overlain by the *B. cuneatus* Zone.

Hoploscaphites nodosus and *H. brevis* are widespread in the *Baculites compressus–B. cuneatus* zones of the Western Interior of North America (fig. 2). They also extend into the upper part of the underlying *Didymoceras cheyennense* Zone and into the lower part of the overlying *Baculites reesidei* Zone, but their exact distribution in these zones is not yet known. These four zones occupy the middle of the upper Campanian, according to the informal tripartite subdivision of the Campanian in North America (Cobban et al., 2006), and represent what is known as the Bearpaw cycle (Kauffman and Caldwell,

1993). Cobban et al. (2006) reported the radiometrically determined ages of bentonites from these zones as follows: 74.67 ± 0.15 Ma for a bentonite from the *Didymoceras cheyennense* Zone, 73.52 ± 0.39 Ma for a bentonite in the lower part of the *Baculites compressus* Zone, and 72.94 ± 0.45 Ma for a bentonite from an unspecified level in the *B. reesidei* Zone. Thus, the duration of the *B. compressus–B. cuneatus* zones (= the difference in age between the bentonite in the lower part of the *B. compressus* Zone and the bentonite from an unspecified level in the *B. reesidei* Zone) is approximately 580,000 years. The range of *H. nodosus* and *H. brevis* (= the difference in age between the bentonite in the upper part of the *D. cheyennense* Zone and the bentonite at an unspecified level in the *B. reesidei* Zone) is approximately 1.73 Ma. Both species show a slight increase in size throughout this interval, expecially in the *B. cuneatus* Zone, but are otherwise unchanged.

The *Baculites compressus–B. cuneatus* zones are present in western Canada. They have been reported from the Bearpaw Shale in southern Alberta (Williams, 1930; Williams and Dyer, 1930; Russell and Landes, 1940; Russell, 1950; Gill and Cobban, 1966; Riccardi, 1983; Larson et al., 1997; Tsujita and Westermann, 1998) and southern Saskatchewan (Fraser et al., 1935; Robinson, 1945; Caldwell, 1968; Riccardi, 1983). In addition, Wickenden (1945: 49) noted the presence of the *Baculites compressus* Zone in the Riding Mountain Formation in southwestern Manitoba, which is equivalent to the Bearpaw Shale in Alberta and Saskatchewan.

The *Baculites compressus–B. cuneatus* zones are also present in central and eastern Montana (figs. 7, 8) (Dobbin and Erdmann, 1955; Cobban, 1962a, 1962b; Jensen and Varnes, 1964; Izett et al., 1971; Gill et al., 1972; Larson et al., 1997). They occur in the Bearpaw Shale in Glacier, Chouteau, Meaghar, Blaine, Fergus, Wheatland, Golden Valley, Musselshell, Stillwater, Big Horn, Rosebud, Garfield, Teton, and Valley counties; in the Livingston Formation in Park County; and in the Pierre Shale in Carter County. The combined thickness of the two zones near Mosby, Garfield County, and Porcupine Dome, Rosebud County, is 30 m and 45 m, respectively (figs. 8, 9).

The *Didymoceras cheyennense–Baculites cuneatus* zones are absent in east-central Wyoming. In their study of the Red Bird section of the Pierre Shale in Niobrara County, Wyoming, Gill and Cobban (1966: 32) noted that "only 6 feet of shale in the upper part of the lower unnamed shale member (unit 68) seems to be assignable to these zones." No phosphatic pebbles or other features indicating slow deposition are present. They hypothesized that the absence of these ammonite zones may be due to submarine erosion. Gill et al. (1970) documented a widespread unconformity farther west in the south-central part of Wyoming at the base of the Teapot Sandstone Member of the Mesaverde Formation, which may correspond to this interval. In contrast, the *Baculites compressus–B. cuneatus* zones are present in the Pierre Shale in Weston and Laramie counties, Wyoming.

In South Dakota, the *Baculites compressus–B. cuneatus* zones are well exposed in the western two-thirds of the state. They have been reported from the Pierre Shale in Butte, Pennington, Custer, Shannon, Meade, Haakon, Ziebach, Mellette, Jones, Stanley, Dewy, Hughes, Lyman, Buffalo, and Brule counties (Searight, 1937; Crandell, 1958; Robinson et al., 1959; Cobban, 1962a, b; Cobban and Larson, 1997; Black, 1964; Stoffer, 1998, 2003; Fox, 2007; Hanczaryk and Gallagher, 2007; Martin et al., 2007). The combined thickness of the two zones is approximately 30 m at AMNH locs. 3408 and 3409 along Elk Creek, Meade County. At AMNH loc. 3212, along Cedar Creek, Shannon County, the combined thickness of the two zones is approximately 14 m (Stoffer, 1998). In some exposures in Meade County, e.g., AMNH loc. 3274, we have noted that both *B. compressus* and *B. cuneatus* are present in the same horizon, and even in the same concretion. It is possible that such strata represent a transitional interval between the two zones. The *B. compressus–B. cuneatus* zones are also present in the Pierre Shale in Barnes County, North Dakota, and in Dawes County, Nebraska (Tharalson, 1993).

In Colorado, Scott and Cobban (1965, 1975, 1986a, 1986b) mapped the Pierre Shale along the Front Range of the Rocky

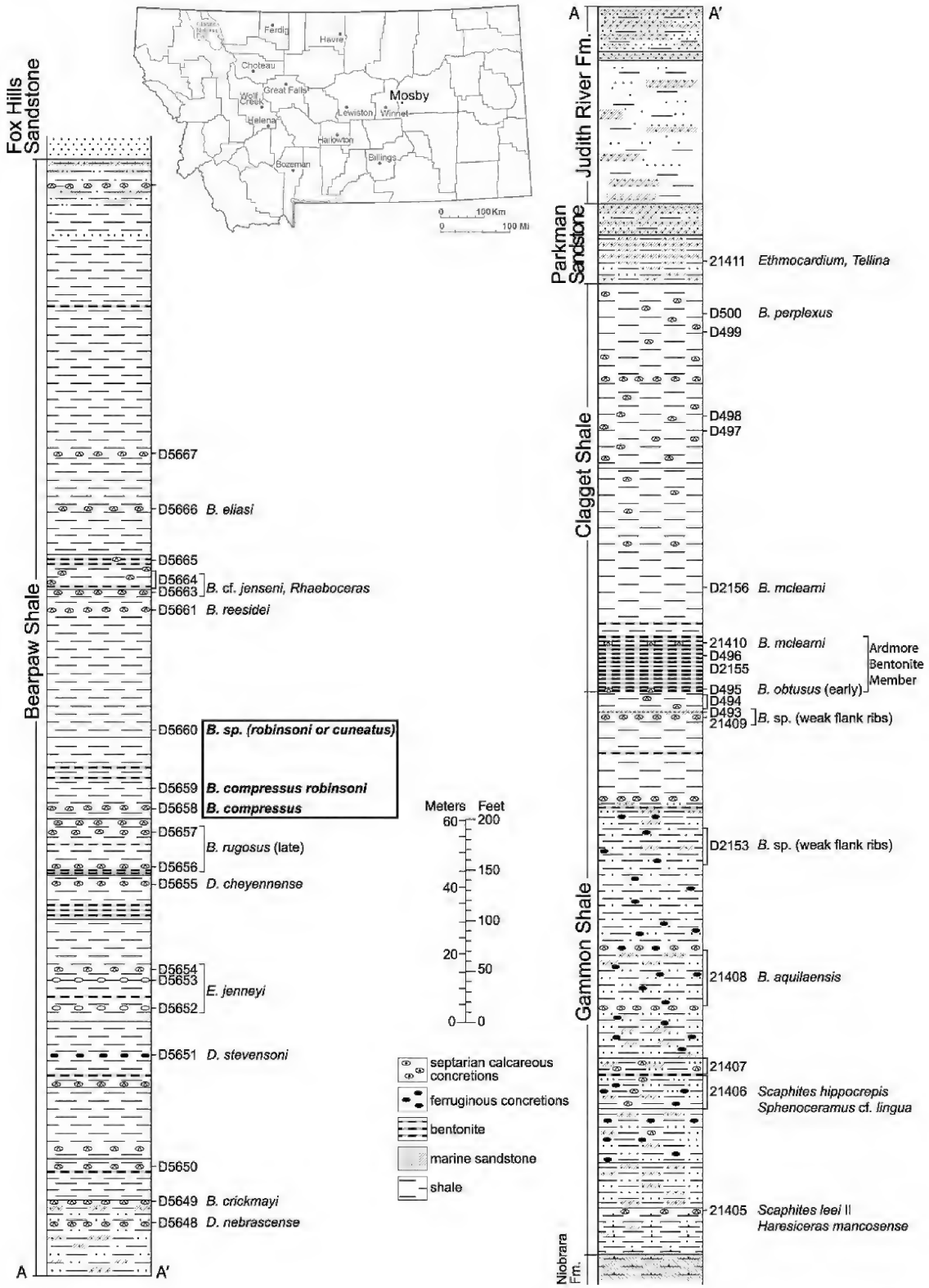
Fox Hills Sandstone
Bearpaw Shale
Judith River Fm.
Parkman Sandstone
Clagget Shale
Gammon Shale
Niobrara Fm.
A
A'
Ferdig
Havre
Choteau
Great Falls
Wolf Creek
Helena
Mosby
Lewiston
Winnet
Harlowton
Bozeman
Billings
0 100 Km
0 100 Mi
D5667
D5666 B. eliasi
D5665
D5664
D5663 B. cf. jenseni, Rhaeboceras
D5661 B. reesidei
D5660 B. sp. (robinsoni or cuneatus)
D5659 B. compressus robinsoni
D5658 B. compressus
D5657
B. rugosus (late)
D5656
D5655 D. cheyennense
D5654
D5653
E. jenneyi
D5652
D5651 D. stevensoni
D5650
D5649 B. crickmayi
D5648 D. nebrascense
Meters Feet
60 200
150
40
100
20
50
0 0
septarian calcareous concretions
ferruginous concretions
bentonite
marine sandstone
shale
21411 Ethmocardium, Tellina
D500 B. perplexus
D499
D498
D497
D2156 B. mclearni
21410 B. mclearni
D496
D2155
Ardmore Bentonite Member
D495 B. obtusus (early)
D494
D493
21409 B. sp. (weak flank ribs)
D2153 B. sp. (weak flank ribs)
21408 B. aquilaensis
21407
21406 Scaphites hippocrepis
Sphenoceramus cf. lingua
21405 Scaphites leei II
Haresiceras mancosense

Mountains. In the Colorado Springs–Pueblo area, the *Baculites compressus* and *B. cuneatus* zones are present in the the cone-in-cone zone of Lavington (1933), and are 24 m and 12 m thick, respectively. Between Loveland and Round Butte, the two zones occur in the unnamed shale member of the Pierre Shale and are 16 m and 8 m thick, respectively. The two zones are also present near Kremmling, Grand County, Colorado, in the unnamed shale member of the Pierre Shale between the Carter Sandstone Member below and the Gunsight Pass Member above (Izett et al., 1971; Izett and Barclay, 1973; Cobban et al., 1992; Kennedy et al., 2000a). The lowest occurrences of *B. compressus*, *B. cuneatus*, and *B. reesidei* in this area are approximately 116 m, 128 m, and 149 m above the top of the Carter Sandstone Member, respectively (Izett et al., 1971), implying that the *B. compressus* and *B. cuneatus* zones are 12 m and 21 m thick, respectively. In Wallace County, Kansas, the *B. compressus–B. cuneatus* zones have been reported from the Weskan Shale Member and lower part of the overlying Lake Creek Shale Member of the Pierre Shale (Elias, 1933).

CORRELATION

The biostratigraphic interval containing *Hoploscaphites nodosus* and *H. brevis* in the Western Interior corresponds to the middle upper, but not uppermost Campanian (fig. 10B). It is useful to correlate this interval with sections elsewhere in North America and Western Europe to determine the geographic and biostratigraphic distribution of these ammonites, as well as related forms. We discuss the biostratigraphy of the Western Interior, the Gulf Coastal Plain, the Atlantic Coastal Plain, Tercis, France, and the Vistula River Valley, Poland, in that order. Correlation between these regions is possible based on the biostratigraphic distribution of nostoceratid ammonites and inoceramids (fig. 10B). In our discussion, certain taxa appear in quotation marks, e.g., "*Acanthoscaphites*," to indicate that the generic name is used informally. The Campanian/Maastrichtian boundary is placed in the upper part of the *Baculites eliasi* Zone, following the interpretation of Walaszczyk et al. (2002) and Walaszczyk (2004), based on the definition of the boundary at the Global Standard stratotype Section and Point (GSSP) for the Campanian/Maastrictian boundary at Tercis, France. On the other hand, strontium isotope analyses have suggested that the boundary actually occurs in the *B. jenseni* Zone (McArthur et al., 1992).

In the Western Interior of North America, the ammonite zonation of the upper Campanian consists of nine zones (Cobban et al., 2006). *Hoploscaphites nodosus* and *H. brevis* range from the upper part of the *Didymoceras cheyennense* Zone to the lower part of the *Baculites reesidei* Zone. Several species that resemble *H. nodosus* and *H. brevis* are present in the *B. reesidei–B. jenseni* zones. They include "*Jeletzkytes*" *furnivali* Riccardi (1983: 19, pl. 4, figs. 3, 4, 7–9; text figs. 7c, 8), and undescribed forms similar to or identical with "*Acanthoscaphites*" *praequadrispinosus* Błaszkiewicz (1980: 38, pl. 19, figs. 2, 3, 6–8; pl. 20, figs. 1–3, 6–8; pl. 21, figs. 1–6) (fig. 10A), *H. vistulensis* Błaszkiewicz (1980: 34, pl. 17, figs. 4–6, 8, 9), and *H. minimus* Błaszkiewicz (1980: 35: pl. 23, fig. 4; pl. 24, fig. 3; pl. 25, figs. 3, 4). In addition, *Nostoceras* (*N.*) *hyatti* Stephenson, 1941, a widespread late Campanian ammonite, has been reported from the *B. jenseni* Zone in Huerfano County, Colorado (Kennedy et al., 1992; Odin and Cobban, 2001). It has since been interpreted as *N.* (*N.*) *hyatti* subspecies II by Küchler and Odin (2001).

Walaszczyk et al. (2001) established five inoceramid zones in the upper Campanian of the Western Interior. The top three zones are, in ascending order, the "*Inoceramus*" *altus* Zone, the "*I.*" *oblongus* Zone, and the "*I.*" *redbirdensis* Zone. The "*I.*" *altus* Zone correlates with the *Didymoceras cheyennense–B. cuneatus* zones (Walaszczyk et al.,

←

Fig. 8. Stratigraphic section of the Bearpaw Shale near Mosby, east-central Montana, spanning the *Scaphites leei* II to *Baculites eliasi* zones. The *Baculites compressus–B. cuneatus* zones are approximately 30 m thick.

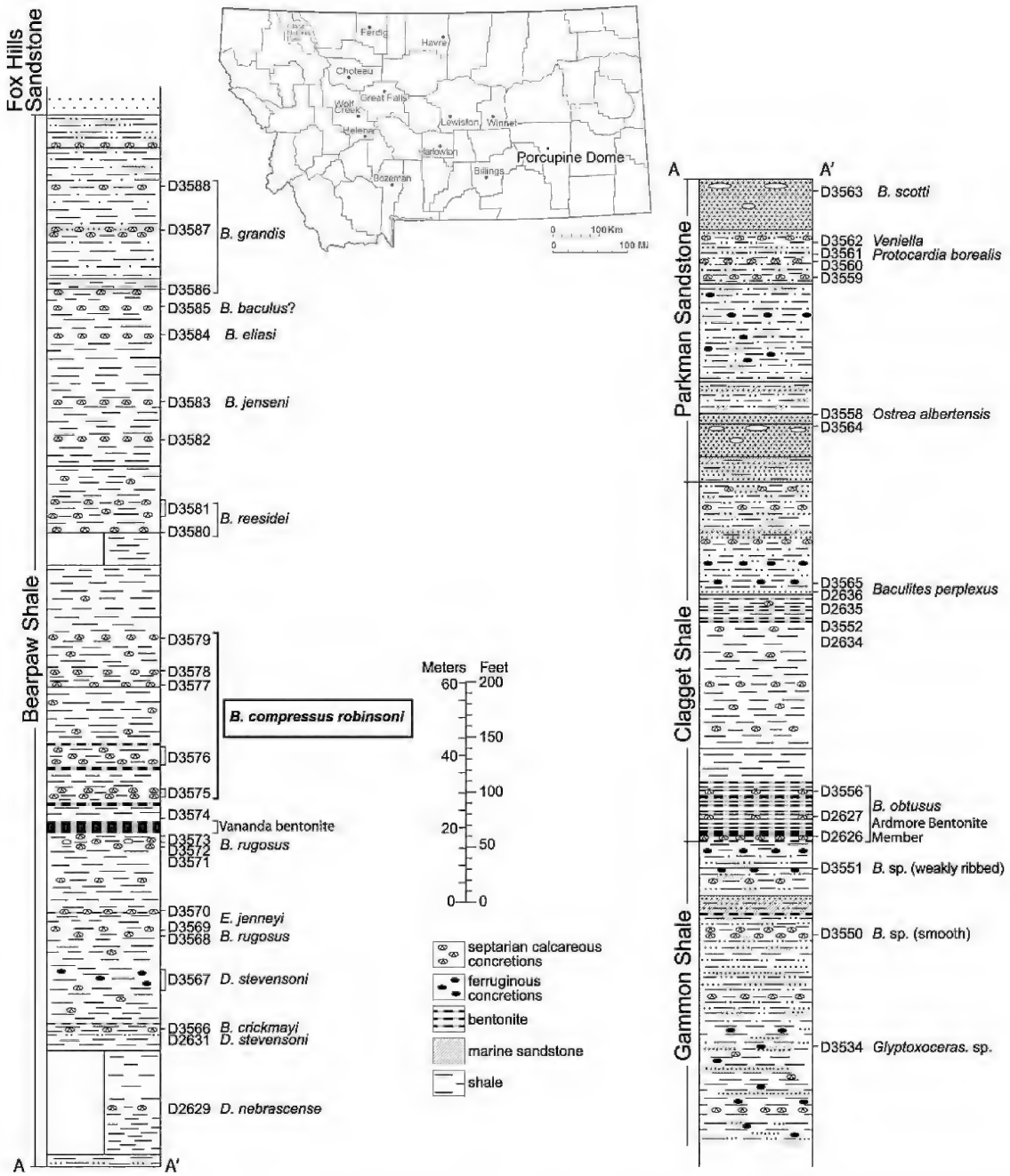

Fig. 9. Stratigraphic section of the Bearpaw Shale on Porcupine Dome, southeast Montana, spanning the *Baculites* sp. (smooth) to *B. grandis* zones. The *Baculites compressus–B. cuneatus* zones are approximately 45 m thick.

2001: fig. 6). Walaszczyk et al. (2002: 277) added that

> In the US Western Interior it [the "*I.*" *altus* Zone] is the assemblage that characterises above all, the *Baculites compressus* ammonite Zone, known from the famous material of the Sage Creek section, as well as from the mass occurrences in western Colorado. The stratigraphically oldest representatives of the assem-

> blage come, however, from the underlying *Didymoceramas cheyenense* [sic] Zone, whereas the youngest come from the basal part of the overlying *Baculites cuneatus* Zone. The precise correlation of the ammonite and inoceramid zonal boundaries at that interval has yet to be worked out.

The "*I.*" *oblongus* Zone correlates with the *B. reesidei* and *B. jenseni* zones (Walaszczyk et al., 2001, fig. 6), although the range of "*I.*" *oblongus* appears to be restricted to the *B. reesidei* Zone (Walaszczyk et al., 2001: fig. 5). Indeed, Walaszczyk et al. (2002: 277) noted that "the '*I.*' *oblongus* Zone characterizes roughly the ammonite zone of *Baculites reesidei*. The precise correlation of its lower and upper boundaries is, however, unknown." The "*I.*" *redbirdensis* Zone approximately correlates with the *B. eliasi* Zone (Walaszczyk et al., 2001: fig. 6).

The biostratigraphic interval corresponding to the ranges of *Hoploscaphites nodosus* and *H. brevis* on the Gulf Coastal Plain is devoid of ammonites and is unzoned. Kennedy et al. (1992) identified the upper Campanian *Nostoceras* (*N.*) *hyatti* Zone in the Saratoga Chalk in southwestern Arkansas (Kennedy and Cobban, 1993), the Coon Creek Tongue of the Ripley Formation in Tennessee (Cobban and Kennedy, 1994), and the Nacatoch Sand in Texas (Kennedy and Cobban, 1993). All three sites contain *N.* (*N.*) *hyatti* subspecies II and *N.* (*N.*) *helicinum* (Shumard, 1861). Species similar to or identical with "*Acanthoscaphites*" *praequadrispinosus* are also present: in Arkansas—called *Jeletzkytes nodosus* by Kennedy and Cobban (1993: fig. 17.22–25); in Tennessee—called *Scaphites reesidei* by Wade (1926: 183, pl. 61, figs. 3–7); *J. nodosus* by Cobban and Kennedy (1994: pl. 9, figs. 7–11); and *J. reesidei* by Larson (in press: pl. 10, figs. 3a–8b); and in Texas—called *S. rugosus* by Stephenson (1941: 425, pl. 89, figs. 15–18).

The biostratigraphic interval corresponding to the ranges of *Hoploscaphites nodosus* and *H. brevis* on the Atlantic Coastal Plain is also devoid of ammonites and is marked by an unconformity at the base of the Navesink Formation. However, the fauna of the Mount Laurel Sand at Biggs Farm, Delaware (Kennedy and Cobban, 1994), includes *Didymoceras cheyennense* Meek and Hayden, 1856b, *Spiroxybeloceras meekanum* (Whitfield, 1877), *Anaklinoceras reflexum* Stephenson, 1941, and *Baculites undatus* Stephenson, 1941. All of these forms suggest a correlation with the *D. cheyennense* Zone and, possibly, the lower part of the *B. compressus* Zone in the U.S. Western Interior. The *Nostoceras* (*N.*) *hyatti* Zone is present in the phosphatized fauna at the base of the Navesink Formation at Atlantic Highlands, New Jersey (Cobban, 1974; Kennedy and Cobban, 1993; Kennedy et al., 1992, 1995, 2000b). The ammonite fauna at this site consists of 11 species including *N.* (*N.*) *hyatti* subspecies II, *N.* (*N.*) *helicinum*, and forms similar to or identical with "*Acanthoscaphites*" *praequadrispinosus* (called *Scaphites nodosus* by Whitfield, 1892: 261: pl. 44, figs. 13, 14; *S. nodosus*? by Weller, 1907: pl. 107, figs. 1, 2; *S.* aff. *S. leei* by Reeside, 1962: 126, 127, pl. 71, figs. 8–11; *Hoploscaphites* sp. by Cobban, 1974: 18, pl. 11, figs. 13–19; text fig. 14; and *Jeletzkytes* cf. *nodosus* by Kennedy et al., 2000b: 20, figs. 9J–P, 10, 11, 12C–F).

At Tercis, France, the *Nostoceras* (*N.*) *hyatti* Zone marks the top of the Campanian, although Walaszczyk (2004: fig. 5) suggested that it also extends into the lower Maastrichtian. Küchler and Odin (2001: fig. 2) analyzed the biostratigraphic distribution of the index species in this section, as well as that of other nostoceratids and diplomoceratids, indicating the position of fossils by level numbers, spaced at intervals of approximately 1 m. The base of the *N.* (*N.*) *hyatti* Zone, marked by the lowest occurrence of *N.* (*N.*) cf. *hyatti*, is at level 66.4. The lowest occurrences of *N.* (*N.*) *hyatti* subspecies I and II are at levels 66.5 and 94.2, respectively. The lowest occurrence of *N.* (*N.*) *helicinum* is at level 67, but this species is more abundant higher up in the section in association with *N.* (*N.*) *hyatti* subspecies II (thicker range bars, fig 10B).

Walaszczyk et al. (2002: 276, chart) recognized five inoceramid zones in the upper Campanian–lower Maastrichtian at Tercis, the uppermost four of which are, in ascending order, the "*Inoceramus*" *altus* Zone, the "*I.*" *oblongus* Zone, the *Trochoceramus costaecus* Zone, and the "*I.*" *redbirdensis* Zone. The bases of these four zones, defined by the

Fig. 10. **A.** *Acanthoscaphites praequadrispinosus* Błaszkiewicz, 1980 (38: pl. 19, figs. 6–8), holotype, IG 1.310.II.17, macroconch, left lateral, *Nostoceras* (*N.*) *hyatti* Zone, Piotrawin, Vistula River Valley, Poland. Forms similar or identical to this species occur in the *Baculites reesidei-B. jenseni* zones of the Western Interior of North America. The specimen is illustrated natural size.

lowest occurrences of their respective index fossils, are at level 66.5, between levels 80 and 88, at level 96.7, and at level 108.

Walaszczyk et al. (2002) correlated these inoceramid zones to the ammonite zones in the U.S. Western Interior. According to them, the "*Inoceramus*" *altus* Zone corresponds to the *Didymoceras cheyennense–Baculites cuneatus* zones. However, there is some confusion regarding the correlation of

B

	Western Interior			Gulf and Atlantic Coastal Plains		Tercis, France			Vistula River Valley, Poland		
	Cephalopod Zonation[1]	Inoceramid Zonation[2]	Key Species[3-5]	Cephalopod Zonation[4]	Key Species[4]	Cephalopod Zonation[6]	Inoceramid Zonation[7]	Key Species[6]	Cephalopod Zonation[8]	Inoceramid Zonation[9]	Key Species[8]
Maastrichtian (part)	*B. eliasi*	*"I." redbirdensis*	*"J." furnavali* *"A." praequadrispinosus* *N. (N.) hyatti* II	unzoned	*"S." reesidei* *"S." rugosus* *"J." nodosus / "J." cf. nodosus* *N. (N.) hyatti* II *N. (N.) helicinum*		*"I." redbirdensis*	*N. (N.) helicinum* *N. (N.) hyatti* II	*Belemnella occidentalis (part)*	*"I." redbirdensis*	*"A." praequadrispinosus* *H. vistulensis* *H. minor* *N. (N.) hyatti* II
Campanian (part)	*B. jenseni*			*N. (N.) hyatti*		*N. (N.) hyatti*	*T.costaecus*		*Belemnella lanceolata lanceolata*	*T.costaecus*	
	B. reesidei	*"I." oblongus*					*"I." oblongus*		*N. pozaryski= N. (N.) hyatti*	*"I." inkermanensis*	
	B. cuneatus	*"I." altus*	*H. nodosus* *H. brevis*	unzoned	*D. cheyennense* *Sp. meekanum* *A. reflexum* *B. undatus*		*"I". altus*			*"I". altus*	
	B. compressus										
	D. cheyennense			*D. cheyennense*							

Abbreviations: "A." = "*Acanthoscaphites*"; A = *Anaklinoceras;* B = *Baculites;* D = *Didymoceras;* H = *Hoploscaphites;* "I" = "*Inoceramus*"; J = *Jeletzkytes;* N = *Nostoceras; Sp.* = *Spiroxybeloceras;* S = *Scaphites;* T= *Trochoceramus.*

Fig. 10. **B.** Comparison of the biostratigraphy of the upper part of the Campanian in the Western Interior of North America, the Gulf and Atlantic Coastal plains, Tercis, France, and the Vistula River Valley, Poland. The shaded area indicates the biostratigraphic interval corresponding to the ranges of *Hoploscaphites nodosus* and *H. brevis*. The Campanian/Maastrichtian boundary is placed in the upper part of the B. eliasi Zone, following the interpretation of Walaszczyk et al. (2002) and Walaszczyk (2004), based on the definition of the boundary at Tercis, which is the site of the global standard stratotype section and point (GSSP) for the Campanian/Maastrictian boundary. The thicker range bars for *N.* (*N.*) *helicinum* and *N.* (*N.*) *hyatti* II indicate a higher abundance. [1]Cobban et al. (2006); [2]Walaszczyk et al. (2001); [3]Riccardi (1983); [4]Kennedy et al. (1992); [5]Odin and Cobban (2001); [6]Küchler and Odin (2001); [7]Walaszczyk et al. (2002); [8]Błaszkiewicz (1980); [9]Walaszczyk (2004).

the "*I.*" *oblongus*, *Trochoceramus costaecus*, and "*I.*" *redbirdensis* zones. In Walaszczyk et al. (2002: 276, chart), the "*I.*" *oblongus* Zone correlates with the *B. reesidei* Zone, the *T. costaecus* Zone correlates with the *Baculites jenseni* Zone, and the "*I.*" *redbirdensis* Zone correlates with the *B. eliasi* Zone. In contrast, in Walaszczyk (2004: fig. 5), the"*I.*" *oblongus* Zone correlates with the *B. reesidei* Zone and the lower two-thirds of the *B. jenseni* Zone, the *T. costaecus* Zone correlates with the upper one-third of the *B. jenseni* Zone and the lower one-third of the *B. eliasi* Zone, and the "*I.*" *redbirdensis* Zone correlates with the upper two-thirds of the *B. eliasi* Zone. We have followed the correlation scheme in Walaszczyk (2004: fig. 5), since this publication presumably reflects the latest thinking on the subject (fig. 10B).

In the Vistula River Valley, Poland, Błaszkiewicz (1980) established the *Didymoceras donezianum* and *Nostoceras pozaryski* zones at the top of the Campanian. Kennedy et al. (1992) synonymized *N. pozaryski* with *N.* (*N.*) *hyatti*, and Küchler and Odin (2001) further assigned this species to *N.* (*N.*) *hyatti* subspecies II. Błaszkiewicz (1980: 14) noted that "In the assumed concept of the zone, its lower boundary is determined by the appearance of *Acanthoscaphites praequadripinosus* sp. nov., while the first occurrence of the index species is considered as pronouncedly later." Walaszczyk (2004: 97) added that *N. (N). hyatti* "first appears distinctly higher and ranges up to approximately the top of the zone" (although elsewhere Walaszczyk [2004: 100], based on a personal communication from M. Machalski, stated that this species may actually appear at the base of the zone). According to Walaszczyk (2004: fig. 5), the *N.* (*N.*) *hyatti* Zone is upper but not uppermost Campanian, and is immediately overlain by the *Belemnella lanceolata lanceolata* Zone, which was previously assigned to the lower Maastrichtian by Błaszkiewicz (1980).

In Poland, the *Nostoceras* (*N.*) *hyatti* Zone contains "*Acanthoscaphites*" *praequadrispinosus* (fig. 10A), *Hoploscaphites vistulensis*, and *H. minimus*. In addition, Machalski (personal commun., 2009) reported the presence of scaphites that are "transitional between *nodosus* and *praequadrispinosus*" from either the top of the *Didymoceras donezianum* Zone or the bottom of the *N.* (*N.*) *hyatti* Zone. The ribbing in these specimens is similar to that in *H. nodosus*, but the size of the adult shell more closely matches that of "*A.*" *praequadrispinosus*.

Walaszczyk (2004: fig. 5) recognized five inoceramid zones in the upper Campanian in the Vistula River Valley, Poland, the uppermost four of which are, in ascending order, the "*Inoceramus*" *altus* Zone, the "*I.*" *inkermanensis* Zone, the *Trochoceramus costaecus* Zone, and the "*I.*" *redbirdensis* Zone, each of which is defined at the base by the lowest occurrence of the respective index fossil. The "*I.*" *altus* and "*I.*" *inkermanensis* zones correspond to the *Nostoceras* (*N.*) *hyatti* Zone, the *T. costaecus* Zone correlates with the lower part of the *Belemnella lanceolata lanceolata* Zone, and the "*I.*" *redbirdensis* Zone correlates with the upper part of the *B. lanceolata lanceolata* Zone and the lower part of the *B. occidentalis* Zone. In terms of the ammonite zonation of the Western Interior, the "*I.*" *altus* Zone correlates with the *Didymoceras cheyennense–Baculites cuneatus* zones, the "*I.*" *inkermanensis* Zone correlates with the *B. reesidei* Zone and the lower two-thirds of the *B. jenseni* Zone, the *T. costaecus* Zone correlates with the upper one-third of the *B. jenseni* Zone and the lower one-third of the *B. eliasi* Zone, and the "*I.*" *redbirdensis* Zone correlates with the upper two-thirds of the *B. eliasi* Zone (Walaszczyk, 2004: fig. 5).

In summary, based on the proposed correlation using inoceramids and nostoceratid ammonites (Błaszkiewicz, 1980; Kennedy et al., 1992; Küchler and Odin, 2001; Walaszczyk, 2004; Walaszczyk et al., 2001, 2002; Cobban et al., 2006), there is a slight discrepancy in the position of the interval containing *Hoploscaphites nodosus and H. brevis* between North America and Western Europe (fig. 10B). In the Western Interior of North America, this interval correlates with the "*Inoceramus*" *altus* Zone, which, by indirect correlation, corresponds to unzoned strata *below* the *Nostoceras (N.) hyatti* Zone on the Gulf and Atlantic Coastal plains. In contrast, in Western Europe, the interval containing *H. nodosus and H. brevis* (= "*I.*" *altus* Zone) correlates with the *lower part* of

the *N.* (*N.*) *hyatti* Zone. In Poland, this zone contains "*Acanthoscaphites*" *praequardripinosus*, *H. vistulensis*, and *H. minimus*. Similar forms are present in the *N.* (*N.*) *hyatti* Zone in North America above the interval containing *H. nodosus* and *H. brevis*.

The biostratigraphic discrepancy between North America and Western Europe raises several questions. Why are *H. nodosus* and *H. brevis* present in North America but absent in Poland? Does this difference reflect biogeographic factors or is it the result of differential preservation? With respect to the inoceramid-nostoceratid biostratigraphy, why is the lowest occurrence of "*A.*" *praequadrispinosus* and related species lower in Poland than in North America? Does this indicate a real difference in the timing of appearance of these species, with implications for ammonite migration, or is it simply the result of imprecision in the biostratigraphic correlation? How well integrated are the ammonite and inoceramid biostratigraphies? How similar are the ranges of the index species between North America and Western Europe? How do unfossiliferous intervals contribute to the uncertainty of the correlation?

Answering these questions involves further study on several fronts: (1) The taxonomy of the scaphites on both sides of the Atlantic (e.g., "*Acanthoscaphites*" *praequadrispinosus*, *Hoploscaphites vistulensis*, *H. minimus*, "*Jeletzkytes*" *furnivali*, *Scaphites reesidei*, and *S. rugosus*) must be reexamined to determine whether these species are the same or different. (2) The biostratigraphy of the inoceramids and nostoceratids must be reevaluated with the goal of specifying areas of uncertainty. For example, in Poland, the base of the *Nostoceras* (*N*). *hyatti* Zone is unclear. In addition, the ranges of scaphites in this zone are not well documented due, undoubtedly, to the rarity of material. (3) Future biostratigraphic studies must take into account unfossiliferous portions of the section, and the common practice, at least in the U.S. Western Interior, of drawing zonal boundaries at horizons lacking index fossils, which invariably leads to some uncertainty. For example, in the Western Interior, the correlation of the "*Inoceramus*" *oblongus* Zone with the *Baculites reesidei* and *B. jenseni* zones requires further analysis, including a more precise determination of the lowest and highest occurrences of these species, as well as gaps in their ranges. (4) The relative abundance of a species in the section can provide additional data, perhaps permitting a more refined zonation (as per Küchler and Odin, 2001). For example, if the relative abundance of *N.* (*N*). *hyatti* is taken into account (see thicker range bars, fig. 10B), rather than simply its range, the biostratigraphic distribution of this species would line up better between North America and Western Europe. These points will be further addressed in future studies.

MODE OF OCCURRENCE

Hoploscaphites nodosus and *H. brevis* generally occur in carbonate-cemented concretions that are distributed in discontinuous layers (fig. 11). They are usually associated with a rich molluscan fauna, dominated by inoceramids and baculites. The scaphites are generally preserved in three dimensions, with the phragmocone filled with sparry calcite, and the body chamber filled with sediment. In the concretions from the *Baculites compressus–B. cuneatus* zones of the Pierre Shale in western South Dakota and east-central Montana, most specimens retain their original aragonitic shell structure, although the quality of preservation varies (Cochran et al., 2010). In contrast, in the sandstone concretions from the *B. compressus–B. cuneatus* zones of the Pierre Shale along the Front Range of the Rocky Mountains, Colorado, the original shell is usually missing.

To better understand concretion formation, we examined concretions from the *Baculites compressus–B. cuneatus* zones of the Pierre Shale in Meade and Pennington counties, South Dakota. These concretions cover an area of at least 1,000 km^2, based on our observations of outcrops along Elk, Sage, and Cedar creeks, all of which are tributaries of the Cheyenne River. This area represents a relatively offshore environment approximately 250 km from the western shoreline of the Western Interior Seaway (fig. 1). However, the position of the shoreline in this area is not well constrained and it may have been farther east than supposed. Although it is difficult to establish the exact

Fig. 11. Fossiliferous concretion BHI 4788 from the *Baculites cuneatus* Zone of the Pierre Shale, Meade County, South Dakota. The concretion contains an adult specimen of *B. cuneatus* Cobban, 1962, an adult macroconch of *Hoploscaphites brevis* (Meek, 1876), and "*Inoceramus*" *sagensis* Owen, 1852.

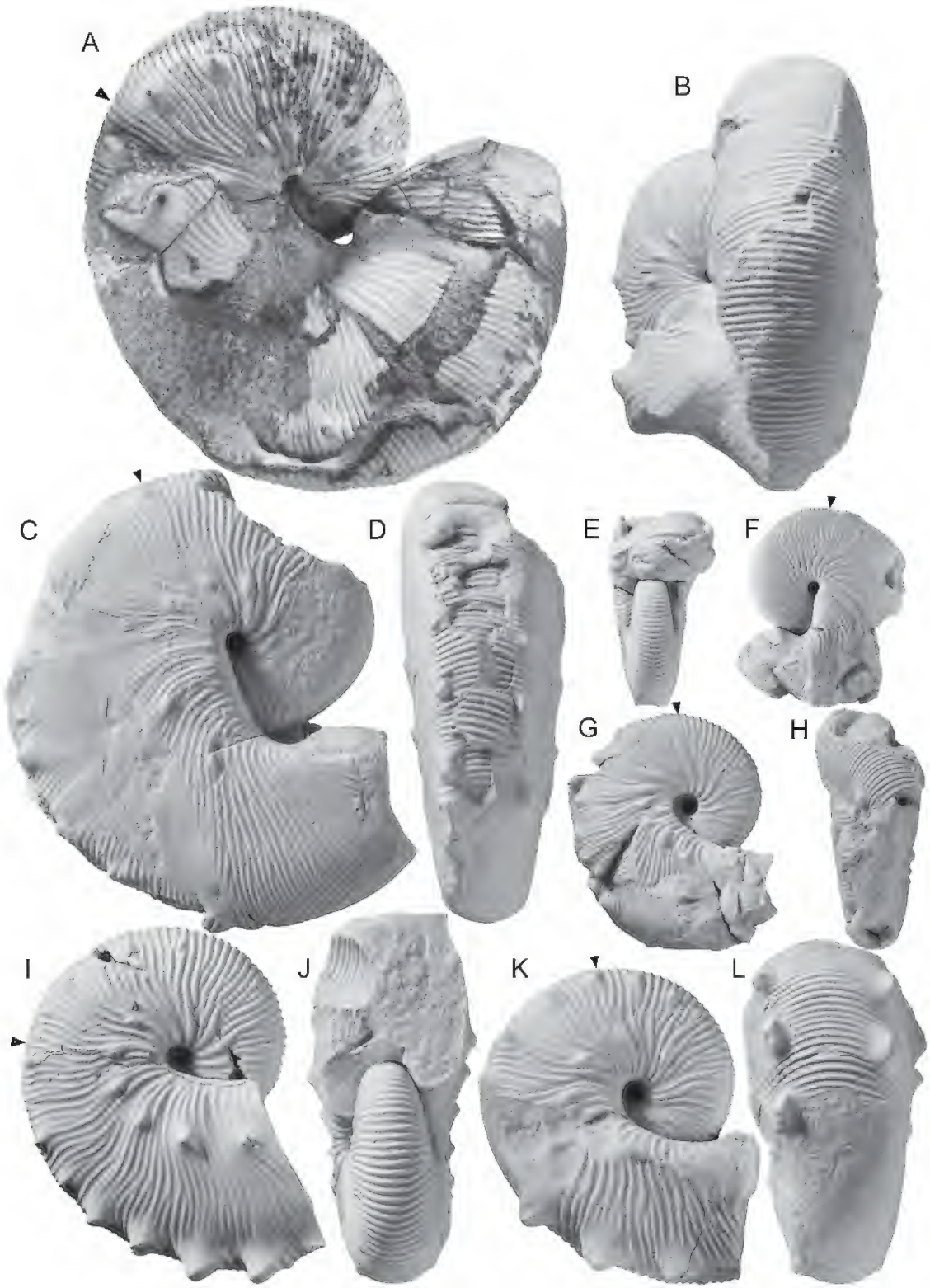
A
B
C
D
E
F
G
H
I
J
K
L

depth of the water in this area, Gill and Cobban (1966) suggested that the seaway was probably less than 70 m deep at this time. As a comparison, Feldman (1972) estimated that the Timber Lake Member of the Fox Hills Formation, which also contains abundant scaphitiferous concretions, was deposited at a depth of 18–55 m.

Landman and Klofak (2006) reported the results of a detailed analysis of a concretion (Kathy's concretion) from AMNH loc. 3274 from the *Baculites compressus –B. cuneatus* zones in the Pierre Shale, Meade County, South Dakota (figs. 12, 13). The concretion is ovoid, and approximately 1 m long by 0.5 m wide. It consists of light grey, finely bioturbated mud, without any indication of bedding structures. In addition to *Hoploscaphites nodosus* and *H. brevis*, the concretion contains approximately 40 macroinvertebrate species including *Baculites compressus* and *B. cuneatus*, which represent the most abundant group in terms of numbers of specimens, one species of placenticeratid, 16 species of bivalves (both infauna and epifauna), 10 species of gastropods, 2 species of scaphopods, and evidence of crustaceans, bryozoans, encrusting algae, foraminifera, small tubes, and fish scales, and bits of wood. In most of the molluscs, the original mineralogy of the shells is preserved.

The distribution of fossils in the concretion is patchy, with concentrations of shelly material surrounded by less fossiliferous matrix. In these concentrations, the shells are loosely packed but in contact, so that, for example, the broken phragmocone of a baculite abuts the broken body chamber of a scaphite. Adult scaphites of both dimorphs are present. The body chambers of these specimens are always broken, although enough of the body chamber is still preserved in these specimens to identify them as adults. The concretion also contains large scaphite phragmocones in which only a small piece of body chamber is still attached. These specimens cannot be unequivocably identified as adults, and could represent instead large juvenile or submature individuals. In addition, there are juvenile scaphites as small as 4 mm in diameter, with most of the body chamber intact. In large scaphites, the chambers of the phragmocone are either hollow or filled with sediment or calcite, whereas in small scaphites, the chambers of the phragmocone are usually filled with calcite. The shell wall of the scaphites consists of a thin, outer prismatic layer and a thicker nacreous layer (e.g., 15 μm versus 200 μm in AMNH 66261). The body chambers of large baculites (adults?) are always broken. Smaller specimens are more complete and include juveniles 5–10 mm in length with the ammonitella still attached. Some of the smaller specimens (10–20 mm in length) are oriented approximately parallel to each other. As in the scaphites, the chambers of large baculite phragmocones are either hollow or filled with sediment or calcite, whereas the chambers of small baculite phragmocones are always filled with calcite.

The concretion contains dozens of isolated ammonite jaws, almost all of which are deformed. The outer calcitic layer is usually missing or recrystallized. In those specimens in which it is missing, the chitinous part of

←

Fig. 12. Scaphites from a single concretion (Kathy's concretion), *Baculites compressus–B. cuneatus* zones, Pierre Shale, AMNH loc. 3274, Meade County, South Dakota. **A, B.** *Hoploscaphites brevis* (Meek, 1876), large macroconch, AMNH 50429. **A.** Left lateral, uncoated; **B.** ventral hook. A chunk of shell is missing from the adapical part of the body chamber, probably due to an injury, and the rest of the shell is broken and deformed. **C, D.** *Hoploscaphites brevis* (Meek, 1876), large macroconch, AMNH 51068. **C.** Right lateral; **D.** ventral. **E, F.** *Hoploscaphites brevis* (Meek, 1876), small macroconch, AMNH 51067. **E.** Apertural; **F.** left lateral. **G, H.** *Hoploscaphites brevis* (Meek, 1876), small microconch, AMNH 55876. **G.** Right lateral; **H.** ventral. **I, J.** *Hoploscaphites brevis* (Meek, 1876), large microconch, AMNH 51065. **I.** Right lateral; **J.** apertural. **K, L.** *Hoploscaphites nodosus* (Owen, 1852), microconch, AMNH 55873. Note that the base of the body chamber is 90° adapical of the line of maximum length. **K.** Right lateral; **L.** ventral. Specimens are illustrated natural size.

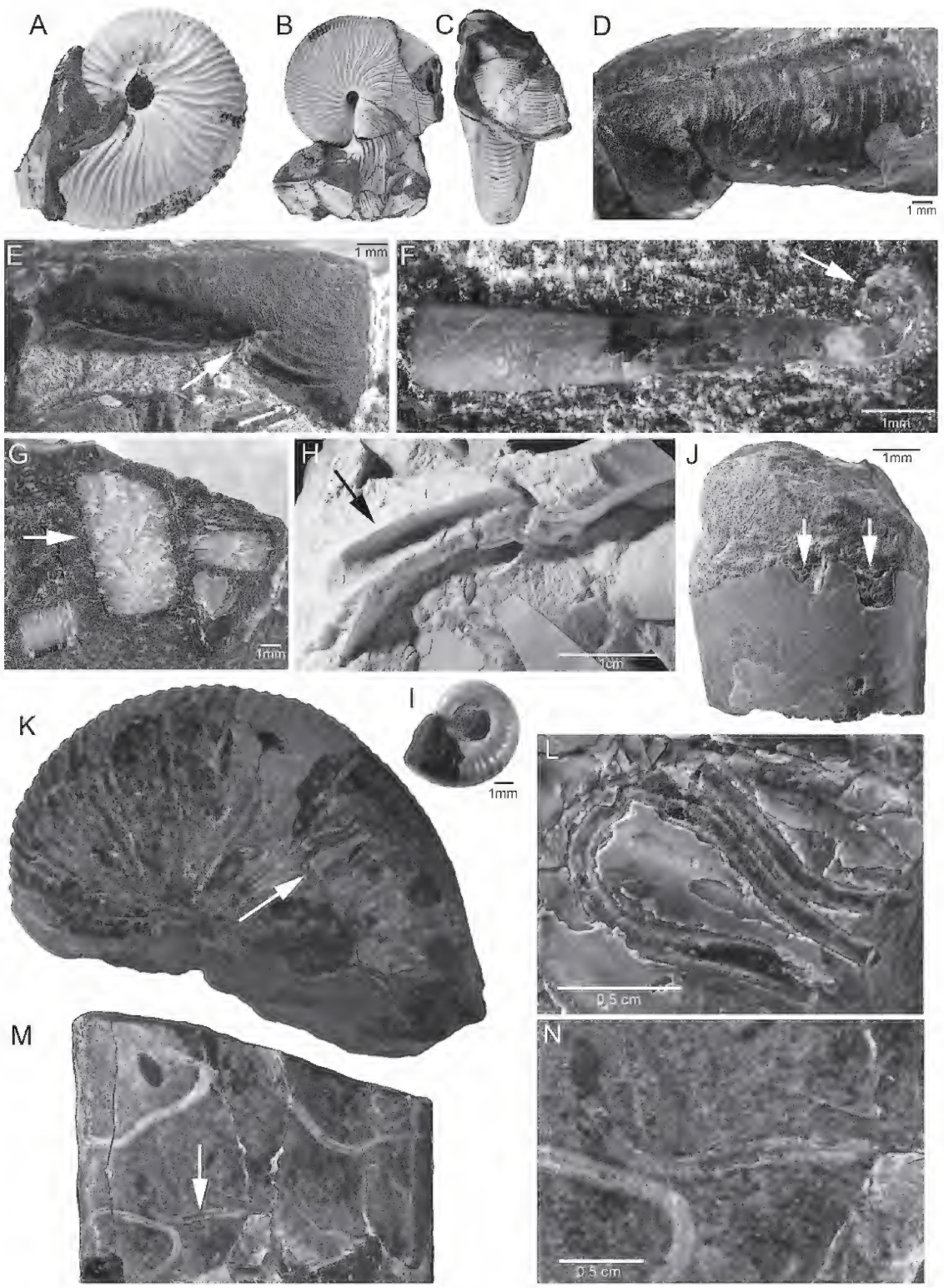
A
B
C
D
1 mm
E
1 mm
F
1mm
G
1mm
H
1cm
J
1mm
I
1mm
K
L
0.5 cm
M
N
0.5 cm

the jaws lies in direct contact with the rest of the concretion, without any gap. After ammonites, the most abundant fossils are bivalves including a mixture of epifaua (e.g., *Limopsis parvula* [Meek and Hayden, 1856c], "*Inoceramus*" *altus* Meek, 1871) and infauna (e.g., *Protocardia subquadrata* [Evans and Shumard, 1857], *Solemya subplicata* [Meek and Hayden, 1856c]). The epifaunal bivalves are always disarticulated, whereas the infaunal bivalves are nearly always articulated, although not in life position. In large inoceramid shells, the beak is usually preserved, but the commissure is broken. In general, the inner nacreous layer (composed of aragonite) is still present, but the outer prismatic layer (composed of calcite) is broken up and scattered as pieces throughout the concretion (fig. 13G).

Most of the breakage in the adult scaphites is probably due to predation. In general, a lethal injury in these forms is manifested by the loss of the adapical end of the body chamber, precluding repair of the shell (Radwański, 1996; Larson, 2003; Keupp, 2006; Klompmaker et al., 2009). Usually, what remains is the phragmocone and a small part of the adapical end of the body chamber terminating in a jagged edge. For example, both AMNH 66238 and 66252 are subadult to adult specimens of *Hoploscaphites brevis* that consist of only the phragmocone and a small piece of the body chamber. In other specimens, the adapical part of the body chamber is missing, but the rest of the shell is still intact, although deformed due to subsequent compaction. For example, in AMNH 50429 (fig. 12A, B), a large macroconch of *H. brevis*, a chunk of shell is missing from the adapical end of the body chamber, but the rest of the shell is intact. The broken pieces were probably held together by the periostracum or the mantle tissue lining the inside of the shell. Similarly, in AMNH 55876 (fig. 12G, H), a small microconch of *H. brevis*, a chunk is missing from the venter and left side of the adapical end of the body chamber, but the right side of the body chamber is intact, although fractured in multiple places. Many of the adult baculites in the concretion exhibit the same pattern of breakage near the base of the body chamber, suggesting that these animals also suffered from a similar form of predation. The shells of the scaphites and baculites may have floated for a short time following an injury. Specimens in which most of the shell is still intact probably settled to the bottom soon after death.

Thus, these shells may have been added to the sea floor through attrition by predation from fish or mosasaurs. Other shells may have been added as a consequence of an environmental disturbance, such as a turbidity current caused by a storm or river discharge. Such turbidity currents may have entrained and killed small baculites and scaphites living just a few meters above the

←

Fig. 13. Preservation of fossils from the *Baculites compressus–B. cuneatus* zones, Pierre Shale, Meade County, South Dakota. **A–J.** Single concretion (Kathy's concretion), AMNH loc. 3274. **A.** Left lateral of a phragmocone of *Hoploscaphites brevis* (Meek, 1876), AMNH 56778. The specimen is broken at the adapical end of the body chamber, probably due to an injury. **B, C.** *Hoploscaphites brevis* (Meek, 1876), small macroconch, AMNH 51067. **B,** Left lateral; **C.** apertural. A chunk of shell is missing from the adapical end of the body chamber, but the rest of the specimen is still intact. **D.** Lower jaw attributed to *Hoploscaphites*, with a tear in the right wing, AMNH 56808. **E.** Lower jaw attributed to *Hoploscaphites* showing damage (arrow) along the lateral margin, AMNH 56803. **F.** Juvenile of *Baculites*, with the ammonitella (arrow) still attached, AMNH 56824. **G.** Isolated piece of *Inoceramus* shell (arrow) with prismatic microstructure, AMNH 56798. **H.** *Agerostrea falcata* (Morton, 1830) with the impression of a baculite (arrow), AMNH 56797. **I.** Juvenile of *Hoploscaphites* with most of the body chamber preserved, AMNH 56842. **J.** Fragment of *Baculites* with scalloped edges (arrows) along the margin, AMNH 56833. **K, L.** *Hoploscaphites nodosus* (Owen, 1852), large macroconch, with the impression of a worm tube (arrow) on the body chamber, AMNH 56763, AMNH loc. 3274. **M, N.** *Baculites compressus* (Say, 1820) with impressions of worm tubes (arrow), on the body chamber, AMNH 56870, AMNH loc. 3408. Specimens are illustrated natural size unless indicated otherwise by a scale bar.

bottom, resulting in minor breakage at the aperture and the current alignment of some of the baculites. Shells may have accumulated in one spot due to irregularities on the sea floor. Such irregularities may have been produced by current induced scours, burrows, or scouring around preexisting shell debris (see Tsujita, 1995, for a similar explanation for the formation of fossiliferous concretions in the Campanian-Maastrichtian Bearpaw Shale in southern Alberta). In contrast to the cephalopods that lived in the water, the gastropods and bivalves lived on the bottom, probably at or near the site. However, they were slightly reworked after death due to currents and bioturbation, as indicated by the fact that epifaunal bivalves are disarticulated and infaunal bivalves are not in life position.

Shells must have rested on the sea floor for some time before burial, or else were buried and then exhumed. For example, in AMNH 56763, a macroconch of *Hoploscaphites nodosus* from another concretion at the same site, a calcareous worm tube is present on the inside surface of the body chamber, indicating that the empty shell must have rested on the sea floor before burial (fig. 13K, L). In AMNH 56797, a specimen of *Agerostrea falcata* (Morton, 1830), the left valve shows the impression of a small baculite, indicating that the oyster must have settled on the dead ammonite (fig. 13H). In AMNH 56833, a fragment of the adapical part of the body chamber of a small baculite, the aperture shows a series of irregular notches, suggesting that it was peeled back by a crab to consume the soft tissue (fig. 13J). In many ammonite jaws, the calcitic layer is missing with no gap between the chitinous part of the jaw and the rest of the concretion, implying that the calcitic layer was destroyed prior to concretion formation. Most of these jaws are deformed with ragged margins, and some of them are even pierced with holes, suggesting that they may have been eaten by a predator, and subsequently secreted as faecal matter.

The sequence of concretion formation has been studied at many sites, e.g., Reeside and Cobban (1960)—the Albian Mowry Shale in Wyoming; Waage (1964)—the upper Maastrichtian Fox Hills Formation in north-central South Dakota; Raiswell (1976)—the lower Lias in northeast England; Gautier (1982)—the Campanian Gammon Ferruginous Member of the Pierre Shale in Montana and the Black Hills region; Maeda (1987)—the Upper Cretaceous Yezo Group in northwestern Hokkaido; Carpenter et al. (1988) – the Fox Hills Formation in south-central North Dakota; and Ludvigson et al. (1994)—the Upper Cretaceous Greenhorn marine cycle in Iowa and South Dakota (see also Berner, 1968; Allison, 1990; and Maeda and Seilacher, 1996). These studies suggest that the cementation of concretions occurred at shallow burial depths below the sediment-water interface. This conclusion probably applies to the concretions in our study as well.

In summary, Kathy's concretion represents a time-averaged deposit of organisms derived from the local community. The shells probably accumulated in irregularities on the sea floor and were reworked by bioturbation and weak currents. Some ammonites, such as the adult scaphites, may have died as a result of predation and settled to the bottom. Other ammonites, such as the juvenile baculites, may have died following short-term environmental disturbances. Therefore, this accumulation reflects successive additions derived from multiple sources. Some material may have been buried rapidly, while other material, such as the ammonite jaws, may have rested on the sea floor for some time. However, taphonomic experiments with modern coleoid jaws (Kear et al., 1995) suggest that, by analogy, the ammonite jaws could not have survived exposure on the sea floor for more than several tens of years, and possibly less.

Other concretions from the *Baculites compressus–B. cuneatus* zones in the Pierre Shale in Meade and Pennington Counties, South Dakota, vary in shape, size, and fossil content, but contain some or all of the same faunal elements. These concretions represent the same biofacies extending over an area of at least 1,000 km^2. These accumulations can be interpreted as mixed death assemblages, similar to the "within habitat time averaged assemblages" of Kidwell and Bosence (1991) and the "Type C assemblages" of Tsujita (1995). They formed during relatively short periods of time (months to years) and reflect a composite mixture of material derived from

both background attrition (predation) and mass mortalities (environmental disturbances).

Given the rate of accumulation of the shells, these concretions can provide valuable information about the structure and composition of scaphite populations. For example, examining the scaphites in single concretions provides a more accurate method of determining the range of variation within a single species, and the size difference between conspecific dimorphs, than examining a sample of specimens from different horizons in the same zone. Nevertheless, it is important to bear in mind that these concretions do not represent census assemblages. Such concretions are present elsewhere, for example, in the Lower Nicolletti Assemblage Zone in the Fox Hills Formation of north-central South Dakota (Waage, 1964; Landman et al., 2003). These concretions are characterized by monospecific clusters of macroconchs (presumably females) of a single species of scaphite, occasionally with jaws preserved inside the body chamber. The interpretation is that the females probably died immediately after spawning, and were rapidly buried.

REPOSITORIES

Specimens are identified by species, museum repository number, study number, locality number, geographic area, and stratigraphic unit. Study numbers range from 1 to approximately 2000. The repository is indicated by a prefix, as follows: Department of Geology, University of Alberta (UA), Edmonton, Alberta, Canada; Division of Paleontology (Invertebrates), American Museum of Natural History (AMNH), New York, New York; Academy of Natural Sciences of Philadelphia (ANSP), Philadelphia, Pennsylvania; Black Hills Museum of Natural History (BHI), Hill City, South Dakota; Geological Survey of Canada (GSC), Ottawa, Ontario, Canada; Department of Geology, the Field Museum (variously given as FMNH, FMUC, UC, and UCP), Chicago, Illinois; Geological Museum of the Polish Geological Institute (IG), Warsaw, Poland; Memphis Pink Palace Museum (MPPM), Memphis, Tennessee; Museum of Paleontology, University of Kansas (KUMIP), Lawrence, Kansas; Museum of Paleontology, University of Michigan (UMMP), Ann Arbor, Michigan; Timber Lake and Area Museum (TLAM), Timber Lake, South Dakota; Tyrrell Museum of Paleontology (TMP), Drumheller, Alberta; the U.S. Geological Survey (USGS), Denver, Colorado; U.S. National Museum (USNM), Washington, D.C.; and Yale Peabody Museum (YPM), New Haven, Connecticut. Locality numbers are listed in appendix 1.

TERMS AND METHODS

Most of the terms used to describe scaphites are reviewed by Riccardi (1983), Landman and Waage (1993), Landman and Cobban (2007), and Machalski (2005b). The adult shell consists of a closely coiled phragmocone and a slightly to strongly uncoiled body chamber (fig. 14A, B). The adult phragmocone is the part of the phragmocone that is exposed in the adult shell, as compared to the part that is concealed inside. The point of exposure is the most adapical point of the adult phragmocone. The body chamber consists of the shaft, beginning near the last septum, and a hook terminating at the aperture. The point of recurvature is the point at which the hook curves backward.

Several measurements were made on the adult shell (fig. 14, tables 1–10). The maximum length of the adult shell (LMAX) was measured from the venter of the adult phragmocone to the venter of the hook. The umbilical diameter of the adult shell (UD) was measured in two ways: (1) through the center of the umbilicus, parallel to the line of maximum length (UD_L), and (2) through the center of the umbilicus, passing through the position of the last septum (UD_P), as indicated on the umbilical shoulder. Whorl width (W) and whorl height (H) were measured at seven points on the adult shell: (1) on the phragmocone 90° adapical of the line of maximum length, (2) on the phragmocone, along the line of maximum length, (3) at the position of the last septum, (4) at midshaft, (5) just adapical of the point of recurvature, (6) at the point of recurvature, and (7) at the aperture. The width of the venter at midshaft (V_4) was measured be-

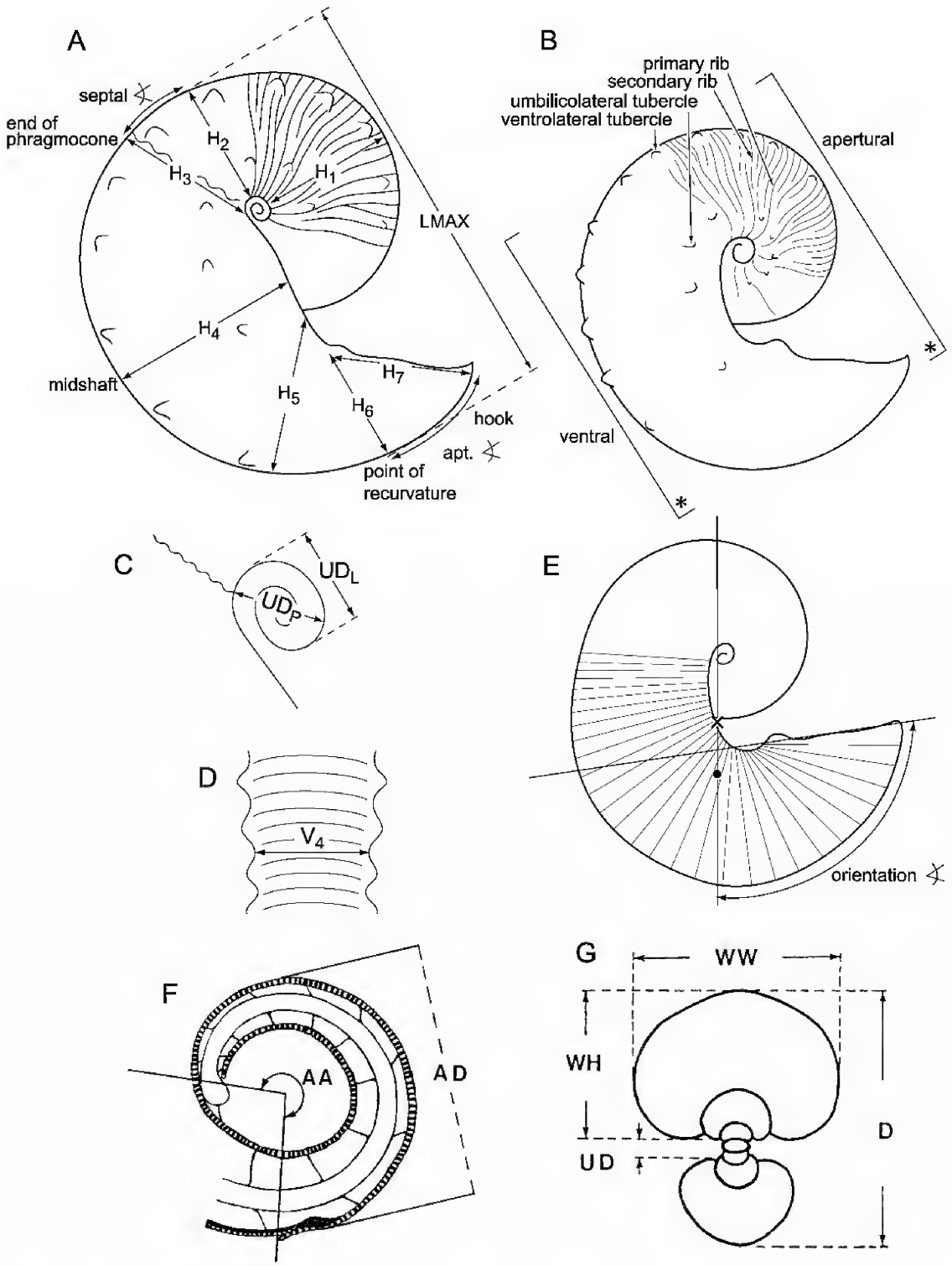

Fig. 14. Scaphite terminology. **A.** Macroconch, right lateral view. The shell is oriented in the probable floating position when the body was withdrawn into the body chamber. The umbilical seam of the shaft in

tween the ventrolateral margins on opposite sides of the venter. All measurements were made using electronic calipers on actual specimens, rather than on photos. Some measurements were estimated (as indicated by asterisks in tables 1–10) in cases of poor preservation. These estimates were not used in computing averages and standard deviations or in plotting graphs.

We calculated several ratios to describe the shape of the adult shell and facilitate comparisons among specimens. The ratios of whorl width to whorl height were calculated at seven points on the shell (W_1/H_1–W_7/H_7), as described above, and provide a measure of the degree of whorl compression. The ratio of ventral width to whorl height at midshaft (V_4/H_4) and the ratio of ventral width to whorl width at midshaft (V_4/W_4) were also calculated and provide additional measures of the degree of whorl compression. The ratio of whorl height at midshaft to whorl height on the phragmocone along the line of maximum length (H_4/H_2), and the ratio of whorl height at midshaft to whorl height at the point of recurvature (H_4/H_6) both describe the ontogenetic change in whorl height. The ratio of maximum length to whorl height on the phragmocone along the line of maximum length ($LMAX/H_2$) is a measure of the degree of uncoiling. For example, Landman (1987: 211) used this ratio to characterize the degree of uncoiling in Turonian-Santonian scaphites in the U.S. Western Interior. The mean value ranged from 3.31 in the most primitive species (*Scaphites larvaeformis* Meek and Hayden, 1859) to 2.55 in the most advanced species (*C. vermiformis* [Meek and Hayden, 1862]), reflecting an evolutionary trend toward tighter coiling. The ratio of maximum length to whorl height at midshaft ($LMAX/H_4$) is a measure of the degree of curvature of the body chamber in lateral view. For example, if the outline of the body chamber in lateral view is a semicircle, the ratio of $LMAX/H_4$ equals 2. This ratio only applies to macroconchs because the umbilical seam of the body chamber usually coincides with the line of maximum length in these forms, and thus the whorl height is the distance from the line of maximum length to the venter of the body chamber (equivalent to the radius in the case of a semicircle).

The apertural angle is defined as in Landman and Waage (1993) and Machalski (2005b). This angle is measured on photographs of specimens in lateral view. A line is drawn along the umbilical shoulder and another line is drawn along the apertural margin. The apertural angle is the angle of intersection between these two lines, extending from approximately the point of recurvature to the end of the shell. We restricted this measurement to macroconchs, but even in these forms, there is room for error. The umbilical shoulder sometimes shows a bulge or sag, making it difficult to know where to draw the line.

←

macroconchs is straight with a slight umbilical bulge. Abbreviations: H_1 = whorl height ¼ whorl adapical of the long axis; H_2 = whorl height along the long axis; H_3 = whorl height at the ultimate septum; H_4 = whorl height at midshaft; H_5 = whorl height right before the point of recurvature; H_6 = whorl height at the point of recurvature; H_7 = whorl height at the aperture; LMAX= maximum length along the long axis; apt. < = apertural angle; septal. < = septal angle. **B.** Microconch, right lateral view. The microconch is approximately 85% of the size of the macroconch or, inversely, the macroconch is approximately 120% the size of the microconch. The umbilical seam of the shaft in microconchs is curved and follows the curvature of the venter. Specimens are photographed from lateral, ventral, and apertural views, as shown. Asterisks indicate the up position in ventral and apertural views. **C.** Close-up of the umbilicus of the macroconch showing the umbilical diameter measured parallel to the long axis (UD_L) and the umbilical diameter measured at the base of the body chamber (UD_P). **D.** View of the venter of the body chamber at midshaft, with the adoral direction toward the top, showing the width of the venter (V_4). **E.** The angle of orientation of the aperture (orientation <) is defined as the angle of the aperture with respect to the vertical, as determined using the method in Trueman (1941). x = center of buoyancy; · = center of mass. **F.** Median cross section through the ammonitella showing measurements of the ammonitella diameter (AD) and ammonitella angle (AA). **G.** Dorsoventral cross section of a juvenile specimen. Abbreviations: D = diameter, WH = whorl height, WW = whorl width, UD = umbilical diameter.

The septal angle describes the position of the last septum relative to the line of maximum length. As in the apertural angle, the septal angle is measured on photographs of specimens in lateral view. The position of the last septum is defined as the position of the median saddle in the ventral (external) lobe. A line is drawn through the position of the last septum (marked on the flanks for convenience) and the center of the umbilicus. Another line is drawn through the center of the umbilicus parallel to the line of maximum length. The septal angle is the angle of intersection between these two lines, extending from the position of the last septum to the line of maximum length. Negative angles are defined as above (adapical of) the line of maximum length; positive angles are defined as below (adoral of) the line of maximum length.

A number of terms are used to describe ornamentation. Primary ribs originate near the umbilicus, whereas secondary ribs originate on the flanks or venter, either by splitting or intercalation (strictly speaking, the latter are called intercalatories). The density of ribs is measured in three ways (Landman and Cobban, 2007). The first method is to count the number of ribs/cm on the venter at a particular spot on the shell, for example, on the midshaft or hook. When the ribs are widely spaced, the rib number may be a fraction (usually ending in 0.25, 0.50, or 0.75), but when ribs are closely spaced, the number is usually an integer. The second method is to count the number of secondary ribs between a given number of primary ribs, and divide the former by the latter. In practice, the number of secondary ribs is usually regarded as the number of ventral ribs, although this actually includes primary ribs. The third method is to count the number of secondary ribs into which a primary rib splits and the number of secondary ribs intercalated between consecutive primary ribs. These three methods yield slightly different information.

In addition to ribs, the ornamentation includes tubercles, which are small conical swellings. They may develop into bullae (elongated in a radial direction), nodes (swollen and blunt), clavi (elongated in a spiral direction), or spines (elongated and pointed) (for an illustration of these ornamental features, see Arkell et al., 1957: L90, fig. 133). Bullae are sometimes difficult to distinguish from raised ribs. Umbilicolateral tubercles occur near the umbilicolateral margin and ventrolateral tubercles occur near the ventrolateral margin (fig. 14). We counted the number of both types of tubercles on the phragmocone and body chamber of the adult shell. We recorded the distance between tubercles, as measured between tubercle crests, following the curvature of the shell on the umbilicolateral margin for umbilicolateral tubercles, and on the ventrolateral margin for ventrolateral tubercles. The height of a tubercle is measured from its base to its tip, although this measurement is usually an underestimate due to imperfect preservation. We also recorded the number of ribs that join a tubercle dorsally, the number of ribs that branch from it ventrally, and the number of ribs that intercalate between consecutive tubercles.

Septal approximation was measured as described in Landman and Waage (1993). We introduced three refinements to their method. (1) In each specimen studied, we measured the interseptal distances two or three times to determine the measurement error. This error was usually less than 0.3 mm, representing less than 5% of the value of the interseptal distance. (2) We measured the interseptal distances in several specimens representing juvenile and submature stages in order to determine the pattern of change during "normal" growth, and thus, by comparison, to give a better idea of septal approximation at maturity. In general, in the early ontogeny of these scaphites, the septa are evenly spaced (in contrast, septal crowding is common in the early ontogeny of Carboniferous ammonoids, see Kraft et al., 2008). Our results indicate that during "normal" growth, the change in interseptal distance between successive chambers is ± 1 mm. Therefore, septal approximation at maturity is defined at the point at which the reduction in interseptal distance is >1 mm. (3) The variation in the magnitude of septal approximation is the ratio, expressed as a percentage, of the interseptal distance of the last chamber to that of the last "normal" chamber. Values between 30% and 40% indicate strong approximation, values

around 50% indicate moderate approximation, and values between 60% and 80% indicate weak approximation.

Sutures were drawn using a camera lucida. In general, the last suture or next to last suture is illustrated. Most of our discussion about sutures refers to the shape of the first lateral saddle and lobe. The suture terminology is that of Wedekind (1916), as reviewed by Kullmann and Wiedmann (1970). However, as Korn et al. (2003) have pointed out, this terminology requires revision, based on their study of the evolution of the suture line in prolecanitids.

In addition to describing adult morphology, we also described the ontogenetic development of these scaphites. The methods are reviewed by Landman and Waage (1993) and Landman and Cobban (2007). In general, adult shells were incrementally broken down to expose earlier and earlier whorls. Specimens were photographed at each stage of this process to document the ontogenetic change in whorl shape and ornamentation. In addition, we prepared dorsoventral cross sections perpendicular to the plane of symmetry and passing through the axis of coiling. We measured the ontogenetic change in the degree of whorl compression, W/H; the relative umbilical diameter, UD/LMAX; and the whorl expansion rate, $(LMAX_{\theta}/LMAX_{\theta-\pi})^2$, where θ is the angle at any given diameter.

Photographs of adult shells are natural size unless otherwise indicated. Small tick marks on the photos mark the base of the body chamber, where visible. The base of the body chamber is defined as the position of the median saddle in the ventral lobe. Specimens are photographed in lateral, ventral, and apertural views (fig. 14B). In lateral view, specimens are photographed with the aperture near the bottom, approximating their position in life.

SHELL MORPHOLOGY

The ammonitella consists of the initial chamber and approximately two-thirds of a whorl (figs. 15, 16). In two specimens of *Hoploscaphites brevis* (AMNH 58522 and 58523), the ammonitella diameter is 678 μm and 742 μm and the ammonitella angle is 281° and 302°, respectively. These values are similar to those reported for scaphites from the Fox Hills Formation by Landman and Waage (1993). The outer whorls of the ammonitella are covered with a tuberculate microornamentation (fig. 15). Such tubercles were first observed in scaphites by Smith (1905: 642, fig. 1.13) in what he called *S. nodosus* var. *brevis*, and have since been documented in nearly all Mesozoic ammonites (Landman et al., 1996). The ammonitella is prismatic in microstructure except for the primary varix, which consists of nacre. Internally, the first septum (proseptum) in scaphites bears a necklike attachment (fig. 16), as previously described in Landman and Bandel (1985) and Landman and Waage (1993).

The juvenile shell is planispirally coiled with a small umbilicus. The whorl section is initially depressed and becomes more compressed through early ontogeny. This change is similar to that in many other ammonites and may correlate with changes in habitat and/or swimming ability (Jacobs, 1992). The ratio of umbilical diameter to shell diameter decreases steeply in early ontogeny until a shell diameter of approximately 10–20 mm, after which the ratio remains nearly the same until the beginning of the mature body chamber. The rate of whorl expansion in juveniles is approximately 2.60.

It is difficult to determine the angle of the body chamber in juveniles because the apertural margin is very thin and almost never preserved intact. We measured an angle of 217.5° in a juvenile of *Hoploscaphites brevis* (D = 25.1 mm), and an angle of 202° in a juvenile of *H. nodosus* (D = 37.5 mm), although the apertural margin is broken in both of these specimens (AMNH 58559 and 58560, respectively). In a study of 37 well-preserved juveniles of *Hoploscaphites comprimus* (Owen, 1852) ranging from 1.8 to 9.6 mm in phragmocone diameter, Landman and Waage (1993) reported an average body chamber angle of 237° with a range from 220° to 264°. Based on all these measurements, we estimate that the body chamber angle in juveniles of *H. nodosus* and *H. brevis* is nearly two-thirds of a whorl (230°), which is referred to as mesodomic in the terminology of Westermann (1996). In contrast,

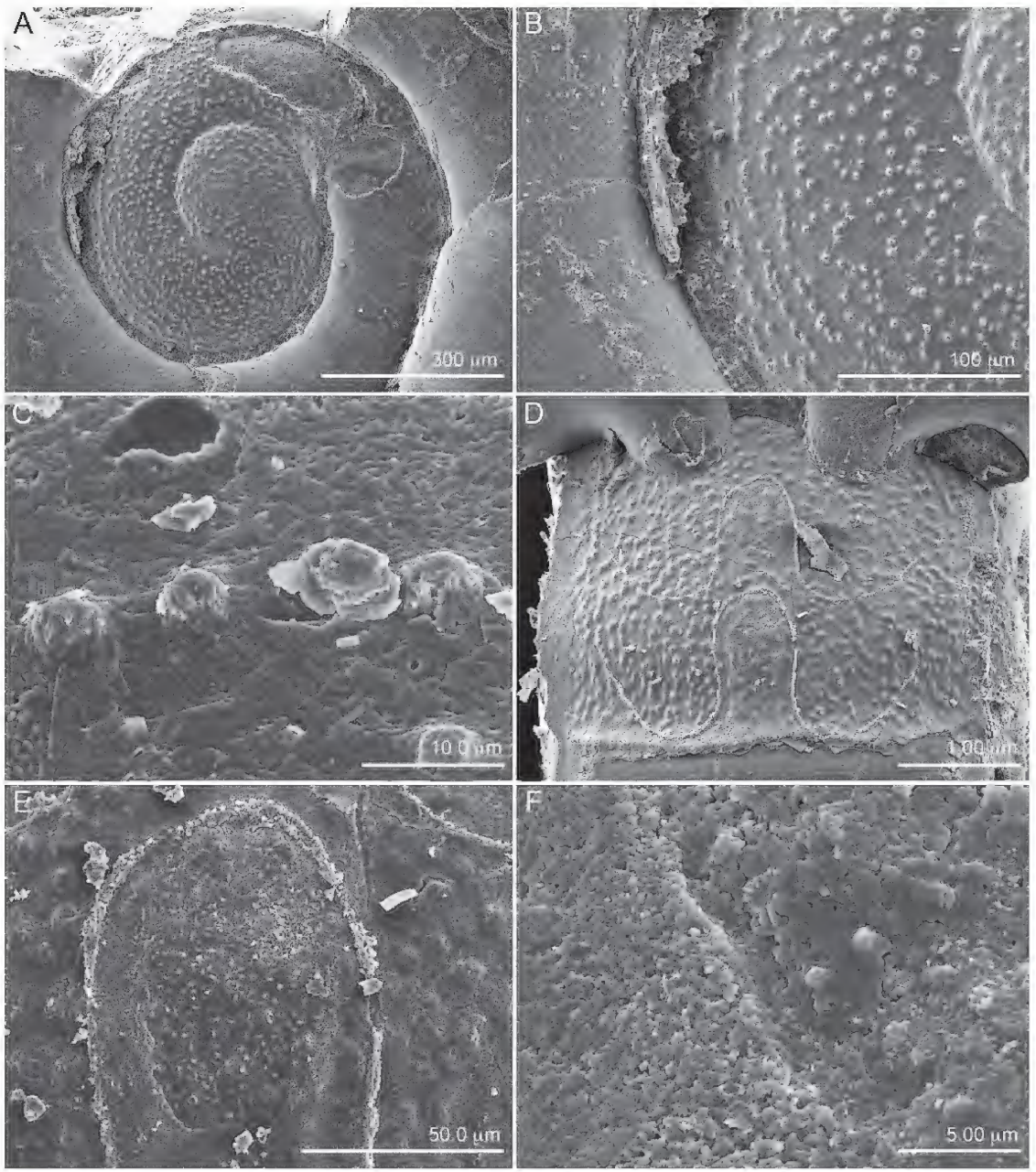

Fig. 15. Embryonic whorls of *Hoploscaphites nodosus* (Owen, 1852) and *H. brevis* (Meek, 1876), AMNH loc. 3274, *Baculites compressus–B. cuneatus* zones, Pierre Shale, Meade County, South Dakota. **A–C.** *Hoploscaphites brevis* (Meek, 1876), AMNH 58539. **A.** The embryonic shell is covered with tubercles. **B.** Most of the tubercles are irregularly distributed but some are aligned in longitudinal rows. **C.** The tubercles vary in diameter and range from 5–10 µm. **D–F.** *Hoploscaphites nodosus* (Owen, 1852), AMNH 66259. **D.** Ventral surface of the embryonic shell just adapical of the primary constriction. The surface is covered with a thin dorsal layer and retains the outline of the dorsal sutures of the succeeding whorl. **E.** Muscle scar in the dorsal lobe. **F.** The muscle scar is demarcated by a fine-grained texture.

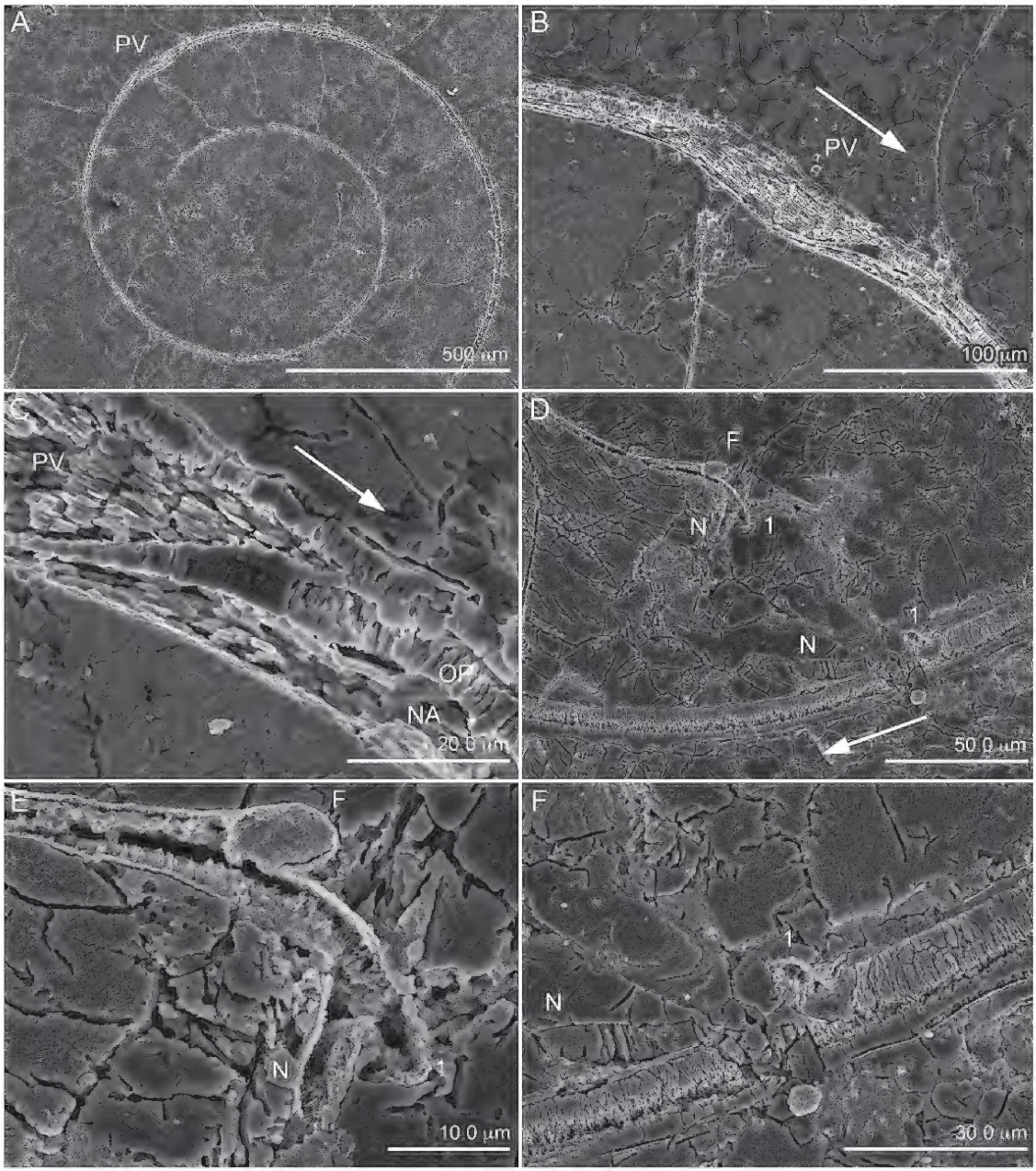

Fig. 16. Embryonic whorls of *Hoploscaphites brevis* (Meek, 1876), AMNH loc. 3274, *Baculites compressus–B. cuneatus* zones, Pierre Shale, Meade County, South Dakota. **A–C.** Median cross section, AMNH 58522. **A.** The embryonic shell ends in the primary varix (PV). The ammonitella diameter is 742 µm and the ammonitella angle is 281°. **B.** Close-up of the primary varix (PV). The arrow here and in C and D indicates the adoral direction. **C.** The postembryonic shell emerges from beneath the primary varix (PV) and consists of an outer prismatic (OP) and inner nacreous layer (NA). **D–E.** Median cross section, AMNH 58531. **D.** The proseptum (1), its necklike attachment (N), and the flange (F) are visible. **E.** Close-up of the dorsal portion of the proseptum (1), its necklike attachment (N), and the flange (F). **F.** Close-up of the ventral portion of the proseptum (1) and its necklike attachment (N).

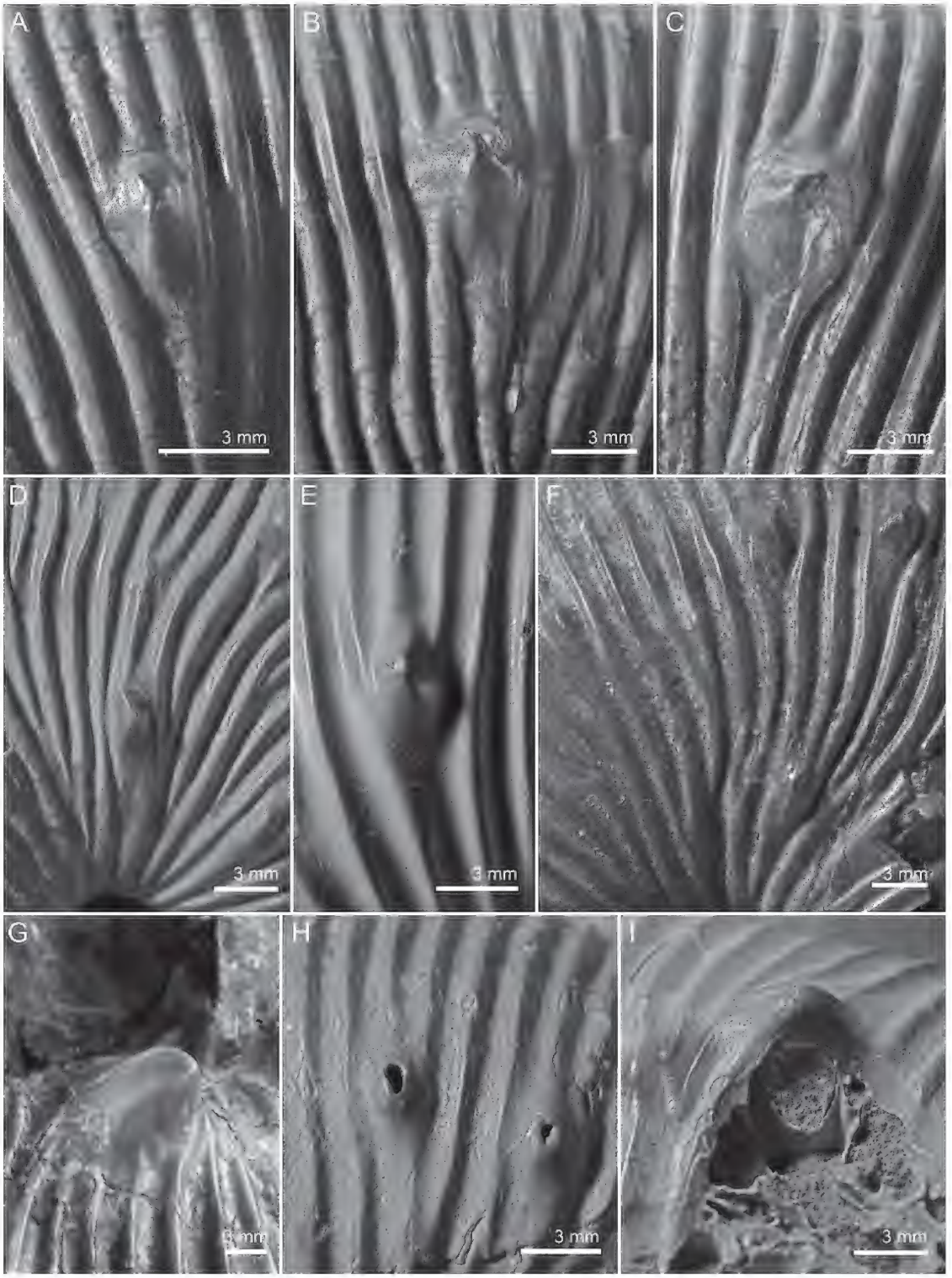
A
3 mm
B
3 mm
C
3 mm
D
3 mm
E
3 mm
F
3 mm
G
3 mm
H
3 mm
I
3 mm

Landman (1987) documented a higher body chamber angle in juveniles of *Scaphites preventricosus* and *Clisoscaphites vermiformis*. In a sample of 31 juveniles of *C. vermiformis* and 9 juveniles of *S. preventricosus*, the body chamber angle averages 266° and ranges from 235° to 302°.

The ornament consists of ribs and umbilicolateral and ventrolateral tubercles (fig. 17). The ribs represent flexures in the shell wall and are, therefore, expressed on the steinkern. However, they are sharper on the actual shell. Ribs beome slightly more closely spaced in passing from the adapical to the adoral part of the exposed phragmocone (fig. 18). Thereafter, they become slightly more widely spaced on the midshaft and slightly more closely spaced again on the hook. Ribs are rectiradiate to slightly rursiradiate on the adapical portion of the shaft, becoming more prorsiradiate on the adoral portion of the shaft. They bend backward on the inner flanks, forward on the midflanks, back again on the outer flanks, and weakly forward at the ventrolateral margin. Ribs become straight or slightly concave near the point of recurvature. Branching and intercalation occur at the umbilical shoulder, on the inner one-third of the flanks at the site of the umbilicolateral tubercles, if they are present, and on the outer one-third of the flanks at the site of the ventrolateral tubercles. Ribs cross the venter of the shaft with a slight forward projection, which weakens on the hook.

The tubercles are hollow (nonfloored) and are, therefore, expressed on the steinkern. The umbilicolateral tubercles usually appear midway on the exposed phragmocone whereas the ventrolateral tubercles usually appear in early ontogeny. The umbilicolateral and ventrolateral tubercles increase in size in passing from the phragmocone to the body chamber. One of the distinctive features of the scaphites from the *Baculites compressus–B. cuneatus* zones is the distribution of the ventrolateral tubercles on the exposed phragmocone. The tubercles in this area are widely and irregularly spaced and commonly occur in pairs or clusters (fig. 19). This contrasts, for example, with *Hoploscaphites crassus* (Coryell and Salmon, 1934) from the *B. baculus* Zone in which the tubercles are closely and regularly spaced.

The ventrolateral tubercles attain their maximum size at midshaft. In *Hoploscaphites nodosus*, these tubercles develop into subspinose clavi, with a flattened, steep adapical face and a more gently sloping adoral face. This implies that during tubercle formation, the apertural lip flared backward and outward along the ventrolateral margin. Al-

←

Fig. 17. Details of the ornamentation in *Hoploscaphites nodosus* (Owen, 1852). The venter is toward the top in all views except for G in which it is toward the bottom. **A–C.** BHI 4216, macroconch, *Baculites compressus* Zone, Pierre Shale, Meade County, South Dakota. **A.** Umbilicolateral tubercle on the right side of the exposed phragmocone. One rib joins it dorsally and three ribs branch from it ventrally. **B.** Ventrolateral tubercle on the right side of the exposed phragmocone. Two ribs join it dorsally and three ribs branch from it ventrally. **C.** Ventrolateral tubercle on the right side of the exposed phragmocone. One rib joins it dorsally and three ribs branch from it ventrally. **D, E.** BHI 4178, macroconch, *Baculites compressus–B. cuneatus* zones, Pierre Shale, Meade County, South Dakota. **D.** Umbilicolateral tubercle on the right side of the exposed phragmocone. The tubercle occurs in the interspace between ribs, with one rib joining it dorsally and three ribs branching from it ventrally. **E.** Ventrolateral tubercle on the left side of the exposed phragmocone. The tubercle occurs in the interspace between ribs, with one rib joining it dorsally and three ribs branching from it ventrally. **F.** BHI 4121, macroconch, *Baculites compressus–B. cuneatus* zones, Pierre Shale, Meade County, South Dakota. Umbilicolateral and ventrolateral tubercles on the left side of the exposed phragmocone. **G.** AMNH 9520/3, microconch, Pierre Shale, Belle Fourche River, South Dakota. Umbilicolateral tubercle on the left side of the body chamber, with a steeply dipping adapical side on the right and a more gently sloping adoral side on the left. **H–I.** AMNH 45343, macroconch, AMNH loc. 3212, *Baculites compressus–B. cuneatus* zones, Pierre Shale, Shannon County, South Dakota. **H.** Ventrolateral tubercles on the right side of the exposed phragmocone. The tips of the tubercles are broken revealing that the tubercles are hollow. **I.** Ventrolateral tubercle on the left side of the exposed phragmocone broken in half and filled with matrix.

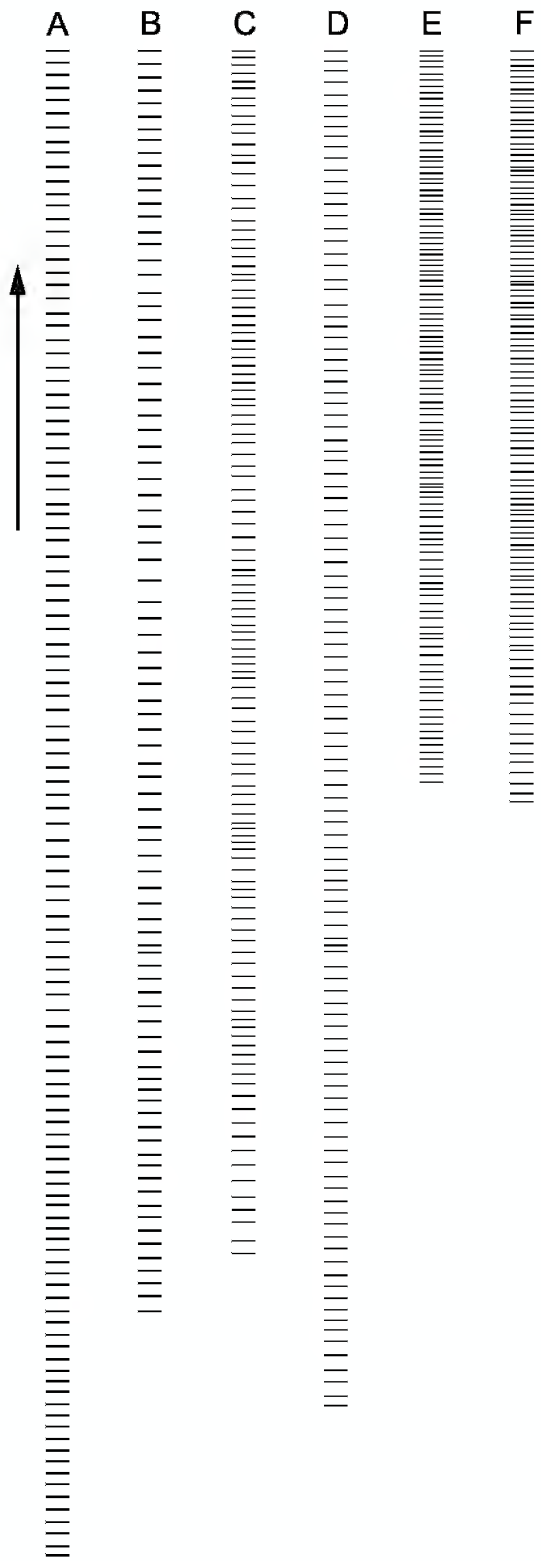
A
B
C
D
E
F

though the pattern of growth lines is not visible on any of these tubercles, the mode of tubercle formation may have been similar to that in *Aspidoceras*, as described by Checa and Martin-Ramos (1989: fig. 4A–C). Starting on the adoral end of the shaft, the ventrolateral tubercles abruptly diminish in size, much more so than the umbilicolateral tubercles. In general, there is an increase in rib density at the sites of the umbilicolateral and ventrolateral tubercles. Several ribs join an umbilicolateral or ventrolateral tubercle dorsally, and an additional number of ribs branch from it ventrally. Occasionally, a tubercle occurs in the interspace between ribs.

Muscle attachment areas are indicated by thin layers of myostracum on steinkerns of the body chambers (fig. 20). The ventral muscle attachment area is ovoid and appears several millimeters adoral of the midventral saddle. It is 1–5 mm in length, depending on the size of the adult shell. The dorsal muscle attachment area is wedge shaped and drapes over the umbilical shoulder on each side of the shell just adoral of the last suture.

The sutures in *Hoploscaphites nodosus* and *H. brevis* do not differ significantly from those of other Campanian and Maastrichtian species of *Hoploscaphites* (fig. 21). The ventral lobe (E) is broad and contains a median saddle. The first lateral sadde (E/L) is broad and asymmetrically bifid. The first lateral lobe (L) is symmetrically to asymmetrically bifid, owing to the relative enlargement of its inner branch.

Scaphites, like many other ammonites, exhibit determinate growth (Bucher et al., 1996). Seilacher and Gunji (1993: 241) have described the phenomenon of "mophogenetic countdown," which they defined as "an irrevocable sequence, or program, of morphogenetic events that proceeds step by step and terminates with growth cessation as the final command." This sequence reflects the growth of the reproductive organs and the attainment of maturity. It is also expressed in the morphology of the shell. For example, in modern nautilus, the disappeance of the color bands on the venter indicates the beginning of the countdown. It also coincides with a reduction in septal spacing and an increase in septal thickness (Collins and Ward, 1987). Landman (1989) discussed this phenomenon in *Pteroscaphites* from the Turonian-Santonian of the U.S. Western Interior. The countdown began in these scaphites at an unusually small size, initiating a set of mature modifications. However, because of the small size of these scaphites, their mature modifications closely reflect the morphology of the juvenile shell and, therefore, differ from the mature modifications of closely related, but larger species.

The morphogenetic countdown begins in scaphites at the point at which the shell departs from the spiral coil and develops into the shaft. This marks the beginning of an essentially irreversible process, unless a fatal injury intervenes, culminating in the formation of the mature shell. The shaft passes into the hook, which recurves backward forming an apertural angle of 35°–85°, depending on the species. The apertural opening is reduced relative to the whorl section of the hook, due to a constriction in the shell (fig. 22). The shell wall bends sharply inward, at nearly a right angle, forming a thick varix, and then reflects outward, terminating in a flared lip.

←

Fig. 18. Spacing of ribs on the venter starting from near the adoral end of the phragmocone (bottom) to the aperture (top). Ribs become more widely spaced on the midshaft and more closely spaced on the hook. **A.** *Hoploscaphites nodosus* (Owen, 1852), macroconch, BHI 4257, *Baculites cuneatus* Zone, Pierre Shale, Meade County, South Dakota. **B.** *Hoploscaphites nodosus* (Owen, 1852), macroconch, AMNH 9520/2, Pierre Shale, Sage Creek, Pennington County, South Dakota. **C.** *Hoploscaphites brevis* (Meek, 1876), macroconch, holotype, USNM 367, Pierre Shale, probably from the Sage Creek area, Pennington County, South Dakota. **D.** *Hoploscaphites brevis* (Meek, 1876), macroconch, YPM 35576, YPM loc. A6520, Pierre Shale, Sage Creek, Pennington County, South Dakota. **E.** *Hoploscaphites brevis* (Meek, 1876), macroconch, BHI 4235, *Baculites compressus* Zone, Pierre Shale, Meade County, South Dakota. **F.** *Hoploscaphites brevis* (Meek, 1876), macroconch, YPM 35584, YPM loc. A6520, Pierre Shale, Sage Creek, Pennington County, South Dakota.

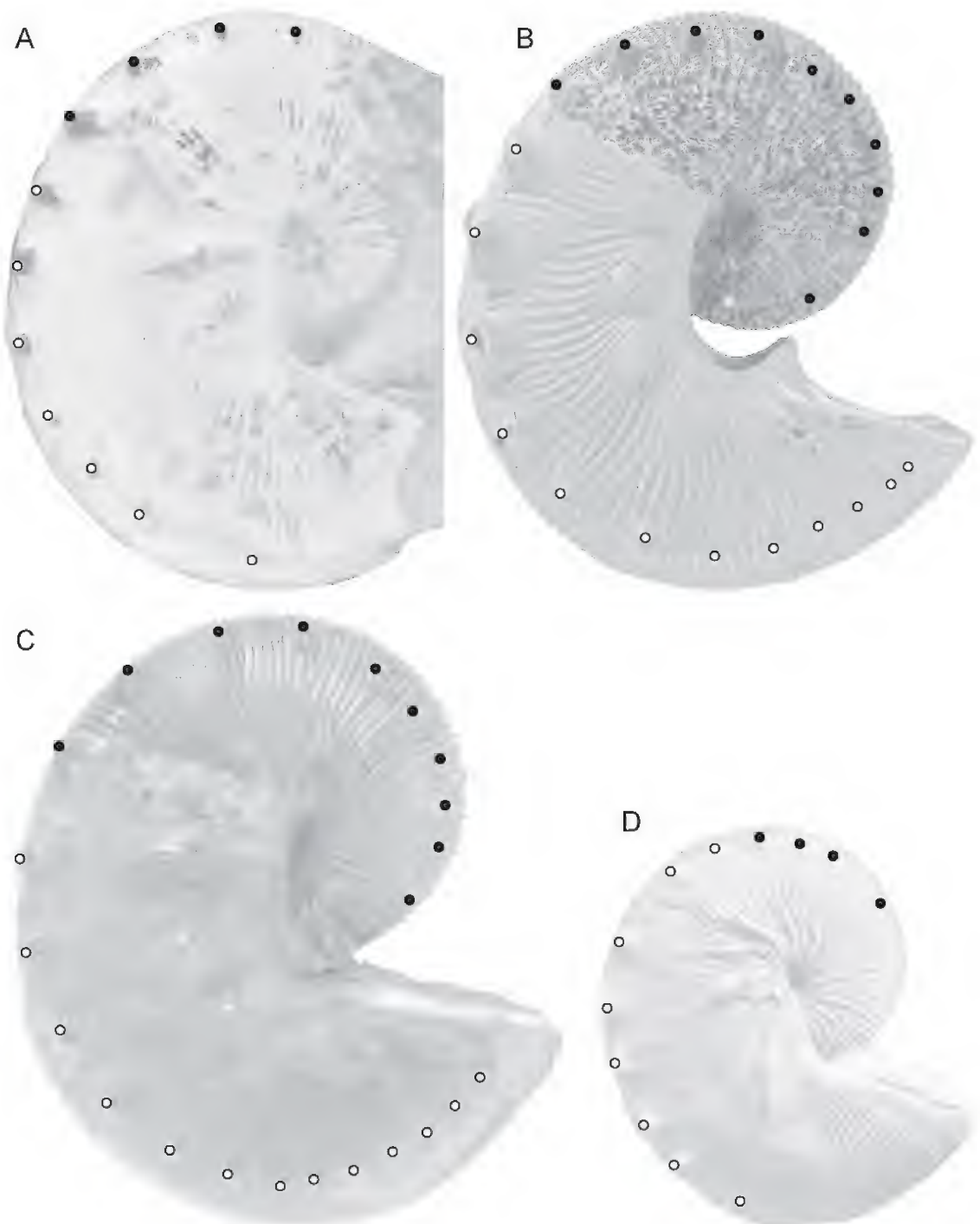

Fig. 19. Spacing of ventrolateral tubercles on the adult shells of *Hoploscaphites nodosus* (Owen, 1852) and *H. brevis* (Meek, 1876). **A.** *Hoploscaphites brevis* (Meek, 1876), large macroconch, BHI 4790, *Baculites compressus–B. cuneatus* zones, Pierre Shale, Meade County, South Dakota. **B.** *Hoploscaphites nodosus* (Owen, 1852), large microconch, BHI 4222, *Baculites compressus* Zone, Pierre Shale, Meade County, South Dakota. **C.** *Hoploscaphites nodosus* (Owen, 1852), large macroconch, BHI 4216, *Baculites*

The formation of a varix is generally interpreted as reflecting a pause in growth (Bucher et al., 1996). Sediments commonly accumulate in the narrow gap between the flared lip and the rest of the shell wall. The constriction and varix disappear on the dorsum where the apertural margin forms an elongate, broadly rounded projection (fig. 22). In steinkerns, the constriction and varix in the shell wall appear as a constriction at the apertural margin.

In the 19th century, it was not universally accepted that the formation of an uncoiled body chamber implied a cessation of growth. Hyatt (1894: 613) argued that the uncoiled body chamber in scaphites and other heteromorph ammonites was resorbed during ontogeny. He based this on the fact that he observed small shells with uncoiled body chambers, which he interpreted as belonging to the same species as large shells with similarly uncoiled body chambers, thus concluding that the uncoiled body chamber must have been resorbed and reformed several times during ontogeny. However, it is much more likely that these small and large shells simply represented adults of different species or dimorphs of the same species. In contrast to Hyatt, Pompeckj (1894) stated that he did not find any evidence for resorption in his study of ammonites with "abnormal" body chambers. Smith (1905), based on his ontogenetic study of scaphites, agreed with Pompeckj's conclusion, and reported that uncoiled body chambers never appeared at early ontogenetic stages. However, like Hyatt, Smith argued that the presence of an uncoiled body chamber indicated that scaphites showed "degeneration or senility."

The initiation of the morphogenetic countdown in scaphites, as indicated on the shell by the beginning of the shaft, corresponds internally to the secretion of the septum approximately two-thirds of a whorl back, based on our observations of the angular length of the body chamber in juveniles (see above). Therefore, the last seven or so septa must have been secreted during the formation of the adult body chamber. Of these, the last two or three septa correspond to the formation of the hook, culminating in the development of the constriction and varix at the apertural margin. Commonly, these last few septa are more closely spaced, which is generally interpreted as an indication of a decrease in the rate of growth, beginning at the onset of maturation (Bucher et al., 1996).

Scaphites occur as dimorphs, which are referred to as macroconchs (M) and microconchs (m). They are interpreted as sexual in nature, the macroconch being the female, and the microconch being the male, following the traditional view as outlined by Lehmann (1981) and Davis et al. (1996). The dimorphs in scaphites are distinguished by differences in size and morphology (Makowski, 1962; Cobban, 1969; Landman and Waage, 1993; Machalski, 2005a, 2005b; but see Kin, 2009, for a counterargument, and Machalski, in press, for a rebuttal). Dimorphism is more marked in Campanian-Maastrichtian scaphites such as *Hoploscaphites* than in older scaphites such as *Clioscaphites*. In general, dimorphism appears only in adult shells. Juvenile shells of conspecific dimorphs are nearly identical, except in rare instances. For example, Landman and Waage (1993: fig. 67) noted that in *Hoploscaphites nicolletii*, the ventral ribs starting at approximately 10 mm shell diameter, are coarser and stubbier in microconchs than in macroconchs. In scaphites from the *Baculites compressus–B. cuneatus* zones, the dimorphs are distinguished at maturity by (1) the presence or absence of an umbilical bulge, (2) the outline of the umbilical shoulder relative to that of the venter in side view, (3) the umbilical diameter, (4) the change in whorl height from the mature phragmocone to the midshaft of the body chamber (H_4/H_2), (5) the change in whorl height from the midshaft of the body chamber to the hook (H_4/H_6), (6) the change

←

compressus Zone, Pierre Shale, Meade County, South Dakota. **D.** *Hoploscaphites brevis* (Meek, 1876), small macroconch, BHI 4292, *Baculites compressus–B. cuneatus* zones, Pierre Shale, Meade County, South Dakota. The photo in D has been flipped so that it faces the same way as the others. Symbols: • = tubercle on the phragmocone; o = tubercle on the body chamber.

A
B
C
D
E
F
G
H

in the degree of whorl compression from the point of recurvature to the aperture, and (7) the adult size. Some of these criteria are more reliable than others in distinguishing between dimorphs.

The presence of a bulge on the umbilical shoulder indicates that the specimen is a macroconch. However, the absence of a bulge is equivocal. Although this feature is invariably absent in microconchs, it is also absent in many specimens that are identified as macroconchs on the basis of other criteria. The umbilical bulge appears on the adapical end of the shaft and extends adorally for several millimeters. In some specimens, the umbilical bulge is so large that it occludes part of the umbilicus. The significance of the bulge is unknown, but it may be related to the position of the reproductive organs, in analogy with the nidamental gland in present-day nautilus.

The outline of the umbilical shoulder of the body chamber relative to that of the venter in side view is usually a reliable means of distinguishing between dimorphs. In general, the umbilical shoulder of the body chamber is straight in macroconchs whereas it is curved in microconchs, matching the curvature of the venter. However, there is some variation in this feature, especially in small, compressed specimens of *Hoploscaphites brevis*. The umbilical shoulder is straight in these specimens, suggesting that they are macroconchs, but other features of the shell, including a gradual rather than abrupt increase in whorl height in passing from the phragmocone to the midshaft, suggest that they are microconchs instead (listed as "microconchs, transitional to macroconchs," in table 9). In a few instances, these specimens appear as macroconchs on the right side and microconchs on the left side, although the reason for this disparity is unknown.

Landman and Waage (1993: 90, fig. 48L–P) documented a similar phenomenon (straight umbilical shoulder and a gradual increase in whorl height) in small specimens of *Hoploscaphites nicolletii*. However, they interpreted these specimens as macroconchs rather than microconchs because the umbilical shoulder of the body chamber is sharply rather than broadly rounded, which is more characteristic of macroconchs. Examples of other ammonites showing a mixture of features of both dimorphs have been reported from the Jurassic of Europe. Parent et al. (2008: 186) noted this phenomenon in aspidoceratids and speculated that it may be due to "a weak sexual determination (hermaphroditism?) or a sex change in the subadult stage." These authors also cited an example of a perisphinctid that was identified as a macroconch on the basis of its ornament in the subadult stage, but which developed an apertural lappet at maturity, suggesting to them that the specimen had changed into a microconch during ontogeny. However, in modern cephalopods, hermaphroditism is unknown (Hanlon and Messenger, 1996).

In general, the umbilical diameter is larger in microconchs than in macroconchs. For example, a plot of UD_P versus LMAX in

←

Fig. 20. Muscle scars and other features on the adult shells of *Hoploscaphites nodosus* (Owen, 1852) and *H. brevis* (Meek, 1876). **A, B.** Unpaired ventral muscle scar (arrows) just adoral of the last suture. **A.** *Hoploscaphites nodosus* (Owen, 1852), macroconch, BHI 4948, *Baculites compressus* Zone, Pierre Shale, Meade County, South Dakota. **B.** *Hoploscaphites nodosus* (Owen, 1852), microconch, BHI 4949, *Baculites compressus* Zone, Bearpaw Shale, Rosebud County, Montana. **C.** Dorsal muscle scar (arrows) on the umbilical shoulder on the right side of the body chamber just adoral of the last suture, *Hoploscaphites brevis* (Meek, 1876), microconch, BHI 4283, *Baculites cuneatus* Zone, Pierre Shale, Meade County, South Dakota. **D.** Septal approximation (arrow), *Hoploscaphites nodosus* (Owen, 1852), macroconch, BHI 4948, *Baculites compressus* Zone, Pierre Shale, Meade County, South Dakota. **E.** Absence of septal approximation (arrow), *Hoploscaphites nodosus* (Owen, 1852), macroconch, BHI 4215, *Baculites cuneatus* Zone, Pierre Shale, Meade County, South Dakota. **F.** Trace of ventral muscle scar (arrow) on the phragmocone, *Hoploscaphites brevis* (Meek, 1876), BHI 4393, microconch, *Baculites compressus–B. cuneatus* zones, Pierre Shale, Meade County, South Dakota. **G, H.** Constriction (arrows) at the apertural margin, *Hoploscaphites brevis*, macroconch, BHI 5130, *Baculites compressus–B. cuneatus* zones, Pierre Shale, Pennington County, South Dakota. **G.** Ventral view; **H.** left lateral view.

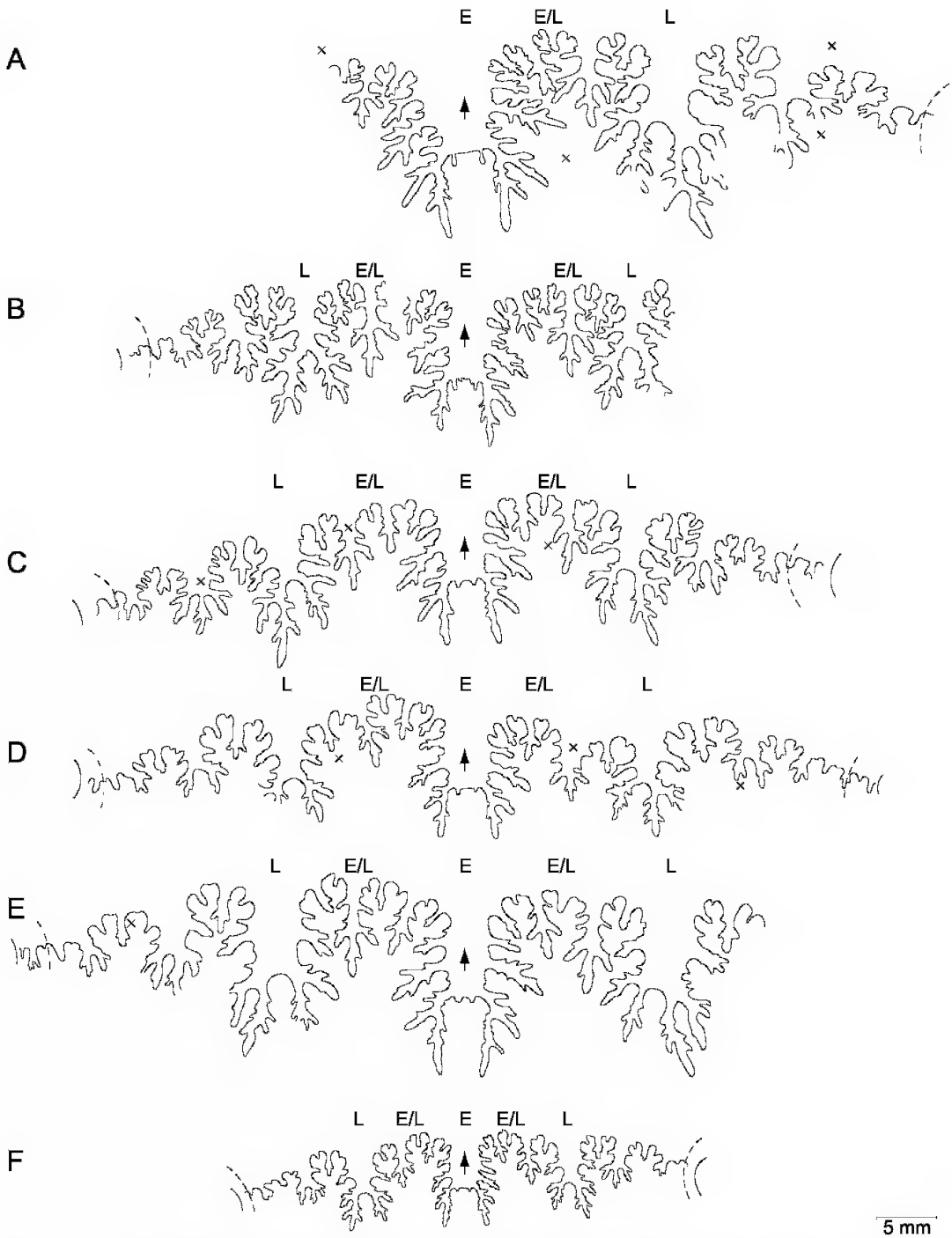

Fig. 21. Sutures in *Hoploscaphites nodosus* (Owen, 1852) and *H. brevis* (Meek, 1876). **A.** *Hoploscaphites brevis* (Meek, 1876), macroconch, third from last suture, BHI 7034, Pierre Shale, *Baculites cuneatus* Zone, Pennington County, South Dakota. **B.** *Hoploscaphites brevis* (Meek, 1876), macroconch, next to last suture, BHI 4205, *Baculites compressus* Zone, Pierre Shale, Meade County, South Dakota. **C.** *Hoploscaphites nodosus* (Owen, 1852), microconch, fourth from last suture, USNM 536232, USGS Mesozoic loc. 21224, Bearpaw Shale, Big Horn County, Montana. **D.** *Hoploscaphites nodosus* (Owen,

Hoploscaphites nodosus reveals a cluster of microconchs on the upper left characterized by high values of UD_P and low values of LMAX, and a cluster of macroconchs on the lower right characterized by lower values of UD_P and higher values of LMAX (fig. 23A). The umbilical diameter measured through the center of the umbilicus passing through the position of the last septum (UD_P) is a more reliable means of distinguishing between dimorphs than the umbilical diameter measured through the center of the umbilicus parallel to the line of maximum length (UD_L). The reason is that UD_P takes into account the difference in the curvature of the umbilical shoulder, provided that the base of the body chamber occurs below the line of maximum length. For example, in *H. nodosus*, the average value of UD_P is significantly higher in microconchs (7.2 mm) than in macroconchs (4.1 mm), whereas the average value of UD_L is nearly the same in both dimorphs (tables 3 and 5). Similary, a plot of UD_P versus UD_L in this species mostly differentiates the two dimorphs based on differences in UD_P (fig. 23B).

In addition to the curvature of the umbilical shoulder and the size of the umbilical diameter, dimorphs differ in the shape of their shells. The whorl height of the body chamber increases more markedly in macroconchs than in microconchs. This difference is expressed in the ratio of whorl height at midshaft to whorl height on the phragmocone along the line of maximum length (H_4/H_2) and by the ratio of whorl height at midshaft to whorl height at the point of recurvature (H_4/H_6). In our sample of *Hoploscaphites nodosus*, the average values of H_4/H_2 and H_4/H_6 are significantly higher in macroconchs (1.32 and 1.06, respectively) than in microconchs (1.21 and 0.99, respectively) (tables 3 and 5). In a plot of H_4/H_6 versus H_4/H_2, the two dimorphs appear as distinct clusters with some overlap between them (fig. 24A). Similarly, in our sample of *H. brevis*, the average values of H_4/H_2 and H_4/H_6 are significantly higher in macroconchs (1.37 and 1.18, respectively) than in microconchs (1.30 and 1.07, respectively) (tables 7 and 9). In a plot of H_4/H_6 versus H_4/H_2 in this species, the two dimorphs also appear as distinct clusters (fig. 24B). However, there is more overlap between them because of the existence of "transitional" specimens.

In both dimorphs, the shell becomes more compressed in passing from the end of the phragmocone to the body chamber (fig. 25). The ratio of whorl width to whorl height reaches a minimum value at midshaft. The whorl section becomes more depressed in passing into the hook, but the two dimorphs diverge thereafter. In macroconchs, the whorl section maintains the same degree of depression or becomes slightly more depressed toward the aperture, whereas in microconchs, the whorl section becomes less depressed. The fact that the whorl section at the aperture is more depressed in macroconchs than in microconchs may be related to differences in the pattern of sexual maturation. It is possible that the more depressed aperture in macroconchs reflects the development of the ovaries and the formation of eggs.

As in other scaphites, dimorphs differ in the size of the adult shell. Macroconchs attain a larger size than microconchs but the size ranges of the two dimorphs overlap. The extent of size overlap depends upon the number of specimens in the sample, with larger samples showing a greater degree of overlap. The extent of size overlap also depends on the geographic and temporal range of the sample. For example, in our sample of *Hoploscaphites nodosus* from the *Baculites compressus–B. cuneatus* zones, the extent of size overlap is 44% of the total combined size range of both dimorphs. However, this sample

---

←

1852), microconch, second from last suture, BHI 4122, *Baculites compressus–B. cuneatus* zones, Pierre Shale, Meade County, South Dakota. **E.** *Hoploscaphites brevis* (Meek, 1876), microconch, third from last suture, USNM 536262, Pierre Shale, Pennington County, South Dakota. **F.** *Hoploscaphites brevis* (Meek, 1876), microconch, third from last suture, BHI 4255, *Baculites compressus–B. cuneatus* zones, Pierre Shale, Meade County, South Dakota. Abbreviations: x = tubercle; E = ventral lobe; E/L = first lateral saddle between ventral and lateral lobes; L = lateral lobe.

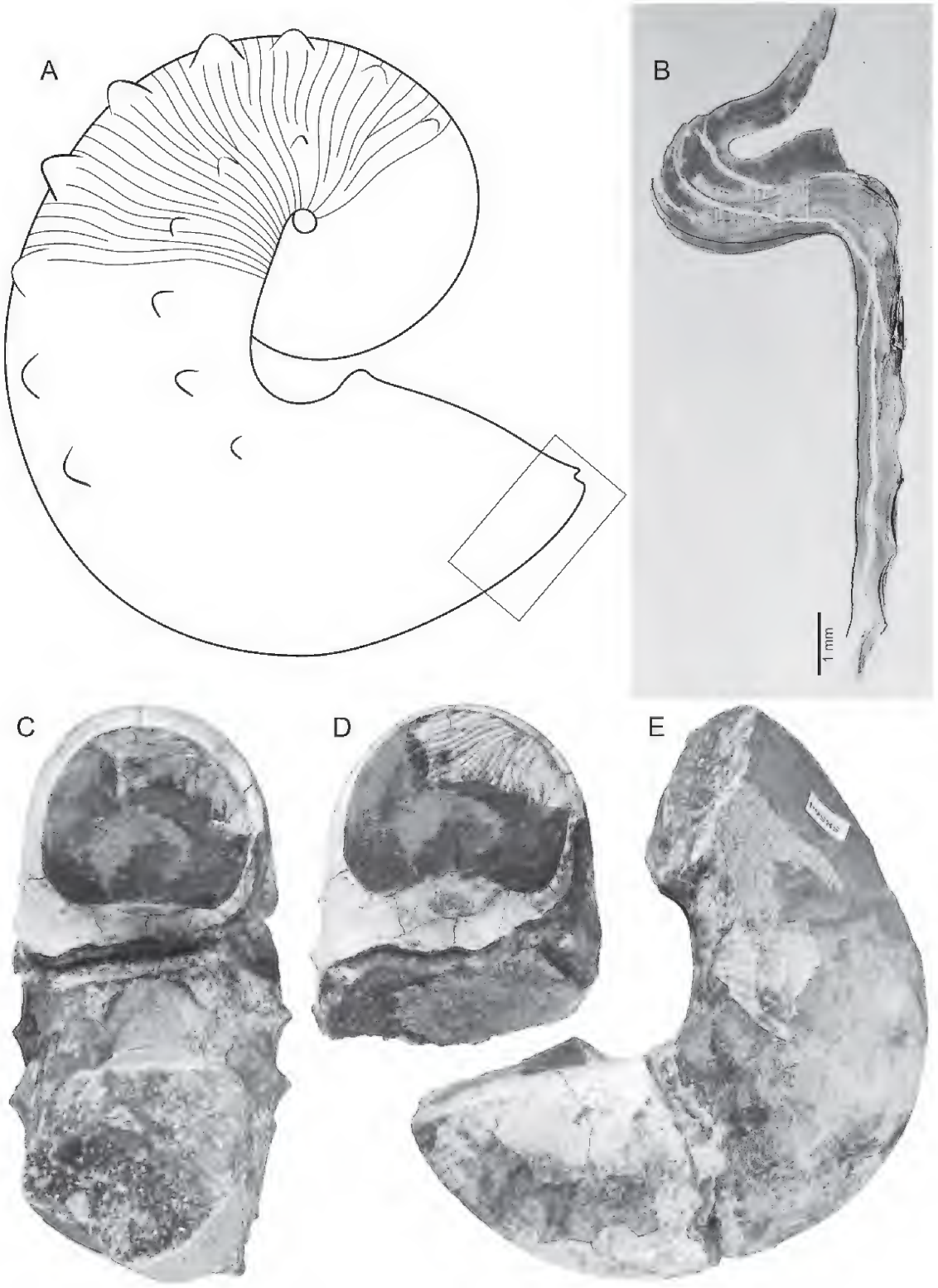
A
B
1 mm
C
D
E

contains an unusually small macroconch. If this specimen is excluded, the extent of size overlap decreases to 22%.

It is perhaps of greater biological interest to determine the size difference between dimorphs within the same species that lived in the same area at the same time and would have potentially mated with each other. The best approximation of these conditions is obtained in a concretion in which both dimorphs are preserved together. As a reminder, however, the cooccurrence of dimorphs in the same concretion does not guarantee that they lived together, only that they were preserved together. A concretion from Pennington County, South Dakota, contains both dimorphs of *Hoploscaphites brevis* preserved side by side (YPM 35581 and 35582). The macroconch is 15% larger than the microconch. Concretion S from AMNH loc. 3274 from Meade County, South Dakota, also contains both dimorphs of *H. brevis* (figs. 26, 27). The average size of two macroconchs is 23% larger than that of two microconchs. We therefore conclude that, on average, the macroconch is 20% larger than the conspecific microconch ("the 20% size rule").

Closer spacing or approximation of the last few septa is common in both dimorphs (fig. 28). We examined the pattern of septal approximation in 13 specimens each of *Hoploscaphites nodosus* and *H. brevis* (4 macroconchs and 9 microconchs in *H. nodosus*, and five macroconchs and eight microconchs in *H. brevis*) (table 1). In *H. nodosus*, the pattern of septal approximation is the same in both dimorphs. Septal approximation either does not occur or occurs over only one or two chambers. The magnitude of approximation is more or less the same in both dimorphs and ranges broadly from 23% to 73%. In contrast, septal approximation occurs in nearly all specimens of *H. brevis* and the pattern of septal approximation differs between dimorphs. In macroconchs, septal approximation occurs over two or three chambers and the magnitude of approximation is strong, ranging from 33% to 38%. In microconchs, approximation usually occurs over only one or two chambers and the magnitude of approximation is weak, ranging from 57% to 86%.

Landman and Waage (1993) observed the pattern of septal approximation in species of *Hoploscaphites* from the Fox Hills Formation, including *H. nicolletii* (Morton, 1842) and *H. spedeni* (Landman and Waage, 1993). They discovered that in *H. nicolletii*, septal approximation tends to occur over more chambers in macroconchs than in microconchs. In macroconchs, septal approximation generally occurs over the last two chambers, whereas in microconchs, it occurs over only the last chamber. In contrast, there is no difference in the pattern of septal approximation between dimorphs in *H. spedeni*. Like *H. nodosus*, *H. spedeni* is a robust species with an inflated whorl section. It is possible that septal approximation is more strongly manifested in specimens with compressed whorl sections, like *H. brevis* and *H. nicolletii*. In such specimens, changes in cameral volume more directly translate into differences in interseptal distance.

Dimorphs also differ in the ratio of the volume of the phragmocone to the volume of the body chamber at maturity. Neige (1996) investigated this relationship in dimorphs of *Hoploscaphites nicolletii*. He dissected adult

←

Fig. 22. Morphology of the apertural margin. **A, B.** Cross section of the shell wall at the apertural margin of a mature macroconch of *Hoploscaphites plenus* (Meek, 1876), BHI 4807, Bearpaw Shale, Garfield County, Montana. **A.** Sketch showing the location of the cross section (rectangle). **B.** Close up of the apertural margin. The exterior direction is toward the right (note the outline of the ribs) and the adoral direction is toward the top. As the shell approaches the apertural margin, it bends sharply inward, at nearly a right angle, forming a thick varix, and then reflects outward, terminating in a flared lip. Sediments commonly accumulate in the narrow gap behind the flared lip. **C–E.** *Hoploscaphites nodosus* (Owen, 1852), large macroconch, AMNH 58564, AMNH loc. 3274, Pierre Shale, Meade County, South Dakota. **C.** Apertural view showing the kidney-shaped aperture filled with dark matrix. **D.** Apertural view, slightly rotated, showing the broadly rounded projection on the dorsal side. **E.** Left lateral view.

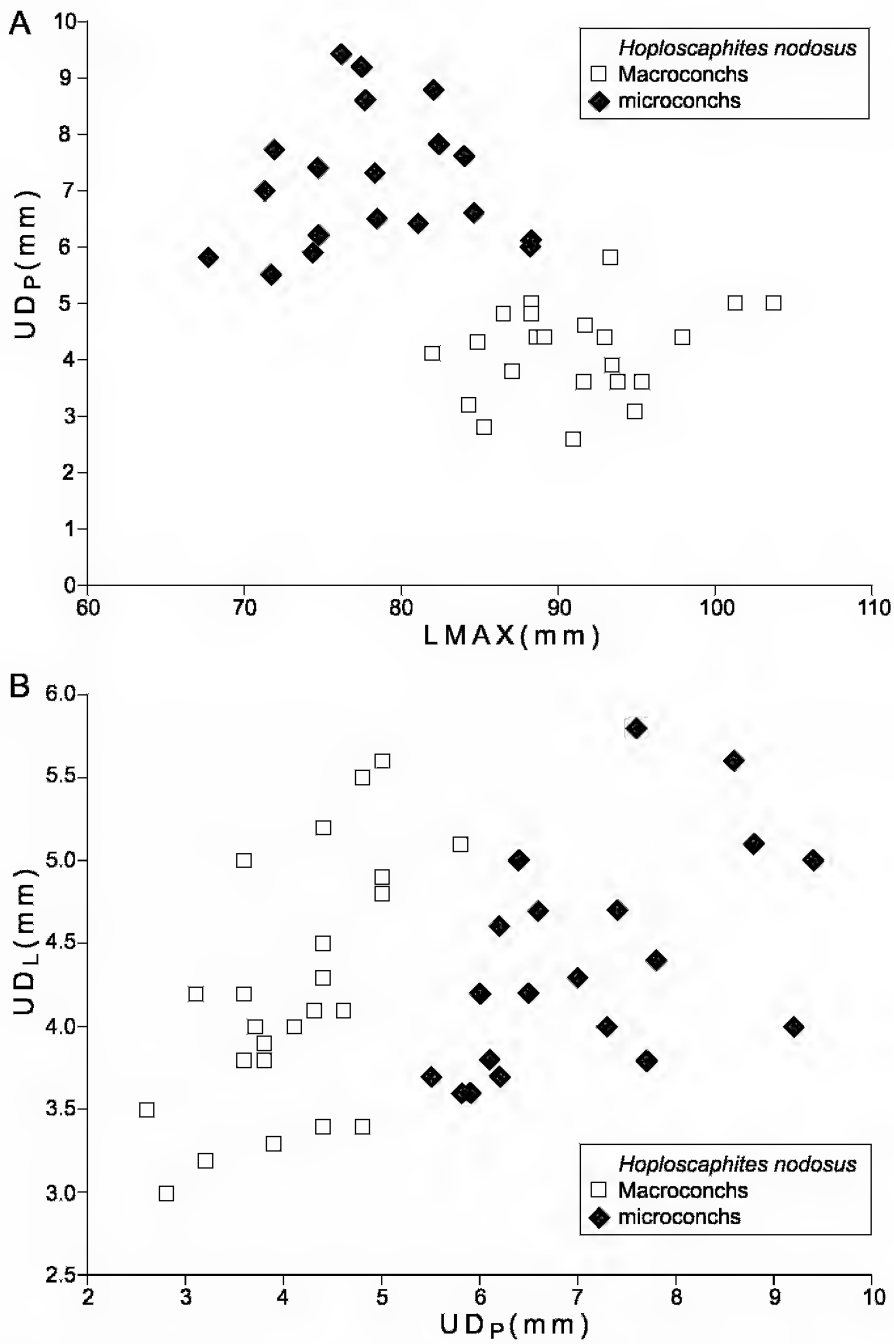

Fig. 23. **A.** Plot of LMAX (mm) versus UD_P (mm) in *Hoploscaphites nodosus* (Owen, 1852) reveals a cluster of microconchs on the upper left and a cluster of macroconchs on the lower right. **B.** Plot of UD_P (mm) versus UD_L (mm) in *Hoploscaphites nodosus* (Owen, 1852) distinguishes the two dimorphs mainly on the basis of UD_P.

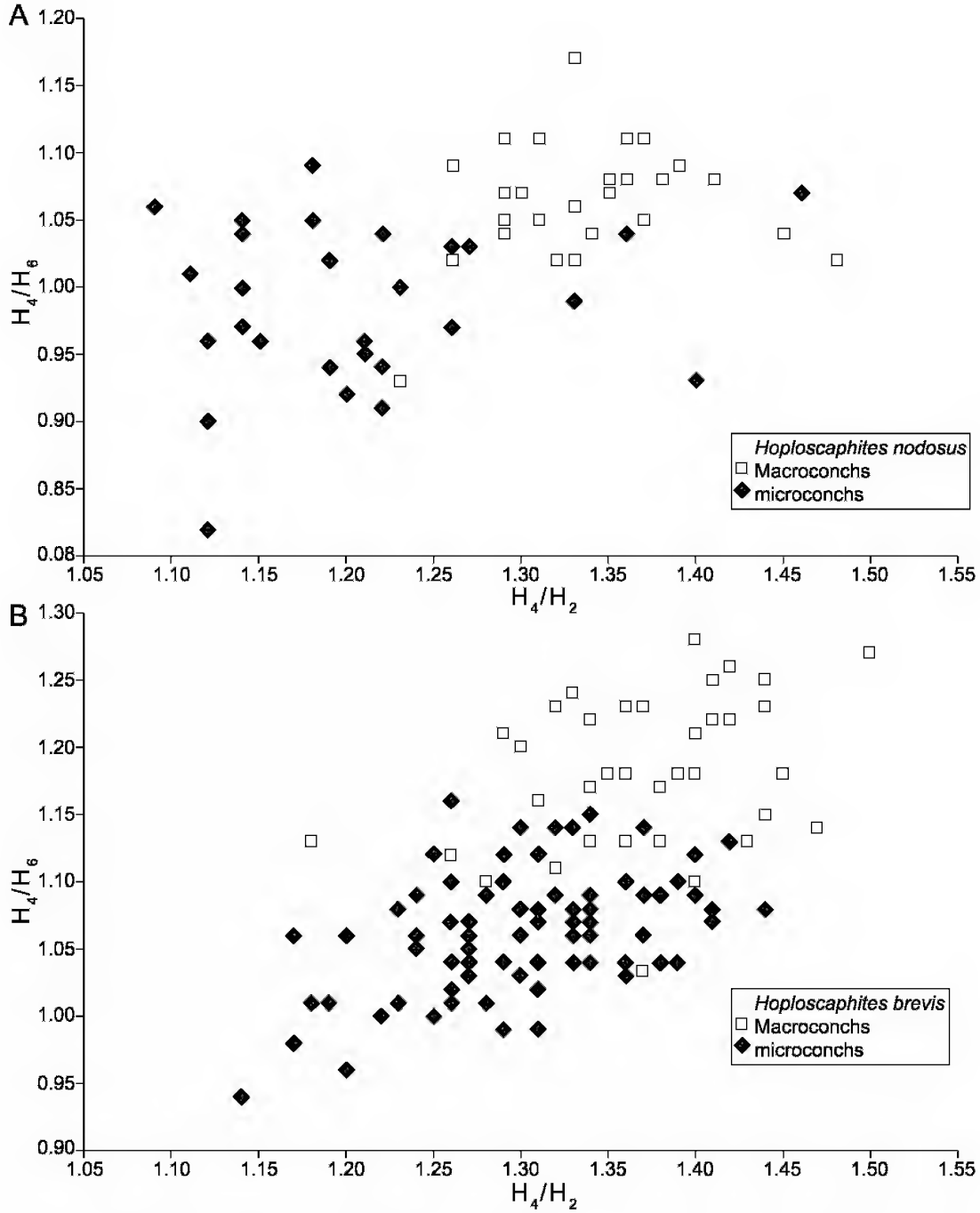

Fig. 24. **A.** Plot of H_4/H_2 versus H_4/H_6 in *Hoploscaphites nodosus* (Owen, 1852). **B.** Plot of H_4/H_2 versus H_4/H_6 in *H. brevis* (Meek, 1876). In each species, the two dimorphs appear as distinct clusters with some overlap between them.

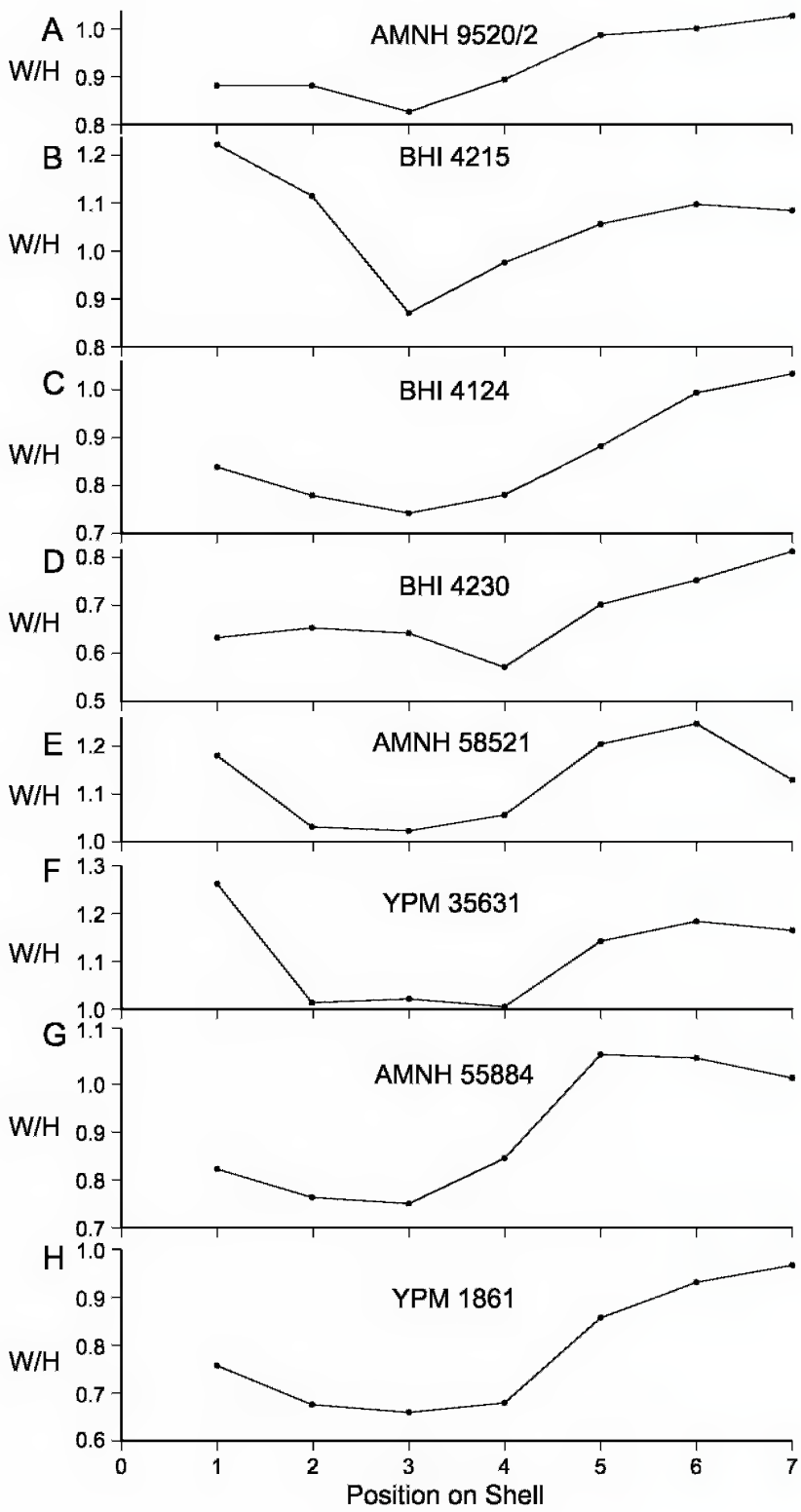
A
AMNH 9520/2
B
BHI 4215
C
BHI 4124
D
BHI 4230
E
AMNH 58521
F
YPM 35631
G
AMNH 55884
H
YPM 1861
W/H
Position on Shell

shells to expose earlier stages in order to calculate this ratio through ontogeny. He assumed a body chamber angle of 230°, based on the average value in 37 juveniles of the closely related species *H. comprimus* as documented by Landman and Waage (1993: fig. 25). At each stage, he measured the volume of the phragmocone and the volume of the body chamber and calculated the ratio between them. In juveniles of both dimorphs, the ratio is constant throughout ontogeny (0.21). However, at maturity, the two dimorphs diverge. In microconchs, the ratio remains the same whereas in macroconchs it increases (0.39). Neige assumed that both dimorphs maintained neutral buoyancy throughout their lifetime and, therefore, the higher ratio in macroconchs did not indicate an increase in buoyancy at maturity. He argued instead that the higher ratio in macroconchs may have served to compensate for (1) the retention of liquid in some of the last few chambers of the phragmocone, (2) an increase in the density of tissues at maturity, for example, related to the formation of the enigmatic "hooks" in macroconchs as described by Landman and Waage (1993: figs. 43–46), or (3) an increase in the volume of tissues at maturity, which protruded outside the aperture.

JAWS

Scaphite jaws occur in the *Baculites compressus–B. cuneatus* zones, but generally are not as well preserved as those in the *B. baculus* Zone in the Pierre Shale near Glendive, Montana (Grier and Grier, personal commun., 2003), nor in the *Hoploscaphites nicolletii* and *H. nebrascensis* zones in the Fox Hills Formation in north-central South Dakota (Landman and Waage, 1993). These differences may reflect differences in the rate of burial of the ammonites after death. In all of these deposits, the lower jaw is more common than the upper jaw, probably due to the larger size and bulkier shape of the lower jaw.

The morphology of the scaphite jaws in the *Baculites compressus–B. cuneatus* zones is similar to that of scaphite jaws described elsewhere by Landman and Waage (1993) and Kennedy et al. (2002, and references therein). The terminology of the jaws is reviewed by Landman et al. (2006, 2007b). The upper jaw is U-shaped and consists of two narrow wings that converge anteriorly to a beaklike apex (fig. 29E). The lower jaw is convex on the ventral side and consists of two mirror-image triangular wings that meet along the plane of bilateral symmetry, called the commissure (also symphysis or central groove). The commissure is bordered on each side by a flange, which increases in height in a posterior direction, reaching its maximum height just before the posterior margin (fig. 29F). The apex of the lower jaw is weakly projected forward, and the anterior margin is slightly concave on either side. The lateral margins are broadly rounded, and the posterior margin is bilobate, with a slight indentation at the commissure (fig. 29H).

Each wing of the lower jaw is composed of two layers. The inner layer consists of coarsely crystalline black material, which presumably represents diagenetically altered chitin (Gupta

←

Fig. 25. Plot of the ratio of whorl width to height (W/H) at seven points on the adult shell of *Hoploscaphites nodosus* (Owen, 1852) and *H. brevis* (Meek, 1876) from ¼ whorl adapical of the long axis (1) to the aperture (7), as shown in figure 14. The shell attains the maximum degree of compression near midshaft (points 3 and 4). **A–D.** Macroconchs. **A.** *H. nodosus*, AMNH 9520/2, Pierre Shale, Pennington County, South Dakota. **B.** *H. nodosus*, BHI 4215, *Baculites cuneatus* Zone, Pierre Shale, Meade County, South Dakota. **C.** *H. brevis*, BHI 4124, *Baculites compressus–B. cuneatus* zones, Pierre Shale, Meade County, South Dakota. **D.** *H. brevis*, BHI 4230, *Baculites compressus* Zone, Pierre Shale, Meade County, South Dakota. **E–H.** Microconchs. **E.** *H. nodosus*, AMNH 58521, *Baculites compressus* Zone, Pierre Shale, Meade County, South Dakota. **F.** *H. nodosus*, YPM 35631, YPM loc. A1461, Bearpaw Shale, Rosebud County, Montana. **G.** *H. brevis*, AMNH 55884, AMNH loc. 3415, *Baculites compressus* Zone, Pierre Shale, Meade County, South Dakota. **H.** *H. brevis*, YPM 1861,YPM loc. A6520, Pierre Shale, Sage Creek, Pennington County, South Dakota.

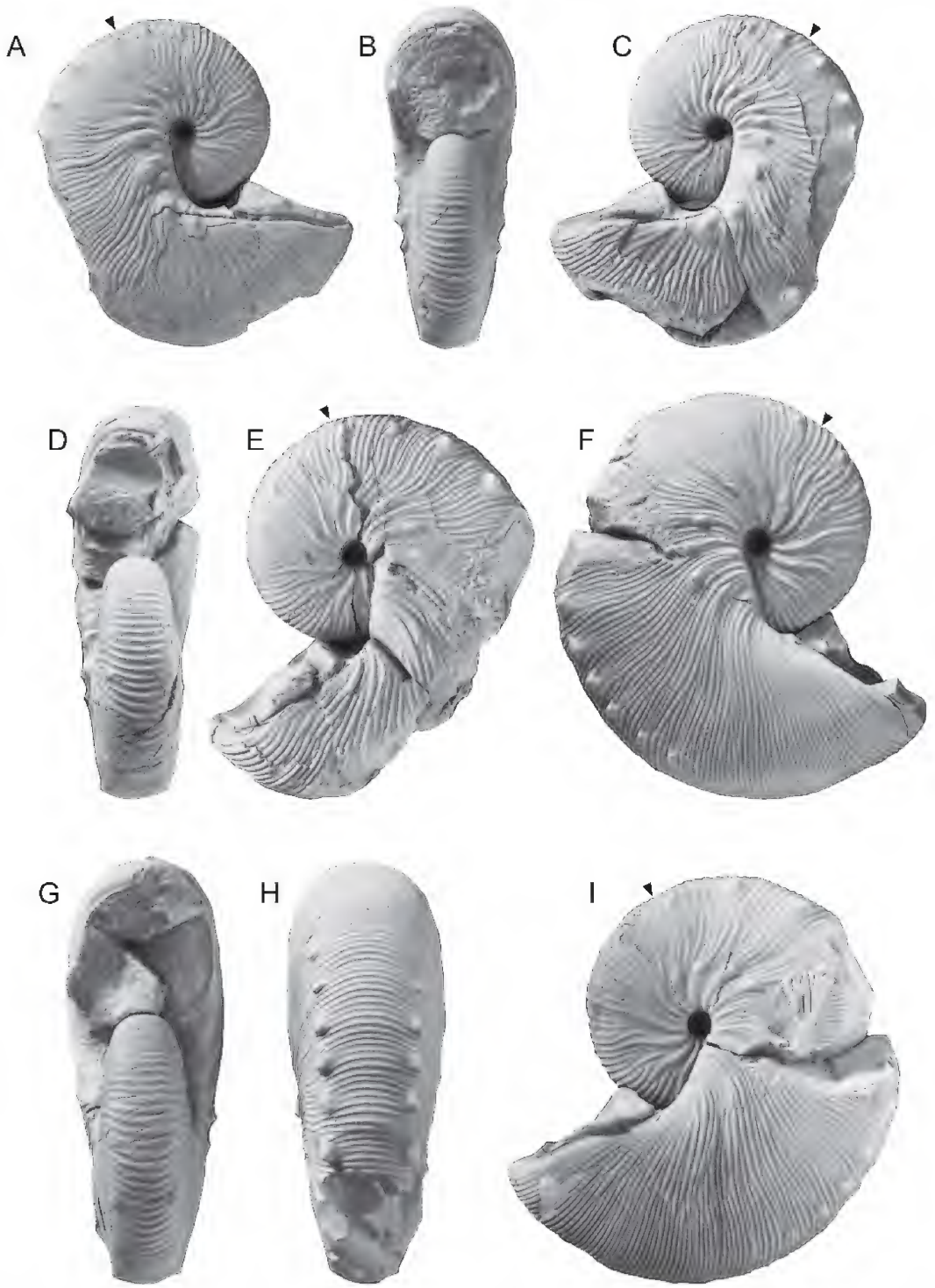

Fig. 26. *Hoploscaphites brevis* (Meek, 1876) from a single concretion (Concretion S), AMNH loc. 3274, Pierre Shale, *Baculites compressus–B. cuneatus* zones, Meade County, South Dakota. **A–C.** Small microconch, AMNH 58518. **A.** Right lateral; **B.** apertural; **C.** left lateral. **D, E.** Small macroconch, AMNH 58517. **D.** Apertural; **E.** left lateral. **F–I.** Small macroconch, AMNH 58515. **F.** Right lateral; **G.** apertural; **H.** ventral; **I.** left lateral. Specimens are illustrated natural size.

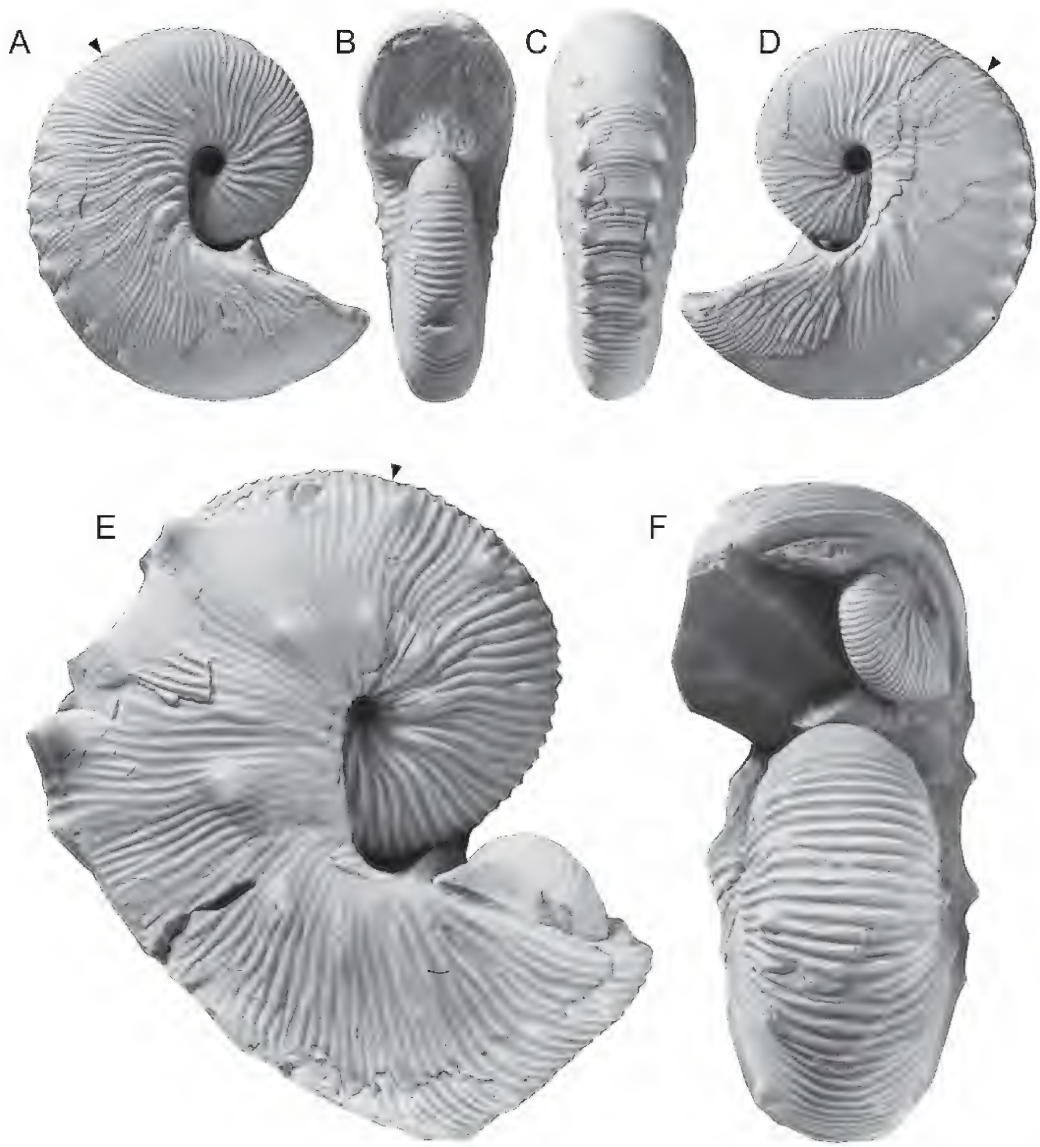

Fig. 27. *Hoploscaphites brevis* (Meek, 1876) from a single concretion (Concretion S), AMNH loc. 3274, Pierre Shale, *Baculites compressus–B. cuneatus* zones, Meade County, South Dakota (continuation of fig. 26), containing a mixture of macroconchs and microconchs. **A–D.** Small microconch, AMNH 58514. **A.** Right lateral; **B.** apertural; **C.** ventral; **D.** left lateral. **E–F.** Large, coarsely ornamented macroconch, AMNH 58516. Note the small scaphite in the aperture. **E.** Right lateral; **F.** apertural. Specimens are illustrated natural size.

et al., 2008). The ventral surface of this layer is ornamented with radial striations, and lirae and growth lines that parallel the posterior margin (fig. 29F, G). The lirae and growth lines slant diagonally forward on the flange. The outer layer consists of calcite and represents the aptychus. This layer is 110 μm thick in AMNH 56883 (fig 29H) and 140 μm thick in AMNH 58563. The ventral surface of the aptychus is not exposed on any of our specimens, but the dorsal surface reflects the ornamentation on the ventral surface of the black layer (fig. 29H). Based on investigations of the lower jaw in other scaphites, the

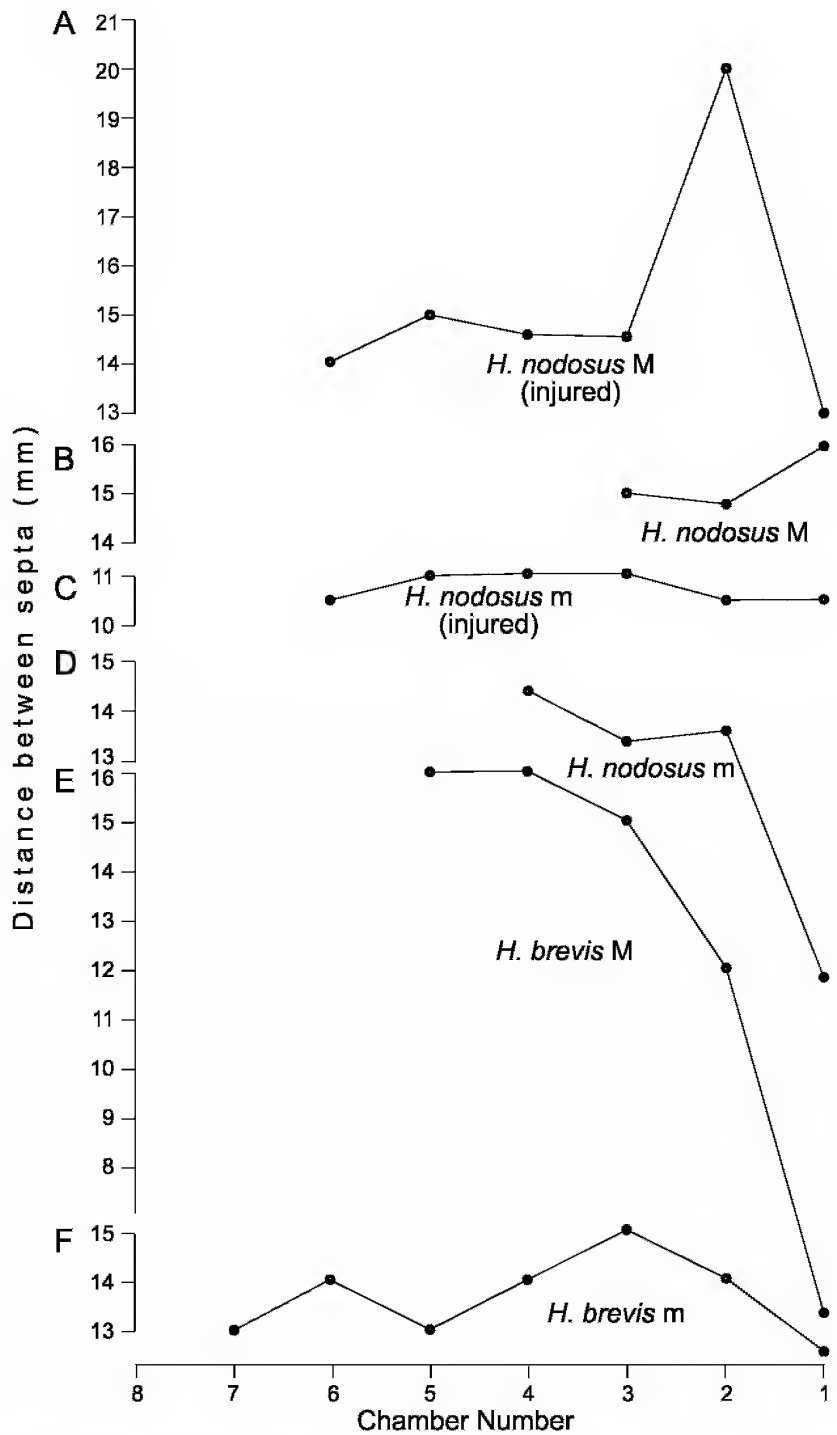

Fig. 28. Septal approximation at maturity in *Hoploscaphites nodosus* (Owen, 1852) and *H. brevis* (Meek, 1876). **A, B.** *H. nodosus*, macroconchs. **A.** YPM 35598, YPM loc. C3347, Pierre Shale, Belle Fourche River, South Dakota. Septal approximation occurs over one chamber and is relatively weak (the interseptal distance of the last chamber is 65% that of the last "normal" chamber). This specimen also exhibits a marked pathology due to an injury, which probably explains the large variation in septal

TABLE 1
Septal approximation at maturity in *Hoploscaphites nodosus* (Owen, 1852) and *Hoploscaphites brevis* (Meek, 1876)

Species	Number	M/m	Number of chambers	Approximation	Magnitude	Comments
H. nodosus	AMNH 58511	M	3	1	53	—
H. nodosus	BHI 4215	M	3	0	—	Last septum adapical of line of LMAX
H. nodosus	BHI 4948	M	7	2	36	—
H. nodosus	YPM 35598	M	6	1	65	Severe injury
H. nodosus	BHI 4122	m	6	0	—	Slight injury
H. nodosus	BHI 4222	m	7	2	48	—
H. nodosus	BHI 4278	m	6	2	73	—
H. nodosus	BHI 4895	m	4	1	63	—
H. nodosus	BHI 4949	m	6	1	67	—
H. nodosus	USNM 536232	m	6	2	48	—
H. nodosus	USNM 536245	m	6	1	23	—
H. nodosus	USNM 538103	m	6	2	54	—
H. nodosus	YPM 1868	m	5	0	—	—
H. brevis	BHI 4164	M	4	3	38	—
H. brevis	BHI 4202	M	5	2	33	—
H. brevis	BHI 4203	M	4	2	34	—
H. brevis	BHI 4205	M	5	2	—	Break at last septum
H. brevis	BHI 7034	M	4	3	38	—
H. brevis	BHI 4210	m	4	1	64	—
H. brevis	BHI 4211a	m	4	1	75	—
H. brevis	BHI 4223	m	5	1	35	—
H. brevis	BHI 4314	m	3	0	—	—
H. brevis	BHI 4725	m	5	2	57	—
H. brevis	BHI 5789b	m	5	1	86	—
H. brevis	FMNH PE8917	m	6	2	58	—
H. brevis	USNM 536262	m	7	1	83	—

M = macroconch; m = microconch; number of chambers = number of chambers over which septal spacing was measured; approximation = number of chambers over which septal approximation occurs; magnitude = ratio of the interseptal distance of the last chamber relative to that of the last "normal" chamber, expressed as a percentage. The interseptal distance between the last two septa in BHI 4205 cannot be measured, but the trend of septal approximation shown between septa 2 and 3 is assumed to have continued.

←

spacing. **B.** BHI 4215, *Baculites cuneatus* Zone, Pierre Shale, Meade County, South Dakota. No septal approximation is apparent, but the base of the body chamber is adapical of the line of maximum length. **C, D.** *H. nodosus*, microconchs. **C.** BHI 4122, *Baculites compressus–B. cuneatus* zones, Pierre Shale, Meade County, South Dakota. No septal approximation is apparent. Note that the values of the interseptal distances in successive chambers are within ± 1 mm of each other. This specimen also exhibits an injury. **D.** BHI 4895, *Baculites compressus–B. cuneatus* zones, Pierre Shale, Meade County, South Dakota. Septal approximation occurs over one chamber and is weak (the interseptal distance of the last chamber is 63% that of the last "normal" chamber). **E.** *H. brevis*, macroconch, BHI 4202, *Baculites compressus* Zone, Pierre Shale, Meade County, South Dakota. Septal approximation occurs over two chambers and is strong (the interseptal distance of the last chamber is 33% that of the last "normal" chamber). **F.** *H. brevis*, macroconch, USNM 536262, Pierre Shale, Pennington County, South Dakota. Septal approximation occurs over one chamber and is weak (the interseptal distance of the last chamber is 83% that of the last "normal" chamber). Measurements are listed in table 1.

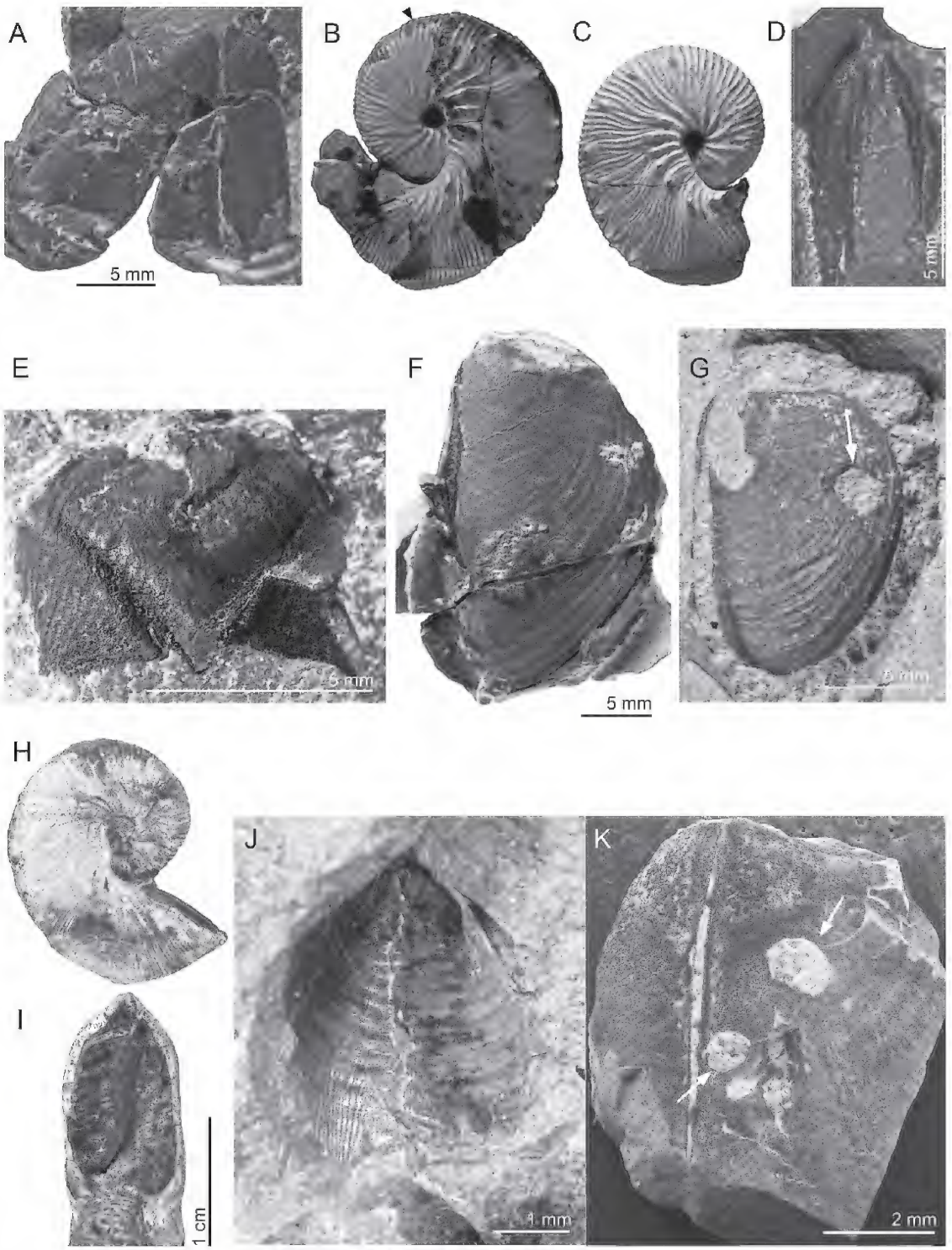

Fig. 29. Jaws of *Hoploscaphites*. **A, B.** Lower jaw near the aperture of *Hoploscaphites brevis* (Meek, 1876), small microconch, BHI 4264, *Baculites compressus* Zone, Pierre Shale, Meade County, South Dakota. **A.** Ventral view of the lower jaw, splayed out in the aperture, anterior direction of the jaw toward

microstructure of the aptychus consists of thin lamellae that parallel the dorsal surface (Kruta et al., 2009).

The chitinous layer of the lower jaw is much more commonly preserved than the calcitic layer. Landman and Waage (1993) noted this same phenomenon in scaphite jaws from the Fox Hills Formation and stated that "The calcitic layer is usually absent on even slightly weathered surfaces, and in freshly exposed specimens it may be partly or entirely absent as a result of removal prior to formation of the enclosing concretion." Similarly, Landman et al. (2006) noted that the calcitic layer is invariably absent on the lower jaws of *Placenticeras* from North America. However, because such a layer is present on the lower jaws of the closely allied genus *Metaplacenticeras* from Hokkaido, Japan, these authors hypothesized that the calcitic layer in *Placenticeras* was diagenetically lost. The rarity of calcitic aptychi in concretions that otherwise contain aragonitic fossils suggests that the calcitic plates were susceptible to mechanical breakage and chemical dissolution during fossilization.

The jaws in the *Baculites compressus–B. cuneatus* zones usually occur as isolated elements in association with whole or broken scaphites. Landman and Klofak (2006) recorded dozens of jaw fragments in association with broken scaphites and other molluscs in a concretion from the Pierre Shale of Meade County, South Dakota. These jaws show evidence of compaction, warping, folding, tearing, puncturing, and exfoliation (fig. 28 I), indicating that they must have remained on the sea floor for an extended period of time, perhaps months to years. In taphonomic experiments with modern coleoids, which were designed to simulate the conditions following death and before burial, Kear et al. (1995) reported that the jaws of these animals were still more or less intact after a year (= the duration of the experiments), although the posterior edges of the jaws had begun to fracture and disintegrate after 10 weeks. The fragmentary nature of the ammonite jaws may also indicate that they were redepoited as faecal matter, having first been consumed and digested by a predator.

Although isolated jaw fragments are abundant, occurrences of jaws inside or closely associated with the body chambers are relatively rare. We have observed only a few specimens, all of which are microconchs of *Hoploscaphites brevis*, in which the jaws occur just inside or just outside the aperture. In AMNH 56874, the lower jaw is folded together folio style, and is oriented diagonally across the broken aperture (fig. 29C, D). The two wings are separated at the commissure, and it appears that the upper jaw is nestled within the gape of the lower jaw. In

←

the top; **B.** left lateral view. **C, D.** Lower jaw near the aperture of *Hoploscaphites brevis* (Meek, 1876), small microconch, AMNH 56874, AMNH loc. 3415, *Baculites compressus* Zone, Pierre Shale, Meade County, South Dakota. **C.** Right lateral; **D.** lower jaw folded together, folio style, showing a gap at the commissure, anterior direction of the jaw toward the top. **E.** Isolated upper jaw attributed to *Hoploscaphites*, anterior view, AMNH 56805, Kathy's concretion, AMNH loc. 3274, *Baculites compressus–B. cuneatus* zones, Pierre Shale, Meade County, South Dakota. **F.** Left lateral view of a lower jaw associated with *Hoploscaphites brevis* (Meek, 1876), anterior direction of the jaw toward the top, BHI 5795, *Baculites compressus–B. cuneatus* zones, Pierre Shale, Meade County, South Dakota. **G.** Left lateral view of an isolated lower jaw attributed to *Hoploscaphites*, with postmortem damage including a puncture (arrow), anterior direction of the jaw toward the top, AMNH 56866, AMNH loc. 3408, *Baculites compressus* Zone, Pierre Shale, Meade County, South Dakota. **H, I.** *Hoploscaphites brevis* (Meek, 1876), small microconch, GSC 5342c, "?Demaine Member, South Saskatchewan River opposite mouth Swift Current Creek, Sask." (= paratype, *Hoploscaphites landesi* Riccardi, 1983, pl. 1, figs. 20–22). **H.** Right lateral; **I.** close up of the left side of the lower jaw in the aperture, anterior direction of the jaw toward the bottom. **J.** Dorsal (inner) surface of the aptychus of an isolated lower jaw attributed to *Hoploscaphites*, anterior direction of the jaw toward the top, AMNH 56883, AMNH loc. 3274, *Baculites compressus–B. cuneatus* zones, Pierre Shale, Meade County, South Dakota. **K.** Isolated lower jaw attributed to *Hoploscaphites*, anterior direction of the jaw toward the top, with postmortem damage including punctures (arrows), AMNH 56846, Kathy's concretion, AMNH loc. 3274, *Baculites compressus–B. cuneatus* zones, Pierre Shale, Meade County, South Dakota.

BHI 4264, the lower jaw is splayed out butterfly style, exposing the ventral surface and the commisure (fig. 29A, B). The edge of the left wing is folded inward and the edge of the right wing is torn. The jaw is oriented perpendicularly to the broken aperture. In GSC 5342c, the left wing of the lower jaw, including the flange, is almost perfectly preserved, except for minor abrasion along the lateral margin (fig. 29H, I). The jaw covers more than half of the aperture, with the apex of the jaw touching the dorsal projection of the shell.

The function of the calcitic layer in the lower jaw is unknown. It may have served as reinforcement to strengthen the jaw for crushing or biting, but the layer is relatively thin (100–150 μm thick). In addition, the presence of a groove, rather than a thickening, along the middle of the lower jaw would have compromised any structural benefit from a mineralized layer (Landman et al., 2007b). Alternatively, the calcitic layer may have served as an operculum for protection against predators. However, it is unclear how the lower jaw would have rotated into a position to fulfill this function (for a review of the various arguments, see Lehmann and Kulicki, 1990; Lewy, 2000; Engeser and Keupp, 2002; Landman et al., 2007b; and Kruta and Landman, 2008).

VARIATION WITHIN AND BETWEEN SPECIES

The scaphites from the *Baculites compressus–B. cuneatus* zones show a wide range of variation from compressed, finely ribbed forms to robust, coarsely ribbed forms. Meek and Hayden (1856e: 281, footnote) noted this high degree of variability from the outset and commented:

> We find it exceedingly difficult to define limits between species amongst these Nebraska *Scaphites*. The position and relative size of nodes and costae, as well as the more or less compressed form of the shell and relative size of the umbilicus, are not, within a considerable range of limits, characters that can always be relied upon. One of our specimens of *S. nodosus* (Owen), for example, has near the dorsolateral [= ventrolateral] margin of one side, the usual row of nodes, and none at all on the other.

The question of how to partition variation among these scaphites or, in other words, how much variation to admit within a single species, is difficult to answer. Such taxonomic decisions are obviously influenced by previous studies of scaphites, in particular, those of Owen (1852), Meek (1876), and Riccardi (1983). However, these studies were handicapped in two important ways: (1) sexual dimorphism was unknown in the 19th century, and (2) the number of specimens available to these authors was limited, providing only a narrow picture of the total range of variation within a species.

Currently, in taxonomic studies, a single ammonite species encompasses a broad range of variation (Kennedy and Cobban, 1976). This approach, called horizontal classification (Dzik, 1985), requires information about the stratigraphic distribution of the specimens. If they occur at the same stratigraphic horizon and geographic locality, and show an intergradation in morphology, however broad, they are interpreted as representing a single species. Alternatively, if they occur at different stratigraphic horizons and geographic localities, and show gaps in morphology, they are interpreted as representing two or more species.

This approach has been used in a number of recent studies on ammonites. For example, Haas (1946) subdivided a sample of collignoniceratids from the Upper Cretaceous of the U.S. Western Interior into seven forms or varieties, based on differences in the suture and ornamentation. Cobban and Hook (1979), using additional specimens with more detailed stratigraphic data, argued that these differences simply reflected variation within a single species. In fact, Jorgensen and Larson (in prep.) noted that most of these varieties occur together in a single concretion. Kennedy et al. (2001: 29) reemphasized this point, adding:

> The present authors have observed considerable intraspecific variation in all of the larger collections of Collignoniceratinae studied. Most species seem to consist of two major forms, a gracile one that has whorls higher than wide, and a more robust form that has broader whorls, a wider umbilicus and stronger ornamentation. These may be sexual dimorphs, but we generally lack sufficient complete adult

individuals to determine if robust and gracile variants differ in adult size.

Reeside and Cobban (1960) adopted the same approach in their study of Albian gastroplitids from the Mowry Shale of Wyoming. In large collections from the same stratigraphic horizon and, even from the same concretion, they observed a wide variety of morphologic types, ranging from compressed costate to stout nodose to subglobose spinose. These morphologic types were connected by a nearly complete gradation and were, therefore, included in the same species. Reeside and Cobban (1960: 52) hesitated about this decision and commented: "Undoubtedly the writers, influenced by the more or less traditional interpretation of systematic relations among the ammonites, would at one time have put the specimens with the seemingly large range of morphologic character shown in each of the assemblages into several genera, and would have proposed numerous species in each, in spite of the seemingly obvious continuity of variation in each group." However, in the end, Reeside and Cobban opted for a more biological interpretation.

Other studies have also recognized the importance of intraspecific variation in ammonites. The practical consequence is a simplification of nomenclature and a reduction in the number of taxa. Examples of this approach include, in the Triassic, Bucher (1992) and Monnet and Bucher (2005) on Anisian ceratitids from Nevada, and Dagys and Weitschat (1993) on Anisian ceratitids from Siberia; in the Jurassic, Westermann (1966) on Bajocian sonniniids from Western Europe, and Chandler and Calloman (2009) on Aalenian leioceratids from England; and in the Cretaceous, Ploch (2003) on Valanginian perisphinctids from Poland, Kennedy and Hancock (1970) on Cenomanian acanthoceratids from France, Wiese and Schulze (2005) on Cenomanian engonoceratids from Africa and the Middle East, and Tanabe (1993) on Turonian prionocyclids from Hokkaido. This subject has not been as extensively treated in the Paleozoic, with the notable exception of Korn and Klug (2007) on Frasnian manticoceratids from France and Germany.

A similar approach has been used in recent studies of scaphites. For example, Cobban (1969) reviewed the taxonomy of *Scaphites hippocrepis* (DeKay, 1827) and *S. leei* Reeside, 1927b, from the Campanian of the U.S. Western Interior based on collections from single concretions or from multiple concretions at approximately the same stratigraphic horizon. Analysis of these samples revealed the presence of two morphs, which Cobban interpreted as sexual dimorphs but which would have previously been assigned to separate species. Cooper (1990) explicitly took intraspecific variation into account in his study of *Scaphites hugardianus* d'Orbigny, 1840, from the Albian of England and, as a result, synonymized several species and varieties. Kennedy (1986b) redescribed *Hoploscaphites constrictus* (J. Sowerby, 1817) from the upper Maastrichtian of the Cotentin Peninsula, France, and, based on large collections, recognized a wide range of variation within this species including compressed, finely ornamented forms and depressed, more coarsely ornamented forms. Kennedy and Summesberger (1987) studied *Acanthoscaphites tridens* (Kner, 1848) from the lower Maastrichtian of the Ukraine, and reinterpreted most of Nowak's named variants as one dimorphic species. Machalski (2005b) described species of *Acanthoscaphites* and *Hoploscaphites* from the upper Maastrichtian of central Europe, and emphasized a population approach relying on large numbers of specimens wherever possible. In explaining his methodology, Machalski (2005b: 659) commented that "a given sample has been assigned to a particular subspecies when it is dominated by individuals possessing the diagnostic features of that subspecies."

These studies all admit a broad range of variation within a single ammonite species. Such variation reflects a correlation between coarseness of ornament and degree of whorl compression, which has been called Buckman's Law of Covariation by Westermann (1966). This correlation has been widely documented (Guex et al., 2003; Yacobucci, 2004; Hammer and Bucher, 2005), and has been interpreted as an outcome of the developmental constraints involved in ammonite growth. It may also reflect variation

in the rate of growth. For example, in their study of muricid gastropods, Urdy et al. (2008) demonstrated that the size of ornamental features, such as spines, is related to pauses in growth. They suggested that similar factors may have played a role in ammonite ontogeny, and may help explain the observed correlation between coarsenss of ornament and degree of whorl compression.

Four scaphite species or varieties have been described from the *Baculites compressus–B. cuneatus* zones of the Pierre Shale and Bearpaw Shale. As originally described, they are *Scaphites nodosus* Owen, 1852, *S. nodosus* var. *brevis* Meek, 1876, *S. nodosus var. quadrangularis* Meek, 1876, and *Hoploscaphites landesi* Riccardi, 1983. The holotype of *S. nodosus* (Owen, 1852: 581, pl. 8, fig. 4), herein referred to as *H. nodosus* (fig. 4), is a stout macroconch 101.5 mm in maximum length, with fairly coarse ornament consisting of ribs and umbilicolateral and ventrolateral tubercles. The holotype of *S. nodosus* var. *brevis* (Meek, 1876: 426, pl. 25, fig. 1a–c), herein referred to as *H. brevis* (fig. 5), is a macroconch 78.4 mm in maximum length, with a more slender shell and finer ornament. The holotype and one of the paratypes of *S. nodosus* var. *quadrangularis* (Meek, 1876: 428, pl. 25, fig. 3a–c = USNM 366; fig. 4 = USNM 365) are microconchs of *H. plenus* (fig. 6A–C, H–K, respectively), and will be further discussed in a future publication. The other paratype of *S. nodosus* var. *quadrangularis* (Meek, 1876, pl. 25, figs. 2a-c = USNM 36690) is a microconch of *H. brevis* (fig. 6D–G). It is 54.1 mm in maximum length with ornament similar to that of the holotype of *H. brevis*. The holotype of *H. landesi* (Riccardi, 1983: 10, pl. 1, figs. 12–22) is a smaller, more compressed microconch of *H. brevis* 49.0 mm in maximum length, with slightly finer ornament (fig. 7E–H).

It is difficult to distinguish among these species on the basis of their early whorls. In his study of the fossils of the Bearpaw Shale, Warren (1934: 94) expressed his frustration at attempting to identify small or incomplete specimens without an adult body chamber:

> These three varieties [*brevis*, *quadrangularis*, and *plenus*] are present in our collections, but the process of differentiating them was not attended with entirely satisfactory results. Complete, well-preserved specimens offer no difficulty in identification, but as the great majority of specimens collected lacked the living chamber, the problem that presented itself was the identification of the different varieties from the initial whorls. The problem was aggravated by the fact that the different varieties varied considerably within themselves. This variation was apparent not only in the shape of the whorl but in the character of the costae and nodes and in the minor features of the suture line. No feature mentioned by Meek in his original differentiation of the varieties is constant throughout, but some features are fairly so.... The shape of the whorl or the character of the costae were found to be unsatisfactory, on the whole, in attempting to identify the different varieties from the initial whorls.

The final body chamber in scaphites uncoils slightly, but remains in the same plane of symmetry, forming a short shaft and recurved hook. As noted above, this modification is interpreted as marking the attainment of maturity, and permits the unequivocal separation of variation due to disparity in developmental stage from phenotypic variation among adults. In addition, because sexual dimorphs in scaphites can be more or less easily distinguished, it is also possible to separate out variation due to sex. The best estimate of the size difference between conspecific dimorphs is obtained by comparing specimens in the same concretion, inasmuch as such accumulations represent relatively short intervals of time (months to years). Our studies indicate that macroconchs are approximately 20% larger than microconchs ("the 20% size rule"), based on an examination of conspecific dimorphs in single concretions from the *Baculites compressus–B. cuneatus* zones,

Thanks to collecting efforts by various institutions over the past 150 years, several hundred specimens from the *Baculites compressus–B. cuneatus* zones are now available for study, allowing us to more fully explore the range and pattern of variation within and among species. The characters examined below are maximum length, degree of uncoiling of the adult body chamber (expressed as the ratio of maximum length of the shell to whorl height of the phragmocone along the axis of maximum length), degree of whorl

compression (expressed as the ratio of whorl width to whorl height and the ratio of ventral width to whorl height), the ontogenetic change in whorl width and height in passing from the point of exposure to the aperture, the apertural angle, the density of ribbing (expressed as the number of ribs/cm on the venter), the size and distribution of umbilicolateral and ventrolateral tubercles, and the complexity of the suture. Our discussion emphasizes macroconchs rather than microconchs because species-specific characters are better expressed in macroconchs, probably due to their larger size (Landman and Waage, 1993; Machalski, 2005b).

We measured the maximum length (LMAX) of all the macroconchs in our sample from the *Baculites compressus–B. cuneatus* zones and constructed several size-frequency histograms (fig. 30D). We labeled specimens as either *Hoploscaphites nodosus* or *H. brevis*, taking into account all available data, and bearing in mind the existence of transitional specimens between species, as well as between dimorphs in *H. brevis* (see above). Each size interval (5 mm) is defined so that LMAX is greater than or equal to *a* but less than *b*. For example, the 50–55 mm size interval represents values of LMAX greater than or equal to 50 mm and less than 55 mm (in effect, less than or equal to 54.9 mm). The measured set of all macroconchs consists of 84 specimens. In *H. nodosus*, LMAX ranges from 70 to 105 mm (fig. 30E). The distribution is unimodal with a peak at 85–95 mm. The holotype of *H. nodosus* falls on the right side of this peak. In *H. brevis*, LMAX ranges from 25 to 105 mm (fig. 30F). The distribution is bimodal with a primary peak at 80–85 mm ("large" macroconchs), and a secondary peak at 60–65 mm ("small" macroconchs). The holotype of *H. brevis* falls just on the left side of the peak at 80–85 mm. The macroconchs that correspond to the paratype of *Scaphites nodosus* var. *quadrangularis* (USNM 36690) and the holotype of *H. landesi* (GSC 5342a), assuming "the 20% size rule," fall just on the left side and within the peak at 60–65 mm, respectively.

We also measured LMAX of all the microconchs in our sample, labeled as either *Hoploscaphites nodosus* or *H. brevis* (fig. 30A). The measured set consists of 117 specimens. In *H. nodosus*, LMAX ranges from 60 to 90 mm (fig. 30B). The distribution is unimodal, with a peak at 70–80 mm. The microconch that corresponds to the holotype of *H. nodosus*, assuming "the 20% size rule," falls to the right side of this peak. In *H. brevis*, LMAX ranges from 25 to 85 mm (fig. 30C). The distribution is bimodal with peaks at 40–45 mm ("small" microconchs) and 65–70 mm ("large" microconchs). The microconch that corresponds to the holotype of *H. brevis*, assuming "the 20% size rule," falls in the peak at 65–70 mm. The paratype of *Scaphites nodosus* var. *quadrangularis* (USNM 36690) and the holotype of *H. landesi* (GSC 5342a), both of which are microconchs, fall on the right side of the peak at 40–45 mm.

As a measure of the morphological variation in our sample, we prepared six graphs, as described below. The specimens are labeled as either *Hoploscaphites nodosus* or *H. brevis*, taking into account all available data (and bearing in mind the existence of transitional specimens between species, as well as between dimorphs in *H. brevis*).

(1) Degree of compression of the adult phragmocone perpendicular to the line of maximum length (W_1/H_1) versus degree of compression of the body chamber at midshaft (V_4/H_4) in macroconchs (fig. 31A). The degree of compression of the phragmocone perpendicular to the line of maximum length is expressed as the ratio of whorl width to whorl height (W_1/H_1), with higher values indicating a more depressed whorl section. The degree of compression of the body chamber at midshaft is expressed as the ratio of ventral width to whorl height (V_4/H_4), with higher values also indicating a more depressed whorl section. Two clusters of specimens are visible in this plot, one on the upper right and one on the lower left. In the cluster on the upper right, the phragmocone and body chamber are more depressed than in the cluster on the lower left. In the cluster on the upper right, W_1/H_1 ranges from approximately 0.9 to 1.3 and V_4/H_4 ranges from approximately 0.6 to 0.9. In the cluster on the lower left, W_1/H_1 ranges from approximately 0.6 to 1.1 and V_4/H_4 ranges from approximately 0.3 to 0.5. Thus, the two clusters show more overlap in W_1/H_1 than in

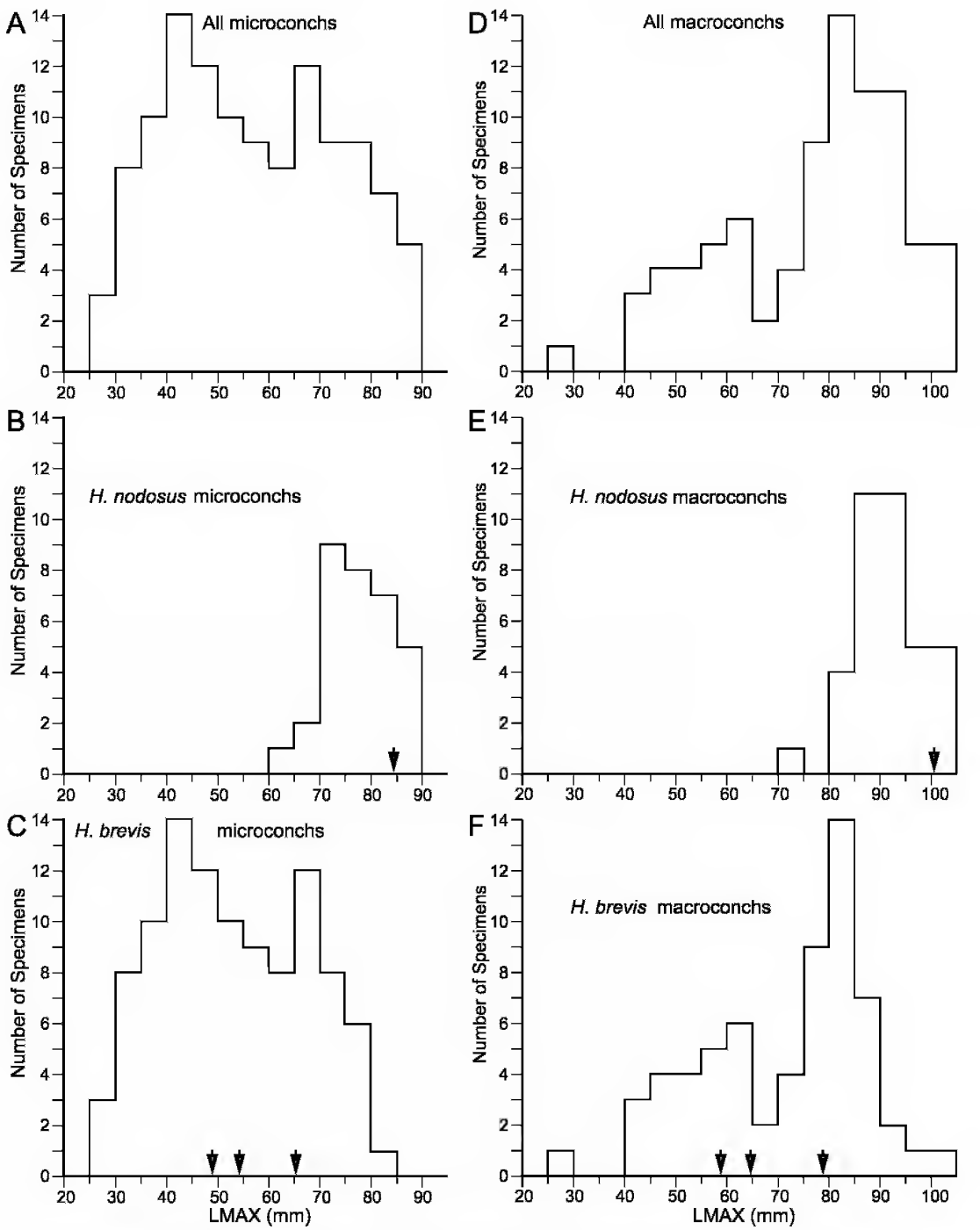

Fig. 30. Size-frequency histograms of *Hoploscaphites nodosus* (Owen, 1852) and *H. brevis* (Meek, 1876), Pierre Shale and Bearpaw Shale, *Baculites compressus–B. cuneatus* zones. **A.** Size-frequency histogram of the microconchs in the combined sample of *H. nodosus* and *H. brevis*. **B.** Size-frequency histogram of *H. nodosus* microconchs. The arrow represents the microconch corresponding to the holotype of *Scaphites nodosus* (0.83 × 101.5 mm = 84.6 mm). **C.** Size-frequency histogram of *H. brevis* microconchs. The three arrows represent, from left to right, the holotype of *Hoploscaphites landesi* Riccardi, 1983

V_4/H_4. The holotype of *H. nodosus* plots in the cluster on the upper right and the holotype of *H. brevis* plots in the cluster on the lower left. This plot suggests that these two groups of specimens are distinct and can be treated as separate taxa.

(2) Curvature of the body chamber in side view ($LMAX/H_4$) versus degree of compression of the body chamber at midshaft (V_4/H_4) in macroconchs (fig. 31B). The curvature of the body chamber in side view is expressed as the ratio $LMAX/H_4$, with higher values indicating less curvature, that is, a more elongate rather than circular shape. The degree of compression at midshaft is expressed as the ratioV_4/H_4, with higher values indicating a more depressed whorl section. Two clusters of specimens are visible in this plot, one on the upper right and one on the lower left. In the cluster on the upper right, the body chamber is less curved in side view, and the whorl section of the body chamber is more depressed, than in the cluster on the lower left. In the cluster on the upper right, $LMAX/H_4$ ranges from approximately 2.2 to 2.5 and V_4/H_4 ranges from approximately 0.6 to 0.9. In the cluster on the lower left, $LMAX/H_4$ ranges from approximately 2.0 to 2.3 and V_4/H_4 ranges from approximately 0.3 to 0.5. Thus, the two clusters show more overlap in $LMAX/H_4$ than in V_4/H_4. The holotype of *H. nodosus* plots in the cluster on the upper right and the holotype of *H. brevis* plots in the cluster on the lower left. As in the previous plot, this graph suggests that the two groups of specimens are distinct and can be treated as separate taxa.

(3) Curvature of the body chamber in side view ($LMAX/H_4$) versus degree of uncoiling of the body chamber ($LMAX/H_2$) in macroconchs (fig. 32A). The curvature of the body chamber in side view is expressed as the ratio $LMAX/H_4$. The degree of uncoiling of the body chamber is expressed as the ratio $LMAX/H_2$, with higher values indicating a greater degree of uncoiling. The specimens form two intergradational clusters, one on the upper right and one on the lower left. In the cluster on the upper right, the body chamber is more elongate and more loosely uncoiled than in the cluster on the lower left. In the cluster on the upper right, $LMAX/H_4$ ranges from approximately 2.2 to 2.5 and $LMAX/H_2$ ranges from approximately 2.8 to 3.2. In the cluster on the lower left, $LMAX/H_4$ ranges from approximately 2.0 to 2.3 and $LMAX/H_2$ ranges from approximately 2.7 to 3.1. The holotype of *H. nodosus* plots on the upper right and the holotype of *H. brevis* plots on the lower left. On the basis of this plot, the two taxa intergrade, so that distinguishing between them is difficult.

(4) Curvature of the body chamber in side view ($LMAX/H_4$) versus apertural angle in macroconchs (fig. 32B). The curvature of the body chamber in side view is expressed as the ratio ($LMAX/H_4$), as above. The specimens form two intergradational clusters, one on the upper right and one on the lower left. In the cluster on the upper right, the apertural angle is higher and the body chamber is more elongate than in the cluster on the lower left. In the cluster on the upper right, $LMAX/H_4$ ranges from approximately 2.2 to 2.5 and the apertural angle ranges from approximately 60° to 85°. In the cluster on the lower left, $LMAX/H_4$ ranges from approximately 2.0 to 2.3 and the apertural angle ranges from approximately 45° to 80°. The holotype of *H. brevis* plots on the lower left. The apertural angle cannot be measured in the holotype of *H. nodosus* because the specimen is broken. However, the apertural angle in specimens that closely match the holotype in size, degree of compression, and ornamentation, is high (65°–85°) and plots on the upper right. As in the previous plot, the two taxa intergrade, so that distinguishing between them is difficult.

←

(49.0 mm), the paratype of *Scaphites nodosus* var. *quadrangularis* Meek, 1876 (pl. 25, fig. 2a–c) (54.1 mm), and the microconch corresponding to the holotype of *Scaphites nodosus* var. *brevis* Meek, 1876 (0.83 × 78.4 mm = 65.3 mm). **D.** Size-frequency histogram of the macroconchs in the combined sample of *H. nodosus* and *H. brevis*. **E.** Size-frequency histogram of *H. nodosus* macroconchs. The arrow represents the holotype of *Scaphites nodosus* Owen, 1852 (101.5 mm). **F.** Size-frequency histogram of *H. brevis* macroconchs. The three arrows represent, from left to right, the macroconch that corresponds to the holotype of *Hoploscaphites landesi* Riccardi, 1983 (1.2 × 49.0 mm = 58.8 mm), the macroconch that corresponds to the paratype of *Scaphites nodosus* var. *quadrangularis* Meek, 1876 (pl. 25, fig. 2a–c) (1.2 × 54.1 mm = 64.9 mm), and the holotype of *Scaphites nodosus* var. *brevis* Meek, 1876 (78.4 mm).

(5) Degree of compression of the adult phragmocone perpendicular to the line of maximum length (W_1/H_1) versus degree of compression of the body chamber at midshaft (V_4/H_4) in microconchs (fig. 33A). The degree of compression of the adult phragmocone perpendicular to the line of maximum length is expressed as the ratio W_1/H_1, and the degree of compression of the body chamber at midshaft is expressed as the ratio V_4/H_4, as above. Two clusters of specimens are visible in this plot, one on the upper right and one on the lower left. In the cluster on the upper right, the phragmocone and body chamber are more depressed than in the cluster on the lower left. In the cluster on the upper right, W_1/H_1 ranges from approximately 0.8 to 1.3 and V_4/H_4 ranges from approximately 0.65 to 0.90. In the cluster on the lower left, W_1/H_1 ranges from approximately 0.65 to 0.95 and V_4/H_4 ranges from approximately 0.30 to 0.55. The paratype of *Scaphites nodosus* var. *quadrangularis* (USNM 386690) plots in the cluster on the lower left. W_1/H_1 cannot be measured in the holotype of *Hoploscaphites landesi* because the specimen is slightly crushed. This plot suggests that the two groups of specimens (*H. nodosus and H. brevis*) are distinct and can be treated as separate taxa.

(6) Relative degree of inflation of the body chamber at midshaft (V_4/W_4) versus degree of compression of the body chamber at midshaft (V_4/H_4) in microconchs (fig. 33B). The relative degree of inflation of the body chamber at midshaft is expressed as the ratioV_4/W_4, with higher values indicating a more inflated body chamber, and the degree of compression of the body chamber at midshaft is expressed as the ratio V_4/H_4, as above. Two clusters of specimens are visible in this plot, one on the upper right and one on the lower left. In the cluster on the upper right, the body chamber is more inflated and depressed than in the cluster on the lower left. In the cluster on the upper right, V_4/W_4 ranges from approximately 0.65 to 0.85 and V_4/H_4 ranges from approximately 0.65 to 0.90. In the cluster on the lower left, V_4/W_4 ranges from approximately 0.45 to 0.75 and V_4/H_4 ranges from approximately 0.30 to 0.55. The paratype of *Scaphites nodosus* var. *quadrangularis* (USNM 386690) and the holotype of *Hoploscaphites landesi* (GSC 5342a) plot on the lower left. This plot suggests that the two groups of specimens (*H. nodosus and H. brevis*) are distinct and can be treated as separate taxa.

We also investigated the range of variation in the size and shape of specimens within single concretions. We examined two concretions from AMNH loc. 3274 in the Pierre Shale, Meade County, South Dakota. These concretions only contain *Hoploscaphites brevis*. Although our samples are small, the variation in size is surprisingly large. In Kathy's concretion, the values of LMAX in four macroconchs of *H. brevis* are 31.6, 74.9, 75.5, and 82.0 mm. In Concretion S from the same locality, the values of LMAX in three macroconchs of the same species are 59.0, 61.0, and 89.0 mm. Thus, the sample in each concretion encompasses most of the size range of the species (fig. 30C).

As an index of shell shape in these specimens, we selected W_1/H_1 because it is measurable in all the specimens, even those that are incomplete. In Kathy's concretion, the values of W_1/H_1 for the four macroconchs of *Hoploscaphites brevis* are 0.71, 0.72, 0.72, and 0.95. In Concretion S, the values of W_1/H_1 for the three macroconchs of the same species are 0.74, 0.75, and 0.99. This range of variation, although not negligible, is slightly less than that of the entire sample from the *Baculites compressus–B. cuneatus* zones (horizontal arrow, fig. 31A).

The pattern of ornament on the adult shell is similar in all specimens, regardless of species. Ribs are weakly to strongly biconcave, with the degree of flexuosity covarying with the flatness of the flanks. The rib density, as measured by the number of ribs/cm on the venter, varies depending on the size and degree of compression of the shell, with larger, more depressed specimens having more widely spaced ribs. However, the ontogenetic pattern of rib spacing is the same in all specimens (fig. 18).

The size and expression of the umbilicolateral and ventrolateral tubercles also covary with the size and degree of compression of the shell, especially in *Hoploscaphites brevis*. In smaller and more compressed specimens of this species, the tubercles are smaller and sometimes appear as bullae. In addition, although the distribution of tubercles is similar in all specimens, the actual distance between tubercles covaries with the size of the shell. The point of appearance and disap-

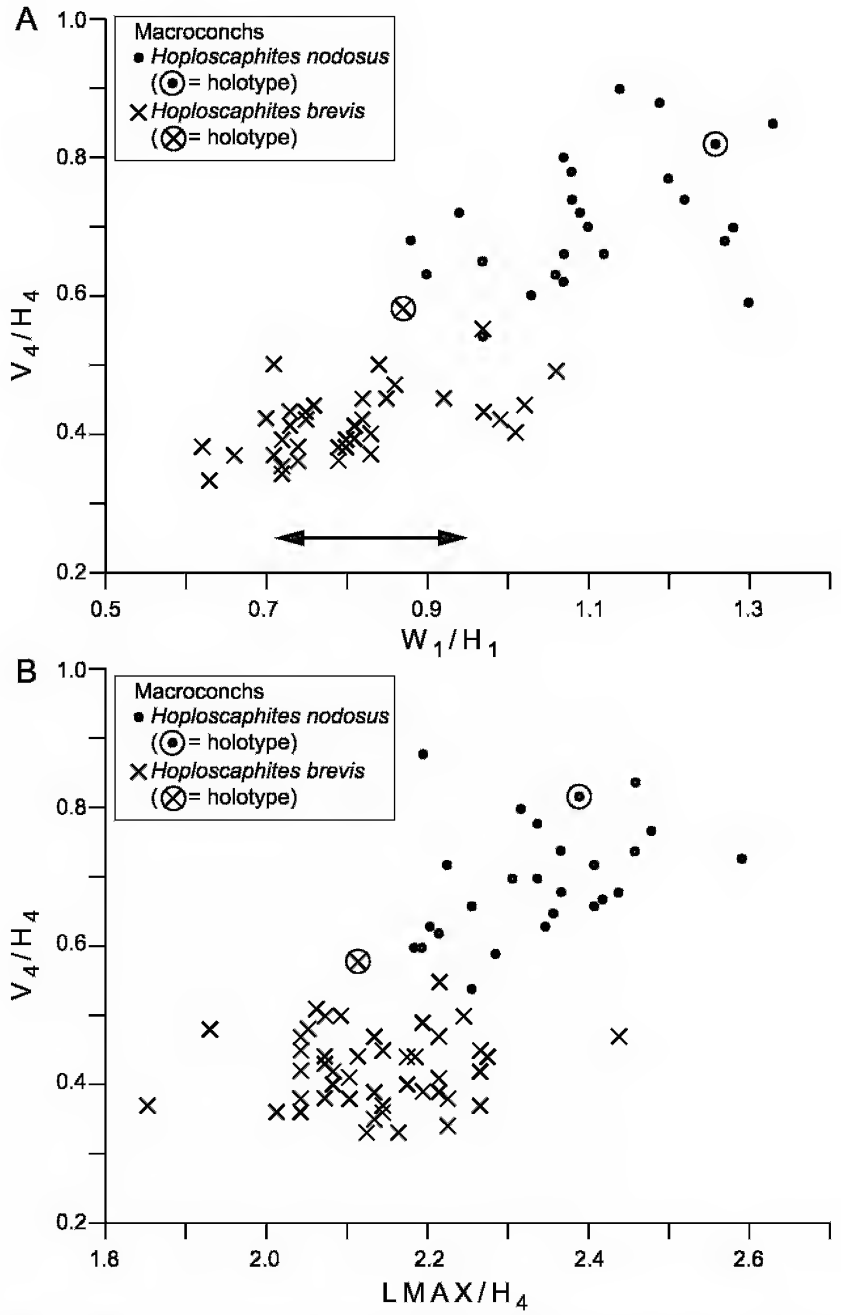

Fig. 31. **A.** Plot of W_1/H_1 versus V_4/H_4 in macroconchs of *Hoploscaphites nodosus* (Owen, 1852) and *H. brevis* (Meek, 1876), Pierre Shale and Bearpaw Shale, *Baculites compressus–B. cuneatus* zones. The arrow represents the variation in W_1/H_1 in seven specimens from two concretions in the Pierre Shale, AMNH loc. 3274, Meade County, South Dakota. **B.** Plot of $LMAX/H_4$ versus V_4/H_4 in macroconchs of *Hoploscaphites nodosus* and *H. brevis*, Pierre Shale and Bearpaw Shale, *Baculites compressus–B. cuneatus* zones.

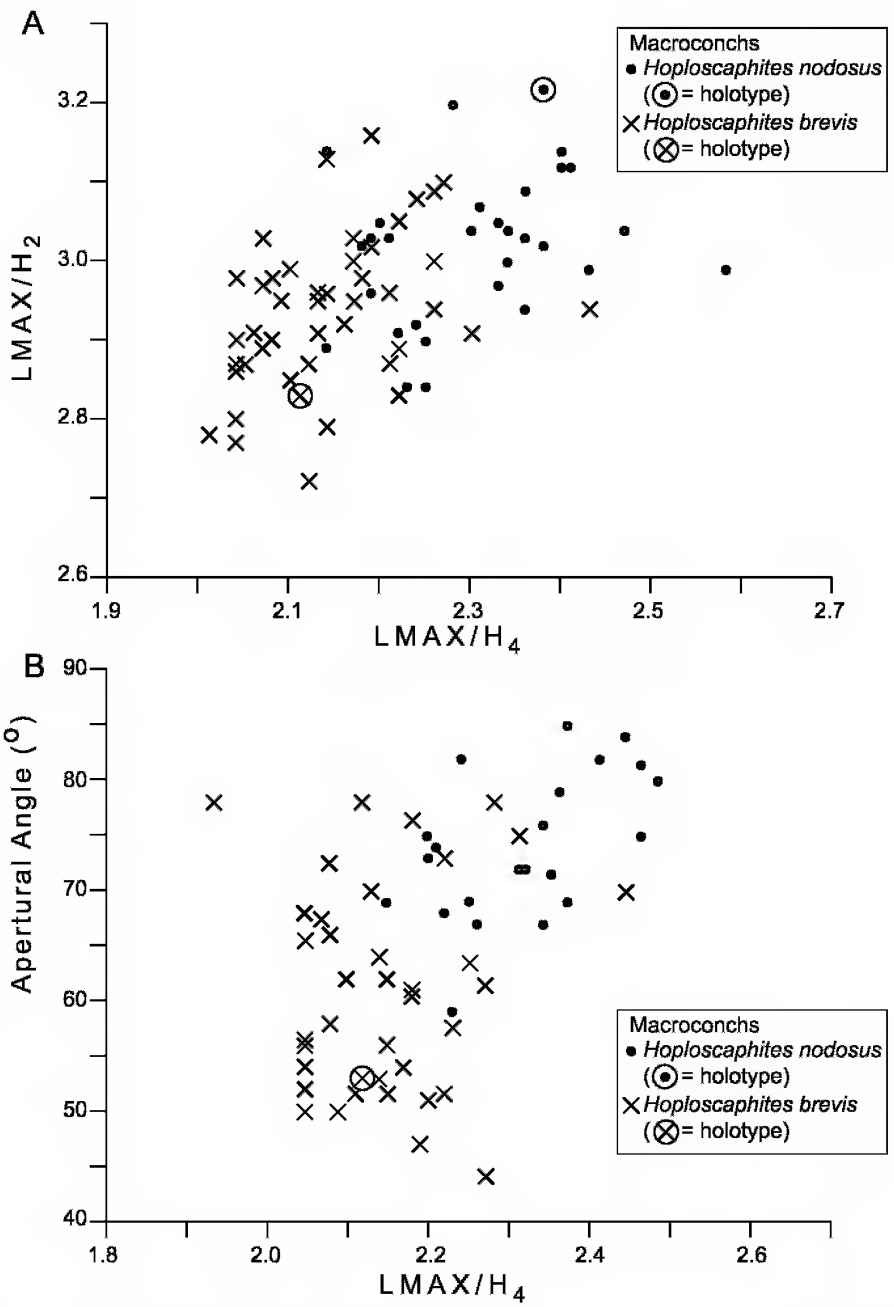

Fig. 32. **A.** Plot of $LMAX/H_4$ versus $LMAX/H_2$ in macroconchs of *Hoploscaphites nodosus* (Owen, 1852) and *H. brevis* (Meek, 1876), Pierre Shale and Bearpaw Shale, *Baculites compressus–B. cuneatus* zones. **B.** Plot of $LMAX/H_4$ versus apertural angle in macroconchs of *Hoploscaphites nodosus* and *H. brevis*, Pierre Shale and Bearpaw Shale, *Baculites compressus–B. cuneatus* zones.

pearance of the tubercles also correlates with shell size. Umbilicolateral tubercles are absent on the phragmocone in small specimens of *H. brevis*, but appear one-third to one-half way onto the exposed phragmocone in large specimens. In small specimens of *H. brevis*, ventrolateral tubercles appear as late as the adoral end of the phragmocone and disap-

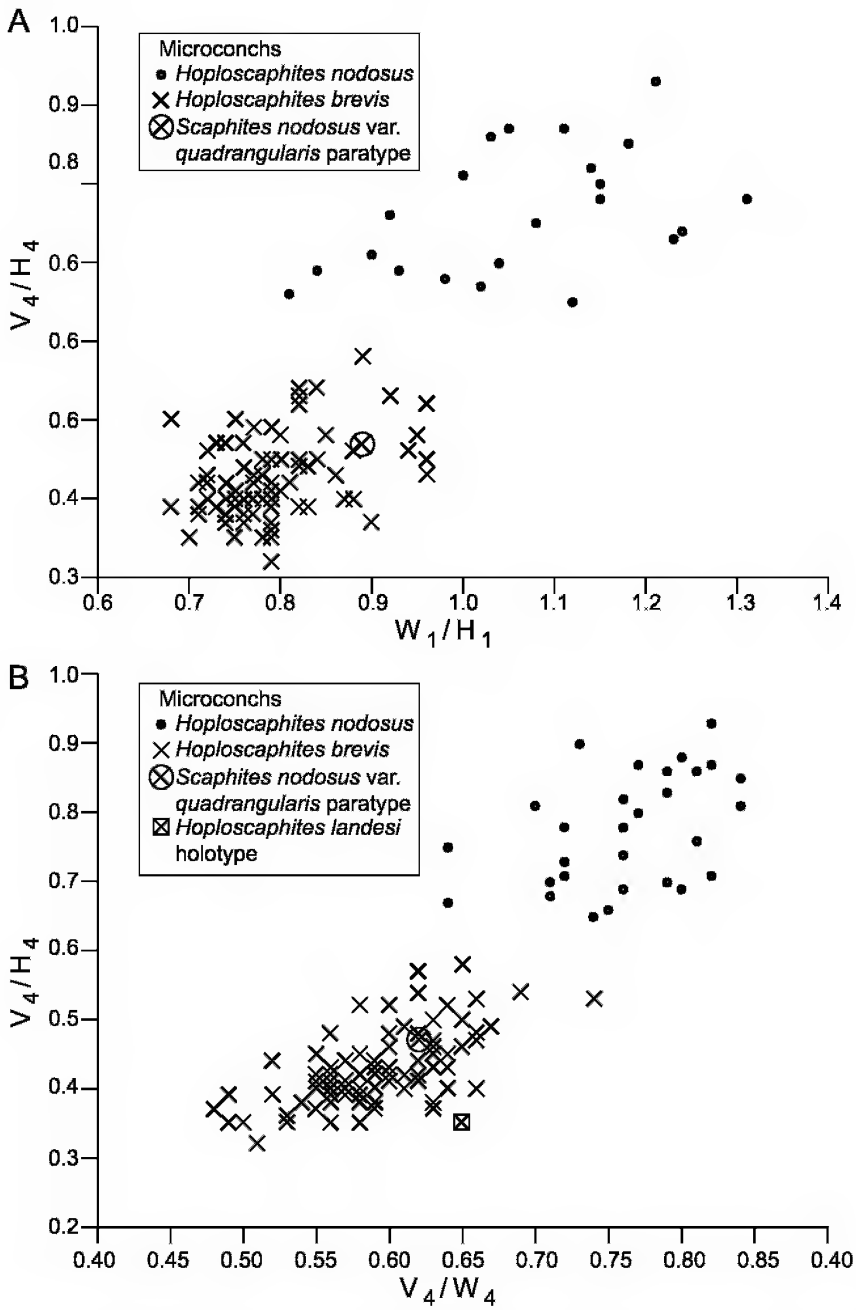

Fig. 33. **A.** Plot of W_1/H_1 versus V_4/H_4 in microconchs of *Hoploscaphites nodosus* (Owen, 1852) and *H. brevis* (Meek, 1876), Pierre Shale and Bearpaw Shale, *Baculites compressus–B. cuneatus* zones. **B.** Plot of V_4/W_4 versus V_4/H_4 in microconchs of *Hoploscaphites nodosus* and *H. brevis*, Pierre Shale and Bearpaw Shale, *Baculites compressus–B. cuneatus* zones.

pear near the point of recurvature, whereas in large specimens of *H. nodosus*, they usually appear near the point of exposure and persist to the aperture.

The suture is similar in all specimens and cannot be used to distinguish among species (fig. 21). The suture consists of a broad ventral or external lobe (E) with a narrow

median saddle, a broad asymmetrically bifid first lateral saddle (E/L), and a symmetrically to slightly asymmetrically bifid first lateral lobe (L). Sutures are more complex in larger specimens, simply reflecting an ontogenetic increase in complexity. However, this increase in complexity does not involve the introduction of new lobes or saddles.

Examination of the variation among these specimens suggests the presence of only two species. The plot of the degree of compression of the adult phragmocone perpendicular to the line of maximum length (W_1/H_1) versus the degree of compression of the body chamber at midshaft (V_4/H_4) in macroconchs reveals two clusters of specimens (fig. 31A). The plot of the curvature of the body chamber in side view ($LMAX/H_4$) versus the degree of compression of the body chamber at midshaft (V_4/H_4) in macroconchs also reveals two clusters (fig. 31B). In both graphs, the holotype of *Hoploscaphites nodosus* plots in the cluster on the upper right and the holotype of *H. brevis* plots in the cluster on the lower left. We therefore treat the cluster on the upper right, which includes specimens with an elongate shell and a relatively depressed whorl section, as *H. nodosus*, and the cluster on the lower left, which includes specimens with a more circular shell and a more compressed whorl section, as *H. brevis*.

The holotype of *Hoploscaphites landesi* is a microconch. In the size-frequency histogram of the microconchs in our sample, it falls on the right side of the peak at 40–45 mm, along with the paratype of *Scaphites nodosus* var. *quadrangularis* (USNM 386690 = *H. brevis*, microconch). In the graph of the degree of compression of the body chamber at midshaft (V_4/H_4) versus the relative degree of inflation of the body chamber at midshaft (V_4/W_4) in microconchs, the holotype of *H. landesi* plots on the lower right side of the cluster on the lower left (fig. 33B). It is slightly more compressed than the other specimens in this cluster (lower value of V_4/H_4), but this difference may be partly due to postmortem crushing. However, the degree of compression of this specimen is similar to the rest of the specimens in the cluster, and this specimen is therefore interpreted as a small microconch of *H. brevis*.

Our expanded definition of *Hoploscaphites brevis* implies the acceptance of a wide range of variation in the adult size of this species. This variation may reflect differences in the time at which individuals mature. Assuming that all specimens grew at approximately the same rate, smaller specimens would have attained maturity at younger ages. The presence of small and large specimens in the same concretion may indicate that they reached maturity at nearly the same time (but at different ages). Alternatively, they may have reached maturity at different times and are simply preserved together because the concretions represent deposition over a long time interval. Our studies suggest that the concretions in the *Baculites compressus–B. cuneatus* zones may have formed over a time period of months to years. Therefore, it is likely that many of these individuals lived contemporaneously and reached maturity at nearly the same time (but at different ages).

Several studies have documented wide variation in the size at maturity in a single ammonite species (for a review, see Davis et al., 1996). In a provocative study on Jurassic ammonites, Matyja (1986) noted the presence of as many as three size classes in the same species. He argued that these classes represented individuals that matured at different sizes due to differences in their rate of growth and age at maturity, and called this phenomenon "developmental polymorphism" (but see Calloman, 1988, for a counterargument). Parent et al. (2008) described two size classes in macroconchs of Late Jurassic aspidoceratids from Germany, which they interpreted as reflecting variation in the age at maturity. In contrast, a study of size variation in adult macroconchs of *Hoploscaphites nicolletii* from the Upper Cretaceous Fox Hills Formation revealed only a single size class in samples of specimens from individual concretions (Landman et al., 2003). Variation in the size at maturity is common in many modern cephalopods (e.g., Richard, 1970; LeGoff et al., 1998), and has been attributed to variation in the timing of maturation controlled by the release of a hormone from the optic gland (Mangold, 1987).

It is entirely possible that all of the scaphites in the *Baculites compressus–B. cuneatus* zones represent a single very vari-

able species (*Hoploscaphites nodosus*). For example, the size histogram of all the macroconchs from this interval can be interpreted as a single sample with a unimodal distribution skewed to the left (fig. 30). The differences in size, degree of compression, and coarseness of ornament may simply reflect differences in the rate of growth and age at maturity, keyed to changes in the environment. In practice, the assignment of transitonal specimens to *H. nodosus* rather than to *H. brevis* or vice versa is sometimes arbitrary. This problem is even more serious with respect to the definition of genera (*Hoploscaphites* versus *Jeletzkytes*), occasionally resulting in the assignment of almost identical specimens to different genera (see discussion about genera below).

PATHOLOGIC SPECIMENS

Pathologic specimens are common among the scaphites in the *Baculites compressus–B. cuneatus* zones (figs. 34, 35). Pathologies have been widely documented in both Paleozoic and Mesozoic ammonites (Holder, 1956; Guex, 1967, 1968; Landman and Waage, 1986; Bond and Saunders, 1989; Kröger, 2002a, 2002b; Larson, 2003, 2007; Keupp, 2006). Many descriptive terms, known as "forma-types," have been introduced to categorize the type of pathology, as recently reviewed by Hengsbach (1996).

If the pathology cannot be attributed to an injury, it may be due to disease, attachment of epizoans to the shell, or infestation by parasites. Examples of such deformities include specimens that depart from bilateral symmetry, without any evidence of a scar in the shell (Landman and Waage, 1986: "Morton's syndrome"; Hengsbach, 1996: "symmetropathy"; Keupp and Ilg, 1992: "forma *undaticarinata*"). In BHI 4896, a microconch of *Hoploscaphites brevis*, the right row of ventrolateral tubercles on the body chamber disappears, although the left row persists (fig. 34F, G). There is no indication of a scar in the shell, suggesting that the disappearance of the tubercles may be due to a parasitic infestation or disease. A similar explanation may account for the deformity in YPM 35631 (fig. 35A), a microconch of *H. nodosus* (?). In this specimen, both rows of ventrolateral tubercles migrate toward the center, beginning just adoral of the point of exposure. The two rows subsequently merge into a single row, which oscillates back and forth before stabilizing on the midventer on the adoral part of the phragmocone. At the point of recurvature, the tubercles abruptly diminish in size and reappear as two closely spaced rows. This deformity also produced a bulge on the midventer on the adoral end of the phragmocone, which caused a displacement of the ventral lobe of the suture to the left side. In addition, there is a scar 3.5 cm long $\times$1.5 cm wide, part of which is inflated, on the dorsal half of the flanks on the left side of the adoral part of the phragmocone and adapical part of the body chamber. It is possible that this scar represents a repaired break at the aperture. However, this scar is adoral of the initial displacement of tubercles, suggesting that the original cause of this displacement was disease or parasitic infestation.

A pathology due to an injury is easier to recognize because of the presence of a scar, which formed during the lifetime of the animal. Some of these scars are the results of injuries at the apertural margin. If the injury was minor, the ornament on the repaired shell is "normal," but is ususally offset with respect to the ornament on the adapical side of the break. If the injury was severe, the ornament on the repaired shell may be distorted or absent altogether, depending upon the ability of the mantle to withdraw to the position of the break, as documented in other ammonites (Kröger, 2002a). If the ornament is absent, it implies that the epithelial mantle could not withdraw, probably because the shell break was too extensive, and that the shell was repaired instead by a part of the mantle that could not secrete ornament. The repaired shell is sometimes inflated, indicating that the mantle expanded to fill the broken part of the shell. If the scar persists to the aperture, it suggests that the mantle edge was permanently damaged. If the scar eventually disappears and merges with the rest of the shell, it suggests that the mantle was able to recover following the attack.

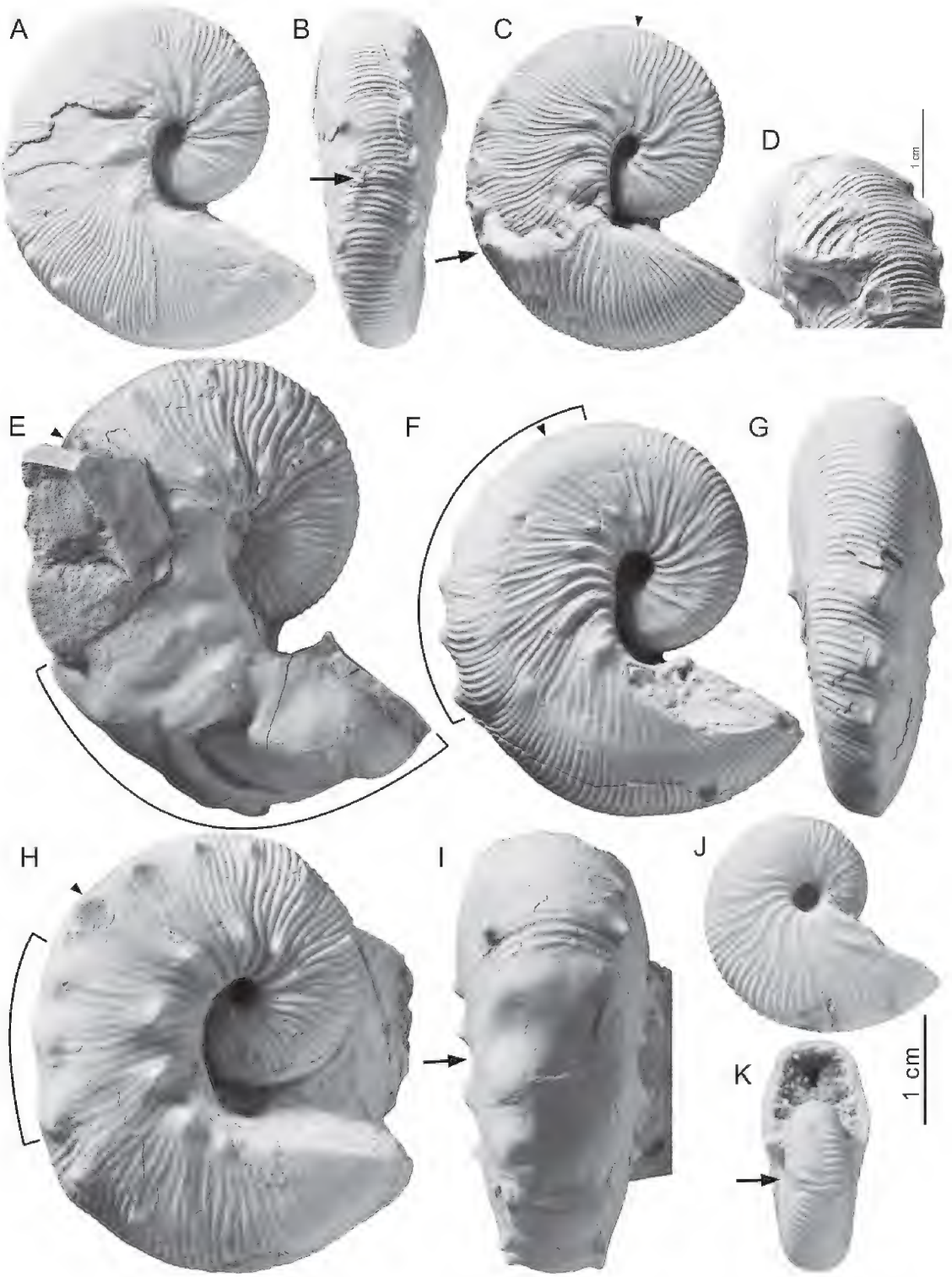

Fig. 34. Sublethal injuries in *Hoploscaphites nodosus* (Owen, 1852) and *H. brevis* (Meek, 1876), *Baculites compressus–B. cuneatus* zones, Pierre Shale, Meade County, South Dakota. **A, B.** *Hoploscaphites*

Examples of repairs at the aperture involving permanent damage to the mantle are grooves that follow the spiral growth of the shell (Hölder, 1956: forma *verticata*; Landman and Waage, 1986: spiral furrow). In general, the injury also affects the surrounding ornament, sometimes resulting in the loss of ribs or tubercles (Guex, 1967: "compensation ornamentale"). YPM 35598, a macroconch of *Hoploscaphites nodosus*, shows a spiral furrow on the right side of the shell (fig. 35B). The furrow originates just adoral of the point of exposure and extends to the point of recurvature. The ribs on the flanks bend backward at the furrow, which runs along the lateral side of the ventrolateral tubercles. The right side of the venter and most of the right flanks of the hook are missing, suggesting a fatal injury of the already weakened specimen. USNM 12284, a macroconch of *H. nodosus*, which was originally illustrated by Whitfield (1880, 441, pl. 13, fig. 12), shows a spiral furrow on the left side (the side not figured by Whitfield). The furrow originates on the middle of the exposed part of the phragmocone at approximately the line of maximum length and continues to the point of recurvature. The ventrolateral tubercles and associated ribs are absent along the furrow, but the rest of the ornamentation on the left side is unaffected. Most of the apertural part of the shell is missing, again perhaps due to a fatal injury.

Examples of repairs at the aperture involving nonpermanent damage to the mantle include BHI 4898 and BHI 4316, both of which are microconchs of *Hoploscaphites brevis*. In BHI 4898, there is a quadrangular patch of repaired shell 1 cm long on the left side of the adapical end of the body chamber (fig. 34A, B). The scar is slightly inflated and stands out from the rest of the shell. The ornament is distorted on the adapical end of the scar, but becomes more "normal" toward the adoral end of the scar. In addition, there is a temporary loss of symmetry on the shaft, with the ventrolateral tubercles migrating first to the left side and then to the right side, before reestablishing themselves on the hook. In BHI 4316, there is a swollen scar on the right side of the adoral part of the shaft (fig. 34C, D). The scar is approximately 1.5 cm long and spans an angle of approximately 40°. The scar is smooth on the dorsal side but is ribbed on the lateral and ventral sides. The ribs on the scar are coarser and more widely spaced than those on the adjacent part of the shell, but become more "normal" toward the adoral end of the scar. The presence of ornament on the scar indicates that the mantle epithelium must have been able to withdraw an angular distance of 40° back from the aperture in order to repair the break.

Scars in the shell also result from damage to the body chamber adapical of the aperture. Such injuries have been referred to as "back breaking" if they occur on the adapical part of the body chamber and "body piercing" if they occur on the flanks of the body chamber (Larson, 2003, 2007). Keupp (2006) introduced the term "forma aegra

---

←

brevis, microconch, BHI 4898. **A.** Right lateral; **B.** ventral, showing temporary loss of symmetry on the shaft (arrow), with the ventrolateral tubercles migrating to the left side and then to the right side, before reestablishing themselves on the hook. **C, D.** *Hoploscaphites brevis*, microconch, transitional in morphology to macroconch, BHI 4316. **C.** Right lateral; **D.** close-up of swollen scar (arrow in C) on the right side of the adoral part of the shaft, with widely spaced ribs. **E.** *Hoploscaphites brevis*, microconch, BHI 4256, showing a V-shaped scar, followed by a large inflated area with distorted ribs, terminating at the aperture (area enclosed in brackets). A large piece of shell is also missing from the adapical part of the body chamber. **F, G.** *Hoploscaphites brevis*, microconch, BHI 4896, with a single row of ventrolateral tubercles (area enclosed in brackets). **F.** Right lateral; **G.** ventral. **H, I.** *Hoploscaphites nodosus*, microconch, BHI 4895, with a smooth healed area on the venter of the body chamber (area enclosed in brackets). **H.** Right lateral; **I.** ventral. **J, K.** *Hoploscaphites brevis*, AMNH 56871, broken phragmocone with an inflated scar (arrow) at a whorl height of 6.5 mm. **J.** Right lateral; **K.** apertural. The scar is covered with distorted ribs that point backward, forming an acute angle with the midventer. Specimens are illustrated natural size unless indicated otherwise by a scale bar.

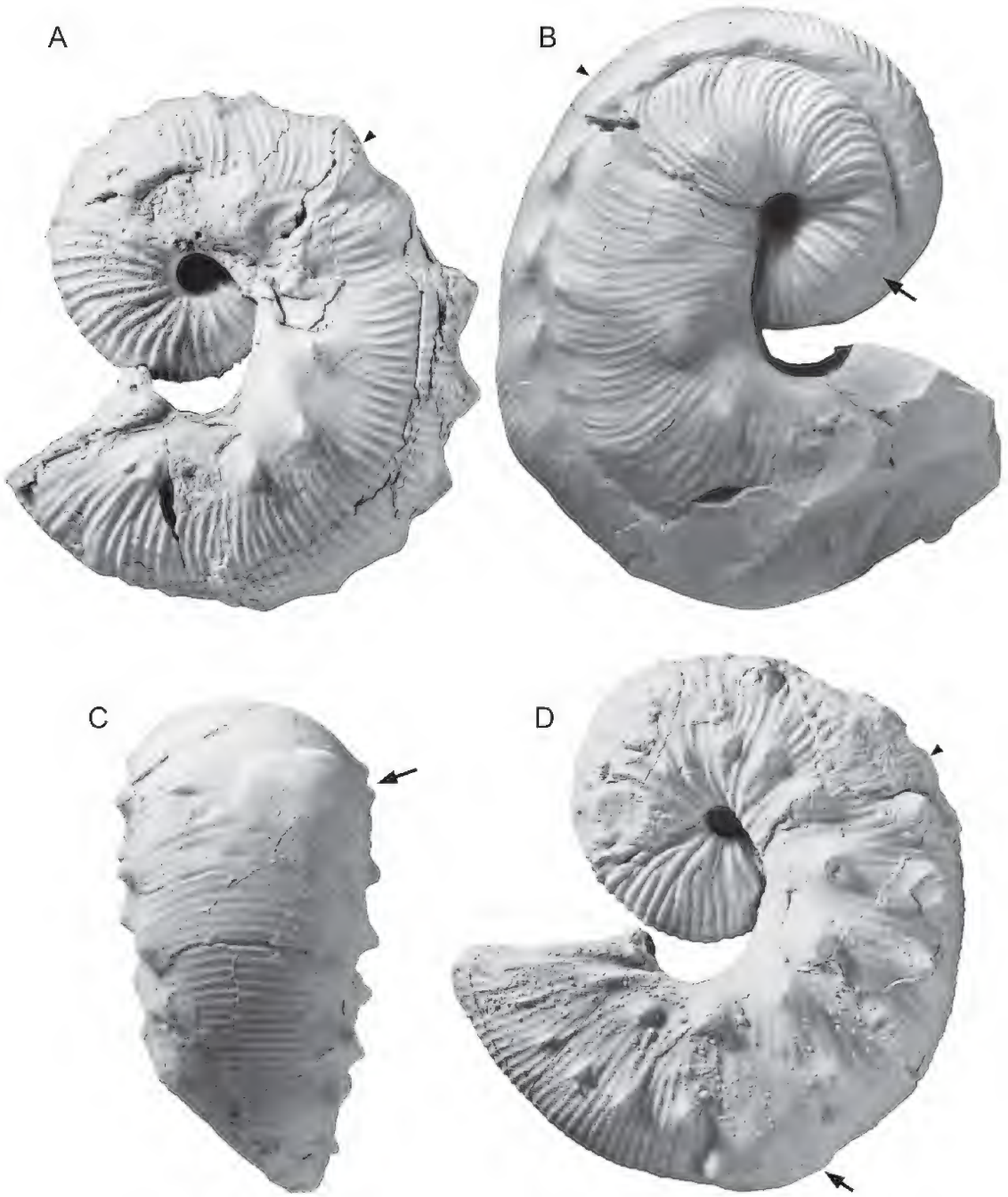

Fig. 35. Sublethal injuries in *Hoploscaphites nodosus* (Owen, 1852). **A.** *Hoploscaphites nodosus* (?), microconch, left lateral view, YPM 35631, with a single row of midventral tubercles instead of two rows of ventrolateral tubercles, YPM loc. A1461, Bearpaw Shale, Rosebud County, Montana. **B.** *Hoploscaphites nodosus*, macroconch, right lateral view, YPM 35598, with a spiral furrow on the right side of the shell beginning just adoral of the point of exposure, YPM loc. C3347, Pierre Shale, Belle Fourche River, South Dakota. **C, D.** *Hoploscaphites nodosus*, microconch, BHI 4912, with a round "blister" (arrow) on the venter just adapical of the point of recurvature, *Baculites compressus–B. cuneatus* zones, Pierre Shale, Meade County, South Dakota. **C.** Ventral; **D.** left lateral. Specimens are illustrated natural size.

fenestra" for these windowlike scars. As with injuries at the aperture, the presence of ornament on the scar indicates that the break was repaired by the mantle edge. If, on the other hand, the scar is smooth, it was repaired by the posterior part of the mantle, which could not secrete ornament. The repaired area is usually inflated and appears as a "blister" surrounded by a sharp fracture (Keupp, 2006: "forma *inflata*"). However, the demarcation between the blister and the rest of the shell is not as apparent if the outer shell has spalled off, leaving an internal mold.

There are several specimens that show "blisters" on the body chamber. In BHI 4912, a large microconch of *Hoploscaphites nodosus*, there is a round "blister" approximately 2.5 cm in diameter at an angular distance of approximately 80° from the mature aperture (fig. 35C, D). The blister extends from the middle of the venter to the middle of the left flanks. It is smooth and surrounded by "normally" ornamented shell. This scar represents the repair of a hole in the body chamber by the posterior part of the mantle. In BHI 4895, a microconch of *H. nodosus*, there is a smooth area along the venter approximately 4 cm long (fig. 34H, I). The ventrolateral tubercles are present on the right side but are missing on the left side. Ribs appear on the flanks, as well as on the venter on the adapical and adoral ends of the blister. Although much of the outer shell has spalled off, the most likely explanation is that this scar represents the repair of a hole in the body chamber by the posterior part of the mantle. In addition, there is a jagged hole on the venter and part of the left side of the body chamber at the point of recurvature, which probably represents the final, fatal injury.

Similar scars are also present in juvenile shells. In AMNH 56871, a broken phragmocone presumably of *Hoploscaphites brevis*, there is an inflated scar at a whorl height of 6.5 mm (fig. 34J, K). The scar is approximately 6 mm long and extends from the middle of the venter to the outer flanks on the left side. The scar is covered with distorted ribs that point backward, forming an acute angle with the midventer. The scar is sharply demarcated on the adapical, adoral, and ventral sides and is surrounded by more "normal" ornament. The presence of distorted ribs suggests that the break occurred close enough to the aperture that the peristomal epithelium was able to withdraw far enough back to repair it.

In BHI 4256, a microconch of *Hoploscaphites brevis*, the coiled portion of the shell is perfectly intact, but the body chamber is severely deformed (fig. 34E). The pathology is probably due to two injuries, implying that the animal was attacked, survived, repaired its shell, and was attacked again. However, the exact sequence of events is difficult to piece together. The adoral part of the body chamber is ornamented on the flanks, but the venter is bumpy and devoid of ornament. In addition, on the right side on the adoral end of the shaft, there is a sharp V-shaped chevron, followed by a large inflated area with distorted ribs, terminating at the aperture. The first attack may have occurred adapical of the aperture and was repaired by the posterior part of the mantle. The second attack may have occurred at the aperture and resulted in the formation of the V-shaped scar and blister with distorted ribs, culminating at the aperture. This specimen also suffered a third, fatal injury, as indicated by a break in the adapical part of the body chamber.

Lethal injuries are indicated by missing pieces of shell, although it is not always easy to distinguish these breaks from postmortem damage. In addition, incomplete shells are generally overlooked because of the tendency to collect whole, perfect specimens. However, the consistent position of the injuries is a clue that they occurred during life, rather than after death (Radwański, 1996; Larson, 2003, 2007; Keupp, 2006; Klompmaker et al., 2009). In general, lethal injuries in scaphites occur on the venter and sides on the adapical part of the body chamber, precluding repair of the shell. The resulting accumulation of shell fragments on the sea bottom is sometimes difficult to distinguish from a shell hash produced by hydrodynamic processes. However, the presence of jagged shell fragments in association with scaphites showing lethal injuries suggests that such an accumulation is a result of predation rather than mechanical breakage (fig. 36F; for further discussion about "kitchen middens," see Radwański, 1996). Lethal injuries have been documented in Late Cretaceous scaphites from the West-

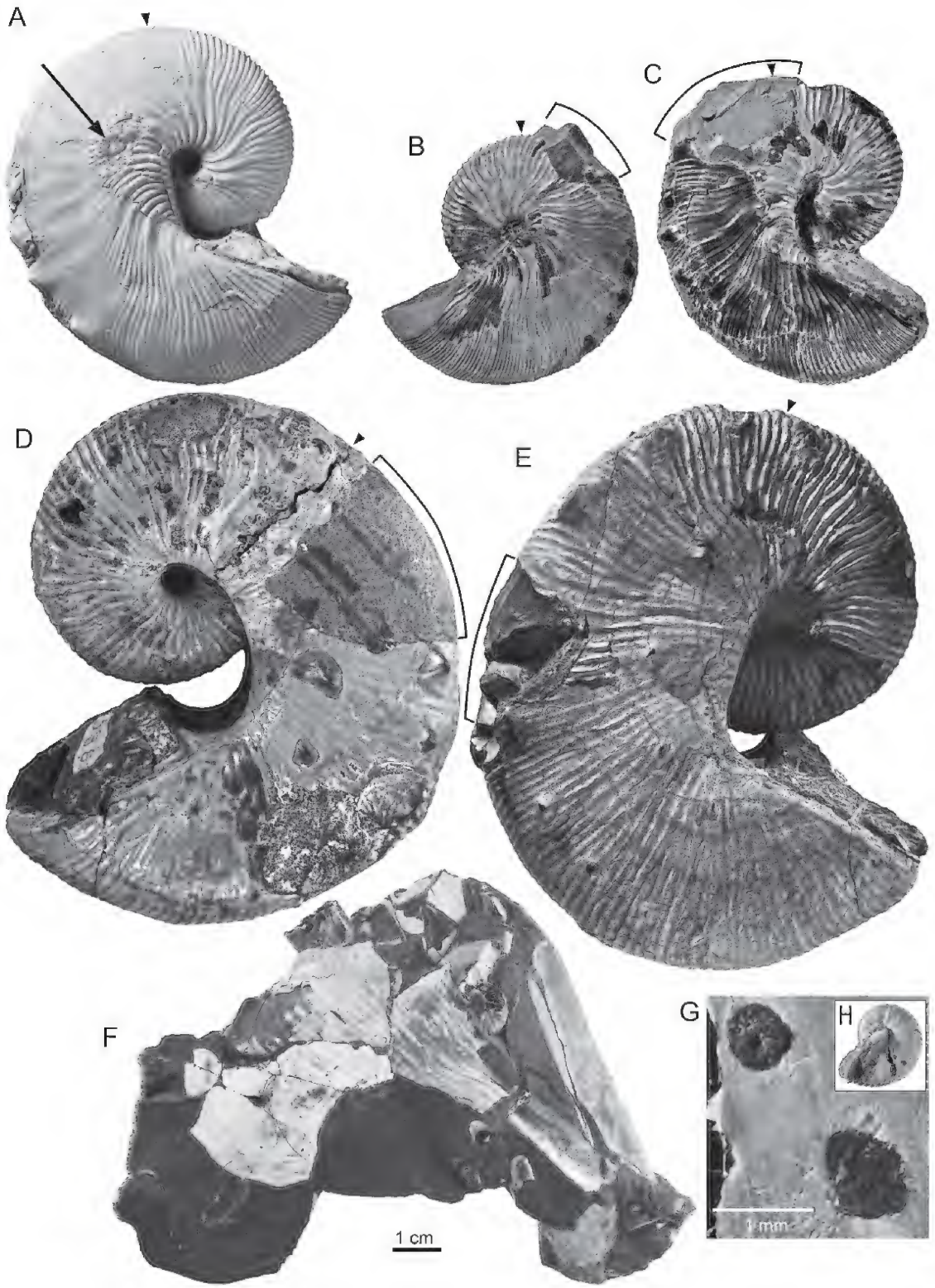
A
B
C
D
E
F
G
H
1 cm
1 mm

ern Interior (Larson, 2003), the Atlantic Coastal Plain (Landman et al., 2007a), and the Vistula River Valley, central Poland (Radwański, 1996).

Lethal injuries are common in *Hoploscaphites nodosus*. In USNM 536235, a large macroconch, there is a triangular gap approximately 4 cm long on the venter and ventrolateral part of the right side of the body chamber at midshaft (fig. 36E). In USNM 536234, a large macroconch, a chunk of shell 3 cm × 4 cm is missing from the venter and the ventrolateral parts of both flanks on the adapical end of the body chamber (fig. 37C, D). In BHI 4287a, a large macroconch, the venter and nearly all of the right side of the shaft of the body chamber is missing (fig. 37A, B). However, despite the removal of such a large part of the body chamber, the rest of the specimen is perfectly intact. In BHI 7033, a large microconch, there is a triangular gap spanning the venter and most of the flanks on the left side on the adapical end of the body chamber (fig. 36D). This specimen also shows a chunk of shell missing on the left side of the body chamber near the point of recurvature.

Lethal injuries are equally common in *Hoploscaphites brevis*. In BHI 4900, a small macroconch, there is a gap approximately 1 cm long on the venter and the ventrolateral flanks on the adapical end of the body chamber (fig. 36B). The edges of the gap are sharp and irregular. In BHI 4901, a small microconch, there is a similar gap, almost 2.5 cm long, on the adapical end of the body chamber, affecting both the venter and ventrolateral parts of the flanks (fig. 36C). In AMNH 50429, a large macroconch, most of the shaft of the body chamber was removed by a predator (fig. 12A, B). Subsequently, during fossilization, this specimen was twisted and crushed, producing a jigsaw of shell fragments, which were probably held together by the remaining pieces of periostracum. In BHI 4267, a macroconch, there is a rectangular hole 1 cm long at one-third whorl height on the right flanks on the adapical end of the body chamber (fig. 36A). In AMNH 56819 (fig. 36G, H), a small piece of a phragmocone, two tiny holes, 0.75 mm and 1 mm in diameter, appear on the left flanks at a shell diameter of 12 mm. These holes may represent lethal injuries but, surprisingly, they occur on the phragmocone and not on the body chamber.

The position of injuries on the scaphite shell provides clues about the mode of life of these animals including the kind of predator and direction of attack. Injuries at the

←

Fig. 36. **A–E.** Lethal injuries in *Hoploscaphites nodosus* (Owen, 1852) and *H. brevis* (Meek, 1876). **A–C.** *Hoploscaphites brevis*. **A.** BHI 4267, macroconch, right lateral view, with a puncture at one-third whorl height (arrow) on the right flanks on the adapical end of the body chamber, *Baculites compressus–B. cuneatus* zones, Pierre Shale, Meade County, South Dakota. **B.** BHI 4900, macroconch, left lateral view, with a gap approximately 1 cm long on the venter and the ventrolateral flanks on the adapical end of the body chamber (area enclosed in brackets), *Baculites compressus* Zone, Pierre Shale, Meade County, South Dakota. **C.** BHI 4901, microconch, transitional in morphology to macroconch, right lateral view, with a gap almost 2.5 cm long on the adapical end of the body chamber, including both the venter and ventrolateral part of the shell (area enclosed in brackets), *Baculites compressus–B. cuneatus* zones, Pierre Shale, Meade County, South Dakota. **D.** *Hoploscaphites nodosus*, large microconch, BHI 7033, left lateral view, with a triangular shaped gap spanning the venter and most of the flanks on the left side on the adapical end of the body chamber (area enclosed in brackets), *Baculites compressus–B. cuneatus* zones, Pierre Shale, Meade County, South Dakota. **E.** *Hoploscaphites nodosus*, macroconch, USNM 536235, right lateral view, with a triangular shaped gap approximately 4 cm long on the venter and ventrolateral part of the right side of the body chamber at midshaft (area enclosed in brackets), USGS Mesozoic loc. 9154, Pierre Shale, near Kremmling, Grand County, Colorado. **F–H.** Postmortem shell damage. **F.** AMNH 63449, fragments of the body chamber of *Hoploscaphites nodosus*, probably resulting from predation, AMNH loc. 3274, *Baculites compressus–B. cuneatus* zones, Pierre Shale, Meade County, South Dakota. **G, H.** Minute holes on the left flanks of the phragmocone of a juvenile of *Hoploscaphites brevis*, AMNH 56819, AMNH loc. 3274, *Baculites compressus–B. cuneatus* zones, Pierre Shale, Meade County, South Dakota. **G.** Close-up of holes; **H.** left lateral view. Specimens are illustrated natural size unless indicated otherwise by a scale bar.

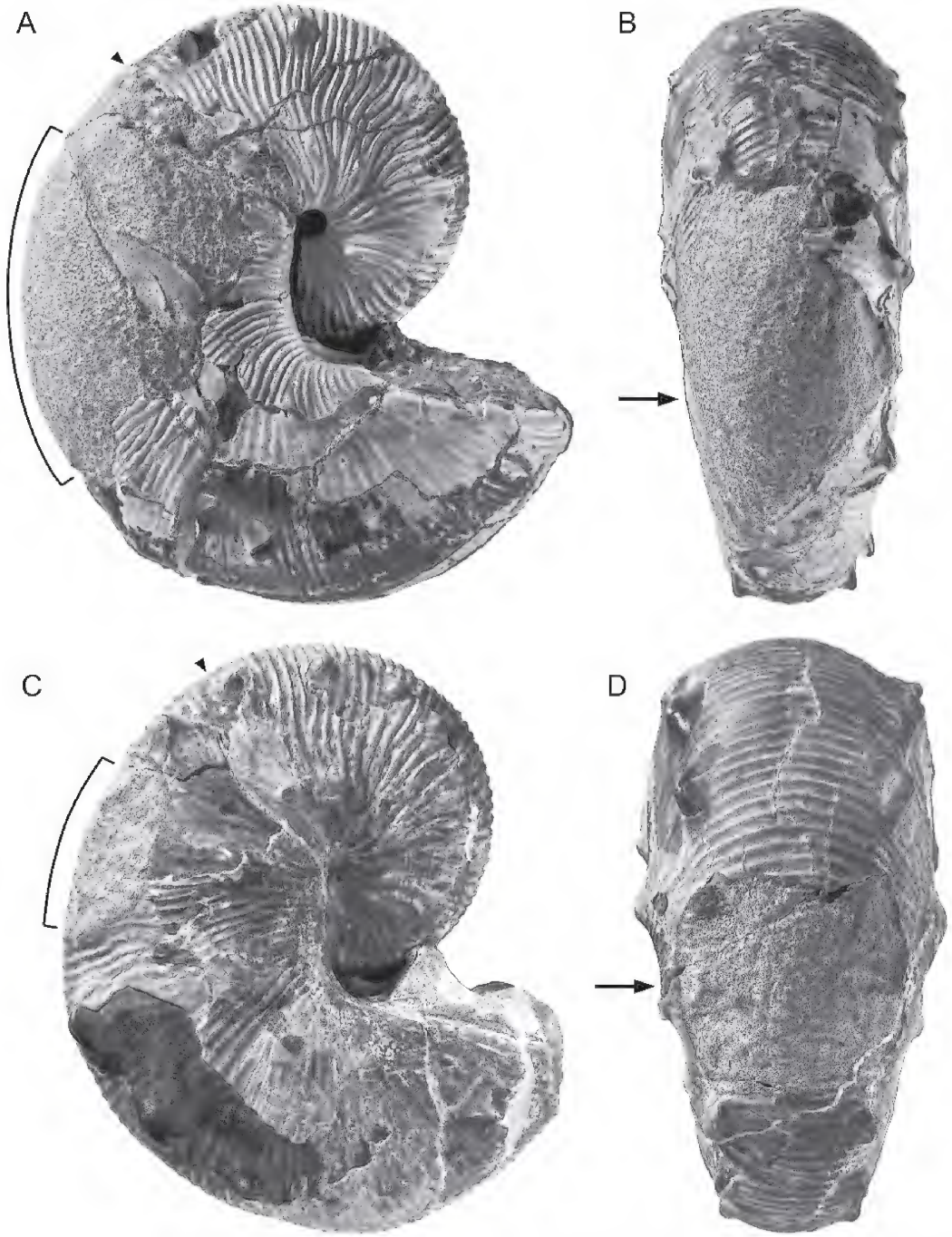

Fig. 37. *Hoploscaphites nodosus* (Owen, 1852), macroconchs, lethal injuries with chunks of shell missing from the adapical part of the body chamber (areas enclosed in brackets in lateral views, arrows in ventral views). Despite the removal of large pieces of shell, the specimens are otherwise intact. **A, B.** BHI 4287a, *Baculites cuneatus* Zone, Pierre Shale, Meade County, South Dakota. **A.** Right lateral; **B.** ventral. **C, D.** USNM 536234, USGS Mesozoic loc. D5034, Pierre Shale, *Baculites compressus* Zone, Larimer County, Colorado. **C.** Right lateral; **D.** ventral. Specimens are illustrated natural size.

aperture indicate that scaphites were sometimes attacked from the front, based on the orientation of the living animal (see section on mode of life). Such injuries in ammonites have been attributed to fish, reptiles, crustaceans, and cephalopods (Landman and Waage, 1986; Larson, 2003; Keupp, 2006; Klompmaker et al., 2009). Injuries on the venter and ventrolateral flanks on the adapical end of the body chamber indicate that scaphites were also attacked from behind (Larson, 2003). This is a particularly vulnerable area because it is out of eyesight, although the exact position of the eyes is unknown. In addition, the whorl section of the body chamber is subquadrate and compressed, making it relatively easy for a predator to grasp and bite the shell. As a result, these injuries are usually fatal. It is, therefore, no coincidence that the adapical end of the body chamber is the most heavily armored part of the scaphite shell, featuring subspinose ventrolateral tubercles (Riccardi, 1983; Landman and Waage, 1993; Monks, 2000). Such tubercles effectively increased the size of the scaphite, discouraging small predators (for a discussion of the antipredatory function of ammonite ornamentation, see Kröger, 2002b). Injuries on the venter and ventrolateral flanks on the adapical end of the body chamber in ammonites have been attributed to fish, reptiles, and cephalopods (Larson, 2003; Klompmaker et al., 2009).

Holes in the flanks of the body chamber indicate that scaphites were also attacked from the side. Radwański (1996) noted such holes in late Maastrichtian scaphites from Poland, and attributed them to crabs, lobsters, and stomatopods. Larson (2003) described similar holes in Campanian and Maastrichtian scaphites from the U.S. Western Interior and attributed them to fish and reptiles. Keupp (2006) reviewed the occurrence of such punctures in a wide variety of ammonites and pointed out that in many specimens, the holes are restricted to only one side. He argued that such holes could not have been produced by grasping predators, such as vertebrates and claw-bearing crustaceans, but rather by stomatopods that would have inflicted ballistic damage on one or both sides of the body chamber. Because all living stomatopods are benthic, he reasoned that ammonites exhibiting such punctures must have lived close to the bottom. This conclusion is consistent with other evidence about the habitat of scaphites (see below).

MODE OF LIFE

Inferences about the mode of life of scaphites are based on observations of their morphology (shell, septa, muscle scars, jaws, hooks, radula), in analogy with modern cephalopods whose mode of life is known. Assuming that scaphites maintained near neutral buoyancy during life, we calculated the angle of orientation of the aperture in embryonic, juvenile, submature, and mature shells (fig. 14). We estimated the centers of buoyancy and mass using the same approach as Trueman (1941). Because scaphites are bilaterally symmetrical, we used photos of specimens in lateral view and cut out the whole specimen and body chamber separately (requiring two photos). Using a computer program (Image J), we determined the centers of the areas of the whole specimen and of the body chamber, and treated these as proxies for the centers of buoyancy and mass, respectively. We then drew a line through the centers of mass and buoyancy (= the vertical) and another line through the apertural margin. The angle of orientation of the aperture is defined as the angle of the aperture with respect to the vertical.

In an embryonic shell of *Hoploscaphites brevis*, the angle of orientation of the aperture is 106.0° (table 2). In a juvenile shell of the same species, the angle of orientation of the aperture is 87° (table 2). In a specimen of *H. nodosus* in which the adult body chamber was removed to expose the phragmocone, the angle of orientation of the aperture of the "juvenile," assuming a body chamber angle of 230°, is 88° (table 2). Determination of the angle of orientation of the aperture in submature shells with incomplete shafts is difficult because of the lack of specimens preserved at this stage. In AMNH 55873, a broken microconch of *H. nodosus*, the base of the body chamber is approximately 90° adapical of the line of maximum length (fig. 12K, L), presumably corresponding to the aperture at the point of recurvature. In principle, the apertural margin at this point

TABLE 2
Angle of orientation of the aperture in *Hoploscaphites nodosus* (Owen, 1852) and *Hoploscaphites brevis* (Meek, 1876)

Species	Number	M/m	LMAX (mm)	Angle (°)
H. nodosus	BHI 4121	M	88.7	102.0
H. nodosus	BHI 4178	M	97.0	108.0
H. nodosus	BHI 4948	M	86.5	100.0
H. nodosus	USNM 536234	M	85.3	100.0
H. nodosus	YPM 35598	M	88.3	90.5
H. nodosus	AMNH 58521	m	77.7	94.0
H. nodosus	BHI 4723	m	78.4	101.0
H. nodosus	USNM 536232	m	74.4	96.0
H. nodosus	USNM 536245	m	71.9	108.5
H. nodosus	YPM 1868	m	91.5	101.0
H. nodosus	USNM 536232	juvenile	45.0[a]	88.0
H. brevis	AMNH 56865	M	61.2	103.5
H. brevis	AMNH 56882	M	82.7	106.0
H. brevis	BHI 4292	M	61.2	102.0
H. brevis	BHI 4311	M	40.7	109.0
H. brevis	BHI 7034	M	99.6	102.0
H. brevis	AMNH 55884	m	71.6	104.0
H. brevis	BHI 4123	m	66.0	107.0
H. brevis	BHI 4211a	m	63.1	100.0
H. brevis	BHI 4249	m	38.6	104.5
H. brevis	BHI 4283	m	53.6	105.0
H. brevis	AMNH 55884	submature[b]	71.7	125.0
H. brevis	BHI 4123	submature[b]	66.2	117.5
H. brevis	AMNH 56871	juvenile[c]	38.2	87.0
H. brevis	AMNH 58522	ammonitella	0.678	106.0

See figure 14 for description of measurements; M = macroconch; m = microconch; [a] shell diameter of adult phragmocone, assumes a body chamber angle of 230°; [b] hypothetical, with base of body chamber 90° adapical of the line of maximum length and aperture at point of recurvature; [c] broken, assumes a body chamber angle of 230°.

would have followed the outline of the ribs (for a similar assumption in nostoceratid ammonites, see Okamoto, 1988: 275). Using this specimen as a model, we reconstructed the "submature" shell in two microconchs of *H. brevis*. The angle of orientation of the aperture in these two "submature" specimens averages 121° and ranges from 117.5° to 125° (table 2). Determination of the angle of orientation of the aperture in mature shells is much easier because the base of the body chamber is usually visible. We examined 10 mature specimens each of *H. nodosus* and *H. brevis* (five macroconchs and five microconchs in each sample for a total of 20 specimens). The angle of orientation of the aperture averages 102.2° and ranges from 90.5° to 109° (table 2).

In summary, our results indicate that the angle of orientation of the aperture is approximately 90° throughout ontogeny. However, the method employed involves at least three assumptions: (1) The phragmocone is completely filled with air. Liquid in the last few chambers effectively decreases the size of the phragmocone and increases the size of the body chamber (Saunders and Shapiro, 1986). We recalculated the centers of buoyancy and mass in a few of the specimens in our sample assuming a smaller phragmocone (minus the last two chambers) and a larger body chamber. The angle of orientation of the aperture increases by approximately 10°. (2) There is a uniform distribution of soft tissues in the body chamber. The presence of an aptychus-type jaw near the aperture effectively lengthens the body chamber, reducing the angle of orientation. Similarly, an extension of the soft body outside of the aperture decreases the

angle of orientation (Kakabadzė and Sharikadzė, 1993; Monks and Young, 1998). (3) There is no variation in shell thickness. The presence of a varix at the apertural margin decreases the angle of orientation.

The angle of orientation of the aperture probably varies within an acceptable range of values throughout ontogeny. This assumption lies at the foundation of most studies about the theoretical morphology of ammonoids (e.g., Okamoto, 1988). In the scaphites from the *Baculites compressus–B. cuneatus* zones, we have noted a correlation between the septal angle and the apertural angle in adults. This correlation is stronger in macroconchs of *Hoploscaphites brevis* than in macroconchs of *H. nodosus* (fig. 38A, B). It is particularly apparent in the combined sample of both species (fig. 38C). The apertural angle is higher in specimens in which the last septum occurs below the line of maximum length. This suggests that the two angles covary such that the aperture achieved a preferred orientation at maturity irrespective of the position of the last septum.

The high angle of orientation of the aperture in adult scaphites is incompatible with a nektobenthic mode of life involving scavenging or searching for food on the bottom, as exemplified by modern nautilus (Klinger, 1981; cf. Monks, 2000). This interpretation is supported by several morphological features of the adult shell. The apertural margin exhibits a constriction ending in a very thin lip. If the soft body extended downward to feed off the bottom, the lip would have easily broken off. In fact, the apertural margin is commonly intact in the thousands of specimens we have examined. In addition, the apertural opening is reduced in size by the constriction and accompanying varix as well as the dorsal extension of the shell. This reduction in the size of the opening would have impeded unrestricted movement of the soft body, further reducing access to the bottom. Trueman (1941: 374) reached this same conclusiton in his study of the mode of life of scaphites: "it is extremely difficult to understand how these forms could have been benthonic crawlers, as has commonly been suggested; the buoyant effect of the air-chambers would make such a mode of life almost impossible."

Lewy (1996) proposed an alternative explanation for the shape of the scaphite body chamber at maturity. According to him, the upwardly facing aperture and terminal constriction would have so impeded movement of the soft body that it would have resulted in death. Subsequently, the body chamber would have served as a floating egg case, wth the newly hatched young feeding on the carcasse of the dead female. He based this interpretation on the similarity of the scaphite body chamber to the egg case of present-day argonauts. Although the resemblance between these two shells is striking, as noted by previous authors, it is due to evolutionary convergence. The ammonite shell is secreted by the mantle, whereas the argonaut egg case is secreted by the glands of the expanded dorsal arms (Saul and Stadum, 2005).

Using nautilus as a model for swimming in ammonites suggests that scaphites were probably poor swimmers (but nautilus may not be the best model to use; see Jacobs and Landman, 1993). Scaphites lack large retractor muscles, which would have provided the propulsive power necessary for strong swimming. Such muscles may have existed in other ammonites based on the presence of scars on the internal surfaces of the shells (Doguzhaeva and Mutvei, 1996). In scaphites, there are only two types of muscle scars, the paired dorsal muscle scars and the unpaired midventral muscle scar (fig. 20). In addition, scaphites lack a hyponomic sinus on the midventer, which would have prevented the animal from extending its hyponome below the shell in order to swim forward. Therfore, scaphites may have been limited in their movement to swimming backward or downward (Westermann, 1996). Juvenile scaphites, with their compressed, closely coiled shells, may have been relatively efficient at slow, continuous swimming (Jacobs, 1992; Jacobs and Chamberlain, 1996). The uncoiling of the body chamber at maturity undoubtedly increased the stability and coefficient of drag, and decreased the hydrodynamic efficiency.

The poor swimming ability of scaphites, especially as adults, may have prevented them from migrating over long distances.

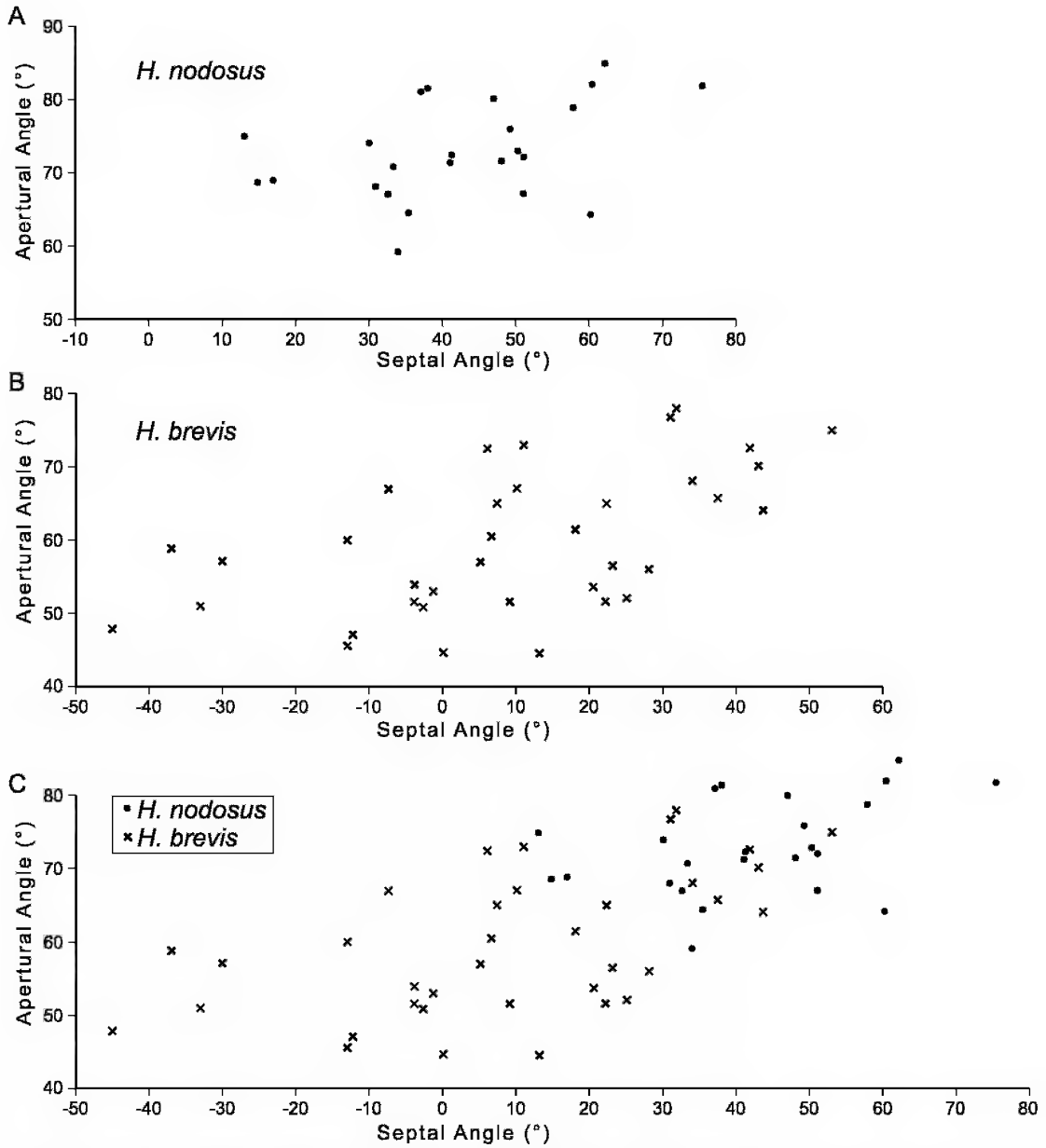

Fig. 38. Plot of septal angle versus apertural angle in macroconchs of *Hoploscaphites nodosus* (Owen, 1852) and *H. brevis* (Meek, 1876). The apertural angle is higher in specimens in which the last septum falls below the line of maximum length. This suggests that the two angles covary such that the aperture achieved a preferred orientation at maturity irrespective of the position of the last septum. Estimates are excluded. **A.** *Hoploscaphites nodosus* (Owen, 1852). (The smallest macroconch of *H. nodosus* [USNM 536270] is excluded). **B.** *Hoploscaphites brevis* (Meek, 1876). **C.** Total sample of *Hoploscaphites nodosus and H. brevis*.

Instead, they may have exploited a low-energy lifestyle, remaining at a single site for an extended period of time, subject to current activity. This interpretation is supported by two studies of scaphite species in the Western Interior Seaway. Jacobs et al. (1994) documented subtle but distinct differences in the shape of the adult shells of *Scaphites whitfieldi* from two regions approximately 225 km apart in South Dakota and Wyo-

ming. If the sites are time equivalent, it suggests that the populations from the two regions did not intermingle. In addition, Cochran et al. (2003) investigated strontium isotope ratios in *Hoploscaphites nebrascensis* (Meek, 1876) from various biofacies (e.g., brackish water, nearshore, offshore) in the Pierre Shale and Fox Hills Formation in South Dakota. The strontium isotope ratios in specimens from a single biofacies are similar to each other, and different from those in specimens from other biofacies. If the sites are time equivalent, this suggests that the scaphites did not migrate among biofacies.

The rate of growth, up to the onset of maturity, was probably the same in both dimorphs within a species, as indicated by the fact that the early whorls are indistinguishable between them. The uncoiling of the body chamber indicates the initiation of the mature growth program. One remarkable observation is that, after many years of study, we have never found a single scaphite preserved at the submature stage, that is, with the shaft of the body chamber in the process of formation. It is possible that the apertural margin at this stage was very thin and easily fragmented during fossilization. Another explanation is that the animal was very vulnerable to predation at this stage, and did not commonly survive. An example of a specimen that was killed at this stage is AMNH 55873 (fig. 12K, L). It is a broken microconch of *Hoploscaphites nodosus* with a lethal break on the adapical part of the shaft. What is unusual about this specimen is that the base of the body chamber is approximately 90° adapical of the line of maximum length, implying that the aperture was at the point of recurvature when the injury was inflicted. An additional explanation for the lack of shells at the submature stage is that the shaft may have formed rapidly, so that the chances of preserving it in the process of formation were low. Landman and Waage (1993) documented a reduction in the thickness of the shell wall and a weakening of the ribbing at midshaft in macroconchs of *H. nicolletii*, possibly reflecting an increase in the rate of growth. Of course, the growth rate decreased and eventually stopped at the attainment of maturity, as indicated by a reduction in the spacing of ribs and tubercles on the hook and the formation of a constriction and varix at the aperture. This stage also coincides with a decrease in septal spacing. The differences in the patterns of septal spacing between dimorphs, as described above, further imply that macroconchs experienced a longer period of slower growth. The larger size of macroconchs generally implies that they reached maturity later than microconchs. Depending on the age difference between them, macroconchs may have mated with microconchs from another year's cohort.

One of the most notable features of the scaphites from the *Baculites compressus–B. cuneatus* zones is that the largest ventrolateral tubercles appear on the midshaft (Riccardi, 1983; Landman and Waage, 1993; Monks, 2000) (fig. 17). In *Hoploscaphites nodosus*, these tubercles usually develop into subspinose clavi. The presence of such large tubercles on the midshaft would have protected the animal against predation from behind, presumably from its blind side. (The eyes may have been located in the reentrant on each side of the dorsal projection.) The ventrolateral tubercles diminish in size near the adult aperture. This may imply that attacks from below and from the front were less common. It is possible that the calcified aptychi of the lower jaws may have provided additional protection in the apertural region.

The presence of epizoans on ammonite shells also provides clues to the mode of life of these animals. Surprisingly, we have never observed a scaphite encrusted with epizoans that grew on it during its lifetime. The absence of such epizoans may be due to antifouling adaptations such as a thick periostracum or mucuslike covering (Landman et al., 1987). In contrast, specimens of scaphites with epizoans that settled on the ammonites after they died are not uncommon. For example, AMNH 56763 is a macroconch of *Hoploscaphites nodosus* with worm tubes on the inside surface of the body chamber, indicating that the specimen must have rested on the sea floor for an extended period of time (fig. 13K, L). There are reports of epizoans on the shells of other cephalopods in the Western Interior Seaway, but most of these specimens were encrusted by epizoans after death. Gill and

Cobban (1966) documented calcareous worm tubes and traces of other organisms on the steinkerns of body chambers of baculites from the Pierre Shale at Red Bird, Wyoming. Kase et al. (1998) reported limpets on *Placenticeras meeki* from the Pierre Shale of South Daktoa and Montana. One specimen is covered with 102 limpets on the left side and 21 on the right side. In most of these specimens, the limpets settled on the shells after the animals died and floated to the surface. Specimens of *Placenticeras* are also commonly encrusted with bryozoans (L. Larson and T. Linn, personal commun., 2008), but it is unclear whether the bryozoans settled on the ammonites before or after death. Dunbar (1928) documented bryozoans on a specimen of what he called *Sphenodiscus lenticularis mississippiensis* Hyatt from the Ripley Formation of Mississippi. The bryozoans settled on the ammonite while it was still alive based on the fact that the bryozoans are partly covered by the secretion of the next whorl. Landman et al. (1987) illustrated a specimen of *Eutrephoceras dekayi* (Morton, 1834) from the Fox Hills Formation encrusted by bryozoans and serpulids. These epizoans settled on the animal while it was alive and were later overgrown by subsequent whorls.

There is no direct evidence about the feeding habits of scaphites based on finds of stomach contents. Like many other members of the Aptychophora Engeser and Keupp, 2002 (= the aptychus-bearing ammonites), scaphites may have preyed upon small organisms in the water column, including decapod crustaceans, copepods, and newly hatched ammonites (Kennedy et al., 2002; Landman et al., 2007b). They may have also eaten larger prey, including juvenile ammonites and fish (Larson, 2003: 10, 11, fig. 13). Recent finds of radulae in *Baculites* and the scaphite *Rhaeboceras* have shed new light on this subject (Kruta et al., in prep). Although the morphology of the radula is basically the same in both genera, the teeth are shorter and more robust in *Rhaeboceras* than in *Baculites* (the large hooklike elements in *Rhaeboceras* previously interpreted as radulae are something else; see below). The difference in the shape of these teeth suggest that *Rhaeboceras*, and perhaps scaphites, in general, fed on slightly larger prey than did *Baculites*.

Reproduction in scaphites has received little attention. The high angle of orientation of the aperture in scaphites, as in many other heteromorphs (e.g., didymoceratids) presents challenges to copulation. In modern nautilus, the aperture is oriented at an angle of 30 ± 15°, allowing the two sexes to meet head on, with the male grasping the female using its jaws and cirri (Arnold, 1987). However, this method of copulation would not have been possible in scaphites without considerable gymnastics. It is much more likely that in scaphites, as in many modern coleoids, the male possessed a specially modified arm (the hectocotylus) that delivered the spermatophores to the female. The deployment of such an arm would have allowed the two sexes to mate head on or side by side. The best evidence of the existence of such a specially modified arm in scaphites is the presence of hooklike structures in association with *Hoploscaphites nicolletii* and *H. nebrascensis* from the upper Maastrichtian Fox Hills Formation (Landman and Waage, 1993: figs. 43–46) and the much larger, but otherwise similar structures in association with *Rhaeboceras* from the Campanian Bearpaw Shale (Kennedy et al., 2002). Hooklike structures are also present in association with species of *Hoploscaphites* from methane seeps in the Pierre shale in the *Baculites scotti–B. compressus* zones.

HABITAT

Hoploscaphites nodosus and H. brevis inhabited the central and northern part of the Western Interior Seaway. During the late Campanian, the sea flooded southern Alberta and central Montana, but the western two-thirds of Wyoming were emergent. The migration of the western shoreline at the time is illustrated in Gill and Cobban (1973). The western shoreline does not show a consistent pattern of displacement along strike due to local variation in tectonic activity, sedimentation rates, sediment supply, and accommodation rates (Krystinik and DeJarnett, 1995). Gill and Cobban (1973: 34) calculated that the transgression of the strandline across Montana occurred at a rate of approximately 115 km per million years (Gill and Cobban, 1973: 34).

Reconstructing the habitat of scaphites is difficult because these animals lived in the water column but are preserved in the sediments. We are interested in determining the environment in which the scaphites lived and, in particular, the depth below the sea surface and the height above the bottom. This information is derived from five sources: (1) the biofacies distribution of the scaphites; (2) the geographic distribution of the scaphites in the basin; (3) the presence of fauna associated with the scaphites and the inferred habitat and mode of life of such fauna; (4) the isotopic composition of the scaphites, especially in comparison with that of other faunal elements whose habitat and mode of life are known; and (5) the mechanical properties of the scaphite shells, as indicators of implosion depths and, by implication, habitat depths.

In evaluating most of this information, it is important to determine the origin of the fossil deposit. Is it a condensed sequence spanning hundreds of thousands of years? Do the fossils represent animals that lived at approximately the same time and in the same place or do they represent a time average of successive generations? In brief, does the fossil deposit reflect the living community? These issues have been widely discussed with respect to benthic organisms (e.g., Kidwell, 1991; Kidwell and Bosence, 1991). Ammonites pose special problems because they lived in the water column and, by definition, represent transported or "exotic" elements, necessarily creating a mixed fossil assemblage on the sea floor (Maeda and Seilacher, 1996). In addition, ammonites are prone to postmortem drift, in analogy with modern nautilus (House, 1987).

The most important piece of evidence to help distinguish between ammonites that sank soon after death and those that floated for an extended period of time is the presence of jaws preserved nearby or inside the ammonite shells. This association has generally been interpreted as indicating that the animals lived, died, and were preserved at approximately the same site (Tanabe, 1979; Landman et al., 2007a; Wani et al., 2005; Wani, 2007). If an ammonite floated after death, its soft body would have fallen out, and the jaw would have either been lost or preserved at a different site than the shell. Field studies of ammonite assemblages have suggested that postmortem drift is not as important a phenomenon as previously thought. In his study of the distribution of ammonite shell morphotypes in the Western Interior Seaway, Batt (1989) noted that certain mophotypes were restricted to particular parts of the basin and, therefore, concluded that postmortem drift was a relatively insignificant factor for most ammonites in shallow epicontinental seas.

Hoploscaphites nodosus and *H. brevis* occur in Alberta, Saskatchewan, Montana, North Dakota, South Dakota, Wyoming, Colorado, and Kansas. They are unknown outside of the Western Interior Basin of North America, including the Gulf Coastal Plain, although their absence in this area may be due to a lack of preservation. The abundance of scaphites diminishes toward the north. Such a decrease in molluscan diversity has previously been observed by Kauffman and Caldwell (1993), and presumably reflects the global decrease in diversity from the tropics to the poles. For example, at Porcupine Dome in east central Montana, scaphites are abundant and are associated with a rich molluscan fauna (Cobban, 1962a). This fauna becomes sparser toward the north, consisting mostly of only baculites and placenticeratids. Tsujita and Westermann (1998) noted that in the *Baculites compressus* Zone, scaphites are absent in western Alberta, and rare in eastern Alberta (Cypress Hills area). According to them, scaphites are absent altogether in Alberta in the transitional beds between the *B. compressus* and *B. cuneatus* zones and in the *B. cuneatus* Zone. They postulated that this absence was due to the existence of stagnant bottom waters trapped on the west side of the Sweetgrass Arch, which may have formed a slight submarine high during this time (Stelck, 1975).

The scaphites occur in a variety of biofacies ranging from nearshore to offshore environments. They are present in sandy, nearshore environments, as represented by the unnamed shale member of the Pierre Shale along the Front Range of the Rocky Mountains (Scott and Cobban, 1965, 1975, 1986a, 1986b), and the unnamed shale

member of the Pierre Shale near Kremmling, Colorado (Izett et al., 1971; Izett and Barclay, 1973; Cobban et al., 1992; Kennedy et al., 2000a). They are also present in more offshore deposits, as represented by the Pierre Shale and Bearpaw Shale in South Dakota and Montana, respectively. For example, they occur in the DeGrey Member of the Pierre Shale in Buffalo County, South Dakota, which was located several hundred kilometers to the east of the shoreline at the time (fig. 1). This site may have represented a shallow area east of the forebulge region (Cross and Pilger, 1978; Metz, 2008). The scaphites also occur in methane seep facies in the Pierre Shale in Custer County, South Dakota (see below).

In all probability, *Hoploscaphites nodosus* and *H. brevis* occupied all biofacies simultaneously. However, the level of biostratigraphic resolution available is inadequate to determine whether there is any diachroneity, that is, whether species appeared first in nearshore facies and subsequently migrated to offshore facies, or vice versa. The upper Maastrichtian Fox Hills Formation in north-central South Dakota is subdivided into assemblage zones, with several assemblage zones per ammonite zone (Landman and Waage, 1993), permitting a higher biostratigraphic resolution. The bio- and lithostratigraphic distributions of the scaphites in these strata were compiled by C. MacClintock (personal commun., 2008). According to his data, the lowest occurrence of both *H. nicolletii* and *H. spedeni* is in the offshore muds of the Mobridge Member of the Pierre Shale. Both species range into the nearshore silts of the Little Eagle lithofacies of the Trail City Member of the Fox Hills Formation and then disappear. These species are replaced by *H. comprimus* and *H. nebrascensis*. However, the lowest occurrence of these species differs depending on the lithofacies. In the upper part of the Little Eagle lithofacies, the lowest occurrence of these species is in the *Abyssinus* concretions, whereas in the muddy Irish Creek lithofacies, the lowest occurrence of these species is higher (just below the *Cucullaea* Assemblage Zone). This discrepancy may imply that these two species originated in the environment represented by the Little Eagle lithofacies, and then migrated into the environment represented by the Irish Creek lithofacies, perhaps reflecting a change in living conditions.

The scaphites in the *Baculites compressus–B. cuneatus* zones are almost always associated with an abundant, diverse benthic fauna. A rich association of scaphites and benthic fauna has been documented in sandstones and sandy shales in the Pierre Shale in Grand County, Colorado (Izett et al., 1971). These deposits represent a nearshore environment and contain 72 species, most of which are bivalves, in addition to 13 species of cephalopods (Sava, 2007), so that the total number of species equals 85 (this figure might be slightly inflated due to the assignment of incomplete specimens to new species [S. Klofak, personal commun., 2009]). The excellent preservation of the fossils suggests that they did not experience much postmortem transport. We have documented a more depauperate fauna consisting of 26 benthic species in addition to scaphites and baculites in a single concretion from the *Baculites compressus–B. cuneatus* zones in the Pierre Shale, Meade County, South Dakota, which represents a more offshore environment (Landman and Klofak, 2006). The concretion contains dozens of ammonite jaw fragments, indicating that the fauna was buried rapidly (within months to years). An association of scaphites and benthic fauna has also been observed by Tsujita and Westermann (1998) from the same biostratigraphic interval in the Bearpaw Shale in Montana. In other horizons in the Pierre Shale, for example, in the *B. grandis* Zone, scaphites are also usually associated with a diverse benthic fauna (Gill and Cobban, 1966).

The common association of scaphites and benthic species has generally been interpreted as indicating hospitable, that is, oxygen-rich episodes in the history of the Western Interior Seaway (Tsujita and Westermann, 1998: fig. 12). These faunal associations suggest that the same environmental factors that promoted the development of the benthic community also favored the proliferation of scaphites. Both the scaphites and the benthic species were probably part of a larger community including worms, crustaceans, fish, and mosasaurs. The association between scaphites and benthic

species further suggests that scaphites lived close to the sea floor (Landman and Waage, 1993: 25; Tsujita and Westermann, 1998: 144), but this interpretation is difficult to prove (see below). During periods of dysoxia, the scaphites, as well as the rest of the community, were excluded from the habitat.

The baculites provide an interesting comparison with the scaphites. The baculites are the most common ammonites in the Pierre Shale and Bearpaw Shale. They occur in association with benthic species but are not restricted to such associations. A notable example is the Sharon Springs Member of the Pierre Shale at Red Bird, Wyoming (Gill and Cobban, 1966). This unit contains fishes, mosasaurs, and baculites, with little or no benthic fauna aside from large flat-shelled inoceramids. The environment is interpreted as representing an anaerobic bottom with oxygenated water above (Byers, 1979). The presence of baculites in this unit suggests that they were relatively independent of the bottom. The baculites are also more geographically widespread than the scaphites in the Western Interior Seaway, making them more useful as index fossils. For example, in the *Baculites compressus–B. reesidei* zones in the Bearpaw Shale in Alberta, the baculites are much more widespread than the scaphites (Tsujita and Westermann, 1998: fig. 10). All this evidence suggests that the baculites lived higher up in the water column than the scaphites, and possibly made occasional forays into the dysoxic bottom waters below (Westermann, 1996).

The habitat of scaphites has also been determined on the basis of isotopic analyses of the shells (Forester et al., 1977; Tourtelot and Rye, 1969; Rye and Sommer, 1980; Wright, 1987). Whittaker et al. (1987) analyzed the oxygen and carbon isotopic composition of molluscs, including scaphites, from the lower Campanian Lea Park Formation of south-central Saskatchewan. They noted that the isotopic composition of scaphites was more similar to that of benthic inoceramids than to that of baculites, which suggested to them that scaphites lived closer to the sea floor than did baculites. He et al. (2005) examined the isotopic composition of molluscs from the *Baculites scotti–B. clinolobatus* zones in the Pierre Shale and Bearpaw Shale of the Western Interior. They noted that the isotopic composition of scaphites was very variable and overlapped that of didymoceratids and baculites. They assumed that baculites lived in the upper part of the water column and that didymoceratids, whose isotopic values were similar to those of benthic inoceramids, lived near the bottom. They, therefore, concluded that scaphites lived throughout the water column. Moriya et al. (2003) investigated the isotopic composition of ammonites as well as planktic and benthic foraminifera and benthic molluscs in the Campanian Yezo Group of Hokkaido, Japan. Although they did not explicitly analyze scaphites, they sampled a wide variety of ammonites including uncoiled heteromorphs. They concluded that the oxygen isotopic values of the ammonites more closely matched those of the benthic organisms than those of the planktic foraminifera, suggesting that the ammonites lived near the sea floor.

In such isotopic studies, it is important to consider the state of preservation of the samples. For example, in Whittaker et al. (1987), the samples consist of aragonitic shell material with nacreous microstructure. The authors used X-ray diffraction analysis to determine the suitability of these samples for isotopic study. However, Cochran et al. (2010) have argued that even material that is still mostly aragonite may have neverthess undergone alteration, yielding erroneous isotopic values. They proposed a screening protocol emphasizing scanning electron microscopy to assess the state of preservation of the nacre. In addition, in studies that compare the isotopic compositions of different organisms to document their respective habitats, it is important that the samples represent the same time interval. This can be approached through the examination of material from the same biostratigraphic zone or, even better, from the same concretion. Otherwise, the results can be misleading, reflecting variation in both environment and time. For example, He et al. (2005) compared the isotopic values of didymoceratids and scaphites in order to document their respective habitats, but the specimens they analyzed were collected from different biostratigraphic zones.

Habitat depths of scaphites have also been calculated based on the mechanical properties of the scaphite shell, especially its septa and siphuncle. Hewitt (1996: table 2) calculated the maximum habitat depth of several hundred ammonites including nine specimens of what he called *Hoploscaphites* spp. and *Jeletzkytes* spp. He stated that the most precise estimates were based on the mechanical strength of the septa. For *Hoploscaphites* spp., he reported a range of values from 53 to 185 m (both of these values are preceded by a question mark in his table). For *Jeletzkytes* spp., he reported a range of values from 20 (preceded by a question mark in his table) to 133 m. Tsujita and Westermann (1998) also calculated the maximum habitat depth of 11 scaphite specimens from the *Baculites compressus–B. reesidei* zones of the Bearpaw Shale using the same equations for septal strength as employed by Hewitt (1996). They calculated an average of 118 m for seven specimens of *Hoploscaphites nodosus*, 74.4 m for three specimens of *H. furnivali*, and 71.5 m for one specimen of *H.* sp. α. All these values represent maximum habitat depths and the scaphites may have, in fact, lived in shallower water. Landman et al. (2007a) estimated a habitat depth of 20–30 m for *Discoscaphites iris* (Conrad, 1858) from the upper Maastrichtian Tinton Formation of New Jersey, based on stratigraphic evidence and an estimate of sea level at the time.

METHANE SEEPS

Among the most interesting occurrences of scaphites in the Western Interior of North America are the Tepee Buttes. These unusual features in the Pierre Shale have been recognized since the late 19th century (Gilbert and Gulliver, 1895). Tepee Buttes are conical hills usually composed of limestone, up to 60 m in diameter, and 10 m in height (Fenneman, 1931). They have been documented from Montana to the Colorado–New Mexico border, and from the Front Range of the Rocky Mountains to western Kansas. They range in age from the late middle Campanian to the early Maastrichtian (Howe, 1987; Kauffman et al., 1996; Metz, 2008).

The presently accepted interpretation of the Tepee Buttes is that they were the sites of cold methane seeps. The source of the methane was nutrient rich brines or connate waters from the Pierre Shale and, possibly, the underlying Niobrara Formation. The methane was oxidized by chemosynthetic bacteria thereby increasing the concentration of CO_2 in the water, thus promoting authigenic precipitation of carbonate minerals. The presence of methane has been confirmed by isotopic analyses of the carbonate cements. Kauffman et al. (1996) reported that the carbonate cements in vent deposits from Colorado are extremely depleted in δ^{13} C (−40‰ to −45‰). Similarly negative values have been reported from Cretaceous vents in the Canadian Arctic (Beauchamp and Savard, 1992). Such negative values indicate that the carbon was derived from methane oxidation.

The seeps support an abundant and diverse community, including bivalves (notably, inoceramids and aggregations of chemosymbiotic-harboring lucinids), gastropods, ammonites, echinoderms, crabs (Bishop, 2000), sponges, tube worms, chemosynthetic bacteria, foraminifera, and radiolarians. Howe (1987) reported a diversity of approximately 30 molluscan species at single seeps from the upper Campanian of Colorado. In their studies of these sites, Kauffman et al. (1996: fig. 3) documented a zonation of macrofaunal and microfaunal assemblages distributed from the center of the vents to the adjacent sea floor, reflecting, according to them, an environmental stress gradient with decreasing H_2S. The most diverse assemblage, consisting mostly of molluscs, occurred on the upper part of the flanks, downcurrent from the immediate vicinity of the methane emissions. In contrast, the sea floor adjacent to the vents was relatively depauperate, and may have been characterized by dysoxic water conditions.

It is unknown if these seeps represented topographical highs on the sea floor, or formed below or at the sediment-water interface (Shapiro and Fricke, 2002). However, the presence of fallen slump blocks on the sides dipping away from the central conduits suggests some relief (Kauffman et al., 1996). A single seep may have perisisted over a time span of 1.25 million years (Kauffman et al., 1996). During this interval,

the seep may have episodically stopped, started, collapsed, and restarted again nearby, depending on the source of the methane and the intricacies of the plumbing network.

The geographic distribution of cold seep deposits in the Western Interior of North America may be related to underlying structural features, as well as the overall tectonics of the foreland basin. In Colorado, the seep deposits are aligned along early Laramide basement faults parallel to the Front Range of the Rocky Mountains (Howe, 1987). In South Dakota, they form a ring around the Black Hills, suggesting that a series of faults existed in this area during the Late Cretaceous. Metz (2008) analyzed the geographic and temporal distribution of cold seeps in the Western Interor Basin, and suggested that they are associated with the development of the forebulge depozone. She argued that the formation of cold seeps coincided with transgressive episodes, which involved an increase in sediment loading near the orogenic belt, and an increase in the degree of flexure of the forebulge, which, in turn, promoted the migration of cold seep fluids from the underlying sediment. In contrast, the cessation of seep activity coincided with regressive episodes, which involved a decrease in sediment loading near the orogenic belt, and a decrease in the degree of flexure of the forebulge.

We examined and collected from methane seeps in the *Didymoceras cheyennense* and *Baculites compressus* zones in Custer County, South Dakota, as well as from older seeps in Butte County, South Dakota. The seep from the *Didymoceras cheyennense* Zone is exposed in cross section at AMNH loc. 3418. The outcrop is nearly vertical and is approximately 13 m high and 20 m wide. The central area consists of multiple, anastomosing pipelike conduits composed of limestone, surrounded by grey shale with orange-weathering partings. Fossils are abundant for a distance of approximately 6 m on either side of the central area. Some of the fossils are preserved in the sediment and others are preserved in limestone concretions. In both instances, they retain their original shell. The sediments on the outer margins of the vent, up to 20 m away, are much darker black, with fewer fossils.

The fossils immediately surrounding the central area include *Hoploscaphites nodosus*, *H. brevis*, *Baculites corrugatus* Elias, 1933, *Didymoceras cheyennense* (Meek and Hayden, 1856b), *Spiroxybeloceras meekanum*, *Nympholucina occidentalis* (Morton, 1842), "*Inoceramus*" *altus*, "*Inoceramus*" *sagensis* Owen, 1852, crinoids, and sponges (fig. 39). Many of the shells are broken, probably as a result of predatory activity. For example, a microconch of *H. brevis* shows a missing chunk from the adapical end of the body chamber, indicating a lethal injury (fig. 39I, J). In addition, a macroconch of *Baculites corrugatus* shows a series of small scalloped edges along the entire length of the body chamber on both sides, indicating that an animal, possibly a crab, systematically gnawed off pieces of the baculite shell after death (fig. 39A, B). Several pieces of evidence suggest that the shell debris in the seep was buried rapidly: (1) the phragmocones of many baculites are hollow; (2) all of the lucinids are articulated; and (3) isolated jaws of scaphites are present.

The seeps from the *Baculites compressus* Zone appear as carbonate mounds. We recorded five such mounds within a radius of 100 m, representing a vent field. The two largest mounds (AMNH locs. 3419 and 3420) are each approximately 5–10 m across and 3 m high. The three smaller mounds (AMNH locs. 3457, 3457a, 3457b) are grouped around AMNH loc. 3420, and are each 2–4 m across and 1–2 m high. The mounds consist of heavily cemented limestone, superficially resembling Paleozoic reefs. This high degree of cementation suggests a late stage in vent development, as described by Beauchamp and Savard (1992) for Late Cretaceous vents from the Canadian Arctic.

Because of the heavy cementation of the mounds, it is difficult to establish a zonation from the center of the vents to the margins. The mounds are riddled with conduits filled with limestone and deposits of sparry calcite. The fauna in the mounds is extremely diverse (fig. 40) and includes *Hoploscaphites nodosus*, *H. brevis*, *Baculites compressus*, *Baculites corrugatus*, *Placenticeras* sp., *Nympholucina occidentalis*, "*Inoceramus*" *altus*, "*Inoceramus*" *sagensis*, gastropods, boring teredos, sea urchins, articulate crinoids, bryozoans,

Fig. 39. Fossil invertebrates from a cold seep in the Pierre Shale, *Didymoceras cheyennense* Zone, AMNH loc. 3418, Custer County, South Dakota. **A, B.** *Baculites corrugatus* Elias, 1933, mature macroconch, AMNH 58552, uncoated. Note the series of small scalloped edges along the entire length of the body chamber on both sides (arrows), probably reflecting predation. **A.** Ventral, with apertural projection on top; **B.** right lateral, with apertural projection on top. **C.** *Didymoceras cheyennense* (Meek

sponges, serpulid worm tubes, and stromatolitelike sheets (microbialites). In contrast, the surrounding grey shale contains few fossils.

The species of scaphites at the methane seeps are the same as those elsewhere in the Western Interior Seaway. However, the presence of scaphites at these seeps poses some interesting questions: How did the scaphites arrive at the seeps? Did they live their entire lives at the seeps or did they wander back and forth between the seeps and the surrounding sea floor? How did the scaphites die at the seeps—by H_2S poisoning or by predators? Although we are planning further studies in the future, some data are already available to answer these questions. We have recovered juvenile and adult scaphites at the seeps from both the *Didymocerass cheyennense* and *Baculites compressus* zones. Thus, both juvenile and adult scaphites lived, died, and were buried at the seeps, although it is unclear whether a single individual lived its entire life there. In addition, we have observed specimens with both lethal and sublethal injuries, indicating that the scaphites were subject to predators, which must also have lived at the site.

To further answer these questions, we are analyzing the isotopic composition of the scaphites from the seep in the *Didymoceras cheyennense* Zone. Previous studies have shown that carbonate cements precipitated at methane seeps are strongly depleted in carbon (e.g., Kauffman et al., 1996). Presumably, this depletion is also reflected in the shells of the animals living at the vents, provided that the shell material is well enough preserved. These results may reveal whether the scaphites lived at the vents all the time or only visited occasionally.

SYSTEMATIC PALEONTOLOGY

CLASS CEPHALOPODA CUVIER, 1797
ORDER AMMONOIDEA ZITTEL, 1884
SUBORDER ANCYLOCERATINA WIEDMANN, 1966
SUPERFAMILY SCAPHITOIDEA GILL, 1871
FAMILY SCAPHITIDAE GILL, 1871
SUBFAMILY SCAPHITINAE GILL, 1871

Genus *Hoploscaphites* Nowak, 1911

TYPE SPECIES: *Ammonites constrictus* J. Sowerby, 1817: 189, pl. A, fig. 1, by original designation.

EXPANDED DIAGNOSIS: Small to large scaphites, strongly dimorphic, with broad variation in degree of whorl compression ranging from slender to robust, with involute phragmocone, short to long shaft, and weakly recurved hook; apertural angle ranging from approximately 35° to 85°; aperture constricted with dorsal projection; ribs straight to flexuous, increasing by branching and intercalation, with weak to strong adoral projection on venter; adult shell with or without umbilicolateral, flank, and ventrolateral tubercles; suture fairly indented, with symmetrically to slightly asymmetrically bifid first lateral lobe.

DISCUSSION: The scaphites of the "*nodosus* group" have fluctuated in their taxonomic assignment since their original description. Owen (1852) assigned *nodosus* to *Scaphites* Parkinson, 1811, the only genus of scaphites available at the time, although he had misgivings based on his uncertainty about the distinction between *Scaphites* and *Ammonites*. Owen (1852: 580) wrote "Unless some far more persistent character can be found on which to establish the genus *Scaphites*, than has yet been presented to us

---

←

and Hayden, 1856b), fragment, AMNH 63440. **D.** Lower jaw attributed to *Hoploscaphites*, AMNH 63423. **E.** *Nympholucina occidentalis* (Morton, 1842), AMNH 66246. **F.** Whorl cross section at the adoral end of a fragment of *Baculites corrugatus* Elias, 1933, AMNH 66245. **G.** *Crassatella evansi* Hall and Meek, 1856, AMNH 66241. **H.** "*Inoceramus*" *sagensis* Owen, 1852, AMNH 66248. **I, J.** Finely ornamented fragment of a microconch of *Hoploscaphites brevis* (Meek, 1876), AMNH 66242. **I.** Right lateral; **J.** ventral. Specimens are illustrated natural size unless indicated otherwise by a scale bar.

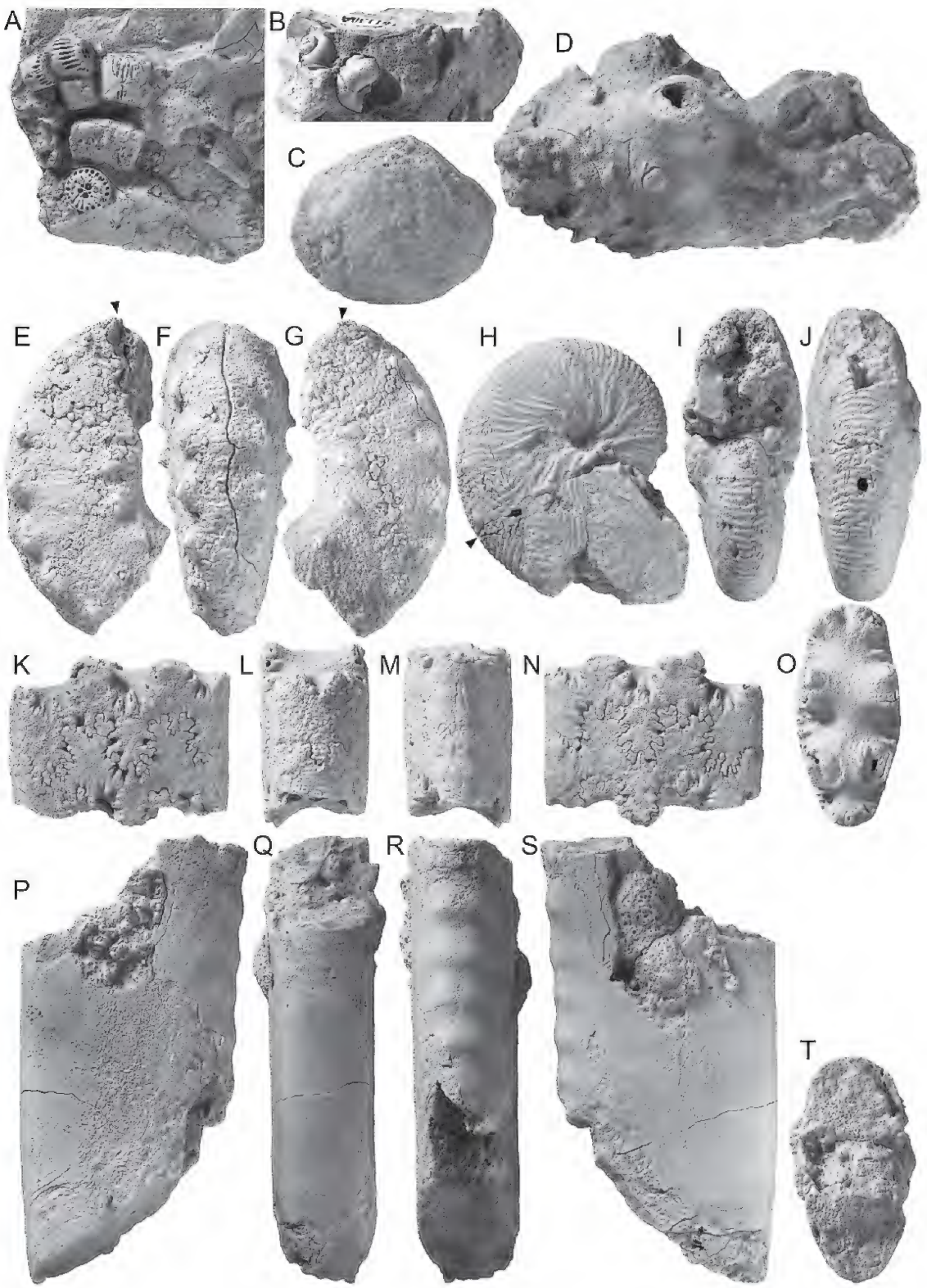
A
B
C
D
E
F
G
H
I
J
K
L
M
N
O
P
Q
R
S
T

by palaeontologists, the genus must be entirely abandoned and merged in the genus Ammonite [sic], and the boat-shaped convolution and absence of septae in the terminal part, must be regarded as *specific* and not *generic* distinctions [Owen's italics]." Meek (1876: 414) accepted Owen's assignment of *nodosus* to *Scaphites* and described *brevis*, *quadrangularis*, and *plenus* as varieties of *nodosus*. He grouped these forms together into the "*nodosus* group" and noted that they differ from other *Scaphites* "chiefly in form, by having the involute part generally proportionally larger, and the deflected part shorter; also in having periphery of body-part more or less flattened, with a row of nodes along each of its margins, and sometimes another near the umbilicus."

Over the succeeding 150 years, the scaphites of the "*nodosus* group" have been variously assigned to *Scaphites* by Whitfield (1880), Gilbert (1896), Logan (1898, 1899), Smith (1905), Weller (1907), Frech (1915), Diener (1916), Stephenson (1941), Donovan (1953), Jeletzky (1960, 1962, 1968, 1970), Birkelund (1965, 1966), and Atabekyan and Khakimov (1976); *Hoploscaphites* by Gill and Cobban (1966), Hirsch (1975), and Kauffman (1977); *Acanthoscaphites* by Nowak (1916), Reeside (1927a), Elias (1933), Coryell and Salmon (1934), Landes (1940), and Cobban and Reeside (1952); and, most recently, *Jeletzkytes* by Riccardi (1983), Cobban et al. (1992, 1994), Kennedy and Cobban (1993), Kennedy et al. (2000b), Landman and Waage (1993), Landman and Cobban (2003), and Larson et al. (1997). Not surprisingly, many of the generic diagnoses themselves have changed over time.

We briefly summarize the taxonomic history of these scaphite genera and reexamine the present assignment of the "*nodosus* group" to *Jeletzkytes*. The genus *Scaphites* has been thoroughly treated by Cobban (1951b), Cobban and Kennedy (1991), Wiedmann (1965), Kennedy (1984, 1988), Cooper (1990), and Landman (1987). In his analysis of the relationships of scaphite genera, Cooper (1994: 166) provided the following description of the genus:

> *Scaphites* (Parkinson 1811)... is the most long ranging (? broadly interpreted) genus in the superfamily. It is characterized by an involute phragmocone, scaphitoid body chamber with moderately long shaft, strongly recurved hook, constricted aperture with acute apertural angle, early whorls that are always depressed but which later may become slightly compressed, and simple straight or flexuous ribs which bifurcate and are joined by intercalatories across the venter. The suture has a bifid L, a pseudolobe (p) to L/U and accessory saddles. In addition, ribbing is commonly interrupted or weakens at the base of the adult body chamber and many species develop umbilical and ventrolateral tubercles on the last part of the phragmocone and body chamber; a few derived species even develop lateral tubercles.

This genus ranges from the Albian to the Campanian.

In a study of Late Cretaceous scaphites from Poland, Nowak (1911: 565) introduced the genus *Hoploscaphites*, which he based primarily on *Scaphites constrictus* J. Sowerby, 1817, and its variants. In his diagnosis of the genus, Nowak cited the compressed, involute shape of the shell and the ornamentation consisting of "arched ribs, which at the

←

Fig. 40. Invertebrate fossils from cold seeps in the Pierre Shale, *Baculites compressus* Zone, AMNH locs. 3419, 3420, Custer County, South Dakota. **A.** Articulate crinoid columnals, AMNH 66260. **B.** Small gastropods, AMNH 61130A. **C.** *Nympholucina occidentalis* (Morton, 1842), AMNH 66251. **D.** Sponge, AMNH 66249. **E–G.** *Hoploscaphites brevis* (Meek, 1876), part of the body chamber of a microconch, AMNH 61122. **E.** Right lateral; **F.** ventral; **G.** left lateral. **H–J.** *Hoploscaphites brevis* (Meek, 1876), phragmocone of a mature macroconch, AMNH 61135. **H.** Right lateral; **I.** apertural; **J.** ventral. **K–O.** *Baculites compressus* (Say, 1820), AMNH 58558. **K.** Right lateral; **L.** dorsal; **M.** ventral; **N.** left lateral; **O.** whorl cross section at the adoral end. **P–T.** *Baculites compressus* (Say, 1820), AMNH 58544. **P.** Right lateral; **Q.** dorsal; **R.** ventral; **S.** left lateral; **T.** whorl cross section at the adoral end. Specimens are illustrated natural size.

middle of the flank and on the venter are bent forward; they fork at different heights on the flank without forming nodes." However, in his description of the type species, Nowak also noted the presence of forms with umbilicolateral and ventrolateral tubercles. The concept of *Hoploscaphites* has been subsequently refined through the work of Reeside (1927a), Cobban and Jeletzky (1965), Birkelund (1965, 1979), Jeletzky and Waage (1978), Landman and Waage (1993), Kennedy (1986b), and Machalski (2005a, 2005b). In its present usage, the genus includes slender nontuberculate species such as *Hoploscaphites greenlandicus* Donovan, 1953, and more robust species with umbilicolateral, ventrolateral, and flank tubercles such as *Hoploscaphites comprimus*. The genus ranges from the lower Campanian to the upper Maastrichtian although Crick (1978: 18) recorded a species of *Hoploscaphites* from the Turonian of Kansas.

Nowak (1911: 565) also introduced the genus *Acanthoscaphites* based on *Scaphites tridens* Kner, 1848, and its variants. The genus has been revised by Reeside (1927a), Kennedy (1987), Kennedy and Summesberger (1987), and Jagt et al. (1999). It includes large specimens, with a slightly uncoiled body chamber that remains in contact with the phragmocone. The number of rows of tubercles on the adult shell varies, but the adoral part of the body chamber almost always bears ventral and ventrolateral tubercles. Machalski (2005b: 681, 682) pointed out that ventral swellings also occur in some species of *Hoploscaphites*, but that such swellings never develop into tubercles, as in *Acanthoscaphites*. The genus is restricted to the Maastrichtian.

Riccardi (1983: 14) reassigned the scaphites of the "*nodosus* group" to his new genus *Jeletzkytes*, with *Scaphites nodosus* Owen, 1852, as type species. He provided the following diagnosis:

> Relatively large scaphitids, with involute phragmocone; body chamber with short shaft extending slightly beyond the phragmocone and weakly recurved hook; whorl section remaining depressed throughout the phragmocone and body chamber, or varying from depressed to slightly compressed during the ontogeny; ribs almost straight to weakly projected and flexuous; earlier representatives with stronger and sparser ribbing and bearing prominent lateral and ventrolateral tubercles on the body chamber; younger representatives with relatively finer and denser ribbing, and 2–3 rows of lateral nodes in the phragmocone, which tend to fade away on the flanks of the body chamber. Suture fairly indented, becoming more complex from older to younger species.

This genus has been reviewed by Cobban et al. (1992), Cobban and Kennedy, (1994), Kennedy and Cobban (1993), Kennedy et al. (1998), Landman and Waage (1993), Landman and Cobban (2003), and Larson et al. (1997). It ranges from the lower Campanian to the upper Maastrichtian.

Riccardi (1983: 14) acknowledged difficulties from the start with his new genus because of its close similarity to the existing genus *Hoploscaphites*. For example, he noted that "the similarities between some of the late representatives of the '*nodosus* group' and *H. constrictus* Sowerby have led on several occasions to identification of some representatives of the former with this latter, or other related, species." He also added that "the similarities between some probable macroconchs, i.e., *J. brevis* and some large specimens of *H. constrictus*, between the probable microconchs, i.e., *J. quadrangularis*, *S. pungens* and some small representatives of *H. constrictus*, is undeniable." Nevertheless, based on an examination of the bulk of Campanian to Maastrichtian material from the Bearpaw Shale, Riccardi (1983: 14) argued that two groups of scaphites were present, one group consisting of slender, finely ornamented forms, which he assigned to *Hoploscaphites*, and another group consisting of robust, coarsely ornamented forms, which he assigned to *Jeletzkytes*. He stated that "when most of the described and figured material of several species is taken into consideration it is possible to recognize two closely related groups of species." This expressed the widely held belief that there were two lineages of scaphites in the Campanian and Maastrichtian that evolved in parallel.

There are three problems with the concept of *Jeletzkytes:*

(1) Intergradation of *Jeletzkytes* and *Hoploscaphites*

One vexing problem in assigning specimens to *Jeletzkytes* or *Hoploscaphites* is the existence of transitional forms, which reflect a morphological continuum. In his discussion of *Hoploscaphites*, Riccardi (1983: 10) noted that some species assigned to this genus, for example, *H. landesi*, exhibit umbilicolateral bullae on the body chamber and are, therefore, "transitional" to *Jeletzkytes*. However, this is only the tip of the iceberg. Riccardi's collection of scaphites from the entire Bearpaw Shale consisted of fewer than 80 specimens, most of which were only parts of phragmocones. In larger collections, transitional forms between the two "genera" are very common, and reflect an intergradation from compressed forms with flexuous ribs and weak tubercles to robust forms with straight ribs and strong tubercles. The assignment of such transitional specimens to one genus or the other is problematic and completely arbitrary. This morphological intergradation is evident in large collections from the *Baculites compressus–B. cuneatus* zones as well as from other biostratigraphic zones in the Pierre Shale and Bearpaw Shale.

A similar range of variation has been documented in the genus *Hoploscaphites* itself. For example, Kennedy (1986b) described specimens of *H. constrictus*, the type species of the genus, from the Maastrichtian of the Cotentin Peninsula, France, which show a range from compressed to depressed forms (compare Kennedy, 1986b: pl 13, fig. 6 and pl. 15, fig. 30). The more robust forms could be assigned to *Jeletzkytes*. Machalski (2005b: fig. 12A–D) has also described subspecies of *H. constrictus* from northern Europe that approach *Jeletzkytes* in terms of the coarseness of their ribs and the size of their tubercles. Landman and Waage (1993: fig. 71A–E) illustrated specimens of *H. comprimus* from the Maastrichtian of South Dakota that bear flank tubercles, a feature usually associated with *Jeletzkytes*. Thus, the genus *Hoploscaphites* itself displays a wide range of variation in degree of whorl compression and coarseness of ornament. This range of variation overlaps with that of *Jeletzkytes*, so that in large collections, the two genera intergrade. Wright (1996: 261, 262) cited the wide range of variation in scaphites as the reason for treating *Jeletzkytes* as a synonym of *Hoploscaphites*. He wrote "Separation of the large and inflated species of the *nodosus* group as *Jeletzkytes* seems unnecessary, given the great variation within most scaphitid species."

(2) Degree of evolutionary convergence

Although an explicit phylogenetic treatment of all species of *Hoploscaphites* and *Jeletzkyte*s is not possible at this time, a stratigraphic examination of specimens based on material from the U.S. Western Interior, reveals that cooccurring species of *Jeletzkytes* and *Hoploscaphites* bear more in common with each other than with congeneric species from other horizons. For example, in species of both "genera" from the *Baculites compressus–B. cuneatus* zones of the Pierre Shale, the ventrolateral tubercles on the exposed phragmocone are widely and irregularly spaced. In contrast, in species of both "genera" from the *B. eliasi–B. baculus* zones of the Pierre Shale, the ventrolateral tubercles on the exposed phragmocone are more closely and evenly spaced. Furthermore, in species of both "genera" from the *B. compressus–B. baculus* zones of the Pierre Shale, only two rows of tubercles are present (the umbilicolateral and ventrolateral tubercles), whereas in species of both "genera" from the *B. grandis* Zone of the Pierre Shale, an additional one or two rows of flank tubercles appear on the exposed phragmocone.

(3) Endemism of *Jeletzkytes*

One rationale for establishing the genus *Jeletzkytes* was the presumption that it was primarily endemic to the Western Interior of North America, a view widely echoed by many other authors, for example, Monks (2000). However, Riccardi (1983: 15) hypothesized that *Jeletzkytes* may also have been present in Europe at the end of the Campanian. In fact, there are many examples of this "genus" outside of the Western Interior of North America. *Jeletzkytes compressus* (Roemer, 1841) is similar to *Hoploscaphites nodosus* but is more finely ribbed with a more ovate whorl section. It is present on the Atlantic Coastal Plain as well as in Europe, including northern Ireland, northern Germany, and the Vistula River Valley, Poland (Kennedy and Cobban, 1994; Kennedy and Christensen, 1997; Kennedy and Kaplan, 1997; Niebuhr,

1996). In fact, it has not been reported from the Western Interior of North America, although it may occur in parts of the *Exiteloceras jenneyi* and *Didymoceras cheyennense* zones in the Pierre Shale. *Acanthoscaphites praequadrispinosus* is also a member of the "*nodosus* group." It is present in the Vistula River Valley, Poland, and, possibly, in the *Baculites reesidei* Zone in the Pierre Shale and Bearpaw Shale in North America. *Jeletzkytes nebrascensis* occurs in the Fox Hills Formation in north-central South Dakota but is also present in the Severn Formation in Maryland. These and other occurrences suggest that *Jeletzkytes* is not restricted to the Western Interior of North America.

We, therefore, provisionally treat *Jeletzkytes* as a junior subjective synonym of *Hoploscaphites*. The shape of the shell, the pattern of ornament, and the complexity of the suture are the same in both genera. The only difference between them is the degree of compression and, as a consequence, the flexuosity of the ribs and the size of the tubercles. As noted, such variation is also present in *Hoploscaphites* itself, including the type species *H. constrictus*. Variation in robustness may be related to the rate of growth and timing of maturation (see the section on variation within and between species). Our broad defintion of *Hoploscaphites* is consistent with the present-day concepts of other scaphite genera such as *Discoscaphites*, which includes both compressed and depressed forms (Jeletzky and Waage, 1978), and *Trachyscaphites*, which also embraces variation in ornament and degree of whorl compression (Cobban and Scott, 1964; Cobban and Kennedy, 1992).

This approach has both practical and theoretical advantages. It eliminates the difficulties of determining the generic assignment of specimens that are transitional between *Jeletzkytes* and *Hoploscaphites*. It also reduces the implied level of convergence necessary to explain the lockstep evolutionary patterns of these scaphites through the Campanian and Maastrichtian. In addition, it reopens the discussion about the degree of endemism of the scaphites in the Western Interior. However, it does not resolve the issue of the relationship between *Hoploscaphites* and *Scaphites*. For example, *S. binodosus* Roemer, 1841, which closely resembles undescribed species of *Hoploscaphites* from the lower Campanian of the Western Interior, is currently assigned to *Scaphites*, as described by Kennedy (1986a) and Kennedy and Kaplan (1995). Similarly, *S. cobbani* Birkelund, 1965, and *S. rosenkrantzi* Birkelund, 1965, from the lower Campanian of Greenland closely resemble undescribed specimens of the "*nodosus* group" from equivalent age strata in the Western Interior. These and other problems will be confronted in future work on the phylogeny of the Campanian-Maastrictian scaphites.

Hoploscaphites nodosus (Owen, 1852)
Figures 4, 12K, L, 13K, L, 15D–F, 17, 18A, B, 19B, C, 20A, B, D, E, 21C, D, 22C–E, 34H, I, 35B–D, 36D–F, 37, 38A, 41–57, 58D–F, 59D, E, 60–77

1852. *Scaphites* (*Ammonites*?) *nodosus* (N.S.). Owen, p. 581, pl. 8, fig. 4 (printed at less than ×1, in mirror image).
1856. *Scaphites nodosus*, Owen. Hall and Meek, p. 405.
1856e. *Scaphites nodosus*, Owen. Meek and Hayden, p. 281.
? 1859. *Scaphites nodosus* (?) var. Meek, p. 185, pl. 2, figs. 7, 8 (unidentifiable because the drawing is inaccurate).
? 1879. *Scaphites nodosus* Owen. White, p. 186.
1880. *Scaphites nodosus* Owen. Whitfield, p. 441, pl. 13, fig. 12.
pars 1885. *Scaphites nodosus*, Owen. Whiteaves, p. 52.
? 1887. *Scaphites nodosus*, Owen. Stanton, p. 185.
? 1889. *Scaphites nodosus*, Owen. Whiteaves, p. 182.
non 1892. *Scaphites nodosus* Owen. Whitfield, p. 261, pl. 44, figs. 13, 14.
non 1896. *Scaphites nodosus*. Gilbert, pl. 63, fig. 3; pl. 65, fig. 2.
? 1899. *Scaphites nodosus* Meek. Logan, pl. 22, fig. 2 (= ?*Hoploscaphites plenus* M); pl. 23, figs. 1–4, 6–12 (unidentifiable because they are only sutures and drawings of ontogenetic stages).
non 1903. *Scaphites nodosus*. Barbour, pl. 6, fig. 6 (= *Scaphites nodosus* var. *brevis* Meek, 1876, p. 426, pl. 25, fig. 1).
? 1905. *Scaphites nodosus* (Owen). Smith, p. 638, fig. 3.14 (suture).
non 1907. *Scaphites nodosus* Owen. Chamberlin and Salisbury, fig. 417d (=*Scaphites nodosus* var. *brevis* Meek, 1876, p. 426, pl. 25, fig. 1).
non 1907. *Scaphites nodosus* Owen? Weller, p. 824, pl. 107, figs. 1, 2.

non 1911. *Scaphites nodosus* Owen. Haug, pl. 118 (= *Hoploscaphites brevis* m).
? 1916. *Scaphites nodosus* Owen. Diener, p. 565, text fig. 6 (first three sutures only, after Smith, 1905).
1917. *Scaphites nodosus* Owen. Dowling, p. 32, pl. 32, fig. 3 (= Owen, 1852, pl. 8, fig. 4).
non 1933. *Acanthoscaphites nodosus* (Owen). Elias, p. 320, pl. 38, figs. 1–3 (it is listed as "Say" in figure captions and "(Owen)" in text).
1940. *Acanthoscaphites nodosus* (Owen). Landes, p. 177, 178.
1944. *Acanthoscaphites nodosus* (Owen, *non* Lopuski). Shimer and Shrock, p. 591, pl. 246, fig. 3 (= Owen, 1852, pl. 8, fig. 4).
1949. *Scaphites nodosus*. Dunbar, pl. 16, fig. 10 (drawing).
non 1952. *Acanthoscaphites nodosus* (Owen *non* Lopuski). Fisher, p. 9, pl. 4, figs. 1–3 (= ?*Hoploscaphites criptonodosus*).
1960. *Scaphites nodosus*. Dunbar, pl. 16, fig. 10 (drawing).
1962. *Acanthoscaphites*. Rhodes et al., p. 130, unnumbered fig.
1970. *Scaphites nodosus* Owen. Jeletzky, pl. 27, fig. 7.
1974. *Scaphites*. Hamilton et al., p. 259, unnumbered fig.
1975. *Hoploscaphites nodosus* (Owen). Hirsch, p. 111, fig. 9B (locality is probably wrong).
1975. *Scaphites*. Nelson, pl. 64, figs. 1, 2 (= Jeletzky, 1970, pl. 27, fig. 7).
1982. *Acanthoscaphites nodosus* (Owen). Case, p. 83, fig. 12.30.
1982. *Scaphites nodosus*. Fortey, fig. 21.
1983. *Jeletzkytes nodosus* (Owen, 1852). Riccardi, p. 15, pl. 2, figs. 1–3; text figs. 5, 7a (= Owen, 1852, pl. 8, fig. 4); figs. 4–8; text fig. 6 (= Jeletzky, 1970, pl. 27, fig. 7).
non 1983. *Jeletzkytes* aff. *nodosus* (Owen, 1852). Riccardi, p. 18, pl. 3, figs. 2–6; text fig. 7b; pl. 4, figs. 1, 2.
non 1983. *Jeletzkytes cf. nodosus* (Owen, 1852). Riccardi, p. 18, pl. 3, fig. 1.
1991. *Scaphites nodosus*. Fortey, fig. 21.
1992. *Acanthoscaphites nodosus* (Owen). Case, p. 83, fig. 12.30.
1992. *Jeletzkytes nodosus* (Owen, 1852). Cobban et al., p. A8, pl. 3, figs. 2–5, 7–11.
non 1993. *Jeletzkytes nodosus* (Owen, 1852). Kennedy and Cobban, p. 430, figs.? 9.5; 17.22–17.25.
non 1994. *Jeletzkytes nodosus* (Owen, 1852). Cobban and Kennedy, p. B8, pl. 9, figs. 7–11.
non 1995. *Jeletzkytes nodosus* (Owen, 1852). Kennedy and Kaplan, pl. 29.
1997. *Jeletzkytes nodosus* (Owen, 1852). Larson et al., p. 76 and unnumbered figs.
1997. *Scaphites nodosus*. Lebrun, p. 179.
1999. *Jeletzkytes nodosus*. Larson, p. 11.
non 2000b. *Jeletzkytes* cf. *J. nodosus* (Owen, 1852). Kennedy et al.: 20, figs. 9J–P, 10, 11, 12C–F.
2002. *Scaphites nodosus*. Monks and Palmer, p. 74, pl. 15 (? enlarged).
2003. *Jeletzkytes nodosus*. Larson, p. 5, fig. 6; p. 20, fig. 27; p. 21, fig. 32.
2009. *Jeletzkytes nodosus*. Larson, p. 206, unnumbered figure.

DIAGNOSIS: Adult shells robust with relatively long shaft and recurved hook, leaving gap between exposed phragmocone and point of recurvature; apertural angle averaging 73° in macroconchs; ellipsoidal outline in side view, with straight umbilical seam in macroconchs and concave umbilical seam in microconchs; intercostal whorl section of body chamber ovoid to subquadrate with fairly flat flanks; whorl height nearly constant in body chamber reaching a maximum just adoral of midshaft; ornament consisting of slightly flexuous primary and secondary ribs and bullate umbilicolateral and clavate ventrolateral tubercles; ventrolateral tubercles unevenly spaced on exposed phragmocone becoming more or less evenly spaced on shaft, reaching maximum size at midshaft; suture with broad, asymmetrically bifid first lateral saddle and narrow, symmetrically to asymmetrically bifid first lateral lobe.

TYPE: Holotype, by monotypy, is UC 6381, the original of *Scaphites nodosus* Owen (1852: pl. 8, fig. 4). It is probably from the *Baculites cuneatus* Zone of the Pierre Shale near Sage Creek, Pennington County, South Dakota (fig. 4). It was figured by Owen at slightly less than natural size in mirror image, so that the side shown is actually the left side. It is a large macroconch and consists of the phragmocone and most of the body chamber extending beyond the point of recurvature, ending just adapical of the aperture.

MATERIAL: There are approximately 40 complete or nearly complete macroconchs and a nearly equal number of microconchs (tables 3–6). The majority of these specimens come from the same geographic area and stratigraphic interval as the holotype. This permits an examination of the range of variation of the species, based on topotype material. We have also included in our study

TABLE 3
Measurements of the adult shells of *Hoploscaphites nodosus* (Owen, 1852), macroconchs

Specimen Number	Study Number	LMAX	$LMAX/H_2$	$LMAX/H_4$	Sep <	Apt <	UD_P	UD_L	W_1/H_1	W_2/H_2	W_3/H_3	W_4/H_4	W_5/H_5	W_6/H_6	W_7/H_7	V_4/H_4
AMNH 9520/1	300	95.4	3.04	2.34	41.0	71.5	3.6	3.8	1.05	0.89	0.86	—	—	—	—	—
AMNH 9520/2[a]	296	86.3	2.99	2.43	—	84.0	—	4.1	0.88	0.88	0.82	0.89	0.98	0.99	1.02	0.68
AMNH 45343	301	93.0	3.00	2.34	34.0	—	4.4	5.2	1.06	1.00	0.99	1.05	1.08	—	—	0.63
AMNH 45344	488	93.4	2.91	2.22	34.0	59.0	5.8	5.1	1.09	1.08	0.99	1.00	1.12	1.21	1.18	0.72
AMNH 47121[b]	1626	101.3	3.15	—	14.0	54.5*	5.0	5.6	1.33	1.28	—	—	—	—	1.13	0.85
AMNH 58511	654	87.1	3.02	2.18	34.0	71.0	3.8	3.8	—	0.92	0.88	0.98	1.05	—	—	0.60
AMNH 58512[c]	294	82.0	2.98	—	37.0	81.0	4.1	4.0	0.83	0.79	0.83	0.80	0.89	0.96	0.98	—
AMNH 58513	298	93.8	3.04	2.47	47.0	80.0	3.6	5.0	1.20	1.06	1.23	1.14	1.11	1.09	1.36	0.77
BHI 4121	293	88.7	2.97	2.33	32.5	67.0	4.4	4.3	1.08	1.11	1.06	1.03	1.21	1.18	1.19	0.78
BHI 4178	290	97.0	3.12	2.40	16.0	76.0*	—	4.7	1.07	1.10	1.15	1.07	1.12	1.14	1.08	0.66
BHI 4214[c, d]	1647	—	—	—	10.0	—	3.7	4.0	—	0.89	0.84	—	—	—	—	0.59
BHI 4215	291	89.1	3.03	2.36	17.0	69.0	4.4	4.5	1.22	1.11	0.87	0.97	1.05	1.09	1.08	0.74
BHI 4216	287	91.0	2.94	2.36	62.0	85.0	2.6	3.5	1.27	1.01	0.95	0.96	1.04	1.05	1.09	0.68
BHI 4219	1264	—	—	—	—	62.0	—	—	—	—	—	—	1.06	1.13	—	—
BHI 4257	292	94.9	3.04	2.30	51.0	72.0	—	3.4	1.28	1.09	1.16	1.05	1.11	1.11	1.24	0.70
BHI 4287a[c]	451	84.9	3.14	2.14	48.0	69.0	4.3	4.1	0.94	0.82	0.82	0.77*	0.92	0.92	1.04	—
BHI 4699	490	91.8	3.02	2.38	−5.0	59.0*	4.6	4.1	—	1.26	1.08	1.09	—	—	—	—
BHI 4773[e]	637	93.5	3.16	—	60.0	64.0	3.9	3.3	1.09	1.08	—	—	1.24	1.11	1.19	—
BHI 4787	583	98.0	3.03	2.19	13.0	75.0	4.4	3.4	1.19	1.27	—	1.12	1.28	1.37	1.30	0.88
BHI 4800	645	101.8	—	2.45	61.0*	75.0	—	—	—	0.88	—	—	1.24	1.12	—	0.84
BHI 4948	1648	86.5	3.05	2.33	49.0	76.0	4.8	3.4	1.10	0.97	0.97	1.04	1.15	1.15	1.15	0.70
UC 6381	Type	101.5	3.22	2.38	79.0	—	—	—	1.26	1.21	1.10	1.02	1.13	1.05	—	0.82
UCP 3692	1290	84.3	3.03	2.21	31.0	68.0	3.2	3.2	1.07	0.95	0.91	0.94	1.07	1.06	—	0.62
UMMP 43126	520	88.6	2.99	2.58	—	—	—	—	—	1.08	—	1.09	—	—	—	0.73
USNM 536216	113	87.1	3.20	2.28	34.0	—	3.8	3.9	1.30	1.05	0.94	0.96	1.03	1.10	—	0.59
USNM 536218	131	98.6	2.92	2.24	15.0	69.0	—	3.8	1.17	—	1.06	—	—	—	—	—
USNM 536219[f]	1167	103.8	3.12	2.41	44.0	—	5.0	4.9	—	0.94	0.96	0.94	—	1.04	—	0.67
USNM 536230	1330	103.9	2.78	—	8.0	—	—	—	—	—	—	—	—	—	—	—
USNM 536233[c]	241	84.8	2.84	2.25	41.0	66.0*	—	3.0	0.97	0.81	0.86	0.85	0.94	1.01	—	0.54
USNM 536234	110	85.3	3.05	2.20	30.0	74.0	2.8	3.0	0.90	0.86	0.99	0.95	1.05	1.03	—	0.63
USNM 536235[c]	242	89.0	2.84	2.23	60.5	82.0	—	—	1.06	0.76	0.92	0.88	0.95	1.02	1.07	—
USNM 536236	1640	88.3	2.89	2.14	9.0	51.0*	5.0	4.8	—	—	1.03	—	1.12	1.14	1.27	—
USNM 536237[a]	123	—	—	—	—	—	—	—	1.14	1.10	1.17	1.11	1.18	—	—	0.90
USNM 536270[g]	325	72.5	3.09	2.36	−3.0	81.0	3.0*	2.4	1.08	1.04	1.07	1.08	1.00	1.09	1.20	0.74
YPM 6078	—	94.9	2.96	2.19	50.0	73.0	3.1	4.2	1.03	0.93	0.94	0.94	1.06	1.09	1.04	0.60
YPM 8924[h]	—	96.8	3.05*	2.45	38.0	81.5	—	—	—	—	0.90	0.95	0.96	0.92	1.02	0.74

TABLE 3
(*Continued*)

Specimen Number	Study Number	LMAX	LMAX/H_2	LMAX/H_4	Sep <	Apt <	UD_P	UD_L	W_1/H_1	W_2/H_2	W_3/H_3	W_4/H_4	W_5/H_5	W_6/H_6	W_7/H_7	V_4/H_4
YPM 35575	295	91.7	2.90	2.25	51.0	67.0	3.6	4.2	1.12	0.98	0.96	0.92	1.02	1.03	1.15	0.66
YPM 35578[d]	1649	—	—	—	35.5	64.5	—	3.6	1.15	1.01	1.05	1.01	—	—	—	—
YPM 35580	356	91.6	3.14	2.40	75.5	82.0	—	—	0.94	—	—	0.90	1.02	1.05	—	0.72
YPM 35593	299	94.4	3.07	2.31	41.0	72.0	—	4.2	1.07	1.09	1.06	1.06	1.19	1.28	—	0.80
YPM 35598[d]	297	88.3	3.40	2.35	58.0	79.0	4.8	5.5	0.97	1.08	0.97	0.98	1.02	—	—	0.65

See figure 14 for description of measurements. All measurements are in mm except for septal angle and apertural angle, which are in degrees. *Estimate.
[a]Used for ontogenetic study.
[b,f]*Baculites reesidei* Zone.
[c]Transitional to *H. brevis*.
[d]Injury.
[e]Dorsal muscle scar.
[f]*Baculites cuneatus–B. jenseni* Zones.
[g]Very small specimen (pathologic?).
[h]Elongate outline.

many incomplete specimens, which provide information about ontogenetic development.

MACROCONCH DESCRIPTION: The specimens in our collection exhibit a range of variation in the degree of robustness, tightness of coiling, and coarseness of ornament. The holotype (fig. 4) and BHI 4699 (fig. 45A, B) represent the more robust, more loosely coiled, and more coarsely ornamented end of the spectrum, while AMNH 58512 (figs. 43C, 55D–F) and USNM 536234 (figs. 37C–D, 56D–F) represent the more slender, more tightly coiled, and more finely ornamented end of the spectrum.

Adults are relatively large. In the measured set, LMAX averages 91.8 mm and ranges from 72.5 to 103.9 mm (table 3). The ratio of the size of the largest macroconch to that of the smallest is 1.43. The size distribution is unimodal (fig. 41). It is possible that specimens from the *Baculites cuneatus* Zone are larger than those from the *B. compressus* Zone. For example, the largest macroconchs in our collection whose locality is known, namely, AMNH 47121 (fig. 48), USNM 536218 (fig. 51A, B), 536219, and 536230 (fig. 50A, B), are from the *B. cuneatus* or *B. cuneatus–B. reesidei* zones.

Specimens are robust with an ellipsoidal outline in side view. The exposed phragmocone occupies most of the coiled portion and is approximately two-thirds of a whorl in angular length; it generally ends below the line of maximum length. The septal angle averages 35.9° and ranges from −5.0° to 79.0°. The umbilicus is tiny and averages 4.1 mm in diameter, both as measured parallel to the line of maximum length, and at the end of the phragmocone. The ratio of umbilical diameter to shell diameter averages 0.04.

The body chamber consists of a long shaft and recurved hook. In side view, the umbilical seam of the shaft is straight and the venter of the shaft is broadly rounded. Occasionally, a small bulge appears on the umbilical seam, as in YPM 35575 (fig. 50C, D). LMAX/H_4 averages 2.32. In some specimens, the venter is more broadly rounded than in others (for example, compare the less rounded venter in YPM 35575 [fig. 50C, D] with the more rounded venter in BHI 4178 [figs. 17D, E, 46A, B] and 4257 [figs. 18A, 53C, D]). The body chamber extends beyond

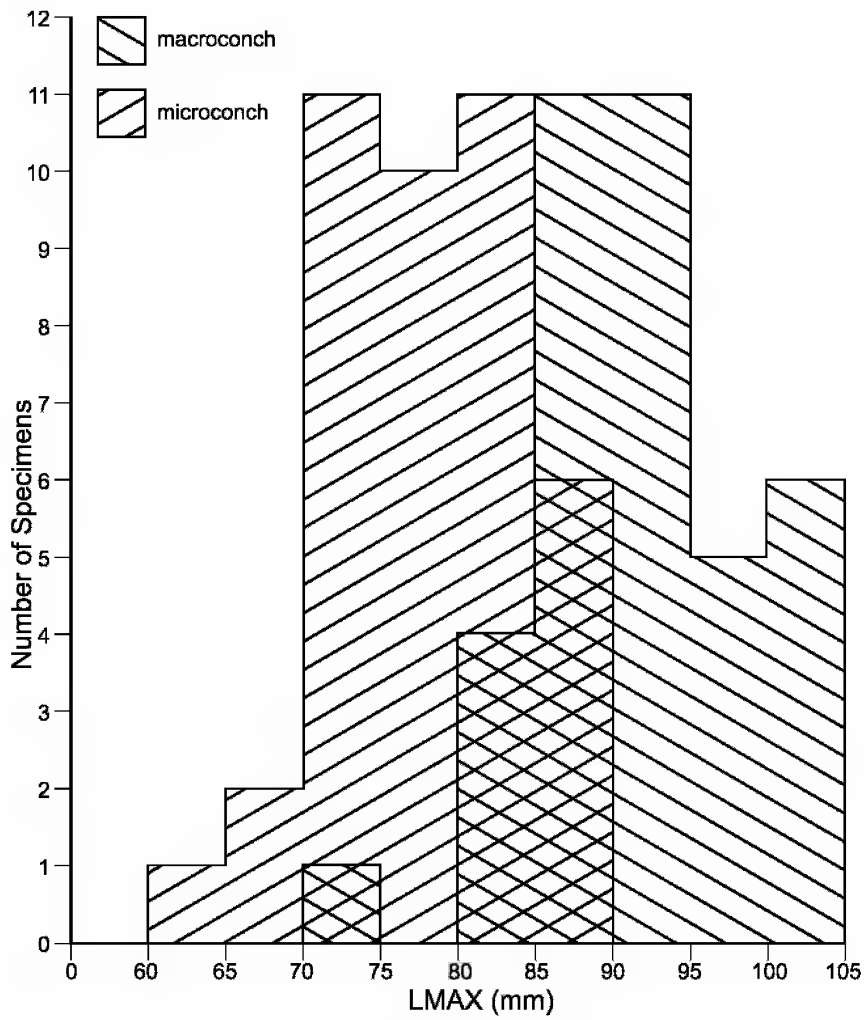

Fig. 41. Size-frequency histogram of *Hoploscaphites nodosus* (Owen, 1852), Pierre Shale and Bearpaw Shale, *Baculites compressus–B. cuneatus* zones, based on the samples in tables 3 and 5, including additional unnumbered specimens in the BHI collections.

the coiled portion, leaving a slight gap. LMAX/H_2 averages 3.01. Variation in the degree of uncoiling is reflected in shell shape, yielding a range from more elongate shapes, as in the holotype (fig. 4) and BHI 4699 (fig. 45A, B), to more compact shapes, as in BHI 4121 (figs. 17F, 43B, 46C, D). The hook is strongly reflected, as indicated by the high apertural angle, which averages 73.3° and ranges from 59° to 85° in well-preserved specimens. The apertural margin is flexuous with a dorsal projection. The apertural lip is thickened and shows a constriction.

Starting at the point of exposure, the width and height of the shell steadily increase. The whorl section of the phragmocone ranges from slightly compressed to slightly depressed. The ratio of whorl width to whorl height near the point of exposure (W_1/H_1) averages 1.09 (1.26 in the holotype). The whorl section becomes less depressed toward the adoral end of the phragmocone. The ratio of whorl width to whorl height at the ultimate septum (W_3/H_3) averages 0.98 (1.10 in the holotype).

The intercostal whorl section of the exposed phragmocone varies from subqua-

drate/ovoid to weakly reniform, with the greatest width at one-third whorl height. The umbilical wall of the phragmocone is steep, and the umbilical shoulder is broadly rounded, becoming more sharply rounded toward the end of the phragmocone. The flanks are very broadly rounded in subquadrate sections. However, in weakly reniform sections, the inner flanks are broadly rounded and the outer flanks are nearly flat. The ventrolateral shoulder is relatively well rounded, and the venter is sharply to broadly rounded.

The shell continues to expand as it passes into the shaft of the body chamber. Whorl width and height reach their maximum values on the adoral part of the shaft, and remain nearly the same or decrease slightly to the point of recurvature, and decrease slightly thereafter to the aperture. The whorl section of the body chamber at midshaft is equally or slightly more depressed that at the last septum (fig. 42). The ratio of whorl width to whorl height at midshaft averages 0.99 (1.02 in the holotype). V_4/H_4 averages 0.71 (0.82 in the holotype). Thereafter, in many specimens, but not all, the body chamber becomes slightly more depressed. The ratio of whorl width to whorl height at the aperture averages 1.14.

The intercostal whorl section of the body chamber at midshaft is similar to that of the phragmocone. It is subquadrate/ovoid or, more commonly, weakly reniform, with the greatest width at one-third whorl height. The umbilical wall of the shaft is steep and the umbilical shoulder is narrowly rounded. The inner flanks are broadly rounded and the outer flanks are nearly flat and convergent. In some specimens, there are broad elevations linking the umbilicolateral and ventrolateral tubercles, as in the holotype (fig. 4) and YPM 35575 (fig. 50C, D). The venter is broadly rounded on the shaft, becoming more narrowly rounded on the hook, and, as a result, the intercostal whorl sections at the point of recurvature and at the aperture are more ovoid than at midshaft.

The ornament consists of primary and secondary ribs, with rows of prominent umbilicolateral and ventrolateral tubercles (table 4). There are no flank tubercles. As in the shape of the shell, specimens display a range of variation in the coarseness of the ornament. For example, more robust specimens, such as the holotype, are characterized by larger umbilicolateral and ventrolateral tubercles than are more slender specimens.

Starting at the point of exposure, primary ribs arise at the umbilical seam and strengthen across the umbilical wall and shoulder. They are either rectiradiate or, more commonly, rursiradiate. They branch at the umbilical shoulder to form secondary ribs, with additional ribs arising on the flanks by branching and intercalation, especially at the sites of the umbilicolateral and ventrolateral tubercles. Ribs swing backward on the inner flanks, weakly forward on the midflanks, and back again on the outer flanks. They become more flexuous toward the adoral end of the phragmocone.

Ribs cross the venter with a slight forward projection. They are sharp, narrow, and equally strong. On the adapical portion of the phragmocone, the rib density ranges from 5 ribs/cm, as in the holotype (fig. 4), to 7 ribs/cm, as in BHI 4800. In some specimens, but not all, the ribs become slightly more closely spaced adorally. There are 6–8 ribs/cm on the venter on the adoral portion of the phragmocone (6 ribs/cm on the venter in the holotype). The ratio of ventral to primary ribs is 3–4:1 (3.5:1 in the holotype) on the adapical portion, and 4–5:1 (4:1 on the holotype) on the adoral portion, of the phragmocone.

On the body chamber, ribs arise at the umbilical seam and are rursiradiate on the umbilical wall and shoulder, becoming more rectiradiate toward the adoral end of the shaft. There are 5–9 ribs/cm on the umbilical shoulder of the shaft (6 ribs/cm on the holotype). In some specimens, such as the holotype (fig. 4) and AMNH 45343 (figs. 17H, I, 53A, B), a few of these ribs are raised into relatively weak bullae, which is reminiscent of more primitive scaphite species. Ribs branch near the umbilical shoulder, and additional branching and intercalation occur on the flanks, especially at the site of the umbilicolateral and ventrolateral tubercles.

Ribs are rectiradiate to slightly rursiradiate on the flanks on the adapical portion of the shaft, becoming more prorsiradiate on the

TABLE 4
Ornament of the adult shells of *Hoploscaphites nodosus* (Owen, 1852), macroconchs

		Rib Density (ribs/cm)							
		Phragmocone		Body Chamber		Number of Umbilicolateral Tubercles		Number of Ventrolateral Tubercles	
Specimen Number	Study Number	Adapical	Adoral	Midshaft	Hook	Phragmocone	Body Chamber	Phragmocone	Body Chamber
AMNH 9520/1	300	6	6.5	6	7	6	5	12	11*
AMNH 9520/2	296	—	6	5	5	4	5*	5	10
AMNH 45343	301	6	6	7	7	4	5	12	8*
AMNH 45344	488	—	—	7	7	—	8	—	11
AMNH 47121	1626	5	5.25	5.75	6	4	6	10	10
AMNH 58512	294	6	—	—	6	2	5	6/7[b]	10
AMNH 58513	298	5	6	5	—	5	4	7	11
BHI 4121	293	5	6	6	6	3	4	7	10
BHI 4178	290	5	6	6	6	3	6	9	13
BHI 4214	1647	6	6	6.5	—	4	4*	7	6*
BHI 4215	291	6	6	6	6	3	6	6	12
BHI 4216	287	6	7	7	6.5	4	5	9	14
BHI 4219	1264	—	—	7	6	—	4*	7	13
BHI 4257	292	6	7	6	6	2	8	6	15
BHI 4287a	451	7	7.25	—	7.75	6	4	9	13
BHI 4699	490	5	6	6	—	4	8	7	15
BHI 4773	637	5	—	—	6	6	6	—	—
BHI 4787	583	6	6	5.75	6	4	6	—	—
BHI 4800	645	7	8	7.25	7	—	6	—	14
BHI 4948	1648	6	8	7	8	5	4	10	14
UC 6381	Type	5	6	6	6	4	4*	7	9*
UCP 3692	1290	6	7	6	6	7	6	10	11
UMMP 43126	520	—	6.25	7	—	—	—	—	—
USNM 315704[a]	621	—	—	8	8	—	8	—	13
USNM 536216	113	6	7	6	6	—	6	—	—
USNM 536218	131	5	5.5	5	4.5	3*	6	—	8*
USNM 536219	1167	6	6	5.5	5.5	6	8*	13	9
USNM 536230	1330	—	6	5.25	—	—	—	7*	8*
USNM 536233	241	6	6	7	7	2	6	5	9
USNM 536234	110	6	6	5	—	6	5	8	—
USNM 536235	242	7	7	6	6	3	5	7	10
USNM 536237	123	5.25	6	5.25	—	—	—	—	—
YPM 35575	295	5	6	7	8	5	5	10	11
YPM 35578	1649	6	8	7	—	5	7	11*	8*

TABLE 4
(*Continued*)

Specimen Number	Study Number	Rib Density (ribs/cm)					Number of Umbilicolateral Tubercles		Number of Ventrolateral Tubercles	
		Phragmocone		Body Chamber			Phragmocone	Body Chamber	Phragmocone	Body Chamber
		Adapical	Adoral	Midshaft	Hook					
YPM 35580	356	5.5	6	5	6.5		—	6	—	12
YPM35593	299	—	7	8	7		4	6	12	12*
YPM35598	297	—	7	7	7		—	4	2*	12

For additional comments, see footnotes in table 3. * Estimate due to incomplete or poor preservation.
[a]Only the body chamber is preserved.
[b]The number is different on each side of the shell.

adoral portion of the shaft. They are weakly biconcave, with the degree of flexuosity covarying with the flatness of the flanks. Ribs swing gently backward on the inner flanks, forward on the midflanks, and backward again on the outer flanks. This weak biconcavity disappears toward the point of recurvature where the ribs become straight or slightly concave.

Ribs cross the venter of the body chamber with a marked forward projection at midshaft, which usually attenuates on the hook. In general, rib density remains the same or increases slightly toward the aperture. There are 5–7.25 ribs/cm on the venter at midshaft (6 ribs/cm in the holotype [fig. 4]; 8 ribs/cm in USNM 315704 [fig. 51C, D], but this is rare) versus 5–8 ribs/cm on the venter on the hook (6 ribs/cm in the holotype). The ratio of ventral to primary ribs averages 3–4:1 at midshaft.

The umbilicolateral tubercles usually appear midway on the exposed phragmocone, but may already be present near the point of exposure. They occur at one-third whorl height and are relatively evenly spaced, with the two most widely spaced tubercles on the adoral part of the phragmocone. The maximum distance between adjacent tubercles ranges from 6 to 11 mm. The tubercles are bullate, and increase in size toward the adoral end of the phragmocone. The size of the largest tubercle ranges from 1 to 2 mm in height. There are 2–6 umbilicolateral tubercles on the exposed phragmocone, averaging 4 (4 on the holotype). Commonly, one to three ribs join a tubercle dorsally and two or three ribs branch from it ventrally. A maximum of five ribs intercalate between tubercles on the adoral end of the phragmocone.

The umbilicolateral tubercles on the body chamber occur at one-third to one-half whorl height at midshaft. In general, a large gap (14–19 mm long) appears between the most adoral tubercle on the phragmocone and the most adapical tubercle on the shaft, which usually exceeds the spacing between subsequent tubercles. At midshaft, the umbilicolateral tubercles are relatively evenly spaced at intervals ranging from 11 to 19 mm, averaging 14 mm (14.5 mm in the holotype). They attain a uniformly large size at midshaft ranging from 1.5 to 3 mm in height,

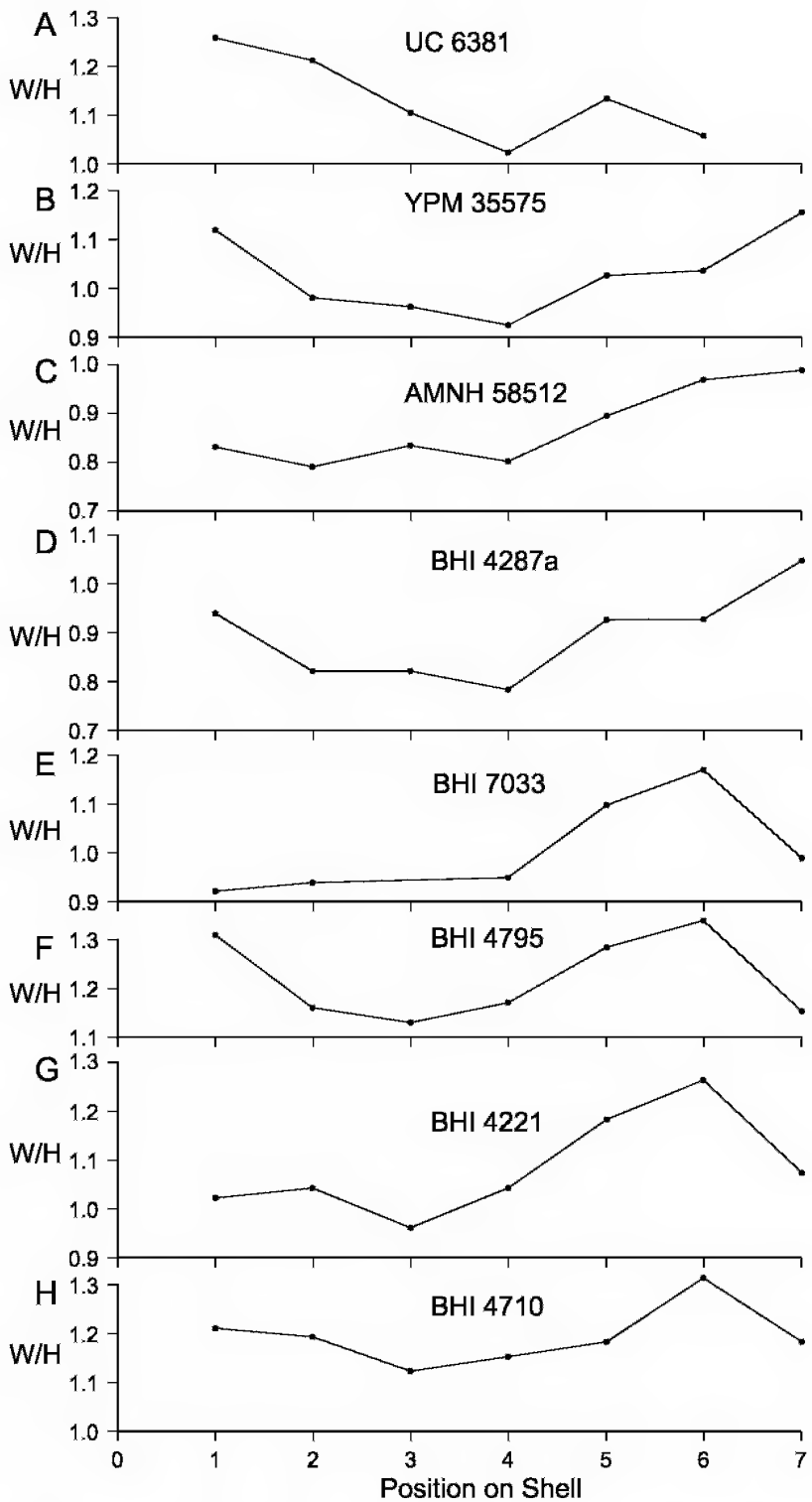

Fig. 42. Plot of the ratio of whorl width to height (W/H) at seven points on the adult shell of *Hoploscaphites nodosus* (Owen, 1852) from ¼ whorl adapical of the long axis (1) to the aperture (7), as

averaging 2 mm. Toward the point of recurvature, the umbilicolateral tubercles decrease slightly in size and spacing, and extend almost or up to the aperture.

The umbilicolateral tubercles are nodate on the shaft, becoming more bullate on the hook. They sometimes show an asymmetrical profile in cross section, with a steep adapical face and a more gently sloping adoral face. At midshaft, two to four ribs join a tubercle dorsally and three to seven ribs branch from it ventrally. A maximum of seven ribs intercalate between tubercles at midshaft. The number of umbilicolateral tubercles on the body chamber ranges from 4 to 8, averaging 6 (4 tubercles on the holotype, but it is incomplete; 8 tubercles on BHI 4257 [figs. 18A, 53C, D], but the base of the body chamber is above the line of maximum length). The total number of umbilicolateral tubercles on the adult shell averages 10.

The ventrolateral tubercles are usually already present at the point of exposure. They occur at 90% whorl height. They are initially small and bullate, but become larger and more clavate toward the end of the phragmocone, with the largest tubercle ranging from 1.5 to 3.5 mm in height (average = 2.6 mm). In general, the tubercles on the phragmocone are unevenly distributed and commonly occur in pairs or clusters. For example, in BHI 4121 (figs. 17F, 43B, 46C, D), starting at the point of exposure, the distance between successive tubercles on the phragmocone, as measured in an adoral direction, is 7, 10, 15, 9, and 12 mm. The maximum distance between the two most adoral tubercles on the exposed phragmocone in the measured set of specimens ranges from 9.5 to 26.5 mm and averages 15 mm. Tubercles match or alternate on opposite sides of the venter. Commonly, one to four ribs join a tubercle dorsally and two to five ribs branch from it ventrally. Tubercles also occur in the interspaces between ribs, as in BHI 4178 (figs. 17D, E, 46A, B) and 4257 (figs. 18A, 53C, D). A maximum of nine ribs intercalate between tubercles, as in BHI 4178 (figs. 17D, E, 46A, B). There are 5–12 tubercles on the exposed phragmocone, averaging 8 (7 on the holotype).

In some specimens, the largest gap between ventrolateral tubercles occurs between the most adoral tubercle on the phragmocone and the most adapical tubercle on the body chamber. This gap ranges from 16 to 26 mm. On the rest of the shaft, the tubercles are evenly spaced. In the measured set of specimens, the distance between adjacent tubercles on the shaft averages 16 mm and ranges from 12 to 22 mm.

The ventrolateral tubercles attain their maximum size on the shaft, forming large, subspinose clavi that project to the side. The bases of the tubercles occur at 90% whorl height. The tubercles commonly show an asymmetrical profile in cross section, with a flattened, steep adapical face and a more gently sloping adoral face. In the measured set of specimens, the height of the largest tubercle averages 3.5 mm and ranges from 2 to 4.5 mm. In general, the ventrolateral tubercles are always larger than the umbilicolateral tubercles. At midshaft, four to seven ribs join a ventrolateral tubercle dorsally and an additional one to three ribs branch from it ventrally. A maximum of eight ribs intercalate between tubercles.

←

shown in figure 14. The shell attains its maximum degree of compression near midshaft (points 3, 4), becoming less compressed thereafter. However, in microconchs, the shell becomes more compressed again at the aperture. **A–D.** Macroconchs. **A.** UC 6381, holotype, probably from the Pierre Shale, Sage Creek, Pennington County, South Dakota. **B.** YPM 35575, YPM loc. A6520, Pierre Shale, Sage Creek, Pennington County, South Dakota. **C.** AMNH 58512, locality unknown. **D.** BHI 4287a, *Baculites cuneatus* Zone, Pierre Shale, Meade County, South Dakota. **E–H.** Microconchs. **E.** BHI 7033, *Baculites compressus–B. cuneatus* zones, Pierre Shale, Meade County, South Dakota. **F.** BHI 4795, *Baculites compressus–B. cuneatus* zones, Pierre Shale, Meade County, South Dakota. **G.** BHI 4221, *Baculites cuneatus* Zone, Pierre Shale, Meade County, South Dakota. **H.** BHI 4710, *Baculites compressus–B. cuneatus* zones, Pierre Shale, Meade County, South Dakota.

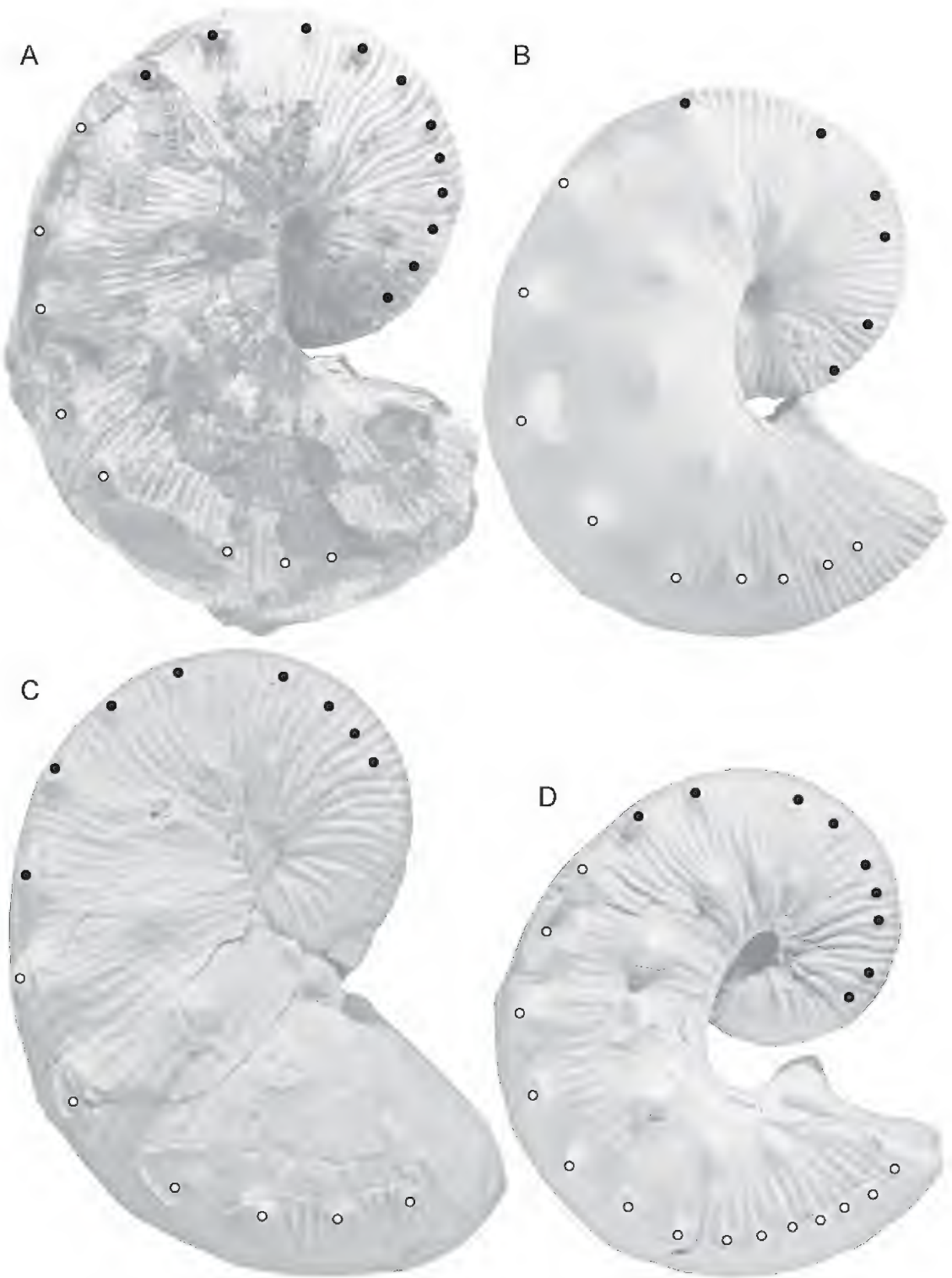

Fig. 43. Spacing of ventrolateral tubercles on the adult shell of *Hoploscaphites nodosus* (Owen, 1852). **A.** AMNH 9520/1, slender macroconch, possibly one of the original specimens collected by Meek and

The ventrolateral tubercles undergo several changes starting on the adoral end of the shaft. First, they migrate dorsally so that they occur at two-thirds to three-quarters whorl height. This change coincides with the narrowing of the venter on the hook. Second, the tubercles decrease abruptly in size. This reduction in size is much more marked than that in the umbilicolateral tubercles. Third, the ventrolateral tubercles become much more closely spaced, and either maintain this close spacing or show a slight approximation thereafter. Fourth, they develop a more bullate appearance, especially on the adoral end of the hook. In most specimens, the ventrolateral tubercles persist to the aperture although in exceptional specimens, such as USNM 536235, they end at the point of recurvature (figs. 36E, 56A–C).

The ventrolateral tubercles on the body chamber are paired or offset from one side of the venter to the other. When they are paired, they commonly form broad elevations across the venter, as in BHI 4121 (figs. 17F, 43B, 46C, D). The number of ventrolateral tubercles on the body chamber averages 12 and ranges from 9 to 15 (9 on the preserved portion of the body chamber of the holotype; 15 on BHI 4257 [figs. 18A, 53C, D], but the base of the body chamber is above the line of maximum length; 15 on BHI 4699 [fig. 45A, B], where a series of small, evenly spaced tubercles occur adoral of an injury and extend almost to the aperture). The total number of ventrolateral tubercles on the adult shell averages 20. The number of ventrolateral tubercles is twice that of the umbilicolateral tubercles, and generally two of the former bracket one of the latter.

The suture (fig. 61) is deeply incised; E/L is asymmetrically bifid, with a broader ventral half, and L is asymmetrically to symmetrically bifid.

MICROCONCH DESCRIPTION: Microconchs show the same range of variation in size, degree of robustness, and coarseness of ornament as macroconchs do, with specimens ranging from large, robust, coarsely ornamented forms, for example, BHI 4220 (fig. 64A, B) and 4710 (figs. 42H, 62) to smaller, more slender, more finely ornamented forms, for example, USNM 536232 (fig. 70A, B). The maximum size of microconchs averages 78.0 mm, which is approximately 85% of the maximum size of macroconchs (table 5). The ratio of the largest microconch to that of the smallest is 1.36. The size distribution is nearly unimodal (fig. 41).

As in macroconchs, shells are robust with an elongate shape. The mature phragmocone occupies approximately three-quarters of a whorl. It always ends below the line of maximum length. The umbilicus is small. UD_L averages 4.3 mm, nearly the same as that in macroconchs (4.1 mm). However, UD_P averages 7.2 mm, which is much larger than that in macroconchs (4.1 mm), due to the concave outline of the umbilical seam (fig. 22). The ratio of UD_P to LMAX averages 0.09, larger than that in macroconchs (0.04).

The body chamber consists of a relatively long shaft and recurved hook. The outline of the umbilical seam of the shaft parallels the curvature of the venter. The body chamber extends well beyond the coiled portion, leaving a large gap. $LMAX/H_2$ averages 3.16, which is slightly greater than that in macroconchs (3.01). The hook is strongly reflected and, as in macroconchs, the apertural lip is flexuous, with a short dorsal projection.

The whorl section of the exposed phragmocone is nearly equidimensional. The ratio of whorl width to whorl height near the point

---

←

Hayden in 1853 from the Pierre Shale, Sage Creek, Pennington County, South Dakota. **B.** BHI 4121, robust macroconch, *Baculites compressus–B. cuneatus* zones, Pierre Shale, Meade County, South Dakota. **C.** UC 6381, holotype, robust macroconch, probably from the Pierre Shale, Sage Creek, Pennington County, South Dakota. **D.** BHI 4723, large microconch, *Baculites compressus–B. cuneatus* zones, Pierre Shale, Pennington County, South Dakota. The photo in B has been flipped so that it appears the same way as the others. Symbols: • = tubercle on the phragmocone; o = tubercle on the body chamber.

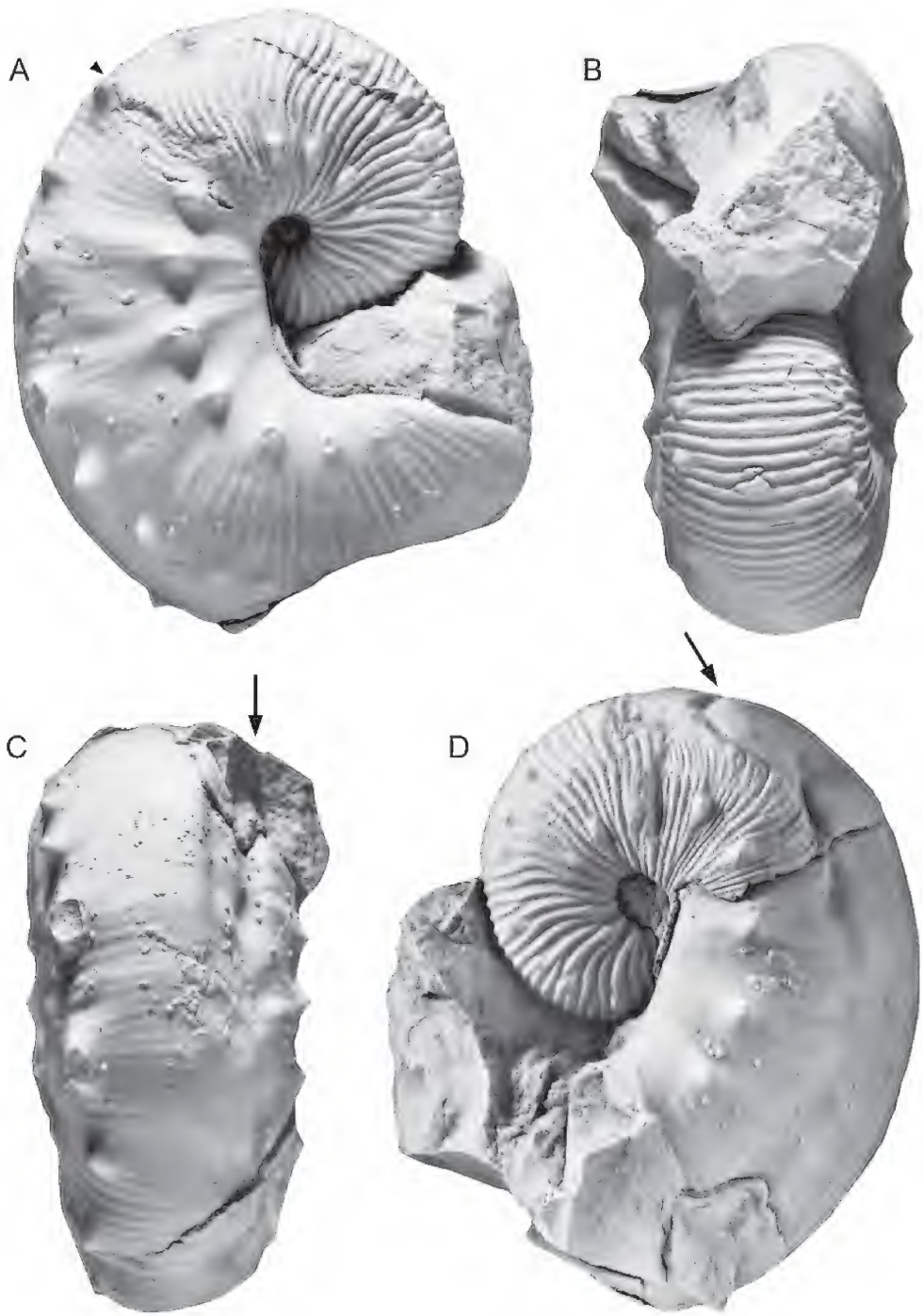

Fig. 44. *Hoploscaphites nodosus* (Owen, 1852), small slender macroconch, USNM 12284 (= Whitfield, 1880: pl. 13, fig. 12) (cast = YPM 35578), from "the Fort Pierre Group, on the Cheyenne River, near Rapid Creek, Black Hills, Dakota." A spiral furrow (arrows) extends from the middle of the exposed phragmocone to the point of recurvature on the left side. **A.** Right lateral; **B.** aperture; **C.** ventral; **D.** left lateral. Specimen is illustrated natural size.

TABLE 5
Measurements of the adult shells of *Hoploscaphites nodosus* (Owen, 1852), microconchs

Specimen Number	Study Number	LMAX	LMAX/H_2	UD_P	UD_L	W_1/H_1	W_2/H_2	W_3/H_3	W_4/H_4	W_5/H_5	W_6/H_6	W_7/H_7	V_4/W_4	V_4/H_4
AMNH 9520/3	489	88.2	—	—	—	—	—	—	1.22	1.30	1.34	1.13	0.73	0.90
AMNH 56765	323	78.3	3.24	7.3	4.0	0.98	0.92	0.88	0.91	1.07	1.13	—	0.71	0.68
AMNH 58521	556	77.7	3.36	8.6	5.6	1.18	1.03	1.02	1.05	1.20	1.24	1.12	0.84	0.85
AMNH 58554	1676	88.3	3.63	6.0	4.2	1.00	1.13	1.03	1.05	1.21	1.27	1.07	0.84	0.81
BHI 4122	304	71.3	3.26	7.0	4.3	1.03	1.03	1.04	1.12	1.03	1.06	0.99	0.79	0.86
BHI 4220	303	84.6	3.18	6.6	4.7	1.05	1.05	1.04	1.07	1.19	1.23	1.16	0.77	0.87
BHI 4221	322	64.7	3.10	4.1*	3.5	1.02	1.04	0.96	1.04	1.18	1.26	1.07	0.64	0.67
BHI 4222	305	82.1	3.42	8.8	5.1	0.90	1.02	1.08	0.95	1.02	1.10	1.03	0.82	0.71
BHI 4710	461	82.4	4.10	7.8	4.4	1.21	1.19	1.12	1.15	1.18	1.31	1.18	0.82	0.93
BHI 4721a	539	88.3	3.23	6.1	3.8	1.14	1.12	1.07	1.01	—	—	—	0.76	0.82
BHI 4723	552	78.4	3.05	6.5	4.2	1.15	1.17	1.11	1.04	1.18	1.21	—	0.77	0.80
BHI 4792	640	75.7	2.79	—	—	—	0.93	—	—	1.09	0.97	1.01	0.79	0.83
BHI 4795	306	81.1	3.24	6.4	5.0	1.31	1.16	1.13	1.17	1.28	1.34	1.15	0.76	0.78
BHI 4798	642	71.3	2.98	—	—	—	—	0.94	1.07	1.11	1.14	—	0.72	0.71
BHI 4799	643	74.1	3.04	—	—	—	—	—	1.18	1.23	1.05	1.18	0.80	0.88
BHI 4801	639	74.2	3.10	—	—	—	1.13	1.14	1.06	—	—	—	0.76	0.82
BHI 4895	1269	67.7	3.13	5.8	3.6	—	0.98	0.92	0.93	1.09	1.14	1.16	0.79	0.70
BHI 4912[a]	1276	77.5	—	9.2	4.0	—	—	—	1.04	1.26	1.30	1.15	0.81	0.86
BHI 4949	1656	74.7	2.79	7.4	4.7	1.12	0.91	0.94	0.91	1.09	1.11	1.14	0.74	0.65
BHI 7033	536	84.0	3.52	7.6	5.8	0.92	0.94	0.86	0.95	1.10	1.17	0.99	0.81	0.76
USNM 536220	128	84.5	2.92	—	—	1.23	1.10	1.14	1.09	1.27	1.29	—	0.72	0.73
USNM 536226[b]	1327	81.0	2.64	—	—	—	0.78	—	0.83	1.03	1.03	—	—	—
USNM 536227	1653	85.2	3.20	—	—	—	—	—	—	—	1.22	1.02	—	—
USNM 536228[b]	1328	—	3.03*	—	—	—	—	—	0.88*	0.92*	0.96*	—	—	—
USNM 536229	1329	76.6	3.10	4.9*	4.7	1.24	1.08	—	1.05	1.11	1.07	1.07	0.76	0.74
USNM 536232	121	74.4	3.06	5.9	3.6	1.08	0.99	1.03	1.04	1.07	1.17	1.17	0.64	0.75
USNM 536245[c]	101	71.9	3.20	7.7	3.8	0.93	0.80	0.83	0.82	0.97	1.00	1.05	0.80	0.69
USNM536246[d]	116	85.6	—	—	4.0	—	—	—	—	—	—	—	0.70	0.81
USNM 536248	1652	76.7	2.78	—	—	0.84	0.88	0.97	0.88	—	—	—	0.76	0.69
USNM 536260	115	69.9	2.95	—	3.0	0.81	0.83	0.86	0.88	0.94	1.01*	—	0.75	0.66
USNM 538103	120	71.7	3.17	5.5	3.7	1.04	0.89	0.95	0.97	1.14	1.17	1.14	0.71	0.70
YPM 1868	307	74.7	3.15	6.2	4.6	1.15	1.07	1.14	1.11	1.15	1.20	1.20	0.72	0.78
YPM 35631[a]	569	76.2	3.30	9.4	5.0	1.26	1.01	1.02	1.00	1.14	1.18	1.16	—	—

See figure 14 for a description of the measurements. All measurements are in mm except for septal angle and apertural angle, which are in degrees. *Estimate.
[a]Injury;
[b]Distorted;
[c]*Didymoceras cheyennense* Zone;
[d]Used in ontogenetic study.

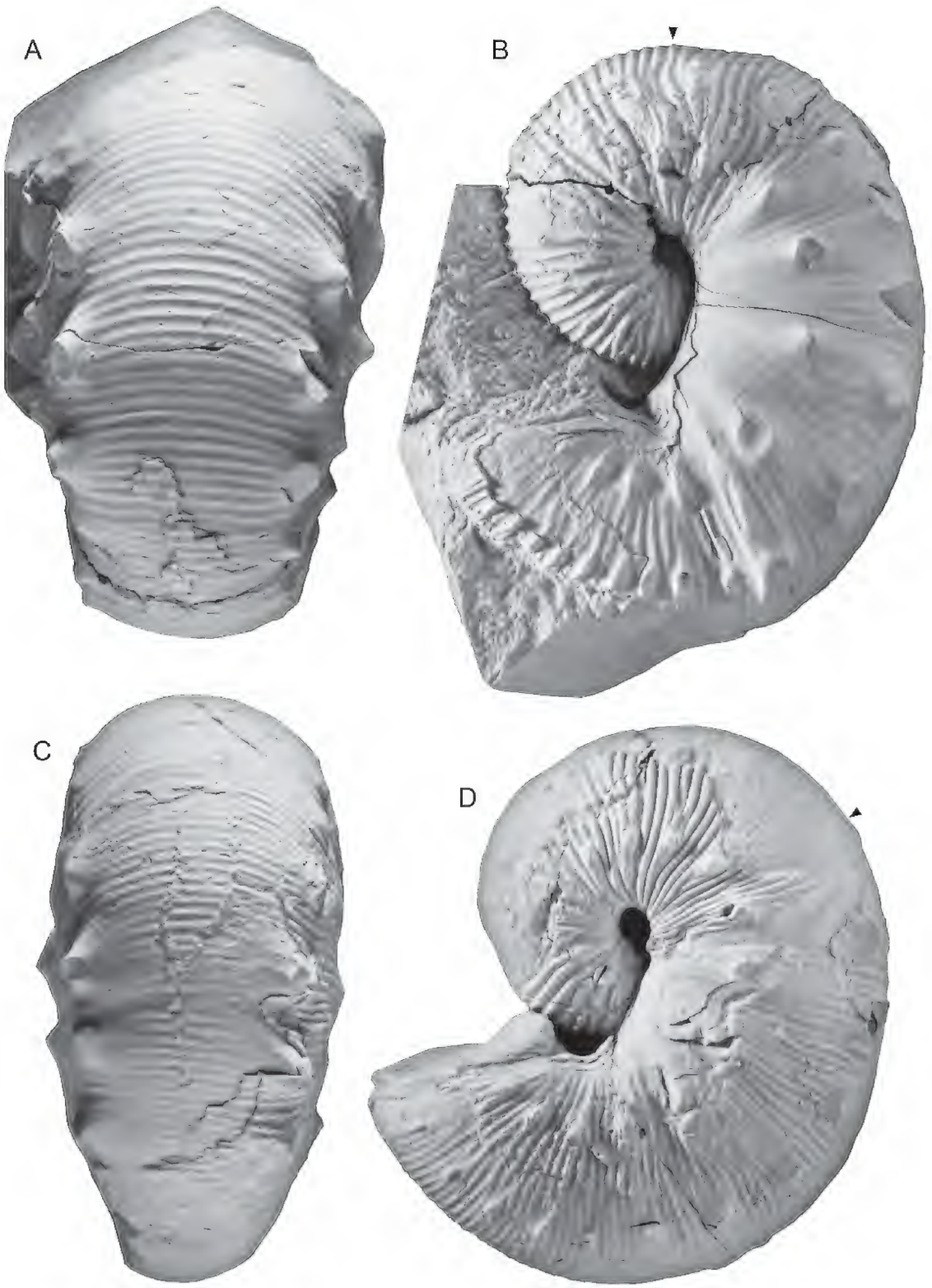
A
B
C
D

of exposure (W_1/H_1) averages 1.07, and remains nearly the same until the end of the phragmocone. In general, the intercostal whorl section of the exposed phragmocone is subquadrate/ovoid but, more rarely, it is weakly reniform, with the greatest width at one-third whorl height (see, for example, USNM 536220). The umbilical wall of the exposed phragmocone is steep and subvertical. The umbilical shoulder is broadly rounded, becoming more sharply rounded toward the end of the phragmocone. In subquadrate/ovoid whorl sections, the flanks are broadly rounded, while in weakly reniform whorl sections, the inner flanks are broadly rounded and the outer flanks are nearly flat. The ventrolateral shoulder is well rounded and the venter is broadly rounded.

Whorl width gradually increases and reaches its maximum value at the point of recurvature, slightly adoral of the point at which it occurs in macroconchs, and either remains the same or decreases slightly thereafter. Whorl height gradually increases and reaches its maximum value at midshaft, although the increase in whorl height is much less than that in macroconchs. The whorl height remains the same or decreases slightly thereafter. The ratio of whorl width to whorl height at midshaft averages 1.02, only slightly more than that in macroconchs (0.98). The ratio is slightly higher at the point of recurvature, averaging 1.17, and remains the same or decreases slightly thereafter.

The intercostal whorl section of the shaft is slightly different from that in macroconchs. In general, it is subquadrate/ovoid, with few examples of weakly reniform whorl sections. The umbilical wall of the shaft is steep, and the umbilical shoulder, unlike that in macroconchs, slopes gently outward. The flanks are broadly rounded, the ventrolateral shoulder is well rounded, and the venter is broadly rounded to flat. As in macroconchs, the ventrolateral shoulder and the venter become more broadly rounded on the hook. The intercostal whorl section at the point of recurvature and at the aperture is ovoid.

The ornamentation in microconchs is similar to that in macroconchs (table 6). There is a range of variation from more coarsely ornamented specimens to more finely ornamented specimens. Differences in the number of tubercles between dimorphs reflect differences in adult size.

On the phragmocone, ribs are sharp and swing backward on the inner flanks, forward on the midflanks, and back again on the outer flanks. Branching and intercalation occur at the site of the umbilicolateral and ventrolateral tubercles. In crossing the venter, ribs are straight or projected slightly forward. There are 6–8 ribs/cm on the venter on the adapical portion, and 6–9 ribs/cm on the venter on the adoral portion, of the phragmocone. The ratio of ventral to primary ribs is approximately 3–4:1 on the adapical portion, and 3–6:1 on the adoral portion, of the phragmocone.

The pattern of ribbing on the body chamber of microconchs is similar to that in macroconchs. Ribs are rursiradiate on the umbilical wall and shoulder. There are 7–9 ribs/cm on the umbilical shoulder of the shaft. Ribs are weakly flexuous, and swing gently backward on the inner third of the flanks, gently forward on the middle third, and gently back again on the outer third. They become less flexuous toward the point of recurvature. Branching and intercalation occur near the umbilical and ventrolateral shoulders, and especially at the umbilicolateral and ventrolateral tubercles.

As in macroconchs, ribs cross the venter of the shaft with a strong forward projection, which diminishes on the hook. There are 6–8 ribs/cm on the venter on the midshaft and on the hook. The ratio of

←

Fig. 45. *Hoploscaphites nodosus* (Owen, 1852), macroconchs, Pierre Shale, *Baculites compressus–B. cuneatus* zones, South Dakota. **A, B.** BHI 4699, similar to holotype, partly embedded in matrix, Meade County. **A.** Ventral; **B.** left lateral. **C, D.** AMNH 45344, with flatter flanks and finer ribbing than holotype, AMNH loc. 3207a, Pennington County. **C.** Ventral; **D.** left lateral. Specimens are illustrated natural size.

TABLE 6
Ornament of the adult shells of *Hoploscaphites nodosus* (Owen, 1852), microconchs

		Rib Density (ribs/cm)							
		Phragmocone		Body Chamber		Number of Umbilicolateral Tubercles		Number of Ventrolateral Tubercles	
Specimen Number	Study Number	Adapical	Adoral	Midshaft	Hook	Phragmocone	Body Chamber	Phragmocone	Body Chamber
AMNH 9520/3	489	—	—	6	6	—	6	—	9
AMNH 55879*	—	—	—	6.5	7	—	7	—	11
AMNH 56765	323	8	9	8	7	4	6	—	4
AMNH 58521	556	6	7	6	6	6	7	8	8
BHI 4122	304	6	8	7	8	5	6	12[a]	9
BHI 4220	303	6	6–7	6	7	6	5	11	9
BHI 4221*	322	6	7	7	8	2	8	3	11
BHI 4222	305	6	8	6	6	7	6	10	12
BHI 4710	461	7	7	6	7	6	6	8	9
BHI 4721a	539	6	6	5	5	5	5	9	11
BHI 4723	552	6.5	9	7	6	6	5	10	14
BHI 4792	640	5	6	7.5	7	2	7	5	11
BHI 4795	306	6	7	6	6.5	6	7	8	8
BHI 4798	642	7	8	—	7	—	3	5	5
BHI 4799	643	—	—	7	7	—	6	—	9
BHI 4801*	639	6	7.5	8	7	4	4	—	8
BHI 4895	1269	8	9	—	9	5	5	7	7
BHI 4912*	1276	—	—	7	7	5	6	—	10
BHI 4949	1656	6	7.5	8	7	5	7	3	6
BHI 7033*	536	6	8	6	6	5	7	—	11
USNM 536220*	128	5.5	6.5	6	7	4	6	6	7
USNM 536226*	1327	6	7	6.5	7	—	7	6	10
USNM 536227	1653	6	6	5	6	—	8	—	12
USNM 536228	1328	7	7	7	7	3	4	7	12
USNM 536229*	1329	5	6	6	7	5	7	9	13
USNM 536232	121	7	7	7	7	3	6	8/9[c]	5
USNM 536245	101	7	8	7	6	6	7	9	8
USNM 536248*	1652	6	7	7	8	2	6	9	9
USNM 536260*	115	7	9	8	8	4	6	8	10
USNM 538103	120	6	7	8	7	5	6	6	6
YPM 1868	307	6	8	7	6	2	5	6	7
YPM 35631[b]	569	7	—	—	6	6	7	8	12

For additional comments, see footnotes in table 5. *Estimate because base of body chamber is uncertain, or aperture is missing, or preservation is poor.
[a]Some of the tubercles are very small.
[b]Injury.
[c]The number is different on each side of the shell.

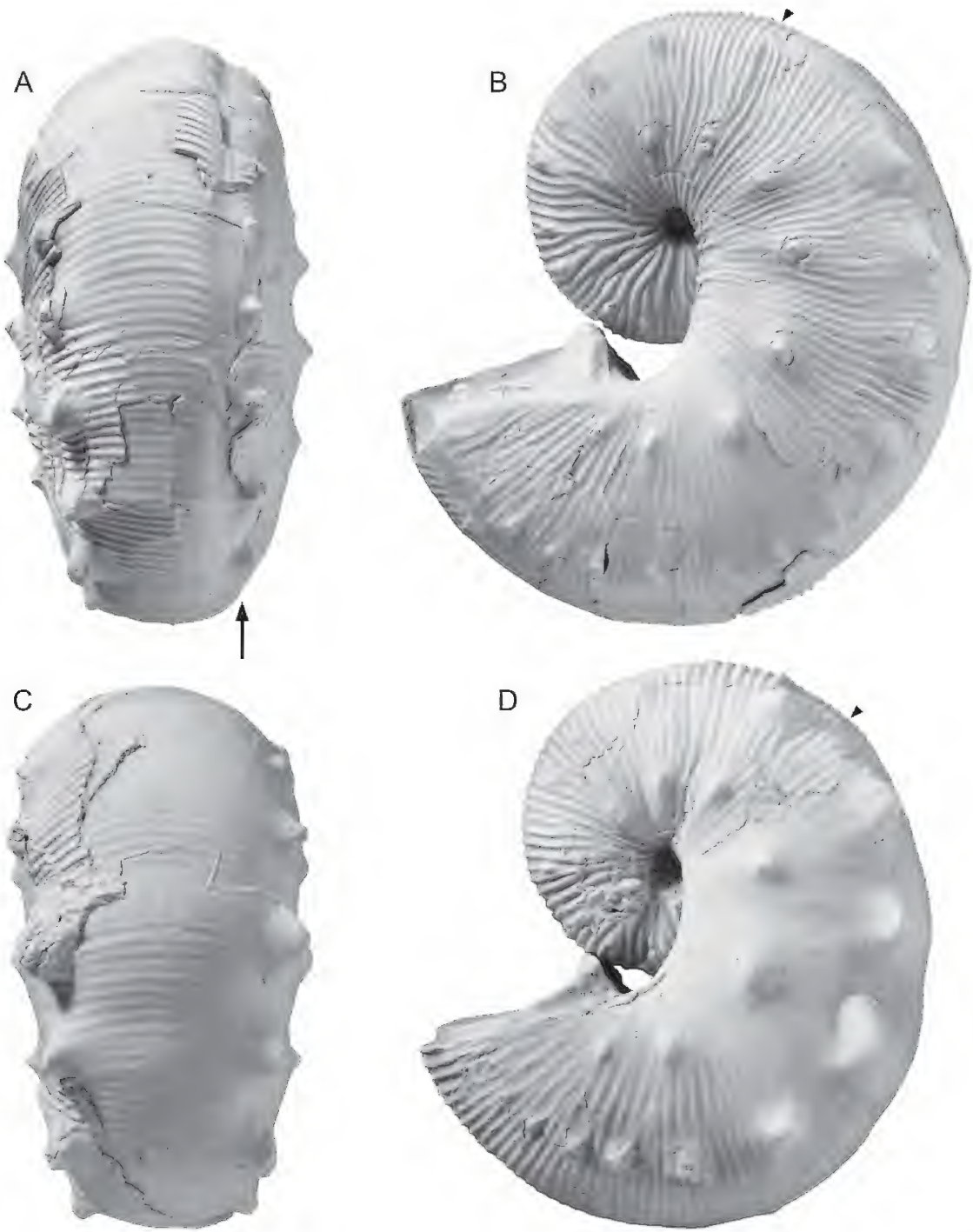

Fig. 46. *Hoploscaphites nodosus* (Owen, 1852), macroconchs, *Baculites compressus–B. cuneatus* zones, Pierre Shale, South Dakota. **A, B.** BHI 4178, with a spiral furrow (arrow) extending from midshaft to the aperture on the left side of the shell. **A.** Ventral hook; **B.** left lateral. **C, D.** BHI 4121. **C.** Ventral; **D.** left lateral. Specimens are illustrated natural size.

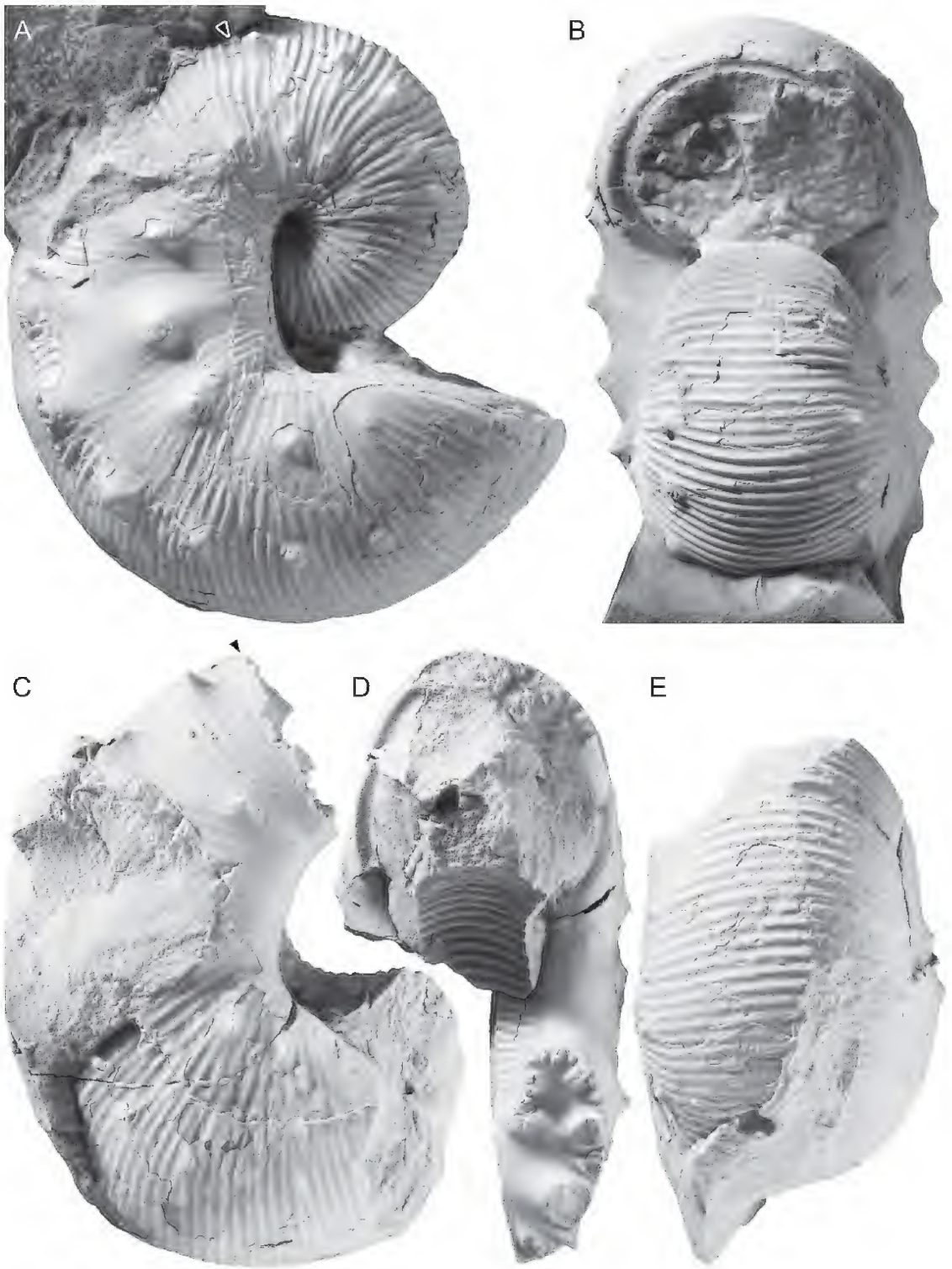

Fig. 47. *Hoploscaphites nodosus* (Owen, 1852), macroconchs, *Baculites compressus–B. cuneatus* zones. **A, B.** BHI 4787, robust but with fine ribbing, Meade County, Pierre Shale, South Dakota. **A.** Right lateral;

ventral to primary ribs is approximately 2–4:1 at midshaft and 3–4:1 at the point of recurvature, approximately the same values as in macroconchs.

The umbilicolateral tubercles appear one-third to one-half way onto the exposed phragmocone. They are more or less evenly spaced, although they are sometimes clustered into pairs. The maximum distance between umbilicolateral tubercles on the exposed phragmocone averages 8.3 mm and ranges from 7 to 9.5 mm. The height of the largest umbilicolateral tubercle ranges from 1 to 3.5 mm. One or two ribs join an umbilicolateral tubercle on the dorsal side, and as many as three ribs branch from it on the ventral side. The total number of umbilicolateral tubercles on the exposed phragmocone averages 5 and ranges from 2 to 7, similar to that in macroconchs.

The umbilicolateral tubercles on the body chamber maintain nearly the same position on the flanks as they do on the phragmocone, that is, at approximately one-third whorl height. This contrasts with macroconchs, in which the umbilicolateral tubercles change their position in passing from the phragmocone to the body chamber, so that they sometimes occur at almost one-half whorl height on the shaft. In general, the umbilicolateral tubercles on the body chamber are evenly spaced, with a slightly wider spacing at midshaft. The maximum distance between umbilicolateral tubercles averages 11 mm and ranges from 10 to 12 mm. The largest umbilicolateral tubercle appears at midshaft and ranges from 2 to 4 mm in height. The umbilicolateral tubercles usually extend to the aperture, decreasing slightly in size and spacing at the point of recurvature. As many as three ribs join an umbilicolateral tubercle dorsally and as many as four ribs branch from it ventrally. There are 5–8 umbilicolateral tubercles on the body chamber, averaging 6. The total number of umbilicolateral tubercles on the adult shell ranges from 7 to 15, averaging 11, slightly more than that in macroconchs (average = 9).

In most specimens, ventrolateral tubercles are already present at the point of exposure. They are more or less evenly spaced on the phragmocone, but an uneven distribution with clustering in pairs is very common. For example, in BHI 4220 (fig. 64A, B), starting at the point of exposure, the distance between consecutive tubercles, as measured in an adoral direction, is 10, 13, 6, 7, 6, 8.5, 7.5, 10, 10, and 14 mm. The maximum distance between consecutive tubercles on the exposed phragmocone in the measured set of specimens ranges from 12 to 21 mm, averaging 14.9 mm, similar to that in macroconchs (average = 15 mm). The maximum height of ventrolateral tubercles ranges from 2 to 4 mm. As many as four ribs join a ventrolateral tubercle dorsally, and an additional one or two ribs branch from it ventrally, looping to ventrolateral tubercles on the opposite side. A maximum of four ribs intercalate between ventrolateral tubercles. The total number of ventrolateral tubercles on the exposed phragmocone ranges from 5 to 12, averaging 8, the same number as in macroconchs.

The ventrolateral tubercles are more or less evenly spaced on the body chamber. They attain their widest spacing at midshaft. The maximum distance between consecutive ventrolateral tubercles ranges from 13.5 to 16 mm, averaging 14.7 mm, slightly less than that in macroconchs (average = 16 mm). The ventrolateral tubercles also attain their maximum size at midshaft, ranging from 2.5 to 4 mm in height. As many as four ribs join a ventrolateral tubercle dorsally and an additional one to three ribs branch from it ventrally, looping to ventrolateral tubercles on the opposite side. A maximum of four ribs intercalate between tubercles.

The ventrolateral tubercles diminish abruptly in size as they approach the point of recurvature. In most specimens, they persist to the aperture, but occasionally, they

---

←

B. apertural. **C–E.** TMP PI 80.13.76, Bearpaw Shale, near Manyberries, Alberta, Canada. **C.** Right lateral; **D.** apertural; **E.** ventral hook. Specimens are illustrated natural size.

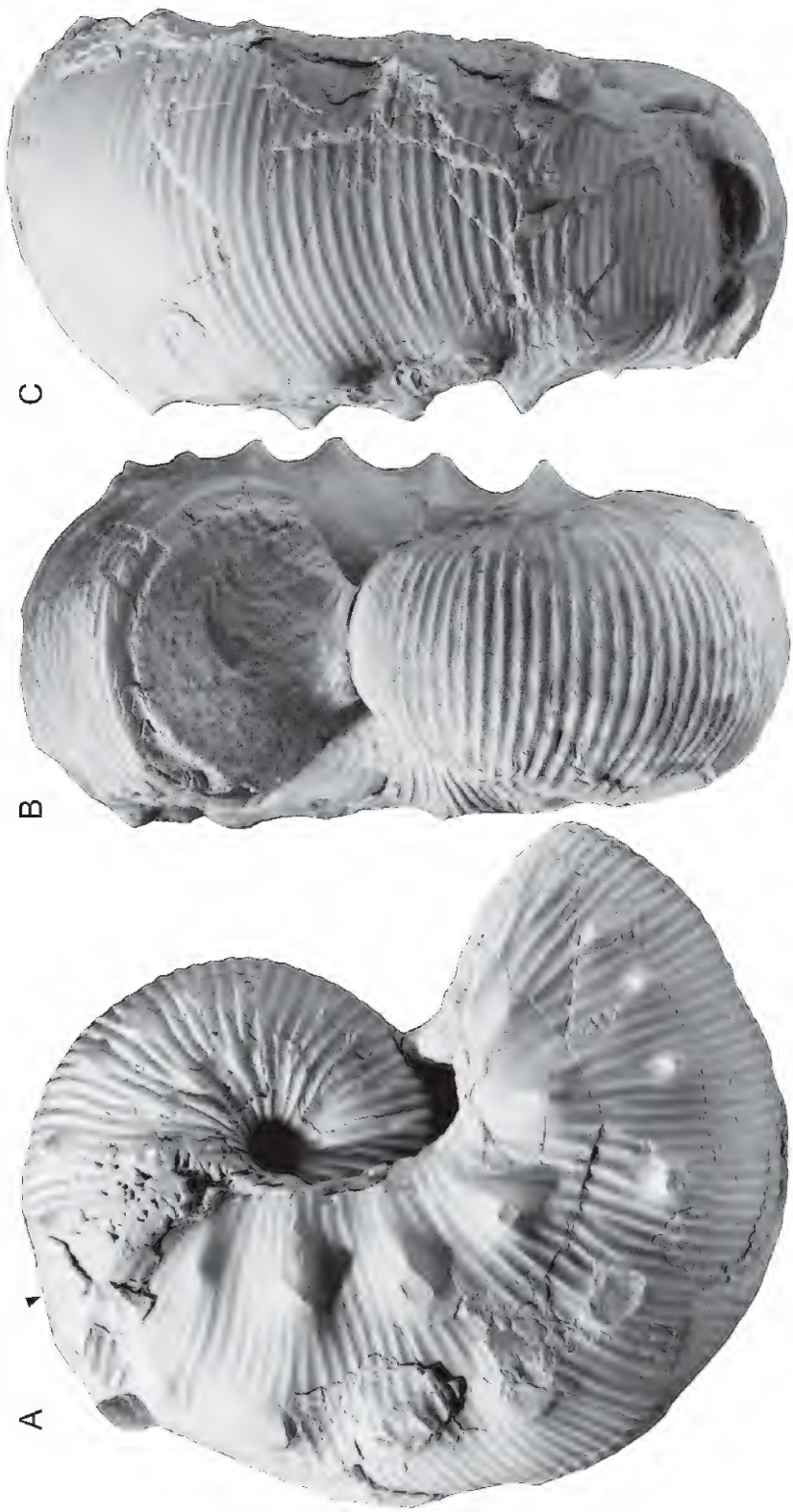

Fig. 48. *Hoploscaphites nodosus* (Owen, 1852), large macroconch, AMNH 47121, *Baculites cuneatus–B reesidei* zones, Bearpaw Shale, AMNH loc. 3368, Rosebud County, Montana. **A.** Right lateral; **B.** apertural; **C.** ventral. Specimen is illustrated natural size.

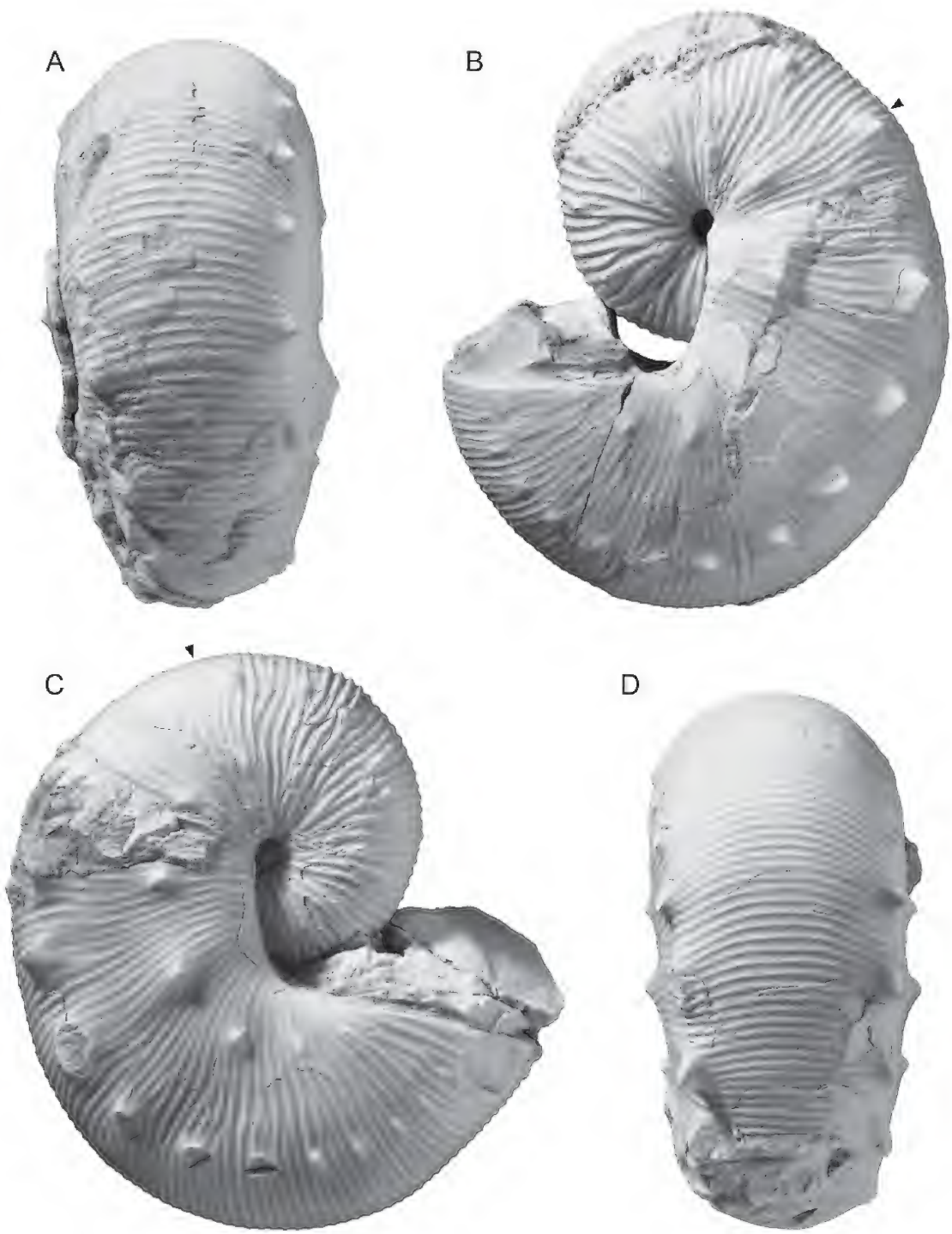

Fig. 49. *Hoploscaphites nodosus* (Owen, 1852), macroconchs. **A, B.** AMNH 58513, locality unknown, probably Pennington County, South Dakota. **A.** Ventral; **B.** left lateral. **C, D.** BHI 4215, *Baculites cuneatus* Zone, Meade County, South Dakota. **C.** Right lateral; **D.** ventral hook. Specimens are illustrated natural size.

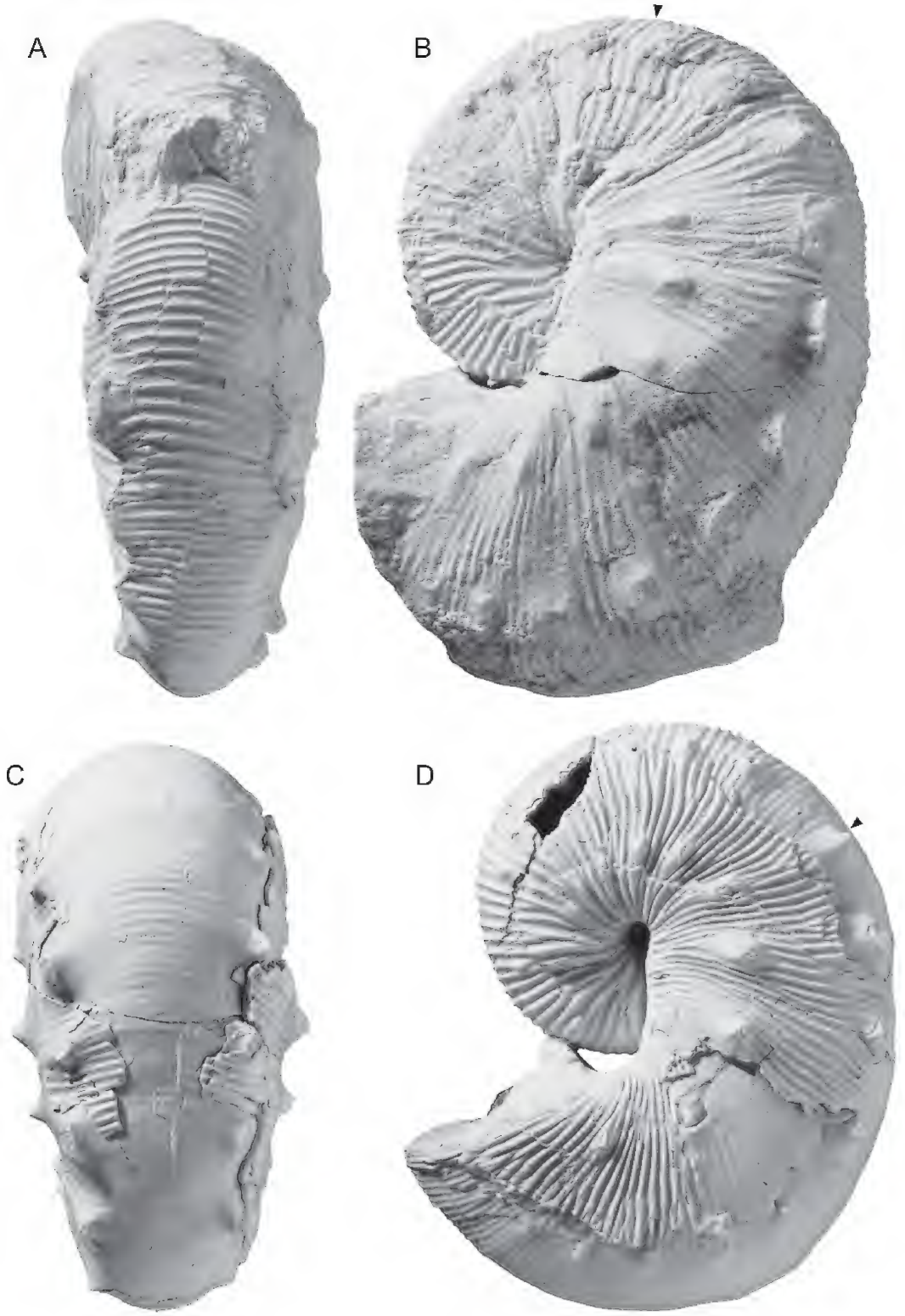
A
B
C
D

disappear at the point of recurvature. The ventrolateral tubercles are paired or offset from one side of the venter to the other. When they are paired, they commonly form broad elevations across the venter, as in BHI 4710 (fig. 63) and USNM 536232 (fig. 70A, B). The number of ventrolateral tubercles on the body chamber ranges from 4 to 14, averaging 9, less than that in macroconchs (average = 12). The total number of ventrolateral tubercles on the adult shell ranges from 9 to 26, averaging 17, only slightly less than that in macroconchs (average = 20).

The suture of microconchs is similar to that of macroconchs (fig. 61).

ONTOGENY: The ontogenetic change in whorl shape in this species is illustrated in two dorsoventral cross sections, with accompanying graphs (figs. 72–75). At a shell diameter of approximately 3 mm, the whorl section is reniform with a ratio of whorl width to height of 1.3–1.4, and a ratio of umbilical diameter to shell diameter of 0.35–0.40. The umbilical wall is nearly flat and slanted outward and the umbilical shoulder is sharply rounded. The flanks are broadly rounded, the ventrolateral shoulder is sharply rounded, and the venter is very broadly rounded. The ratio of whorl width to whorl height decreases through most of ontogeny until the beginning of the mature phragmocone, after which it sometimes increases. At a shell diameter of 10–20 mm, the ratio ranges from 1.0 to 1.3, depending upon the robustness of the specimen. The whorl section is subquadrate with a sharply rounded umbilical wall and shoulder. The flanks are broadly rounded, the ventrolateral shoulder is sharply rounded, and the venter is broadly rounded. The ratio of umbilical diameter to shell diameter also decreases through most of ontogeny until a shell diameter of approximately 20 mm, after which the ratio remains nearly the same until the beginning of the mature body chamber.

The ontogenetic development of the ornamentation is illustrated in a dissection of a macroconch (fig. 76). The early whorls are smooth. At a shell diameter of 3.5 mm, corresponding to 2.4 whorls adoral of the primary constriction, small swellings appear on the flanks, and soon thereafter, weak ribs appear on the venter. The swellings on the flanks become more elongate and develop into convex, prorsiradiate ribs. They cross the venter with a broad adoral projection. Additional ribs appear by intercalation at the ventrolateral shoulder, so that the ratio of ventral to primary ribs is 3:1 at a shell diameter of approximately 10 mm. Over the next 0.75 whorl, terminating at a diameter of approximately 20 mm, corresponding to 0.5–0.75 whorl adapical of the point of exposure, the ribs become slightly more flexuous. Ribs swing forward on the inner flanks and backward again on the outer flanks, crossing the venter with a broad adoral projection. There are 8.5 ribs/cm on the venter. Branching and intercalation occur at the umbilicolateral and ventrolateral shoulders, so that the ratio of ventral to primary ribs is 4:1.

Over the next 0.5 whorl, corresponding to 0.25–0.5 whorl adapical of the point of exposure, terminating at a diameter of approximately 30 mm, the rib density decreases to 6.25 ribs/cm on the venter. In addition, ventrolateral tubercles appear on every other rib to every fourth rib. A single rib or pair of ribs loops between ventrolateral tubercles on opposite sides of the venter. At the point of exposure, ribs are prorsiradiate and nearly straight on the flanks. They swing gently backward on the inner flanks, gently forward on the midflanks, and gently backward on the outer flanks, crossing the venter with only a slight forward projection. There are approximately 6 ribs/cm on the venter. Branching and intercalation occur near the umbilicolateral and ventrolateral shoulders,

←

Fig. 50. *Hoploscaphites nodosus* (Owen, 1852), macroconchs. **A, B.** USNM 536230, USGS Mesozoic loc. D 1353, Pierre Shale, *Baculites cuneatus* Zone, Grand County, Colorado. **A.** Ventral; **B.** left lateral. **C, D.** YPM 35575, G.A. Clarke Collection, YPM loc. A6520, Pierre Shale, Sage Creek, Pennington County, South Dakota. **C.** Ventral; **D.** left lateral. Specimens are illustrated natural size.

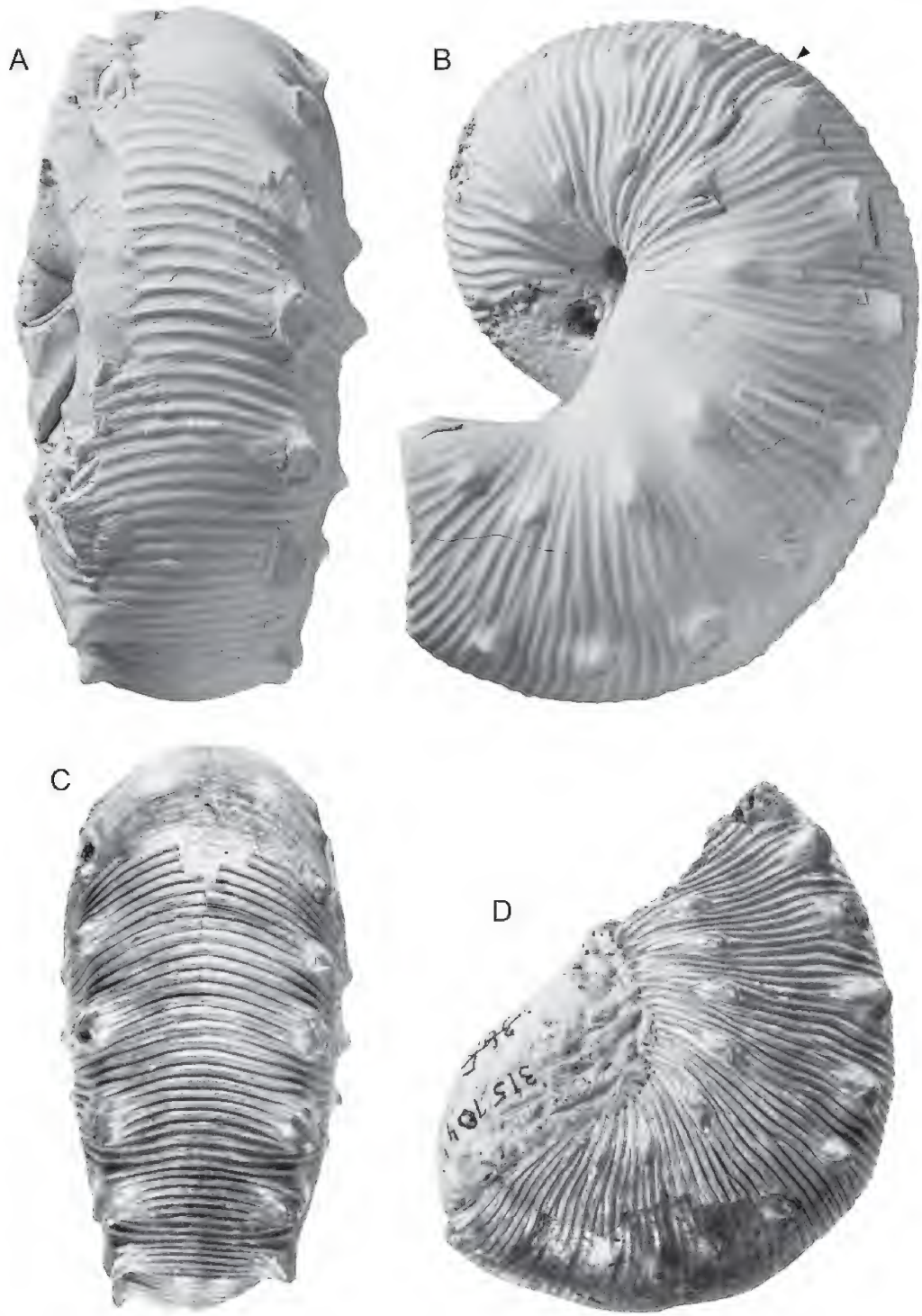

Fig. 51. *Hoploscaphites nodosus* (Owen, 1852), macroconchs. **A, B.** USNM 536218, USGS Mesozoic loc. 22182, Bearpaw Shale, *Baculites cuneatus–B. reesidei* zones, Fergus County, Montana. **A.** Ventral; **B.** left lateral. **C, D.** USNM 315704, uncoated, said to be from the "Yellowstone River, 150 mi above river mouth, Montana," but more probably from the Pierre Shale, Pennington County, South Dakota. **C.** Ventral; **D.** left lateral. Specimens are illustrated natural size.

so that the ratio of ventral to primary ribs is 3:1. Ventrolateral tubercles occur sporadically on every third to every ninth rib. Umbilicolateral tubercles appear at one-third whorl height on the last one-third whorl of the exposed phragmocone.

Septal approximation at maturity occurs in most, but not all, specimens (fig. 77, table 1). The pattern between dimorphs is not markedly different, perhaps because the whorl section in this species is depressed and, therefore, variation in chamber volume is not necessarily expressed as variation in chamber length. We examined four macroconchs and nine microconchs involving the last three to seven chambers (two specimens with three chambers, one with four chambers, one with five chambers, seven with six chambers, and two with seven chambers).

In macroconchs, septal approximation either occurs over the last one or two chambers or not at all. In specimens with septal approximation, the magnitude of approximation ranges from 36% to 65%. In the specimen with the weakest approximation (YPM 35598), there is a pathology due to an injury. In the specimen without septal approximation (BHI 4215), the last septum occurs adapical of the line of maximum length. In microconchs, septal approximation occurs either over the last one or two chambers or not at all. The magnitude of septal approximation ranges from 48% to 73%, with one exception (23% in USNM 536245). In one of the specimens without septal approximation, there is a pathology due to an injury.

DISCUSSION: The ontogeny of this species has previously been treated by several authors. Hall and Meek (1856) examined the development of sutures in this species based on material collected by Meek and Hayden in 1853. However, due to changes in nomenclature, it is difficult to confirm that the species they examined is, indeed, *Hoploscaphites nodosus*, because there are no accompanying illustrations of adult specimens. The authors noted an increase in the complexity of the suture during ontogeny. They observed a similar pattern in other ammonites that they studed from the same region, and extrapolated this pattern to ammonites in general. They interpreted this evidence as supporting one of the prevailing theories at the time, namely recapitulation. Hall and Meek (1856: 404) stated:

> these facts have an important bearing upon the study of this family of fossils [ammonites], and show in a remarkable degree how beautifully the progression from lower to higher forms of animal organization, as exhibited in the introduction of successive creations upon the same general plan from the older to the more recent geological epochs, is here simulated and illustrated by the phases of development in a single individual in its progress from the young state to maturity.

Logan (1899: pl. 22, fig. 2; pl. 23, figs. 1–4, 6–12) studied the ontogeny of what he called *Scaphites nodosus*, but, again, it is impossible to confirm the identity of the species. The adult specimen he illustrated more closely resembles *Hoploscaphites plenus*, and Riccardi (1983: 17) noted that the catalog number cited by Logan (3653) for the adult whose sutures he illustrated currently refers to two specimens in the Field Museum, both of which are *H. plenus*. However, the specimen that Logan broke down for study is probably no longer intact. Logan examined the ontogenetic development of the shell shape, ornamentation, and suture. The drawings of the sutures are not very detailed, and are illustrated upside down from a modern perspective. Logan compared the ontogenetic development of *Scaphites nodosus* with that of the older species *Scaphites warreni* Meek, 1876, in the context of the theory of recapitulation, as propounded by Hyatt (1894). Logan concluded that a comparison between these two species in terms of their suture, shape, and ornamentation indicated an evolutionary progression in form, rather than a retrogression, as predicted by Hyatt's theories.

Smith (1905: figs. 1.1–7, 9–16; 2.1; 3.1–10, 14) published a study on the ontogenetic development of *Scaphites*, including what he called *Scaphites nodosus*, *S. nodosus* var. *plenus*, *S. nodosus* var. *quadrangularis*, and *S. nodosus* var. *brevis*, in addition to several species from the Upper Cretaceous of California. However, in the introduction to his paper, he stated that the Western Interior material was collected from the vicinity of

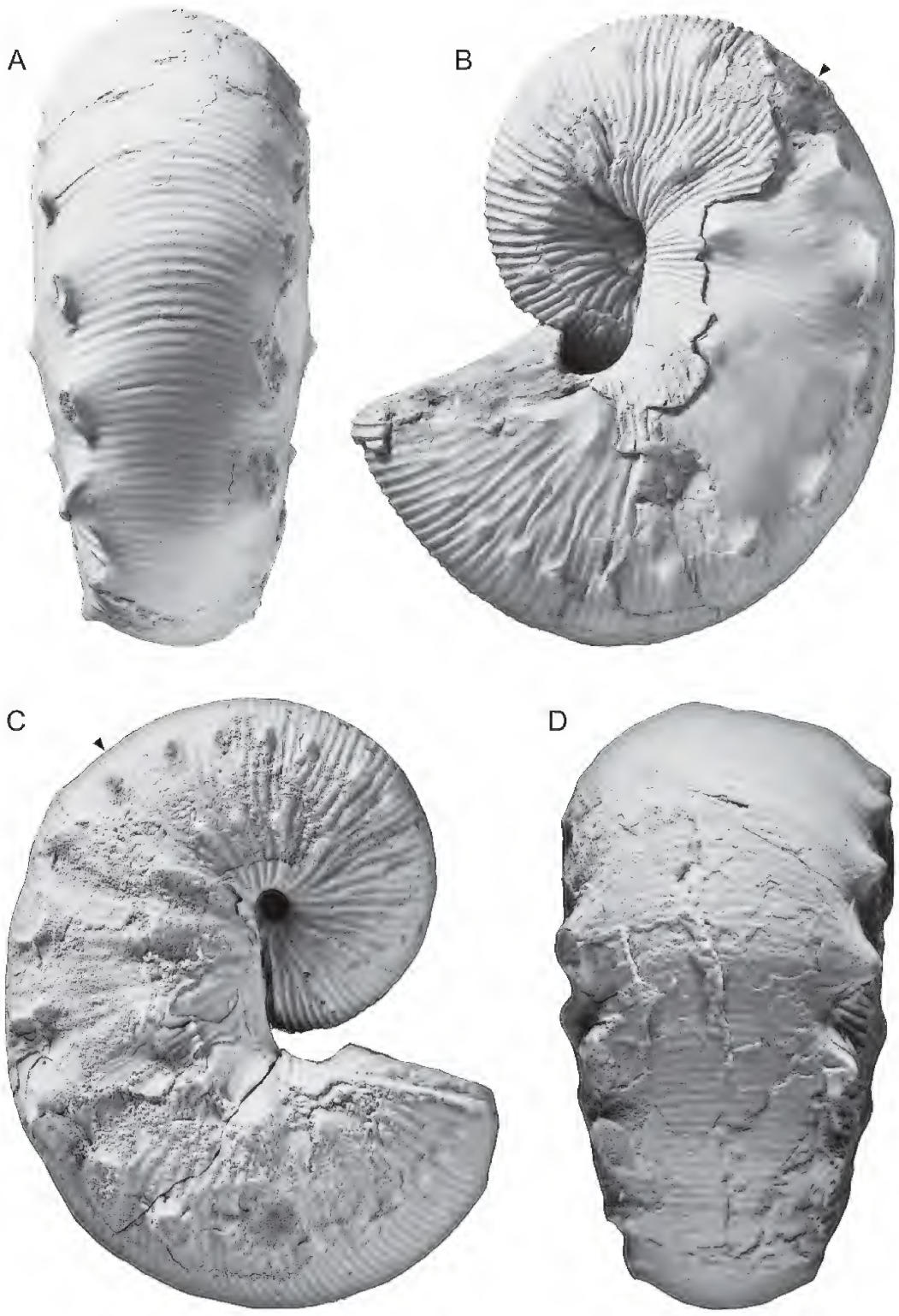
A
B
C
D

Wibaux, Montana. The rocks in this area do not contain *Hoploscaphites nodosus*, but rather closely related forms that appear higher up in the stratigraphic section. Like Logan, Smith examined the ontogeny of these species in the context of the theory of recapitulation, but unlike Logan (1899), he concluded that scaphites were not progressive, but "degenerate forms," in accordance with the then prevailing views of Cope and Hyatt. Smith (1905: 651) listed four reasons why these species were degenerate: "(1) in the possession of an abnormal body chamber, they show degeneration or senility; (2) in the dicranidian [bifid] lobes; (3) in the reduced number of lobes and saddles; [and] (4) in the fact that they have, so far as we know, left no trace of a descendant."

Since the original description of *Hoploscaphites nodosus* by Owen in 1852, this species has become one of the best-known fossils from the Upper Cretaceous of the Western Interior. One of the reasons for its popularity is that it has been illustrated in many geology textbooks and guides to invertebrate fossils (Dunbar, 1960; Case, 1992; Monks and Palmer, 2002). Even so, as Riccardi (1983: 16) noted, it is still a poorly known species, because its range of variability has not been well established.

Meek (1859: pl. 2, figs. 7, 8) illustrated a specimen that he called *Scaphites nodosus* (?) var. from the "South Branch of the Saskatchewan," Canada. However, he noted in his explanation that "the specimen figured shows the remains of two rows of tubercles on the dorsum [= venter]—one on each side. They are much worn, and have been unfortunately omitted altogether by the artist." As a result, the specimen is difficult to identify, and to further complicate matters, it appears to be lost (fide Riccardi, 1983: 16). In the following years, *Hoploscaphites nodosus* has frequently been reported from Canada. Dowling (1917: 32) listed *S. nodosus* from the Cypress Hills area, southwestern Saskatchewan. Landes (1940: 177–178) described material as *Acanthoscaphites nodosus* from the Sandy Shale of the Bearpaw Shale in the Manyberries area, southeastern Alberta, but did not illustrate it. Jeletzky (1970: pl. 27, fig. 7) identified a specimen of *S. nodosus* (GSC 5369a) from the "Elbow of the Saskatchewan River," which was originally mentioned by Whiteaves (1885: 52). This specimen was refigured by Nelson (1975: pl. 64, figs. 1, 2) and Riccardi (1983: pl. 2, figs. 4–8), the last of whom called it *Jeletzkytes nodosus*. It is a broken microconch that conforms to *H. nodosus* in terms of size, shape, and rib spacing. We illustrate a similar specimen (TMP 80.13.76) from the Manyberries area, Alberta (fig. 47C–E). It is a macroconch and consists of most of the body chamber, with a piece of shell missing from the adapical part, probably due to an injury.

Riccardi (1983: 18, text fig. 7b, pl. 3, figs. 2–6; pl. 4, figs. 1, 2) assigned two specimens from the Bearpaw Shale to *Jeletzkytes* aff. *nodosus*: UA 748 (fig. 78A, B) from the north side of the Milk River, near Groton, Alberta, and UA 03944 (fig. 78C, D) from an unknown locality in Alberta. The first of these, UA 748, is a complete macroconch with a maximum length of 111 mm and an apertural angle of 51°. It bears straight, sharp ribs, and 12 umbilicolateral and 17 ventrolateral tubercles. The second of these, UA 03944, is also a macroconch, 101 mm in maximum length, with the adoral part of the shaft and hook missing. There are 16 umbilicolateral and 18 ventrolateral tubercles on the preserved portion of the shell. Riccardi (1983: pl. 3, fig. 1) also assigned a specimen, originally mentioned by Whiteaves (1885: 52) from the South Saskatchewan River, opposite the mouth of Swift Current Creek, to what he called *Jeletzkytes* cf. *nodosus*. It is 107.5 mm in maximum length, with widely spaced

←

Fig. 52. *Hoploscaphites nodosus* (Owen, 1852), macroconchs. **A, B.** YPM 8924, O.C. Marsh Collection, YPM loc. A6560, Pierre Shale, Box Elder Creek, Pennington County, South Dakota. **A.** Ventral; **B.** left lateral. **C, D.** YPM 35593, more compact and finely ribbed than holotype, YPM loc. C3346, Pierre Shale, locality unknown. **C.** Right lateral; **D.** ventral. Specimens are illustrated natural size.

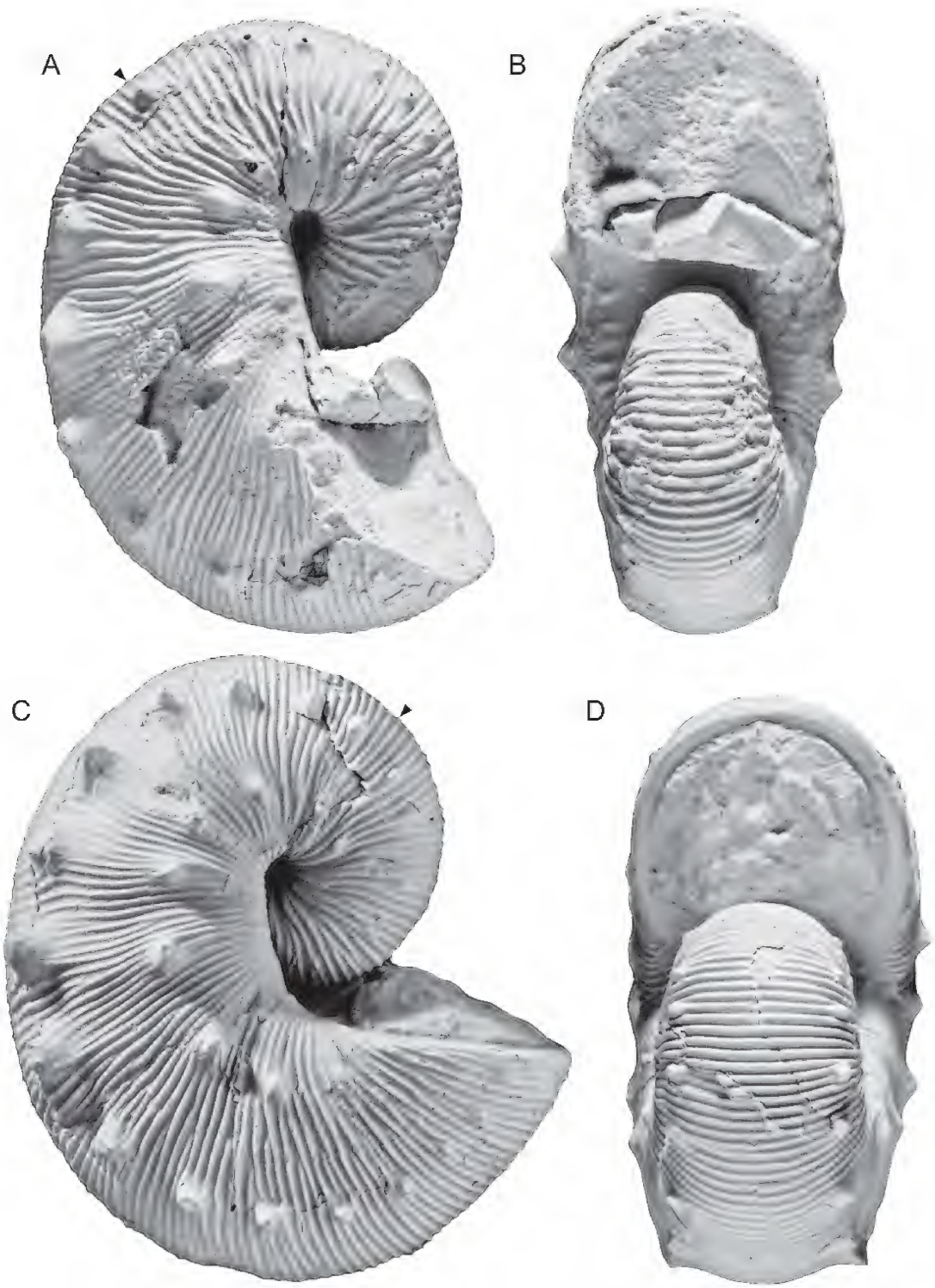

Fig. 53. A, B. *Hoploscaphites nodosus* (Owen, 1852), macroconchs. **A, B.** AMNH 45343, more compact and finely ribbed than holotype, AMNH loc. 3212, *Baculites compressus–B. cuneatus* zones, Shannon

ribbing. All three of these specimens are larger and more coarsely ornamented than *H. nodosus*, and probably represent a closely related species from the *Baculites reesidei–B. jenseni* zones. Similar specimens appear in the same biostratigraphic interval in the Bearpaw Shale, Montana.

Several specimens have been attributed to *Hoploscaphites nodosus* from the Pierre Shale of Wallace County, Kansas, but also differ from it in their larger size and coarser ribbing. The Pierre Shale in this region consists, in part, of the Weskan Shale Member, which represents the *B. compressus–B. cuneatus* zones, and the overlying Lake Creek Shale Member, which represents the *B. reesidei* Zone. Elias (1933: pl. 38, figs. 1–3) described two macroconchs from the Weskan Shale and Lake Creek Shale members that he assigned to *Acanthoscaphites nodosus*: KUMIP 59651 (fig. 79A–D) consists of the internal whorls and part of the body chamber, and KUMIP 59652 (fig. 79F, G) consists of part of the body chamber. Both specimens are very coarsely ornamented and are provisionally referred to *Hoploscaphites* aff. *H. nodosus*. We illustrate two similar specimens from the Lake Creek Shale Member: USNM 538096 (fig. 80C) is part of a body chamber, probably of a macrconch, and USNM 538097 (fig. 79E) is part of a body chamber, probably of a microconch. Elias (1933: pl. 41, fig. 3) also illustrated a specimen of what he called *Acanthoscaphites nodosus* var. *brevis* from the lower part of the Lake Creek Shale Member (fig. 80E, F). It consists of most of the body chamber of a large macroconch. It closely resembles *H. nodosus*, although its flat flanks are reminiscent of forms from the *B. reesidei–B. jenseni* zones.

Hoploscaphites nodosus is common in South Dakota. In all probability, the holotype was collected from the Pierre Shale at Sage Creek, Pennington County. Subsequently, Whitfield (1880: 441, pl. 13, fig. 12) illustrated a remarkable specimen from the Cheyenne River, near Rapid Creek (fig. 41). It was collected by the U.S. Geological and Geographical Survey of the Black Hills in 1875, with Walter P. Jenney as geologist in charge (the same expedition that confirmed the presence of gold in the Black Hills, thus encouraging miners to come to the region, and eventually leading to the Great Sioux War of 1876–1877). It is a macroconch with a long spriral furrow on the left side starting on the middle of the phragmocone. Whitfield (1880: 442) noted that the specimen "appears to be intermediate between Mr. Meek's varieties *brevis* and *plenus*." Riccardi (1983: 16) further noted that this specimen differs from the holotype of *H. nodosus* in its more compressed whorl section, less conspicuous umbilicolateral and ventrolateral tubercles, and longer shaft. In terms of the range of variation in *H. nodosus*, this specimen represents the smaller, more compressed, and more finely ornamented end of the spectrum. Recently, Larson et al. (1997: 76, unnumbered figs.) illustrated a macroconch and microconch of *H. nodosus* from the Pierre Shale of South Dakota. In fact, as a generality, most of the specimens of this species illustrated in fossil guidebooks are from the Pierre Shale of South Dakota (e.g., Case, 1992: fig. 12.30).

Hoploscaphites nodosus has previously been reported from Colorado. Cobban et al. (1992: A8, pl. 3, figs. 2–5, 7–11) described this species in association with *Baculites compressus* and *B. cuneatus* from the unnamed shale member of the Pierre Shale near Kremmling and Granby in north-central Colorado. The specimens they illustrated are nearly identical to those we describe from the same localities (figs. 36E, 50A, B, 56A–E, 68, 73, 93A, B, 101). Scott and Cobban (1986b) also recorded *H. nodosus* from the Pierre Shale east of the Front Range near Fort Collins, in association with *Baculites cuneatus* in the unnamed shale member, and in association

---

←

County, South Dakota. **A.** Right lateral; **B.** apertural. **C, D.** BHI 4257, more compact and finely ribbed than holotype, *Baculites cuneatus* Zone, Pierre Shale, Meade County, South Dakota. **C.** Right lateral; **D.** apertural. Specimens are illustrated natural size.

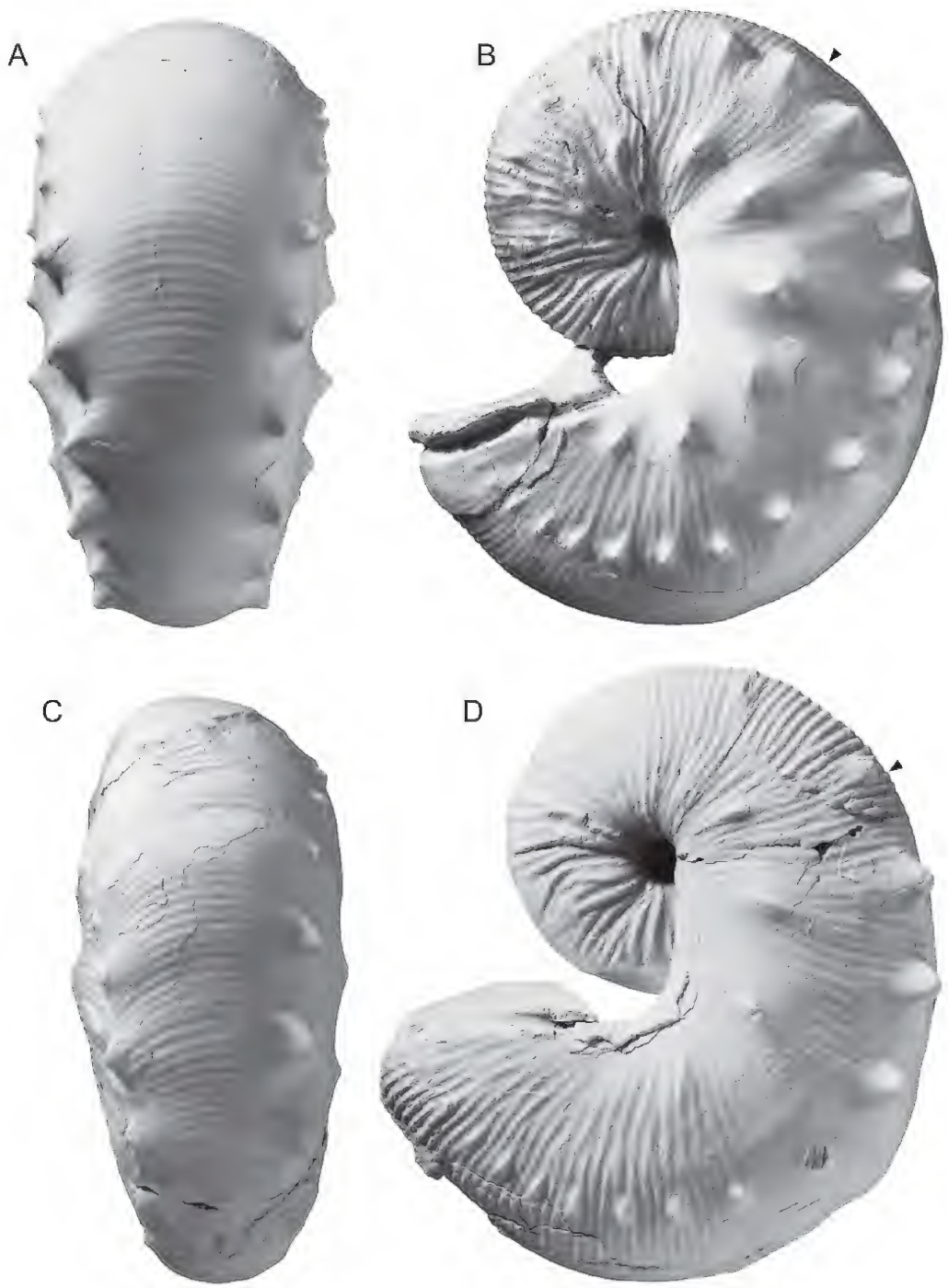

Fig. 54. *Hoploscaphites nodosus* (Owen, 1852), macroconchs. **A, B.** BHI 4948, *Baculites compressus* Zone, Pierre Shale, Meade County, South Dakota. **A.** Ventral; **B.** left lateral. **C, D.** YPM 35598, YPM loc. C3347, Pierre Shale, Belle Fourche River, South Dakota. A spiral furrow extends from the point of exposure to the aperture on the right side of the shell (fig. 35B). **C.** Ventral; **D.** left lateral. Specimens are illustrated natural size.

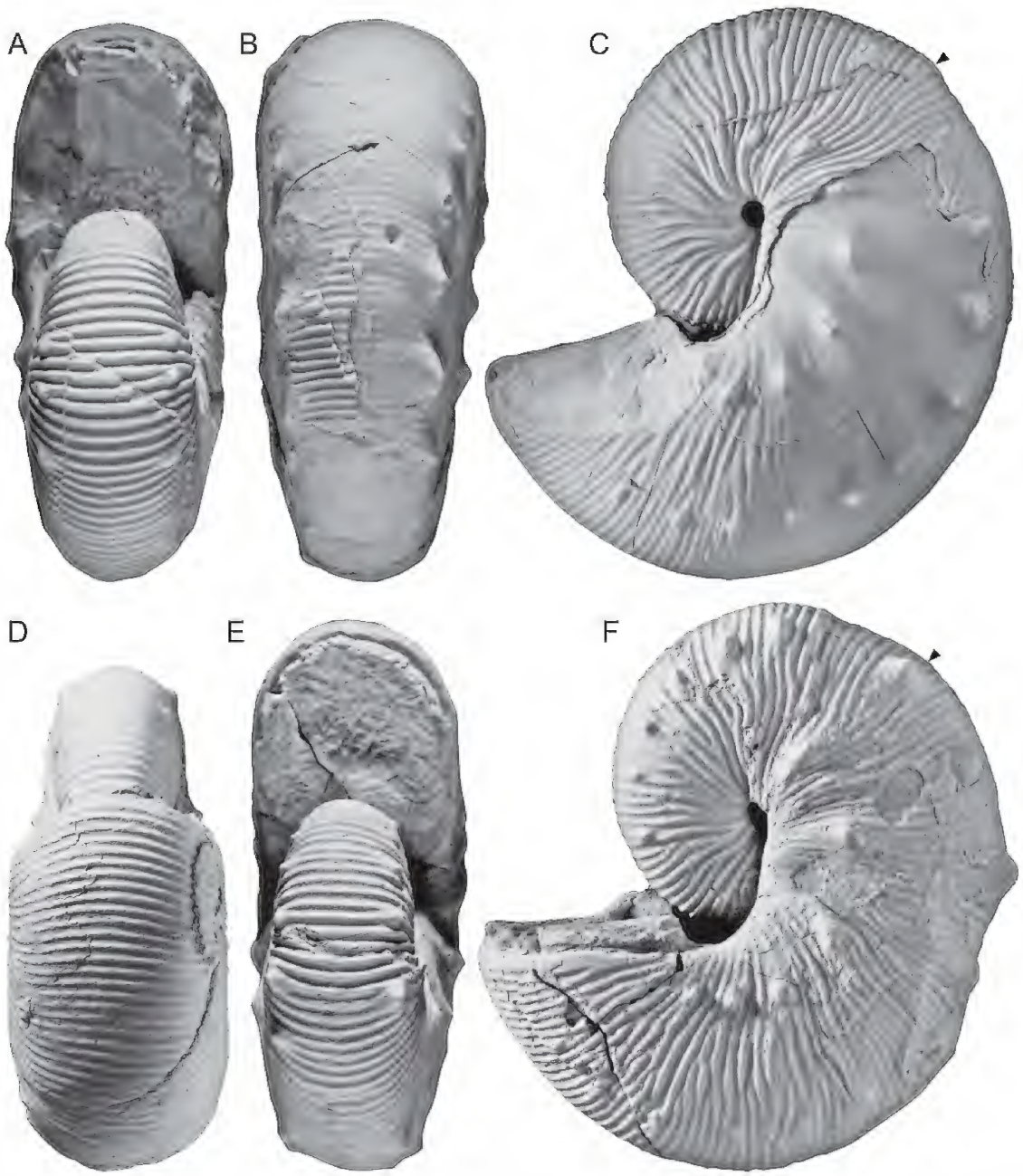

Fig. 55. *Hoploscaphites nodosus* (Owen, 1852), macroconchs, transitional to *H. brevis*. **A–C.** USNM 536233, USGS Mesozoic loc. 23072, Pierre Shale, near Sage Creek, Pennington County, South Dakota. A chunk of shell is missing from the adapical part of the body chamber. **A.** Apertural; **B.** ventral; **C.** left lateral. **D–F.** AMNH 58512, more slender and finely ribbed than holotype, locality unknown. **D.** Ventral hook; **E.** apertural; **F.** left lateral. These specimens are assigned to *H. nodosus* rather than *H. brevis* because the body chamber is elongate and the ventrolateral tubercles persist to the aperture. Specimens are illustrated natural size.

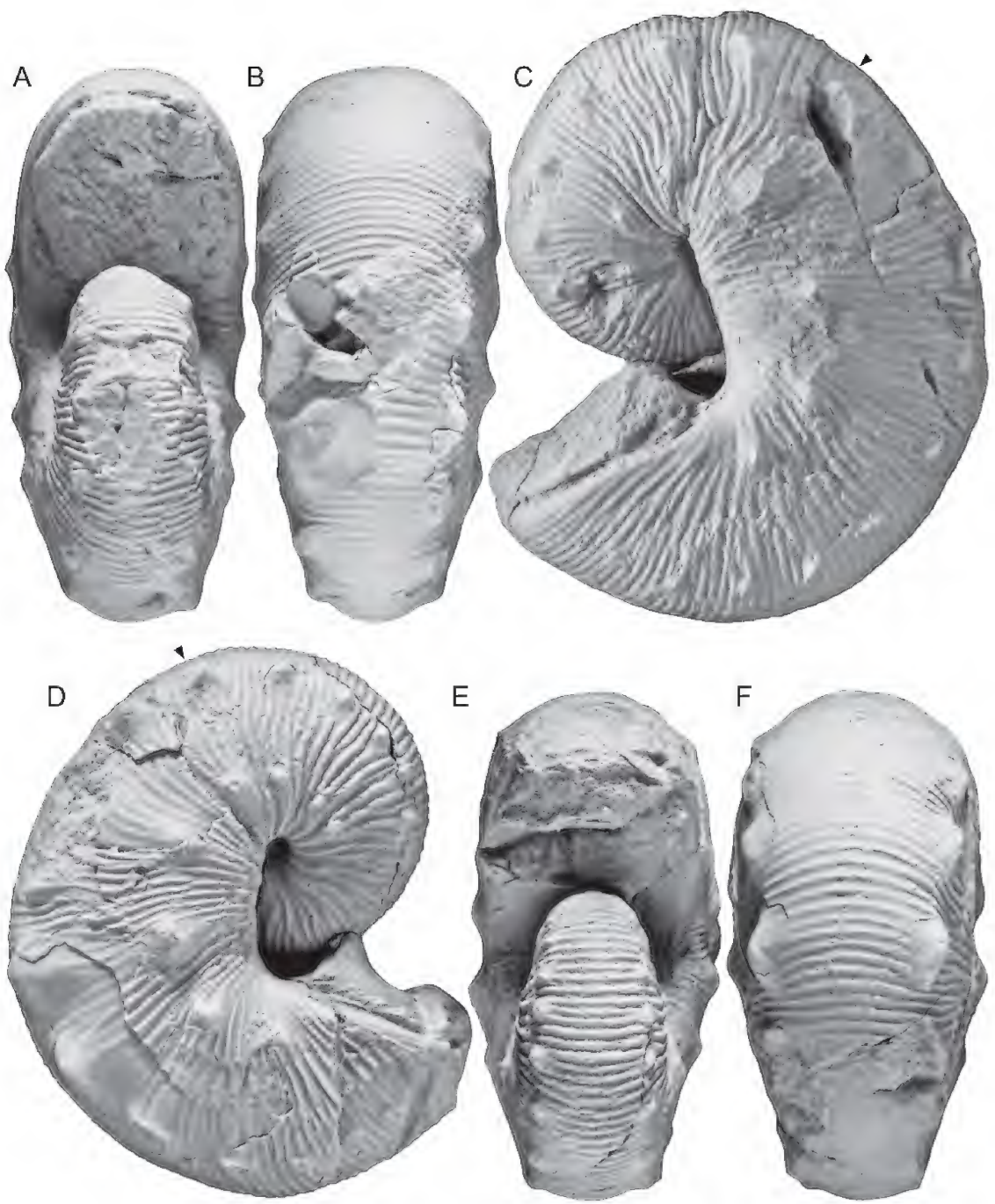

Fig. 56. *Hoploscaphites nodosus* (Owen, 1852), macroconchs, Pierre Shale. **A–C.** USNM 536235, USGS Mesozoic loc. 9154, Pierre Shale, near Kremmling, Grand County, Colorado. A piece of shell is missing from the venter of the midshaft. **A.** Apertural; **B.** ventral; **C.** left lateral. **D–F.** USNM 536234, smaller and more compressed than holotype, USGS Mesozoic loc. D5034, *Baculites compressus* Zone, Round Butte, Larimer County, Colorado. A large chunk of shell is missing from the adapical part of the body chamber. **D.** Right lateral; **E.** apertural; **F.** ventral. Specimens are illustrated natural size.

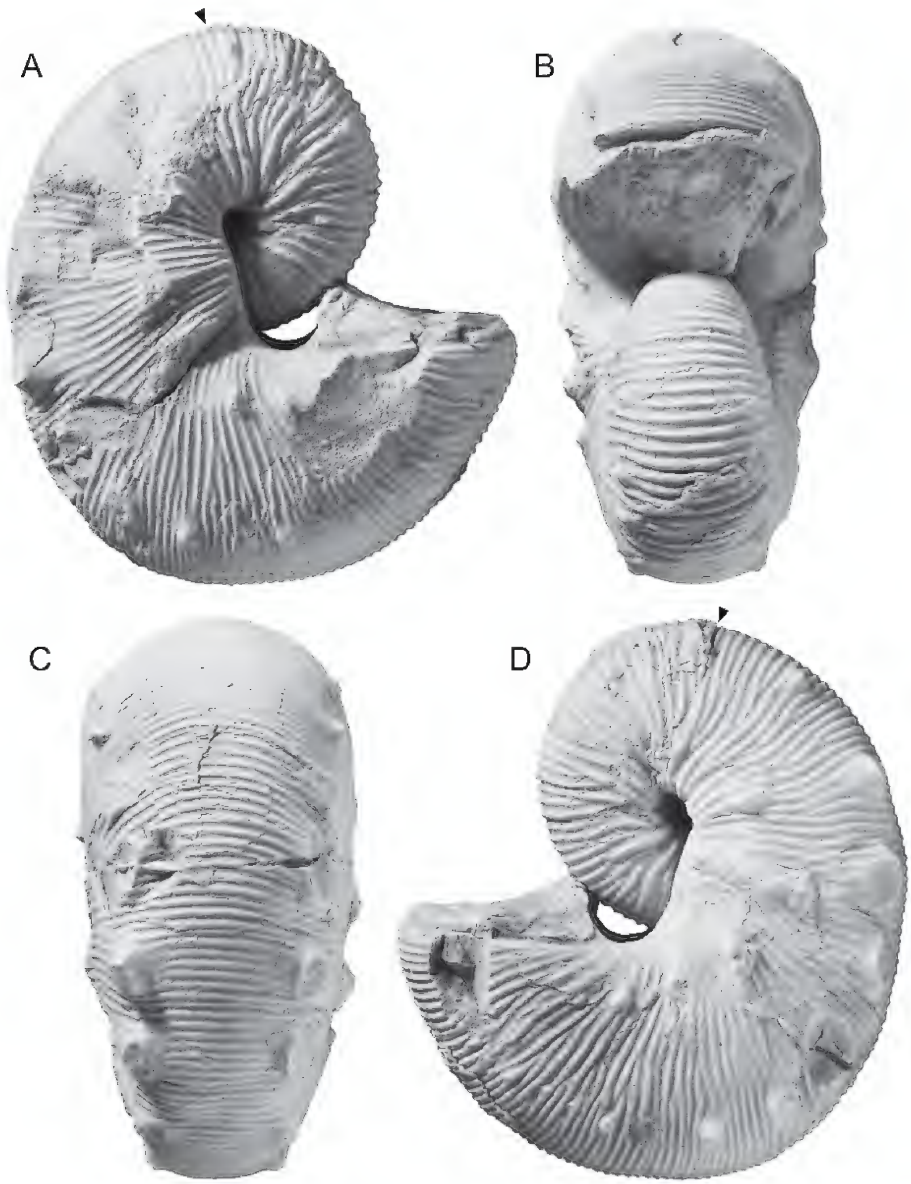

Fig. 57. *Hoploscaphites nodosus* (Owen, 1852), macroconch, USNM 536270, locality unknown. **A.** Right lateral; **B.** apertural; **C.** ventral; **D.** left lateral. This is the smallest macroconch known of this species and closely resembles *Hoploscaphites compressus* (Roemer, 1841). Specimen is illustrated natural size.

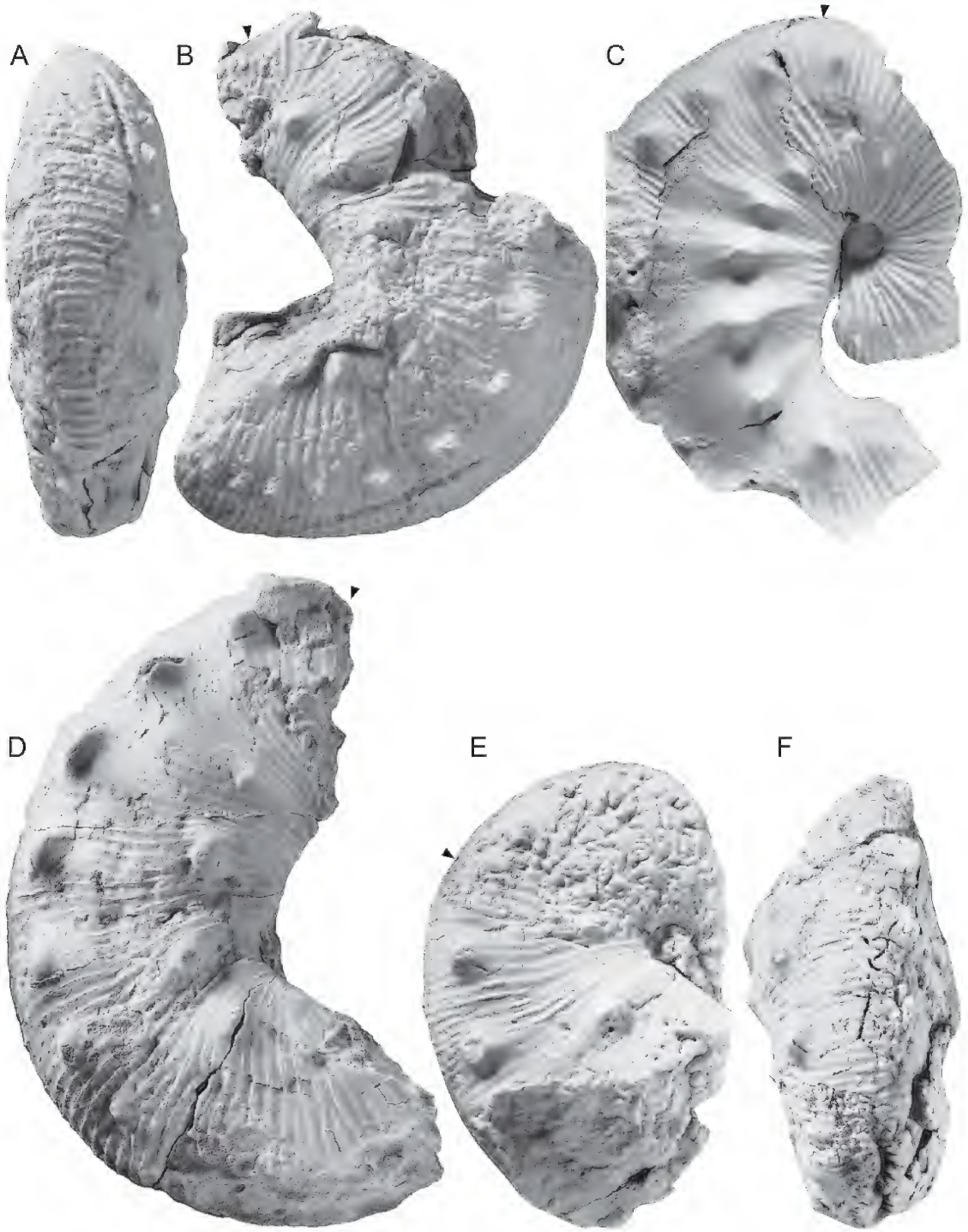

Fig. 58. Scaphites from the Oacoma Member, *Baculites compressus* Zone, Pierre Shale, east-central South Dakota. **A–C.** *Hoploscaphites brevis* (Meek, 1876), macroconchs. **A, B.** USNM 536268, USGS Mesozoic loc. D13686, Buffalo County. **A.** Ventral; **B.** left lateral. **C.** USNM 536269, left lateral, USGS Mesozoic loc. D13583, Lyman County. **D–F.** *Hoploscaphites nodosus* (Owen, 1852), macroconchs. **D.**

with *B. reesidei* in the overlying Rocky Ridge Sandstone Member, the unnamed sandy shale member, the Larimer Sandstone Member, and the unnamed shaly sanstone member. Gilbert (1896: pl. 65, fig. 2) illustrated a specimen (USNM 28363) that he called *Scaphites nodosus* from the Larimer Sandstone Member in the same area. It is a large macroconch 106 mm in maximum length, with flattened flanks and coarse ribbing. This specimen, as well as those reported by Scott and Cobban (1986b) from the *B. reesidei* Zone in this area, all probably belong to a closely related species of *H. nodosus*. Gilbert (1896: pl. 63, fig. 3) also illustrated a small specimen from a Tepee Butte in the "Tepee zone of the Pierre shale," Colorado, which he called a small variety of *S. nodosus*. It is 36 mm in maximum length and is a microconch of another, as yet undescribed, species.

In the Gulf Coastal Plain, many specimens have been assigned to *Hoploscaphites nodosus*, but differ from it in their coarser ribbing. Kennedy and Cobban (1993: 430: fig. 17.22–25) identified three specimens from the Saratoga Chalk, Arkansas, as *Jeletzkytes nodosus*. The most complete specimen of the three (USNM 445291) is a body chamber with widely spaced ribbing. In assigning these specimens to *J. nodosus*, Kennedy and Cobban (1993: 431) cited comparable material from the U.S. Western Interior that also shows widely spaced ribbing, including USNM 445292. However, this specimen is from USGS Mesozoic loc. 22182, which represents the *Baculites reesidei* Zone. Cobban and Kennedy (1994: B8, pl. 9, figs. 7–11) described two specimens as *J. nodosus* from the Coon Creek Tongue of the Ripley Formation at Coon Creek, McNairy County, Tennessee. One of them, BHI 1981, is a phragmocone and part of the body chamber of a macroconch. We illustrate two nearly identical specimens from the same locality (fig. 81) (see Larson, in press, for illustrations of additional specimens). The specimens from both the Coon Creek and Saratoga Chalk are more coarsely ornamented than *H. nodosus*, and belong to one of several species including *Hoploscaphites rugosus* (Stephenson, 1941: 425, pl. 89, figs. 15–18), *Hoploscaphites reesidei* (Wade, 1926: 183, pl. 61, figs. 3–7), or a closely related form.

In the Atlantic Coastal Plain, *Hoploscaphites nodosus* has been reported from the base of the Navesink Formation, New Jersey. Whitfield (1892: 261: pl. 44, figs. 13, 14) illustrated a fragment of a body chamber that he called *Scaphites nodosus* (ANSP 19499). The locality of this specimen was unknown, but Whitfield argued, based on its lithology, that it came from the "green sands" of New Jersey. It was refigured by Weller (1907: pl. 107, figs. 1, 2) who called it *Scaphites nodosus* ?, and by Reeside (1962: 126, 127, pl. 71, figs. 8–11), who noted that it "has nothing in common, morphologically or stratigraphically, with *S. nodosus*" and called it *Scaphites* aff. *S. leei*. Cobban (1974: 18, pl. 11, figs. 13–19; text fig. 14) illustrated similar specimens from the base of the Navesink Formation at Atlantic Highlands, New Jersey, which he attributed to *Hoploscaphites* sp. Kennedy et al. (2000b: 20, figs. 9J–P, 10, 11, 12C–F) illustrated still other specimens, including some nearly complete adults, from the same stratigraphic horizon, which they identified as *Jeletzkytes* cf. *nodosus*. All of these specimens resemble forms from the *Baculites reesidei–B. jenseni* zones in the Western Interior of North America.

Of the material Meek (1876) illustrated as *Scaphites nodosus* var. *quadrangularis*, none appears to represent *Hoploscaphites nodosus*. Meek (1876: pl. 25, figs. 2–4) illustrated three specimens, all of which are said to be from the "Yellowstone River, Montana, 150 miles above its mouth." USNM 386690 is a microconch of *H. brevis* and is probably from southwestern South Dakota (fig. 6G–D). USNM 365 and 366 are microconchs of *H. plenus*, and the stated locality is probably

---

←

USNM 536267, right lateral, USGS Mesozoic loc. D4968, Lyman County. **E, F.** USNM 536266, USGS Mesozoic loc. D13686, Buffalo County. **E.** Right lateral; **F.** ventral. Specimens are illustrated natural size. The position of the base of the body chamber is estimated.

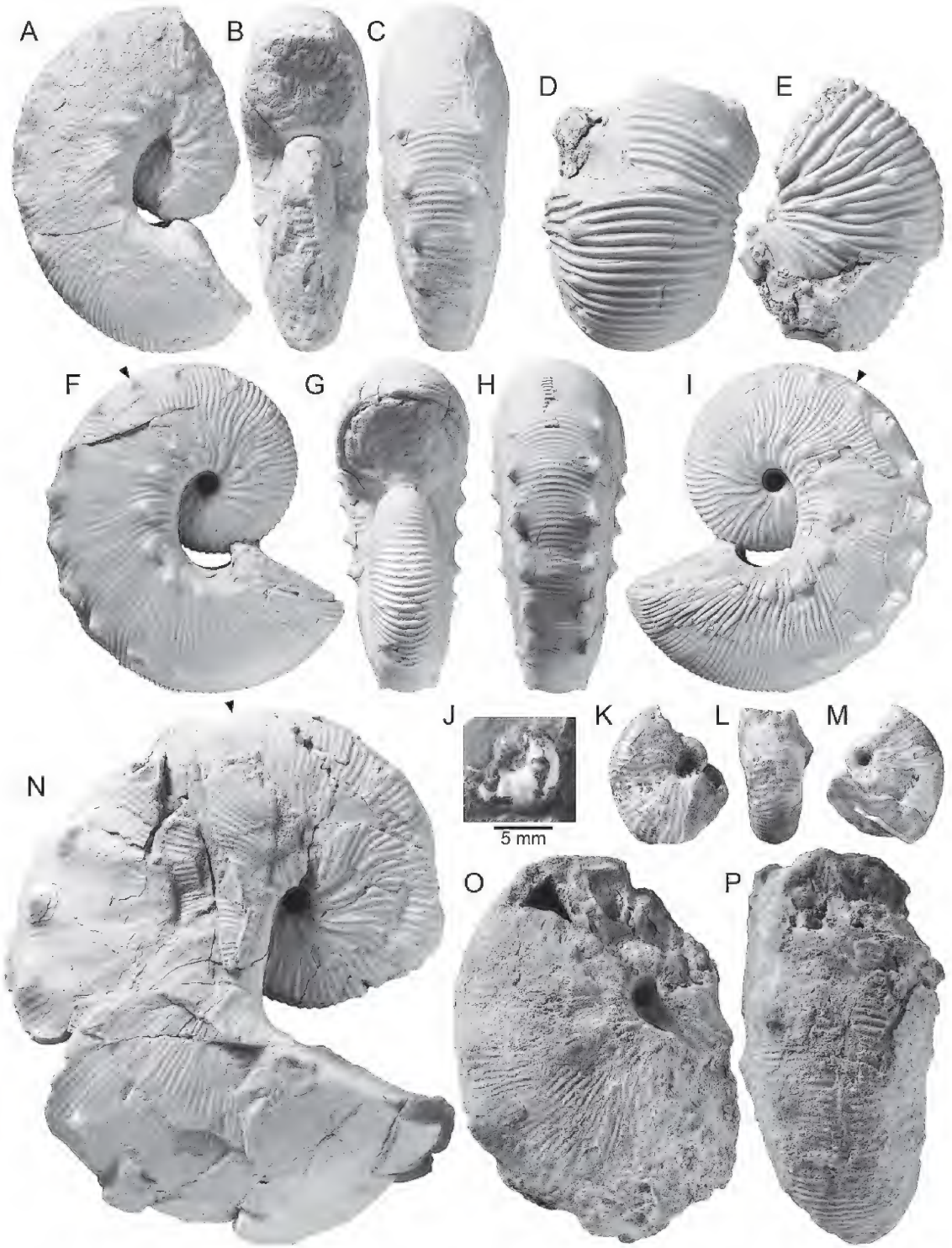

Fig. 59. Scaphites, cold seep, AMNH loc. 3418, *Didymoceras cheyennense* Zone, Pierre Shale, Custer County, South Dakota. **A–C.** *Hoploscaphites brevis* (Meek, 1876), small microconch, AMNH 56885. **A.** Right lateral; **B.** apertural; **C.** ventral. **D–E.** Fragment of a phragmocone of *Hoploscaphites nodosus*

close to the original source (fig. 6A–C and H–K, respectively). The specimen illustrated by Whitfield (1880: pl. 13, figs. 10, 11) as *Scaphites nodosus* var. *quadrangularis* (USNM 12291) from the "Fort Pierre Group" on the Cheyenne River, South Daktoa, is a microconch of *H. brevis* (fig. 7A–D). In contrast, there is an unfigured specimen in the USNM collections (USNM 315704) that is labeled as a paratype of *S. nodosus* var. *quadrangularis*, which is, in fact, a body chamber of a macroconch of *H. nodosus* (fig. 51C, D). The label states that the specimen is part of the original lot (365) described by Meek (1876) and, indeed, the number "365" is crossed out on the specimen. It is said to be from the "Fort Pierre Group, 150 miles above the mouth of the Yellowstone River, Montana," but is probably from southwestern South Dakota instead.

Hoploscaphites nodosus differs from *H. brevis*, which occurs in the same biostratigraphic interval, by its larger size, more robust whorl section, higher apertural angle, and more extended shaft, producing a more elongate outline in lateral view. In macroconchs, maximum whorl height occurs on the adoral part of the shaft in *H. nodosus*, whereas it occurs at midshaft in *H. brevis*. The pattern of ornamentation also differs between the two species. The ribs on the flanks of the body chamber are nearly straight in *H. nodosus*, whereas they are more flexuous in *H. brevis*. In addition, the ventrolateral tubercles are large and usually extend almost to the aperture in *H. nodosus*, whereas they are smaller and generally disappear at the point of recurvature in *H. brevis*. However, transitional specimens are present that link the two species (figs. 31, 32, 36E, 37A,B, 42D, 55, 56A–C; marked as transitional to *H. brevis* in table 3).

In the overlying *Baculites reesidei–B. jenseni* zones in the Western Interior, several species are present that superficially resemble *Hoploscaphites nodosus*. These include *H. furnivali* Riccardi, 1983 (19, pl. 4, figs. 3, 4, 7–9; text figs. 7c, 8), and undescribed forms close to or identical with "*Acanthoscaphites*" *praequadrispinosus*. As noted above, similar species also occur in age-equivalent strata on the Gulf Coastal Plain including the Saratoga Chalk in southwestern Arkansas, the Coon Creek Tongue of the Ripley Formation in Tennessee, and the Nacotoch Sand in Texas. In general, these forms differ from *H. nodosus* in their more widely spaced ribbing and flatter flanks. We plan a more thorough analysis of these species and their relationships to *H nodosus* and *H. brevis* in the future.

In the succeeding zones of *Baculites eliasi–B. grandis*, other species of *Hoploscaphites* are present, all of which are easily distinguished from *H. nodosus*, including *H. plenus* (Meek, 1876), *H. crassus* (Coryell and Salmon, 1934), and *H. criptonodosus* (Riccardi, 1983). *Hoploscaphites plenus* is a robust form, with a short shaft and a low apertural angle (Riccardi, 1983: pl. 9, figs. 1, 2). The ribs are nearly straight on the flanks of the body chamber, and the ventrolateral tubercles are closely spaced. *Hoploscaphites crassus* is a subglobose form with the same pattern of ornamentation as *H. plenus* (Riccardi, 1983: pl. 9. figs. 3, 4). *Hoploscaphites criptonodosus* is smaller and more compressed than either of these two species (Riccardi, 1983: pl. 6, fig. 10; pl. 7, figs. 1, 2; pl. 8, figs. 7–9). It is

←

(Owen, 1852), AMNH 56886. **D.** Ventral; **E.** left lateral. **F–I.** *Hoploscaphites brevis* (Meek, 1876), small microconch, AMNH 56884. **F.** Right lateral; **G.** apertural; **H.** ventral; **I.** left lateral. **J.** *Hoploscaphites* juvenile, AMNH 66244, left lateral. **K–M.** Part of a phragmocone of *Hoploscaphites brevis* (Meek, 1876), AMNH 66243. **K.** Right lateral; **L.** ventral; **M.** left lateral. **N.** *Hoploscaphites brevis* (Meek, 1876), macroconch, AMNH 63438, larger and more finely ornamented than holotype, right lateral. **O, P.** *Hoploscaphites brevis* (Meek, 1876), fragment of large macroconch, AMNH 63437, more finely ornamented than holotype. **O.** Right lateral; **P.** ventral. Specimens are illustrated natural size unless indicated otherwise by a scale bar.

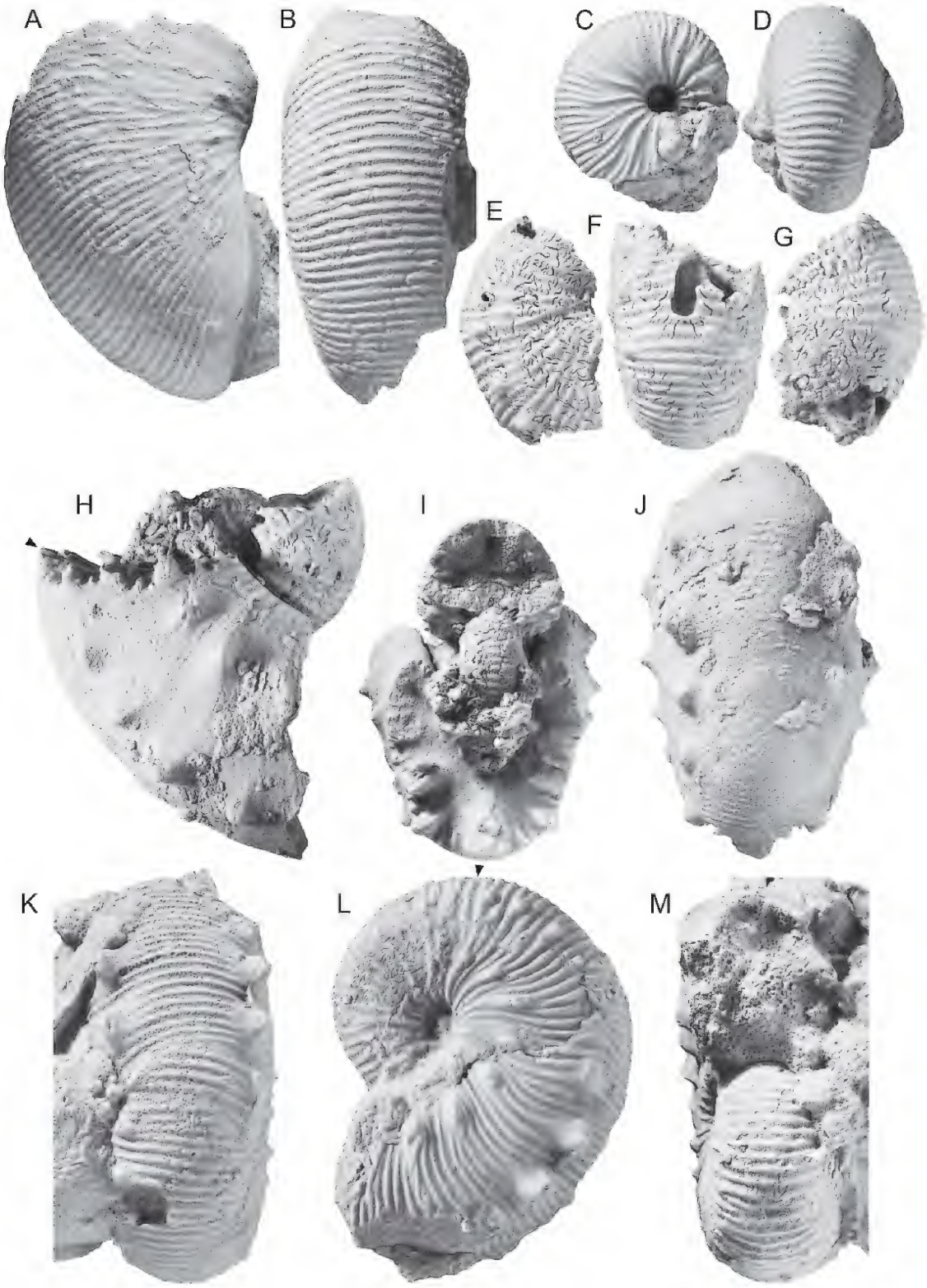
A
B
C
D
E
F
G
H
I
J
K
L
M

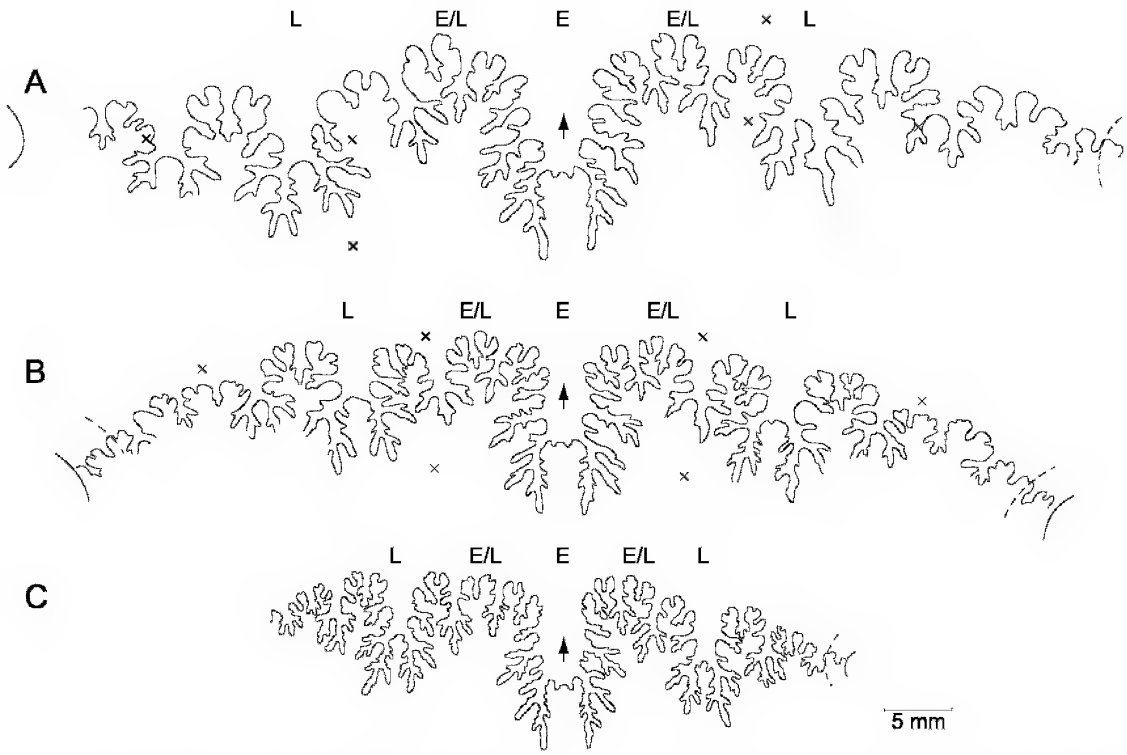

Fig. 61. Sutures of *Hoploscaphites nodosus* (Owen, 1852). **A.** YPM 35593, macroconch, next to last suture, YPM loc. C3346, Pierre Shale, locality unknown. **B.** BHI 4222, microconch, third from last suture, *Baculites compressus* Zone, Pierre Shale, Meade County, South Dakota. **C.** AMNH 56880, juvenile, last suture, WH = 16.2 mm, AMNH loc. 3274, *Baculites compressus–B. cuneatus* zones, Pierre Shale, Meade County, South Dakota. Abbreviations: x = tubercle; E = ventral lobe; E/L = first lateral saddle between ventral and lateral lobes; L = lateral lobe.

←

Fig. 60. *Hoploscaphites nodosus* (Owen, 1852), cold seep, AMNH locs. 3419, 3420, *Baculites compressus* Zone, Pierre Shale, Custer County, South Dakota. **A, B.** Fragment of a macroconch (?), AMNH 61133. **A.** Right lateral; **B.** ventral. **C, D.** Juvenile, AMNH 61121, **C.** Right lateral; **D.** ventral. **E–G.** Fragment of a phragmocone, AMNH 61119. **E.** Right lateral; **F.** ventral; **G.** left lateral. **H–J.** Macroconch, AMNH 61126. **H.** Right lateral; **I.** apertural; **J.** ventral. **K–M.** Microconch, BHI 5964. **K.** Ventral, with repaired injury; **L.** left lateral; **M.** apertural. Specimens are illustrated natural size. The position of the base of the body chamber in H and L is estimated.

distinguished by the presence of several weak tubercles on the flanks of the exposed phragmocone.

Outside of the Western Interior, *Hoploscaphites nodosus* resembles *Scaphites binodosus* Roemer, 1841, from northern Europe (for recent illustrations, see Kennedy and Kaplan, 1995: 32, pl. 21, fig. 13; pl. 22, figs. 1–10; pl. 23, figs. 1–9; pl. 24, figs. 1–4; pl. 25, figs. 1–4; pl. 26, figs. 1–7; pl. 27, figs. 1–4; pl. 28, figs. 1–4; Kaplan et al., 2005: pl. 59, figs. 1, 2; pl. 60, figs. 1, 2; pl. 61, figs. 7–9; pl. 62, figs. 7–9; pl. 64, figs. 8, 9). Some of the differences between these two species may be due to differences in preservation because the European material commonly shows postmortem crushing and compaction, whereas the North American material usually retains its original shape. However, *S. binodosus* can be distinguished from *H. nodosus* in at least two ways. In *S. binodosus*, there are broad ribs connecting the umbilicolateral and ventrolateral tubercles on the flanks of the body chamber. Such swellings are also present in *H. nodosus*, but are not as prominent. In addition, in many microconchs of *S. binodosus*, there are barlike ribs extending from the umbilical seam to the umbilical shoulder, terminating in the umbilicolateral tubercles. These features are absent in *H. nodosus*, but are present in undescribed species from the middle Campanian of the Pierre Shale.

Hoploscaphites nodosus is also similar to *H. compressus* (Roemer, 1841), which has been reported from the Atlantic Coastal Plain and northern Europe (see redescriptions of this species by Kennedy and Cobban, 1994: 1300, figs. 8.4, 16.1–18, 17.1–5, 8–11, 15–20; Niebuhr, 1996: 271, pl. 1, figs. 1–9; pl. 2, figs. 1–12; Kennedy and Kaplan, 1997: 74: pl. 80, figs. 1, 4–7; pl. 81, figs. 1–3, 5–7; pl. 82, figs. 9, 11–13). The pattern of ribbing and the distribution of umbilicolateral and ventrolateral tubercles are the same in both species. However, the ribs are more closely spaced and the tubercles are smaller in *H. compressus*. For example, in a macroconch of *H. compressus* from the Mount Laurel Sand of New Jersey (USNM 445143), there are 9 ribs/cm on the venter of the hook (Kennedy and Cobban, 1994: fig. 16.15–18). In contrast, in macroconchs of *H. nodosus*, the maximum rib density on the hook is 8 ribs/cm (table 4). The whorl section is also more inflated in *H. compressus* than in *H. nodosus*. In USNM 536270 (fig. 57), which is the smallest macroconch of *H. nodosus* in our collection, the ornamentation is similar to *H. compressus*, but the flanks of the body chamber are much flatter.

Of all the European species, *Hoploscaphites nodosus* most closely resembles *Acanthoscaphites praequadrispinosus* from the Vistula River Valley, Poland (Błaszkiewicz, 1980: 38, pl. 19, figs. 2, 3, 6, 8; pl. 20, figs. 1–3, 6–8; pl. 21, figs. 1–6; Kennedy and Kaplan, 1995: pl. 29). As first pointed out by Riccardi (1983), the inclusion of *A. praequadrispinosus* in *Acanthoscaphites* is incorrect, because *Acanthoscaphites* is characterized by the presence of nodes on the midventer of the body chamber, which are absent in *A. praequadrispinosus*. We similarly exclude this species from *Acanthoscaphites*, but until we complete a more thorough analysis of it and its relationships to *H. nodosus* and members of the closely related genus *Rhaeboceras*, we treat the name *Acanthoscaphites* informally and enclose it in quotation marks.

Kennedy and Cobban (1993: 430) regarded "*Acanthoscaphites*" *praequadrispinosus* as a junior synonym of *H. nodosus*, but the results of our present study suggest that the two species are distinct. The overall pattern of ornamentation is, indeed, the same in both species. For example, the marked reduction in size of the ventrolateral tubercles in passing from the shaft to the hook in *H. nodosus* also occurs in "*A.*" *praequadrispinosus*. In describing the ornamentation on the body chamber of this species, Błaszkiewicz (1980: 39) noted that the "lateroventral [= ventrolateral] tubercles are large and conspicuously represent the 'clavi' type. The dimensions of these tubercles violently diminish over the hooked sector of some specimens." The two species differ, however, in maximum size and density of ribbing. "*Acanthoscaphites*" *praequadrispinosus* attains prodigious sizes. The holotype (Błaszkiewicz, 1980: pl. 19, figs. 6–8), a macroconch, is 184 mm in maximum length, whereas the largest macroconch of *H. nodosus* in our collection is 104 mm in maximum

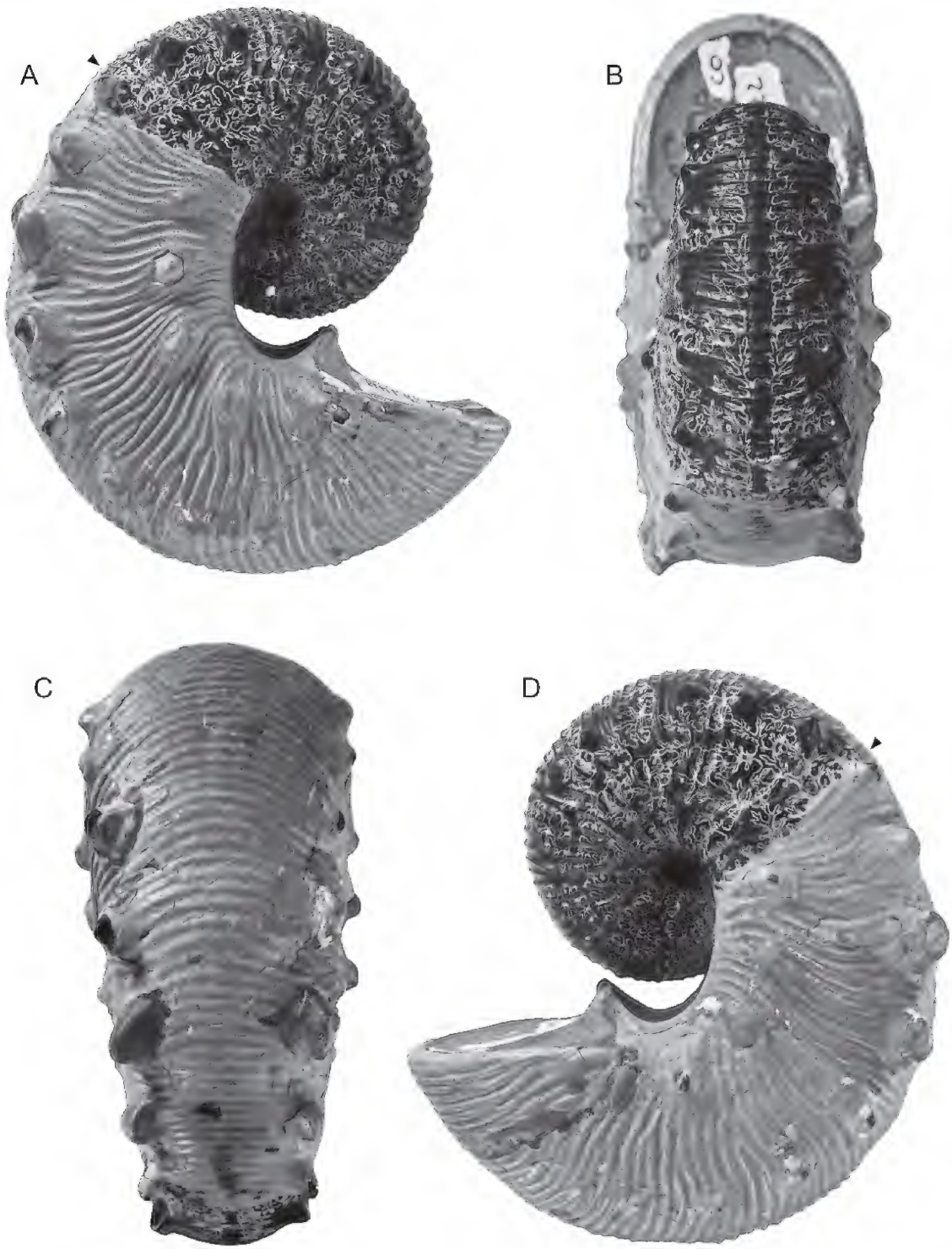

Fig. 62. *Hoploscaphites nodosus* (Owen, 1852), large microconch, BHI 4222, uncoated, *Baculites compressus* Zone, Pierre Shale, Meade County, South Dakota. **A.** Right lateral; **B.** apertural; **C.** ventral; **D.** left lateral. The shell on the phragmocone was removed to expose the sutures. Specimen is illustrated natural size.

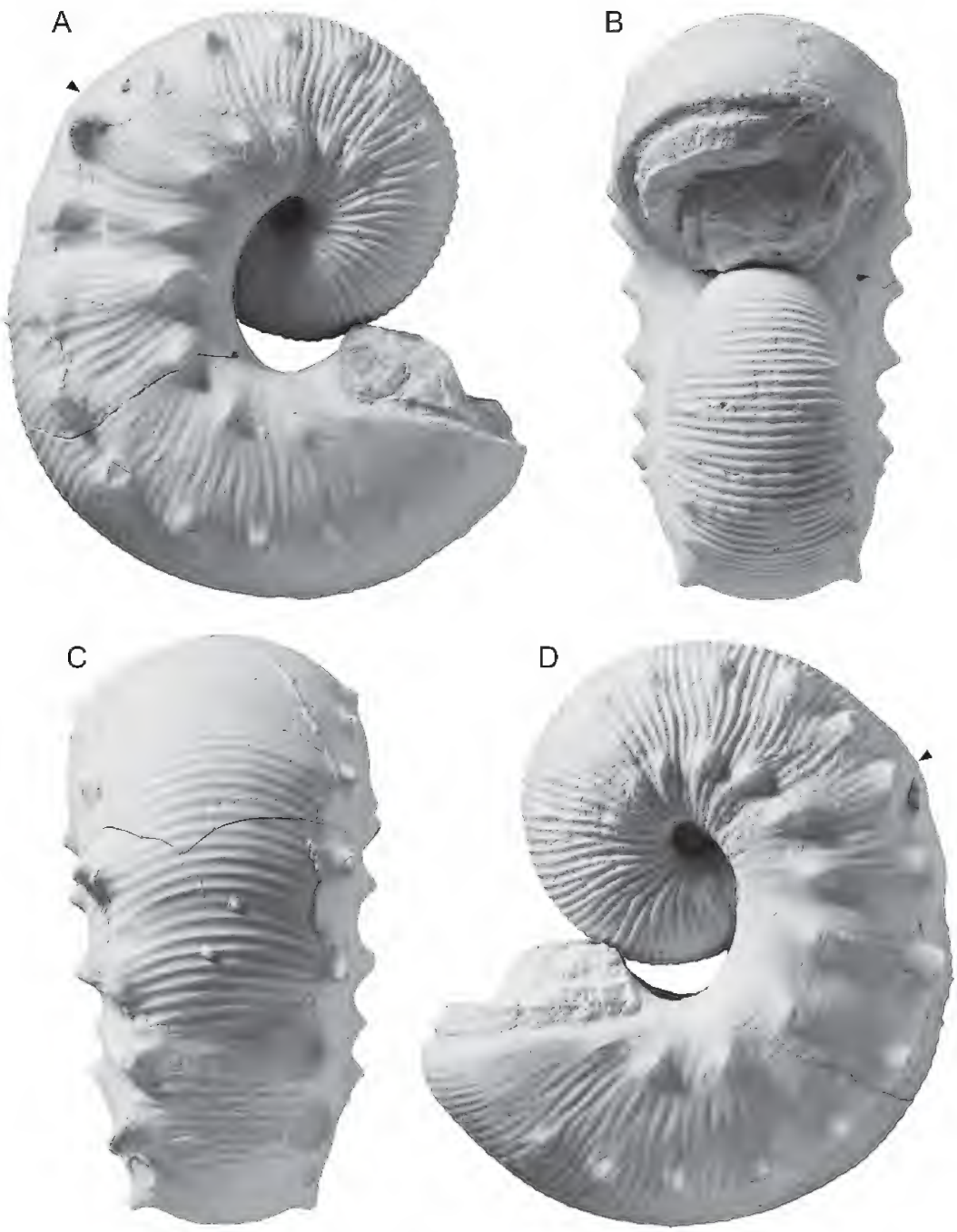

Fig. 63. *Hoploscaphites nodosus* (Owen, 1852), large microconch, BHI 4710, *Baculites compressus–B. cuneatus* zones, Pierre Shale, Meade County, South Dakota. **A.** Right lateral; **B.** apertural; **C.** ventral; **D.** left lateral. Specimen is illustrated natural size.

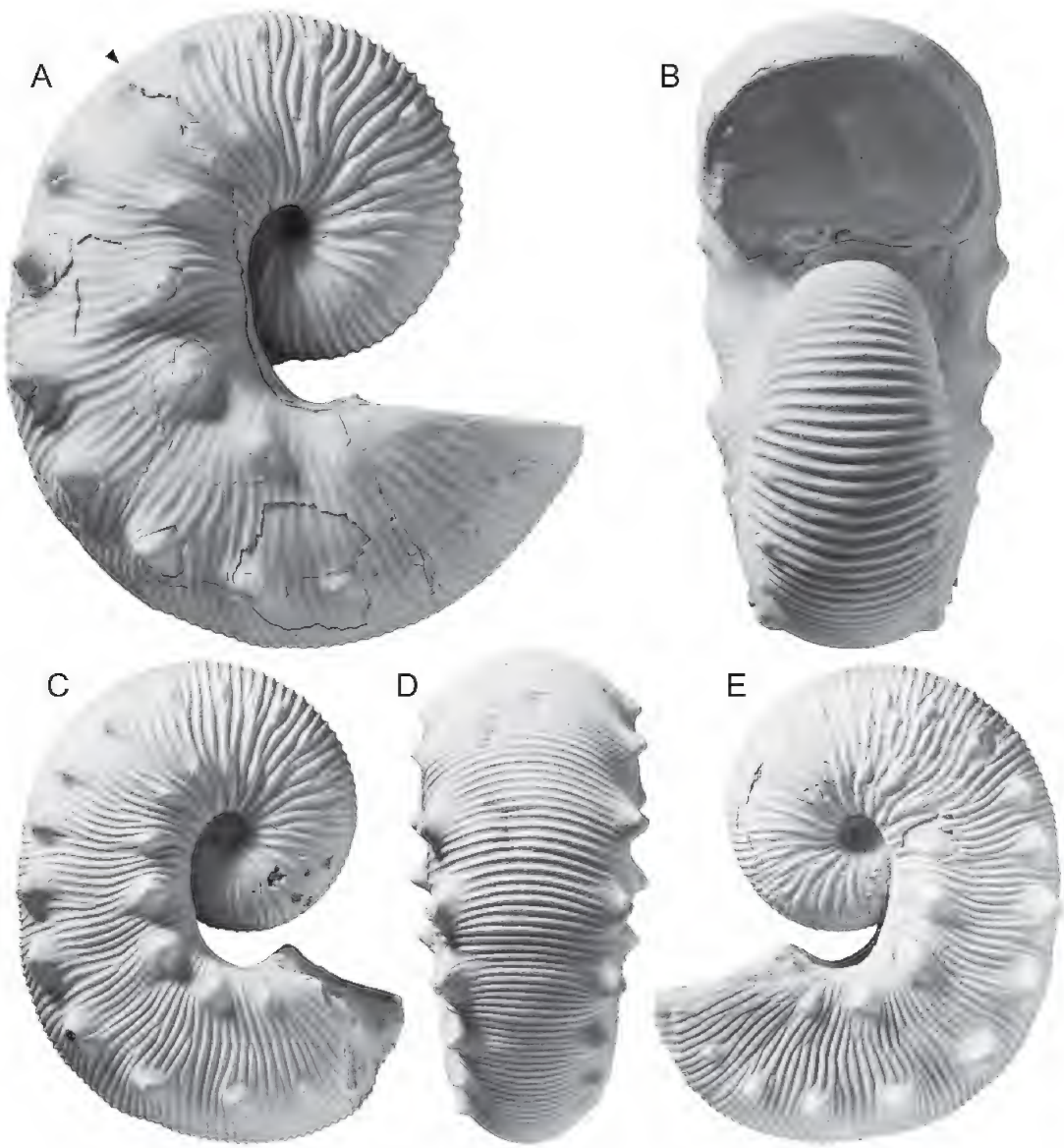

Fig. 64. *Hoploscaphites nodosus* (Owen, 1852), microconchs. **A, B.** BHI 4220, *Baculites compressus* Zone, Pierre Shale, Meade County, South Dakota. **A.** Right lateral; **B.** apertural. The apertural margin was accidentally ground down during preparation. **C–E.** BHI 7004, Pierre Shale, *Didymoceras cheyennense* Zone, Pierre Shale, Custer County, South Dakota. **C.** Right lateral; **D.** ventral; **E.** left lateral. Specimens are illustrated natural size.

Fig. 65. *Hoploscaphites nodosus* (Owen, 1852), large microconch, BHI 4723, *Baculites compressus–B. cuneatus* zones, Pierre Shale, Pennington County, South Dakota. **A.** Right lateral; **B.** apertural; **C.** ventral; **D.** left lateral. Specimen is illustrated natural size.

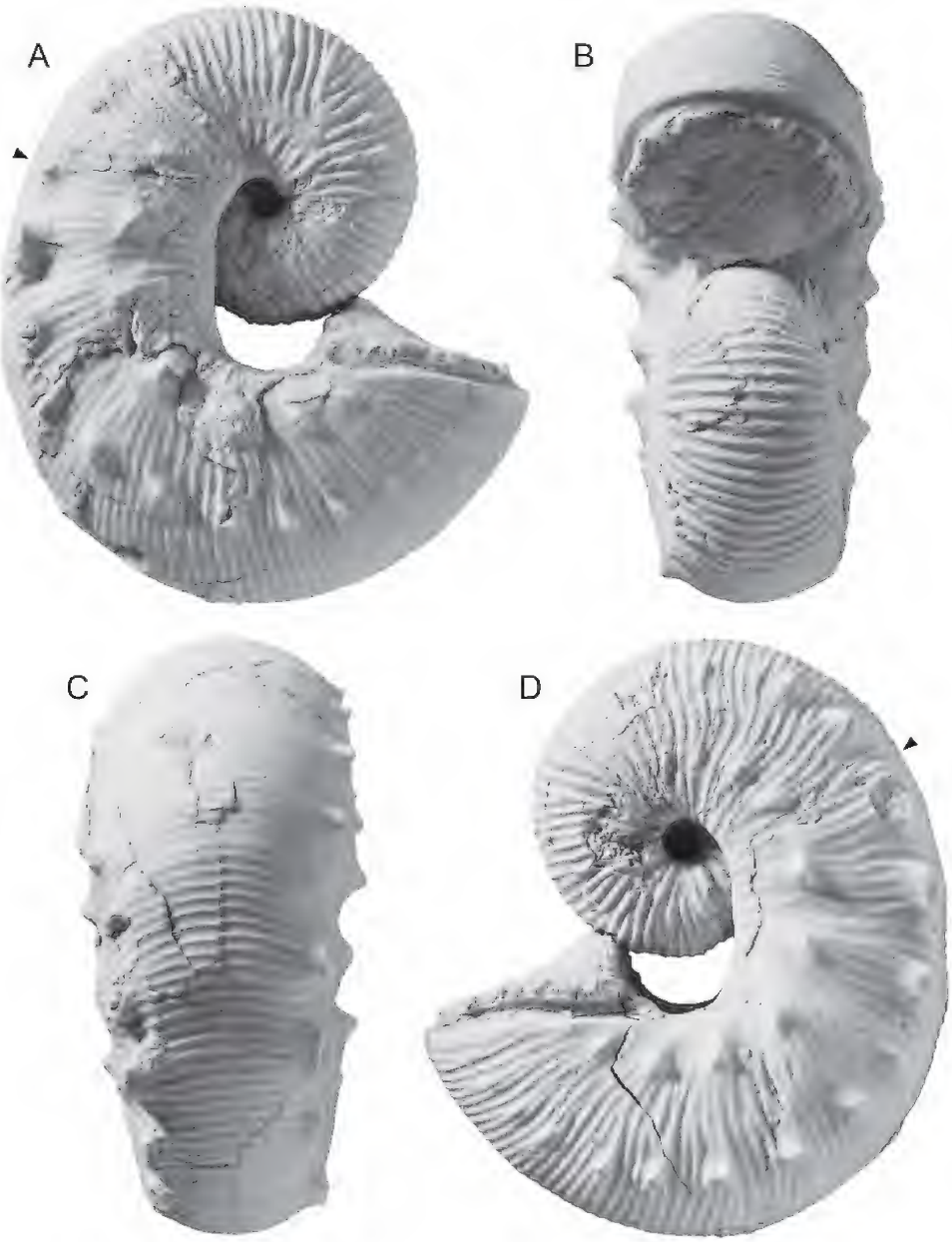

Fig. 66. *Hoploscaphites nodosus* (Owen, 1852), large microconch, AMNH 58521, Pierre Shale, *Baculites compressus* Zone, Meade County, South Dakota. **A.** Right lateral; **B.** apertural; **C.** ventral; **D.** left lateral. Specimen is illustrated natural size.

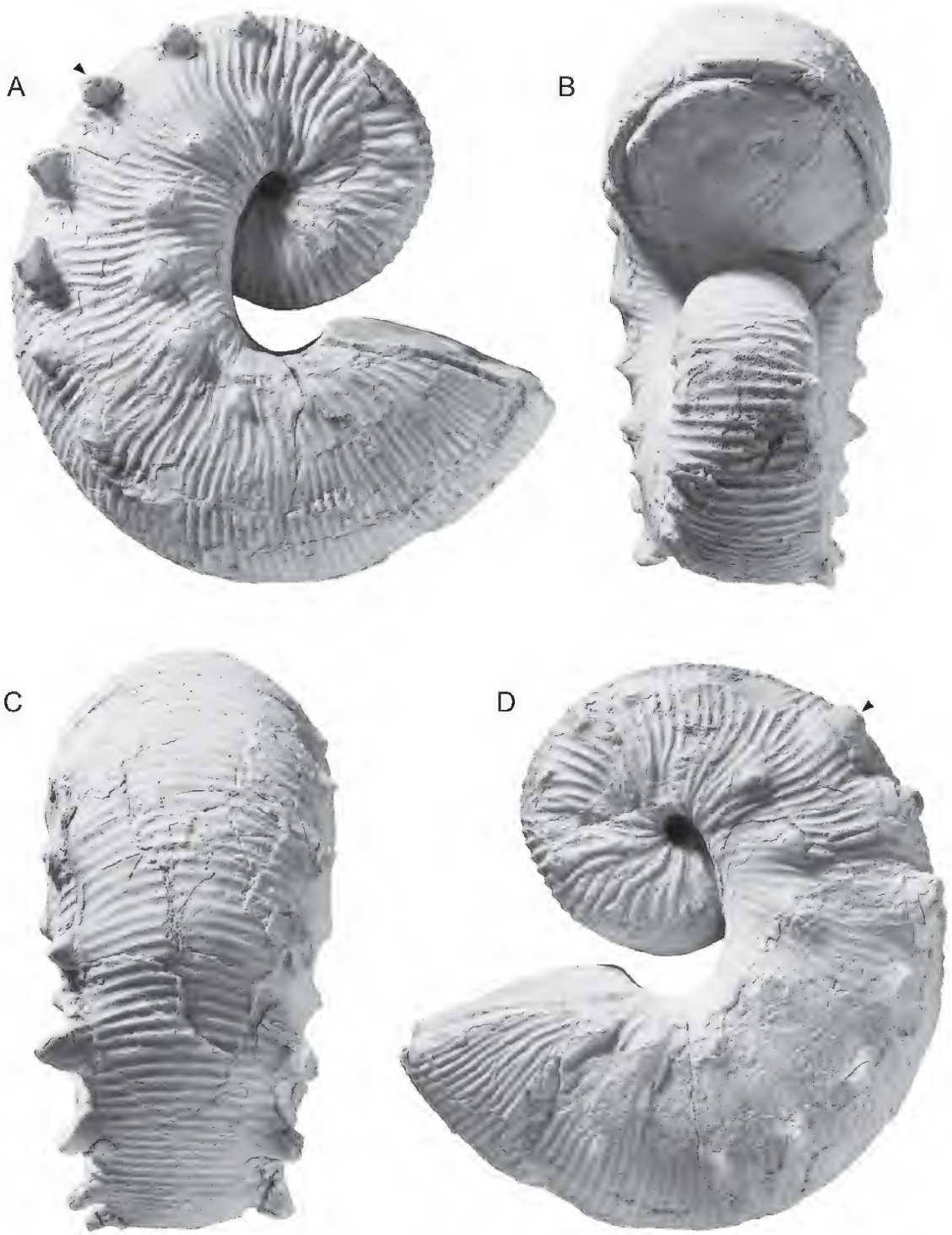

Fig. 67. *Hoploscaphites nodosus* (Owen, 1852), large microconch, AMNH 58554, AMNH loc. 3409, *Baculites cuneatus* Zone, Pierre Shale, Meade County, South Dakota. **A.** Right lateral; **B.** apertural; **C.** ventral; **D.** left lateral. Specimen is illustrated natural size.

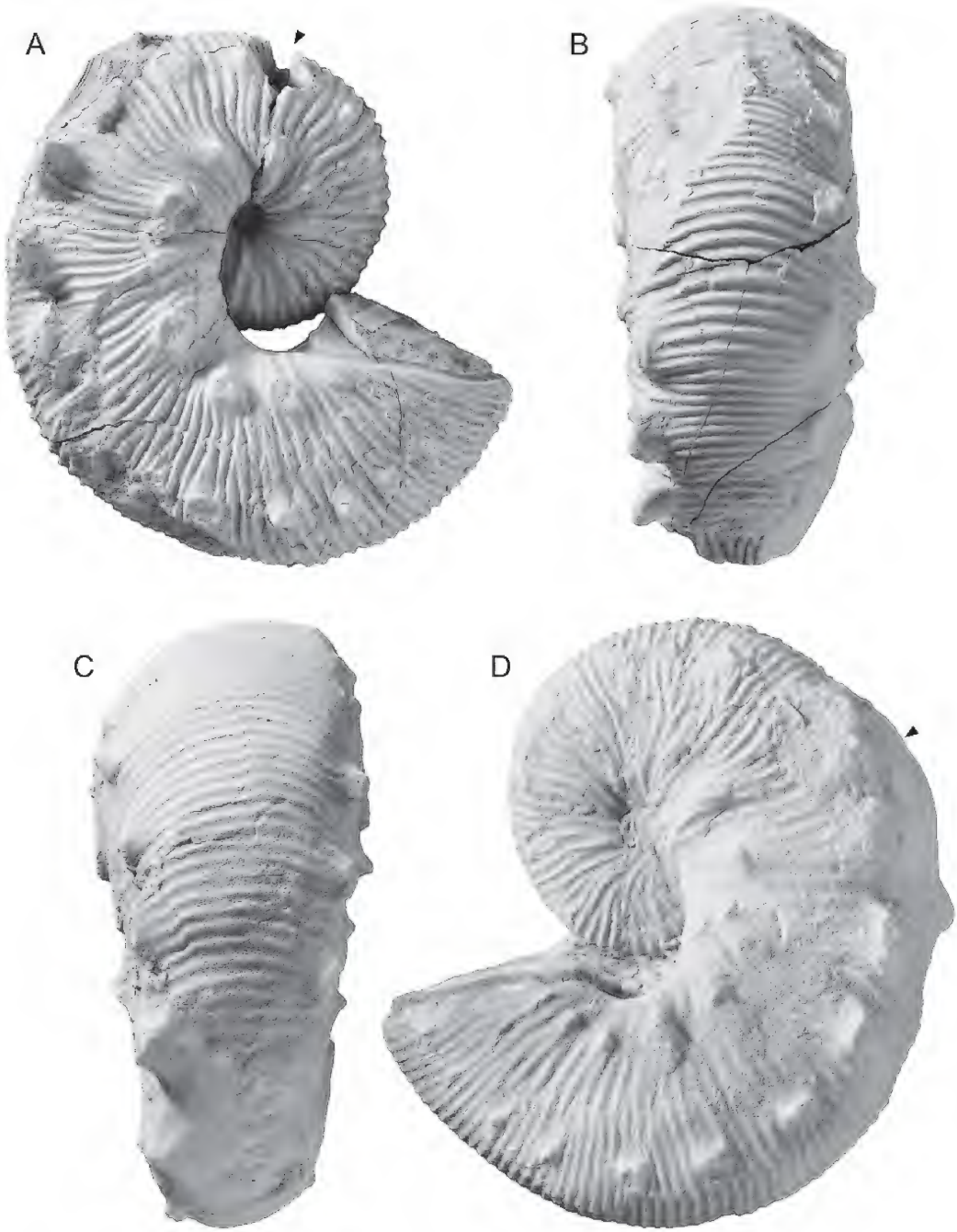

Fig. 68. *Hoploscaphites nodosus* (Owen, 1852), microconchs. **A, B.** USNM 536229, USGS Mesozoic loc. D1785, *Baculites cuneatus* Zone, Pierre Shale, Grand County, Colorado. **A.** Right lateral; **B.** ventral. **C, D.** USNM 536227, USGS Mesozoic loc. D1353, *Baculites cuneatus* Zone, Pierre Shale, Grand County, Colorado. **C.** Ventral; **D.** left lateral. Specimens are illustrated natural size.

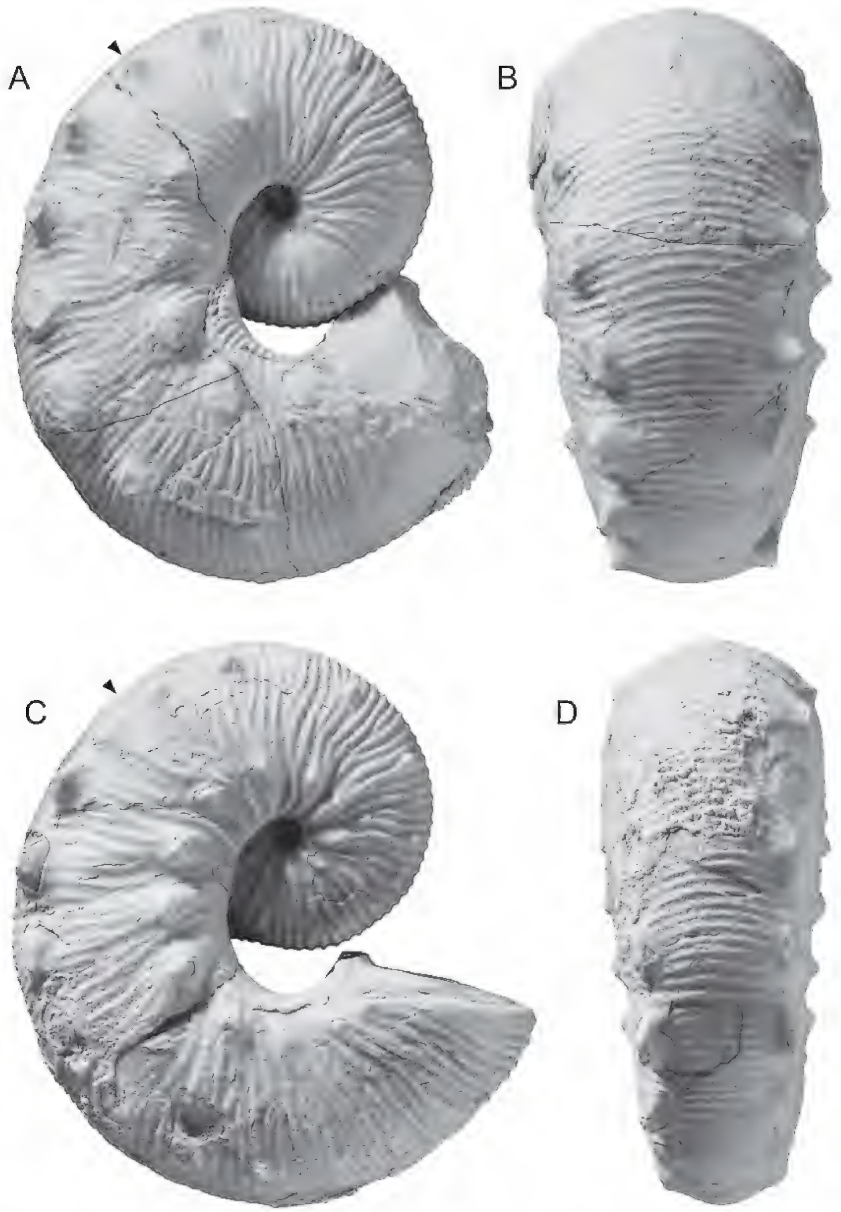

Fig. 69. *Hoploscaphites nodosus* (Owen, 1852), microconchs. **A, B.** YPM 1868, YPM loc. A6520, Pierre Shale, Sage Creek, Pennington County, South Dakota. **A.** Right lateral; **B.** ventral. **C, D.** USNM 536245, USGS Mesozoic loc. D 221, *Didymoceras cheyennense* Zone, Pierre Shale, Dawes County, Nebraska. **C.** Right lateral; **D.** ventral. Specimens are illustrated natural size.

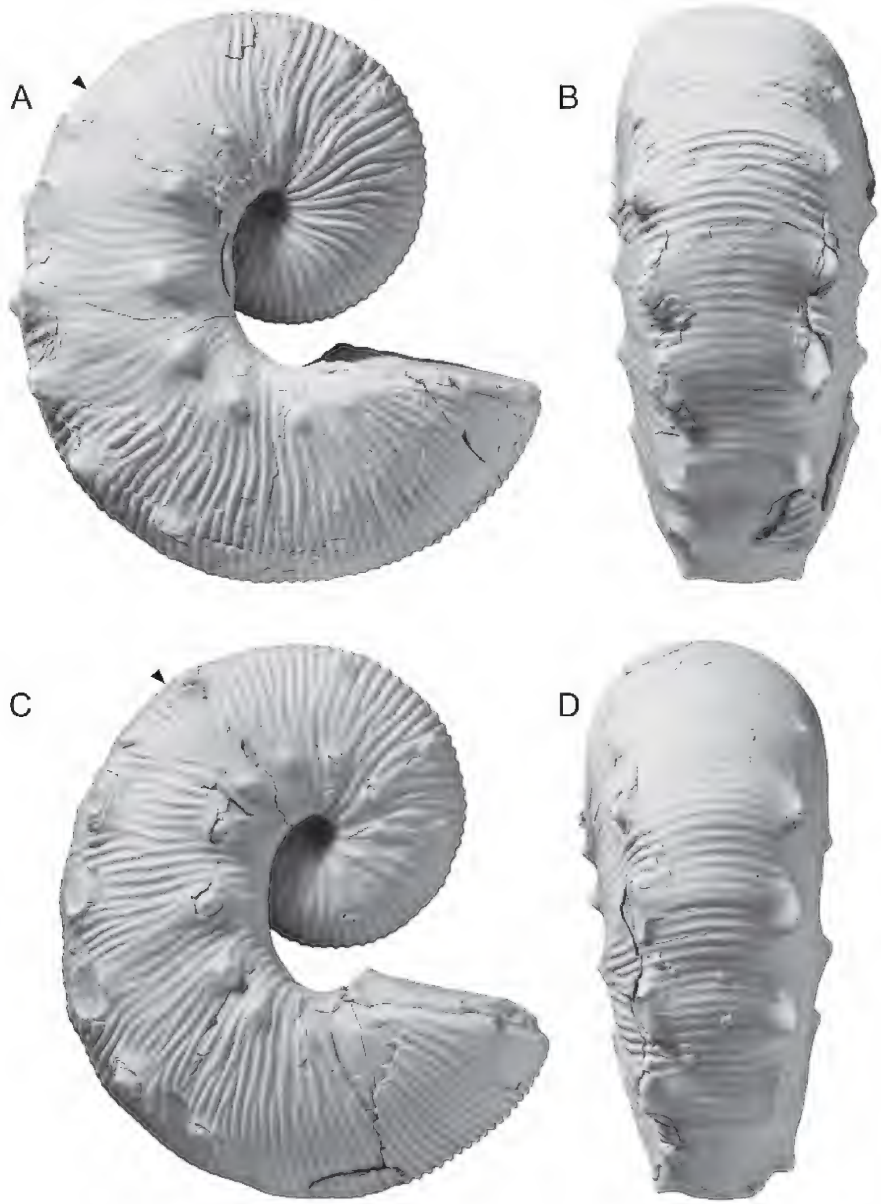

Fig. 70. *Hoploscaphites nodosus* (Owen, 1852), microconchs, USGS Mesozoic loc. 21224, Bearpaw Shale, near Hardin, Big Horn County, Montana. **A, B.** USNM 536232. **A.** Right lateral; **B.** ventral. **C, D.** USNM 538103. **C.** Right lateral; **D.** ventral. Specimens are illustrated natural size.

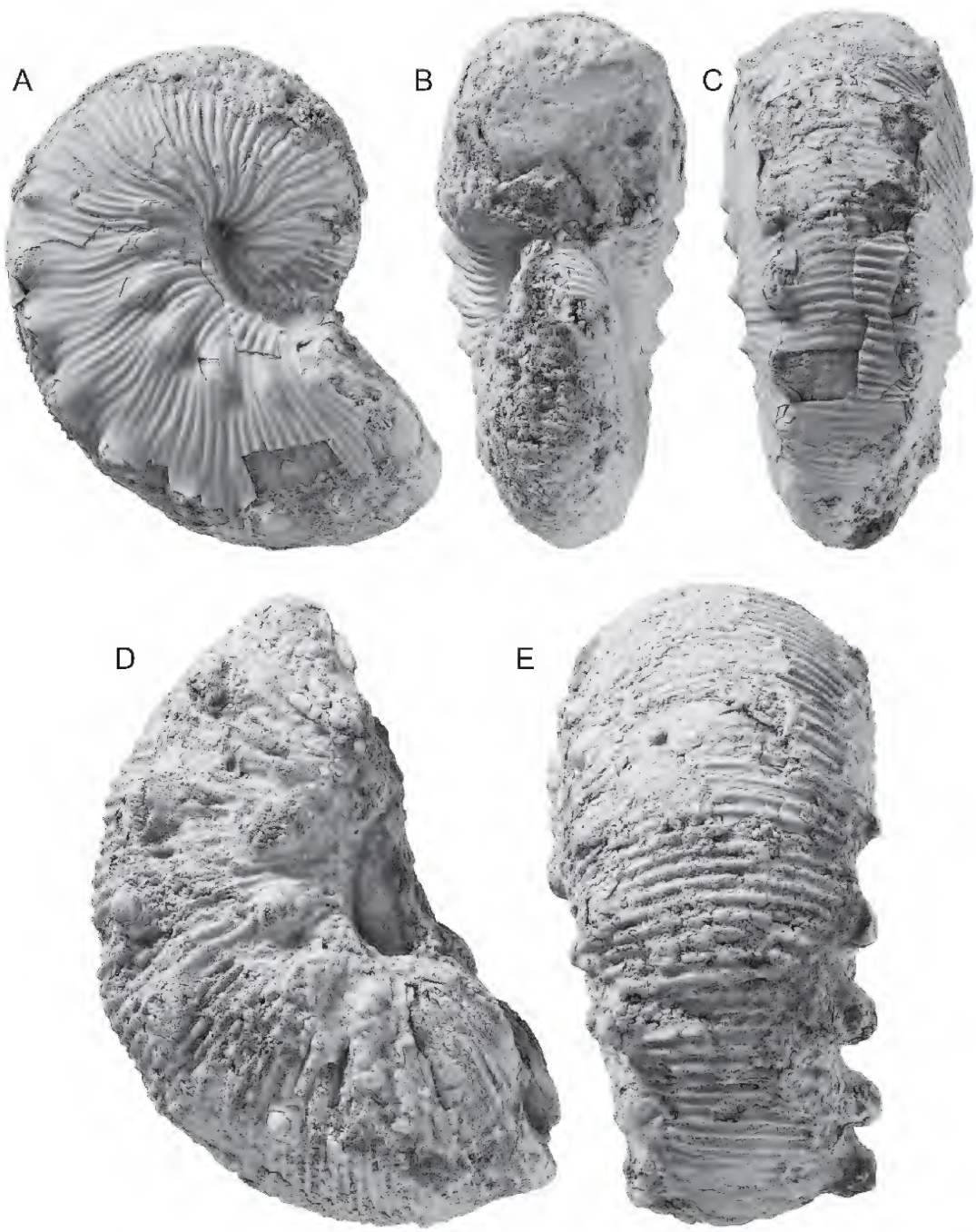

Fig. 71. *Hoploscaphites nodosus* (Owen, 1852), microconchs, *Baculites cuneatus* Zone, Pierre Shale, near the junction of the Belle Fourche and Cheyenne Rivers, Meade County, South Dakota. **A–C.** BHI 4791. **A.** Right lateral; **B.** apertural; **C.** ventral. **D, E.** BHI 4794, massive body chamber. **D.** Right lateral; **E.** ventral. Specimens are illustrated natural size.

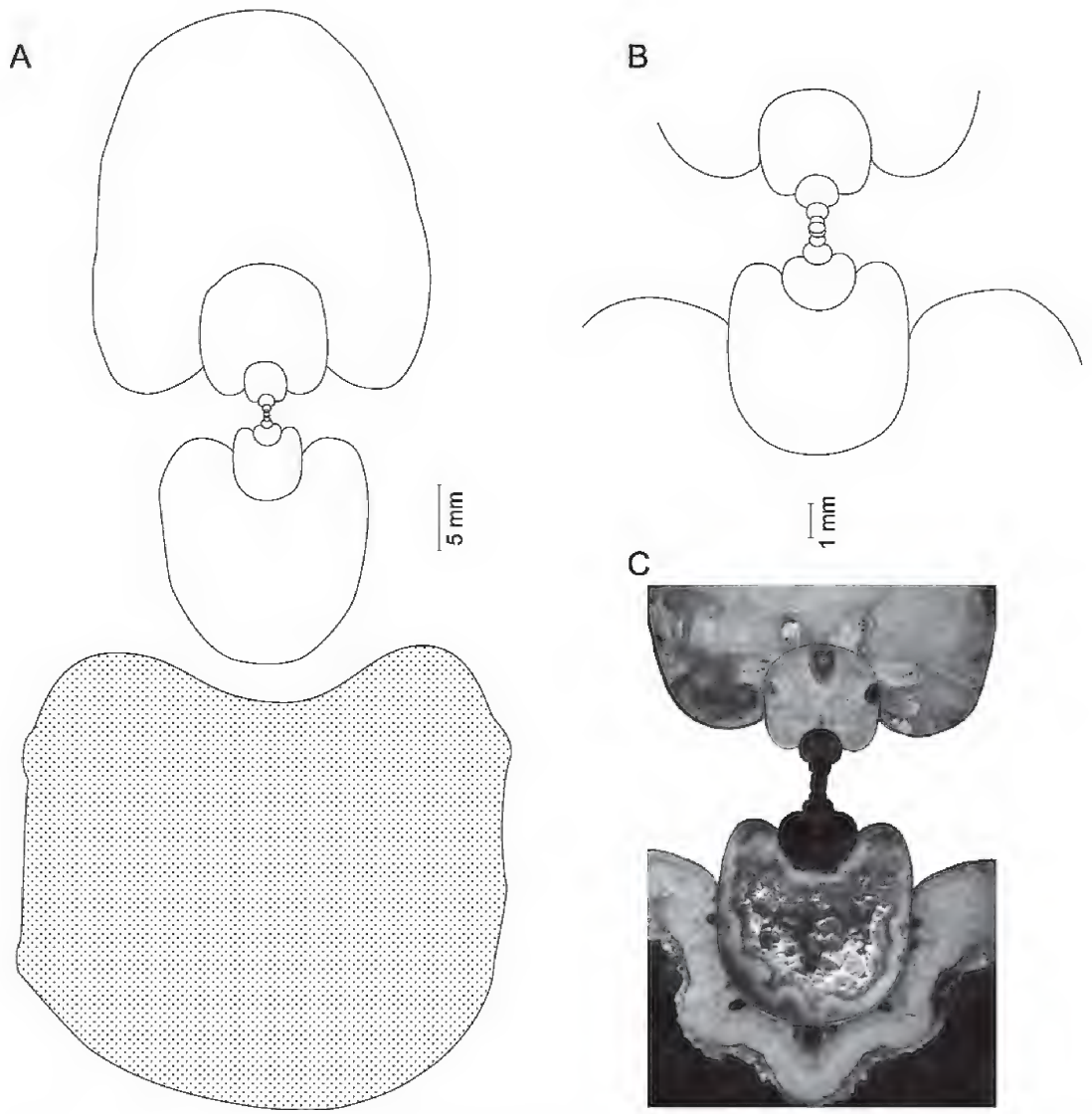

Fig. 72. Dorsoventral cross section through a slender macroconch of *Hoploscaphites nodosus* (Owen, 1852), AMNH 9520/2, Pierre Shale, Sage Creek, Pennington County, South Dakota. The plane of the cross section approximately coincides with the line of maximum length. **A.** Camera lucida of cross section of the adult shell. The stippled area demarcates the mature body chamber. **B.** Camera lucida of cross section of the inner whorls. **C.** Photo of cross section of the inner whorls. Measurements are listed in appendix 2, table 1.

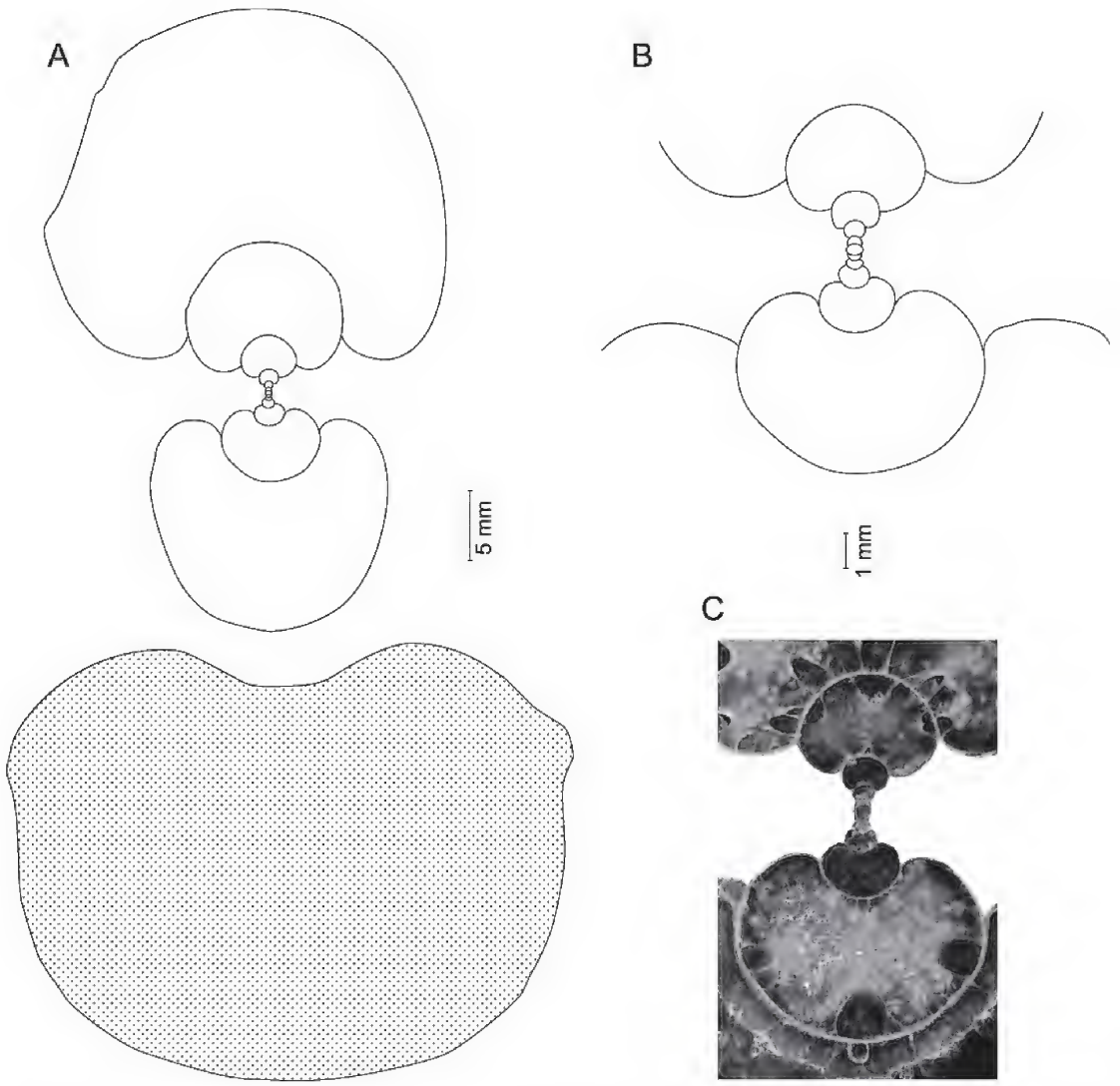

Fig. 73. Dorsoventral cross section through a robust microconch of *Hoploscaphites nodosus* (Owen, 1852), USNM 536246, USGS Mesozoic loc. 9133, Pierre Shale, near Kremmling, Grand County, Colorado. The plane of the cross section approximately coincides with the line of maximum length. **A.** Camera lucida of cross section of the adult shell. The stippled area demarcates the mature body chamber. **B.** Camera lucida of cross section of the inner whorls. **C.** Photo of cross section of the inner whorls. Measurements are listed in appendix 2, table 3.

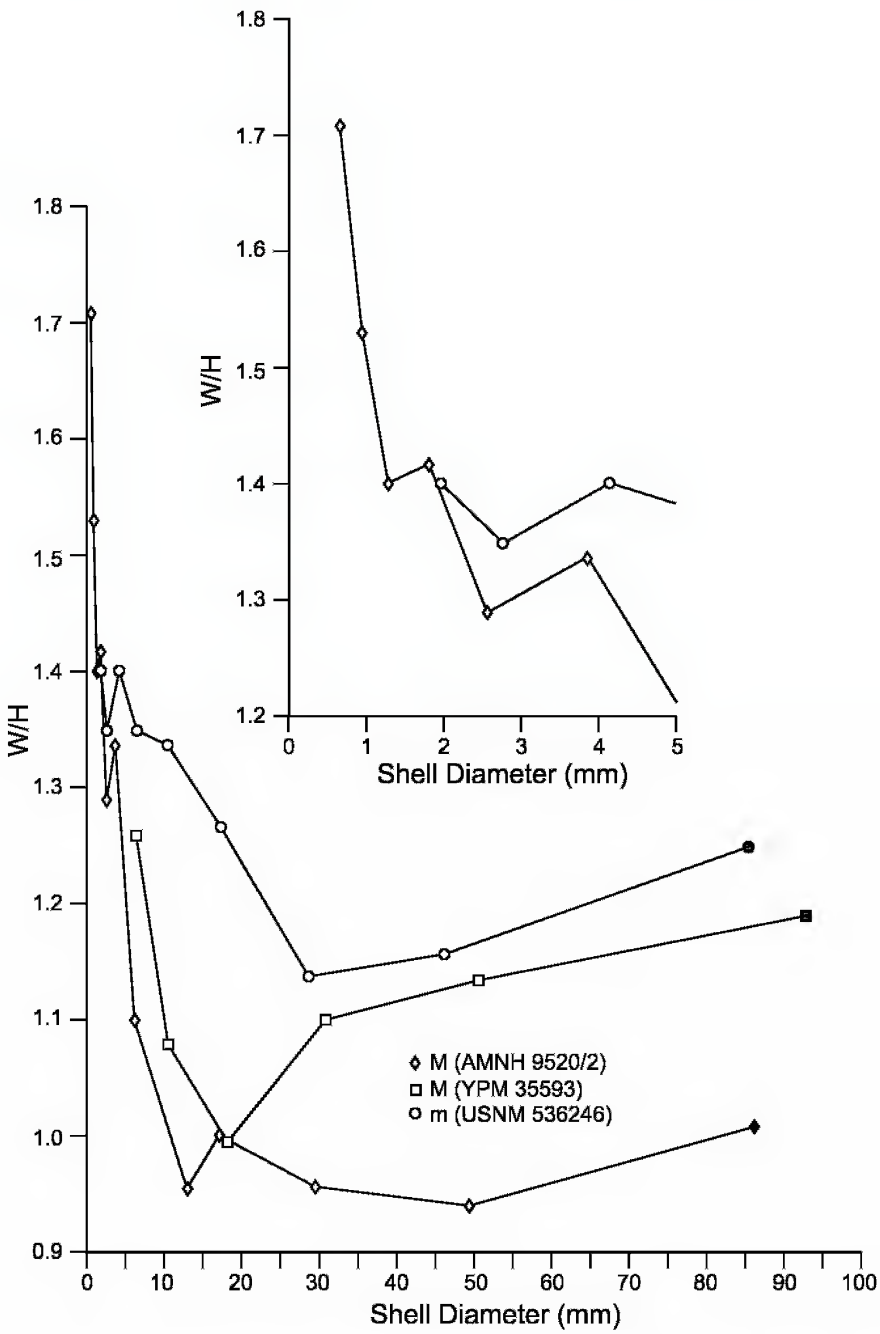

Fig. 74. Plot of the ratio of whorl width to height (W/H) versus shell diameter (mm) in *Hoploscaphites nodosus* (Owen, 1852) in early (top graph) and later ontogeny (bottom graph; see figs. 72, 73 for illustrations of cross sections on which these graphs are based, and appendix 2, tables 1–3, for a list of measurements). The ratio of whorl width to height decreases through most of ontogeny until the beginning of the mature phragmocone, after which it increases. Filled symbols indicate measurements in the mature body chamber.

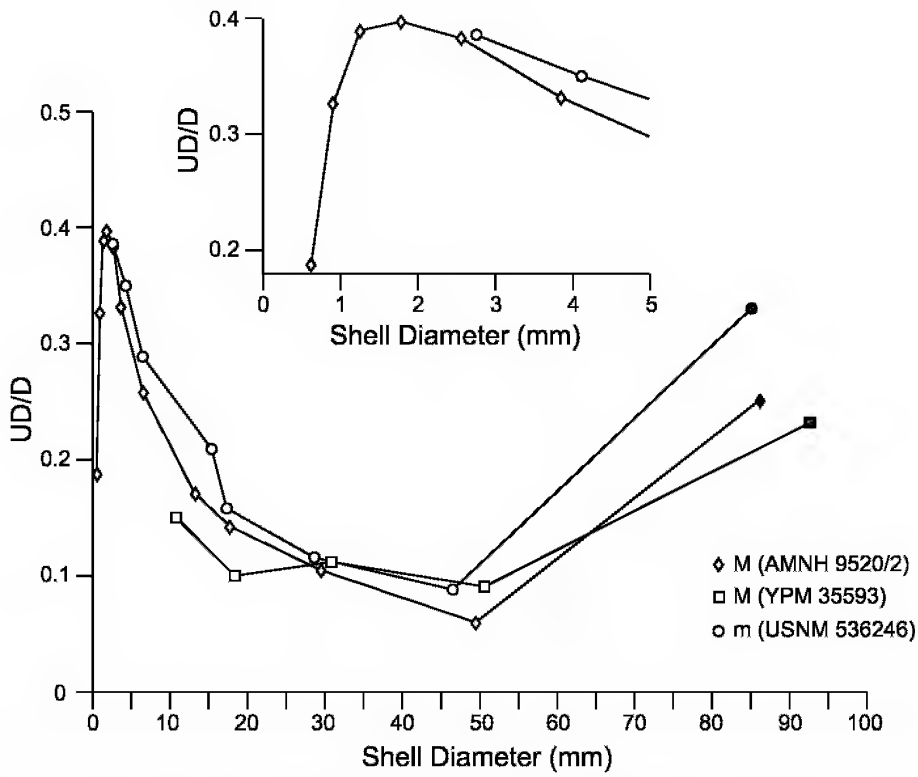

Fig. 75. Plot of the ratio of umbilical diameter (UD/D) to shell diameter versus shell diameter (mm) in *Hoploscaphites nodosus* (Owen, 1852) in early (top graph) and later ontogeny (bottom graph; see figs. 72, 73 for illustrations of cross sections on which these graphs are based, and appendix 2, tables 1–3, for a list of measurements). The ratio decreases through most of ontogeny until a shell diameter of approximately 20 mm, after which it remains nearly the same until the beginning of the mature body chamber. Filled symbols indicate measurements in the mature body chamber.

length (e.g., USNM 536219 and 536230). In addition, the ribs are more widely spaced in "*A.*" *praequadrispinosus* than in *H. nodosus*. For example, in a macroconch of "*A.*" *praequadrispinosus* from Piotrawin, Poland (Błaszkiewicz, 1980: pl. 21, figs. 1, 2), there are 4 ribs/cm on the venter of the shaft, whereas in the most coarsely ornamented macroconchs of *H. nodosus* in our collection (USNM 536230 and 536237), there are 5.25 ribs/cm on the same area of the shell.

OCCURRENCE: *Hoploscaphites nodosus* is present in the *Baculites compressus–B. cuneatus* zones in the Western Interior of North America. It is also present in part of the underlying *Didymoceras cheyennense* Zone and in part of the overlying *B. reesidei* Zone, but its exact distribution in these zones is not yet known. In Canada, *Hoploscaphites nodosus* is reported from the Bearpaw Shale of Alberta and Saskatchewan, although only one of the previously illustrated specimens from Saskatchewan (GSC 5369a), and the specimen we illustrate from Alberta (TMP PI 80.13.76), are unequivocably included in this species. All of the other specimens from Canada represent forms from slightly higher biostratigraphic zones. In Montana, *H. nodosus* occurs in the Bearpaw Shale in Glacier, Chouteau, Meaghar, Blaine, Fergus, Wheatland, Golden Valley, Musselshell, Stillwater, Big Horn, Rosebud, Garfield, Teton, and Valley counties; in the Livingston Formation in Park County; and in the Pierre Shale in Carter County. In North Dakota, it occurs in the Pierre Shale in Barnes County. In South Dakota, it occurs in the Pierre Shale in Butte, Pennington, Custer, Shannon, Meade, Haakon, Ziebach, Mellette, Jones, Stanley, Dewy, Hughes, Lyman, Buffalo, and

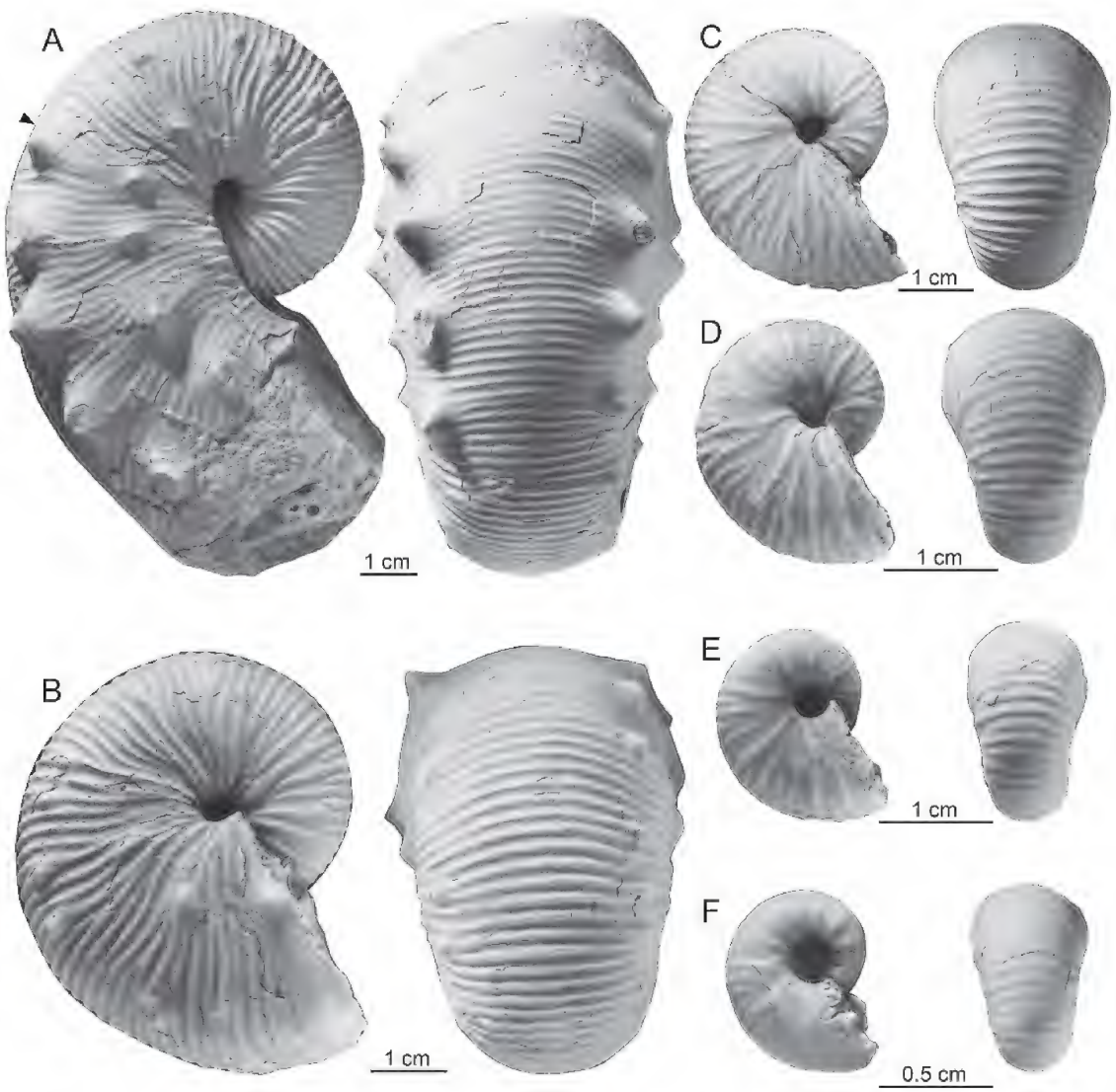

Fig. 76. Ontogenetic breakdown of *Hoploscaphites nodosus* (Owen, 1852), macroconch, USNM 536231, USGS Mesozoic loc. D12201, ?*Didymoceras cheyennense* Zone, Bearpaw Shale, Big Horn County, Montana. **A–F.** Six sizes through ontogeny in lateral and ventral views showing the change in ornamentation from early ontogeny (F) to maturity (A). Note that A is reduced and all the other photos are either natural size or enlarged.

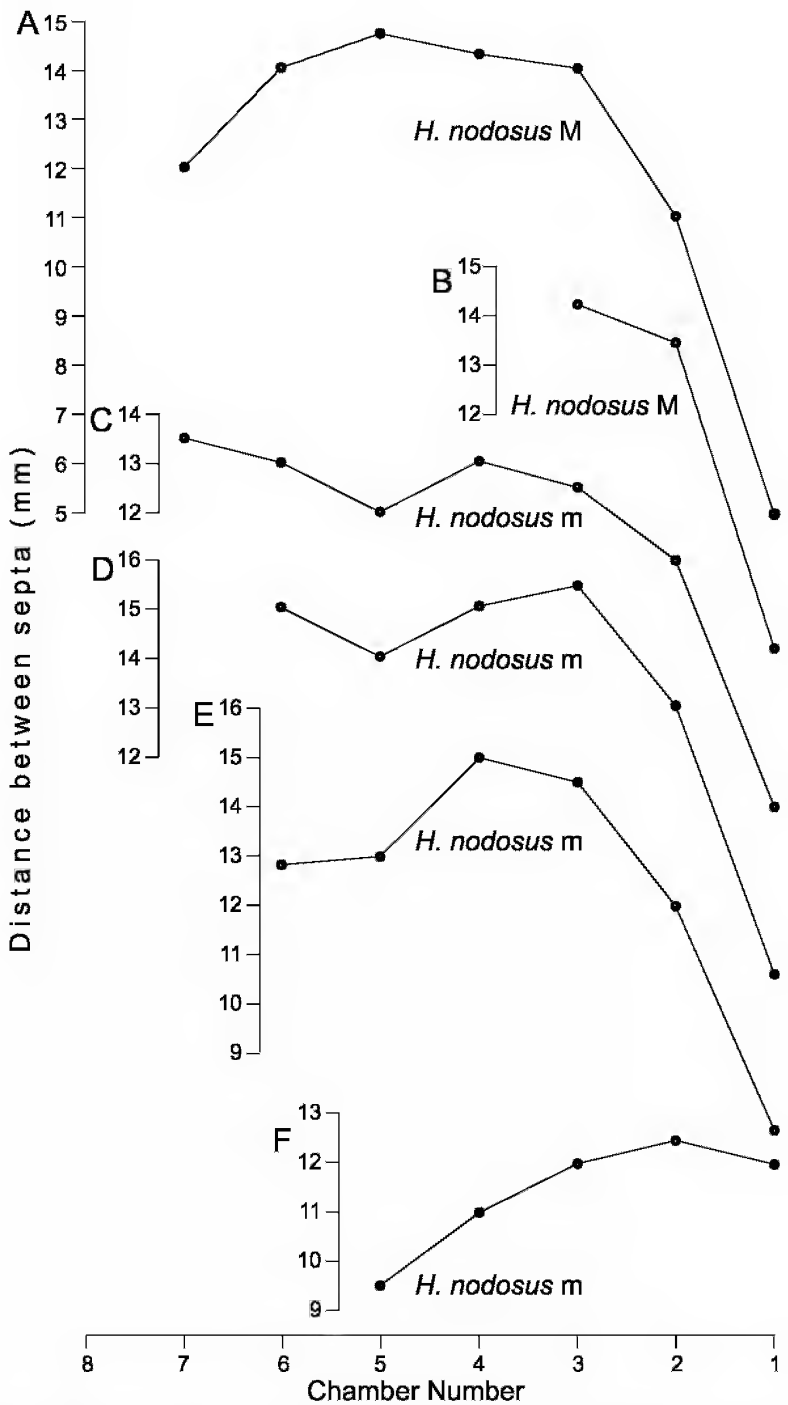

Fig. 77. Septal approximation at maturity in *Hoploscaphites nodosus* (Owen, 1852). **A, B.** Macroconchs. **A.** BHI 4948, *Baculites compressus* Zone, Pierre Shale, Meade County, South Dakota. Septal approximation occurs over two chambers and is strong (the interseptal distance of the last chamber is 36% that of the last "normal" chamber). **B.** AMNH 58511, Pierre Shale, Meade County, South Dakota. Septal approximation occurs over one chamber and is modest (the interseptal distance of the last chamber is 53% that of the last "normal" chamber). **C–F.** Microconchs. **C.** BHI 4222, *Baculites compressus* Zone,

Brule counties. In Wyoming, it occurs in the Pierre Shale in Weston and Laramie counties. In Colorado, it occurs in the Pierre Shale in Boulder, El Paso, Fremont, Grand, Huerfano, Jackson, Jefferson, Larimer, and Pueblo counties. In Kansas, it is reported from the Weskan Shale and Lake Creek Shale members of the Pierre Shale in Wallace County, but most of the previously illustrated specimens from this area represent forms from the *Baculites reesidei* Zone.

Hoploscaphites nodosus, as described herein, is absent in the Gulf and Atlantic Coastal plains and northern Europe, although this may be due to a taphonomic bias. However, forms closely resembling *H. nodosus* are present in these areas in strata below and above the biostratigraphic interval containing *H. nodosus*, for example, the *Nostoceras* (*N.*) *hyatti* Zone in New Jersey (Kennedy et al., 2000b). Thus, although *H. nodosus* is endemic to the Western Interior of North America, it is part of a more broadly distributed clade. The phylogenetic relationships of *H. nodosus* and the other species in this clade are yet to be resolved, but this clade is evidently not restricted to the Western Interior of North America, contrary to popular thought (Monks, 2000).

Hoploscaphites brevis (Meek, 1876)
Figures 5, 6D–G, 7, 11, 12A–J, 13A–C, 15A–C, 16, 18C–F, 19A, D, 20C, F, G, H, 21A, B, E, F, 26, 27, 29A–D, F, H, I, 34A–G, J, K, 36A–C, G, H, 39I, J, 40E–G, H–J, 58A–C, 59A–C, F–I, K–M, N–P, 79H–J, 80A, B, D, 82–116

?1859. *Scaphites nodosus*? var. Meek, p. 185, pl. 2, figs. 7, 8. (It is unidentifiable because the drawing is inaccurate as stated by Meek.)

1860. *Scaphites nodosus* var. *quadrangulus* Meek and Hayden, p. 420 (nomen nudum).

1860. *Scaphites nodosus* var. *exilis* Meek and Hayden, p. 420 (nomen nudum).

1860. *Scaphites nodosus* var. *brevis* Meek and Hayden, p. 420.

1864. *Scaphites nodosus* var. *brevis* Meek and Hayden. Meek, p. 24.

1864. *Scaphites nodosus* var. *exilis* Meek and Hayden. Meek, p. 24 (nomen nudum).

1864. *Scaphites nodosus* var. *quadrangularis* Meek and Hayden. Meek, p. 24.

1876. *Scaphites nodosus* var. *brevis* Meek, p. 426, pl. 25, fig. 1a–c.

pars 1876. *Scaphites nodosus* var. *quadrangularis* Meek, p. 428, pl. 25, fig. 2; *non* figs. 3, 4 (= *Hoploscaphites plenus* m).

1880. *Scaphites nodosus* var. *brevis* Meek. Whitfield, p. 443, pl. 13, figs. 8, 9.

1880. *Scaphites nodosus* var. *quadrangularis* Meek and Hayden. Whitfield, p. 443, pl. 13, figs. 10, 11.

1898. *Scaphites nodosus* var. *brevis* Meek. Logan, p. 511, pl. 108, fig. 3 (= Meek, 1876: pl. 25, fig. 1).

?1899. *Scaphites nodosus* Meek. Logan, pl. 22, fig. 2 (= ?*Hoploscaphites brevis* M).

?1905. *Scaphites nodosus* var. *brevis* Meek. Smith, p. 640, fig. 1.2 (very poor photo), 1.4–7 (ontogenetic dissection), 1.9–18 (drawings of early whorls); 3.1–3 (suture only), 5 (drawing of early whorls), 6 (suture only), 9 (drawing of early whorls).

?1905. *Scaphites nodosus* var. *quadrangularis* Meek. Smith, fig. 1.3 (poor photo); 2. 1 (drawing of early whorls).

1907. *Scaphites nodosus* Owen. Chamberlin and Salisbury, fig. 417d (= *Scaphites nodosus* var. *brevis* Meek, 1876, p. 426, pl. 25, fig. 1).

1910. *Scaphites nodosus* var. *brevis* Meek. Grabau and Shimer, p. 177, fig. 1428 (= Meek, 1876: pl. 25, fig. 1).

non 1910. *Scaphites nodosus quadrangularis* (Meek). Grabau and Shimer, p. 177, 178, figs. 1429, 1430 (= Meek, 1876, pl. 25, fig. 3a, b, c = *Hoploscaphites plenus* m).

←

Pierre Shale, Meade County, South Dakota. Septal approximation occurs over two chambers and is modest (the interseptal distance of the last chamber is 48% that of the last "normal" chamber). **D.** USNM 536232, USGS Mesozoic loc. 21224, Bearpaw Shale, Big Horn County, Montana. Septal approximation occurs over two chambers and is modest (the interseptal distance of the last chamber is 48% that of the last "normal" chamber). **E.** USNM 538103, USGS Mesozoic loc. 21224, Bearpaw Shale, near Hardin, Big Horn County, Montana. Septal approximation occurs over two chambers and is modest (the interseptal distance of the last chamber is 52% that of the last "normal" chamber). **F.** YPM 1868, YPM loc. A6520, Pierre Shale, Sage Creek, Pennington County, South Dakota. No septal approximation is apparent. Measurements are listed in table 1.

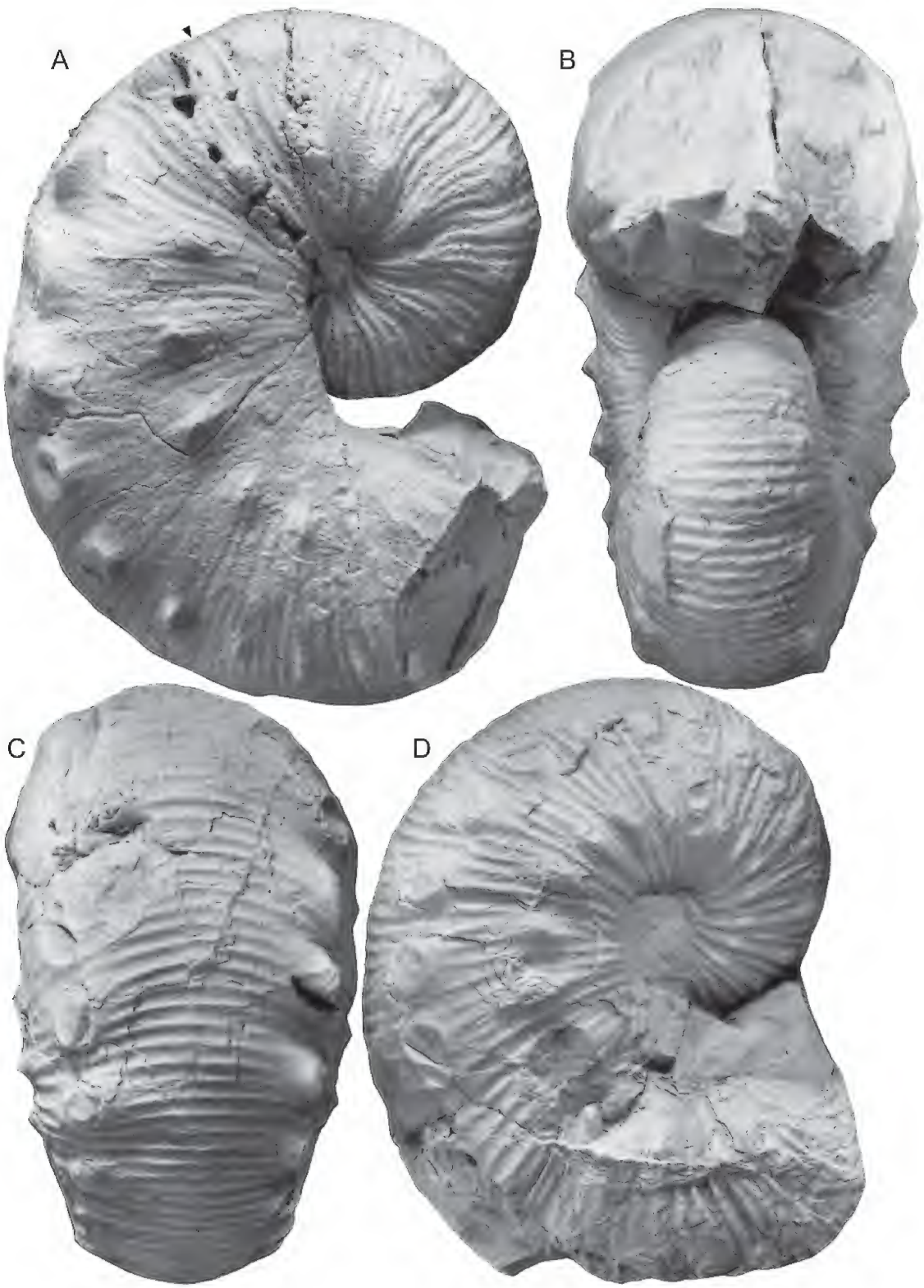
A
B
C
D

1915. *Scaphites binodosus* F.A. Roemer var. *brevis* Meek. Frech, p. 560, fig. 7.
non 1915. *Scaphites binodosus* F.A. Roemer var. *quadrangularis* Meek. Frech, p. 559, fig. 5 (=*Hoploscaphites plenus* m).
1921. *Scaphites nodosus* var. *brevis*. Grabau, p. 701, fig. 1698f, g (= Meek, 1876: pl. 25, fig. 1).
non 1921. *Scaphites nodosus* var. *quadrangularis*. Grabau, p. 701, fig. 1698h (= Meek, 1876, pl. 25, fig. 3c = *Hoploscaphites plenus* m).
1924. *Scaphites nodosus*, var. *brevis* Meek. Shimer, p. 267, fig. 119 (= Meek, 1876: pl. 25, fig. 1).
non 1931. *Acanthoscaphites nodosus* var. *quadrangularis* (Meek and Hayden). Warren, pl. 1, fig. 2 (= *Hoploscaphites plenus* m).
?1933. *Acanthoscaphites nodosus* var. *quadrangularis* Meek. Elias, p. 322, pl. 37, fig. 3.
pars 1933. *Acanthoscaphites nodosus* var. *brevis* Meek. Elias, p. 321, pl. 37, fig. 2; *non* pl. 41, fig. 3.
1933. *Scaphites nodosus*, var. *brevis* Meek. Shimer, p. 319, fig. 146 (= Meek, 1876: pl. 25, fig. 1).
non 1941. *Scaphites brevis* Meek. Stephenson, p. 426, pl. 90, figs. 7, 8.
1944. *Acanthoscaphites nodosus brevis*. Shimer and Shrock, p. 591, pl. 246, figs. 1, 2 (= Meek, 1876, pl. 25, fig. 1).
non 1944. *Acanthoscaphites nodosus quadrangularis*. Shimer and Shrock, p. 591, pl. 246, figs. 4–6 (= Meek, 1876, pl. 25, fig. 3 = *Hoploscaphites plenus* m).
?1952. *Scaphites* (*Scaphites*) *elegans* Tate, 1865. Jeletzky in Cobban and Reeside, p. 1027.
1953. *Scaphites*. Shrock and Twenhofel, text fig. 10.76, P1, P2 (= Meek, 1876, pl. 25, fig. 1).
1960. *Acanthoscaphites nodosus* var. *brevis* Meek. Easton, p. 453, fig. 11.27-3 (= Meek, 1876, pl. 25, fig. 1).
?1968. *Scaphites elegans* Tate. Jeletzky, p. 49 (= ?*Hoploscaphites plenus* m).
non 1970. *Scaphites brevis* Meek. Jeletzky, pl. 27, fig. 9.
non 1975. *Scaphites*. Nelson, p. 668, pl. 64, figs. 3, 4 (= Jeletzky, 1970: pl. 27, fig. 9).
1977. *Hoploscaphites nodosus brevis* (Meek and Hayden). Kauffman, pl. 32, fig. 9 (= Meek, 1876: pl. 25, fig. 1).
non 1977. *Hoploscaphites nodosus quadrangularis* (Meek and Hayden). Kauffman, pl. 32, fig. 8 (= Meek, 1876: pl. 25, fig. 4 = *Hoploscaphites plenus* m).
1980. *Hoploscaphites nodosus quadrangularis* (Meek). Thomel, p. 63, fig. 112.
non 1982. *Acanthoscaphites nodosus quadrangularis* (Owen, *non* Lopuski). Case, p. 83, fig. 12.28 (= *Hoploscaphites plenus* m).
1983. *Jeletzkytes brevis* (Meek). Riccardi: pl. 5, figs. 1, 2; text fig. 24a (= Meek, 1876: pl. 25, fig. 1).
non 1983. *Jeletzkytes* cf. *brevis* (Meek, 1876) ♀. Riccardi: p. 22, pl. 5, figs. 3–9 (figs. 5–7 = Jeletzky, 1970: pl. 27, fig. 9); pl. 6, figs. 5–9 (phragmocones); text figs. 14–19 (sutures), 24b (cross section).
pars 1983. *Jeletzkytes* cf. *brevis* (Meek, 1876) ♂. Riccardi, p. 25, pl. 10, figs. 3, 4 (= Meek, 1876: pl. 25, fig. 2), figs. 7–9, text fig. 22a; *non* pl. 10, figs. 1, 2 (= Meek, 1876: pl. 25, fig. 4 = *Hoploscaphites plenus* m); figs. 5, 6 (= Meek, 1876: pl. 25, fig. 3a = *Hoploscaphites plenus* m); figs. 10–18, text figs. 21b, 22b (= *Hoploscaphites plenus* m or *H. criptonodosus* m); figs. 19–21, text fig. 21a (= *Hoploscaphites plenus* m or *H. criptonodosus* m); ? text fig. 20 (sutures with no illustrated specimen).
non 1983. *Jeletzkytes* aff. *brevis* (Meek) ♀. Riccardi, p. 27, pl. 6, figs. 1–4, text fig. 23 (suture); text fig. 24 (cross section) (= ? *Hoploscaphites plenus*).
1983. *Hoploscaphites landesi* Riccardi, p. 10, pl. 1, figs. 12–22.
1983. *Hoploscaphites* sp. α Riccardi, p. 11, pl. 1, figs. 1–11; text figs. 3, 4.
non 1992. *Acanthoscaphites nodosus quadrangularis* (Owen, *non* Lopuski). Case, p. 83, fig. 12.28 (= *Hoploscaphites plenus* m).
1992. *Hoploscaphites* cf. *landesi* Riccardi, 1983. Cobban et al., p. A9, pl. 3, fig. 6.
1994. *Jeletzkytes nodosus brevis*. Emerson et al., p. 335 (= Meek, 1876: pl. 25, fig. 1).
1997. *Jeletzkytes brevis* (Meek, 1876). Larson et al., p. 77, unnumbered figs.
1997. *Jeletzkytes* "*quadrangularis*" (Meek and Hayden, 1860). Larson et al., p. 78, lower left fig.
1997. *Hoploscaphites landesi* Riccardi, 1983. Larson et al., p. 74, unnumbered figs.
2007. *Jeletzkytes brevis*. Fox, fig. 19b.

←

Fig. 78. *Hoploscaphites* aff. *H. nodosus* (Owen, 1852), Bearpaw Shale, Alberta, Canada. **A, B.** UA 748, macroconch (= *Jeletzkytes* aff. *nodosus* [Owen], Riccardi, 1983, pl. 3, figs. 2–6), north side of Milk River, near Groton, T. 3, R. 10, W4th. **A.** Right lateral; **B.** apertural. **C, D.** UA 03944, macroconch (= *Jeletzkytes* aff. *nodosus* [Owen], Riccardi, 1983, pl. 4, figs. 1, 2), locality unknown. **C.** Ventral; **D.** right lateral. These specimens are larger than *Hoploscaphites nodosus* and are probably from the *Baculites reesidei* Zone. Specimens are illustrated natural size.

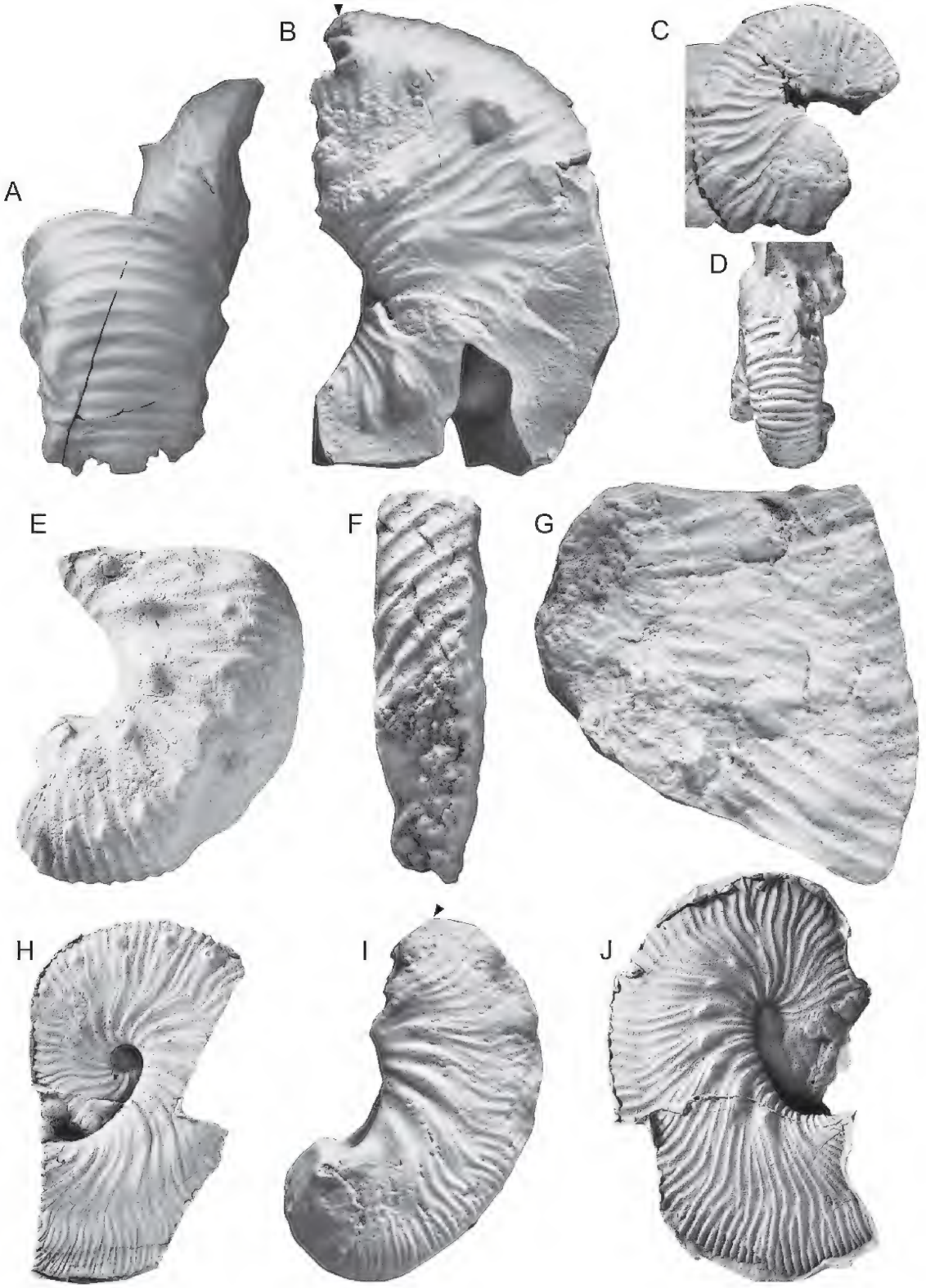
A
B
C
D
E
F
G
H
I
J

2009. *Jeletzkytes brevis*. Larson, p. 206, unnumbered fig.

DIAGNOSIS: Adult shell compressed, with rounded to ellipsoidal outline in lateral view; strongly dimorphic; in macroconchs, shaft relatively short with recurved hook, leaving small gap between exposed phragmocone and hook; apertural angle averaging 59°; umbilical seam straight in lateral view; in microconchs, shaft longer with more recurved hook, leaving larger gap between exposed phragmocone and hook; umbilical seam concave in lateral view; in both dimorphs, intercostal whorl section of body chamber subquadrate with fairly flat flanks; ornament consisting of flexuous primary and secondary ribs; umbilicolateral bullae/tubercles appearing on adoral end of exposed phragmocone and extending onto body chamber; ventrolateral tubercles stronger than umbilicolateral tubercles and unevenly spaced on exposed phragmocone, becoming more or less evenly spaced on shaft, usually terminating at point of recurvature; suture with broad, asymmetrically bifid first lateral saddle and narrow, symmetrically to asymmetrically bifid first lateral lobe.

TYPE: The holotype, by monotypy and original designation is USNM 367, the original of *Scaphites nodosus* var. *brevis* Meek, 1876: 428, pl. 25, fig. 1 (fig. 5). Meek wrote that "Dr. Owen's type specimen [*Scaphites nodosus*] came from near Cheyenne River, Dakota, where it was found in the upper part of the Fort Pierre group. Ours [*Scaphites nodosus* var. *brevis*] is from the same horizon on Yellowstone River, Montana, 150 miles above its mouth." In the *Catalogue of the Type Specimens of Fossil Invertebrates in the Department of Geology, U.S. National Museum* (Schuchert, 1905: 588), the locality is further restricted to the Yellowstone River, near Miles City, Montana. However, the entry for this specimen in the handwritten catalog of the Department of Paleobiology at the U.S National Museum states that the specimen was collected from the south fork of the Cheyenne River in South Dakota. This locality is much more in agreement with the source of most of our specimens and that of the type of *Hoploscaphites nodosus*.

Meek (1876: 428) illustrated three specimens as *Scaphites nodosus* var. *quadrangularis*, and listed their locality as the same as *S. nodosus* var. *brevis* ("Yellowstone River, Montana, 150 miles above its mouth"). The holotype, by original designation, is USNM 366, the original of Meek (1876: 428, pl. 25, fig. 3a–c), and is a microconch of *Hoploscaphites plenus* Meek, 1876 (fig. 6H–K). Similarly, USNM 365 (Meek, 1876: 428, pl. 25, fig. 4), a paratype, is also a microconch of *H. plenus* (fig. 6A–C). As such, the original stated locality of the Yellowstone River, Montana, is probably correct for both of these specimens. USNM 386690 (Meek, 1876: 428, pl. 25, fig. 2a–c), another paratype,

←

Fig. 79. *Hoploscaphites* aff. *H. nodosus* (Owen, 1852) and *Hoploscaphites brevis* (Meek, 1876), Pierre Shale, Wallace County, Kansas. **A–D.** *Hoploscaphites* aff. *H. nodosus* (Owen, 1852), macroconch, KUMIP 59651 (= Elias, 1933: 320, *Acanthoscaphites nodosus* [Owen], s.s.; pl. 38, figs. 1a, 1b, 2, *Acanthoscaphites nodosus* Say [s.s.]), upper part of Weskan Shale Member. **A.** Ventral; **B.** left lateral; **C.** right lateral of fragment of the internal whorls; **D.** ventral of fragment of the internal whorls. **E.** *Hoploscaphites* aff. *H. nodosus* (Owen, 1852), microconch, USNM 538097, left lateral of part of a body chamber, USGS Mesozoic loc. D615, Lake Creek Shale Member, *Baculites reesidei* Zone. **F, G.** *Hoploscaphites* aff. *H. nodosus* (Owen, 1852) (= Elias, 1933: 320, *Acanthoscaphites nodosus* [Owen], s.s.; pl. 38, fig. 3, *Acanthoscaphites nodosus* Say [s.s.]), KUMIP 59652, middle part of Lake Creek Shale Member. **F.** Ventral; **G.** left lateral. **H.** *Hoploscaphites brevis* (Meek, 1876), microconch, USNM 538098, rubber peel, left lateral, unnumbered USGS Mesozoic loc. **I.** *Hoploscaphites brevis* (Meek, 1876), microconch, KUMIP 59655 (= Elias, 1933: 322, pl. 37, fig. 3, *Acanthoscaphites nodosus* var. *quadrangularis* Meek and Hayden), part of body chamber, left lateral, upper part of Lake Creek Shale Member. **J.** *Hoploscaphites brevis* (Meek, 1876), microconch, USNM 538099, rubber peel, right lateral, USGS Mesozoic loc. D 615, Lake Creek Shale Member, *Baculites reesidei* Zone. Specimens are illustrated natural size. The position of the base of the body chamber is estimated in B and I.

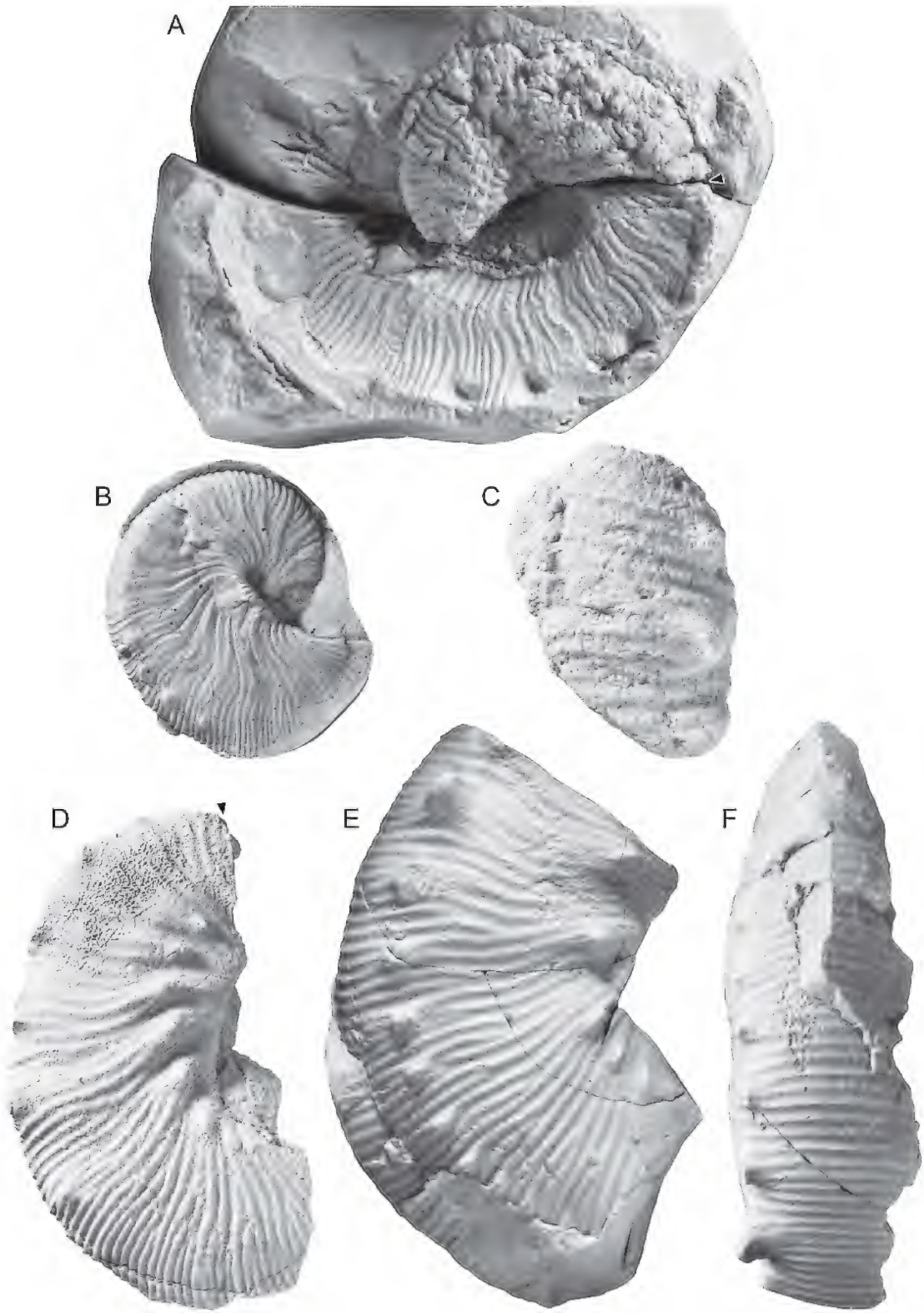
A
B
C
D
E
F

is a microconch of *H. brevis* (fig. 6D–H), and is probably from the south fork of the Cheyenne River, South Dakota. The taxonomic relationship between *S. nodosus* var. *quadrangularis* and *H. plenus* will be treated at greater length in a future publication.

Hoploscaphites landesi Riccardi, 1983, is a junior subjective synonym of *H. brevis*. The holotype of *H. landesi* (Riccardi, 1983: 10, pl. 1, figs. 12–14 = GSC 5342a) is from the "? Demaine Sandstone, Bearpaw Formation, and South Saskatchewan River opposite mouth of Swift Current River, Saskatchewan." It is a small microconch (LMAX = 49.0 mm) of *H. brevis* (fig. 7E–H). The three paratypes of *H. landesi* (Riccardi, 1983: 10, pl. 1, figs. 15–17 = GSC 5342b; pl. 1, figs. 18, 19 = GSC 5342d; pl. 1, figs. 20–22 = GSC 5342c) are from the same locality as the holotype and are also small microconchs of *H. brevis* (LMAX ranges from 34.7 to 38.7 mm). GSC 5342b and c (fig. 7I–L and M–Q, respectively) are nearly complete, and GSC 5342d consists of only part of the body chamber.

MATERIAL: There are approximately 300 specimens in our collection of which approximately 65 macroconchs and 105 microconchs comprise the measured set (tables 7–10). We have also included in our study many incomplete specimens, which provide information on ontogenetic development. Most of the material is from the *Baculites compressus–B. cuneatus* zones, Pierre Shale, South Dakota.

MACROCONCH DESCRIPTION: LMAX averages 71.5 mm and ranges from 29.5 to 101.5 mm (fig. 82, table 7). The ratio of the size of the largest macroconch to that of the smallest is 3.44. The size distribution is bimodal with a primary peak at 80–85 mm ("large" macroconchs) and a secondary peak at 60–65 mm ("small" macroconchs). All the specimens display the same pattern of ornamentation consisting of fine, flexuous ribs, small umbilicolateral tubercles, and larger ventrolateral tubercles, which are usually restricted to the shaft. Although the pattern of ornamentation is the same, the spacing of the ribs and the size of the umbilicolateral and ventrolateral tubercles covary with adult size.

Adults are slender, with a rounded to elongate outline in lateral view. For example, the outline is rounded in BHI 4203 (LMAX/H_4 = 2.04), whereas it is elongate in YPM 35584 (LMAX/H_4 = 2.26). The exposed phragmocone occupies approximately one-half to two-thirds of a whorl. It terminates slightly above or slightly below the line of maximum length. The septal angle averages 8.8° and ranges from −45.0° to 53.0°. There is a small, deep umbilicus, which averages 3.6 mm in diameter, both as measured parallel to the line of maximum length, and at the end of the phragmocone. The ratio of the average umbilical diameter to the average shell diameter is 0.05.

The body chamber consists of a short shaft and recurved hook, extending slightly beyond the coiled portion, leaving a small gap. LMAX/H_2 averages 2.93 and ranges from 2.72 to 3.16 (2.83 in the holotype). The hook is weakly reflected, as indicated by a low

←

Fig. 80. *Hoploscaphites* aff. *H. nodosus* (Owen, 1852) and *Hoploscaphites brevis* (Meek, 1876), Pierre Shale, Wallace County, Kansas. **A.** *Hoploscaphites brevis* (Meek, 1876), microconch (?), KUMIP 59653 (= Elias, 1933: 322, pl. 37, fig. 2, *Acanthoscaphites nodosus* var. *brevis* Meek), right lateral impression, upper part of Lake Creek Shale Member. **B.** *Hoploscaphites brevis* (Meek, 1876), macroconch, USNM 538095, right lateral impression, rubber peel, USGS Mesozoic loc. D615, Lake Creek Shale Member, *Baculites reesidei* Zone. **C.** *Hoploscaphites* aff. *H. nodosus* (Owen, 1852), fragment of part of the venter of a macroconch, USNM 538096, USGS Mesozoic loc. D4905, lower part of Lake Creek Shale Member. **D.** *Hoploscaphites brevis* (Meek, 1876), macroconch, USNM 538100, right lateral, USGS Mesozoic loc. D615, Lake Creek Shale Member, *Baculites reesidei* Zone. **E, F.** *Hoploscaphites* aff. *H. nodosus* (Owen, 1852), macroconch, KUMIP 59654 (= Elias, 1933: 321, pl. 41, fig. 3, *Acanthoscaphites nodosus* var. *brevis* Meek), lower part of Lake Creek Shale Member. **E.** Right lateral; **F.** ventral. Specimens are illustrated natural size. The position of the base of the body chamber is estimated in A and D.

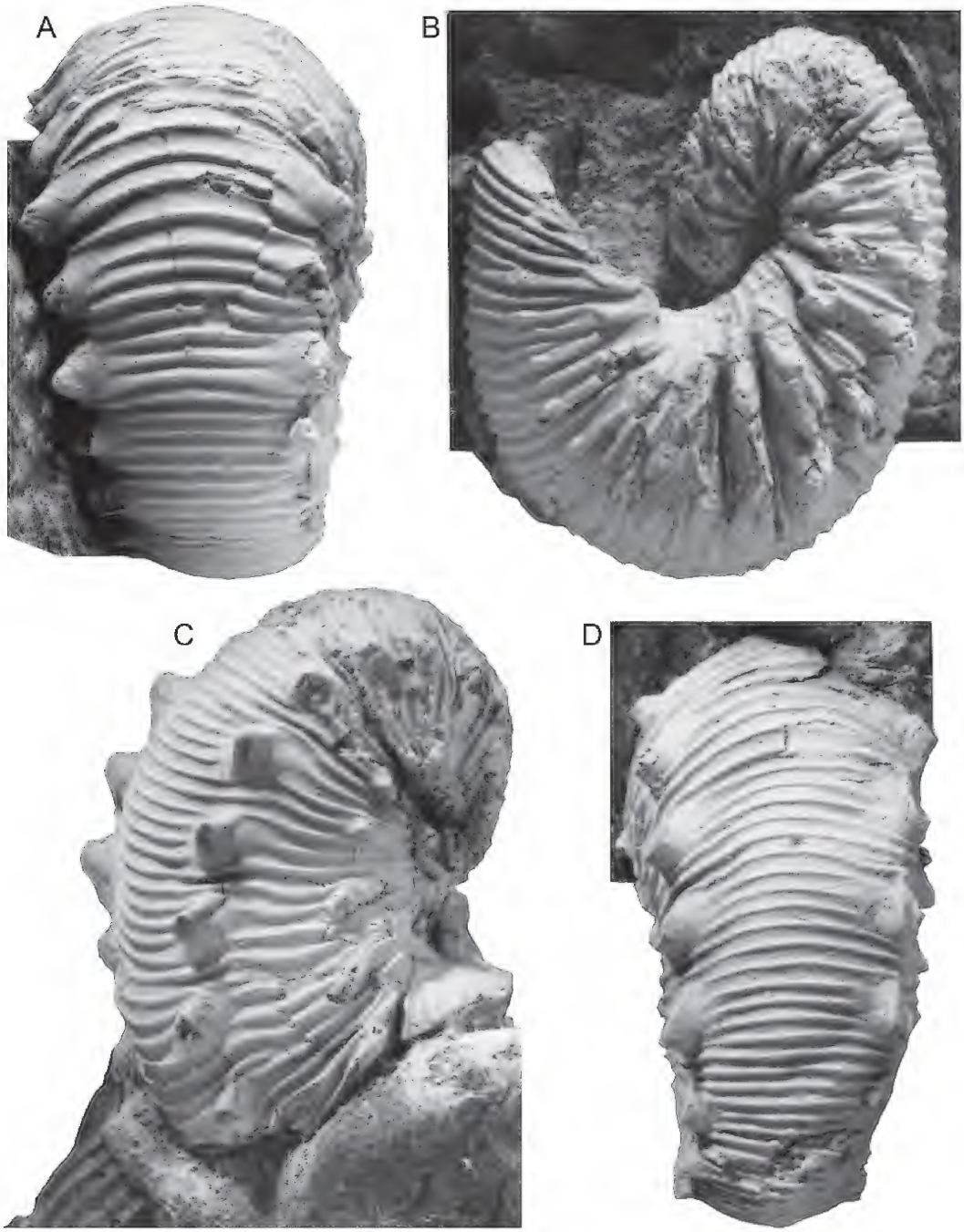

Fig. 81. *Hoploscaphites* aff. *H. nodosus* (Owen, 1852), Coon Creek Tongue, Ripley Formation, *Nostoceras* (*N.*) *hyatti* Zone, Coon Creek, McNairy County, Tennessee. **A, B.** MPPM 1996.39.1, macroconch. **A.** Ventral; **B.** left lateral. **C, D.** MPPM 1996.39.3, macroconch. **C.** Right ventrolateral; **D.** ventral. These specimens are more coarsely ribbed than *Hoploscaphites nodosus* (Owen, 1852). Specimens are illustrated natural size.

apertural angle, averaging 59.0° and ranging from 36.0° to 78.0°. There is a weak correlation between the septal angle and the apertural angle (fig. 38B). The apertural angle is higher in specimens in which the last septum falls below, rather than above, the line of maximum length. The apertural lip is thickened and shows a constriction.

In lateral view, the umbilical shoulder of the shaft is convex or straight, depending on the presence or absence of an umbilical swelling. This feature is one of the most reliable criteria to help identify macroconchs. The umbilical swelling appears as an elongate bulge that extends several millimeters on the shaft. In some specimens, for example, BHI 4234 (fig. 97I–K), it occludes part of the umbilicus. An umbilical swelling is present in approximately 30% of our specimens. It is more common in small specimens with low apertural angles.

The whorl section of the phragmocone near the point of exposure is compressed. W_1/H_1 averages 0.82 and ranges from 0.62 to 1.06 (0.87 in the holotype). There is a weak correlation with size, with larger specimens showing slightly more depressed whorl sections. The intercostal whorl section is subquadrate with maximum width at one-third whorl height. The umbilical wall is steep and subvertical and the umbilical shoulder is sharply rounded. The flanks are very broadly rounded to flat, converging toward the venter. The ventrolateral shoulder is sharply rounded and the venter is broadly rounded.

The ratio of whorl width to whorl height is nearly the same at the adoral end of the phragmocone. W_3/H_3 averages 0.76 and ranges from 0.64 to 0.91 (0.89 in the holotype). The intercostal whorl section is also subquadrate with maximum width at one-third whorl height. The umbilical wall is steep and inclined slightly outward, and the umbilical shoulder is sharply rounded. The inner flanks are broadly rounded and the outer flanks are nearly flat and converge toward the venter. The ventrolateral shoulder is sharply rounded and the venter is broadly rounded.

There is a small increase in whorl width but a substantial increase in whorl height as the shell passes into the shaft of the body chamber. Whorl width attains a maximum value on the adoral part of the shaft, after which it remains the same or decreases slightly. Whorl height attains a maximum value at midshaft, after which it also decreases slightly. The whorl section at midshaft is slightly more compressed than that at the base of the body chamber (fig. 83). W_4/H_4 averages 0.72 and ranges from 0.61 to 0.92 (0.78 in the holotype). There is a weak correlation with LMAX, with larger specimens showing slightly more depressed whorl sections. The ratio of V_4/H_4 averages 0.43 and ranges from 0.33 to 0.58 (0.58 in the holotype). The intercostal whorl section is subquadrate. The umbilical shoulder is sharply rounded on the shaft, becoming more broadly rounded on the hook. The flanks are very broadly rounded to nearly flat, with maximum width at one-third whorl height. In some specimens such as AMNH 56882 (fig. 90), the inner flanks are broadly rounded, and the outer flanks are flattened and converge toward the venter. The ventrolateral shoulder is sharply rounded and the venter is very broadly rounded.

The whorl section becomes less compressed from midshaft to just adapical of the point of recurvature, and remains more or less the same thereafter (fig. 83). The ratio of whorl width to whorl height at the aperture averages 0.97 and ranges from 0.81 to 1.20 (0.98 in the holotype). At the same time, the intercostal whorl section becomes slightly more ovoid, with maximum width at one-half whorl height. The flanks become more broadly rounded, and the venter becomes more narrowly rounded, coincident with the disappearance of the ventrolateral tubercles.

The ornament consists of fine, flexuous ribs, with rows of umbilicolateral and ventrolateral tubercles (table 8). Ribs are rursiradiate on the umbilical wall and shoulder of the phragmocone. They bend slightly backward on the inner flanks, slightly forward on the midflanks, and slightly backward again on the outer flanks. They cross the venter with a slight forward projection. On the adapical part of the phragmocone, branching and intercalation occur at one-third whorl height at the site of the umbilicolateral tubercles, if they are present, and at two-thirds whorl height. As a result, the inner

TABLE 7
Measurements of the adult shells of *Hoploscaphites brevis* (Meek, 1876), macroconchs

Specimen Number	Study Number	LMAX	LMAX/H_2	LMAX/H_4	Sep <	Apt <	UD_P	UD_L	W_1/H_1	W_2/H_2	W_3/H_3	W_4/H_4	W_5/H_5	W_6/H_6	W_7/H_7	V_4/H_4
AMNH 9519/1	662	84.6	—	1.93*	31.5	78.0	3.6*	3.2*	—	—	—	—	—	—	—	0.48
AMNH 45347[a]	—	78.8	—	2.04	—	68.0	—	4.0	—	—	—	—	—	—	—	—
AMNH 46642	1473	79.2	2.80	—	—	60.0	—	2.4	0.97	0.74	—	0.82*	—	1.04	1.20	0.43*
AMNH 51068	1673	74.9	2.78	2.01	10.0	67.0	3.3	3.4	—	0.71	0.73	0.66	0.87	0.97	—	0.36
AMNH 55882	—	66.2*	2.90*	2.00*	7.0	65.0	3.5	3.6	0.83	0.74	0.76	0.68	0.73*	0.78*	0.79*	0.42*
AMNH 56864	1674	48.9	2.96	2.21	−34.0	—	3.4	3.6	0.73	0.63	0.64	0.61	0.76	0.82	—	0.41
AMNH 56865	1675	61.2	2.91	2.13	−1.5	53.0	3.3	3.1	0.81	0.74	0.74	0.68	0.82	0.86	0.93	0.39
AMNH 56877	—	79.6	2.84	—	—	58.0	—	—	0.93	0.84	0.84	—	—	—	1.07	—
AMNH 56882	—	82.7	2.87	2.12	−30.0	59.0	3.3	4.1	—	0.69	0.63	0.76	0.88	0.93	0.98	
AMNH 58515	1455	62.1	2.90	2.08	−45.0	48.0	3.8	3.7	0.83	0.73	0.76	0.73	0.88	0.91	0.86	0.40
AMNH 58516	1453	87.0	2.84	—	−7.5	67.0	3.2	3.2	0.99	0.92	0.93	—	—	—	—	—
AMNH 58517	1454	57.2	3.05	—	—	52.0	2.6	2.5	0.79	0.72	0.78	—	—	—	—	—
AMNH 58543	1667	53.5	3.11	2.33*	13.0	44.0	—	3.8	0.79	0.72	0.72	0.66	0.84	0.82	—	0.38
AMNH 58561	523	81.5	3.00	2.17	31.0	76.5	2.7	2.8	1.01	0.85	0.85	0.77	0.97	1.00	0.96	0.40
AMNH 58566	566	89.2	—	2.11	—	78.0	—	—	—	—	—	0.82	1.05	1.10	1.02	0.44
BHI 4124	308	83.5	2.97	2.07	42.0	72.5	4.6	4.3	0.84	0.78	0.74	0.78	0.88	0.99	1.03	0.50
BHI 4202	313	80.5	2.79	2.14	28.0	56.0	3.7	4.2	0.82	0.76	0.78	0.74	0.97	1.04	1.02	0.45
BHI 4203	312	72.3	2.87	2.04	23.0	56.5	3.6	3.3	0.92	0.79	0.80	0.80	0.94	1.00	1.02	0.45
BHI 4204	316	78.2	2.97	2.21	11.0	73.0	3.2	3.7	0.86	0.79	0.80	0.74	0.89	0.98	1.08	0.47
BHI 4205	321	80.2	3.10	2.27	—	78.0	4.2	4.2	1.02	0.85	0.88	0.87	0.95	1.02	1.05	0.44
BHI 4206	1263	71.2	2.72	2.12	—	—	3.0	2.6	—	—	—	0.70	0.87	1.09	1.12	0.33
BHI 4230	485	57.0	2.92	2.16	−4.0	54.0	4.4	4.1	0.63	0.65	0.64	0.57	0.70	0.75	0.81	0.33
BHI 4232	439	50.3	3.05	2.22	34.0	68.0	3.6	3.3	0.80	0.74	0.71	0.66	0.87	0.91	0.94	0.39
BHI 4234	338	63.7	2.94	2.26	17.75	61.5	2.8	2.8	0.85	0.76	0.75	0.70	0.93	0.92	0.92	0.45
BHI 4235	332	47.9	2.90	2.04	—	54.0	2.5	2.4	0.74	0.71	0.71	0.63	0.82	0.85	0.87	0.36
BHI 4241	341	29.5	2.98	2.08	—	35.0*	2.9	2.9	0.70	0.72	0.80	0.68	0.86	0.93	—	0.42
BHI 4247	445	49.0	3.02	2.19	−3.0	51.0	3.8	3.5	0.72	0.68	0.75	0.65	0.86	—	—	0.39
BHI 4250	334	42.6	2.98	2.18	−12.0	47.0	4.0	4.2	0.76	0.75	0.72	0.65	0.85	0.92	0.88	0.44
BHI 4267	331	57.4	2.83	2.22	—	57.5	4.5	4.1	0.72	0.67	0.70	0.62	0.78	0.82	0.83	0.34
BHI 4274	311	61.3	2.95	2.17	6.5	60.5	3.4	3.1	0.76	0.71	0.72	0.70	0.90	0.90	0.98	0.44
BHI 4292	309	61.2	2.85	2.10	−4.0	51.5	3.6	3.6	0.81	0.80	0.81	0.68	0.82	0.89	0.86	0.41
BHI 4311	330	40.7	2.99	2.10	—	38.0	3.6	2.6	0.74	0.69	0.67	0.64	0.78	0.83	0.84	0.38
BHI 4324[b]	453	82.6	2.94	2.43	43.0	70.0	2.8	4.0	—	0.77	0.77	0.82	0.88	0.86	—	0.47
BHI 4382	646	57.5	3.03	2.17	—	61.0	—	—	1.09*	0.87*	1.04*	0.85	—	—	1.03	—
BHI 4385	798	92.6	3.08	1.99*	−33.0	51.0	—	—	0.80	0.69	0.69	0.55*	0.59*	0.70*	0.66*	0.30*
BHI 4390[b]	442	86.7	2.95	2.44*	—	—	4.2	4.2	—	0.84	0.76.	—	—	0.92	—	0.51
BHI 4391	444	83.0	3.08	2.24	—	63.5	4.0	3.4	0.71	0.78	0.76	0.84	0.92	0.94	0.96	0.50

TABLE 7
(*Continued*)

Specimen Number	Study Number	LMAX	LMAX/H_2	LMAX/H_4	Sep <	Apt <	UD_P	UD_L	W_1/H_1	W_2/H_2	W_3/H_3	W_4/H_4	W_5/H_5	W_6/H_6	W_7/H_7	V_4/H_4
BHI 4394	443	68.6	3.00	2.26	—	56.0	3.3	3.5	0.71	0.69	0.66	—	—	—	—	0.37
BHI 4776	592	81.9	2.91	2.06	22.0	65.0	—	—	0.67	0.64	0.66	0.69	—	—	0.99	—
BHI 4777	597	54.1	3.01	1.85	6.0	72.5	4.2	4.2	0.66	0.69	0.68	0.62	0.81	0.85	0.94	0.37
BHI 4789	636	80.4*	—	2.06*	—	67.5	—	4.1	—	—	—	—	—	—	—	0.51
BHI 4790	661	88.6	2.95	2.13	43.5	64.0	4.0	4.3	—	0.86	0.80	0.81	0.98	1.05	—	0.47
BHI 4796	521	61.6	3.13	2.14	9.0	51.5	3.0	3.0	0.83	0.78	0.79	0.64	0.76	0.73	—	0.37
BHI 4803	454	73.2	2.89	2.07	—	58.0	—	4.1	0.62	0.64	—	0.64*	0.83*	0.86*	0.77*	0.38
BHI 4900	1670	42.9	—	2.07	—	—	—	3.0	0.73	—	—	0.68	0.97	—	—	0.43
BHI 4902	—	92.9*	2.62*	1.90*	—	63.5	—	—	0.70*	0.70*	0.65*	0.69*	—	—	—	0.40*
BHI 4903	—	78.6	3.03	2.07	—	66.0	—	—	—	0.74	0.66	0.69	0.88	—	—	0.44
BHI 4910a	1273	77.7	2.86	2.04	37.0	65.5	3.0	2.4	0.82	0.80	0.74	0.78	0.95	1.04	1.12	0.42
BHI 4911a	1274	87.4	2.77	2.04	25.0	52.0	4.2	3.5	0.80	0.68	0.71	0.69	0.85	—	—	0.38
BHI 4913	1277	84.2	2.96	2.14	−13.0	60.0	3.8	4.5	—	0.60	0.67	0.61	0.77	0.86	0.87	0.36
BHI 5130	1658	79.3	2.87	—	—	55.0	3.9*	4.5*	0.99	0.79	—	0.72	0.91	0.91	0.94	0.42
BHI 7034	441	99.6	3.16	2.19	53.0	75.0	4.8	4.5	1.06	0.93	0.91	0.89	1.06	1.09	1.11	0.49
USNM 367	Type	78.4	2.83	2.11	20.5	53.0	—	3.0	0.87	0.89	0.89	0.78	0.94	1.00	0.98	0.58
USNM 14912	1651	101.5	2.91	2.30	−37.0	60.0	—	—	0.92	0.87	—	0.92	1.02	1.03	1.05	—
USNM 536221[c]	129	87.8	2.95	2.09	—	62.0	—	3.6	—	0.76	—	0.83	0.90	1.01	1.07	0.50
USNM 536222	243	87.3	2.96	—	5.0	57.0	4.3	3.8	0.76	0.79	0.82	—	0.94	0.94	0.90	—
USNM 536223[c]	147	—	—	—	—	—	4.1	4.4	0.75	0.71	0.82	0.66	—	—	—	0.43
USNM 536224	117	—	—	—	—	—	3.8	3.7	0.92	0.74	0.70	0.70	—	—	—	—
USNM 536225	130	83.0	2.87	2.05	—	—	4.2	4.2	—	0.77	0.75	—	—	—	—	0.48
USNM 536257	260	59.6	2.91	—	—	50.0	—	—	0.72	0.63	0.69	—	—	—	—	—
USNM 536265[c]	144	79.1	2.80	2.04	—	56.0	—	3.7	0.79	0.66	0.69	0.69	0.77	1.02	0.94	0.36
YPM 35576	302	82.8	2.87	2.21	22.0	51.5	3.5	3.5	0.97	0.89	0.90	0.84	0.98	1.05	1.05	0.55
YPM 35582	392	81.4	—	2.25	—	67.0	—	—	—	—	—	0.90	1.00	1.10	1.34*	0.59
YPM 35584 [b]	447	52.3	3.09	2.26	0.0	44.0	3.7	3.6	0.75	0.77	0.77	0.69	0.82	0.90	0.92	0.42
YPM 35585	446	46.2	2.96	2.13	—	36.0	—	3.5	0.72	0.71	0.74	0.66	0.87	0.93	0.91	0.35

See figure 14 for a description of the measurements. All measurements are in mm except for septal angle and apertural angle, which are in degrees. *Estimate.
[a]Used in ontogenetic study.
[b]Elongate outline.
[c]? *Baculites reesidei* Zone.

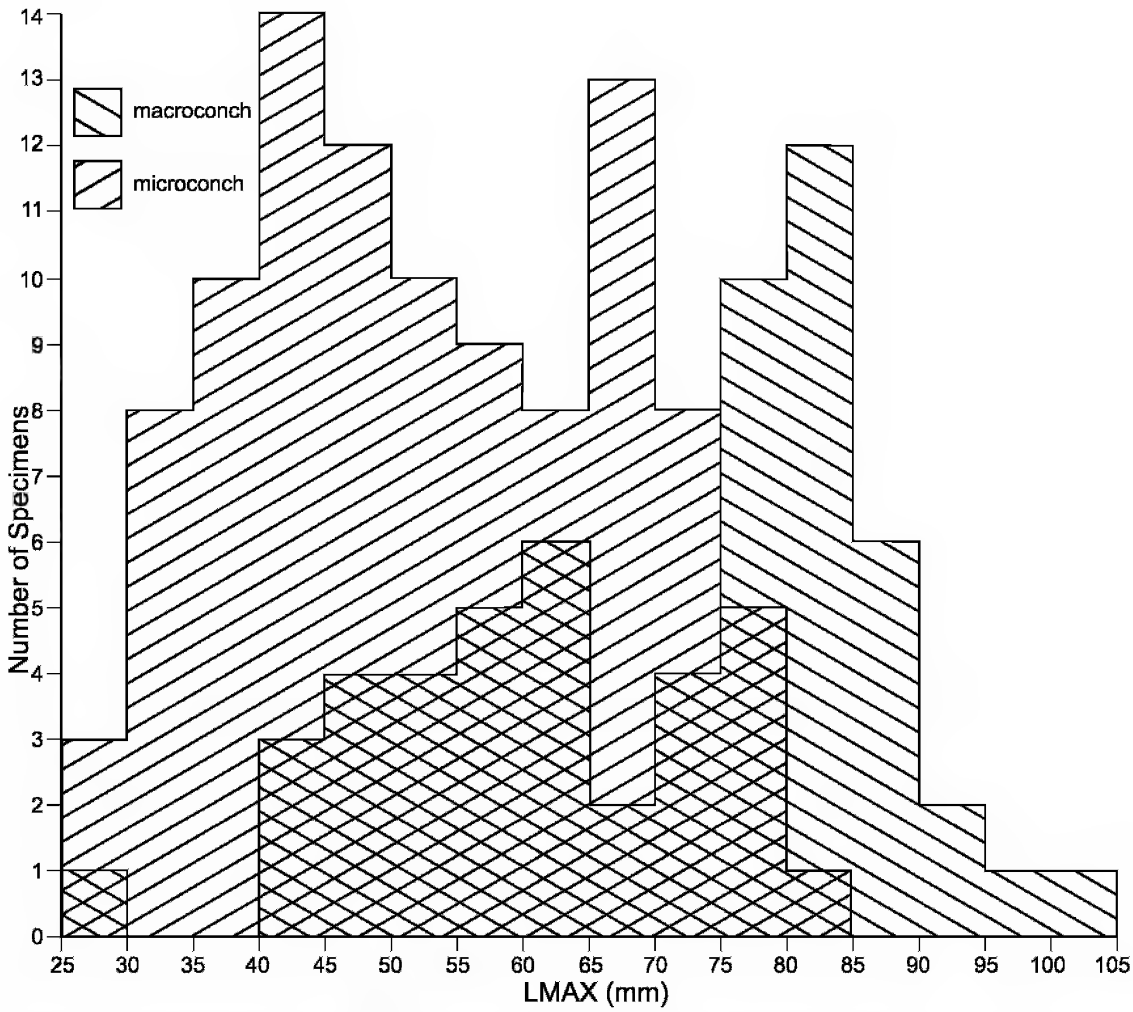

Fig. 82. Size-frequency histogram of *Hoploscaphites brevis* (Meek, 1876), Pierre Shale and Bearpaw Shale, *Baculites compressus–B. cuneatus* zones, based on the samples in tables 7 and 9.

flanks of the shell are relatively bare, with few secondary ribs. This pattern changes on the adoral part of the phragmocone, as additional secondary ribs originate near the umbilical shoulder.

The density of ribbing on the phragmocone either remains the same or increases slightly toward the base of the body chamber. There are 6–10 ribs/cm on the venter on the adapical portion of the phragmocone and 7–10 ribs/cm on the venter on the adoral portion of the phragmocone. In the holotype, the rib density is constant (6 ribs/cm) whereas in BHI 4205 the rib density increases adorally from 6 to 8 ribs/cm. The ratio of secondary to primary ribs on the phragmocone ranges from 4–5:1.

Ribs are narrow, prorsiradiate, and flexuous on the shaft. They arise at the umbilical seam and are rursiradiate on the umbilical wall and shoulder of the shaft, becoming more rectiradiate in an adoral direction. There are 8–14 ribs/cm on the umbilical shoulder of the shaft (7 on the left side and 8 on the right side of the holotype). In some specimens such as YPM 35585 (fig. 99A–D), a few of these ribs develop into weak bullae. Branching and intercalation occur near the umbilical shoulder, at the site of the umbilicolateral tubercles, if they are present, and on

the mid to outer flanks. Ribs swing strongly backward across the inner flanks, strongly forward across the midflanks, weakly backward again across the outer flanks, and weakly forward again at the ventrolateral shoulder. They become less flexuous toward the adoral end of the shaft. They form a distinctive pattern on the hook, with the outer flanks much more densely ribbed than the inner flanks. This pattern is especially striking in specimens lacking ventrolateral tubercles on the hook.

Ribs cross the venter of the shaft with a slight forward projection, which weakens on the hook. The rib density, as measured by the number of ribs/cm on the venter, varies depending on LMAX, with larger specimens showing lower rib densities. However, the ontogenetic pattern of rib density is nearly the same in all specimens. In general, the rib density increases from the adoral part of the phragmocone to the midshaft. In small specimens, the rib density is 7–10 ribs/cm on the adoral part of the phragmocone and 10–14 ribs/cm on the midshaft. In larger specimens, the rib density is 6–8 ribs/cm on the adoral part of the phragmocone and 6–10 ribs/cm on the midshaft.

There are minor variations in the general pattern of increasing rib density. In the holotype (figs. 5, 18C), an initial area of closely spaced ribs (10 ribs/cm) on the adapical part of the shaft is followed by an area of more widely spaced ribs (8 ribs/cm), which is followed, in turn, by another area of closely spaced ribs (10 ribs/cm), which is followed on the adoral part of the shaft by another area of widely spaced ribs (8 ribs/cm). In some specimens, the increase in rib density is gradual. In BHI 4274 (fig. 96A–D), the rib density gradually increases over approximately 0.25 whorl from 7 ribs/cm on the phragmocone at the line of maximum length to 12 ribs/cm just adapical of the midshaft. In other specimens, the increase in rib density is more abrupt. In YPM 35584 (fig. 98A–D), the rib density abruply increases from 9 ribs/cm on the adoral part of the phragmocone to 12 ribs/cm just adapical of the midshaft. In BHI 4311 (fig. 99I–L), the rib density increases abruptly from 10 ribs/cm on the adoral part of the phragmocone to 12 ribs/cm on the midshaft. In BHI 4796 (fig. 97A–D), the rib density abruptly increases from 9 ribs/cm on the adoral part of the phragmocone to 11 ribs/cm on the midshaft. In other specimens, especially those from the *Baculites cuneatus* Zone, the rib density either remains the same or decreases slightly. In USNM 536221 (fig. 94C, D), the rib density decreases from 7 ribs/cm on the adoral part of the phragmocone to 6 ribs/cm on the midshaft. In still other specimens, such as BHI 4250 (fig. 99E–H), a small part of the venter is smooth without any ribs at all.

The rib density generally continues to increase from the midshaft to the hook. In USNM 536222 (fig. 87D, E), the rib density increases from 7 ribs/cm on the midshaft to 9 ribs/cm on the hook. In BHI 4247 (fig. 98E–H), it increases from 12 ribs/cm on the midshaft to 15 ribs/cm on the hook. In BHI 4311 (fig. 99I–L), it increases from 12 ribs/cm on the midshaft to 14 ribs/cm on the hook. More rarely, the rib density remains the same or decreases slightly, although it never reverts to the value on the phragmocone. In BHI 4274 (fig. 96A–C), the rib density on the midshaft (12 ribs/cm) remains the same to the point of recurvature, after which it decreases to 10 ribs/cm near the aperture. In the measured set of specimens, the rib density on the hook ranges from 10–15 ribs/cm in small specimens and 7–11 ribs/cm in large specimens. The highest rib density on the hook (15 ribs/cm) occurs in BHI 4244 and 4247 (fig. 98E–H), both of which are from the *Baculites compressus* Zone.

The ratio of secondary to primary ribs on the midshaft ranges from approximately 3–7:1 (5:1 in the holotype). The ratio of secondary to primary ribs on the hook ranges from approximately 3–6:1 (5:1 in the holotype). This value seems low given the large number of ventral ribs on the hook. However, the number of primary ribs on the hook is also large. The maximum ratio of secondary to primary ribs on the hook is 8:1 in BHI 4247 (fig. 98E–H) due to a combination of a large number of ventral ribs and a small number of primary ribs.

In most small specimens, umbilicolateral tubercles are absent on the phragmocone. Instead, the primary ribs in this area are strong and adorally concave. Umbilicolateral tubercles are more common on the phrag-

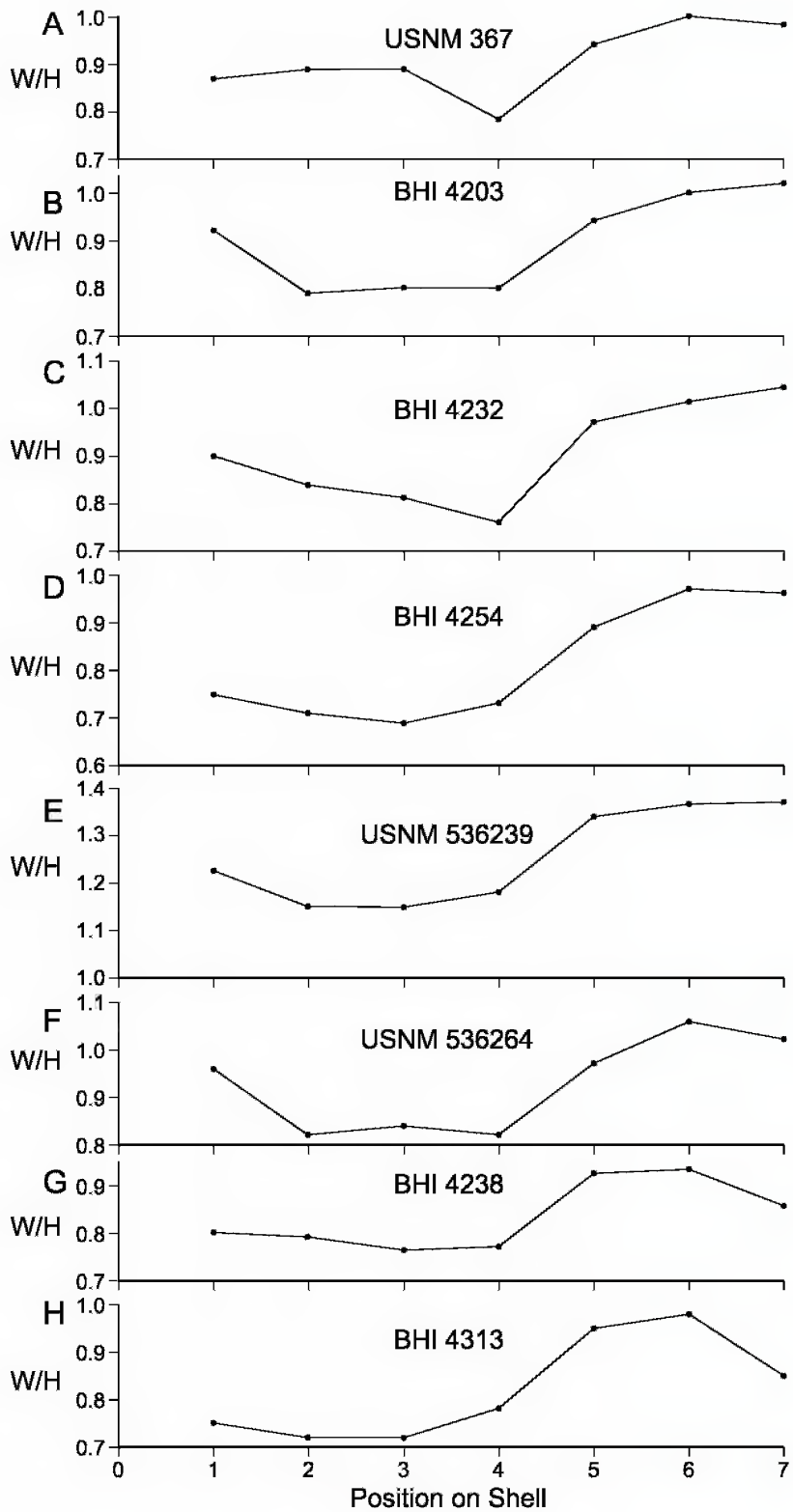
A
W/H
USNM 367
B
W/H
BHI 4203
C
W/H
BHI 4232
D
W/H
BHI 4254
E
W/H
USNM 536239
F
W/H
USNM 536264
G
W/H
BHI 4238
H
W/H
BHI 4313
Position on Shell

mocone in large specimens. However, even among these specimens, umbilicolateral tubercles are sometimes absent. The size of the specimen does not appear to be a determining factor. For example, in BHI 4234 (fig. 97I–K), in which LMAX = 63.7 mm, there are no umbilicolateral tubercles on the phragmocone, whereas in BHI 4274 (fig. 96A–C), which is approximately the same size (LMAX = 61.3 mm), there are five umbilicolateral tubercles on the phragmocone, starting near the point of exposure. By the same token, there are no umbilicolateral tubercles on the phragmocone in BHI 4230 (fig. 97E–H), in which LMAX = 57.0 mm, whereas there are four umbilicolateral tubercles on the phragmocone in BHI 4232 (fig. 108A–D), which is slightly smaller (LMAX = 50.3 mm), but otherwise identical.

The umbilicolateral tubercles usually appear midway or near the adoral end of the exposed phragmocone. More rarely, they appear at the point of exposure. They are relatively evenly spaced, with a few exceptions such as BHI 4203 (fig. 87A–C). The maximum distance between adjacent tubercles ranges from 4 to 9 mm. A total of two to four umbilicolateral tubercles are present on the exposed phragmocone (one in the holotype). The umbilicolateral tubercles are small, less than 1 mm in height, and bullate. In general, one or two ribs join a tubercle dorsally and two or three ribs branch from it ventrally. A maximum of two ribs intercalate between tubercles.

Umbilicolateral tubercles are usually, but not invariably, present on the body chamber. In specimens that are rounded in lateral view, the tubercles are arranged in a broad arc, which is one of the hallmarks of this species. The tubercles are more or less uniformly spaced on the shaft with, occasionally, some approximation near the point of recurvature. For example, in BHI 4274 (fig. 96A–D), there are six umbilicolateral tubercles on the body chamber. They are uniformly spaced, with a distance of 6.5 mm between tubercles at midshaft. In contrast, in BHI 4292 (fig. 96D–F), there are four umbilicolateral tubercles on the body chamber, three of which appear on the adapical end of the shaft, and one of which appears on the adoral end of the shaft. In the measured set of specimens, the maximum distance between adjacent tubercles on the shaft ranges from 2 to 14 mm (14 mm in the holotype).

The umbilicolateral tubercles on the body chamber occur at one-fourth to one-third whorl height. In some specimens, such as USNM 536221 (fig. 94C, D), the tubercles are conical in appearance. In contrast, in the holotype (fig. 5), as well as in BHI 4124 (fig. 89A–C) and USNM 536222 (fig. 87D, E), the tubercles are elongated radially and occur on broad folds that extend from the umbilical shoulder to the midflank. Tubercles attain their maximum height at midshaft (0.25–2.0 mm). One to three ribs join an umbilicolateral tubercle dorsally, and two to four ribs branch from it ventrally. A maxi-

←

Fig. 83. Plot of the ratio of whorl width to height (W/H) at seven points on the adult shell of *Hoploscaphites brevis* (Meek, 1876) from ¼ whorl adapical of the long axis (1) to the aperture (7), as shown in figure 14. The shell attains its maximum degree of compression near midshaft (points 3, 4), becoming less compressed thereafter. However, in microconchs, the shell becomes more compressed again at the aperture. **A–C.** Macroconchs. **A.** USNM 367, holotype, Pierre Shale, probably from the Sage Creek area, Pennington County, South Dakota. **B.** BHI 4203, *Baculites compressus* Zone, Pierre Shale, Meade County, South Dakota. **C.** BHI 4232, *Baculites compressus–B. cuneatus* zones, Pierre Shale, Meade County, South Dakota. **D–H.** Microconchs. **D.** BHI 4254, *Baculites compressus* Zone, Pierre Shale, Meade County, South Dakota. **E.** USNM 536239, USGS Mesozoic loc. 23070, Pierre Shale, Pennington County, South Dakota. **F.** USNM 536264, USGS Mesozoic loc. 23650, *Didymoceras cheyennense* Zone, Pierre Shale, Carter County, Montana. **G.** BHI 4238, *Baculites compressus* Zone, Pierre Shale, Meade County, South Dakota. **H.** BHI 4313, *Baculites compressus–B. cuneatus* zones, Pierre Shale, Meade County, South Dakota.

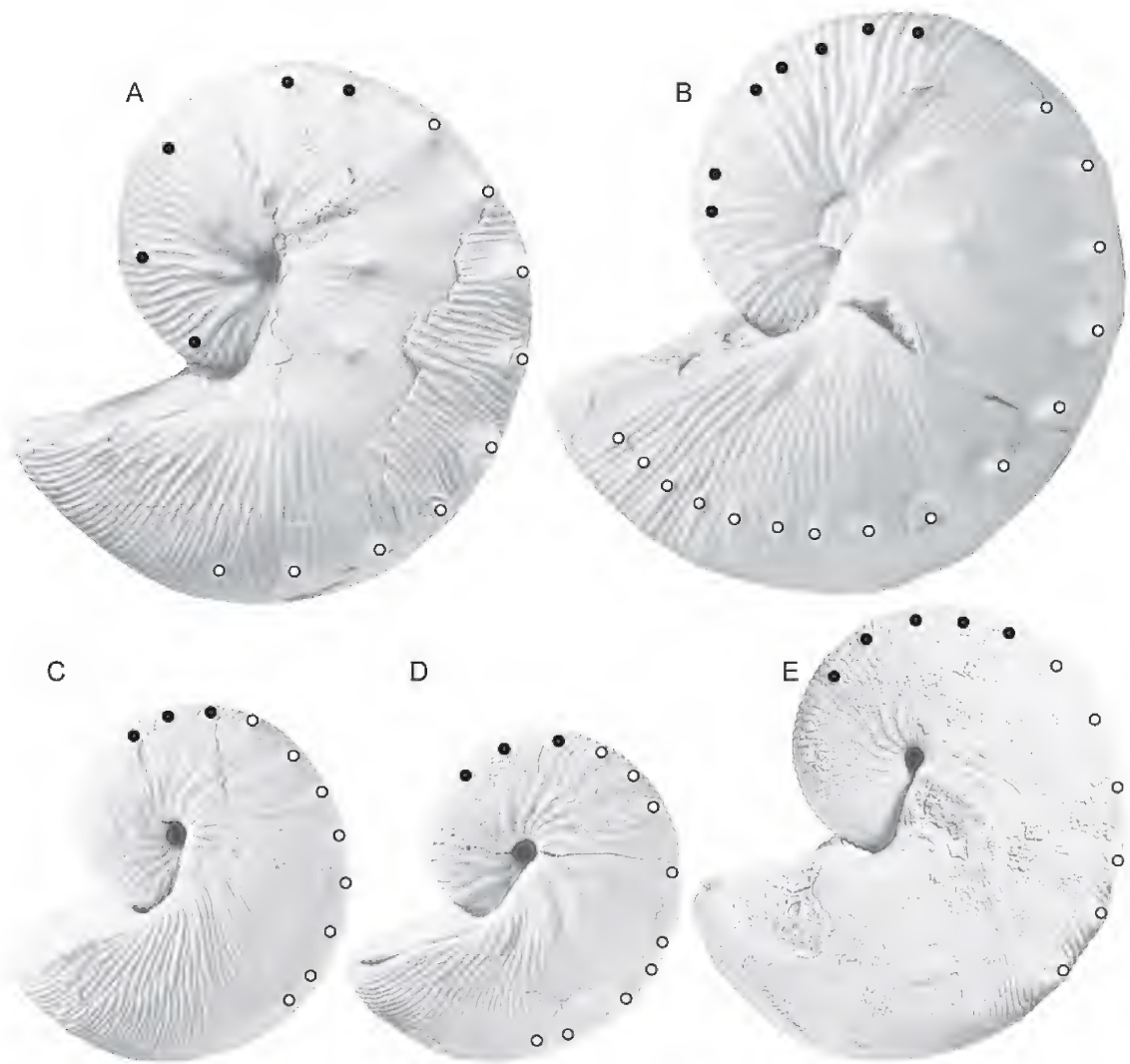

Fig. 84. Spacing of ventrolateral tubercles on the adult shell of *Hoploscaphites brevis* (Meek, 1876), macroconchs. **A.** BHI 4203, *Baculites compressus* Zone, Pierre Shale, Meade County, South Dakota. **B.** USNM 367, holotype, Pierre Shale, probably from the Sage Creek area, Pennington County, South Dakota. **C.** BHI 4235, *Baculites compressus* Zone, Pierre Shale, Meade County, South Dakota. **D.** YPM 35585, YPM loc. A6520, Pierre Shale, Sage Creek, Pennington County, South Dakota. **E.** BHI 4796, *Baculites compressus–B. cuneatus* zones, Pierre Shale, Meade County, South Dakota. The photo in E has been flipped so that it faces the same way as the others. Symbols: • = tubercle on the phragmocone; o = tubercle on the body chamber.

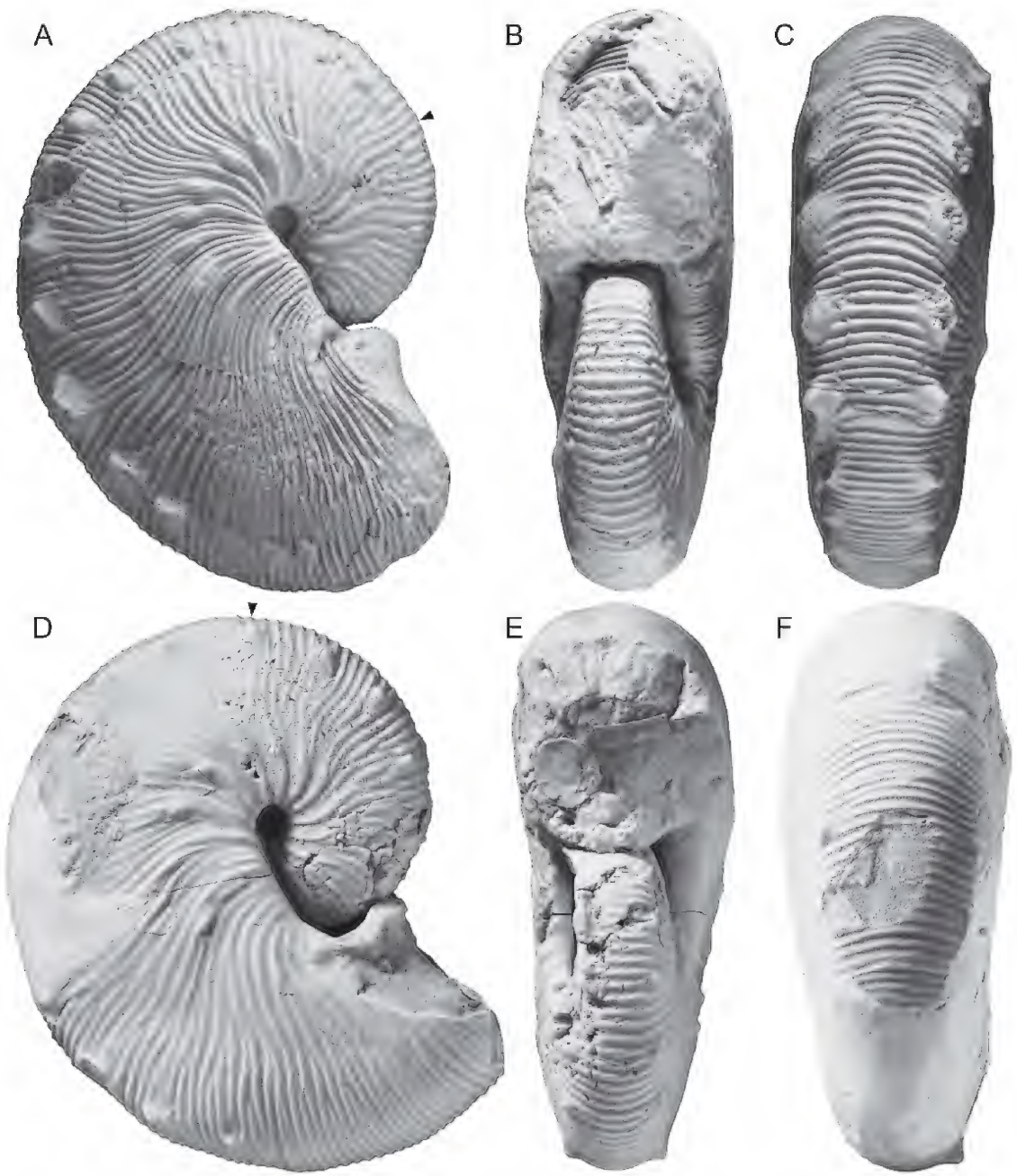

Fig. 85. *Hoploscaphites brevis* (Meek, 1876), large macroconchs. **A–C.** USNM 536223, USGS Mesozoic loc. D1074, *Baculites reesidei* Zone (?), Pierre Shale, Pueblo County, Colorado. **A.** Right lateral; **B.** apertural; **C.** ventral. **D–F.** USNM 536225, USGS Mesozoic loc. 7892, Bearpaw Shale, Musselshell County, Montana. **D.** Right lateral; **E.** apertural; **F.** ventral. Specimens are illustrated natural size.

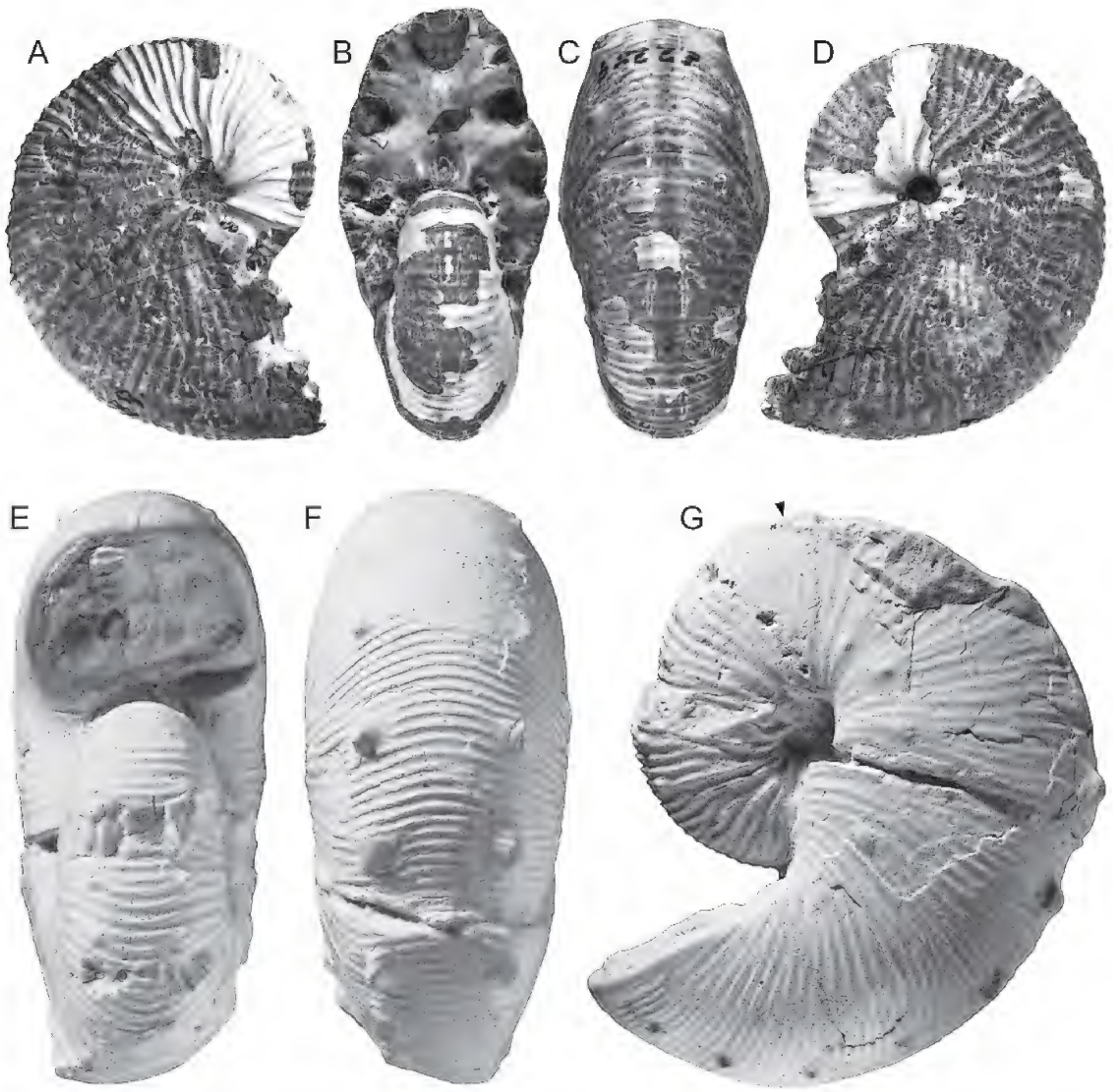

Fig. 86. **A–D.** *Hoploscaphites brevis* (Meek, 1876), macroconch, USNM 12289 (= Whitfield, 1880: pl. 13, figs. 8, 9, *Scaphites nodosus* var. *brevis*), uncoated, from "the Fort Pierre Group, Cheyenne River, near Rapid Creek, Black Hills, Dakota." **A.** Right lateral; **B.** apertural; **C.** ventral; **D.** left lateral. **E–G.** *Hoploscaphites plenus* (Meek, 1876), macroconch, GSC 21852 (= Riccardi, 1983: pl. 5, figs. 5–7, *Hoploscaphites* cf. *brevis* [Meek, 1876]), GSC loc. 97993, Bearpaw Shale, Frenchman (?) River, Saskatchewan, Canada. **E.** Apertural; **F.** ventral; **G.** left lateral. Specimens are illustrated natural size.

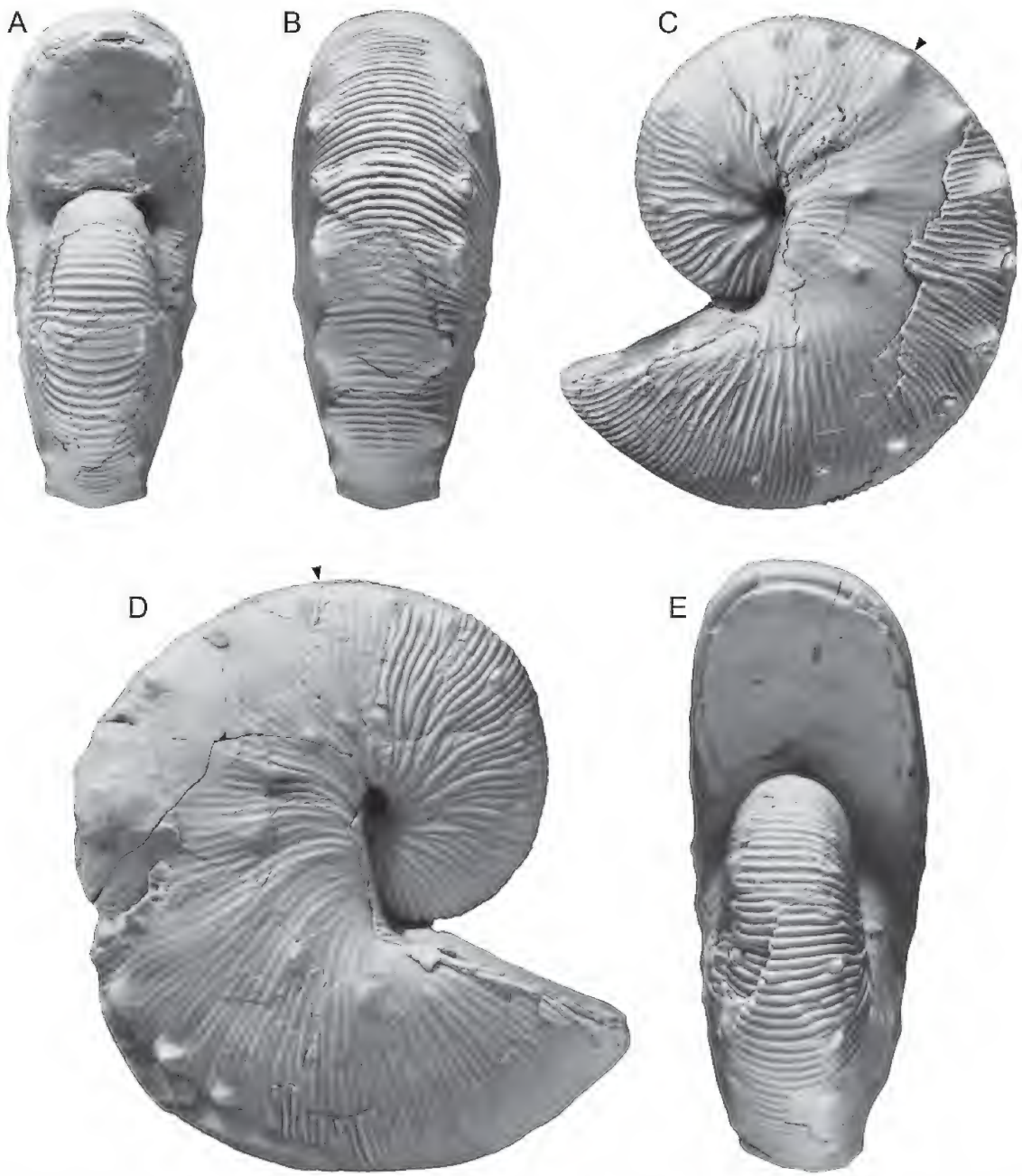

Fig. 87. *Hoploscaphites brevis* (Meek, 1876), large macroconchs. **A–C.** BHI 4203, *Baculites compressus* Zone, Pierre Shale, Meade County, South Dakota. **A.** Apertural; **B.** ventral; **C.** left lateral. **D, E.** USNM 536222, USGS Mesozoic loc. 23537, *Didymoceras cheyennense* Zone, Pierre Shale, Carter County, Montana. A chunk of shell is missing from the back of the body chamber. **D.** Right lateral, **E.** apertural. Specimens are illustrated natural size.

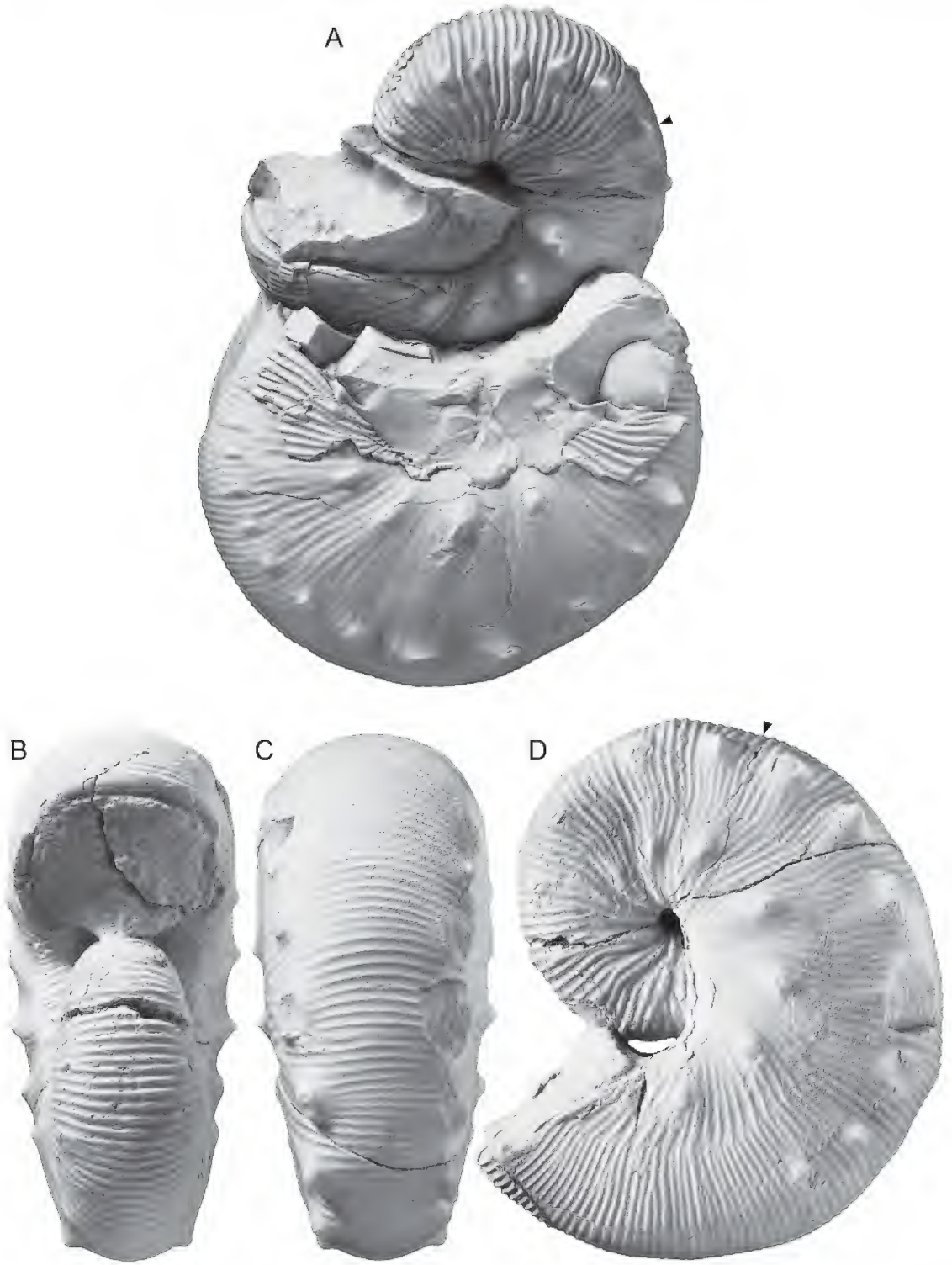

Fig. 88. *Hoploscaphites brevis* (Meek, 1876), YPM loc. A6520, Pierre Shale, Sage Creek, Pennington County, South Dakota. **A.** YPM 355812, 35582, macroconch and microconch, respectively, in the same concretion. **B–D.** YPM 35576, large macroconch. **B.** Apertural; **C.** ventral; **D.** left lateral. Specimens are illustrated natural size.

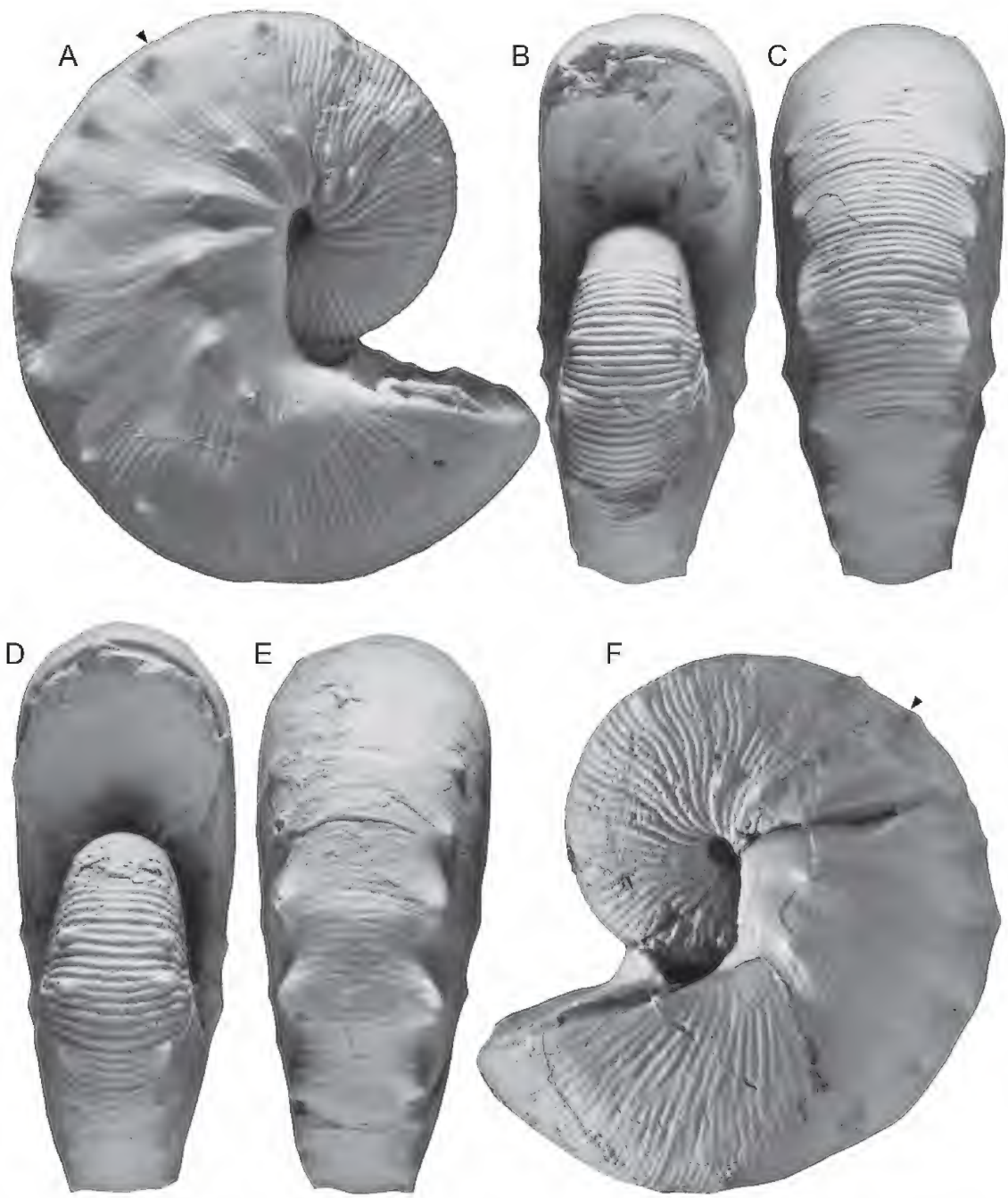

Fig. 89. *Hoploscaphites brevis* (Meek, 1876), large macroconchs. **A–C.** BHI 4124, *Baculites compressus–B. cuneatus* zones, Pierre Shale, Meade County, South Dakota. **A.** Right lateral; **B.** apertural; **C.** ventral. **D–F.** BHI 4202, *Baculites compressus* Zone, Pierre Shale, Meade County, South Dakota. **D.** Apertural; **E.** ventral; **F.** left lateral. Specimens are illustrated natural size.

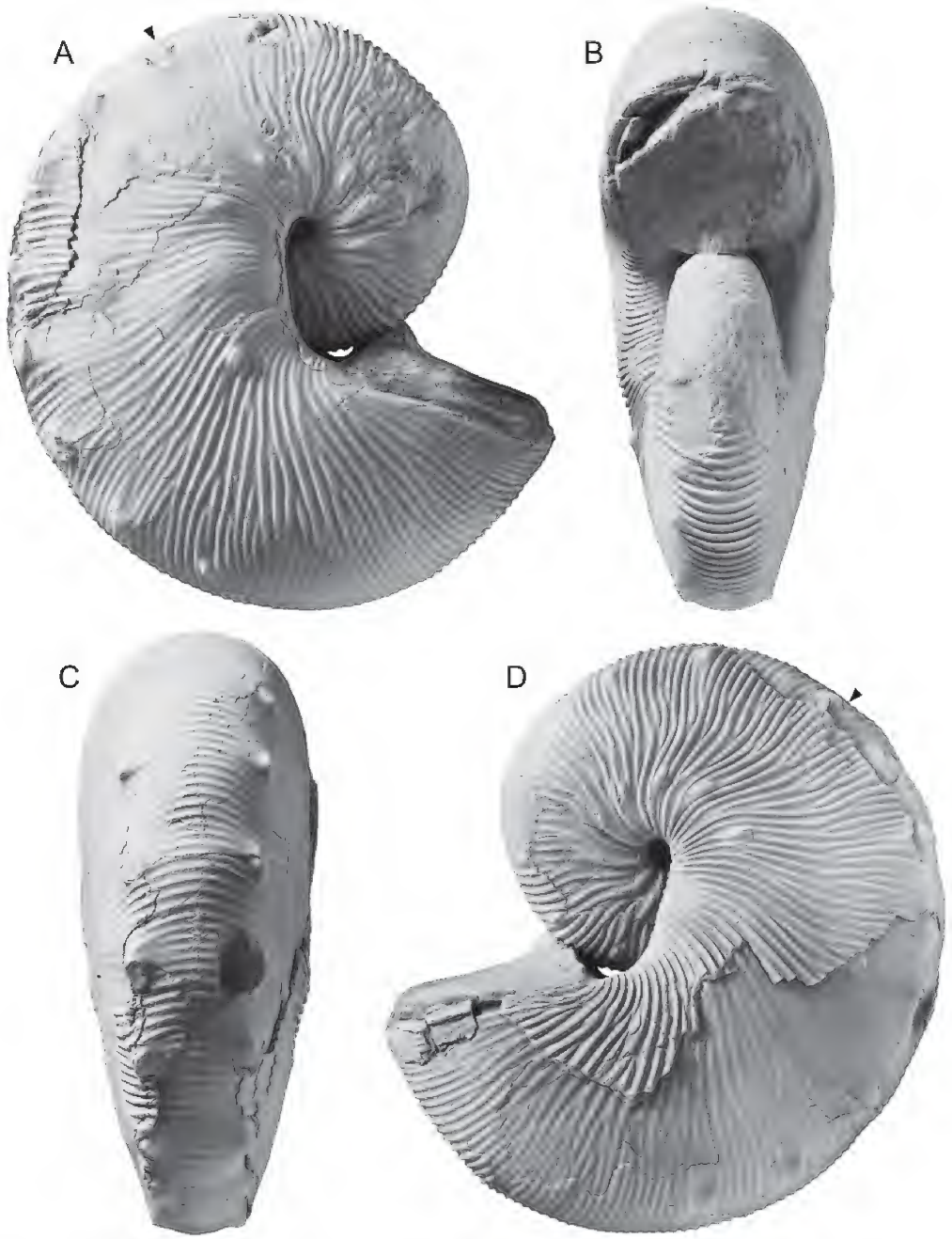

Fig. 90. *Hoploscaphites brevis* (Meek, 1876), large macroconch, AMNH 56882, AMNH loc. 3436, *Baculites compressus* Zone, Pierre Shale, Meade County, South Dakota. **A.** Right lateral; **B.** apertural; **C.** ventral; **D.** left lateral. Specimen is illustrated natural size.

mum of six ribs intercalate between tubercles. The maximum number of umbilicolateral tubercles on the body chamber is 10 (6 in the holotype), and the maximum number of umbilicolateral tubercles on the adult shell is 14 (7 in the holotype).

Ventrolateral tubercles commonly occur on the phragmocone. However, as with umbilicolateral tubercles, the size of the specimen is not a determining factor, at least in small specimens. For example, in BHI 4234 (fig. 97I–K), in which LMAX = 63.7 mm, ventrolateral tubercles are absent, whereas in BHI 4292 (fig. 96D–F), which is nearly the same size (LMAX = 61.2 mm), ventrolateral tubercles are present. In those specimens with ventrolateral tubercles, the tubercles appear anywhere starting from the point of exposure to the adoral end of the phragmocone. For example, in the holotype (fig. 5), they appear midway on the exposed phragmocone, whereas in BHI 4230 (fig. 97E–H), they appear at the adoral end of the exposed phragmocone.

The ventrolateral tubercles on the phragmocone are relatively small, less than 2.0 mm in height. In general, they are unevenly spaced and commonly occur in pairs or clusters. In the holotype (fig. 5), starting midway on the exposed phragmocone, the distance beween successive tubercles, as measured in an adoral direction, is 4, 12, 5, 5, 6, and 7 mm. In BHI 4203 (fig. 87A–C), starting at the point of exposure, the distance between successive tubercles, as measured in an adoral direction, is 14, 14, 18, and 9 mm. In BHI 4232 (fig. 108A–D), starting one-third way on the phragmocone, the distance between successive tubercles, as measured in an adoral direction is 9.5, 3.5, 8, and 4.5 mm. In BHI 4124 (fig. 89A–C), starting at the point of exposure, the tubercles become progressively more widely spaced adorally, attaining a maximum distance of 16 mm at the adoral end of the phragmocone. The maximum distance between ventrolateral tubercles on the exposed phragmocone in our sample ranges from 5 to 18 mm. One or two ribs join a ventrolateral tubercle dorsally and two or three ribs branch from it ventrally. A maximum of seven ribs occurs between ventrolateral tubercles, depending on the distance between tubercles and the density of ribbing.

The largest gap between ventrolateral tubercles usually occurs between the most adoral tubercle on the phragmocone and the most adapical tubercle on the body chamber. Thereafter, the tubercles are more or less uniformly spaced on the shaft. This pattern is exemplified by the holotype: the distance between the most adoral tubercle on the phragmocone and the most adapical tubercle on the body chamber is 19 mm; thereafter, the tubercles are nearly evenly spaced (9–12 mm) until the point of recurvature. Similarly, in BHI 4203 (fig. 89A–C), the largest gap between consecutive tubercles (13.5 mm) appears between the most adoral tubercle on the phragmocone and the most adapical tubercle on the body chamber, after which the tubercles are evenly spaced (9–12 mm). In contrast, in BHI 4274 (fig. 96A–D), the largest gap between consecutive tubercles (11.5 mm) occurs on the adoral part of the shaft, after which the tubercles are uniformly spaced (5.5–7 mm). The maximum distance between consecutive tubercles at midshaft in our sample ranges from 6 to 16 mm.

The ventrolateral tubercles attain their maximum height at midshaft (0.5–2.5 mm). In some specimens, the tubercles are clavate with a flat, steepened adapical face, and a more gently sloping, adoral face. In general, the ventrolateral tubercles die out on the adoral end of the shaft. In specimens in which they persist onto the hook, the tubercles become smaller, more bullate, and more closely spaced. For example, in the holotype (fig. 5), the tubercles on the hook are closely and evenly spaced at intervals of approximately 6 mm. The most adoral tubercle, just adapical of the aperture, consists of a small radial swelling. The number of ventrolateral tubercles on the body chamber in our sample ranges from 4 to 16 (15 in the holotype). The total number of ventrolateral tubercles on the adult shell ranges from 5 to 23 (22 in the holotype). At midshaft, four to six ribs join a ventrolateral tubercle dorsally and five to seven ribs branch from it ventrally. Four to six ribs occur between ventrolateral tubercles, depending on the distance

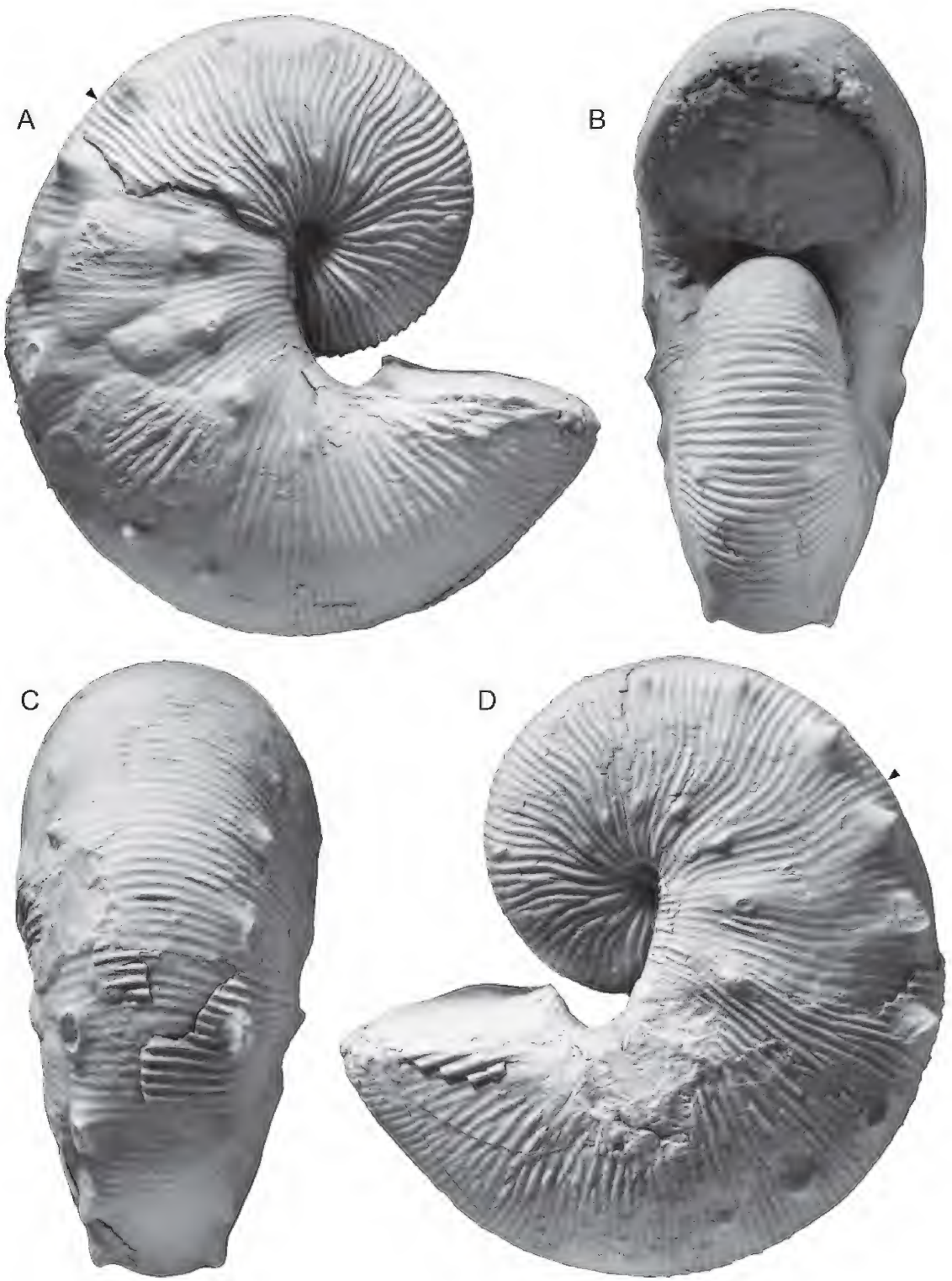
A
B
C
D

between tubercles and the density of ribbing.

The suture is deeply incised (fig. 100). E/L is broad and asymmetrically bifid, and L is asymmetrically to symmetrically bifid.

MICROCONCH DESCRIPTION: Like macroconchs, microconchs show a range in adult size, degree of robustness, and coarseness of ornament (table 9). USNM 536241 (fig. 104D–F) represents an example of a large, robust, coarsely ornamented specimen whereas USNM 536250 (fig. 109M–P) represents an example of a small, slender, finely ornamented specimen. Of the previously designated holotypes and paratypes of *Hoploscaphites landesi*, all are microconchs of *H. brevis*.

LMAX averages 53.0 mm and ranges from 26.7 to 81.2 mm. The size distribution is bimodal, with peaks at 40–45 mm ("small" microconchs) and 65–70 mm ("large" microconchs). This broad size includes the holotype of *Hoploscaphites landesi* (GSC 5342a) and the paratype of *Scaphites nodosus* var. *quadrangularis* (USNM 386690). The ratio of the size of the largest microconch to that of the smallest is 3.04. The average size of microconchs is 74% that of macroconchs. A comparison of the size distribution, rather than just the means, yields similar results. The microconch peak at 40–45 mm potentially corresponds to the macroconch peak at 60–65 mm (size of microconchs = 68% that of macroconchs), and the microconch peak at 65–70 mm potentially corresponds to the macroconch peak at 80–85 mm (size of microconchs = 82% that of macroconchs). However, these results are very dependent on the size and distribution of the sample. A comparison of specimens in the same concretion provides a better estimate of the relative size of dimorphs. YPM 35581 and 35582, a macroconch and microconch, respectively, occur side by side in the same concretion (fig. 88A); the size of the microconch is 87% that of the macroconch. In Concretion S from AMNH loc. 3274, the average size of two microconchs is 81% that of two macroconchs. As an average, therefore, the size of microconchs is approximately 85% that of macroconchs (or inversely, the size of macroconchs is approximately 120% that of microconchs).

Shells range from circular to ellipsoidal in lateral view, clustering more heavily on the ellipsoidal end of the spectrum. The circular end-member is represented by BHI 4253 (fig. 107E–H) and the ellipsoidal end-member is represented by AMNH 55884 (fig. 103A–C). The exposed phragmocone occupies one-half to two-thirds of a whorl. In general, the base of the body chamber occurs below the line of maximum length. The umbilicus of the phragmocone is relatively small. UD_P and UD_L average 3.7 and 3.3 mm, respectively. The ratio of UD_P to LMAX averages 0.07. The body chamber consists of a relatively long shaft and recurved hook, leaving a small gap between the exposed phragmocone and hook. The ratio of $LMAX/H_2$ averages 3.10, which is greater than that in macroconchs (2.93), implying that microconchs are relatively more uncoiled than macroconchs. The apertural lip is flexuous, with a short dorsal projection.

The umbilical seam of the shaft in lateral view varies from concave to nearly straight. In most specimens, such as AMNH 56768 (fig. 102D–F) and BHI 4725 (fig. 106D–L), the curvature of the seam closely follows that of the venter, epitomizing the morphology of microconchs. In many small specimens, however, such as AMNH 55874 (fig. 108I–L), BHI 4239 (fig. 108A–D), and 4240 (fig. 108M–P), the umbilical seam of the shaft is more gently curved in lateral view, approaching the morphology of macro-

←

Fig. 91. *Hoploscaphites brevis* (Meek, 1876), large macroconch, BHI 7034, *Baculites cuneatus* Zone, Pierre Shale, Pennington County, South Dakota. **A.** Right lateral; **B.** apertural; **C.** ventral; **D.** left lateral. This specimen is inflated and, in this respect, closely resembles the macroconch illustrated in Frech (1915: 560, fig. 7). It also shows some bubblelike areas on the flanks of the shaft on the right side, which may be due to parasitism. Specimen is illustrated natural size.

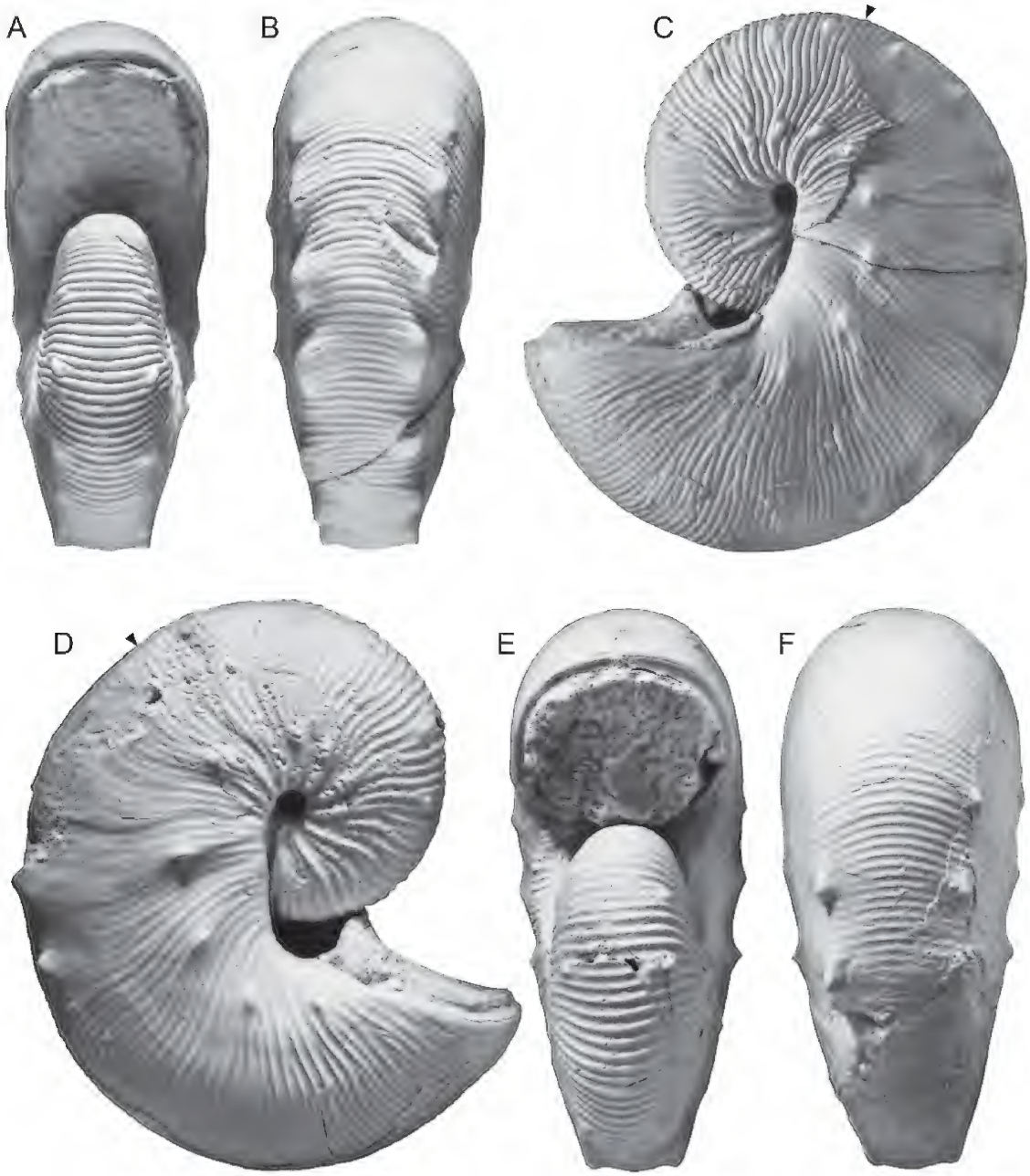

Fig. 92. *Hoploscaphites brevis* (Meek, 1876), large macroconchs, *Baculites compressus* Zone, Pierre Shale, Meade County, South Dakota. **A–C.** BHI 4204, more elongate than holotype. **A.** Apertural; **B.** ventral; **C.** left lateral. **D–F.** BHI 4205, more elongate than holotype. **D.** Right lateral; **E.** apertural; **F.** ventral. Specimens are illustrated natural size.

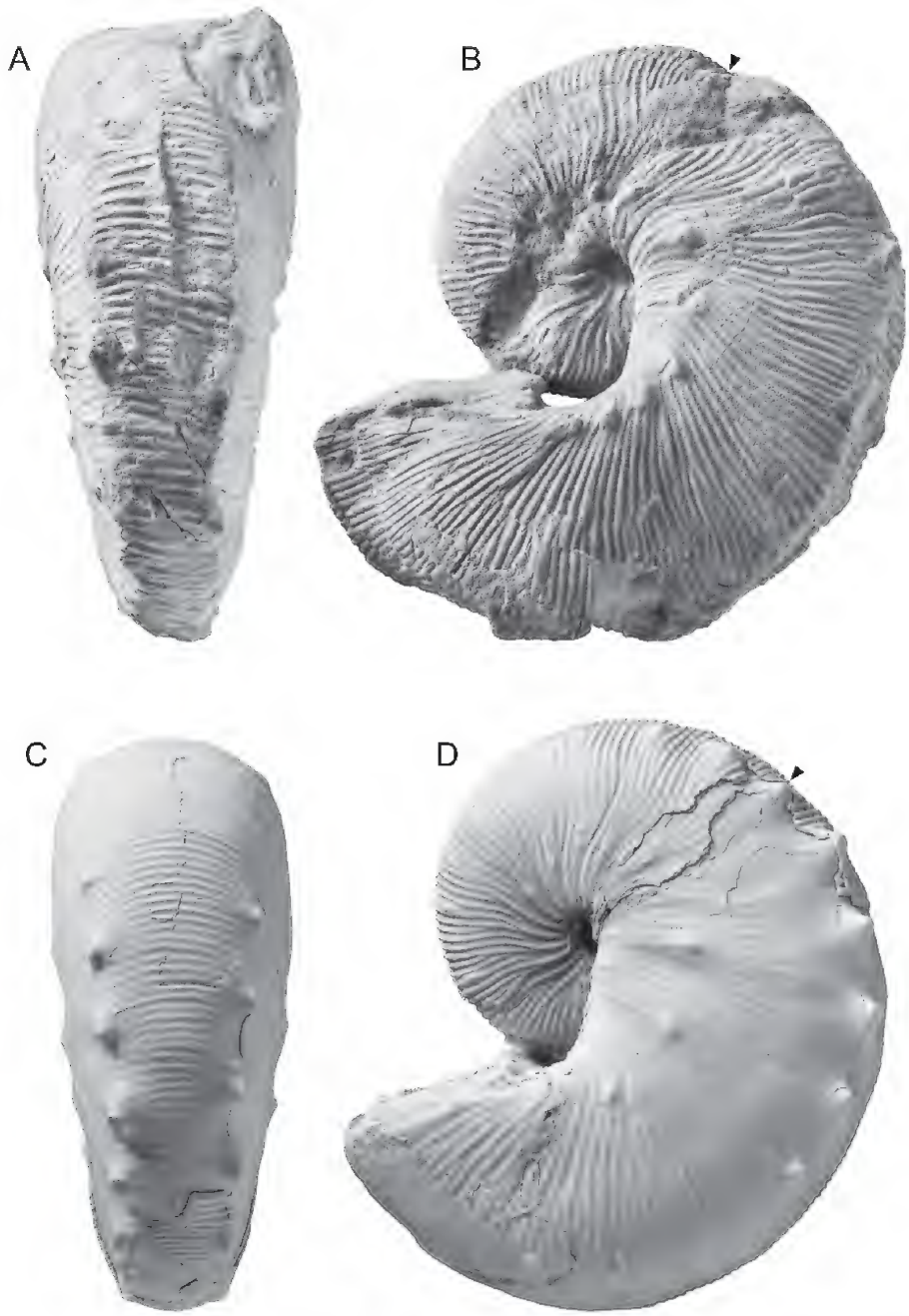

Fig. 93. *Hoploscaphites brevis* (Meek, 1876), large macroconchs. **A, B.** AMNH 63442, slightly distorted, Pierre Shale, near Kremmling, Grand County, Colorado. The position of the base of the body chamber is estimated. **A.** Ventral; **B.** left lateral. **C, D.** BHI 4910a, very similar to holotype, *Baculites compressus–B. cuneatus* zones, Pierre Shale, Pennington County, South Dakota. **C.** Ventral; **D.** left lateral. Specimens are illustrated natural size.

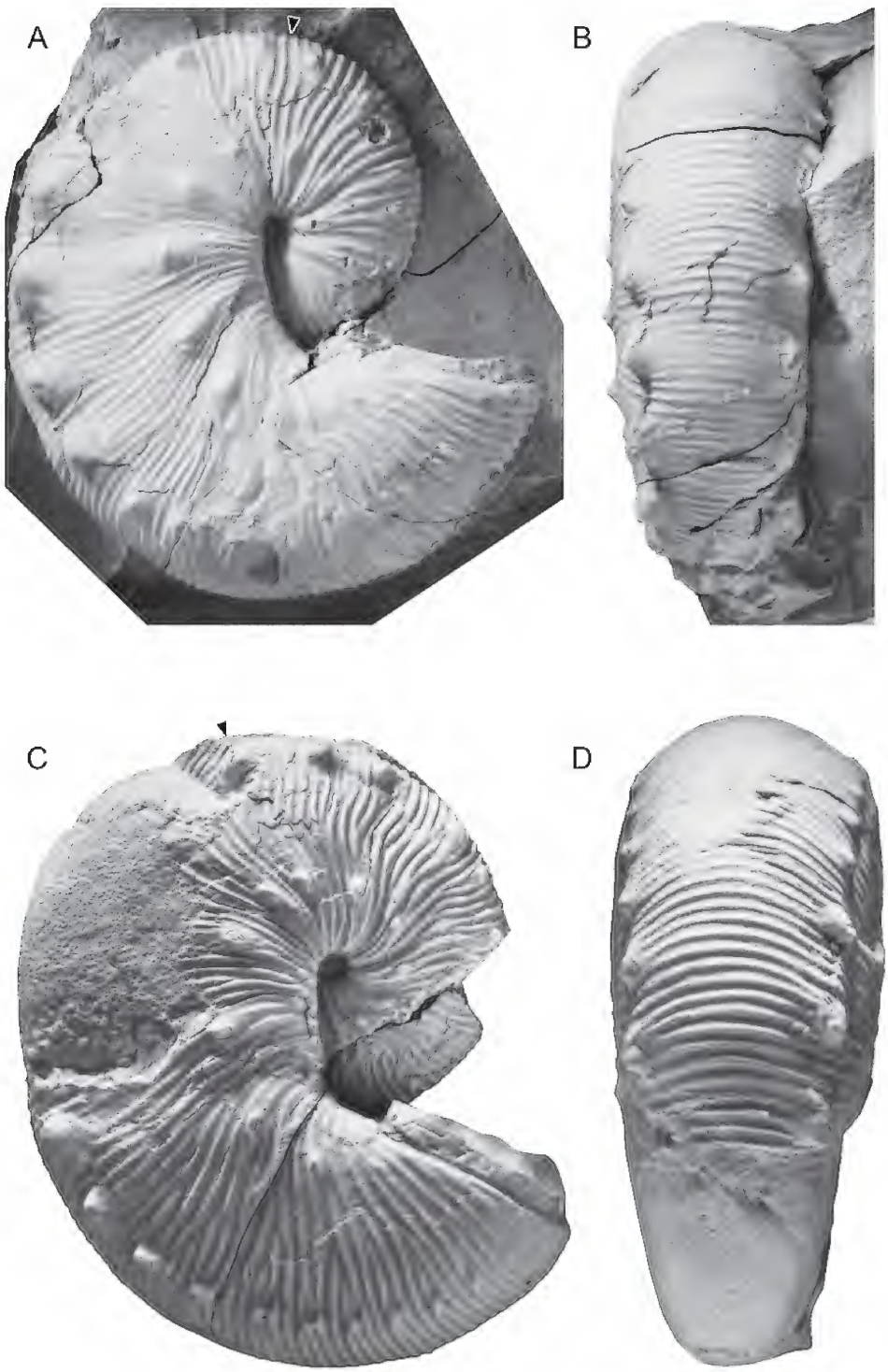

Fig. 94. *Hoploscaphites brevis* (Meek, 1876), large macroconchs. **A, B.** BHI 4789, *Baculites compressus–B. cuneatus* zones, Pierre Shale, Pennington County, South Dakota. **A.** Right lateral; **B.** ventral. **C, D.** USNM 536221, USGS Mesozoic loc. 22182, *Baculites compressus–B. reesidei* zones, Bearpaw Shale, Fergus County, Montana. **C.** Right lateral; **D.** ventral. A piece of shell is missing from the adapical part of the body chamber. Specimens are illustrated natural size.

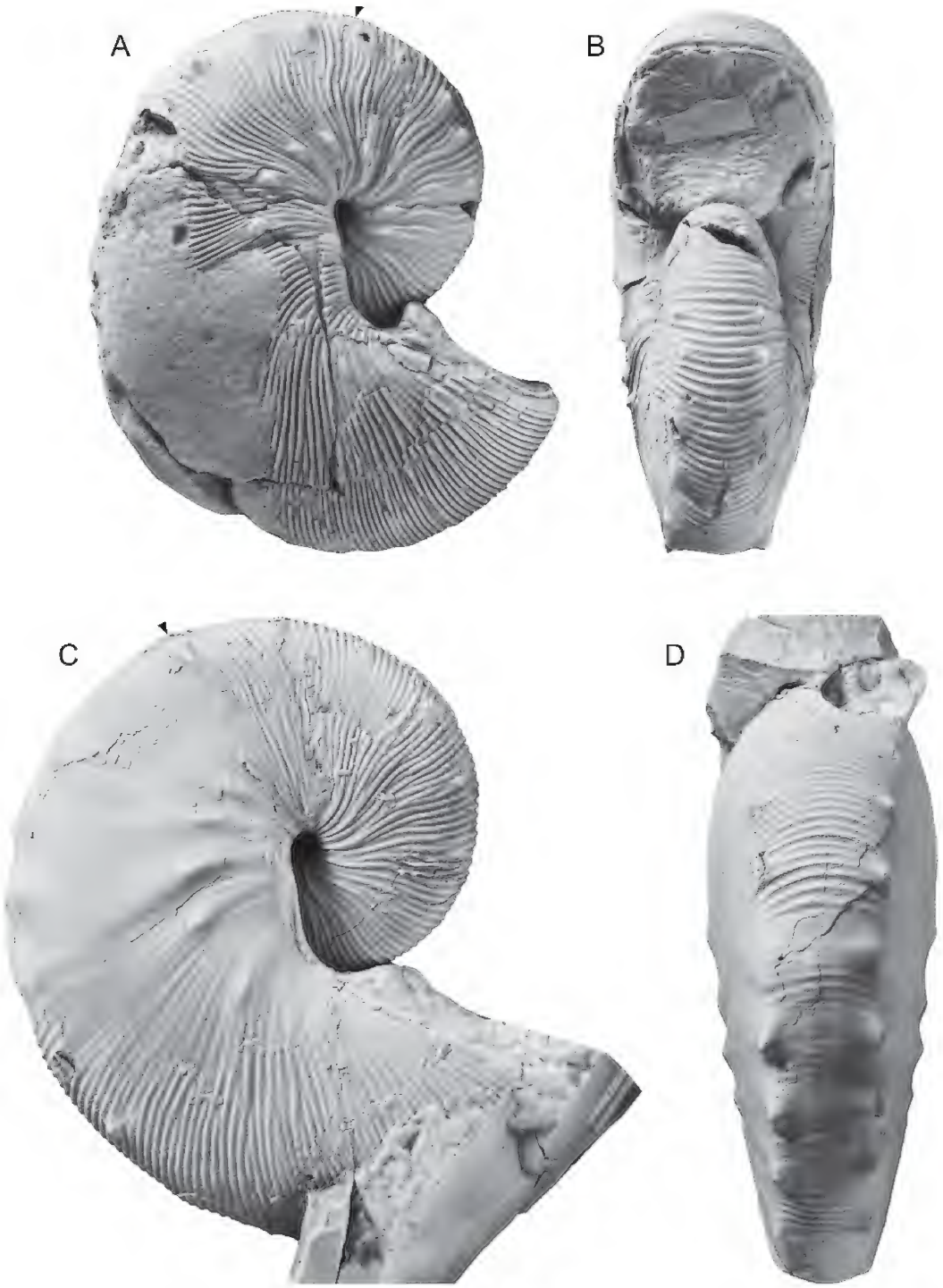

Fig. 95. *Hoploscaphites brevis* (Meek, 1876), large macroconchs. **A, B.** AMNH 46642, AMNH loc. 3207, Pierre Shale, *Baculites compressus–B. cuneatus* zones, Pierre Shale, Pennington County, South Dakota. **A.** Right lateral; **B.** apertural. **C, D.** BHI 4911a, *Baculites compressus–B. cuneatus* zones, Pierre Shale, Pennington County, South Dakota. **C.** Right lateral; **D.** ventral. Specimens are illustrated natural size.

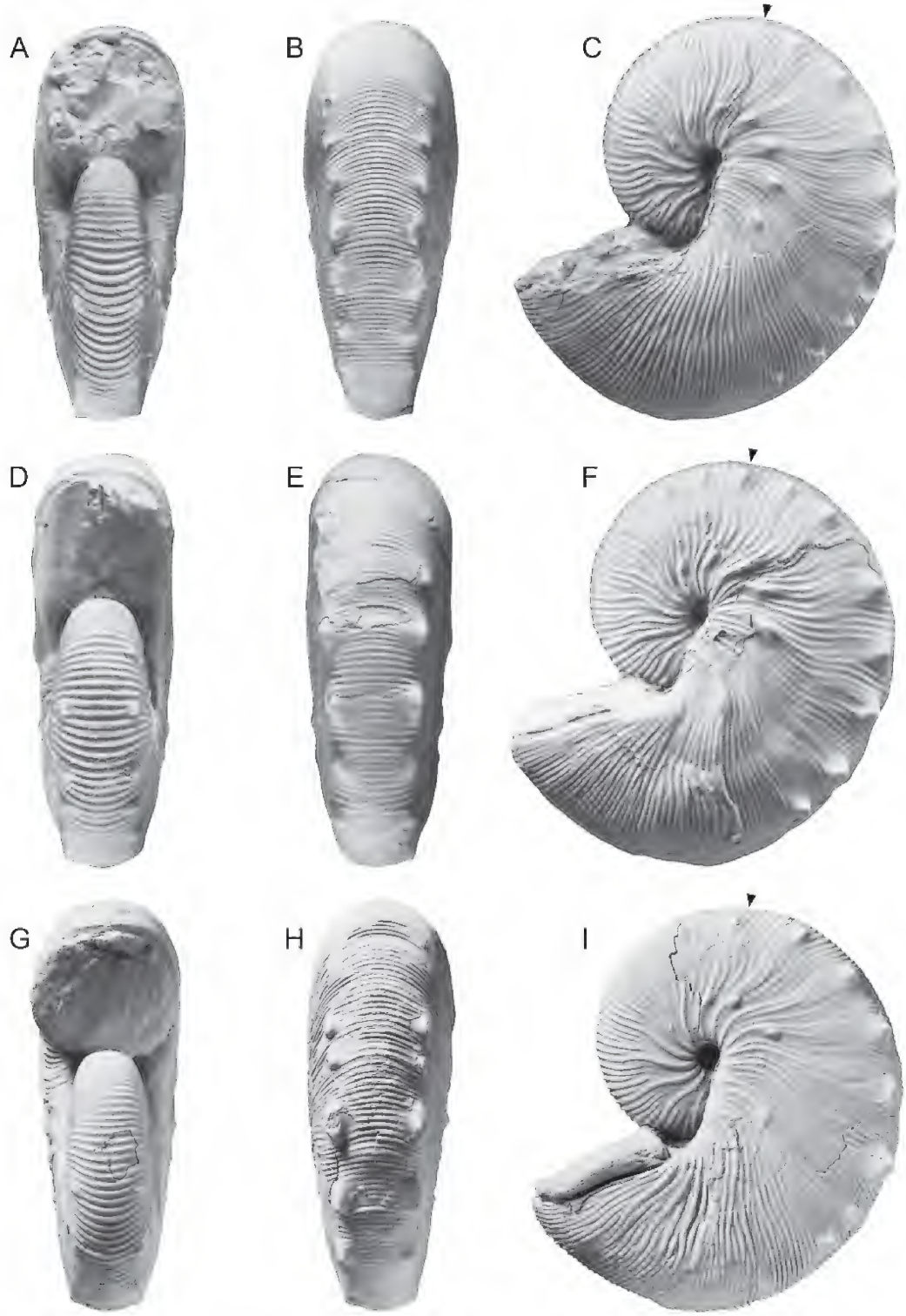

Fig. 96. *Hoploscaphites brevis* (Meek, 1876), small macroconchs. **A–C.** BHI 4274, *Baculites cuneatus* Zone, Pierre Shale, Meade County, South Dakota. **A.** Apertural; **B.** ventral; **C.** left lateral. **D–F.** BHI 4292,

conchs (listed as transitional specimens in table 9). However, other morphologic features, for example, the size of the umbilicus and the whorl height at midshaft, suggest that these specimens are microconchs instead. In a few instances, the specimens appear as macroconchs on the right side and microconchs on the left side (fig. 108A–D).

The intercostal whorl section of the phragmocone is compressed subquadrate. W_1/H_1 averages 0.79 (0.82 in macroconchs) and W_3/H_3 averages 0.73 (0.76 in macroconchs). The umbilical wall is steep and subvertical and the umbilical shoulder is sharply rounded. The inner flanks are broadly rounded and the outer flanks are nearly flat and converge toward the venter. Maximum width occurs at one-third whorl height. The ventrolateral margin is sharply rounded and the venter is broadly rounded to flat.

Whorl width gradually increases and usually attains its maximum value just adapical of the point of recurvature, after which it remains the same. Whorl height gradually increases and attains its maximum value at midshaft, after which it decreases slightly to the point of recurvature, then increases slightly again to the aperture. The increase in whorl height from the phragmocone to the shaft is much more gradual than it is in macroconchs. However, in some specimens, such as BHI 4240 (fig. 108I–L), the increase in whorl height is more abrupt, so that the morphology approaches that of macroconchs (such specimens are listed as transitional in table 9).

The whorl section at midshaft shows the same degree of compression as at the base of the body chamber (W_4/H_4 averages 0.73). The intercostal whorl section is subquadrate to weakly reniform with maximum width at one-quarter to one-third whorl height, corresponding to the site of the umbilicolateral tubercles. The umbilical wall is steep and the umbilical shoulder slopes gently outward. The inner flanks are broadly rounded and the outer flanks are nearly flat and converge toward the venter. The ventrolateral shoulder is sharply rounded and the venter is very broadly rounded to nearly flat.

As in macroconchs, the whorl section becomes slightly less compressed from midshaft to the point of recurvature, after which it remains nearly the same (fig. 83). The ratios of whorl width to height at the point of recurvature (W_6/H_6) and at the aperture (W_7/H_7) both average 0.94. The intercostal whorl section at the point of recurvature is slightly more ovoid than at midshaft. The umbilical wall is nearly flat and the umbilical shoulder is sharply rounded. The flanks are broadly rounded to flat, with maximum width at one-third whorl height. The ventrolateral shoulder is less sharply rounded and the venter is more broadly rounded than at midshaft due to the disappearance of the ventrolateral tubercles.

The ornament in microconchs is similar to that in macroconchs (table 10). Specimens are covered with relatively fine, flexuous ribs, and rows of umbilicolateral and ventrolateral tubercles. However, in many small specimens, tubercles are present only on the shaft of the body chamber.

At the point of exposure, ribs are rursiradiate on the umbilical wall and shoulder. Ribs swing slightly backward on the inner flanks, slightly forward on the midflanks, and then slightly backward again on the outer flanks, crossing the venter with a slight forward projection. Branching and intercalation occur at one-half to two-thirds whorl height, leaving the inner flanks more sparsely ribbed than the outer flanks. In larger specimens, this pattern changes toward the adoral end of the phragmocone, as additional secondary ribs originate at the site of the

---

←

Baculites compressus–B. cuneatus zones, Pierre Shale, Meade County, South Dakota. **D.** Apertural; **E.** ventral; **F.** left lateral. **G–I.** AMNH 56865, AMNH loc. 3408, *Baculites compressus* Zone, Pierre Shale, Meade County, South Dakota. **G.** Apertural; **H.** ventral; **I.** left lateral. Specimens are illustrated natural size.

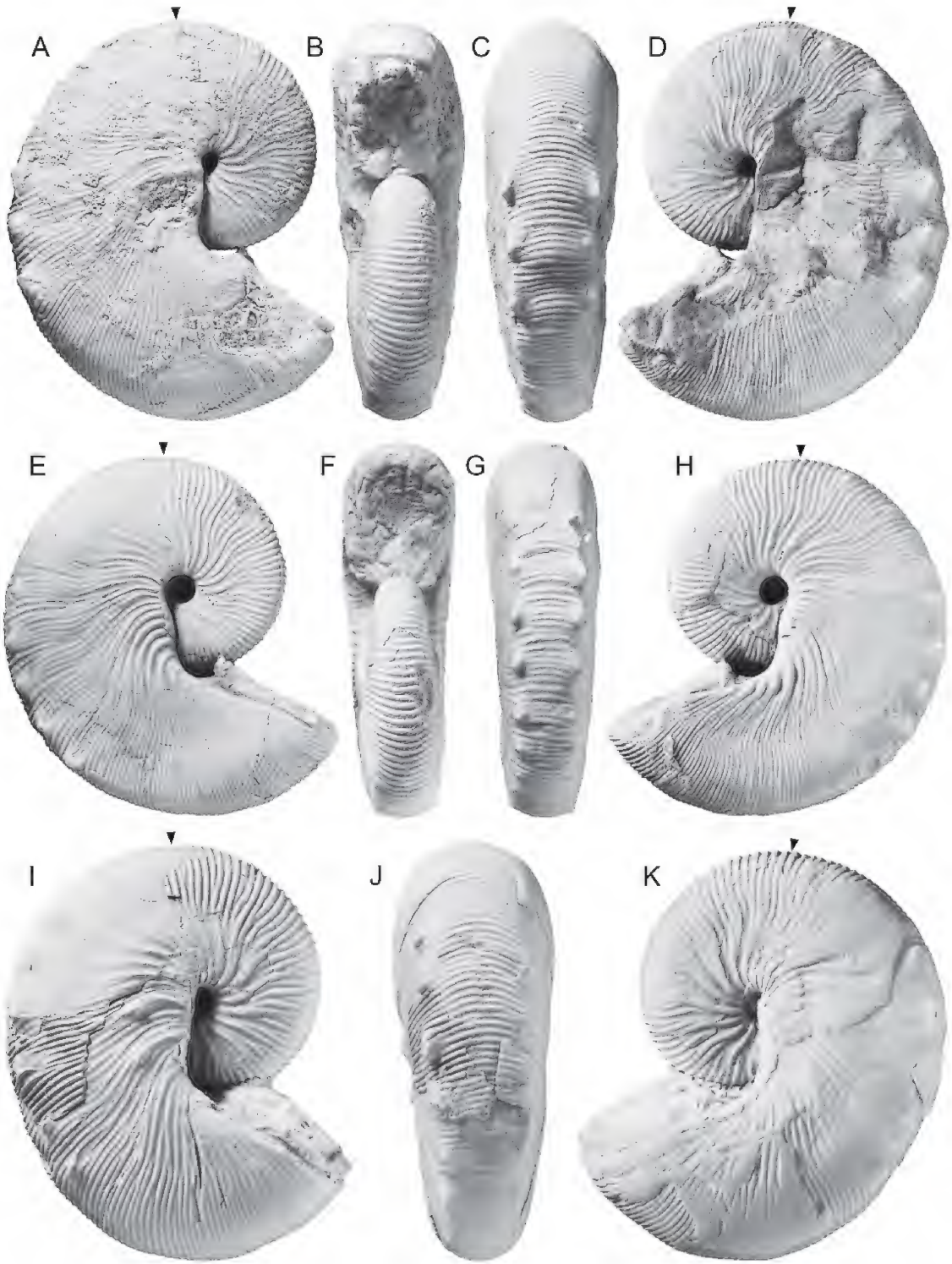

Fig. 97. *Hoploscaphites brevis* (Meek, 1876), small macroconchs. **A–D.** BHI 4796, *Baculites compressus–B. cuneatus* zones, Pierre Shale, Meade County, South Dakota. **A.** Right lateral; **B.** apertural;

umbilicolateral tubercles. The ratio of secondary to primary ribs on the adoral end of the phragmocone ranges from 4–7:1.

The rib density on the phragmocone shows a broad range among specimens, and correlates with adult size. It ranges from 7 to 13 ribs/cm on the venter on both the adapical and adoral portions of the phragmocone. The density of ribbing decreases slightly, remains the same, or increases slightly toward the base of the body chamber (table 10). For example, in GSC 5342b (fig. 7I–L), the rib density decreases from 10 to 9 ribs/cm, in GSC 5342c (fig. 7M–Q), it remains the same (11ribs/cm), and in GSC 5342a (fig. 7E–H), it increases from 8 to 9 ribs/cm.

Ribs are narrow, prorsiradiate, and flexuous on the body chamber. They are rursiradiate on the umbilical wall and shoulder of the shaft, becoming more rectiradiate toward the point of recurvature. Ribs bend backward on the inner flanks, forward on the midflanks, back again on the outer flanks, and weakly forward again at the ventrolateral margin. They cross the venter with a weak adoral projection, which strengthens on the hook. Branching and intercalation occur at one-third whorl height (at the site of the umbilicolateral tubercles, if they are present), and at two-thirds whorl height. As in macroconchs, ribs become less flexuous toward the adoral end of the shaft. Due to the reduced whorl height on the hook, branching and intercalation occur on the midflanks, so that the outer flanks are much more densely ribbed than the inner flanks. This pattern is accentuated due to the disappearance of the ventrolateral tubercles at the point of recurvature.

In general, ribs become more closely spaced in passing from the phragmocone to the shaft of the body chamber. This increase in density usually occurs on the adapical end of the shaft. There are 8–18 ribs/cm on the venter at midshaft, reflecting an increase of as many as 7 ribs/cm from the adoral end of the phragmocone to midshaft. The rib density remains the same or changes slightly from the midshaft to the hook, with 8–18 ribs/cm on the hook. We illustrate two examples of the ontogenetic change in rib density. In USNM 536251 (fig. 106E–H), the rib density changes from 10 ribs/cm on the adoral end of the phragmocone to 14 ribs/cm on the midshaft to 12 ribs/cm on the hook. In USNM 12291 (fig. 7A–D), the rib density changes from 10 ribs/cm on the adoral end of the phragmocone to 11 ribs/cm on the midshaft to 10 ribs/cm on the hook. The ratio of secondary to primary ribs on the body chamber ranges from 4–8:1, with no ontogenetic change from the midshaft to the hook.

Umbilicolateral tubercles are absent on the phragmocone in small specimens and, instead, the ribs in this area are strong and adorally concave. Umbilicolateral tubercles are usually present on the phragmocone in larger specimens and appear at the point of exposure or, more commonly, on the adoral one-half to one-third of the phragmocone. They occur at one-third whorl height and are more or less evenly spaced. The maximum distance between consecutive tubercles ranges from 2 to 7 mm. The umbilicolateral tubercles are small, less than 1.0 mm in height, and are sometimes difficult to distinguish from raised ribs. They are elongated radially, becoming more conical toward the adoral end of the phragmocone, as shown in BHI 4246 (fig. 106M–P). The maximum number of umbilicolateral tubercles on the exposed phragmocone is 8 (6 in USNM 12291). One rib joins a tubercle dorsally, and two ribs branch from it ventrally. One or two ribs intercalate between tubercles.

Umbilicolateral tubercles are present on the body chamber in all of the specimens in our sample. They occur at one-quarter whorl height on the shaft, but migrate closer to the

---

←

C. ventral; **D.** left lateral. **E–H.** BHI 4230, *Baculites compressus* Zone, Pierre Shale, Meade County, South Dakota. **E.** Right lateral; **F.** apertural; **G.** ventral; **H.** left lateral. **I–K.** BHI 4234, *Baculites compressus–B. cuneatus* zones, Pierre Shale, Meade County, South Dakota. **I.** Right lateral; **J.** ventral; **K.** left lateral. Specimens are illustrated natural size.

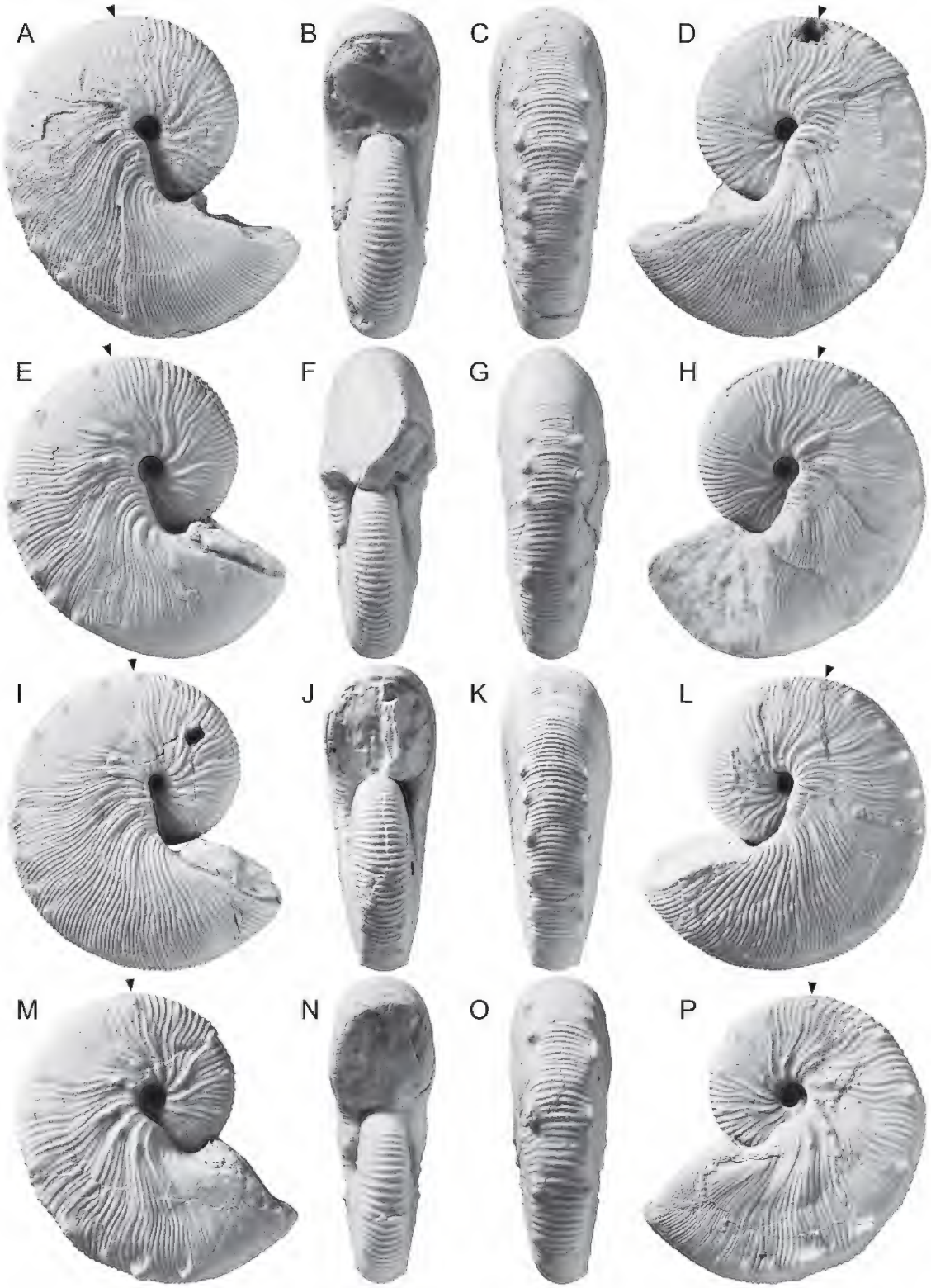
A
B
C
D
E
F
G
H
I
J
K
L
M
N
O
P

umbilical shoulder on the hook. The maximum distance between consecutive umbilicolateral tubercles at midshaft ranges from 3.5 to 10 mm. In general, the umbilicolateral tubercles are more or less evenly spaced, with some approximation near the aperture. In USNM 386690 (fig. 6D–G), starting at the adapical end of the body chamber, the distance between consecutive tubercles, as measured in an adoral direction, is 3, 4, 4, 5, 5, and 3 mm. In GSC 5342a (fig. 7E–H), starting at the adapical end of the body chamber, the distance between consecutive tubercles, as measured in an adoral direction, is 3, 3, 3.5, 4.5, and 5 mm. In general, at midshaft, one or two ribs join an umbilicolateral tubercle dorsally and two to four ribs branch from it ventrally. One to five ribs intercalate between umbilicolateral tubercles, depending on rib density and tubercle spacing.

The umbilicolateral tubercles on the body chamber are small, less than 1.5 mm in height. They are usually bullate in shape, but in larger specimens, they are more conical. One interesting anomaly is BHI 4725 (fig. 106I–L) in which the tubercles on the right side of the shaft are each subdivided into two peaks connected by a short ridge. Tubercles attain their maximum size at midshaft or just adapical of the point of recurvature. For example, in BHI 4252, the tubercles increase in size adorally, culminating in the largest umbilicolateral tubercle just adapical of the point of recurvature. Similarly, in GSC 5342c (fig. 7M–Q), with only three umbilicolateral tubercles, the largest tubercle occurs near the point of recurvature. The number of umbilicolateral tubercles on the body chamber ranges from 3 to 8, so that the total number of umbilicolateral tubercles on the adult shell ranges from 2 to 13.

Ventrolateral tubercles occur on the exposed phragmocone in 70% of the specimens in our sample. The maximum number of tubercles on the exposed phragmocone is 10, with rare exceptions, such as BHI 4315, with 14 tubercles. In general, the tubercles appear near the point of exposure to midway on the phragmocone. The maximum distance between consecutive tubercles ranges from 5 to 12 mm. In some specimens, the tubercles are evenly distributed on the phragmocone. For example, in USNM 12291 (fig. 7A–D), the tubercles occur at nearly equal intervals of 7 mm, with a slight approximation toward the adoral end of the phragmocone. In other specimens, the distribution of tubercles is uneven. For example, in BHI 4283 (fig. 105A–C), starting at the point of exposure, the distance between consecutive tubercles, as measured in an adoral direction, is 7, 7, 7, 11, and 5.5 mm. In AMNH 55884 (fig. 105A–C), starting one-third of the way onto the phragmocone, the distance between consecutive tubercles on the right side of the specimen, as measured in an adoral direction, is 9, 9, 11, 11, 7, and 7 mm. The ventrolateral tubercles on the phragmocone are conical and attain a maximum height of 1.5 mm. Commonly, one or two ribs join a ventrolateral tubercle dorsally and two or three ribs branch from it ventrally.

The ventrolateral tubercles occur on the shaft but do not continue onto the hook. The maximum distance between consecutive tubercles at midshaft ranges from 3.5 to 12 mm. In most specimens, the ventrolateral tubercles are uniformly spaced on the shaft. For example, in GSC 5342a (fig. 7E–H), the tubercles are equally spaced at intervals of approximately 5 mm, starting at the adapical end of the shaft. In other specimens, however, the tubercles are irregularly distributed.

←

Fig. 98. *Hoploscaphites brevis* (Meek, 1876), small macroconchs. **A–D.** YPM 35584, YPM loc. A6520, Pierre Shale, Sage Creek, Pennington County, South Dakota. **A.** Right lateral; **B.** apertural; **C.** ventral; **D.** left lateral. **E–H.** BHI 4247, *Baculites compressus–B. cuneatus* zones, Pierre Shale, Meade County, South Dakota. **E.** Right lateral; **F.** apertural; **G.** ventral; **H.** left lateral. **I–L.** BHI 4235, *Baculites compressus* Zone, Pierre Shale, Meade County, South Dakota. **I.** Right lateral; **J.** apertural; **K.** ventral; **L.** left lateral. **M–P.** AMNH 56864, AMNH loc. 3408, *Baculites compressus* Zone, Pierre Shale, Meade County, South Dakota. **M.** Right lateral; **N.** apertural; **O.** ventral; **P.** left lateral. Specimens are illustrated natural size.

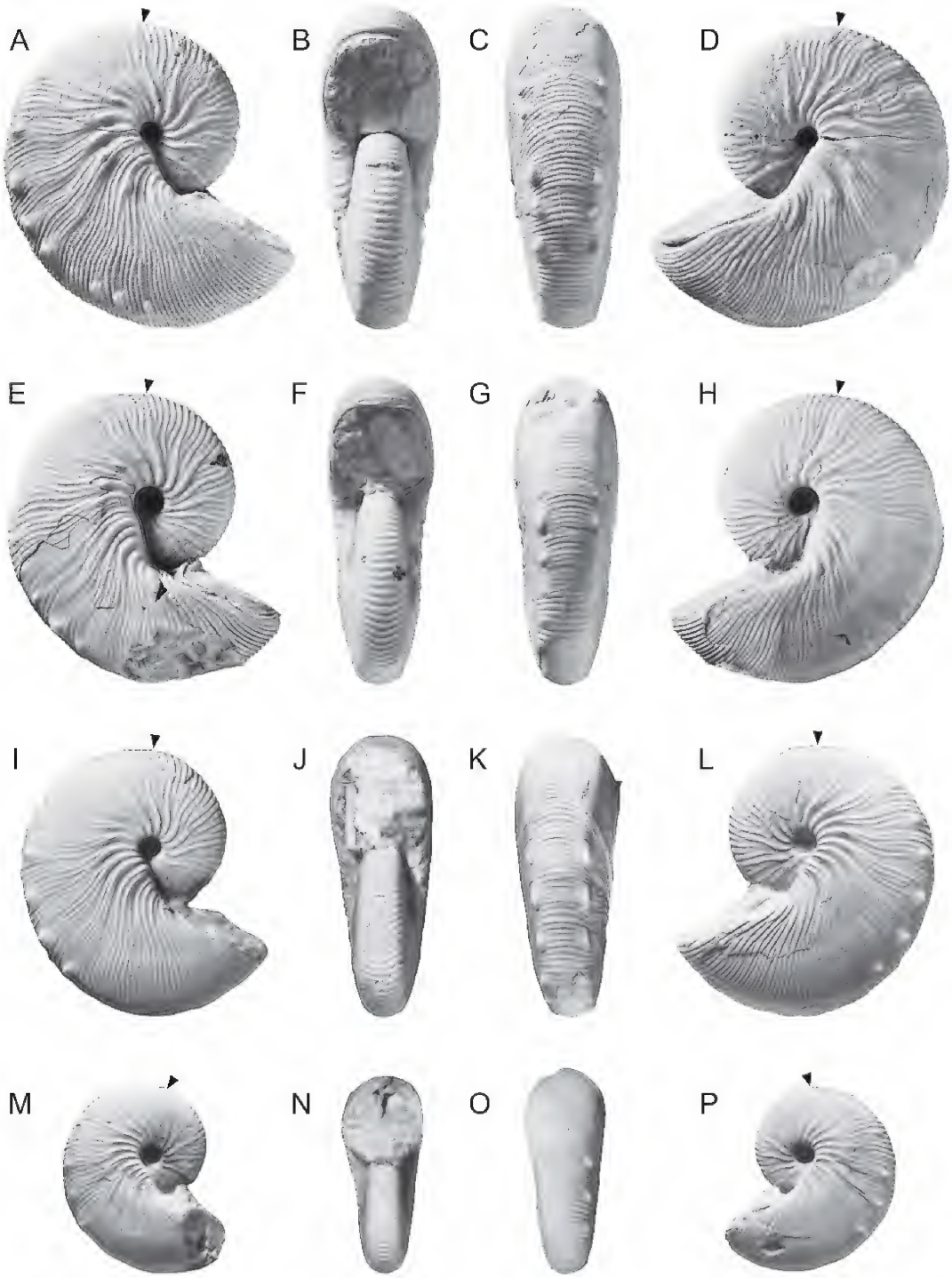

Fig. 99. *Hoploscaphites brevis* (Meek, 1876), small macroconchs. **A–D.** YPM 35585, YPM loc. A6520, Pierre Shale, Sage Creek, Pennington County, South Dakota. **A.** Right lateral; **B.** apertural; **C.** ventral; **D.** left lateral. **E–H.** BHI 4250, *Baculites compressus–B. cuneatus* zones, Pierre Shale, Meade County, South Dakota. **E.** Right lateral; **F.** apertural; **G.** ventral; **H.** left lateral. **I–L.** BHI 4311, *Baculites compressus–B.*

For example, in BHI 4313, the six tubercles on the shaft form three pairs, the distance between tubercles in adjacent pairs equalling 5 mm, and the distance between tubercles in the same pair, 2–3 mm. The one or two most adoral tubercles are commonly more widely spaced than the others. For example, in BHI 4123 (fig. 103D–F), the distance between consecutive tubercles on the left side of the shell, as measured in an adoral direction, starting at the adapical end of the shaft, is 13, 10.5, 14.5, and 22 mm. Similarly, in BHI 4277, the distance between consecutive tubercles on the right side of the shell, as measured in an adoral direction, starting at midshaft, is 3.5, 3, 5, and 7 mm.

The ventrolateral tubercles on the midshaft commonly exhibit an asymmetrical profile in cross section, with a flattened, steep adapical face and a more gently sloping adoral face. The maximum height of a ventrolateral tubercle at midshaft ranges from 0.50–2.75 mm. Two to five ribs join a ventrolateral tubercle dorsally and four to six ribs branch from it ventrally. Three to six ribs intercalate between ventrolateral tubercles, depending on rib density and tubercle spacing. Ventrolateral tubercles are paired or offset from one side of the venter to the other. When they are paired, they commonly form broad elevations across the venter, as in USNM 12291 (fig. 7A–D). The number of ventrolateral tubercles on the body chamber ranges from 5 to 11, so that the total number of ventrolateral tubercles on the adult shell ranges from 5 to 17.

The suture of microconchs is similar to that of macroconchs (fig. 100).

ONTOGENY: The ontogenetic change in whorl shape in this species is illustrated in three dorsoventral sections, with accompanying graphs (figs. 110–114). At a shell diameter of approximately 3 mm, the whorl section is reniform with a ratio of whorl width to whorl height of approximately 1.3, and a ratio of umbilical diameter to shell diameter of approximately 0.35. The umbilical wall is nearly flat and slanted outward, the umbilical shoulder is sharply rounded, the flanks are broadly rounded, the ventrolateral shoulder is sharply rounded, and the venter is very broadly rounded. The ratio of whorl width to whorl height decreases through most of ontogeny until the beginning of the mature phragmocone, after which it usually increases. The ratio ranges from 0.75 to 0.90 at a shell diameter of 10–25 mm. The whorl section at this stage is subquadrate with a steep umbilical wall, a sharply rounded umbilical shoulder, broadly rounded to flat flanks, a sharply rounded ventrolateral shoulder, and a broadly rounded venter. The ratio of umbilical diameter to shell diameter decreases through most of ontogeny until a shell diameter of approximately 10 mm, after which it remains nearly the same until the formation of the mature body chamber.

The ontogenetic development of the ornamentation is illustrated in a macroconch (fig. 115). The early whorls are smooth, but at a shell diameter of approximately 3 mm, small swellings appear on the flanks, which later develop into adorally convex, prorsiradiate ribs. At a shell diameter of approximately 4 mm, ribs appear on the venter and cross it with a weak adoral projection. Additional ribs arise by intercalation at the ventrolateral shoulder, so that the ratio of ventral to primary ribs is 3:1 at a shell diameter of approximately 9 mm. Over the next 0.75 whorl, terminating at a shell diameter of approximately 20 mm (0.25 whorl adapical of the point of exposure), the ribs become increasingly more flexuous. They swing slightly backward on the umbilical wall and shoulder, slightly forward on the inner two-thirds of the flanks, and slightly backward on the outer one-third of the flanks. They cross the venter with a broad

←

cuneatus zones, Pierre Shale, Meade County, South Dakota. **I.** Right lateral; **J.** apertural; **K.** ventral; **L.** left lateral. **M–P.** BHI 4241, *Baculites compressus* Zone, Pierre Shale, Meade County, South Dakota. **M.** Right lateral; **N.** apertural; **O.** ventral; **P.** left lateral. Specimens are illustrated natural size.

TABLE 8
Ornament of the adult shells of *Hoploscaphites brevis* (Meek, 1876), macroconchs

		Rib Density (ribs/cm)							
		Phragmocone		Body Chamber		Number of Umbilicolateral Tubercles		Number of Ventrolateral Tubercles	
Specimen Number	Study Number	Adapical	Adoral	Midshaft	Hook	Phragmocone	Body Chamber	Phragmocone	Body Chamber
AMNH 58561	523	7	8	8	8	4/5	3	7+	8
BHI 4124	308	7	8	7	9	4	6	8	6
BHI 4202	313	7	8	9	9	2	4	9	7
BHI 4203	312	7	8	8	10	5	3	6	8
BHI 4204	316	7	8	8	8	4	7	5	8
BHI 4205	321	6	8	8	7	5	4	4	3+
BHI 4230	485	9	9	11	14	0	1	1	9
BHI 4232	439	10	10	13	14	4	5	5	8
BHI 4234	338	7	8	11	10	0	2	0	8
BHI 4247	445	10	9	12	15	0	3	2	5/6[a]
BHI 4267	331	10	9	11	11	—	2?	2	6/7[a]
BHI 4274	311	7	7	12	10	5	6	3	9
BHI 4292	309	8	8	10	11	2	4	5	8
BHI 4311	330	10	10	12	14	0	1/2[a]	0	6
BHI 4324	453	7	7	10	9	5+	4	5+	4
BHI 4394	443	8	9	12	10	5	5	5	6
BHI 4796	521	10	9	11	12	0	1	3	8
BHI 4803	454	7	8	8	9	4	3	5	—
BHI 7034	441	6	6	6	7	5	4	7	6
USNM 367	Type	6	6	8–10	9	1	6	7	15
USNM 12289	—	7	7	—	—	7	—	13	—
USNM 536222	243	7	7	7	9	3	6	8	5+
USNM 536223	147	6	6	7	8	0	11	4	16
USNM 536225	130	6	6	7	7	4	5	5	7
USNM 536265	144	6	6	6	7	6	8	8	15
YPM 35584	447	9	9	12	13	0	3	0	8

For additional comments, see footnotes in table 7. *Estimate due to incomplete or poor preservation.
[a]The number is different on each side of the shell.

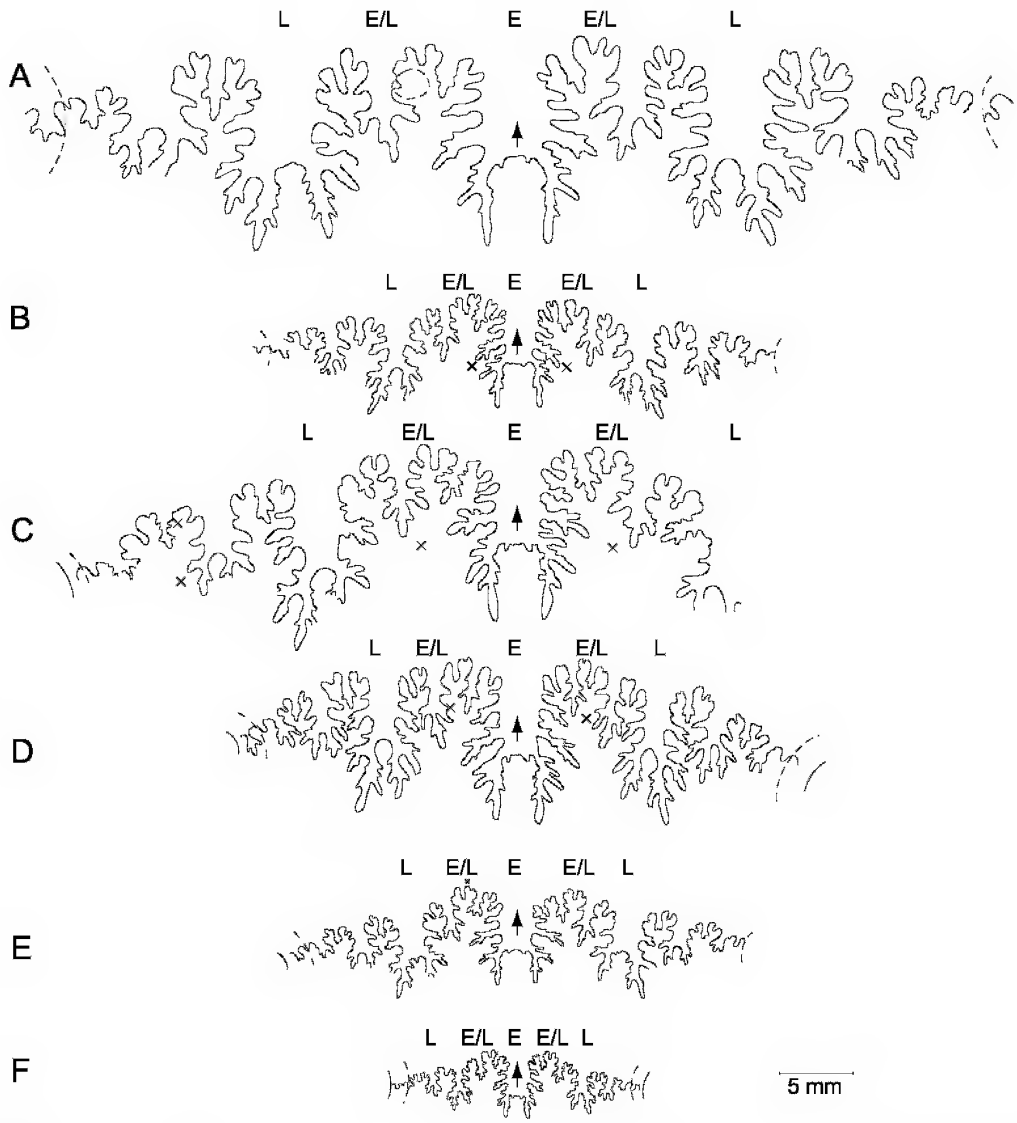

Fig. 100. Sutures of *Hoploscaphites brevis* (Meek, 1876). **A.** BHI 4202, macroconch, third to last suture, *Baculites compressus* Zone, Pierre Shale, Meade County, South Dakota. **B.** BHI 4235, macroconch, next to last suture, *Baculites compressus* Zone, Pierre Shale, Meade County, South Dakota. **C.** USNM 536225, microconch, last suture, WH = 27.2 mm, USGS Mesozoic loc. 7892, Bearpaw Shale, Musselshell County, Montana. **D.** BHI 4314, microconch, third from last suture, *Baculites compressus–B. cuneatus* zones, Pierre Shale, Meade County, South Dakota. **E.** BHI 4261, microconch, next to last suture, *Baculites compressus* Zone, Pierre Shale, Meade County, South Dakota. **F.** AMNH 56881, juvenile, last suture, WH = 6.2 mm, AMNH loc. 3274, *Baculites compressus–B. cuneatus* zones, Pierre Shale, Meade County, South Dakota. Abbreviations: x = tubercle; E = ventral lobe; E/L = first lateral saddle between ventral and lateral lobes; L = lateral lobe.

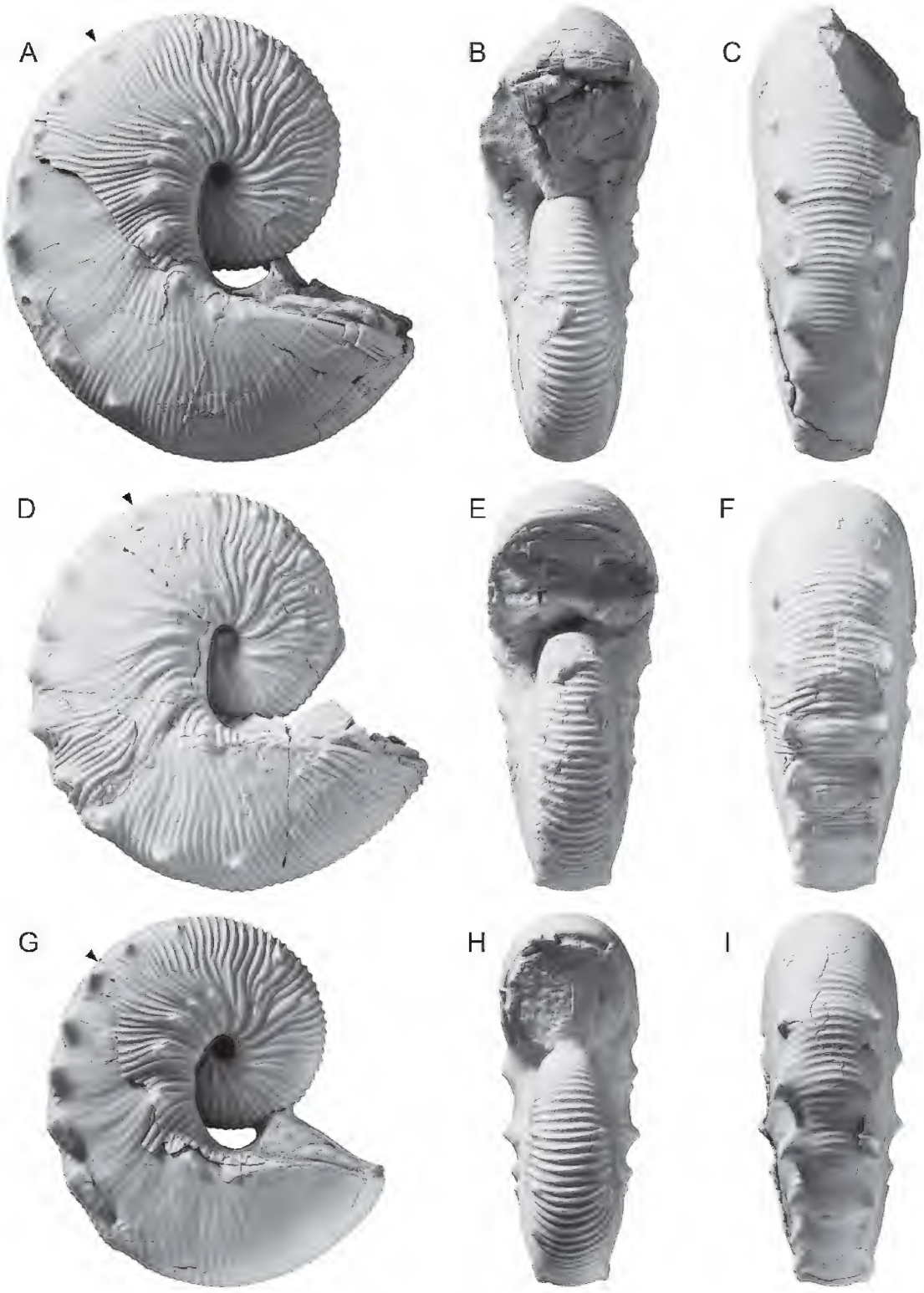
A
B
C
D
E
F
G
H
I

adoral projection. There are 9 ribs/cm on the venter. Branching and intercalation occur on the inner one-third and outer two-thirds of the flanks, so that the ratio of ventral to primary ribs is 4:1. Umbilicolateral and ventrolateral tubercles only appear on the exposed phragmocone.

Most specimens show septal approximation at maturity (fig. 116, table 1). The pattern between dimorphs is slightly different. We examined five macroconchs and eight microconchs involving the last three to seven chambers (one specimen with three chambers, five with four chambers, five with five chambers, one with six chambers, and one with seven chambers).

In macroconchs, septal approximation occurs over either the last two or three chambers. In BHI 4205, the shell is broken at the site of the last septum, so that the interseptal distance between the last two septa cannot be measured. However, the distance between septa 2 and 3 is less than that between septa 3 and 4, and we therefore assumed that the distance between septa 1 and 2 (the last two septa) is less than that between septa 2 and 3. The magnitude of septal approximation is strong and ranges from 33% to 38%. In contrast, in microconchs, septal approximation occurs over only the last one or two chambers or not at all (two specimens with septal approximation over two chambers, five with septal approximation over one chamber, and one with no septal approximation at all). The magnitude of septal approximation is weak. In seven of the eight specimens that show septal approximation, the magnitude of septal approximation ranges from 57 to 86%.

DISCUSSION: *Hoploscaphites brevis* has been frequently reported from the U.S. Western Interior. The holotype has been reprinted in many textbooks, for example, Grabau and Shimer (1910: 177, fig. 1428), Grabau (1921: 701, fig. 1698f, g), Shrock and Twenthofel (1953: text fig. 10.76, P1, P2), and Easton (1960: 453, fig. 11.27-3). It has also been reillustrated in Logan (1898, pl. 108, fig. 3), Kauffman (1977: pl. 32, fig. 9), and Riccardi (1983: pl. 5, figs. 1, 2; text fig. 24a). The specimen illustrated by Meek (1876: pl. 25, fig. 2) as *Scaphites nodosus* var. *quadrangularis* (USNM 386690) is a microconch of *H. brevis*, probably from South Dakota (fig. 6D–G) (reillustrated by Riccardi, 1983: pl. 10, figs. 3, 4). The two specimens figured by Whitfield (1880: 443, pl. 13, figs. 8–11) as *S. nodosus* var. *brevis* (USNM 12289) (fig. 86A–D) and *S. nodosus* var. *quadrangularis* (USNM 12291) (fig. 7A–D) are a macroconch and a microconch of *H. brevis*, respectively. Frech (1915: 560, fig. 7) illustrated a specimen that he called *S. binodosus* F.A. Roemer var. *brevis* Meek from "Bad lands, Dakota." It is a macroconch of *H. brevis* and is remarkably similar to BHI 7034 (fig. 91). The adoral part of the shaft and hook are inflated in both specimens, but the ventrolateral tubercles on Frech's specimen persist to the aperture, whereas they die out at the point of recurvature on BHI 7034. Elias (1933: pl. 37, fig. 2) figured a specimen as *Acanthoscaphites nodosus* var. *brevis* from Wallace County, Kansas (KUMIP 59653) (fig. 80A). It consists of part of the phragmocone and impression of the body chamber and is probably a microconch of *H. brevis*. Elias (1933: pl. 37, fig. 3) also figured a fragment of the shaft of a body chamber, which he called *A. nodosus* var. *quadrangularis* Meek (KUMIP 59655) (fig. 79I). It is probably a microconch of *H. brevis*, although it cannot be identified with certainty.

Most of the other specimens assigned to *Scaphites nodosus* var. *brevis* and *S. nodosus*

←

Fig. 101. *Hoploscaphites brevis* (Meek, 1876), large microconchs. **A–C.** YPM 1861, YPM loc. A6520, Pierre Shale, Sage Creek, Pennington County, South Dakota. **A.** Right lateral; **B.** apertural; **C.** ventral. **D–F.** USNM 536249, USGS Mesozoic loc. D8060, *Baculites compressus* Zone, Pierre Shale, Grand County, north-central Colorado. **D.** Right lateral; **E.** apertural; **F.** ventral. **G–I.** AMNH 56767, AMNH loc. 3274, *Baculites compressus–B. cuneatus* zones, Pierre Shale, Meade County, South Dakota. **G.** Right lateral; **H.** apertural; **I.** ventral. Specimens are illustrated natural size.

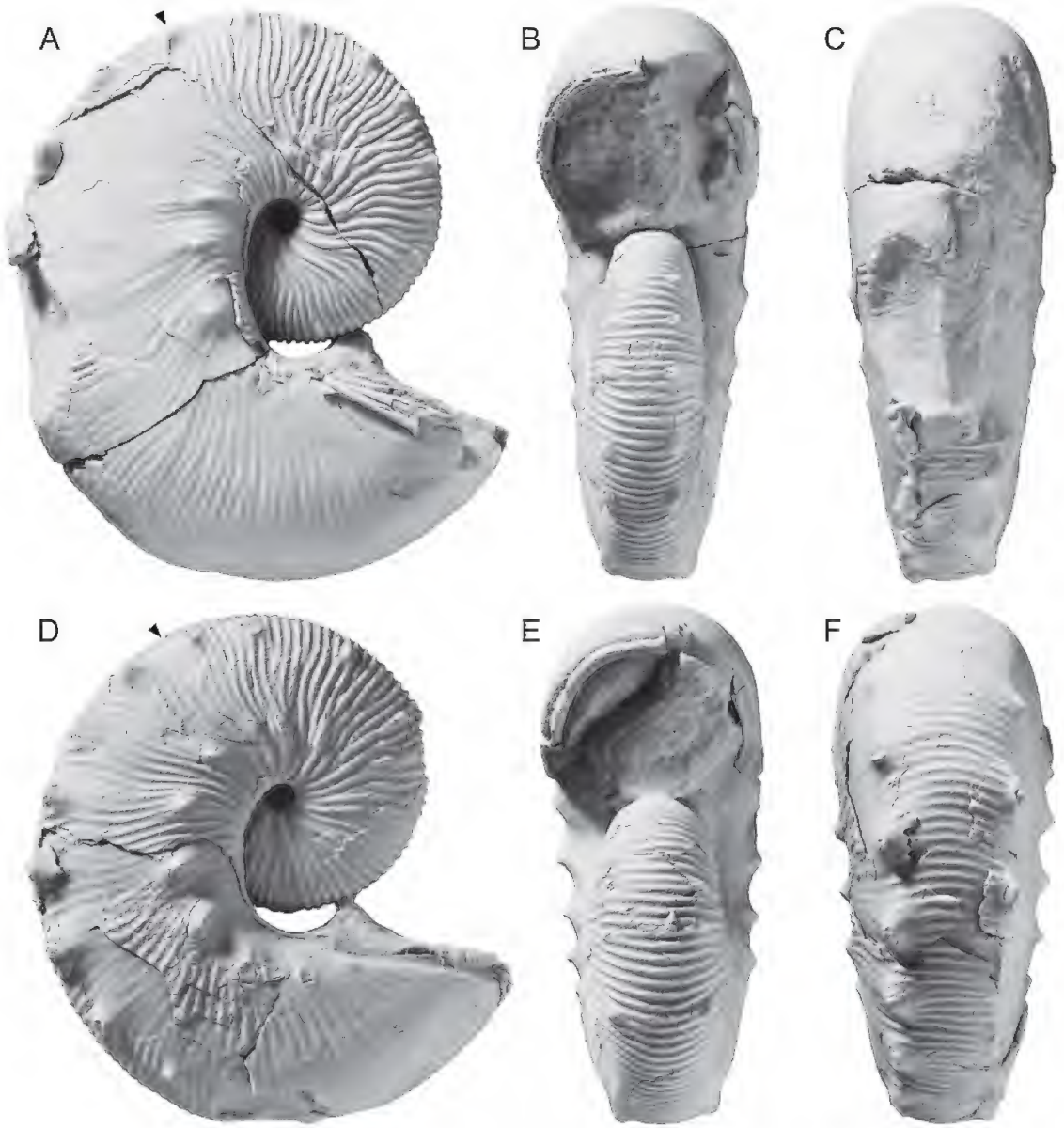

Fig. 102. *Hoploscaphites brevis* (Meek, 1876), large microconchs, AMNH loc. 3274, *Baculites compressus–B. cuneatus* zones, Pierre Shale, Meade County, South Dakota. **A–C.** AMNH 58556. **A.** Right lateral; **B.** apertural; **C.** ventral. **D–F.** AMNH 56768. **D.** Right lateral; **E.** apertural; **F.** ventral. Specimens are illustrated natural size.

var. *quadrangularis* from the U.S. Western Interior are representatives of *Hoploscaphites plenus*. Two of the three specimens figured by Meek (1876: pl. 25, figs. 3, 4) as *S. nodosus* var. *quadrangularis* are microconchs of *H. plenus* (fig. 6A–C, H–K), probably from Montana (reillustrated, in part, by Grabau and Shimer, 1910: figs. 1429, 1430; Grabau, 1921, fig. 1698h; Kauffman, 1977: pl. 32, fig. 8; Riccardi, 1983: pl. 10, figs. 1, 2, 5, 6). Similarly, the specimen illustrated by Frech (1915, fig. 5) as *S. binodosus* F.A. Roemer var. *quadrangularis* Meek is a microconch of *H. plenus*. All of the ontogenetic material

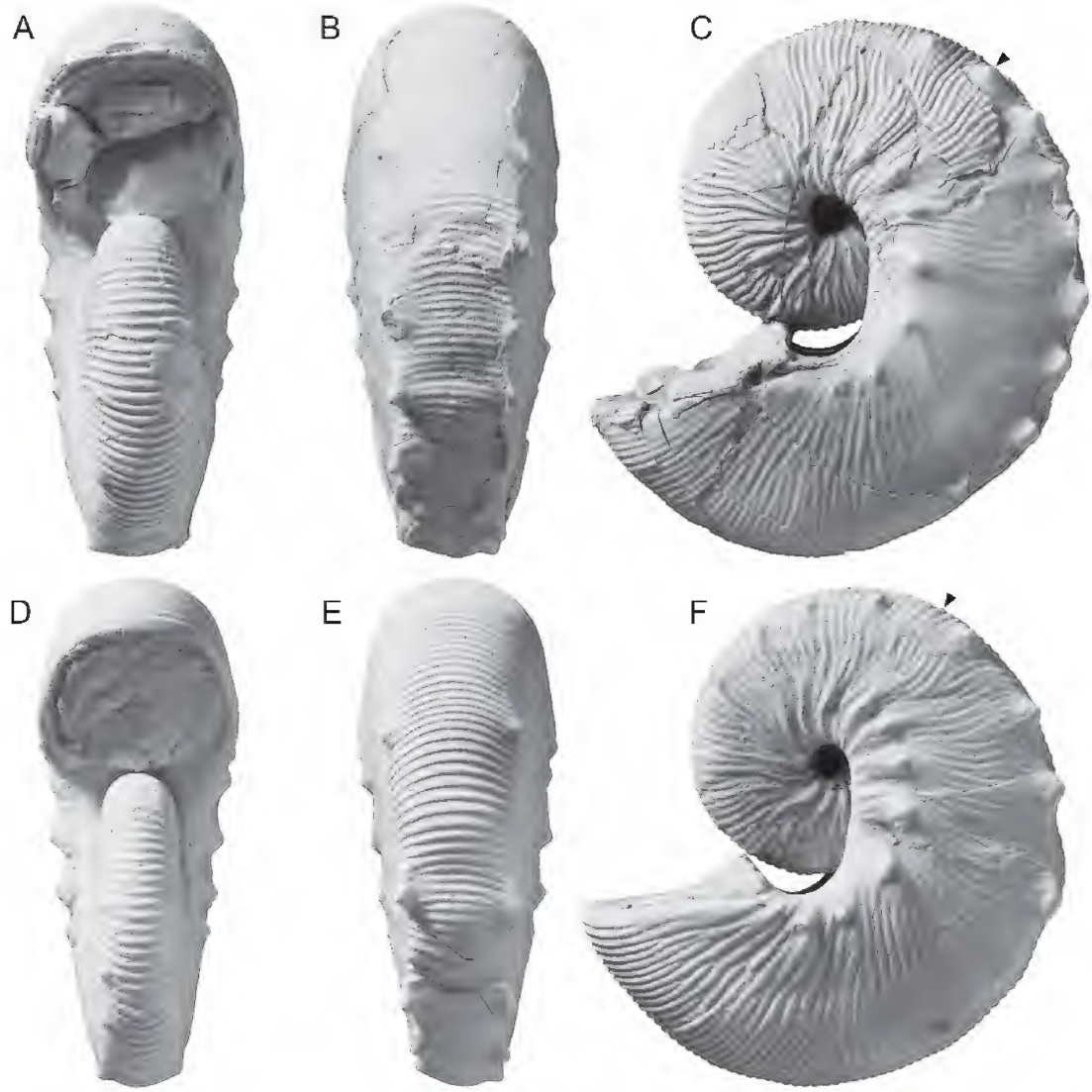

Fig. 103. *Hoploscaphites brevis* (Meek, 1876), large microconchs. **A–C.** AMNH 55884, AMNH loc. 3415, *Baculites compressus* Zone, Pierre Shale, Meade County, South Dakota. **A.** Apertural; **B.** ventral; **C.** left lateral. **D–F.** BHI 4123, *Baculites compressus–B. cuneatus* zones, Pierre Shale, Meade County, South Dakota. **D.** Apertural; **E.** ventral; **F.** left lateral. Specimens are illustrated natural size.

illustrated by Smith (1905: 640, fig. 1.2, 4–7, 9–18, 1.3, 2.1) as *S. nodosus* var. *brevis* and *S. nodosus* var. *quadrangularis* from Wibaux, Montana, also probably belongs to *H. plenus*, or a closely related species. The microconch illustrated by Warren (1931: pl. 1, fig. 2) as *Acanthoscaphites nodosus* var. *quadrangularis* also probably belongs to *H. plenus*. The specimen illustrated by Elias (1933: pl. 41, fig. 3) as *A. nodosus* var. *brevis* is a fragment of a body chamber of a macroconch (KU-MIP 59654) (fig. 80E, F) but differs from *H. brevis* in its larger size and more widely spaced ribs. It probably represents a closely related species from the *Baculites reesidei* Zone.

Hoploscaphites brevis has also been reported from the Western Interior of Canada, but as with the U.S. material, many of the previously described specimens belong to *H.*

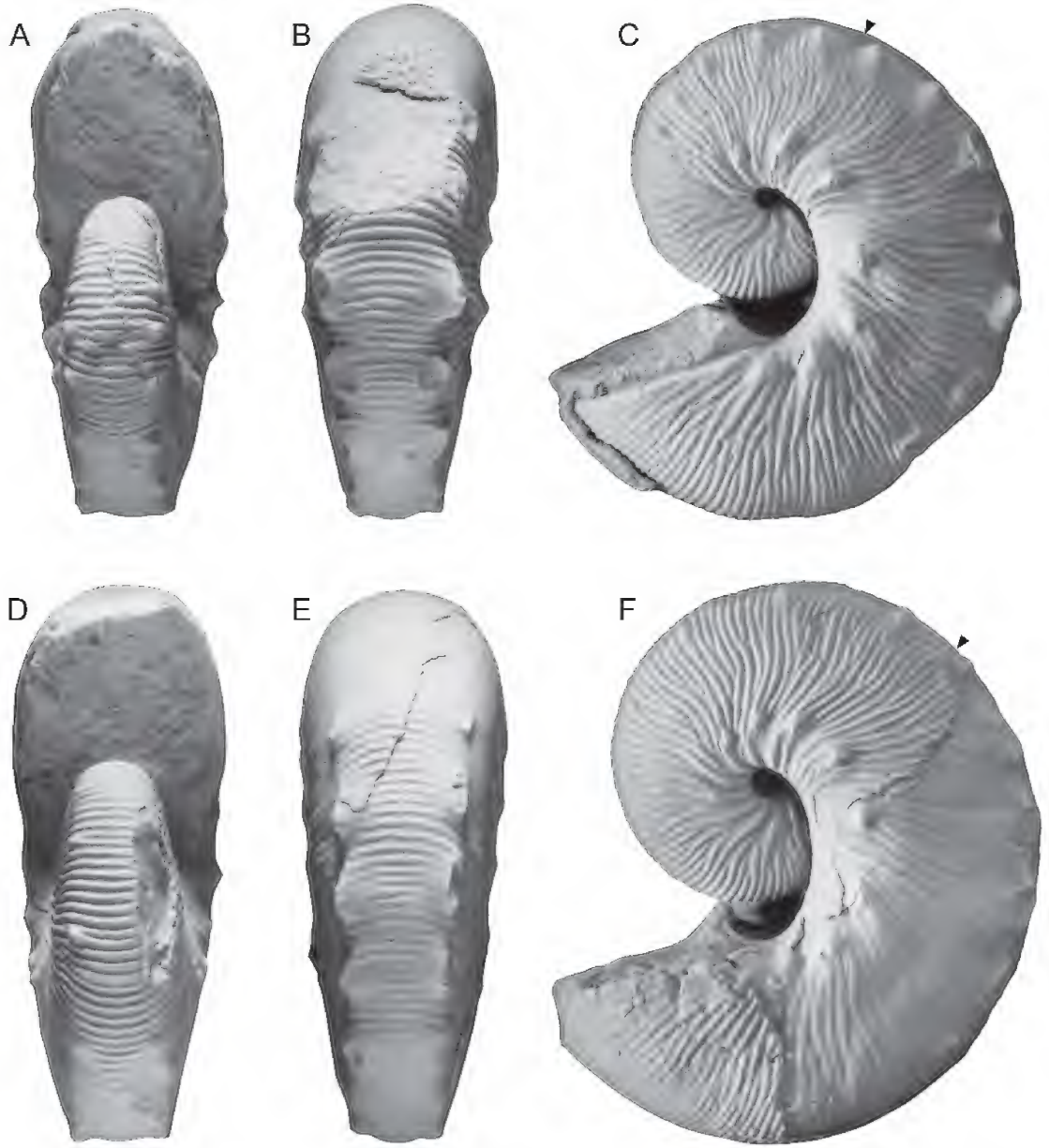

Fig. 104. *Hoploscaphites brevis* (Meek, 1876), large microconchs, locality unknown, but probably Pierre Shale, Pennington County, South Dakota. **A–C.** USNM 536242. **A.** Apertural; **B.** ventral; **C.** left lateral. **D–F.** USNM 536241. **D.** Apertural; **E.** ventral; **F.** left lateral. Specimens are illustrated natural size.

plenus. With respect to macroconchs, Riccardi (1983, pl. 5, figs. 3–9) illustrated three specimens (UA 1199, GSC 21852, and GSC 67099) as *Jeletzkytes* cf. *brevis* ♀ (previously illustrated, in part, by Jeletzky [1970: pl. 27, fig. 9] and Nelson [1975: pl. 64, figs. 3, 4]). However, the adoral part of the shaft in GSC 21852 (fig. 86E–G) is more inflated, and the distance between ventrolateral tubercles on either side of the venter is shorter, than in *H. brevis*. In all probability, all three specimens belong to *H. plenus*. Riccardi (1983: pl. 6,

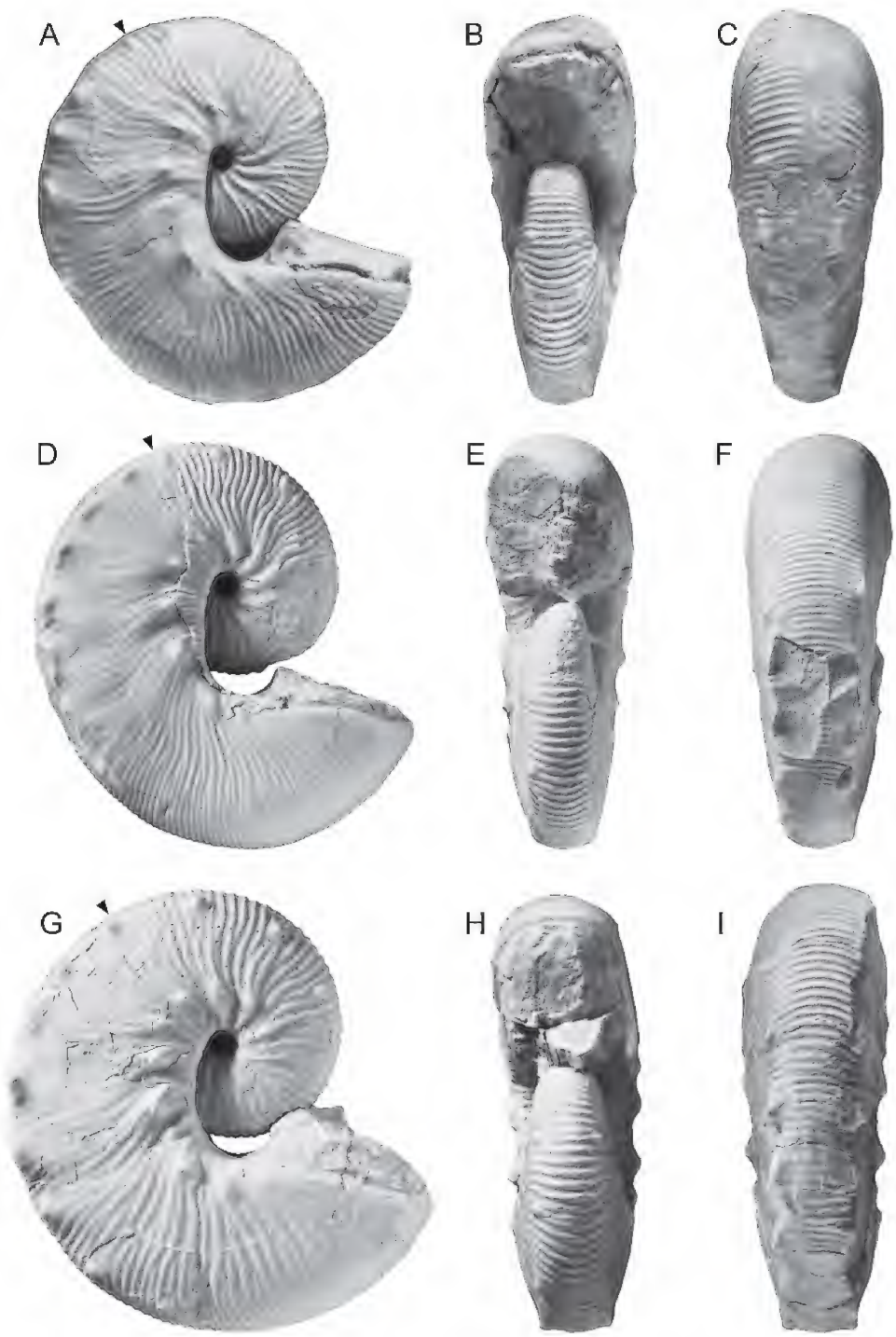

Fig. 105. *Hoploscaphites brevis* (Meek, 1876), small microconchs. **A–C.** BHI 4283, *Baculites cuneatus* Zone, Pierre Shale, Meade County, South Dakota. **A.** Right lateral; **B.** apertural; **C.** ventral. **D–F.** USNM 536243, locality unknown, but probably Pierre Shale, Pennington County, South Dakota. **D.** Right lateral; **E.** apertural; **F.** ventral. **G–I.** BHI 4211a, *Baculites compressus* Zone, Pierre Shale, Meade County, South Dakota. **G.** Right lateral; **H.** apertural; **I.** ventral. Specimens are illustrated natural size.

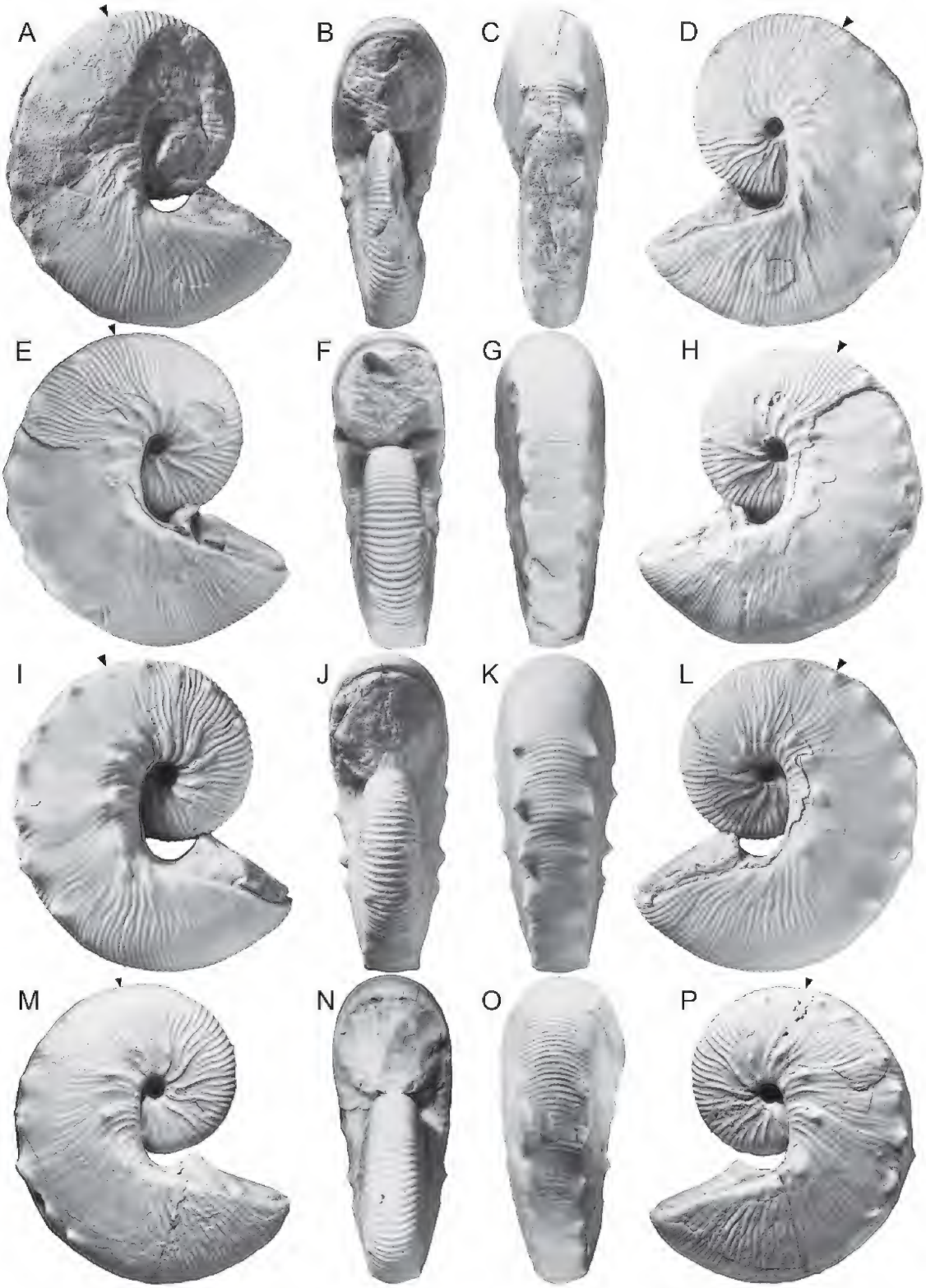
A
B
C
D
E
F
G
H
I
J
K
L
M
N
O
P

figs. 5–9) illustrated two additional specimens (GSC 67097 and GSC 67098) as *Jeletzkytes* cf. *brevis* ♀. They are only phragmocones, and it is difficult to identify them with any certainty. Riccardi (1983: pl. 6, figs. 1–4) also illustrated a specimen (GSC 97995) as *Jeletzkytes* affin. *brevis* ♀. It also belongs to *H. plenus* based on its inflated whorl section, widely spaced ribs, and the short distance between ventrolateral tubercles on either side of the venter.

With respect to microconchs, Riccardi (1983) illustrated five specimens from Canada that he called *Jeletzkytes* cf. *brevis* Meek ♂. Of the two nearly complete specimens, UA 03943 (Riccardi, 1983: pl. 10, figs. 7–9, text fig. 22a) is a large microconch of *Hoploscaphites brevis* and GSC 67102 (Riccardi: 1983: pl. 10, figs. 19–21; text fig. 21a) is a microconch of either *H. plenus* or *H. criptonodosus*, based on the presence of weak flank tubercles on the phragmocone and the inflated whorl section of the body chamber. Of the three fragmentary specimens, GSC 67103 (Riccardi, 1983: pl. 10, figs. 15, 16, text fig. 22b) consists of the adapical part of the phragmocone and adoral part of the body chamber. The ornament on the phragmocone is the same as that in GSC 67102, suggesting that it is also a microconch of either *H. plenus* or *H. criptonodosus*. Of the remaining two specimens, GSC 67101 (Riccardi, 1983: pl. 10, figs. 10–14, text fig. 21b) consists of the early whorls of the phragmocone and most of the body chamber, and GSC 67100 (Riccardi, 1983: pl. 10, figs. 17, 18) consists of part of the shaft and hook. Jeletzky (in Cobban and Reeside, 1952: 1027) assigned GSC 67100 to *Scaphites elegans* Tate, 1865 (= *H. compressus* [Roemer, 1841], Kennedy and Kaplan, 1997). The flanks of the body chamber at the point of recurvature in both of these specimens are narrow and inflated, similar to the condition in GSC 67102, suggesting that both of these specimens are also microconchs of either *H. plenus* or *H. criptonodosus*.

The holotype and paratypes of *Hoploscaphites landesi* Riccardi, 1983 (p.10, pl. 1, figs. 12–22) from the "Bearpaw Formation, ?Demaine Sandstone, South Saskatchewan River, opposite the mouth of Swift Current Creek, Saskatchewan," are small, compressed microconchs of *H. brevis*, with the umbilicolateral and ventrolateral tubercles restricted to the shaft (fig. 7E–Q). These specimens grade into larger, more robust individuals, which bear tubercles on both the phragmocone and the shaft. The specimens called *Hoploscaphites* sp. α by Riccardi (1983: 11, pl. 1, figs. 1–11, text figs. 3, 4) are probably large compressed macroconchs of *H. brevis*.

On the Gulf Coastal Plain, Stephenson (1941: 426, pl. 90, figs. 7, 8)) described a specimen (USNM 77307) as *Scaphites brevis* Meek from the Nacatoch Sand of Texas. It is a macroconch, 57.4 mm in maximum length, and consists of the impression of the adult shell with part of the body chamber preserved in three dimensions, although slightly crushed. It differs from *Hoploscaphites brevis* in three important respects: (1) the apertural angle (44°) is on the low end of the spectrum for this species, (2) the rib density on the venter increases markedly from the midshaft to the hook (6 ribs/cm on the midshaft to 10 ribs/cm on the hook), and, most importantly, (3) the ribs on the body chamber are straight rather than flexuous, although the inner one-third of the flanks are not well preserved. According to Kennedy and Cobban (1993), the Nacatoch Sand in Texas represents the *Nostoceras* (*N.*) *hyatti* Zone, implying that Stephenson's specimen is probably not *H. brevis*.

←

Fig. 106. *Hoploscaphites brevis* (Meek, 1876), small microconchs. **A–D.** BHI 4273, *Baculites cuneatus* Zone, Pierre Shale, Meade County, South Dakota. **A.** Right lateral; **B.** apertural; **C.** ventral; **D.** left lateral. **E–H.** USNM 536251, Pierre Shale, Meade or Pennington County, South Dakota. **E.** Right lateral; **F.** apertural; **G.** ventral; **H.** left lateral. **I–L.** BHI 4725, *Baculites compressus–B. cuneatus* zones, Pierre Shale, Meade County, South Dakota. **I.** Right lateral; **J.** apertural; **K.** ventral; **L.** left lateral. **M–P.** BHI 4246, *Baculites compressus–B. cuneatus* zones, Pierre Shale, Meade County, South Dakota. **M.** Right lateral; **N.** apertural; **O.** ventral; **P.** left lateral. Specimens are illustrated natural size.

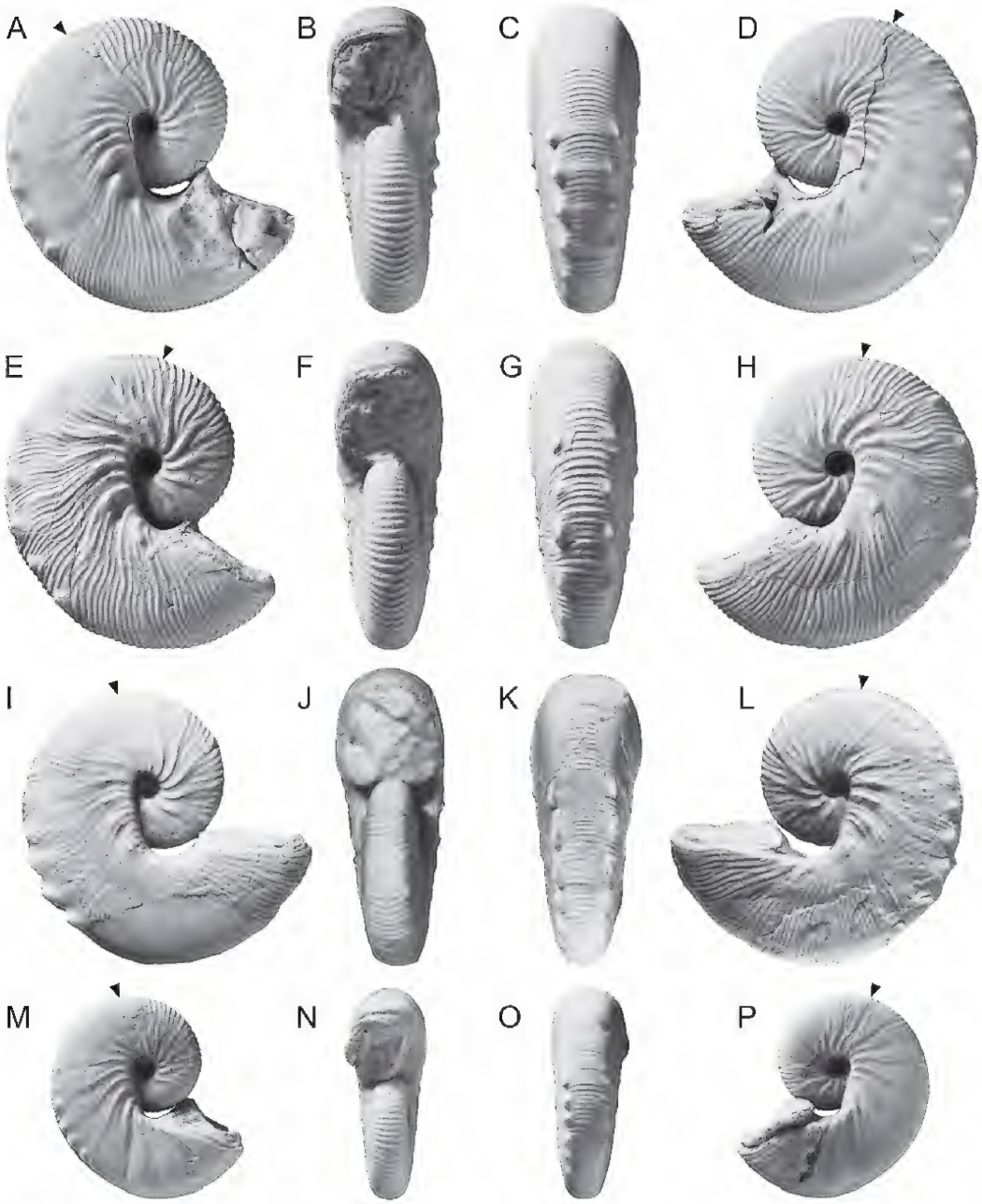

Fig. 107. *Hoploscaphites brevis* (Meek, 1876), small microconchs. **A–D.** BHI 4245, *Baculites cuneatus* Zone, Pierre Shale, Meade County, South Dakota. **A.** Right lateral; **B.** apertural; **C.** ventral; **D.** left lateral. **E–H.** BHI 4253, transitional in morphology to macroconch, *Baculites compressus* Zone, Pierre Shale, Meade County, South Dakota. **E.** Right lateral; **F.** apertural; **G.** ventral; **H.** left lateral. **I–L.** BHI 2155, *Baculites compressus* Zone, Pierre Shale, Meade County, South Dakota. **I.** Right lateral; **J.** apertural; **K.** ventral; **L.** left lateral. **M–P.** BHI 4276, *Baculites compressus–B. cuneatus* zones, Pierre Shale, Meade County, South Dakota. **M.** Right lateral; **N.** apertural; **O.** ventral; **P.** left lateral. Specimens are illustrated natural size.

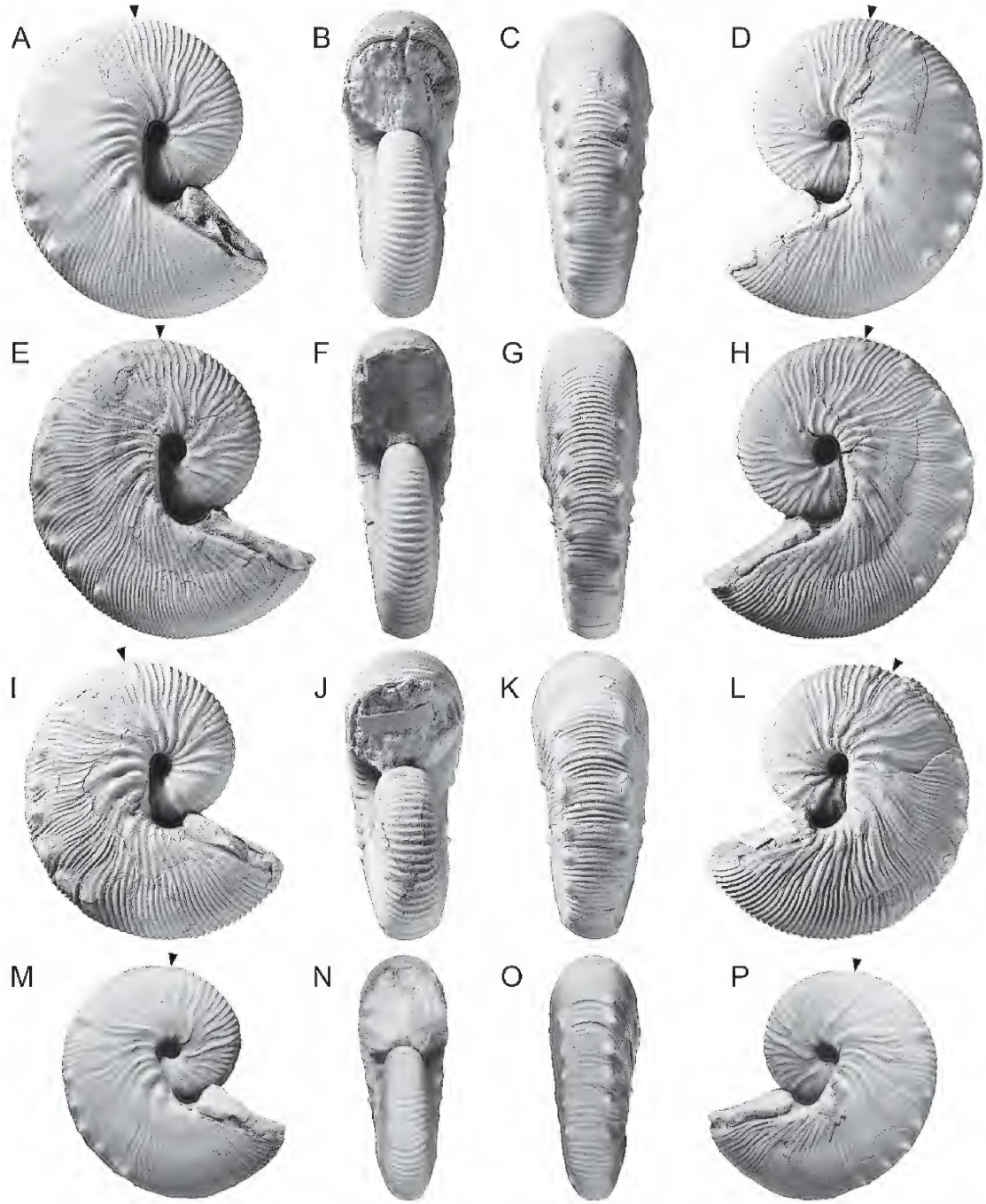

Fig. 108. *Hoploscaphites brevis* (Meek, 1876), small microconchs. **A–D.** BHI 4239, transitional in morphology to macroconch, *Baculites compressus* Zone, Pierre Shale, Meade County, South Dakota. **A.** Right lateral; **B.** apertural; **C.** ventral; **D.** left lateral. **E–H.** BHI 4233, *Baculites compressus* Zone, Pierre Shale, Meade County, South Dakota. **E.** Right lateral; **F.** apertural; **G.** ventral; **H.** left lateral. **I–L.** AMNH 55874, transitional in morphology to macroconch, AMNH loc. 3415, *Baculites compressus* Zone, Pierre Shale, Meade County, South Dakota. **I.** Right lateral; **J.** apertural; **K.** ventral; **L.** left lateral. **M–P.** BHI 4240, transitional in morphology to macroconch, *Baculites compressus–B. cuneatus* zones, Pierre Shale, Meade County, South Dakota. **M.** Right lateral; **N.** apertural; **O.** ventral; **P.** left lateral. Specimens are illustrated natural size.

TABLE 9
Measurements of the adult shells of *Hoploscaphites brevis* (Meek, 1876), microconchs

Specimen Number	Study Number	LMAX	LMAX/H_2	UD_P	UD_L	W_1/H_1	W_2/H_2	W_3/H_3	W_4/H_4	W_5/H_5	W_6/H_6	W_7/H_7	V_4/H_4	V_4/W_4
AMNH 9516/1	—	71.1	3.08*	4.1	4.0	—	—	—	—	—	—	—	0.52	0.60
AMNH 9518/1	—	63.8	2.93	3.6	3.3	0.78	0.74	0.71	0.73	0.95	1.04	—	0.43	0.59
AMNH 45387	651	53.1	3.10	3.3	2.9	0.79	0.74	0.70	0.72	0.84	0.90	—	0.37	0.48
AMNH 45394[a]	561	76.3	3.22	3.3	2.8	0.68	0.67*	—	—	—	—	—	—	—
AMNH 55874[b]	1671	40.4	3.11	2.8	2.7	0.94	0.82	0.77	0.73	0.98	0.99	1.01	0.46	0.63
AMNH 55875	—	47.3	3.07	—	2.9	0.83	0.79	—	0.74	0.95	0.94*	0.99	0.44	0.59
AMNH 55884	1655	71.6	3.09	5.6	5.1	0.82	0.76	0.75	0.84	1.06	1.05	1.01	0.44	0.52
AMNH 55885[b]	1672	32.3	3.14	2.4	2.4	0.96	0.85	0.85	0.75	0.96	0.98	—	0.43	0.60
AMNH 56767	1666	58.0	3.19	5.2	3.8	0.88	0.82	0.86	0.90	0.99	0.94	0.98	0.46	0.60
AMNH 56768	1665	70.2	3.19	4.8	3.7	0.95	0.90	0.90	0.91	1.04	1.08	1.12	0.48	0.56
AMNH 56769	1668	79.6	3.17	6.2*	4.8	0.96	0.94	—	0.89	1.08	1.07	1.11	0.52	0.58
AMNH 58514	1456	49.0	3.16	3.7	3.4	0.82	0.76	0.66	0.69	0.84	0.90	1.00	0.39	0.57
AMNH 58518	—	48.8	—	3.1	2.7	0.76	0.70	0.71	—	—	—	0.94	—	—
AMNH 58519	567	73.4	3.26	—	3.8	—	0.64	0.66	0.70	—	—	—	0.41	0.62
AMNH 58520	653	—	—	—	3.8	0.82	—	—	—	—	—	—	0.54	0.62
AMNH 58537	562	64.8	2.97	3.9	4.1	—	0.63	0.63	0.73	0.86	1.00	0.94	0.38	0.63
AMNH 58555[c]	—	—	—	—	2.7	0.74	0.78	—	0.74	—	—	—	0.42	0.62
AMNH 58556	1443	79.0	2.97	5.4	4.5	0.78	0.66	0.67	—	0.83	0.87	0.93	0.35	0.53
AMNH 58557	—	81.2	3.24	6.0	4.3	0.85	0.83	0.78	0.88	—	—	—	0.48	0.60
BHI 2155	345	39.8	3.32	3.7	3.2	0.84	0.73	0.72	0.71	0.82	0.88	0.91	0.45	0.64
BHI 4118[b]	336	41.4	2.94	3.3	3.2	0.72	0.74	0.75	0.68	0.91	0.91	—	0.43	0.63
BHI 4119	343	35.2	3.01	2.7	2.8	0.78	0.77	0.77	0.77	0.84	0.85	—	0.40	0.56
BHI 4123	288	66.0	3.24	4.2	4.1	0.74	0.69	0.70	0.69	0.91	0.98	1.03	0.40	0.58
BHI 4208	286	52.8	3.05	3.3	2.9	0.92	0.73	0.78	0.82	0.90	0.97	1.04	0.53	0.66
BHI 4209	289	60.8	3.10	4.1	3.5	0.68	0.67	0.65	0.66	0.82	0.87	0.92	0.39	0.58
BHI 4210	315	67.5	3.12	4.4	3.6	0.77	0.72	0.73	0.69	0.76	0.80	0.88	0.43	0.64
BHI 4211a	385	63.1	3.29	3.9	3.4	0.77	0.77	0.75	—	—	—	—	0.40	0.61
BHI 4212[a]	587	64.8	3.10	4.6	4.2	0.71	0.72	0.66	—	0.85	0.90	0.86	—	—
BHI 4223	320	66.4	3.22	6.4	4.8	0.89	0.94	0.86	0.91	1.00	1.07	1.05	0.58	0.65
BHI 4231	354	56.6	3.08	3.3	3.5	0.79	0.65	0.63	0.63	0.84	0.85	0.91	0.45	0.64
BHI 4233	333	43.3	3.21	—	3.6	0.74	0.71	0.71	0.62	0.83	0.83	0.86	0.37*	0.63
BHI 4236	352	40.7	3.26	—	2.2	0.78	0.74	0.74	—	—	—	—	0.39	—
BHI 4238[d]	348	45.6	3.14	3.5	3.5	0.80	0.79	0.76	0.77*	0.92	0.93	0.85	0.45	0.55
BHI 4239[b]	362	44.0	2.91	2.3	2.5	0.82	0.76	0.74	0.70	0.93	0.93	0.96	0.45	0.64
BHI 4240[b]	342	36.1	3.01	2.7	2.7	0.72	0.74	0.78	0.74	0.85	0.90	0.90	0.40	0.57
BHI 4242	360	39.1	3.15	3.5	2.1	0.83	0.73	0.73	0.80	—	—	—	0.44	0.57
BHI 4243	361	30.2	3.21	—	3.1	0.80	0.79	0.81	0.75	—	—	—	0.48	0.62

TABLE 9
(*Continued*)

Specimen Number	Study Number	LMAX	LMAX/H_2	UD_P	UD_L	W_1/H_1	W_2/H_2	W_3/H_3	W_4/H_4	W_5/H_5	W_6/H_6	W_7/H_7	V_4/H_4	V_4/W_4
BHI 4244 [e]	440	45.7	3.01	—	3.4	—	—	—	—	—	—	0.78	0.36	0.48*
BHI 4245	359	41.7	3.09	2.7	2.3	0.79	0.75	0.74	0.71	0.86	0.93	—	0.36	0.53
BHI 4246	337	48.4	3.16	2.5	2.4	0.88	0.74	0.76	0.78	0.94	0.99	0.96	0.40	0.59
BHI 4248[b, c]	1677	36.1	3.11	—	3.0	0.90	0.75	—	0.63	0.86	0.86	0.74	0.37	0.59
BHI 4249	350	38.6	3.22	3.1	2.7	0.76	0.71	0.73	0.70	0.87	0.89	0.86	0.47	0.66
BHI 4251	347	31.6	3.04	2.0	2.1	0.77	0.72	0.72	0.65	0.78	0.84	0.82	0.40	0.58
BHI 4252	353	42.6	3.13	3.8	3.5	0.79	0.70	0.71	0.71	0.84	0.87	0.88	0.49	0.67
BHI 4253	339	41.5	3.07	2.3	2.4	0.75	0.70	0.73	0.67	0.83	0.84	0.83	0.41	0.60
BHI 4254	349	31.7	3.02	1.9	1.9	0.76	0.72	0.70	0.74	0.90	0.98	0.97	0.44	0.62
BHI 4255	355	51.4	3.13	3.4	3.4	0.73	0.67	0.67	0.71	0.91	0.92	—	0.47	0.63
BHI 4261	357	41.3	3.28	3.7	3.4	0.76	0.72	0.71	0.65	0.84	0.83	0.82	0.38	0.59
BHI 4262	351	33.7	2.93	—	3.2	0.78	0.79	0.79	0.76	0.80	0.89	—	0.45	0.63
BHI 4263	484	42.8	2.89	3.3	3.2	—	—	—	0.70	0.79	—	—	0.38	0.61
BHI 4264	344	43.0	2.99	3.9	3.8	0.77	0.74	0.74	0.74	—	0.95	—	—	—
BHI 4268a[f]	376	75.7	3.14	—	4.5	0.70	0.68	—	0.66	0.84	0.96	0.95	0.35	0.50
BHI 4268b[f]	377	75.2	3.23	4.4	4.4	—	—	0.73*	0.73	0.95	0.96	0.95	0.41	0.57
BHI 4273[e]	346	50.2	3.04	3.1	3.1	—	—	—	—	—	0.84	0.93	—	—
BHI 4275	378	67.5	3.10	3.3	3.0	—	—	—	—	—	—	—	0.35	0.56
BHI 4276	335	28.5	3.27	3.1	2.9	0.81	0.73	0.73	0.70	0.78	0.79	0.84	0.42	0.61
BHI 4277	340	26.7	3.18	2.5	2.6	0.72	0.79	0.79	0.63	0.86	0.90	—	0.46	0.65
BHI 4283	310	53.6	3.01	3.3	3.1	0.73	0.74	0.73	0.70	0.98	1.06	0.96	0.39	0.56
BHI 4287b	450	50.6	3.12	2.6	2.8	0.76	0.73	0.73	0.69	0.88	0.98	0.90	0.37	0.55
BHI 4288	285	71.6	3.21	3.8	3.6	0.74	0.77	0.75	0.74	0.95	0.98	1.12	0.47	0.62
BHI 4313	358	28.8	3.10	2.6	2.5	0.75	0.72	0.72	0.78	0.95	0.98	0.85	0.50	0.65
BHI 4314	584	69.6	3.25	4.9	4.8	0.79	0.71	0.71	0.62	0.76	—	—	0.32	0.51
BHI 4315	314	54.0	2.95	4.6	4.2	0.75	0.73	0.69	0.71	0.89	0.98	—	0.39	0.60
BHI 4316[b, g]	482	50.2	2.84	3.2	2.8	0.75	0.71	0.71	0.68	—	1.06	1.04	0.41	0.60
BHI 4383	647	36.1	3.14	2.3	2.4	0.71	0.74	0.73	0.71	0.83	0.91	0.94	0.42	0.60
BHI 4392	1654	62.1	3.03	4.3*	4.5*	0.71	0.72	0.69	0.66	—	—	—	0.38	0.56
BHI 4393	449	71.9	2.96	4.9	3.9	—	0.61	0.65	—	—	—	—	0.35	0.53
BHI 4708[b]	457	32.1	3.15	3.3	2.9	0.77	0.74	0.73	0.71	0.83	0.91	0.88	0.38	0.56
BHI 4709	456	49.2	3.35	3.0	2.8	0.77	0.78	0.70	0.77	0.87	0.94	—	0.49	0.61
BHI 4713[a]	535	58.8	3.01	—	3.2	0.77	0.71	0.76	—	—	1.01	—	—	—
BHI 4719	459	63.8	3.04	3.7	3.0	—	0.69	0.68	0.69	0.92	0.96	0.97	0.38	0.54
BHI 4725	455	49.9	3.10	4.2	3.6	0.71	0.71	0.74	0.75	0.93	1.01	0.96	0.42	0.55
BHI 4727	460	69.1	3.13	4.1	3.6	0.79	0.70	0.76	0.79	0.99	1.00	—	0.42	0.58
BHI 4729	458	33.4	3.01	2.2	2.1	0.86	0.86	0.71	0.80	0.93	0.94	—	0.43	0.60
BHI 4770	616	49.2	3.11	4.0	3.3	0.75	0.71	0.74	0.71	0.84	0.93	—	0.40	0.55

TABLE 9
(*Continued*)

Specimen Number	Study Number	LMAX	LMAX/H_2	UD_P	UD_L	W_1/H_1	W_2/H_2	W_3/H_3	W_4/H_4	W_5/H_5	W_6/H_6	W_7/H_7	V_4/H_4	V_4/W_4
BHI 4896[g]	1262	44.8	3.01	3.6	3.8	0.79	0.66	0.71	0.68*	0.86	0.98	—	—	—
BHI 4898	1271	53.5	2.91	3.7	3.2	0.79	0.71	0.71	0.77*	0.88	0.88	0.94	0.41	0.56
BHI 4899a[h]	1272	65.3	3.04	—	2.8	0.79	0.75	0.72	0.71	1.01	1.02	1.06	0.40	0.56
BHI 4901	1669	46.9	3.15	—	2.6*	0.78	0.78	—	0.74	0.86	0.91	—	0.39	0.58
BHI 4915	1279	65.4	3.22	—	3.6	0.84	0.88	—	0.82	1.01	0.99	0.95	0.54	0.69
GSC 5342a[e]	409	49.0	2.88	—	—	0.52*	0.56*	—	0.57*	0.68*	0.72*	0.73*	0.35	0.65
GSC 5342b[e]	408	38.7	3.23	—	—	—	0.58*	0.58*	0.64*	0.74*	0.78*	0.78*	0.36	—
GSC 5342c[e]	407	38.4	2.95	—	2.8	—	—	0.53*	0.58*	—	0.57*	—	0.40	0.64
USNM 12291	422	55.3	3.35	—	3.6	0.68	0.81	0.74*	0.74	0.91	0.97	0.95	0.50	0.63
USNM 386690	423	54.1	3.11	—	4.1	0.89	0.84	—	0.75	0.95	1.03	0.91	0.47	0.62
USNM 536239	265	58.6	3.08	3.1	3.8	0.83	0.75	0.75	0.78	0.94	0.97	0.97	0.39	0.49
USNM 536240	586	—	—	4.7	3.4	0.88	0.82	—	—	—	—	—	—	—
USNM 536241	118	76.5	2.98	5.2	4.0	0.72	0.71	0.80	0.75	0.94	0.99	1.01	0.42	0.56
USNM 536242	119	68.2	3.13	4.4	3.5	0.77	0.70	0.81	0.72	—	0.98	0.92	0.42	0.58
USNM 536243	104	55.6	3.09	3.6	2.6	—	0.70	0.68	0.70	0.86	—	—	0.44	0.63
USNM 536244	108	55.7	3.04	3.4	3.7	0.79	0.75	0.73	0.75	0.90	0.96	—	0.39	0.52
USNM 536249	1083	61.1	3.07	3.6	3.6	0.80	0.76	0.78	0.74	0.88	0.89	1.00	0.41	0.55
USNM 536250	105	33.4	3.06	2.8	2.7	0.82	0.70	0.70	0.65	0.79	0.92	—	0.53	0.74
USNM 536251	107	47.9	3.03	—	3.0	0.75	0.69	—	0.62	0.83	0.87	—	0.35	0.49
USNM 536253	1660	37.0	3.06	—	—	—	0.72	0.71	0.75	0.95	1.03	1.00	0.42	0.59
USNM 536254[b, c]	1661	43.0	3.12	—	2.3	—	0.80	—	0.84	0.98	1.01	0.95	0.43	0.56
USNM 536259[b]	106	55.1	3.08	3.3	3.3	0.87	0.76	0.70	0.62	0.85	0.96	1.01	0.40	0.66
USNM 536261	259	67.8	—	4.9	4.5	0.71	—	0.64	0.72	0.90	0.92	—	0.39	0.60
USNM 536262	1208	—	—	6.2	5.4	0.82	0.74	0.74	0.80	—	—	—	0.52	0.64
USNM 536263	109	57.4	2.94	3.8	3.7	0.79	0.69	0.70	—	—	—	—	0.35	0.58
USNM 536264[i]	98	66.3	3.19	3.6	3.4	0.96	0.82	0.84	0.81	0.97	1.06	1.02	0.45	0.58
YPM 1861	585	68.8	3.00	3.1	3.2	0.76	0.68	0.66	0.68	0.86	0.93	0.97	0.40	0.58
YPM 35581[j]	393	71.1*	3.12	—	—	—	0.94	—	—	—	—	—	0.57*	0.62*
YPM 35586	522	44.5	3.16	3.6	3.2	0.74	0.70	0.76	0.70	0.86	0.90	—	0.38	0.58
YPM 222477	—	72.4	3.15	3.3	3.2	0.78*	0.78	0.71	0.77	0.92	1.02	1.04	0.48	0.66

See figure 14 for a description of the measurements. All measurements are in mm except for septal angle and apertural angle, which are in degrees. *Estimate.
[a]Lethal injury.
[b]Transitional to macroconch.
[c]Used in ontogenetic study.
[d]Elongate outline.
[e]Distorted.
[f]Next to one another in the same concretion.
[g]Nonlethal injury.
[h]Shows Morton's Syndrome (Landman and Waage, 1986).
[i]*Didymoceras cheyennense* Zone.
[j]Next to a macroconch of *H. brevis* (YPM 35581) in the same concretion.

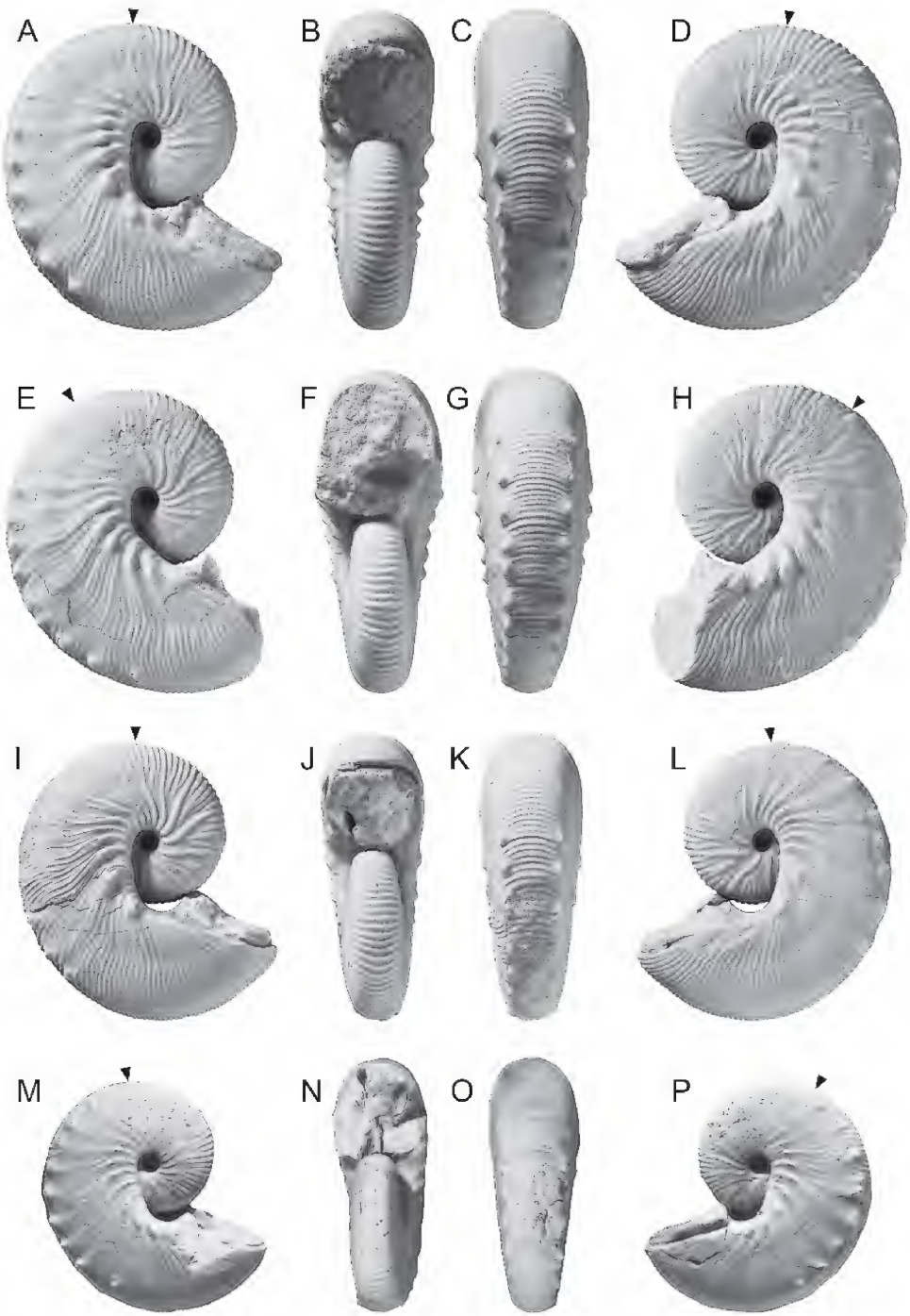

Fig. 109. *Hoploscaphites brevis* (Meek, 1876), small microconchs. **A–D.** BHI 4252, *Baculites cuneatus* Zone, Pierre Shale, Meade County, South Dakota. **A.** Right lateral; **B.** apertural; **C.** ventral; **D.** left lateral. **E–H.** YPM 35586, YPM A6520, Pierre Shale, Sage Creek, Pennington County, South Dakota. **E.** Right lateral; **F.** apertural; **G.** ventral; **H.** left lateral. **I–L.** BHI 4249, *Baculites compressus–B. cuneatus* zones, Pierre Shale, Meade County, South Dakota. **I.** Right lateral; **J.** apertural; **K.** ventral; **L.** left lateral. **M–P.** USNM 536250, locality unknown, but probably Pierre Shale, Pennington County, South Dakota. **M.** Right lateral; **N.** apertural; **O.** ventral; **P.** left lateral. Specimens are illustrated natural size.

TABLE 10
Ornament of the adult shells of *Hoploscaphites brevis* (Meek, 1876), microconchs

		Rib Density (ribs/cm)							
		Phragmocone		Body Chamber		Number of Umbilicolateral Tubercles		Number of Ventrolateral Tubercles	
Specimen Number	Study Number	Adapical	Adoral	Midshaft	Hook	Phragmocone	Body Chamber	Phragmocone	Body Chamber
AMNH 45349	561	7	7	8	8	5	5	6	2+
AMNH 58538	562	8	9	8	9	2	8	10	7
BHI 2155	345	10	12	15	13	1	6	3/5[a]	6
BHI 4123	288	7	7	9	9	2	7	5	5
BHI 4209	289	8	8	10	9	3	7/8[a]	6	5
BHI 4233	333	9	9	13	15	0	10	1	10
BHI 4239	362	9	9	11	12	0	3/5[a]	0	6/7[a]
BHI 4240	342	10	9	10	14	0	8	0	6
BHI 4242	360	11	11	14	15	0	5	2	9
BHI 4244	440	12	10	14	15	0	0	0	5
BHI 4246	337	9	9	12	10	2	5	1	9
BHI 4249	350	10	10	13	16	0	4	0	8
BHI 4251	347	12	13	12	16	0	3	1	6
BHI 4252	353	9	9	12	11	0	6	0	8
BHI 4262	351	10	8	11	13	0	5	0	6
BHI 4264*	344	10	10	10	12	4	5	2	7
BHI 4268a	376	9	8	10	9	7	6	7	8
BHI 4268b	377	8	9	9	8	4	5	9	6
BHI 4276	335	13	12	14	18	0	2	0	6
BHI 4277	340	11	10	11	14	0	6	0	5
BHI 4283	310	8.5	8	—	10	5	5	6	6
BHI 4287	450	9	9	10	11	4	5	5	7
BHI 4313	358	11	10	13	18	0	4	0	6
BHI 4314	584	8	8	8	8	5	6+	3	10
BHI 4315	314	8	8	12	11	5	5	14	7
BHI 4316	482	9	8	12	10	3	6	3	10
BHI 4393	449	9	9	9	10	8	4	8	7
BHI 4708	457	11	10	16	16	0	3	0	7
BHI 4713	535	8	10	11	11	1	9	2	5+
BHI 4719	459	9	10	10	10	5	4	6+	5
BHI 4725	455	9	11	12	10	7	4/6[a]	7	5
BHI 4727	460	7	9	8.75	9	2	5	5	5

TABLE 10
(*Continued*)

		Rib Density (ribs/cm)							
		Phragmocone		Body Chamber		Number of Umbilicolateral Tubercles		Number of Ventrolateral Tubercles	
Specimen Number	Study Number	Adapical	Adoral	Midshaft	Hook	Phragmocone	Body Chamber	Phragmocone	Body Chamber
BHI 4729	458	11	10	11	13	0	3	0	7
BHI 4775	—	8	9	10	10	5	7	5+	8
GSC 5342a	409	8	9	14	12	0	6	6	7
GSC 5342b	408	10	9	14	13	0	3	0	6
GSC 5342c	407	11	11	18	14	0	3	0	5
USNM 12291	422	10	10	11	10	6	5	4	6
USNM 386690	423	9	—	11	10	1	7	—	7
USNM 536241	118	8	8	8	8	7	5	7	5
USNM 536242	119	7	9	8	8	2	6	7	6
USNM 536243	104	9	9	11	11	4	5	5	6
USNM 536244	108	9	9	9	9	4	4	5	9
USNM 536251	107	9	10	14	12	3	5	5	7
USNM 536259	106	9	10	11	10	3	5	3	5
USNM 536256	105	12	11	14	18	0	3	0	8
YPM 1861	585	7	8	10	10	6	6	8	7
YPM 35586	522	10	9	11	13	0	6	1	11

For additional comments, see footnotes in table 9. *Estimate due to incomplete or poor preservation.
[a]The number is different on each side of the shell.

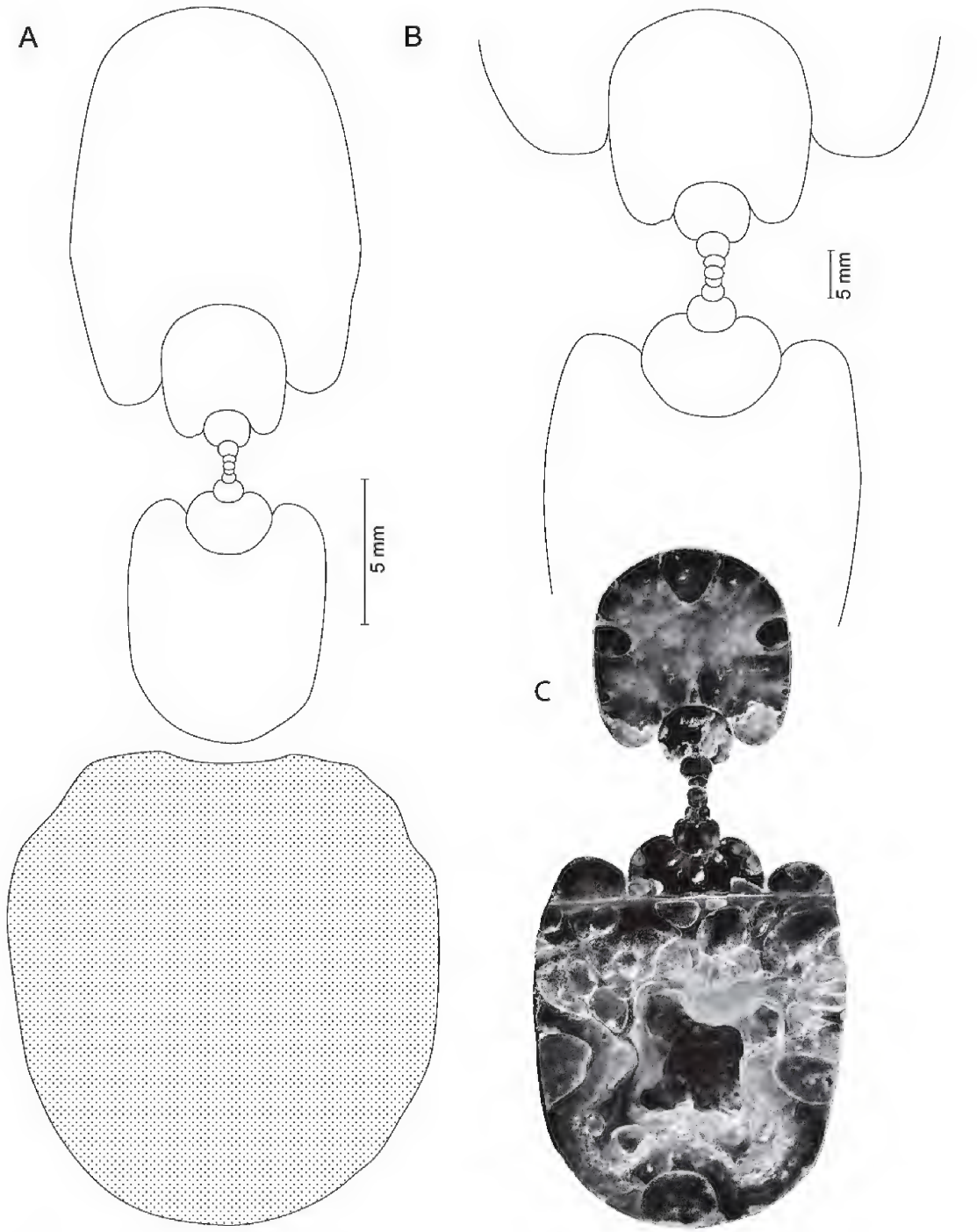

Fig. 110. Dorsoventral cross section through a small microconch of *Hoploscaphites brevis* (Meek, 1876), transitional in morphology to macroconch, USNM 536254, USGS Mesozoic loc. D12203, *Baculites compressus* Zone, Pierre Shale, Pennington County, South Dakota. The plane of the cross section approximately coincides with the line of maximum length. **A.** Camera lucida of cross section of the adult shell. The stippled area demarcates the mature body chamber. **B.** Camera lucida of cross section of the inner whorls. **C.** Photo of cross section of the inner whorls. Measurements are listed in appendix 2, table 5.

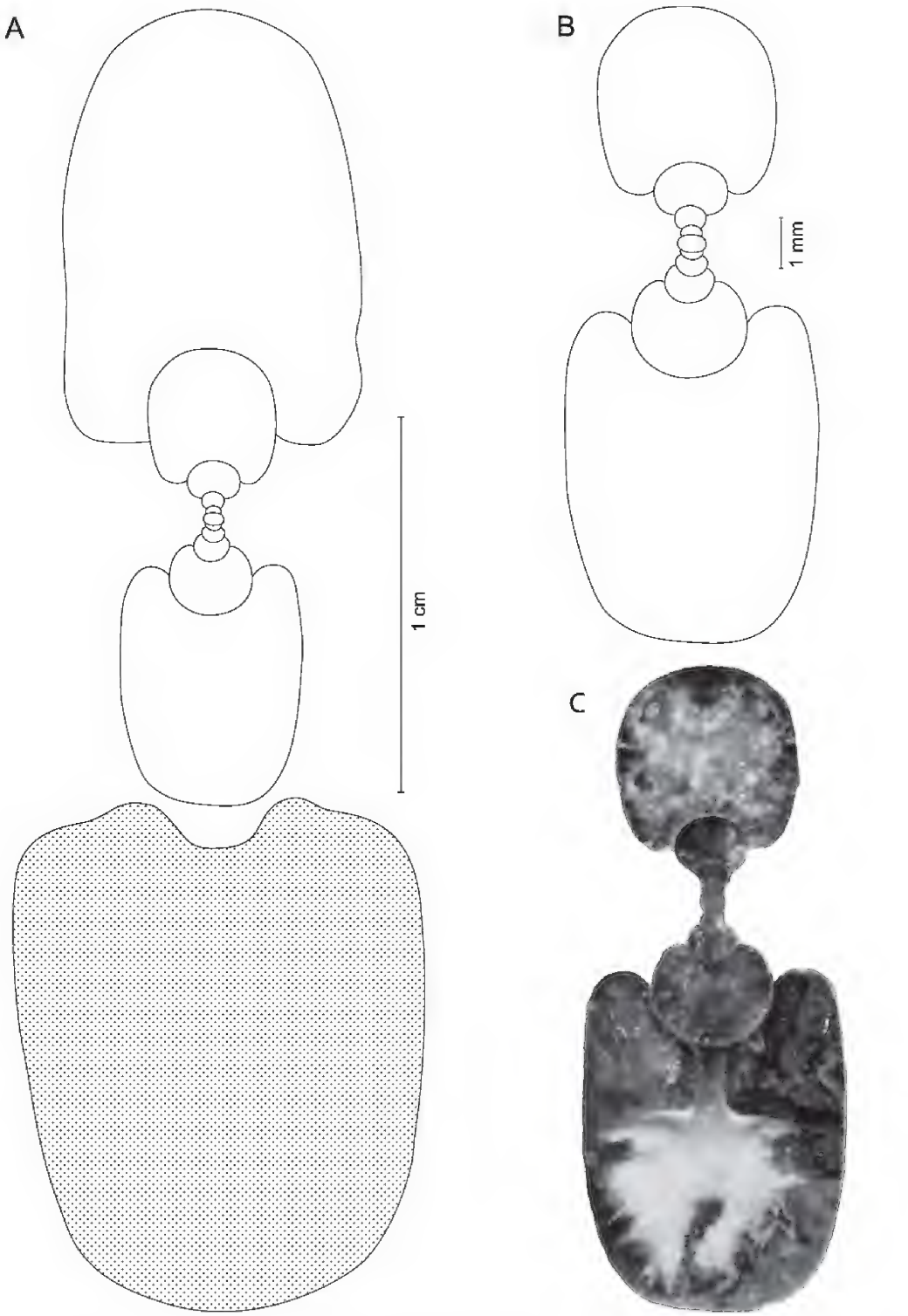

Fig. 111. Dorsoventral cross section through a small microconch of *Hoploscaphites brevis* (Meek, 1876), transitional in morphology to macroconch, BHI 4248, *Baculites compressus–B. cuneatus* zones, Pierre Shale, Meade County, South Dakota. The plane of the cross section approximately coincides with the line of maximum length. **A.** Camera lucida of cross section of the adult shell. The stippled area demarcates the mature body chamber. **B.** Camera lucida of cross section of the inner whorls. **C.** Photo of cross section of the inner whorls. Measurements are listed in appendix 2, table 4.

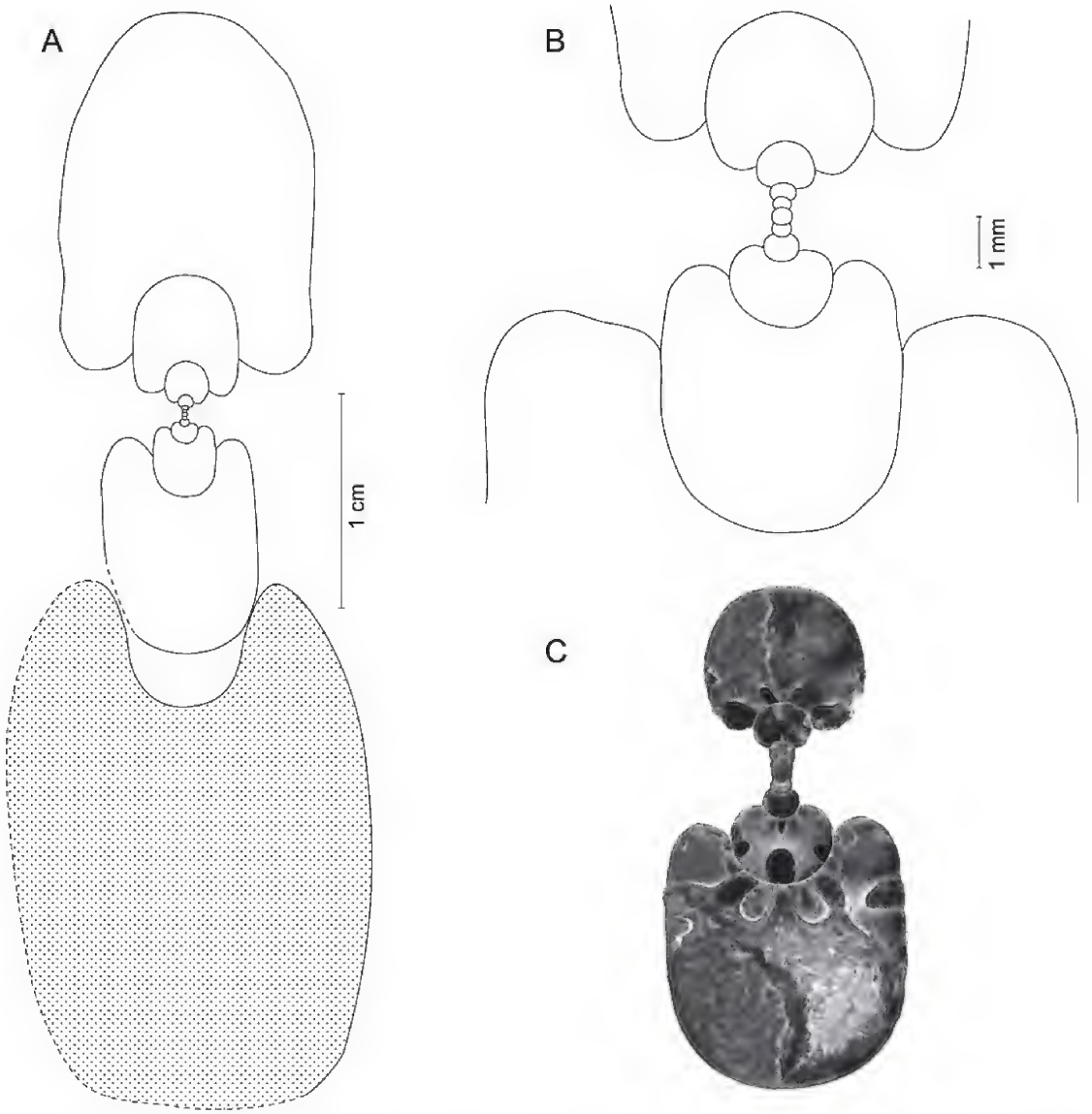

Fig. 112. Dorsoventral cross section through a small microconch of *Hoploscaphites brevis* (Meek, 1876), AMNH 58555, Pierre Shale, Meade or Pennington County, South Dakota. The plane of the cross section approximately coincides with the line of maximum length. **A.** Camera lucida of cross section of the adult shell. The stippled area demarcates the mature body chamber. **B.** Camera lucida of cross section of the inner whorls. **C.** Photo of cross section of the inner whorls. Measurements are listed in appendix 2, table 6.

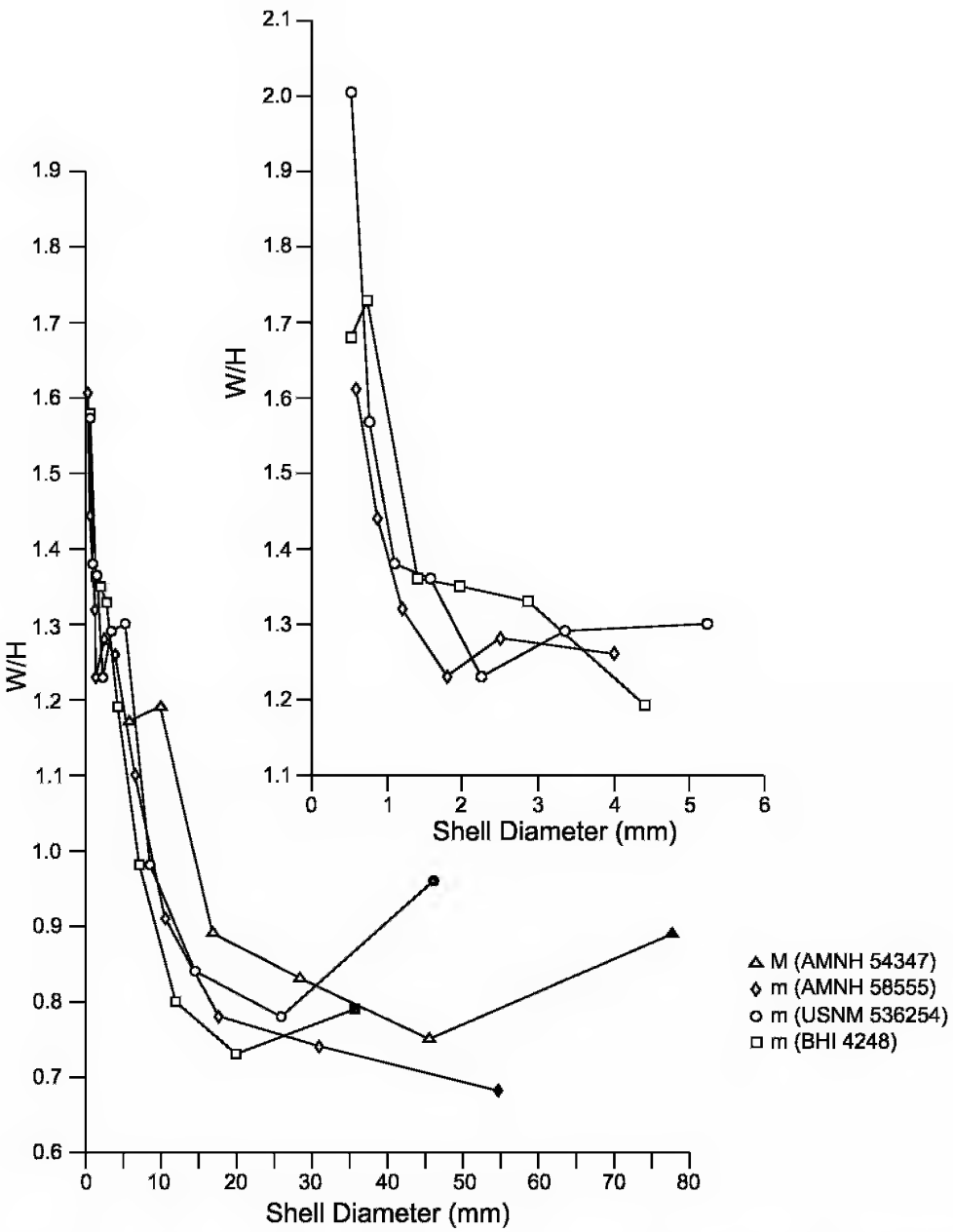

Fig. 113. Plot of the ratio of whorl width to whorl height (W/H) versus shell diameter (mm) in *Hoploscaphites brevis* (Meek, 1876) in early (top graph) and later ontogeny (bottom graph; see figs. 110–112 for illustrations of cross sections on which these graphs are based, and appendix 2, tables 4–6, for a list of measurements). The ratio decreases through most of ontogeny until the beginning of the mature phragmocone, after which it sometimes increases. Filled symbols indicate measurements in the mature body chamber.

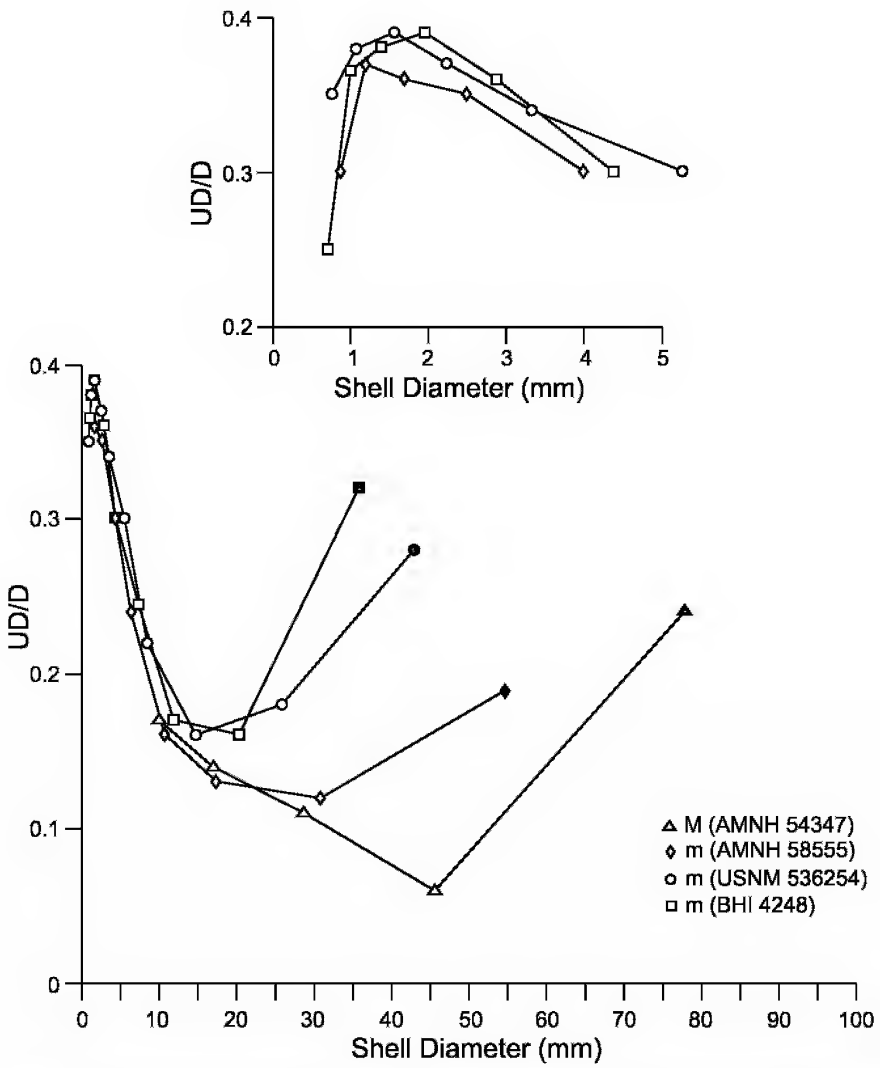

Fig. 114. Plot of the ratio of umbilical diameter to shell diameter (UD/D) versus shell diameter (mm) in *Hoploscaphites brevis* (Meek, 1876) in early (top graph) and later ontogeny (bottom graph; see figs. 110–112 for illustrations of cross sections on which these graphs are based, and appendix 2, tables 4–6, for a list of measurements). The ratio decreases through most of ontogeny until a shell diameter of approximately 10 mm, after which it remains nearly the same until the formation of the mature body chamber. Filled symbols indicate measurements in the mature body chamber.

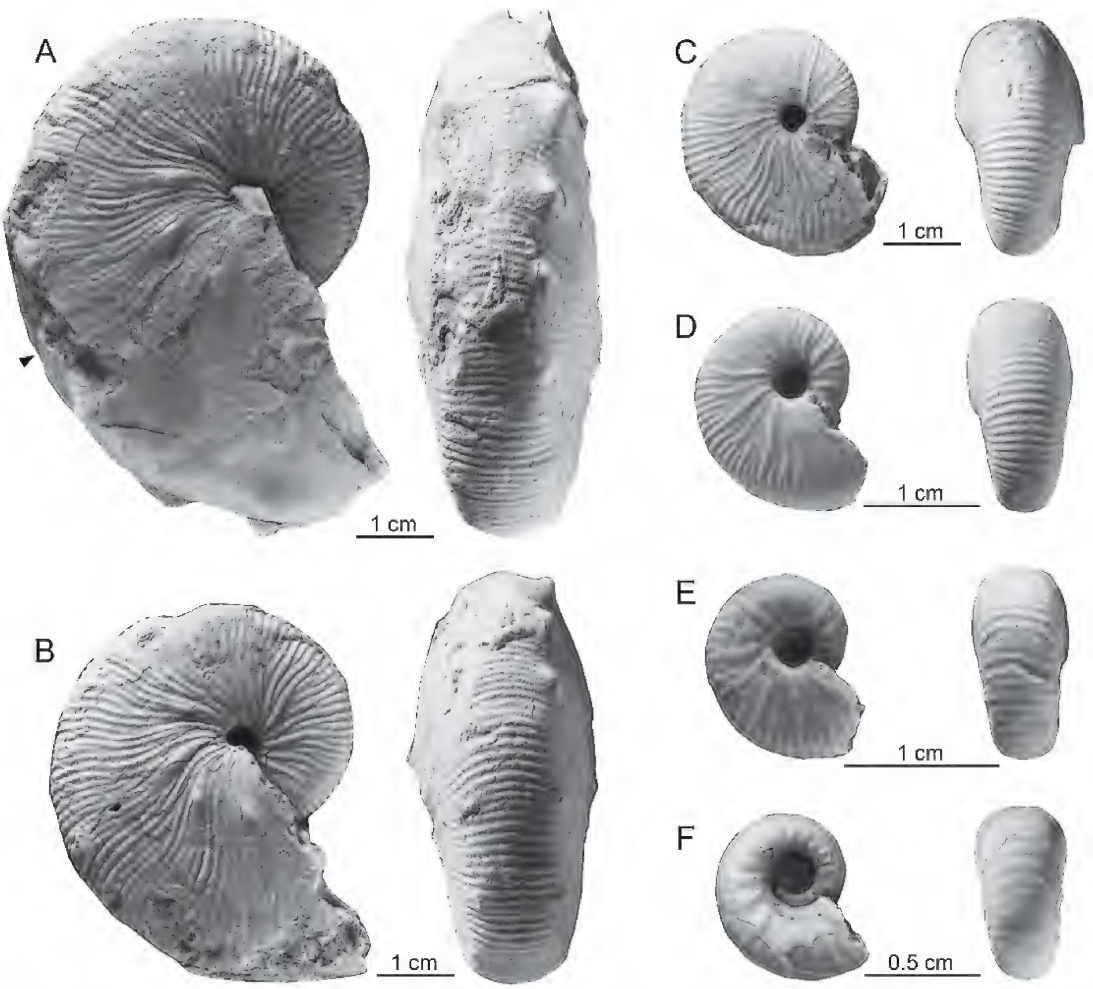

Fig. 115. Ontogenetic breakdown of *Hoploscaphites brevis* (Meek, 1876), macroconch, USNM 536238, locality unknown, but probably Pierre Shale, Meade or Pennington County, South Dakota. **A–F.** Six sizes through ontogeny in lateral and ventral views showing changes in ornamentation from early ontogeny (F) to maturity (A).

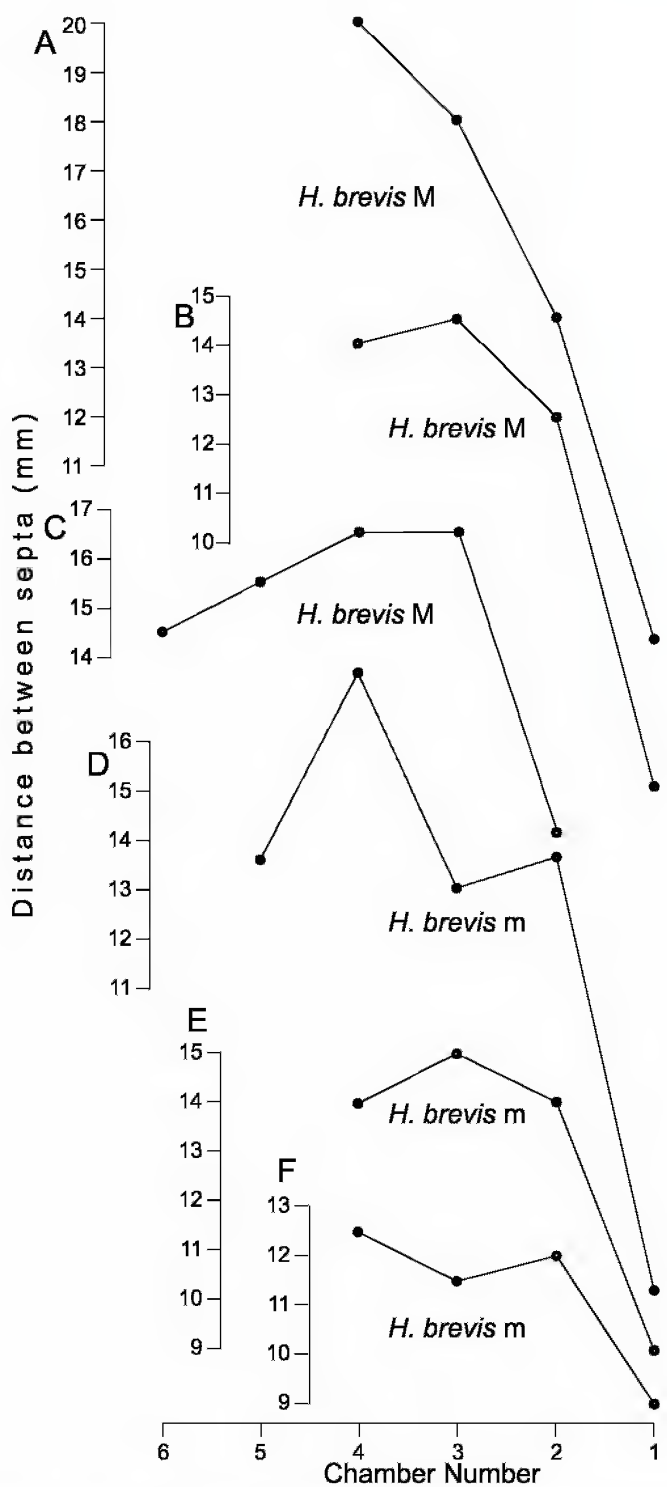

Fig. 116. Septal approximation at maturity in *Hoploscaphites brevis* (Meek, 1876). **A–C.** Macroconchs. **A.** BHI 7034, *Baculites cuneatus* Zone, Pierre Shale, Pennington County, South Dakota. Septal approximation occurs over three chambers and is strong (the interseptal distance of the last chamber is

Hoploscaphites brevis is characterized by a relatively compressed whorl section with flattened flanks, flexuous ribs, and umbilicolateral and ventrolateral tubercles. It differs from the cooccurring species *H. nodosus* in its more compressed whorl section and more flexuous ribs, even in early ontogeny (10–20 mm shell diameter). In addition, the ventrolateral tubercles usually die out at the point of recurvature in *H. brevis*, whereas they extend to the aperture in *H. nodosus*. Outside of North America, *H. brevis* most closely resembles *H. minimus* Błaszkiewicz, 1980, and *H. vistulensis* Błaszkiewicz, 1980, from the Vistula River Valley, Poland. The two nearly complete specimens of *H. minimus* (Błaszkiewicz, 1980: pl. 24, fig. 3; pl. 25, figs. 3, 4) are microconchs and the two specimens of *H. vistulensis* (Błaszkiewicz, 1980: pl. 17, figs. 4, 6, 8, 9) are macroconchs. Both of these species are reported from the *Nostoceras* (*N.*) *hyatti* Zone, which is higher than the biostratigraphic interval containing *H. brevis*. However, similar forms appear in the *Baculites reesidei–B. jenseni* zones in the Western Interior, and we defer further discussion about these species until the completion of our study on the scaphites from these zones.

Several specimens of *Hoploscaphites brevis* contain lower jaws in the adapertural end of the body chamber. In GSC 5342c, a microconch, the left wing of the lower jaw covers more than half of the aperture, with the adapical tip of the jaw touching the dorsal projection of the shell (fig. 29H, I). In BHI 4264, a microconch, the lower jaw is splayed out, butterfly style, with the left wing curled slightly inward (fig. 29A, B). In AMNH 56874, a microconch, the lower jaw is folded together, folio style, and is oriented diagonally across the broken aperture (fig. 29C, D).

OCCURRENCE: *Hoploscaphites brevis* is present in the *Baculites compressus–B. cuneatus* zones in the Western Interior of North America. It is also present in part of the underlying *Didymoceras cheyennense* Zone and in part of the overlying *B. reesidei* Zone, but its exact distribution in these zones is not yet known. *Hoploscaphites brevis* is present in the Bearpaw Shale of Alberta and Saskatchewan, Canada, although the rarity of the closely related species *H. nodosus* in this area is suspicious. In Montana, *H. brevis* occurs in the Bearpaw Shale in Glacier, Chouteau, Meaghar, Blaine, Fergus, Wheatland, Golden Valley, Musselshell, Stillwater, Big Horn, Rosebud, Garfield, Teton, and Valley counties; in the Livingston Formation in Park County; and in the Pierre Shale in Carter County. In North Dakota, it occurs in the Pierre Shale in Barnes County. In South Dakota, it occurs in the Pierre Shale in Butte, Pennington, Custer, Shannon, Meade, Haakon, Ziebach, Mellette, Jones, Stanley, Dewy, Hughes, Lyman, Buffalo, and Brule counties. In Wyoming, it occurs in the Pierre Shale in Weston and Laramie counties. In Colorado, it occurs in the Pierre Shale in Boulder, El Paso, Fremont, Grand, Jackson,

---

←

38% that of the last "normal" chamber). **B.** BHI 4203, *Baculites compressus* Zone, Pierre Shale, Meade County, South Dakota. Septal approximation occurs over two chambers and is strong (the interseptal distance of the last chamber is 34% that of the last "normal" chamber). **C.** BHI 4205, *Baculites compressus* Zone, Pierre Shale, Meade County, South Dakota. Septal approximation occurs over one chamber and is weak (the interseptal distance of the last chamber is 64% that of the last "normal" chamber). This specimen shows a slight pathology. **D–F.** Microconchs. **D.** BHI 4223, *Baculites compressus* Zone, Pierre Shale, Meade County, South Dakota. Septal approximation occurs over one chamber and is strong (the interseptal distance of the last chamber is 35% that of the last "normal" chamber). **E.** BHI 4210, *Baculites compressus* Zone, Pierre Shale, Meade County, South Dakota. Septal approximation occurs over one chamber and is weak (the interseptal distance of the last chamber is 64% that of the last "normal" chamber). **F.** BHI 4211a, *Baculites compressus* Zone, Pierre Shale, Meade County, South Dakota. Septal approximation occurs over one chamber and is weak (the interseptal distance of the last chamber is 75% that of the last "normal" chamber). Measurements are listed in table 1.

Jefferson, Larimer, and Pueblo counties. In Kansas, it is reported from the Weskan Shale and Lake Creek Shale members of the Pierre Shale in Wallace County, but most of the previously illustrated specimens from this area represent forms from the *Baculites reesidei* Zone.

Hoploscaphites brevis, as redescribed here, is absent in the U.S. Gulf and Atlantic Coastal plains and northern Europe, although this may be due to taphonomic reasons. However, forms closely resembling *H. brevis* are present in these areas in strata below and above the biostratigraphic interval containing *H. brevis*, for example, in the *Nostoceras* (*N.*) *hyatti* Zone in New Jersey (Kennedy et al., 2000b). Thus, although *H. brevis* is endemic to the Western Interior of North America, it is part of a more broadly distributed clade.

ACKNOWLEDGMENTS

We thank Peter Harries (University of South Florida, Tampa, Florida), Stephen C. Hook (Socorro, New Mexico), Steven Jorgensen (Denver, Colorado), Kym Larson (Madison, Wisconsin), and Margaret (Peg) Yacobucci (Bowling Green State University, Bowling Green, Ohio) for reviewing an earlier draft of this manuscript and making many valuable suggestions. At the American Museum of Natural History we thank the following individuals for their many years of help on this project: Stephanie Crooms for word-processing the manuscript; Bushra Hussaini for accessioning material, assigning AMNH numbers, and keeping track of loans; Susan Klofak for collecting fossils in the field, preparing and curating specimens, dissecting concretions, breaking down specimens for ontogenetic analysis, and drawing sutures; Mary Knight for editing the manuscript for publication; Kathy Sarg for collecting fossils in the field, measuring specimens, and keeping track of all the material; Stephen Thurston for photographing specimens, preparing figures, and tracing sutures (and, in the past, Portia Rollins and Andrew Modell); and Jamie Newman for X-ray diffraction analysis of samples. Over the years, many students and colleagues have contributed to this project through help in the field or in the lab or both: Jon Allen (Bates College, Lewiston, Maine); Dana Bartolucci (Bryn Mawr College, Bryn Mawr, Pennsylvania); Brett Bennington (Hofstra University, Hempstead, New York); Jay Biederman (AMNH); Sharifah Carter (Kingsborough Community College, Brooklyn, New York); John Chamberlain (Brooklyn College, Brooklyn, New York); Kirk Cochran (Stony Brook University, Stony Brook, New York); Mary Conway (AMNH); Matt Einhorn (Kingsborough Community College, Brooklyn, New York); Tony Frantz (Metropolitan Museum of Art, New York, New York); Matt Garb (Brooklyn College, Brooklyn, New York); James and Joyce Grier (North Dakota State University, Fargo, North Dakota); Peter Harries (University of South Florida, Tampa, Florida); Laura Haug (Hamilton College, Hamilton, New York); Yumiko Iwasaki (AMNH); David Jacobs (University of California, Los Angeles, California); Robert Jenkins (University of Tokyo, Tokyo, Japan); Brian Johnson (Haverford College, Haverford, Pennsylvania); Steven and Susan Jorgensen (Denver, Colorado); Peter Kaplan (Yale University, New Haven, Connecticut); Isabelle Kruta (Muséum National d'Histoire Naturel, Paris, France); Jennifer Lane (New York University, New York, New York); Luke, Lief, Brenda, and Peter Larson, and Marion Zenker (Black Hills Institute of Geological Research, Hill City, South Dakota); Katie Pflaumer (Bryn Mawr College, Bryn Mawr, Pennsylvania); Briana Pobina (Bryn Mawr College, Bryn Mawr, Pennsylvania); Kristen Polizzotto (Kingsborough Community College, Brooklyn, New York); Isabelle Rouget (Université Pierre et Marie Curie, Paris, France); Phil Stoffer (U.S. Geological Survey, Menlo Park, California); Kazushige Tanabe (University of Tokyo, Tokyo, Japan); René Trudel (Korite International and Canada Fossils, Lethbridge, Alberta), Yuki Yoshioka (University of Tokyo, Tokyo, Japan); the late Karl Waage (Yale University, New Haven, Connecticut); David Weinreb (Yale University, New Haven, Connecticut); and Barbara Worcester (AMNH). We thank the following individuals for loans of specimens critical to our study: Ron Brister, Roy Young, Margaret

McNutt, and Louella Weaver (Memphis Pink Palace Museum, Memphis, Tennesee); Talia Karim (University of Kansas Natural History Museum & Biodiversity Research Center, Lawrence, Kansas); Kallie Moore (University of Montana Paleontology Center, Missoula, Montana); Dan Spivak and Brandon Strilisky (Tyrrell Museum of Paleontology, Drumheller, Alberta); Susan Butts, Tim White, and Cope MacClintock (Yale Peabody Museum, New Haven, Connecticut); and Jann Thompson and Dan Levin (National Museum of Natural History, Washington, D.C.). We thank Rachel Benton (Badlands National Park, South Dakota) for arranging permits to collect on park property. Several people have generously donated specimens for our study in addition to having helped in the field: Japh Boyce (Rapid City, South Dakota); Jamie Brezina (Rapid City, South Dakota); Amy and Barry Brown (Curaçao, Venezuela); Tom Linn (Rapid City, South Dakota); Jim Michaud (Rapid City, South Dakota); and Pierre Paré (Korite International and Canada Fossils, Calgary, Alberta). We especially thank Jamie Brezina who discovered the methane seeps from the *D. cheyennense* and *B. compressus* zones in South Dakota, and shared his discovery with us. We are indebted to the following landowners for permission to collect on their property and for their kindness and hospitality on hot summer afternoons: Don Cameron (Manager, Sun Coulee Cattle Co., Ingomar, Montana), John and Kathy Green (Newell, South Dakota), Pierre Paré and René Trudel (Korite International and Canada Fossils, Lethbridge and Calgary, Alberta), Tom and Sheila Trask and their family (Elm Creek, South Dakota), and many, many other landowners who have allowed us access to their property over the past 35 years. We thank K.C. McKinney (U.S. Geological Survey, Denver, Colorado) for help in using the U.S.G.S. collections and retrieving locality data. NHL gratefully acknowledges the support of Nathalie Quay, the Norman D. Newell Fund at the AMNH, and NSF Grant EAR 0308926. Several students have also been supported by the Program for Research Experiences for Undergraduates (NSF Grant DBI 0850543 to Mark Siddall, AMNH).

REFERENCES

Allison, P.A. 1990. Carbonate nodules and plattenkalks. *In* D.E.G. Briggs and P.R. Crowther (editors), Palaeobiology—a synthesis: 250–253. Oxford: Blackwell Science Publications.

Arkell, W.J., B. Kummel, and C.W. Wright. 1957. Mesozoic Ammonoidea. *In* R.C. Moore (editor), Treatise on invertebrate paleontology. Part L, Mollusca 4: 80–465. Lawrence, KS: Geological Society of America.

Arnold, J.M. 1987. Reproduction and embryology of *Nautilus*. *In* W.B. Saunders and N.H. Landman (editors), *Nautilus:* the biology and paleobiology of a living fossil: 353–372. New York: Plenum.

Atabekyan, A.A., and F.K. Khakimov. 1976. Kampanskie i Maastrikhtskie ammonity Srednei Azii (Campanian and Maastrichtian ammonites in Central Asia). Dushanbe: Izd-vo "Donish, 146 pp. [in Russian]

Baadsgaard, H., J.F. Lerbekmo, and J.R. Wijbrans. 1993. Multimethod radiometric age for a bentonite near the top of the *Baculites reesidei* Zone of southwestern Saskatchewan (Campanian-Maastrichtian stage boundary?). Canadian Journal of Earth Sciences 30: 769–775.

Barbour, E.H. 1903. Report of the state geologist. Nebraska Geological Survey 1: 1–258.

Batt, R.J. 1989. Ammonite shell morphotype distribution in the Western Interior Greenhorn Sea and some paleoecological implications. Palaios 4: 32–42.

Beauchamp, B., and M. Savard. 1992. Cretaceous chemosynthetic carbonate mounds in the Canadian Arctic. Palaios 7: 434–450.

Berner, R.A. 1968. Calcium carbonate concretions formed by the decomposition of organic matter. Science 159: 195–197.

Birkelund, T. 1965. Ammonites from the Upper Cretaceous of West Greenland. Meddelelser om Grønland 179 (7): 1–192.

Birkelund, T. 1966. Die Entwicklung der jüngsten Scaphiten und ihre stratigraphische Bedeutung im baltischen Gebiet. Berichte Deutschen Gesellschaft Geologische Wissenschaften, Reike A, Geologie und Paläontologie 11 (6): 737–744.

Birkelund, T. 1979. The last Maastrichtian ammonites. *In* T. Birkelund and R.C. Bromley (editors), Cretaceous-Tertiary Boundary Events Symposium. I, the Maastrichtian and Danian of Denmark: 51–57, University of Copenhagen.

Bishop, G.A. 2000. Fossil crabs from Tepee Buttes, submarine seeps of the Late Cretaceous Pierre Shale, South Dakota and Colorado, USA. Journal of Crustacean Biology 20: 286–300.

Black, D.F.B. 1964. Geology of the Bridger area west-central South Dakota. South Dakota State Geological Survey Report of Investigations 92: 1–17.

Błaszkiewicz, A. 1980. Campanian and Maastrichtian ammonites of the Middle Vistula River Valley, Poland. A stratigraphic-paleontological study. Prace Instytutu Geologicznego 92: 1–63.

Bond, P.N., and W.B. Saunders. 1989. Sublethal injury and shell repair in Upper Mississippian ammonoids. Paleobiology 15 (4): 414–428.

Brown, R.A.C. 1943. Preliminary study of "*Acanthoscaphites*" *nodosus* in the Upper Cretaceous of Western Canada. Unpublished master's thesis, University of Toronto: 1–39.

Bucher, H. 1992. Ammonoids of the *Shoshonensis* Zone (Middle Anisian, Middle Triassic) from northwestern Nevada (USA). Jahrbuch der Geologischen Bundesanstalt 135 (2): 425–465.

Bucher, H., N.H. Landman, S.M. Klofak, and J. Guex. 1996. Mode and rate of growth in ammonoids. *In* N.H. Landman, K. Tanabe, and R.A. Davis (editors), Ammonoid paleobiology: 407–461. New York: Plenum.

Byers, C.W. 1979. Biogenic structures of black shale paleoenvironments. Postilla 174: 1–43.

Caldwell, W.G.E. 1968. The Late Cretaceous Bearpaw Formation in the south Saskatchewan River Valley. Saskatchewan Research Council Geology Division Report 8: 1–86.

Callomon, J.H. 1988. [Review of] Matyja, B.A., 1986, Developmental polymorphism in Oxfordian ammonites. Acta Geologica Polonica 36: 37–68. Cephalopod Newsletter 9: 14–16.

Carpenter, S.J., J.M. Erickson, K.C. Lohmann, and M.R. Owen. 1988. Diagenesis of fossiliferous concretions from the Upper Cretaceous Fox Hills Formation, North Dakota. Journal of Sedimentary Petrology 58 (4): 706–723.

Case, G.R. 1982. A pictorial guide to fossils. New York: Van Nostrand Reinhold, 515 pp.

Case, G.R. 1992. A pictorial guide to fossils. Malabar, FL: Krieger, 514 pp.

Chamberlin, T.C., and R.D. Salisbury. 1907. Geology. Vol. 3. Earth History. 2nd ed., revised. New York: Henry Holt, 624 pp.

Chandler, R., and J. Callomon. 2009. The Inferior Oolite at Coombe Quarry, near Mapperton, Dorset, and a new Middle Jurassic ammonite faunal horizon, Aa-3b, *Leioceras comptocostosum* n. biosp. in the Scissum Zone of the lower Aalenian. Proceedings of the Dorset Natural History and Achaeological Society 130: 99–132.

Checa, A., and D. Martin-Ramos. 1989. Growth and function of spines in the Jurassic ammonite *Aspidoceras*. Palaeontology (London) 32: 645–655.

Cobban, W.A. 1951a. New species of *Baculites* from the Upper Cretaceous of Montana and South Dakota. Journal of Paleontology 25 (6): 817–821.

Cobban, W.A. 1951b. Scaphitid cephalopods of the Colorado Group. U.S. Geological Survey Professional Paper 239: 1–42.

Cobban, W.A. 1958a. Late Cretaceous fossil zones of the Powder River Basin, Wyoming and Montana. Wyoming Geological Association Guidebook, 13th Annual Field Conference: 114–119.

Cobban, W.A. 1958b. Two new species of *Baculites* from the Western Interior region. Journal of Paleontology 32 (4): 660–665.

Cobban, W.A. 1962a. New *Baculites* from the Bearpaw Shale and equivalent rocks of the Western Interior. Journal of Paleontology 36 (1): 126–135.

Cobban, W.A. 1962b. *Baculites* from the lower part of the Pierre Shale and equivalent rocks in the Western Interior. Journal of Paleontology 36 (4): 704–718.

Cobban, W.A. 1969. The Late Cretaceous ammonites *Scaphites leei* Reeside and *Scaphites hippocrepis* (DeKay) in the Western Interior of the United States. U.S. Geological Survey Professional Paper 619: 1–27.

Cobban, W.A. 1974. Ammonites from the Navesink Formation at Atlantic Highlands, New Jersey. U.S. Geological Survey Professional Paper 845: 1–20.

Cobban, W.A., and S.C. Hook. 1979. *Collignoniceras woollgari woollgari* (Mantell) ammonite fauna from Upper Cretaceous of Western Interior, United States. New Mexico Bureau of Mines and Mineral Resources Memoir 37: 1–51.

Cobban, W.A., and J.A. Jeletzky. 1965. A new scaphite from the Campanian rocks of the Western Interior of North America. Journal of Paleontology 39 (5): 794–801.

Cobban, W.A., and W.J. Kennedy. 1992. Campanian *Trachyscaphites spiniger* ammonite fauna in northeast Texas. Palaeontology 35 (1): 63–93.

Cobban, W.A., and W.J. Kennedy. 1994. Upper Cretaceous ammonites from the Coon Creek Tongue of the Ripley Formation at its type locality in McNairy County, Tennessee. U.S. Geological Survey Bulletin 2073-B: B1–B12.

Cobban, W.A., W.J. Kennedy, and G.R. Scott. 1992. Upper Cretaceous heteromorph ammonites from the *Baculites compressus* Zone of the Pierre Shale in north-central Colorado. U.S. Geological Survey Bulletin 2024: A1–A11.

Cobban, W.A., and N.L. Larson. 1997. Marine Upper Cretaceous rocks and their ammonite record along the northern flank of the Black Hills uplift, Montana, Wyoming, and South

Dakota. Contributions to Geology, University of Wyoming 32 (1): 27–35.

Cobban, W.A., E.A. Merewether, T.D. Fouch, and J.D. Obradovich. 1994. Some Cretaceous shorelines in the Western Interior of the United States. *In* M.V. Caputo, J.A. Peterson, and K.J. Franczyk (editors), Mesozoic systems of the Rocky Mountain region, USA: 393–413. Denver, CO: Rocky Mountain Section of Society for Sedimentary Geology.

Cobban, W.A., and J.B. Reeside, Jr. 1952. Correlation of the Cretaceous formations of the Western Interior of the United States. Bulletin of the Geological Society of America 63: 1011–1044.

Cobban, W.A., and G.R. Scott. 1964. Multinodose scaphitid cephalopods from the lower part of the Pierre Shale and equivalent rocks in the conterminous United States. U.S. Geological Survey Professional Paper 483-E: E1–E13.

Cobban, W.A., I. Walaszczyk, J.D. Obradovich, and K.C. McKinney. 2006. A USGS zonal table for the Upper Cretaceous Middle Cenomanian–Maastrichtian of the Western Interior of the United States based on ammonites, inoceramids, and radiometric ages. U.S. Geological Survey Open-File Report 2006-1250: 1–46.

Cochran, J.K., N.H. Landman, K.K. Turekian, A. Michard, and D.P. Shrag. 2003. Paleoceanography of the Late Cretaceous (Maastrichtian) Western Interior seaway of North America: evidence from Sr and O isotopes. Palaeogeography Palaeoclimatology Palaeoecology 191: 45–64.

Cochran, J.K., et al. 2010. Effect of diagenesis on the Sr, O, and C isotopic composition of Late Cretaceous mollusks from the Western Interior of North America. American Journal of Science 310: 69–88.

Collins, D., and P.D. Ward. 1987. Adolescent growth and maturity in *Nautilus*. *In* W.B. Saunders and N.H. Landman (editors), *Nautilus:* the biology and paleobiology of a living fossil: 421–432. New York: Plenum.

Conrad, T.A. 1858. Observations on a group of Cretaceous fossil shells found in Tippah County, Mississippi, with descriptions of fifty-six new species. Journal of the Academy of Natural Sciences of Philadelphia, 2nd ser. 3: 323–336.

Cooper, M.R. 1990. A revision of the Scaphitidae (Cretaceous Ammonoidea) from the Cambridge Greensand. Neues Jahrbuch für Geologie und Paläontologie Abhandlungen 178 (3): 285–308.

Cooper, M.R. 1994. Towards a phylogenetic classification of the Cretaceous ammonites. III. Scaphitaceae. Neues Jahrbuch für Geologie und Paläontologie Abhandlungen 193 (2): 165–193.

Coryell, H.N., and E.S. Salmon. 1934. A molluscan faunule from the Pierre Formation in eastern Montana. American Museum Novitates 746: 1–18.

Crandell, D.R. 1958. Geology of the Pierre area, South Dakota. U.S. Geological Survey Professional Paper 307: 1–83.

Crick, R.E. 1978. Morphological variations in the ammonite *Scaphites* of the Blue Hill Member, Carlile Shale, Upper Cretaceous, Kansas. University of Kansas Paleontological Contributions Paper 88: 1–28.

Cross, T.A., and R.H. Pilger, Jr. 1978. Tectonic controls of late Cretaceous sedimentation, Western Interior, USA. Nature 274: 653–657.

Cuvier, G. 1797. Tableau élémentaire de l'histoire naturelle des animaux. Paris: Baudouin, xvi, 710 pp.

Dagys, A., and W. Weitschat. 1993. Extensive intraspecific variation in a Triassic ammonoid from Siberia. Lethaia 26: 113–121.

Davis, R.A., N.H. Landman, J.-L. Dommergues, D. Marchand, and H. Bucher. 1996. Mature modifications and dimorphism in ammonoid cephalopods. *In* N.H. Landman, K. Tanabe, and R.A. Davis (editors), Ammonoid paleobiology: 463–539. New York: Plenum.

DeKay, J.E. 1827. Report on several multilocular shells from the State of Delaware; with observations of a second specimen of the new fossil genus *Eurypterus*. Annals of the Lyceum of Natural History of New York 2: 273–279.

Diener, C. 1916. Bemerkungen zur Nomenklatur der Gattung *Scaphites*. Zentralblatt für Mineralogie, Geologie und Paläontologie 1916: 525–529.

Dobbin, C.E., and C.E. Erdmann. 1955. Structure contour map of the Montana plains. U.S. Geological Survey Oil and Gas Investigations Map OM 178 B.

Doguzhaeva, L., and H. Mutvei. 1996. Attachment of the body to the shell in ammonoids. *In* Landman, N.H., K. Tanabe, and R.A. Davis (editors), Ammonoid paleobiology: 43–63. New York: Plenum.

Donovan, D.T. 1953. The Jurassic and Cretaceous stratigraphy and paleontology of Traill, Ø, East Greenland. Meddelelser om Grønland 3 (4): 1–150.

Dowling, D.B. 1917. The southern plains of Alberta. Geological Survey of Canada Memoir 93: 1–200.

Dunbar, C.O. 1928. On an ammonite shell investing commensal Bryozoa. American Journal of Science (5th series) 16 (92): 164–165.

Dunbar, C.O. 1949. Historical geology. New York: Wiley, 567 pp.

Dunbar, C.O. 1960. Historical geology. 2nd ed. New York: Wiley, 500 pp.

Dzik, J. 1985. Typologic versus population concepts of chronospecies: implications for ammonite biostratigraphy. Acta Palaeontologica Polonica 30: 71–91.

Easton, W.H. 1960. Invertebrate paleontology. New York: Harper, 701 pp.

Elias, M.K. 1933. Cephalopods of the Pierre Formation of Wallace County, Kansas, and adjacent area. University of Kansas Science Bulletin 21 (9): 289–363.

Emerson, B.L., J.H. Emerson, R.E. Akers, and T.J. Akers. 1994. Texas Cretaceous ammonites and nautiloids. Texas Paleontology Series Publication 5: 1–439.

Engeser, T., and H. Keupp. 2002. Phylogeny of aptychi-possessing Neoammonoidea (Aptychophora nov., Cephalopoda). Lethaia 24: 79–96.

Evans, J., and B.F. Shumard. 1857. On some new species of fossils from Cretaceous formations of Nebraska Territory. Transactions of the Academy of Natural Sciences of Saint Louis 1: 38–42.

Feldmann, R.M. 1972. Stratigraphy and paleoecology of the Fox Hills Formation (Upper Cretaceous) of North Dakota. Bulletin of the North Dakota Geological Survey: 61–65.

Fenneman, N.M. 1931. Physiography of western United States. New York: McGraw-Hill, 714 pp.

Fisher, S.P. 1952. The geology of Emmons County, North Dakota. North Dakota Geological Survey Bulletin 26: 1–47.

Forester, R.W., W.G.E. Caldwell, and F.H. Oro. 1977. Oxygen and carbon isotopic study of ammonites from the Late Cretaceous Bearpaw Formation in southwestern Saskatchewan. Canadian Journal of Earth Sciences 14 (9): 2086–2100.

Fortey, R. 1982. Fossils: the key to the past. New York: Van Nostrand Reinhold, 172 pp.

Fortey, R. 1991. Fossils: the key to the past. New ed. Cambridge, MA: Harvard University Press, 187 pp.

Foster, M. 1994. Strange genius: the life of Ferdinand Vandeveer Hayden. Niwot, CO: Roberts Rinehart, 443 pp.

Fox, J.E. 2007. Mollusks from the late Campanian upper DeGrey Formation of the Pierre Shale group, Missouri River Valley, central South Dakota. *In* J.C. Martin and D.C. Parris (editors), The geology and paleontology of the Late Cretaceous marine deposits of the Dakotas. Geological Society of America Special Paper 427: 85–98.

Fraser, F.J., F.H. McLearn, L.S. Russell, P.S. Warren, and R.T.D. Wickenden. 1935. Geology of southern Saskatchewan. Geological Survey of Canada Memoir 176: 1–137.

Frech, F. 1915. Über *Scaphites*. I. Die Bedeutung von *Scaphites* für die Gliederung der Oberkreide. Zentralblatt für Mineralogie Geologie und Paläontologie 1915: 553–568.

Gautier, D.L. 1982. Siderite concretions: indicators of early diagenesis in the Gammon Shale (Cretaceous). Journal of Sedimentary Petrology 52 (3): 859–871.

Gilbert, G.K. 1896. The underground water of the Arkansas Valley in eastern Colorado. U.S. Geological Survey Annual Report 17 (2): 551–601.

Gilbert, G.K., and F.R. Gulliver. 1895. Tepee Buttes. Geological Society of America Bulletin 6: 333–342.

Gill, J.R., and W.A. Cobban. 1966. The Red Bird section of the Upper Cretaceous Pierre Shale in Wyoming. U.S. Geological Survey Professional Paper 393-A: 1–73.

Gill, J.R., and W.A. Cobban. 1973. Stratigraphy and geologic history of the Montana group and equivalent rocks, Montana, Wyoming, and North and South Dakota. U.S. Geological Survey Professional Paper 776: 1–37.

Gill, J.R., W.A. Cobban, and L.G. Schultz. 1972. Correlation, ammonite zonation, and a reference section for the Montana group, central Montana. *In* Montana Geological Society Guidebook, 21st Annual Field Conference, Crazy Mountains Basin, 1972: 91–97.

Gill, J.R., E.A. Merewether, and W.A. Cobban. 1970. Stratigraphy and nomenclature of some Upper Cretaceous and Lower Tertiary rocks in south-central Wyoming. U.S. Geological Survey Professional Paper 667: 1–53.

Gill, T. 1871. Arrangement of the families of mollusks. Smithsonian Miscellaneous Collections 227: 1–49.

Goetzmann, W.H. 1966. Exploration and empire. New York: Knopf.

Grabau, A.W. 1921. A textbook of geology. Part II: historical geology. New York: D.C. Heath, 976 pp.

Grabau, A.W., and H.W. Shimer. 1910. North American index fossils: invertebrates. Vol. 2. New York: A.G. Seiler, 909 pp.

Guex, J. 1967. Contribution à l'étude des blessures chez les ammonites. Bulletin des Laboratoires de Géologie, Minéralogie, Géophysique et du Musée Géologique de l'Université de Lausanne 165: 1–16.

Guex, J. 1968. Sur deux conséquences particulières des traumatismes du manteau des ammonites. Bulletin des Laboratoires de Géologie, Minéralogie, Géophysique et du Musée Géologique de l'Université de Lausanne 175: 1–6.

Guex, J., A. Koch, and H. Bucher. 2003. A morphogenetic explanation of Buckman's law

of covariation. Bulletin Société Géologique de France 174 (6): 603–606.

Gupta, N.S., D.E.G. Briggs, N.H. Landman, K. Tanabe, and R.E. Summons. 2008. Molecular structure of organic components in cephalopods: evidence for oxidative cross linking in fossil marine invertebrates. Organic Geochemistry 39 (2008): 1405–1414.

Haas, O. 1946. Intraspecific variation in and ontogeny of *Prionotropis woollgari* and *Prionocyclus wyomingensis*. Bulletin of the American Museum of Natural History 86 (4): 141–224.

Hall, J., and F.B. Meek. 1856. Description of new species of fossils, from the Cretaceous formations of Nebraska, with observations upon *Baculites ovatus* and *B. compressus*, and the progressive development of the septa in *Baculites*, *Ammonites*, and *Scaphites*. Memoirs of the American Academy of Arts and Sciences New Series 5: 379–411.

Hamilton, W.R., A.R. Woolley, and A.C. Bishop. 1974. The Larousse guide to minerals, rocks and fossils. New York: Larousse, 320 pp.

Hammer, Ø., and H. Bucher. 2005. Buckman's first law of covariation—a case of proportionality. Lethaia 38: 67–72.

Hanlon, R.T., and J.B. Messenger. 1996. Cephalopod behaviour. New York: Cambridge University Press.

Hanczaryk, P.A., and W.B. Gallagher. 2007. Stratigraphy and paleoecology of the middle Pierre Shale along the Missouri River, central South Dakota. *In* J.C. Martin and D.C. Parris (editors), The geology and paleontology of the Late Cretaceous marine deposits of the Dakotas. Geological Society of America Special Paper 427: 51–69.

Hartman, J.H. 1984. Systematics, biostratigraphy, and biogeography of latest Cretaceous and early Tertiary Viviparidae (Mollusca, Gastropoda) of southern Saskatchewan, western North Dakota, eastern Montana, and northern Wyoming. Unpublished Ph.D. dissertation, University of Minnesota, 928 pp.

Hartman, J.H. 1999. Western exploration along the Missouri River and the first paleontological studies in the Williston Basin, North Dakota and Montana. Proceedings of the North Dakota Academy of Science, Paleontology and Geology Symposium 53: 158–165.

Haug, E. 1911. Traité de géologie. Les périodes géologiques. Paris: Armand Colin.

He, S., T.K. Kyser, and W.G.E. Caldwell. 2005. Paleoenvironment of the Western Interior Seaway inferred from $\delta^{18}O$ and $\delta^{13}C$ values of molluscs from the Cretaceous Bearpaw marine cyclothem. Palaeogeography Palaeoclimatology Palaeoecology 217: 67–85.

Hengsbach, R. 1996. Ammonoid pathology. *In* N.H. Landman, K. Tanabe, and R.A. Davis (editors), Ammonoid paleobiology: 581–605. New York: Plenum.

Hewitt, R.A. 1996. Architecture and strength of the ammonoid shell. *In* N.H. Landman, K. Tanabe, and R.A. Davis (editors), Ammonoid paleobiology: 297–339. New York: Plenum.

Hind, H.Y. 1859. North West Territory. Reports of progress; together with a preliminary and general report on the Assiniboine and Saskatchewan Exploring Expedition, made under instructions from the Provincial Secretary, Canada: 1–201. Toronto: J. Lovell.

Hirsch, K.F. 1975. Die Ammoniten des Pierre Meeres (Oberkreide) in den westlichen USA. Aufschluss 26 (3): 102–113.

Hölder, H. 1956. Über Anomalien an jurassischen Ammoniten. Paläontologische Zeitschrift 30 (1/2): 95–107.

House, M.R. 1987. Geographic distribution of *Nautilus* shells. *In* W.B. Saunders and N.H. Landman (editors), *Nautilus*: the biology and paleobiology of a living fossil: 53–64. New York: Plenum.

Howe, B. 1987. Tepee buttes: a petrological, paleontological, and paleoenvironmental study of Cretaceous submarine spring deposits. Unpublished master's thesis, University of Colorado, Boulder, 218 pp.

Hyatt, A. 1894. Phylogeny of an acquired characteristic. Proceedings of the American Philosophical Society 32 (143): 349–647.

Izett, G.A., and G.S.V. Barclay. 1973. Geologic map of the Kremmling quadrangle, Grand County, Colorado. U.S. Geologic Quadrangle Map GQ-1115, scale 1:24,000.

Izett, G.A., W.A. Cobban, G.B. Dalrymple, and J.D. Obradovich. 1998. $^{40}Ar/^{39}Ar$ age of the Manson impact structure, Iowa, and correlative impact ejecta in the Crow Creek Member of the Pierre Shale (Upper Cretaceous), South Dakota and Nebraska. Geological Society of America Bulletin 110: 361–376.

Izett, G.A., W.A. Cobban, and J.R. Gill. 1971. The Pierre Shale near Kremmling, Colorado, and its correlation to the east and the west. U.S. Geological Survey Professional Paper 684-A: 1–19.

Jacobs, D. 1992. Shape, drag, and power in ammonoid swimming. Paleobiology 18 (2): 203–220.

Jacobs, D.K., and J.A. Chamberlain, Jr. 1996. Buoyancy and hydrodynamics in ammonoids. *In* N.H. Landman, K. Tanabe, and R.A. Davis (editors), Ammonoid paleobiology: 169–224. New York: Plenum.

Jacobs, D.K., and N.H. Landman. 1993. Is *Nautilus* a good model for the function and behavior of ammonoids? Lethaia 26: 1–12.

Jacobs, D.K., N.H. Landman, and J.A. Chamberlain, Jr. 1994. Ammonite shell shape covaries with facies and hydrodynamics: iterative evolution as a response to changes in basinal environment. Geology 22: 905–908.

Jagt, J.W.M., W.J. Kennedy, and M. Machalski. 1999. Giant scaphitid ammonites from the Maastrichtian of Europe. Bulletin de l'Institut Royal des Sciences Naturelles de Belgique Sciences de la Terre 69: 133–154.

Jeletzky, J.A. 1960. Youngest marine rocks in Western Interior of North America and the age of the *Triceratops*-beds, with remarks on comparable dinosaur-bearing beds outside North America. Twenty-first International Geological Congress, Copenhagen, Report 5: 25–40.

Jeletzky, J.A. 1962. Study of *Scaphites* fauna from the Bearpaw Formation of Alberta and Saskatchewan. Geological Survey of Canada Paper 62-3: 1–4.

Jeletzky, J.A. 1968. Macrofossil zones of the marine Cretaceous of the Western Interior of Canada and their correlation with the zones and stages of Europe and the Western Interior of the United States. Geological Survey of Canada Paper 67-72: 1–66.

Jeletzky, J.A. 1970. Cretaceous macrofaunas. *In* Geology and economic minerals of Canada. Pt. B, Economic Geology Report 1: 649–662.

Jeletzky, J.A. 1971. Marine Cretaceous biotic provinces and paleogeography of western and arctic Canada: illustrated by a detailed study of ammonites. Geological Survey of Canada Paper 70-22: 1–92.

Jeletzky, J.A., and K.M. Waage. 1978. Revision of *Ammonites conradi* Morton 1834, and the concept of *Discoscaphites* Meek 1870. Journal of Paleontology 52 (5): 1119–1132.

Jensen, F.S., and H.D. Varnes. 1964. Geology of the Fort Peck area, Garfield, McCone and Valley Counties, Montana. U.S. Geological Survey Professional Paper 414-F: 1–49.

Jerzykiewicz, T. 1996. *Baculites compressus robinsoni* Cobban from the Crowsnest River section at Lundbreck, Alberta: an implication for the timing of the late Cretaceous Bearpaw transgression into the southern foothills of Alberta. Geological Survey of Canada, Current Research 1996-E: 97–100.

Jorgensen, S.D., and N.L. Larson. In prep. Ammonites and sharks of the Upper Cretaceous (Turonian) Carlile Shale of eastern South Dakota: with biostratigraphic correlations to the Black Hills region, South Dakota and Wyoming. Rocky Mountain Geology.

Kakabadzė, M.V., and M.Z. Sharikadzė. 1993. On the mode of life of heteromorph ammonoids (heterocone, ancylocone, ptychocone). *In* S. Elmi, C. Mangold, and Y. Almares (editors), 3ème symposium international: céphalopodes actuels et fossiles. Geobios Mémoire Spécial 15: 209–215.

Kaplan, U., W.J. Kennedy, and M. Hiß. 2005. Stratigraphie und Ammonitenfaunen des Campan im nordwestlichen und zentralen Münsterland. Geologie und Paläontologie in Westfalen 64: 1–171.

Kase, T., P.A. Johnston, A. Seilacher, and J.B. Boyce. 1998. Alleged mosasaur bite marks on Late Cretaceous ammonites are limpet (patellogastropod) home scars. Geology 26 (10): 947–950.

Kauffman, E.G. 1977. Illustrated guide to biostratigraphically important Cretaceous macrofossils, Western Interior Basin, USA. Mountain Geologist 14 (3–4): 225–274.

Kauffman, E.G. 1984. Paleobiogeography and evolutionary response dynamic in the Cretaceous Western Interior Seaway of North America. *In* G.E.G. Westermann (editor), Jurassic-Cretaceous biochronology and palaeogeography of North America. Geological Association of Canada Special Paper 27: 273–306.

Kauffman, E.G., M.A. Arthur, B. Howe, and P.A. Scholle. 1996. Widespread venting of methane-rich fluids in Late Cretaceous (Campanian) submarine springs (Tepee Buttes), Western Interior seaway, U.S.A. Geology 24: 799–802.

Kauffman, E.G., and W.G.E. Caldwell. 1993. The Western Interior Basin in space and time. *In* W.G.E. Caldwell and E.G. Kauffman (editors), Evolution of the Western Interior Basin. Geological Association of Canada Special Paper 39: 1–30.

Kauffman, E.G., et al. 1993. Molluscan biostratigraphy of the Cretaceous Western Interior Basin, North America. *In* W.G.E. Caldwell and E.G. Kauffman (editors), Evolution of the Western Interior Basin. Geological Association of Canada Special Paper 39: 397–434.

Kear, A.J., D.E.G. Briggs, and D.T. Donovan. 1995. Decay and fossilization of non-mineralized tissue in coleoid cephalopods. Palaeontology 38 (1): 105–131.

Kennedy, W.J. 1984. Systematic paleontology and stratigraphic distribution of the faunas of the French Coniacian. Special Papers in Palaeontology 31: 1–160.

Kennedy, W.J. 1986a. Campanian and Maastrichtian ammonites from northern Aquitaine, France. Special Papers in Palaeontology 36: 1–145.

Kennedy, W.J. 1986b. The ammonite fauna of the Calcaire à *Baculites* (Upper Maastrichtian) of the Cotentin Peninsula (Manche, France). Palaeontology 29: 25–83.

Kennedy, W.J. 1987. The ammonite fauna of the type Maastrichtian with a revision of *Ammonites colligatus* Binkhorst, 1861. Bulletin de l'Institut Royal des Sciences Naturelles de Belgique 56: 151–267 (1986 imprint).

Kennedy, W.J. 1988. Late Cenomanian and Turonian ammonite faunas from northeast and central Texas. Special Papers in Palaeontology 39: 1–131.

Kennedy, W.J., and W.K. Christensen. 1997. Santonian to Maastrichtian ammonites from Scania, southern Sweden. Fossils & Strata 44: 75–128.

Kennedy, W.J., and W.A. Cobban. 1976. Aspects of ammonite biology, biogeography, and biostratigraphy. Special Papers in Palaeontology 17: 1–94.

Kennedy, W.J., and W.A. Cobban. 1991. Coniacian ammonite faunas from the United States Western Interior. Special Papers in Palaeontology 45: 5–96.

Kennedy, W.J., and W.A. Cobban. 1993. Ammonites from the Saratoga Chalk (Upper Cretaceous), Arkansas. Journal of Paleontology 67 (3): 404–434.

Kennedy, W.J., and W.A. Cobban. 1994. Upper Campanian ammonites from the Mount Laurel Sand at Biggs Farm, Delaware. Journal of Paleontology 68 (6): 1285–1305.

Kennedy, W.J., W.A. Cobban, and N.H. Landman. 2001. A revision of the Turonian members of the ammonite subfamily Collignoniceratinae from the United States Western Interior and the Gulf Coast. Bulletin of the American Museum of Natural History 267: 1–148.

Kennedy, W.J., W.A. Cobban, and G.R. Scott. 1992. Ammonite correlation of the uppermost Campanian of Western Europe, the U.S. Gulf Coast, Atlantic seaboard and Western Interior, and the numerical age of the base of the Maastrichtian. Geological Magazine 129 (4): 497–500.

Kennedy, W.J., W.A. Cobban, and G.R. Scott. 2000a. Heteromorph ammonites from the Upper Campanian (Upper Cretaceous) *Baculites cuneatus* and *Baculites reesidei* zones of the Pierre Shale in Colorado, USA. Acta Geologica Polonica 50 (1): 1–20.

Kennedy, W.J., and J.M. Hancock. 1970. Ammonites of the genus *Acanthoceras* from the Cenomanian of Rouen, France. Palaeontology 13: 462–490.

Kennedy, W.J., R.O. Johnson, and W.A. Cobban. 1995. Upper Cretaceous ammonite faunas of New Jersey. *In* J.E.B. Baker (editor), Contributions to the paleontology of New Jersey 12: 24–55. Trenton: Geological Association of New Jersey.

Kennedy, W.J., and U. Kaplan. 1995. *Parapuzosia* (*Parapuzosia*) *seppenradensis* (Landois) und die Ammonitenfauna der Dülmener Schichten, unteres Unter-Campan, Westfalen. Geologie und Paläontologie in Westfalen 33: 1–127.

Kennedy, W.J., and U. Kaplan. 1997. Ammoniten aus dem Campan des Stemweder Berges, Dammer Oberkreidemulde, NW-Deutschland. Geologie und Paläontologie in Westfalen 50: 31–245.

Kennedy, W.J., N.H. Landman, W.K. Christensen, W.A. Cobban, and J.M. Hancock. 1998. Marine connections in North America during the late Maastrichtian: palaeogeographic and palaeobiogeographic significance of *Jeletzkytes nebrascensis* Zone cephalopod fauna from the Elk Butte Member of the Pierre Shale, SE South Dakota and NE Nebraska. Cretaceous Research 19: 745–775.

Kennedy, W.J., N.H. Landman, W.A. Cobban, and R.O. Johnson. 2000b. Additions to the ammonite fauna of the Upper Cretaceous Navesink Formation of New Jersey. American Museum Novitates 3306: 1–30.

Kennedy, W.J., N.H. Landman, W.A. Cobban, and N.L. Larson. 2002. Jaws and radulae in *Rhaeboceras*, a Late Cretaceous ammonite. *In* H. Summesberger, K. Histon, and A. Daurer (editors), Cephalopods—present and past. Abhandlungen der Geologischen Bundesanstalt 57: 113–132.

Kennedy, W.J., and H. Summesberger. 1987. Lower Maastrichtian ammonites from Nagoryany (Ukrainian SSR). Beiträge zur Paläontologie von Österreich 13: 25–78.

Keupp, H. 2006. Sublethal punctures in body chambers of Mesozoic ammonites (forma aegra *fenestra* n. f.), a tool to interpret synecological relationships, particularly predator-prey interactions. Paläontologische Zeitschrift 80/2: 112–123.

Keupp, H., and Ilg, A. 1992. Paläopathologie der Ammonitenfauna aus dem Obercallovium der Normandie und ihre palökologische Interpretation. Berliner Geowissenschaftliche Abhandlungen (E) 3: 171–189.

Kidwell, S.M. 1991. The stratigraphy of shell concentrations. *In* P.A. Allison and D.E.G. Briggs (editors), Taphonomy: releasing the data locked in the fossil record: 211–290. New York: Plenum.

Kidwell, S.M., and D.W.J. Bosence. 1991. Taphonomy and time-averaging of marine shelly faunas. *In* P.A. Allison and D.E.G. Briggs (editors), Taphonomy: releasing the data locked in the fossil record: 115–209. New York: Plenum.

Kin, A. 2009. Early Maastrichtian ammonites and nautiloids frorm Hrebenne, southeast Poland, and phenotypic plasticity of *Acanthoscaphites tridens* (Kner, 1848). Cretaceous Research 31 (1): 27–60.

Klinger, H.C. 1981. Speculations on buoyancy control and ecology in some heteromorph ammonites. In M.R. House and J.R. Senior (editors), The Ammonoidea: 337–355. New York: Academic Press.

Klompmaker, A.A., N.A. Waljaard, and R.H.B. Fraaije. 2009. Ventral bite marks in Mesozoic ammonites. Palaeogeography, Palaeoclimatology, Palaeoecology 280 (2009): 245–257.

Kner, R. 1848. Versteinerungen des Kreidemergels von Lemberg und seiner Umgebung. Naturwissenschaftliche Abhandlungen, gesammelt und durch subscription, herausgegeben von W. Haidinger Vol. 3, pt. 2, no. 1: 1–42.

Korn, D., V. Ebbighausen, J. Bockwinkel, and C. Klug. 2003. The A-mode sutural ontogeny in prolecanitid ammonoids. Palaeontology 46 (6): 1123–1132.

Korn, D., and C. Klug. 2007. Conch form analysis, variability, morphological disparity, and mode of life of the Frasnian (Late Devonian) ammonoid *Manticoceras* from Coumiac (Montagne Noire, France). *In* N.H. Landman, R.A. Davis, and R.H. Mapes (editors), Cephalopods present and past: new insights and fresh perspectives: 57–85. Dordrecht: Springer.

Kraft, S., D. Korn, and C. Klug. 2008. Patterns of ontogenetic septal spacing in Carboniferous ammonoids. Neues Jahrbuch für Geologie und Paläontologie Abhandlungen 250/1: 31–44.

Kröger, B. 2002a. On the ability of withdrawing of some Jurassic ammonoids. *In* H. Summesberger, K. Histon, and A. Daurer (editors), Cephalopods—present and past. Abhandlungen der Geologischen Bundesanstalt 57: 199–204.

Kröger, B. 2002b. Antipredatory traits of the ammonoid shell—indications from Jurassic ammonoids with sublethal injuries. Paläontologische Zeitschrift 76 (2): 223–234.

Kruta, I., and N.H. Landman. 2008. Injuries on nautilus jaws: implications for the function of ammonite aptychi. Veliger 50 (3): 241–247.

Kruta, I., I. Rouget, N.H. Landman, K. Tanabe, and A. Cecca. 2009. Aptychi microstructure in Late Cretaceous Ancyloceratina (Ammonoidea). Lethaia 42 (3): 312–321.

Kruta, I., N.H. Landman, I. Rouget, F. Cecca, and P. Tafforeau. In prep. Exceptional preservation of the feeding apparatus in ammonites as a clue to their extinction.

Krystinik, L.F., and B.B. DeJarnett. 1995. Lateral variability of sequence stratigraphic framework in the Campanian and lower Maastrichtian of the Western Interior Seaway. *In* J.C. Van Wagoner and G.T. Bertram (editors), Sequence stratigraphy of foreland basin deposits: outcrop and subsurface examples from the Cretaceous of North America. American Association of Petroleum Geologists Memoir 64: 11–25.

Küchler, T., and G.S. Odin. 2001. Upper Campanian-Maastrichtian ammonites (Nostoceratidae, Diplomoceratidae) from Tercis les Bains (Landes, France). *In* G.S. Odin (editor), The Campanian-Maastrichtian boundary: 500–528. New York: Elsevier.

Kullmann, J., and J. Wiedmann. 1970. Significance of sutures in phylogeny of Ammonoidea. University of Kansas Paleontological Contributions 44: 1–32.

Landes, R.W. 1940. Geology of the southern Alberta plains. Part 2. Palaeontology of the marine formations of the Montana Group. Memoirs of the Canadian Geological Survey 221: 129–217.

Landman, N.H. 1983. Powerful Plains Indian medicine: invertebrate fossils. Discovery 16 (2): 21–23.

Landman, N.H. 1987. Ontogeny of Upper Cretaceous (Turonian-Santonian) scaphitid ammonites from the Western Interior of North America: systematics, developmental patterns, and life history. Bulletin of the American Museum of Natural History 185 (2): 117–241.

Landman, N.H. 1989. Iterative progenesis in Upper Cretaceous ammonites. Paleobiology 15 (2): 95–117.

Landman, N.H., and K. Bandel. 1985. Internal structures in the early whorls of Mesozoic ammonites. American Museum Novitates 2823: 1–21.

Landman, N.H., and W.A. Cobban. 2003. Ammonites from the upper part of the Pierre Shale and Fox Hills Formation of Colorado. American Museum Novitates 3388: 1–45.

Landman, N.H., and W.A. Cobban. 2007. Redescription of the Late Cretaceous (late Santonian) ammonite *Desmoscaphites bassleri* Reeside, 1927, from the Western Interior of North America. Rocky Mountain Geology 42 (2): 67–94.

Landman, N.H., R.O. Johnson, M.P. Garb, L.E. Edwards, and F.T. Kyte. 2007a. Cephalopods from the Cretaceous/Tertiary boundary in New Jersey and Maryland, with a description of the highest ammonite zones in North America. Part 3. Manasquan River Basin, Monmouth County, New Jersey. Bulletin of the American Museum of Natural History 303: 1–122.

Landman, N.H., and S.M. Klofak. 2006. Anatomy of a concretion. *In* A symposium on the paleontology, geology and stratigraphy of the Late Cretaceous Western Interior Seaway: a tribute to the life of William Aubrey "Bill" Cobban, August 26–27, 2006. Abstracts vol.: 30.

Landman, N.H., S.M. Klofak, and K.B. Sarg. 2003. Variation in adult size of scaphitid ammonites from the Upper Cretaceous Pierre Shale and Fox Hills Formation. *In* P.J. Harries (editor), Approaches in high-resolution stratigraphic paleontology: 149–194. Dordrecht: Kluwer Academic Publishers.

Landman, N.H., N.L. Larson, and W.A. Cobban. 2007b. Jaws and radula of *Baculites* from the Upper Cretaceous (Campanian) of North America. *In* N.H. Landman, R.A. Davis, and R.H. Mapes (editors), Cephalopods present and past: new insights and fresh perspectives: 257–298. Dordrecht: Springer.

Landman, N.H., W.B. Saunders, J.E. Winston, and P.J. Harries. 1987. Incidence and kinds of epizoans on the shells of live *Nautilus*. *In* W.B. Saunders and N.H. Landman (editors), *Nautilus*: the biology and paleobiology of a living fossil: 163–177. New York: Plenum.

Landman, N.H., K. Tanabe, and Y. Shigeta. 1996. Ammonoid embryonic development. *In* N.H. Landman, K. Tanabe, and R.A. Davis (editors), Ammonoid paleobiology: 343–405. New York: Plenum.

Landman, N.H., and K.M. Waage. 1986. Shell abnormalities in scaphitid ammonites. Lethaia 19: 211–224.

Landman, N.H., and K.M. Waage. 1993. Scaphitid ammonites of the Upper Cretaceous (Maastrichtian) Fox Hills Formation in South Dakota and Wyoming. Bulletin of the American Museum of Natural History 215: 1–257.

Landman, N.H., and J.E. Winston. 1999. Study of invertebrates at the American Museum of Natural History. *In* J.E. Winston (editor), Libbie Henrietta Hyman: life and contributions. American Museum Novitates 3277: 5–11.

Landman, N.H., et al. 2006. Jaws of Late Cretaceous placenticeratid ammonites: how preservation affects the interpretation of morphology. American Museum Novitates 3500: 1–48.

Larson, N.L. 1999. Discovering the mysterious ammonites. Torreano di Cividale. Italy: Geofin s.r.l., 126 pp.

Larson, N.L. 2003. Predation and pathologies in the Late Cretaceous ammonite family Scaphitidae. MAPS 26 (3): 1–30. Malcolm, IL: Mid-America Paleontology Society.

Larson, N.L. 2007. Deformities in the Late Callovian (Late Middle Jurassic) ammonite fauna from Saratov, Russia. *In* N.H. Landman, R.A. Davis, and R.H. Mapes (editors), Cephalopods present and past: new insights and fresh perspectives: 344–374. Dordrecht: Springer.

Larson, N.L. In press. The Late Campanian (Upper Cretaceous) cephalopod fauna of the Coon Creek Formation at its type locality. *In* M.A. Gibson and S.P. Dunagan (editors), Coon Creek monograph, SE Paleontology Society Field Trip, March 15–16, 2003. Nashville: Tennessee Division of Geology.

Larson, N.L., S.D. Jorgensen, R.A. Farrar, and P.L. Larson. 1997. Ammonites and the other cephalopods of the Pierre Seaway. Tucson, AZ: Geoscience Press, 148 pp.

Lavington, C.S. 1933. Montana Group in eastern Colorado. American Association of Petroleum Geologists Bulletin 17 (4): 397–410.

LeBrun, P. 1997. Ammonites: une histoire naturelle des ammonoïdes. Part 2: Ontogenèse et dimorphisme, locomotion, paléoécologie, origine, évolution et extinction: 101–208. Paris: CEDIM.

LeGoff, R., E. Gauvrit, G. Pinczon du Sel, and J. Daguzan. 1998. Age group determination by analysis of the cuttlebone of the cuttlefish *Sepia officinalis* L. in reproduction in the Bay of Biscay. Journal of Molluscan Studies 64: 183–193.

Lehmann, U. 1981. The ammonites: their life and their world. New York: Cambridge University Press.

Lehmann, U., and C. Kulicki. 1990. Double function of aptychi (Ammonoidea) as jaw elements and opercula. Lethaia 23: 325–331.

Lewy, Z. 1996. Octopods: Nude ammonoids that survived the Cretaceous-Tertiary boundary mass extinction. Geology 24 (7): 627–630.

Lewy, Z. 2000. Neverthess, aptychi are ammonoid opercular plates. GSI (Geological Survey of Israel) Current Research 12: 155–158.

Link, T.A., and A.J. Childerhose. 1931. Bearpaw Shale and contiguous formations in Lethbridge area, Alberta. American Association of Petroleum Geologists Bulletin 15 (10): 1227–1242.

Logan, W.N. 1898. The invertebrates of the Benton, Niobrara and Fort Pierre Groups. Geological Survey of Kansas. 4. Paleontology Pt. 8: 433–518.

Logan, W.N. 1899. Contributions to the paleontology of the Upper Cretaceous series. Field Columbian Museum Publication 36. Geological Series 1 (6): 205–216.

Ludvigson, G.A., B.J. Witzke, L.A. González, R.H. Hammond, and O.W. Plocher. 1994. Sedimentology and carbonate geochemistry of concretions from the Greenhorn marine cycle

(Cenomanian-Turonian), eastern margin of the Western Interior Seaway. *In* G.W. Shurr, G.A. Ludvigson, and R.H. Hammond (editors), Perspectives on the eastern margin of the Cretaceous Western Interior Basin: 145–173. Geological Society of America Special Paper 287.

Machalski, M. 2005a. The youngest Maastrichtian ammonite faunas from Poland and their dating by scaphitids. Cretaceous Research 26: 813–836.

Machalski, M. 2005b. Late Maastrichtian and earliest Danian scaphitid ammonites from central Europe: taxonomy, evolution, and extinction. Acta Palaeontologica Polonica 50 (4): 653–696.

Machalski, M. In press. Early Maastrichtian ammonites and nautiloids from Hrebenne, southeast Poland, and phenotypic plasticity of *Acanthoscaphites tridens* (Kner, 1848): A commentary. Cretaceous Research.

Maeda, H. 1987. Taphonomy of ammonites from the Cretaceous Yezo Group in the Tappu area, northwestern Hokkaido, Japan. Transactions and Proceedings of the Palaeontological Society of Japan New Series 148: 285–305.

Maeda, H., and A. Seilacher. 1996. Ammonoid taphonomy. *In* N.H. Landman, K. Tanabe, and R.A. Davis (editors), Ammonoid paleobiology: 544–578. New York: Plenum.

Makowski, H. 1962. Problem of sexual dimorphism in ammonites. Palaeontologica Polonica 12: 1–92.

Mangold, K. 1987. Reproduction. *In* P.R. Boyle (editor), Cephalopod life cycles. Vol. 2. Comparative reviews: 157–200. New York: Harcourt Brace Jovanovich.

Martin, J.E., J.L. Bertog, and D.C. Parris. 2007. Revised lithostratigraphy of the lower Pierre Shale Group, (Campanian) of central South Dakota, including newly designated members. *In* J.C. Martin and D.C. Parris (editors), The geology and paleontology of the Late Cretaceous marine deposits of the Dakotas: 9–22. Geological Society of America Special Paper 427.

Matyja, B.A. 1986. Developmental polymorphism in Oxfordian ammonites. Acta Geologica Polonica 36 (1–3): 37–68.

McArthur, J.M., et al. 1992. Strontium isotope stratigraphy in the Late Cretaceous: intercontinental correlation of the Campanian/Maastrichtian boundary. Terra Nova 4: 385–393.

Meek, F.B. 1859. Remarks on the Cretaceous fossils collected by Professor Henry Y. Hind, on the Assiniboine and Saskatchewan Exploring Expedition, with descriptions of some new species. *In* H.Y. Hind, 1859, North West Territory. Reports of progress, together with a preliminary and general report on the Assiniboine and Saskatchewan Exploring Expedition, made under instructions from the Provincial Secretary, Canada: 182–185. Toronto: J. Lovell.

Meek, F.B. 1864. Check list of the invertebrate fossils of North America. Cretaceous and Jurassic. Smithsonian Miscellaneous Collections 177: 1–40.

Meek, F.B. 1871. Preliminary paleontological report, consisting of lists of fossils, with descriptions of some new types etc. Preliminary report of the United States Geological Survey of Wyoming and portions of contiguous territories 4: 287–318.

Meek, F.B. 1876. A report on the invertebrate Cretaceous and Tertiary fossils of the upper Missouri country. United States Geological Survey of the Territories Report 9: 1–629, pls. 1–45.

Meek, F.B., and F.V. Hayden. 1856a. Descriptions of new species of Gasteropoda from the Cretaceous formations of Nebraska Territory. Proceedings of the Academy of Natural Sciences of Philadelphia 8: 63–69.

Meek, F.B., and F.V. Hayden. 1856b. Descriptions of new species of Gasteropoda and Cephalopoda from the Cretaceous formations of Nebraska Territory. Proceedings of the Academy of Natural Sciences of Philadelphia 8: 70–72.

Meek, F.B., and F.V. Hayden. 1856c. Descriptions of twenty-eight new species of Acephala and of Gasteropod, from the Cretaceous formations of Nebraska Territory. Proceedings of the Academy of Natural Sciences of Philadelphia 8: 81–87.

Meek, F.B., and F.V. Hayden. 1856d. Descriptions of new species of Acephala and Gasteropoda, from the Tertiary formations of Nebraska Territory, with some general remarks on the geology of the country about the sources of the Missouri River. Proceedings of the Academy of Natural Sciences of Philadelphia 8: 111–126.

Meek, F.B., and F.V. Hayden. 1856e. Descriptions of new species of Mollusca collected by Dr. F.V. Hayden, in Nebraska Territory; together with a complete catalogue of all the remains of Invertebrata hitherto described and identified from the Cretaceous and Tertiary formations of that region. Proceedings of the Academy of Natural Sciences of Philadelphia 8: 265–286.

Meek, F.B., and F.V. Hayden. 1859. Descriptions of new organic remains collected in Nebraska Territory... together with some remarks on the geology of the Black Hills and portions of the surrounding country. Proceedings of the Academy of Natural Sciences of Philadelphia 10: 41–59.

Meek, F.B., and F.V. Hayden. 1860. Systematic catalogue, with synonyma, etc., of Jurassic, Cretaceous and Tertiary fossils collected in Nebraska, by the exploring expeditions under the command of Lieut. G.K. Warren, of U.S. Topograghical Engineers. Proceedings of the Academy of Natural Sciences of Philadelphia 12: 417–432.

Meek, F.B., and F.V. Hayden. 1862. Descriptions of new Cretaceous fossils from Nebraska Territory... for the location and construction of a wagon road from the sources of the Missouri to the Pacific Ocean. Proceedings of the Academy of Natural Sciences of Philadelphia 1862: 21–28.

Metz, C.L. 2008. The paleobiogeography of the Late Cretaceous Western Interior Basin Tepee Butte Mounds (hydrocarbon seeps) of North America and possible tectonic factors controlling their distribution. Geological Society of America, Abstracts with Programs 40 (6): 250–251.

Monks, N. 2000. Functional morphology, ecology, and evolution of the Scaphitaceae Gill, 1871 (Cephalopoda). Journal of Molluscan Studies 66: 205–216.

Monks, N., and P. Palmer. 2002. Ammonites. Washington, DC: Smithsonian Institution Press, 159 pp.

Monks, N., and J.R. Young. 1998. Body position and the functional morphology of Cretaceous heteromorph ammonites. http://palaeo-electronica.pangaea.de/1998_1/monks/text.pdf

Monnet, C., and H. Bucher. 2005. New Middle and Late Anisian (Middle Triassic) ammonoid faunas from northwestern Nevada (USA): taxonomy and biochronology. Fossils and Strata 52: 1–121.

Moriya, K., H. Nishi, H. Kawahala, K. Tanabe, and Y. Takayanagi. 2003. Demersal habitat of Late Cretaceous ammonoids: evidence from oxygen isotopes for the Campanian (Late Cretaceous) northwestern Pacific thermal structure. Geology 31 (2): 167–170.

Morton, S.G. 1830. Synopsis of the organic remains of the Ferruginous Sand Formation of the United States, with geographical remarks. American Journal of Science and Arts 17: 274–295.

Morton, S.G. 1834. Synopsis of the organic remains of the Cretaceous group of the United States. Illustrated by nineteen plates, to which is added an appendix containing a tabular view of the Tertiary fossils hitherto discovered in North America. Philadelphia: Key and Biddle.

Morton, S.G. 1842. Description of some new species of organic remains of the Cretaceous group of the United States: with a tabular view of the fossils hitherto discovered in this formation. Journal of the Academy of Natural Sciences of Philadelphia 8 (2): 207–227.

Neige, P. 1996. Morphométrie des coquilles d'ammonites: applications ontogénétiques, paléobiologiques et phylogénétiques. Unpublished Ph.D. dissertation, Université de Bourgogne, France.

Nelson, S.J. 1975. Paleontological field guides. Northern Canada and Alaska. Bulletin of Canadian Petroleum Geology 23 (3): 428–683.

Niebuhr, B. 1996. Die Scaphiten (Ammonoidea, Ancyloceratina) des höheren Obercampan der Lehrter Westmulde östlich Hannover (N-Deutschland). Berliner Geowissenschaftliche Abhandlungen 18: 267–287.

Nowak, J. 1911. Untersuchungen über die Cephalopoden der oberen Kreide in Polen. II Teil: Die Skaphiten. Bulletin de l'Académie des Sciences de Cracovie Série B 7: 547–589.

Nowak, J. 1916. Zur Bedeutung von *Scaphites* für die Gliederung der Oberkreide. Verhandlungen der Kaiserlichen und Koniglichen Geologischen Reichsanstalt für 1915 3: 55–67.

Odin, G.S., and W.A. Cobban. 2001. Europe-America connection; palaeontological identification of some ammonites from Tercis les Bains (Landes, France). *In* G.S. Odin (editor), The Campanian-Maastrichtian boundary: 483–486. New York: Elsevier.

Okamoto, T. 1988. Developmental regulation and morphological saltation in the heteromorph ammonite *Nipponites*. Paleobiology 14: 272–286.

Orbigny, A.d'. 1840–1842. Paléontologie française. Terrains crétacés. Tome 1, céphalopodes. Paris: Masson, 662 pp.

Owen, D.D. 1852. Report of a geological survey of Wisconsin, Iowa, and Minnesota; and incidentally of a portion of Nebraska Territory made under instructions from the United States Treasury Department. Philadelphia: Lippincott, Grambo, 2 vols., 638 pp.

Parent, H., A. Scherzinger, and G. Schweigert. 2008. Sexual phenomena in Late Jurassic Aspidoceratidae (Ammonoidea). Dimorphic correspondence between *Physodoceras hermanni* (Berckhemer) and *Sutneria subeumela* Schneid, and first record of possible hermaphroditism. Palaeodiversity 1: 181–187.

Parkinson, J. 1811. Organic remains of a former world. London: Sherwood, Neily and Jones, 3 vols., xvi + 479 pp., 22 pls.

Ploch, I. 2003. Taxonomic interpretation and sexual dimorphism in the Early Cretaceous (Valanginian) ammonite *Valanginites nucleus* (Roemer, 1841). Acta Geologica Polonica 53 (3): 201–208.

Pompeckj, J.F. 1894. Die Ammonoideen mit anormaler Wohnkammer. Jahreshefte des Ver-

eins für Vaterlandische Naturkunde 50: 220–290.

Radwański, A. 1996. The predation upon, and the extinction of, the latest Maastrichtian populations of the ammonite species *Hoploscaphites constrictus* (J. Sowerby, 1817) from the Middle Vistula Valley, Poland. Acta Geologica Polonica 46 (1–2): 117–135.

Raiswell, R. 1976. The microbiological formation of carbonate concretions in the Upper Lias of N.E. England. Chemical Geology 18: 227–244.

Reeside, J.B., Jr. 1927a. The scaphites, an Upper Cretaceous ammonite group. U.S. Geological Survey Professional Paper 150-B: 21–40.

Reeside, J.B., Jr. 1927b. The cephalopods of the Eagle sandstone and related formations in the Western Interior of the United States. U.S. Geological Survey Professional Paper 151: 1–87.

Reeside, J.B., Jr. 1957. Paleoecology of the Cretaceous Seas of the Western Interior of the United States. *In* H.S. Ladd (editor), Treatise on marine ecology and paleoecology, vol. 2: 505–542. Paleoecology, Geological Society of America, Memoir 67.

Reeside, J.B., Jr. 1962. Cretaceous ammonites of New Jersey. *In* H.G. Richards, et al. (editors), The Cretaceous fossils of New Jersey. New Jersey Department of Conservation and Economic Development Bulletin 61 Pt. 2: 113–137. Trenton: State of New Jersey Department of Conservation and Economic Development.

Reeside, J.B., Jr, and W.A. Cobban. 1960. Studies of the Mowry Shale (Cretaceous) and contemporary formations in the United States and Canada. U.S. Geological Survey Professional Paper 355: 1–126.

Remin, Z. 2009. Upper Campanian and lower Maastrichtian belemnite stratigraphy of the Vistula River Valley and Kronsmoor sections based on new taxonomical and methodological approach. *In* M.B. Hart (editor), 8th International Symposium on the Cretaceous System, Plymouth University, 6th–12th September 2009, Abstract vol.: 163.

Rhodes, F.H.T., H.S. Zim, and P.R. Shaffer. 1962. Fossils: a guide to prehistoric life. New York: Golden Press, 160 pp.

Riccardi, A.C. 1983. Scaphitids from the Upper Campanian–Lower Maastrichtian Bearpaw Formation of the Western Interior of Canada. Geological Survey of Canada Bulletin 354: 1–51.

Richard, A. 1970. Analyse du cycle sexual chez les céphalopods mise en évidence expérimentale d'un rythme conditionné par les variations des facteurs externs et interns. Bulletin de la Société Zoologique de France 95: 461–469.

Robinson, C.S., W.J. Mapel, and W.A. Cobban. 1959. Pierre Shale along western and northern flanks of Black Hills, Wyoming and Montana. Bulletin of the American Association of Petroleum Geologists 43 (1): 101–123.

Robinson, H.R. 1945. New baculites from the Cretaceous Bearpaw Formation of southwestern Saskatchewan. Transactions of the Royal Society of Canada (ser. 3) 39 (4): 51–54.

Roemer, F.A. 1840–1841. Die Versteinerungen des norddeutschen Kreidegebirges. iv + 145pp, 16 pl. (pp. 1–48, pl. 1–7, 1840; pp. 49–145, pl. 8–16, 1841). Hannover: Hahn'schen Hofbuchhandlung.

Russell, L.S. 1950. Correlation of the Cretaceous-Tertiary transition in Saskatchewan and Alberta. Bulletin of the Geological Society of America 61: 27–42.

Russell, L.S., and R.W. Landes. 1940. Geology of the southern Alberta plains. Geological Survey of Canada Memoir 221: 1–223.

Rye, D.M., and M.A. Sommer, II. 1980. Reconstructing paleotemperature and paleosalinity regimes with oxygen isotopes. *In* D.C. Rhoads and R.A. Lutz (editors), Skeletal growth of aquatic organisms: 169–202. New York: Plenum.

Saul, L.R., and C.J. Stadum. 2005. Fossil argonaut (Mollusca: Cephalopoda: Octopodida) from late Miocene siltstones of the Los Angeles Basin, California. Journal of Paleontology 79: 520–531.

Saunders, W.B., and E.A. Shapiro. 1986. Calculation and simulation of ammonoid hydrostatics. Paleobiology 12 (1): 64–79.

Sava, L.A. 2007. The molluscan and brachiopod fauna of the Late Cretaceous Pierre Shale (*Baculites compressus*/*Baculites cuneatus* biozones) near Kremmling, Colorado. Unpublished master's thesis, Department of Geology, University of South Florida.

Say, T. 1820. Observations on some species of zoophytes, shells, &c. principally fossil. American Journal of Science and Arts 2 (2): 34–45.

Schuchert, C. 1905. Catalogue of the type specimens of fossil invertebrates in the Department of Geology, United States National Museum. Bulletin of the United States National Museum 53 (1): 1–704.

Scott, G.R., and W.A. Cobban. 1965. Geologic and biostratigraphic map of the Pierre Shale between Jarre Creek and Loveland, Colorado. U.S. Geological Survey Miscellaneous Geological Investigations Map I-439, scale 1:48,000, separate text.

Scott, G.R., and W.A. Cobban. 1975. Geologic and biostratigraphic map of the Pierre Shale in the Canon City–Florence Basin and the Twelvemile Park area, south-central Colorado. U.S.

Geological Survey Miscellaneous Geological Investigations Map I-937, scale 1:48,000.

Scott, G.R., and W.A. Cobban. 1986a. Geologic and biostratigraphic map of the Pierre Shale in the Colorado Springs–Pueblo area, Colorado. U.S. Geological Survey Miscellaneous Geological Investigations map I-1627, scale 1:100,000.

Scott, G.R., and W.A. Cobban. 1986b. Geologic, biostratigraphic and structure map of the Pierre Shale between Loveland and Round Butte, Colorado. U.S. Geological Survey Miscellaneous Geologic Investigations map I-1700, scale 1:50,000.

Searight, W.V. 1937. Lithologic stratigraphy of the Pierre Formation in the Missouri valley in South Dakota. South Dakota Geological Survey Report Inventory 27: 1–63.

Seilacher, A., and P.Y. Gunji. 1993. Morphogenetic countdowns in heteromorph shells. Neues Jahrbuch für Geologie und Paläontologie Abhandlungen 190 (2/3): 237–265.

Shapiro, R., and H. Fricke. 2002. Tepee Buttes: fossilized methane-seep ecosystems. *In* E.M. Leonard, et al. (editors), High Plains to Rio Grande Rift: Late Cenozoic evolution of central Colorado. Geological Society of America Annual Meeting Field Trip Guidebook: 94–101. Boulder, CO: Geological Society of America.

Shimer, H.W. 1924. An introduction to the study of fossils (plants and animals). New York: MacMillan, 450 pp.

Shimer, H.W. 1933. An introduction to the study of fossils (plants and animals). Revised ed. New York: MacMillan, 496 pp.

Shimer, H.W., and R.R. Shrock. 1944. Index fossils of North America. Cambridge, MA: M.I.T. Press, 837 pp.

Shrock, R.R., and W.H. Twenhofel. 1953. Principles of invertebrate paleontology. New York: MacGraw-Hill, 816 pp.

Shumard, B.F. 1861. Description of new Cretaceous fossils from Texas. Proceedings of the Boston Society of Natural History 8: 188–205.

Shurr, G.W., G.A. Ludvigson, and R.H. Hammond. 1994. Introductory remarks: perspectives on the eastern margin of the Cretaceous Western Interior Seaway. *In* G.W. Shurr, G.A. Ludvigson, and R.H. Hammond (editors), Perspectives on the eastern margin of the Cretaceous Western Interior Seaway. Geological Society of America Special Paper 287: 1–4.

Smith, W.D. 1905. The development of *Scaphites*. Journal of Geology 13 (7): 635–654.

Sohl, N.F. 1967. Upper Cretaceous gastropods from the Pierre Shale at Red Bird, Wyoming. United States Geological Survey Professional Paper 393-B: 1–46.

Sowerby, J. 1812–1822. The mineral conchology of Great Britain. London: the author.

Stanton, T.W. 1887 [1888]. Palaeontological notes. Proceedings of the Colorado Scientific Society 2 (3): 184–187.

Stelck, C.R. 1975. Basement control of Cretaceous sand sequences in western Canada. *In* W.G.E. Caldwell (editor), The Cretaceous system in the Western Interior of North America. Geological Association of Canada Special Papers 13: 427–440.

Stephenson, L.W. 1941. The larger invertebrates of the Navarro Group of Texas (exclusive of corals and crustaceans and exclusive of the fauna of the Escondido Formation). University of Texas Bulletin 4101: 1–641.

Stoffer, P.W. 1998. Stratigraphy of the upper Pierre Shale and Fox Hills Formation (Campanian and Maastrichtian; Late Cretaceous), the Badlands National Park region, South Dakota: implications for eustatic changes in sea level, tectonism, and marine paleoecology of the Western Interior Seaway. Unpublished Ph.D. dissertation, City University of New York.

Stoffer, P.W. 2003. Geology of Badlands National Park: a preliminary report. U.S. Geological Survey Open-File Report 03-35: 1–63.

Tanabe, K. 1979. Palaeoecological analysis of ammonoid assemblages in the Turonian *Scaphites* facies of Hokkaido, Japan. Palaeontology 22 (3): 609–630.

Tanabe, K. 1993. Variability and mode of evolution of the Middle Cretaceous ammonite *Subprionocyclus* (Ammonitina: Collignoniceratidae) from Japan. *In* S. Elmi, C. Mangold, and Y. Alméras (editors), Geobios Mémoire Spécial 15: 347–357.

Tate, R. 1865. On the correlation of the Cretaceous formations of the northeast of Ireland. Quarterly Journal of the Geological Society of London 21: 15–44.

Tharalson, D. 1993. Cephalopod diversity within a concretionary interval of the Pierre Shale (Upper Cretaceous) in Dawes County, northwestern Nebraska. Transactions of the Nebraska Academy of Sciences 20: 87–95.

Thomel, G. 1980. Ammonites. Nice, France: Serre, 227 pp.

Tourtelot, H.A., and R.O. Rye. 1969. Distribution of oxygen and carbon isotopes in fossils of Late Cretaceous age, Western Interior region of North America. Geological Society of America Bulletin 80: 1903–1922.

Trueman, A.E. 1941. The ammonite body chamber, with special reference to the buoyancy and mode of life of the living ammonite. Quarterly Journal of the Geological Society (London) 96: 339–383.

Tsujita, C.J. 1995. Origin of concretion-hosted shell clusters in the Late Cretaceous Bearpaw Formation, southern Alberta. Palaios 10: 408–423.

Tsujita, C.J., and G.E. Westermann. 1998. Ammonoid habitats and habits in the Western Interior Seaway: a case study from the Upper Cretaceous Bearpaw Shale of southern Alberta, Canada. Palaeogeography, Palaeoclimatology, Palaeoecology 144: 135–160.

Urdy, S., N. Goudeman, H. Bucher, and C. Monnet. 2008. Growth models of Recent gastropod shells: implication for ammonoids. Geological Society of America Abstracts with Programs 40 (6): 103.

Waage, K.M. 1964. Origin of repeated fossiliferous concretion layers in the Fox Hills Formation. Kansas Geological Survey Bulletin 169: 541–563.

Waage, K.M. 1968. The Type Fox Hills Formation, Cretaceous (Maestrichtian), South Dakota, Pt. 1, stratigraphy and paleoenvironments. Peabody Museum of Natural History Bulletin 27: 1–175.

Wade, B. 1926. The fauna of the Ripley Formation on Coon Creek, Tennessee. United States Geological Survey Professional Paper 137: 1–272.

Walaszczyk, I. 2004. Inoceramids and inoceramid biostratigraphy of the Upper Campanian to basal Maastrichtian of the Middle Vistula River section, central Poland. Acta Geologica Polonica 54 (1): 95–168.

Walaszczyk, I., W.A. Cobban, and P.J. Harries. 2001. Inoceramids and inoceramid biostratigraphy of the Campanian and Maastrichtian of the United States Western Interior Basin. Revue Paléobiologie (Genève) 20 (1): 117–234.

Walaszczyk, I., G.S. Odin, and A.V. Dhondt. 2002. Inoceramids from the Upper Campanian and Lower Maastrichtian of the Tercis section (SW France), the Global Stratotype Section and Point for the Campanian-Maastrichtian boundary; taxonomy, biostratigraphy and correlation potential. Acta Geologica Polonica 52 (3): 269–305.

Wani, R. 2007. How to recognize *in situ* fossil cephalopods: evidence from experiments with modern *Nautilus*. Lethaia 40: 305–311.

Wani, R., T. Kase, Y. Shigeta, and R. De Ocampo. 2005. New look at ammonoid taphonomy, based on field experiments with modern chambered nautilus. Geology 33 (11): 849–852.

Warren, P.S. 1931. Invertebrate paleontology of southern plains of Alberta. American Association of Petroleum Geologists Bulletin 15 (10): 1283–1291.

Warren, P.S. 1934. Paleontology of the Bearpaw Formation. Transactions of the Royal Society of Canada (ser. 3) 4 (28): 81–97.

Wedekind, R. 1916. Über Lobus, Suturallobus und Inzision. Zentralblatt für Mineralogie, Geologie und Paläontologie B 1916: 185–195.

Weller, S. 1907. A report on the Cretaceous paleontology of New Jersey. Geological Survey of New Jersey, Paleontology Series 4: 1–871.

Westermann, G.E.G. 1966. Covariation and taxonomy of the Jurassic ammonite *Sonninia adicra* (Waagen). Neues Jahrbuch für Geologie und Paläontologie Abhandlungen 124: 289–312.

Westermann, G.E.G. 1996. Ammonoid life and habitat. *In* Landman, N.H., K. Tanabe, and R.A. Davis (editors), Ammonoid paleobiology: 607–707. New York: Plenum.

White, C.A. 1879. Report on the paleontological field-work for the season of 1877. Eleventh annual report of the United States Geological and Geographical Survey of the Territories, embracing Idaho and Wyoming, being a report of progress of the exploration for the year 1877: 161–272.

Whiteaves, J.F. 1885. Report on the Invertebrata of the Laramie and Cretaceous rocks of the vicinity of the Bow and Belly River and adjacent localities in the Northwest Territory. Contributions to Canadian Palaeontology 1: 1–89.

Whiteaves, J.F. 1889. On some Cretaceous fossils from British Columbia, the Northwest Territory and Manitoba. Contributions to Canadian Palaeontology 1: 151–196.

Whitfield, R.P. 1877. Preliminary report on the paleontology of the Black Hills, containing descriptions of new species of fossils from the Potsdam, Jurassic, and Cretaceous formations of the Black Hills of Dakota. U.S. Geographical and Geological Survey of the Rocky Mountain Region. 49 pp.

Whitfield, R.P. 1880. Paleontology of the Black Hills of Dakota. *In* H. Newton and W.P. Jenney, Report on the geology and resources of the Black Hills of Dakota with atlas: 329–468. Washington, DC: Government Printing Office.

Whitfield, R.P. 1892. Gasteropoda and Cephalopoda of the Raritan Clays and Greensand Marls of New Jersey. United States Geological Survey Monograph 18: 1–402.

Whitfield, R.P., and E.O. Hovey. 1898. Catalogue of the types and figured specimens in the Paleontological Collection of the Geological Department, American Museum of Natural History. Bulletin of the American Museum of Natural History 11: 1–500.

Whittaker, S.G., T.K. Kyser, and W.G.E. Caldwell. 1987. Paleoenvironmental geochemistry of

the Claggett marine cyclothem in south-central Saskatchewan. Canadian Journal of Earth Sciences 24: 967–984.

Wickenden, R.T.D. 1945. Mesozoic stratigraphy of the eastern plains, Manitoba and Saskatchewan. Canada Department of Mines and Resources Geological Survey Memoir 239: 1–87.

Wiedmann, J. 1965. Origin, limits, and systematic position of *Scaphites*. Palaeontology 8 (33): 397–453.

Wiedmann, J. 1966. Stammesgeschichte und System der postriadischen Ammonoideen: ein Überblick. Neues Jahrbuch für Geologie und Paläontologie Abhandlungen 125: 49–79; 127: 13–81.

Wiese, F., and F. Schulze. 2005. The Upper Cenomanian (Cretaceous) ammonite *Neolobites vibrayeanus* (d'Orbigny, 1841) in the Middle East: taxonomic and palaeocologic remarks. Cretaceous Research 26: 930–946.

Williams, M.Y. 1930. New species of marine invertebrate fossils from the Bearpaw Formation of southern Alberta. National Museum of Canada Bulletin 63: 1–6.

Williams, M.Y., and W.S. Dyer. 1930. Geology of southern Alberta and southwestern Saskatchewan. Geological Survey of Canada Memoir 163: 1–160.

Winchell, N.H. 1900. Personal and scientific news. American Geologist 25 (3): 195.

Wright, E.K. 1987. Stratification and paleocirculation of the Late Cretaceous Western Interior Seaway of North America. Geological Society of America Bulletin 99: 480–490.

Wright, C.W. 1996. Treatise on invertebrate paleontology: Mollusca 4, Cephalopoda: Ammonoidea. Boulder, CO: Geological Society of America.

Yacobucci, M.M. 2004. Buckman's paradox: variability and constraints on ammonoid ornament and shell shape. Lethaia 37: 57–69.

Zittel, K.A. von. 1884. Handbuch der Paläontologie. Abteilung 1. Band 2: 329–522. Munich: R. Oldenbourg.

APPENDIX 1
List of Localities

American Museum of Natural History (AMNH) Localities

3183. *Baculites compressus* Zone (?), Pierre Shale, SE¼ sec. 8, T. 1 N., R. 14 E., near Wasta, Pennington County, South Dakota.

3207. *Baculites compressus–B. cuneatus* zones, Pierre Shale, SW¼ sec. 35, T. 1 S., R. 14 E., 43°54′39″N., 102°24′48″W., along Sage Creek, approximately 1.9 km from Sage Creek Campground, Badlands National Park, Pennington County, South Dakota.

3207a. Float, Pierre Shale, SW¼ sec. 35 T. 1 S., R. 14 E., near Sage Creek, Badlands National Park, Pennington County, South Dakota.

3212. *Baculites compressus–B. cuneatus* zones, Pierre Shale, SW¼SE¼ sec. 11, T. 5 S., R. 47 W., Shannon County, South Dakota.

3213. *Baculites compressus–B. cuneatus* zones, Pierre Shale, NE¼ sec. 11, T. 2 S., R. 14 E., cutbank along tributary to Sage Creek, approximately 1.6 km from Sage Creek Campground, Badlands National Park, Pennington County, South Dakota.

3225a. *Baculites cuneatus–B. reesidei* zones, Pierre Shale, NE¼SW¼ sec. 22, T. 3 S., R. 12 E., west of Scenic, 30–37 m above creek level, Pennington County, South Dakota.

3225b. *Baculites cuneatus* Zone, Pierre Shale, NE¼SW¼ sec. 22, T. 3 S., R. 12 E., west of Scenic, cutbank along creek level, Pennington County, South Dakota.

3274. *Baculites compressus –B. cuneatus* zones, Pierre Shale, SE½ sec. 6, T. 3 N., R. 14 E. and S½ SW½ sec. 5, T. 3 N., R. 14 E., Meade County, South Dakota.

3285. *Baculites compressus* Zone, Pierre Shale, SW¼ sec. 11, T. 2 S., R. 14 E., south fork of Sage Creek, Badlands National Park, Pennington County, South Dakota.

3322. Pierre Shale, NW ¼ sec. 6, T. 1 N., R. 80 W., Route 227, 3.5 km north of Kremmling, Grand County, Colorado.

3323. Pierre Shale, NE ¼ sec. 7, T. 1 N., R. 80 W., near Kremmling, Grand County, Colorado.

3330. *Baculites compressus–B. cuneatus* zones, Pierre Shale, SE¼ sec. 17, T. 3 N., R. 80 W., 8 km north of Kremmling, Grand County, Colorado.

3363. *Baculites compressus* Zone, Bearpaw Shale, E½ sec. 18, T. 9 N., R. 36 E., northeast side of Petroleum Road, off Rt. 12, Rosebud County, Montana.

3364. *Baculites compressus* Zone, Bearpaw Shale, N½ sec. 14, T. 9 N., R. 35 E., southwest side of Rt. 12, 6.5–8 km southeast of Ingomar, Rosebud County, Montana.

3365. *Baculites compressus* Zone, Bearpaw Shale, SE¼ sec. 14 and SW½ sec. 13, T. 9 N., R. 35 E, 0.8 km south of AMNH loc. 3364, Rosebud County, Montana.

3366. *Baculites compressus* Zone, Pierre Shale, SW¼ sec. 28 and NW½ sec. 29, T. 9 N., R. 36 E., along ridge 0.8 km southwest of Rt. 12, 4.8 km south of Moreland (Thebes) Rd., Rosebud County, Montana.

3368. *Baculites cuneatus–B. reesidei* zones, Bearpaw Shale, S½ sec. 9, T. 12 N., R. 31 E., northeast of Melstone, Rosebud County, Montana.

3402. *Baculites compressus* Zone, Pierre Shale, NW¼ NW¼ NE¼ sec. 32, T. 1 S., R. 11 E., along cutbank of Rapid Creek, approximately 6 km east-southeast of Farmingdale, Pennington County, South Dakota.

3408. *Baculites compressus* Zone, Pierre Shale, N½SW¼ sec. 5, T. 3 N., R. 14 E., Meade County, South Dakota.

3409. *Baculites cuneatus* Zone, Pierre Shale, NE¼ SE¼ sec. 4, T. 3 N., R. 14 E., Meade County, South Dakota.

3415. *Baculites compressus* Zone, Pierre Shale, SE¼NW¼ sec. 11, T. 3 N., R. 14 E., Meade County, South Dakota.

3418. Bioherm, *Didymoceras cheyennense* Zone, Pierre Shale, 43°47.299′N, 102°53.299′W, near Folsome, Custer County, North Dakota.

3419. Bioherm, *Baculites compressus* Zone, Pierre Shale, 43°45.675′N, 102°51.145′W, near Folsom, Custer County, South Dakota.

3420. Bioherm, *Baculites compressus* Zone, Pierre Shale, 43°45.655′N, 102°51.284′W, near Folsom, Custer County, South Dakota.

3434. *Baculites compressus–B. cuneatus* zones, Pierre Shale, NE ¼ sec. 4, T. 3 N., R. 14 E, Meade County, South Dakota.

3436. *Baculites compressus* Zone, Pierre Shale, NE¼ SE¼ sec. 9, T. 3 N., R. 14 E., Meade County, South Dakota.

3457, a, b. Bioherms. *Baculites compressus* Zone, Pierre Shale. 8–25 m west of AMNH loc. 3420, near Folsome, Custer County, North Dakota.

Geological Survey of Canada (GSC) Localities

The name of the collector and the date of collection are indicated at the end of the entry.

C-186877. *Baculites compressus* Zone, Bearpaw Shale, north bank of the Crowsnest River, LSD 15-26-7-2-W5, near Lundbreck, Alberta, Canada. T. Jerzykiewicz, 1995(?).

U.S. Geological Survey (USGS) Mesozoic Localities

The prefix D refers to Denver locality numbers, which are listed first, and the others refer to Washington, D.C. locality numbers. The names of collectors and dates of collection are indicated at the end of each entry.

D40. Pierre Shale, 1075 m below top, Denver & Salt Lake Railroad cut near center of NW¼SE¼ sec.

20, T. 2 S., R. 70 W., Jefferson County, Colorado. R. Van Horn and W.A. Cobban, 1954.

D76. Bearpaw Shale, approximately 3 km south of Franklin, Golden Valley County, Montana. O.O. Mueller, 1954.

D213. Pierre Shale, SE¼SE¼ sec. 15, T. 35 N., R. 48 W., Shannon County, South Dakota. R.J. Dunham, 1954.

D221. *Didymoceras cheyennense* Zone, Pierre Shale, south bank of White River, NE¼NE¼ sec. 7, T. 34 N., R. 47 W., Dawes County, Nebraska. R.J. Dunham, 1954.

D271. Pierre Shale, SE¼SE¼ sec. 15, T. 6 S., R. 69 W., Jefferson County, Colorado. G.R. Scott, 1955.

D280. Pierre Shale, just above bed of phosphatic pebbles, same locality as D271. G.R. Scott, 1955.

D337. Pierre Shale, NE¼SW¼ sec. 5, T. 2 S., R. 70 W., Jefferson County, Colorado. G.R. Scott, 1959.

D372. *Baculites compressus* Zone, Pierre Shale, Larimer Sandstone equivalent, W½ sec. 19, T. 11 N., R. 68 W., 34–35 km north of Fort Collins, 0.5–2.1 km south of Round Butte, Larimer County, Colorado.

D373. *Baculites compressus* Zone, Pierre Shale, Larimer Sandstone equivalent, 4.6 m higher than D372, SE¼NW¼ sec. 19, T. 11 N., R. 68 W., 34.6 km north of Fort Collins, 0.8 km south of Round Butte, Larimer County, Colorado.

D440. *Baculites compressus*–B. *reesidei* zones, Pierre Shale, "Monument Hill" Bentonitic Member, NE¼NE¼ sec. 24, T. 56 N., R. 69 W, 6.4 km north-northwest of Stroner, Campbell County, Wyoming.

D490. Bearpaw Shale, sec. 10, T. 6 N., R. 17 E., north of bridge over Mud Creek, Wheatland County, Montana. W.A. Cobban, 1955.

D493. Claggett Shale, phosphatic pebble unit 2 m above base, NE¼SE¼ sec. 5, T. 14 N., R. 31 E., Garfield County, Montana. W.A. Cobban, 1955.

D494. Claggett Shale, 4 m above base, same locality as D493. W.A. Cobban, 1955.

D495. Claggett Shale, 8 m above base, same locality as D493. W.A. Cobban, 1955.

D496. Claggett Shale, septarian concretions 18 m above base, NE¼NE¼SE¼ sec. 5, T. 14 N., R. 31 E., 6 km east-northeast of Mosby, Garfield County, Montana. W.A. Cobban, 1955.

D497. Approximately middle of Claggett Shale, SW¼NW¼ sec. 4, T. 14 N., R. 31 E., Garfield County, Montana. W.A. Cobban, 1955.

D498. Claggett Shale, approximately 20 m below top, same locality as D497. W.A. Cobban, 1955.

D499. Claggett Shale, approximately 23 m below top, NW¼SW¼ sec. 4, T. 14 N., R. 31 E., Garfield County, Montana. W.A. Cobban, 1955.

D500. Claggett Shale, approximately 9 m below top, same locality as D499. W.A. Cobban, 1955.

D615. *Baculites reesidei* Zone, Pierre Shale, Lake Creek Shale Member, SE¼ SE¼ sec. 29, T. 11 S., R. 39 W., at curve in road 19.3 km north-northeast of Sharon Springs, Wallace County, Kansas.

D618. *Baculites reesidei* Zone, float, Pierre Shale, Lake Creek Shale Member, NE¼ sec. 31, T. 11 S., R. 39 W. just south of east-west section road, 18.5 km north-northeast of Sharon Springs, Wallace County, Kansas. W.A. Cobban.

D621. *Didymoceras cheyennense* Zone (?), Pierre Shale, gray limestone concretions in upper part of Weskan Shale Member, SW¼ sec. 30, T. 12 S., R. 39 W. and SE¼ sec. 25, T. 12 S., R. 40 W., 9.7 km northeast of Sharon Springs, Wallace County, Kansas.

D732. Pierre Shale, dark gray limy concretions in sandy shale, NW¼SE¼ sec. 9, T. 2 N., R. 70 W., Boulder County, Colorado.

D746. Pierre Shale, sandy concretions in greenish-gray sandstone, NW¼NE¼NW¼NE¼ sec. 16, T. 2 N., R. 70 W., Boulder County, Colorado.

D764. Bearpaw Shale, calcareous concretions 44–48 m above base, near center of south line of sec. 14, T. 6 N., R. 22 E., Golden Valley County, Montana. W.A. Cobban, 1955.

D780. Bearpaw Shale, 168 m above base, NW¼NE¼ sec. 15, T. 11 N., R. 31 E., Rosebud County, Montana. H.R. Smith, 1955.

D782. Bearpaw Shale, 168 m above base, SE¼ sec. 28, T. 13 N., R. 31 E., Garfield County, Montana. H.R. Smith, 1955.

D855. Pierre Shale, 12 m below top of Monument Hill Bentonitic Member, NW¼ sec. 23, T. 9 S., R. 55 E., Carter County, Montana.

D1055. Pierre Shale, gray concretions in soft dark shale, SW¼ sec. 14, T. 14 N., R. 3 E., Butte County, South Dakota. W.A. Cobban, 1956.

D1074. *Baculites reesidei* Zone (?), Pierre Shale, near center of south line of sec. 24, T. 18 S., R. 64 W., approximately 21 km north-northwest of Pueblo, Pueblo County, Colorado. G.R. Scott and W.A. Cobban.

D1080. Pierre Shale, N½ sec. 23, T. 18 S., R. 64 W., Pueblo County, Colorado. G.R. Scott and W.A. Cobban, 1956.

D1349. *Baculites compressus* Zone, Pierre Shale, brown and gray limestone concretions in silty shale, SE¼NE¼ sec. 18, T. 3 N., R. 80 W., ridge of fine sandy shale just north of road and 18 km north of Kremmling, Grand County, north-central Colorado.

D1351. *Baculites compressus* Zone, Pierre Shale, gray and brown sandy calcareous concretions 9–11 km below large conspicuous ridge-forming concretions, NW¼SW¼ sec. 17, T. 3 N., R. 80 W., Grand County, Colorado. G.R. Scott and W.A. Cobban, 1957.

D1352. Pierre Shale, large brown sandstone concretions 10 m above D1351. NW¼ SW¼ sec. 17, T. 3N., R. 80W., Grand County, Colorado. G.R. Scott and W.A. Cobban, 1957.

D1353. *Baculites cuneatus* Zone, Pierre Shale, brown and gray sandy calcareous concretions 4–6 m above the huge concretions of D1352, NW¼ SW¼ sec. 17, T. 3 N., R. 80 W., Grand County, Colorado. G.R. Scott and W.A. Cobban, 1957.

D1594. Pierre Shale, middle part, sec. 31, T. 2 N., R. 15 E., Pennington County, South Dakota. H.A. Tourtelot, 1956.

D1598. Pierre Shale, upper part, SW¼NE¼ sec. 32, T. 5 N., R. 13 E., Meade County, South Dakota. H.A. Tourtelot, 1956.

D1657. Pierre Shale, Verendrye Member, sec. 27, T. 7 N., R. 28 E., Stanley County, South Dakota. L.G. Schultz, 1957.

D1661. Pierre Shale, transition beds between DeGrey and Verendrye Members, sec. 34, T. 13 N., R. 31 E., Dewey County, South Dakota. L.G. Schultz, 1957.

D1785. Pierre Shale, higher than D1353, NW¼SW¼ sec. 17, T. 3 N., R. 80 W., Grand County, Colorado. G.R. Scott and W.A. Cobban, 1957, 1958.

D2153. Gammon Shale, ironstone concretions 74–91 m above base, same locality as 21409. W.A. Cobban, 1959.

D2155. Claggett Shale, brown limestone concretions 38 m above base, E½E½ sec. 4, T. 14 N., R. 31 E., Garfield County, Montana. W.A. Cobban, 1959.

D2156. *Baculites mclearni* Zone, Claggett Shale, brown limestone concretions 37.8 m above basal pebble bed, near center of E½E½ sec. 5, T. 14 N., R. 31 E., 5.8 km ENE of Mosby, Garfield County, Montana.

D2393. Pierre Shale, bed of highly fossiliferous limestone concretions, east side of road near center of west line of NW¼ sec. 20, T. 5 N., R. 13 E., Meade County, South Dakota. W.A. Cobban, 1959.

D2553. Bearpaw Shale, approximately 46 m above base, NE¼NE¼ sec. 4, T. 36 N., R. 8 W., Landslide Butte, Glacier County, Montana. A.E. Roberts, J.R. Gill, and W.A. Cobban, 1960.

D2618. Pierre Shale, SW¼SW¼ sec. 29, T. 45 N., R. 62 W., Weston County, Wyoming. W.J. Mapel, 1960.

D2626. Claggett Shale, lower part of bentonitic member, NE¼ sec. 6, T. 8 N., R. 38 E., Rosebud County, Montana. J.R. Gill, L.G. Schultz, and W.A. Cobban, 1960.

D2627. Claggett Shale, upper part of bentonitic member, same locality as D2626. J.R. Gill, L.G. Schultz, and W.A. Cobban, 1960.

D2629. Bearpaw Shale, gray limestone concretions, approximately 15 m above base, NW¼NW¼ sec. 31, T. 10 N., R. 36 E., Rosebud County, Montana. J.R. Gill, L.G. Schultz, and W.A. Cobban, 1960.

D2631. Bearpaw Shale, limestone concretions approximately 52 m above base, beside road in NW¼NW¼ sec. 31, T. 10 N., R. 36 E., Rosebud County, Montana. J.R. Gill, L.G. Schultz, and W.A. Cobban, 1960.

D2632. Bearpaw Shale, limestone concretions just below Vananda bentonite bed, SE¼ sec. 27, T. 10 N., R. 35 E., east of Ingomar, Rosebud County, Montana. J.R. Gill, L.G. Schultz, and W.A. Cobban, 1960.

D2633. Bearpaw Shale, limestone concretions just below Vananda bentonite bed, same locality as D2632. J.R. Gill, L.G. Schultz, and W.A. Cobban, 1960.

D2634. Claggett Shale, brown septarian limestone concretions 7.6 m below top, NE¼ sec. 6, T. 8 N., R. 38 E., Rosebud County, Montana. J.R. Gill, L.G. Schultz, and W.A. Cobban, 1960.

D2635. Claggett Shale, 1–2 m below top, same locality as D2636. J.R. Gill, L.G. Schultz, and W.A. Cobban, 1960.

D2636. Judith River Formation, phosphatic nodules at base, NE¼ sec. 6, T. 8 N., R. 38 E., Rosebud County, Montana. J.R. Gill, L.G. Schultz, and W.A. Cobban, 1960.

D2654. Sandstone bed in the Pierre Shale, SW¼SE¼ sec. 12, T. 3 N., R. 81 W., Grand County, Colorado. W.R. Brown, 1957.

D2723. Pierre Shale, NW¼SW¼ sec. 5, T. 1 N., R. 70 W., Boulder County, Colorado. G.R. Scott, 1960.

D2941. Pierre Shale, stream bank in SE¼ sec. 31, T. 2 N., R. 70 W., Boulder County, Colorado. W.A. Cobban, 1961.

D3074. Pierre Shale, Verendrye Member (?), Big Canyon, SW¼NE¼ sec. 20, T. 4 N., R. 15 E., Pennington County, South Dakota. H.A. Tourtelot, 1961.

D3083. Livingston Formation, 6 m thick marine sandstone, NE¼ sec. 25, T. 4 N., R. 8 E., Park County, Montana. J.R. Gill and A.E. Roberts, 1961.

D3443. Bearpaw Shale, soft sandstone 14 m above a prominent bed of bentonite, State Rt. 8, SW¼ sec. 16, T. 3 S., R. 35 E., Big Horn County, Montana. J.R. Gill, 1961.

D3534. Mancos Shale, 0.6 m thick limestone bed in lower part, 30–90 m above Frontier Sandstone, N½ sec. 15, T. 5 N., R. 99 W., Moffat County, Colorado. J. Dyni, 1961.

D3550. Gammon Shale, upper part, 7 m below "Ivory band," SW¼ sec. 2, T. 12 N., R. 37 E., Rosebud County, Montana. J.R. Gill and L.G. Schultz, 1961.

D3551. Gammon Shale, upper part, NE¼SW¼ sec. 19, T. 12 N., R. 38 E., Rosebud County, Montana. J.R. Gill and L.G. Schultz, 1961.

D3552. Claggett Shale, 6 m below top, SW¼ sec. 21 T. 12 N., R. 37 E., Rosebud County, Montana. J.R. Gill and L.G. Schultz, 1961.

D3554. Gammon Shale, ironstone 57 m below top, same locality as D3550. J.R. Gill and L.G. Schultz, 1961.

D3556. Claggett Shale, 13 m above base, SW¼ sec. 23, T. 12 N., R. 37 E., Rosebud County, Montana. J.R. Gill and W.A. Cobban, 1961.

D3558. Judith River Formation, appproximately 50 m above base, SW¼ sec. 10, T. 7 N., R. 38 E., Rosebud County, Montana. J.R. Gill and L.G. Schultz, 1961.

D3559. Judith River Formation, approximately 88 m above base, same locality as D3558. J.R. Gill and L.G. Schultz, 1961.

D3560. Judith River Formation, approximately 93 m above base, same locality as D3558. J.R. Gill and L.G. Schultz, 1961.

D3561. Judith River Formation, approximately 69 m above base, SE¼ sec 28, T. 7 N., R. 39 E., Rosebud County, Montana. J.R. Gill and L.G. Schultz, 1961.

D3562. Judith River Formation, approximatley 18 m below top, same locality as D3561. J.R. Gill and L.G. Schultz, 1961.

D3563. Judith River Formation, approximately 3 m below top, same locality as D3561. J.R. Gill and L.G. Schultz, 1961.

D3564. Judith River Formation, top, SW¼NW¼ sec. 25, T. 7 N., R. 39 E., Rosebud County, Montana. J.R. Gill, W.A. Cobban, and L.G. Schultz, 1961.

D3565. Judith River Formation, approximately 3 m above base, NW¼ sec. 8, T. 8 N., R. 38 E., Rosebud County, Montana. J.R. Gill and L.G. Schultz, 1961.

D3566. Bearpaw Shale, 38 m above base, S½ sec. 25, T. 7 N., R. 39 E., Rosebud County, Montana. J.R. Gill, L.G. Schultz, and W.A. Cobban, 1961.

D3567. Bearpaw Shale, 49–55 m above base, same locality as D3566. J.R. Gill, L.G. Schultz, and W.A. Cobban, 1961.

D3568. Bearpaw Shale, dusky-red ferruginous concretions 64 m above base, same locality as D3566. J.R. Gill and W.A. Cobban, 1961.

D3569. Bearpaw Shale, septarian limestone concretion 66 m above base, same locality as D3566. W.A. Cobban, 1961.

D3570. Bearpaw Shale, gray limestone concretions associated with a thick bentonite bed 70 m above base, same locality as D3566. J.R. Gill, 1961.

D3571. Bearpaw Shale, dusky-red ferruginous concretions 88 m above base, same locality as D3566. J.R. Gill and W.A. Cobban, 1961.

D3572. Bearpaw Shale, "tepee butte" limestone and gray and buff septarian limestone concretions, 90 m above base, same locality as D3566. J.R. Gill and W.A. Cobban, 1961.

D3573. Bearpaw Shale, limestone concretions between the first and second bentonite beds of the Vananda Member, 93 m above base, NE¼NE¼ sec. 36, T. 7 N., R. 39 E., Rosebud County, Montana. L.G. Schultz, 1961.

D3574. Bearpaw Shale, 97 m above base, same locality as D3573. J.R. Gill and W.A. Cobban, 1961.

D3575. Bearpaw Shale, limestone concretions 101 m above base, NE¼NE¼ sec. 36, T. 7 N., R. 39 E., Rosebud County, Montana. J.R. Gill and W.A. Cobban, 1961.

D3576. Bearpaw Shale, gray limestone concretions 114 m above base, same locality as D3573. J.R. Gill, L.G. Schultz, and W.A. Cobban, 1961.

D3577. Bearpaw Shale, closely spaced brown limestone concretions 134 m above base, same locality as D3573. J.R. Gill, L.G. Schultz, and W.A. Cobban, 1961.

D3578. Bearpaw Shale, gray limestone concretions 138 m above base, S½ sec. 25, T. 7 N., R. 40 E., Rosebud County, Montana. L.G. Schultz, 1961.

D3579. Bearpaw Shale, grey and brown limestone concretions 147 m above base, S½ sec. 25, T. 7 N., R. 40 E., Rosebud County, Montana. J.R. Gill, L.G. Schultz, and W.A. Cobban, 1961.

D3580. Bearpaw Shale, brown limestone concretions 176 m above base, same locality as D3579. J.R. Gill, L.G. Schultz, and W.A. Cobban, 1961.

D3581. Bearpaw Shale, brown limestone concretions 185 m above base, same locality as D3579. J.R. Gill, L.G. Schultz, and W.A. Cobban, 1961.

D3582. Bearpaw Shale, grey limestone concretions 202 m above base, same locality as D3579. J.R. Gill, L.G. Schultz, and W.A. Cobban, 1961.

D3583. Bearpaw Shale, 213 m above base, same locality as D3579. J.R. Gill, L.G. Schultz, and W.A. Cobban, 1961.

D3584. Bearpaw Shale, very closely spaced limestone concretions 231 m above base, same locality as D3579. W.A. Cobban, 1961.

D3585. Bearpaw Shale, 239 m above base, same locality as D3579. J.R. Gill, L.G. Schultz, and W.A. Cobban, 1961.

D3586. Bearpaw Shale, 243 m above base, same locality as D3579. W.A. Cobban, 1961.

D3587. Bearpaw Shale, 258 m above base, same locality as D3579. J.R. Gill and L.G. Schultz, 1961.

D3588. Bearpaw Shale, 266 m above base, same locality as D3579. J.R. Gill and L.G. Schultz, 1961.

D3595. Bearpaw Shale, 48 m above base, sec. 25, T. 8 N., R. 20 E., Golden Valley County, Montana. J.R. Gill, 1961.

D3599. Bearpaw Shale, 140 m above base, same locality as D3595. J.R. Gill, 1961.

D3600. *Baculites compressus* Zone, Bearpaw Shale, 144 m above base, sec. 25, T. 8 N., R. 20 E., Golden Valley County, Montana.

D3624. Bearpaw Shale, 80 m above base, center sec. 14, T. 6 N., R. 15 E., Wheatland County, Montana. J.R. Gill, 1961.

D3634. Bearpaw Shale, float on lower 15 m, near center of north line of sec. 4, T. 36 N., R. 8 W., Glacier County, Montana. A.E. Roberts and W.A. Cobban, 1960.

D3659. Bearpaw Shale, 146 m above base, center NW¼ sec. 10, T. 14 N., R. 31 E., Garfield County, Montana. J.R. Gill, 1966.

D3819. Bearpaw Shale, center NE¼ sec. 33, T. 27 N., R. 19 E., Blaine County, Montana. W.T. Pecora and B.C. Carter, Jr., 1962.

D3820. Bearpaw Shale, SE¼NW¼ sec. 34, T. 27 N., R. 19 E., Blaine County, Montana. W.T. Pecora and B.C. Carter, Jr., 1962.

D3827. Bearpaw Shale, SW¼NE¼ sec. 1, T. 25 N., R. 17 E., Blaine County, Montana. W.T. Pecora and B.C. Hearn, Jr., 1962.

D4101. Pierre Shale, 8–12 m above base of DeGrey Member, approximately 14 km south of Valley City, SE¼ sec. 4, T. 138 N., R. 58 W., Barnes County, North Dakota. J.R. Gill and A.N. Fatmi, 1963.

D4119. Bearpaw Shale, approximately 46 m above base, SW¼NW¼ sec. 21, T. 11, R. 29, W. 3rd Mer., east of Box Elder Creek, Saskatchewan, Canada. J.R. Gill and W.A. Cobban, 1963.

D4120. Bearpaw Shale, approximatley 58 m above base, same locality as D4119. J.R. Gill. 1963.

D4125. Bearpaw Shale, approximately 43 m above base, center of the N½ sec. 1, T. 11, R. 3, W 4th Mer., east side of Rose Creek Valley, Alberta, Canada. J.R. Gill, A.N. Fatmi, and W.A. Cobban, 1963.

D4126. Bearpaw Shale, concretions 47 m above base, same locality as D4125. J.R. Gill and W.A. Cobban, 1963.

D4127. Bearpaw Shale, approximately 58 m above base, same locality as D4125. J.R. Gill. 1963.
D4129. Bearpaw Shale, shaly ferruginous concretion approximately 6 m above base, south bank of St. Mary River, SE¼ sec. 2, T. 7, R. 22, W. 4th Mer., Alberta, Canada. W.A. Cobban, 1963.
D4130. Bearpaw Shale, concretions 26–38 m above base, same locality as D4129. J.R. Gill and W.A. Cobban, 1963.
D4131. Bearpaw Shale, type locality of Magrath Sandstone Member, east bank of St. Mary River, NE¼ sec. 32, T. 6, R. 22, W. 4th Mer., Alberta, Canada. J.R. Gill, A.N. Fatmi, and W.A. Cobban, 1963.
D4132. Bearpaw Shale, ferruginous concretions between the Magrath Sandstone Member and the "Double ash bed" of Link and Childerhose (1931), same locality as D4131. J.R. Gill, A.N. Fatmi, and W.A. Cobban, 1963.
D4138. Bearpaw Shale, limestone concretions approximately 7.6 m above base, NW¼NE¼ sec. 34, T. 3 N., R. 19 E., Stillwater County, Montana. J.R. Gill and W.A. Cobban, 1963.
D4209. Bearpaw Shale, 30 m above Vananda? Bentonite bed, NE¼NE¼ sec. 1, T. 27 N., R. 36 E., Valley County, Montana. J.R. Gill, 1962.
D4497. Pierre Shale, SW¼NE¼ sec. 34, T. 3 N., R. 77 W., Grand County, Colorado. G.A. Izett, 1964.
D4710. Bearpaw Shale, sec. 11, T. 7 N., R. 8 E., Meagher County, Montana. R.W. Stone, 1907.
D4905. Pierre Shale, lower 6–7.5 m of Lake Creek Member, south side of Lake Creek, SW¼ sec 31, T. 11 S., R. 38 W. and NE¼NE¼NW¼ and NW¼NW¼NE¼ sec. 6, T. 12 S., R 38 W., Wallace County, Kansas. W.A. Cobban, 1964, 1965.
D4965. Pierre Shale, limestone concretions in middle of Verendrye Member, beside State Route 47, NE¼NE¼ sec. 13, T. 102 N., R. 73 W., Lyman County, South Dakota. W.A. Cobban, 1965.
D4968. *Baculites compressus* (?) Zone, Pierre Shale, upper few meters of DeGrey Member, by road 1 km south of south end of Big Bend Dam bridge, Lyman County, South Dakota. W.A. Cobban, 1965.
D4994. Pierre Shale, gray concretions, beside Newell-Fairpoint road at center of south line of SW¼ sec. 9, T. 9 N., R. 9 E., Butte County, South Dakota. W.A. Cobban, 1965.
D5034. *Baculites compressus* Zone, Pierre Shale, Round Butte, Larimer County, Colorado.
D5037. Pierre Shale, NW¼ sec. 17, T. 11 N., R. 68 W., Larimer County, Colorado. G.R. Scott, 1964.
D5415. *Baculites cuneatus* Zone, Pierre Shale, NE¼ NE¼ sec. 13, T. 3 N., R. 81 W., Grand County, Colorado.
D5648. Bearpaw Shale, lowest bed of brown, sandy limestone concretions 15 m above base, NE¼SE¼ sec. 9, T. 14 N., R. 31 E., Garfield County, Montana. J.R. Gill and others, 1966.
D5649. Bearpaw Shale, second bed of brown limestone concretions 23 m above base, same locality as D5648. J.R. Gill and others, 1966.
D5650. Bearpaw Shale, brown, silty limestone concretions above a bed of bentonite that contains small barite nodules 33 m above base, same locality as D5648. R.E. Burkholder and W.A. Cobban, 1966.
D5651. Bearpaw Shale, reddish limestone concretions 66 m above base, same locality as D5648. W.A. Cobban, 1966.
D5652. Bearpaw Shale, "tepee butte" limestone 80 m above base, SW¼NW¼ sec. 10, T. 14 N., R. 31 E., Garfield County, Montana. W.A. Cobban, 1966.
D5653. Bearpaw Shale, "tepee butte" limestone 88 m above base, same locality as D5652. J.R. Gill, 1966.
D5654. Bearpaw Shale, reddish-brown septarian limestone concretions 92 m above base, same locality as D5652. J.R. Gill, 1966.
D5655. Bearpaw Shale, 117 m above base, same locality as D5652. R.E. Burkholder, 1966.
D5656. Bearpaw Shale, 123 m above base, same locality as D5652. R.E. Burkholder, 1966.
D5657. Bearpaw Shale, 133 m above base, same locality as D5652. R.E. Burkholder, 1966.
D5658. Bearpaw Shale, 140 m above base, same locality as D5652. J.R. Gill, 1966.
D5659. Bearpaw Shale, 146 m above base, SW¼NW¼ sec. 10, T. 14 N., R. 31 E., near Mosby, Garfield County, Montana. W.A. Cobban, 1966.
D5660. Bearpaw Shale, 163 m above base, same locality as D5652. R.E. Burkholder and W.A. Cobban, 1966.
D5661. Bearpaw Shale, limestone concretions 197 m above base, same locality as D5652. J.R. Gill and others, 1966.
D5663. Bearpaw Shale, reddish brown ferruginous concretions just below upper bentonitic member approximately 204 m above base, same locality as D3659. J.R. Gill and others, 1966.
D5664. Bearpaw Shale, lower half of upper bentonitic member approximately 206–212 m above base, same locality as D3659. J.R. Gill and others, 1966.
D5665. Bearpaw Shale, upper part of upper bentonitic member, approximately 212–216 m above base, same locality as D3659. J.R. Gill, 1966.
D5666. Bearpaw Shale, 230 m above base, same locality as D3659. R.E. Burkholder and W.A. Cobban, 1966.
D5667. Bearpaw Shale, second conspicuous bed of brown limestone concretions below top, NE¼NW¼ sec. 7, T. 14 N., R. 30 E., Garfield County, Montana. J.R. Gill and others, 1966.
D5862. *Baculites compressus* Zone, Pierre Shale, NW¼ sec. 21, T. 3 N., R. 80 W., Grand County, Colorado.
D5863. Pierre Shale, N½ sec. 20, T. 3 N., R. 80 W., Grand County, Colorado. G.A. Izett, 1967.
D5864. *Baculites* cf. *B. compressus* Zone, Pierre Shale, 4.5 m above D5863.
D5937. Pierre Shale, NW¼ sec. 17, T. 11 N., R. 68 W., Larimer County, Colorado. G.R. Scott, 1964.
D5991. *Baculites compressus* Zone, Pierre Shale, NE¼NW¼ sec. 12, T. 3 N., R. 81 W., Grand County, Colorado. G.A. Izett and W. A. Cobban, 1967.
D6037. Bearpaw Shale, upper part, sec. 5, T. 7 N., R. 9 E., Meagher County, Montana, T.W. Stanton, M.R. Campbell, and W.R. Calvert, 1909.

D6569. Bearpaw Shale, septarian limestone concretions 66 m above base, same locality as D3572. W.A. Cobban, 1961.

D6577. *Baculites compressus* Zone, Pierre Shale, NE¼NW¼ sec. 7, T. 3 N., R. 80 W., Grand County, Colorado.

D6854. Bearpaw Shale, 7.6 m above base, SE¼ sec. 33, T. 24 N., R. 21 E., Blaine County, Montana. B.C. Hearn, Jr., 1967.

D7325. Bearpaw Shale, Coulee Slide Butte, NE¼ sec. 4, T. 36 N., R. 8 W., Glacier County, Montana. E. Stebinger, 1911.

D8004. Pierre Shale, SE¼NE¼ sec. 28, T. 18 S., R. 69 W., Fremont County, Colorado. G.R. Scott, 1971.

D8059. *Baculites compressus* Zone, Pierre Shale, NW¼NW¼SE¼ sec. 12, T. 3 N., R. 81 W., Grand County, Colorado.

D8060. *Baculites compressus* Zone, Pierre Shale, approximately 6 m below 2R zone, same locality as D8059.

D8068. *Baculites compressus* Zone, Pierre Shale, SE¼NE¼ sec. 34, T. 2 N., R. 77 W., Grand County, Colorado.

D8068. Pierre Shale, SE¼NE¼ sec. 34, T. 2 N., R. 77 W., Grand County, Colorado. G.A. Izett, 1971.

D8074. *Baculites compressus* Zone, Pierre Shale, SW¼SW¼ sec. 2, T. 2 N., R. 77 W., Middle Park, Grand County, north-central Colorado.

D8086. *Baculites compressus* Zone, Pierre Shale, a few meters below glauconitic zone, sec. 34, T. 2 N., R. 77 W., Grand County, Colorado.

D8068. Pierre Shale, SE¼NE¼ sec. 34, T. 2 N., R. 77 W., Grand County, Colorado. G.A. Izett, 1971.

D8089. *Baculites compressus* Zone, Pierre Shale, NE¼NW¼ sec. 25, T. 3 N., R. 77 W., Grand County, Colorado. G.A. Izett, 1971; G.R. Scott, 1972.

D8092. *Baculites compressus* Zone, Pierre Shale, SE¼SE¼ sec. 12, T. 3 N., R. 81 W., Middle Park, Grand County, north-central Colorado.

D8378. Pierre Shale, SE¼SW¼ sec. 14, T. 10 N., R. 76 W., Larimer County, Colorado. J.R. Gill, D.L. Blackstone, and W.A. Cobban, 1972.

D8782. Pierre Shale, east of Horse Creek, Laramie County, Wyoming. W.T. Lee, 1914.

D8874. Pierre Shale, SW¼SE¼ sec. 11, T. 16 S., R. 64 W., El Paso County, Colorado. G.R. Scott, 1972.

D9637. Pierre Shale, SE¼SW¼ sec. 26, T. 9 N., R. 78 W., Jackson County, Colorado. D.J. Madden and M.A. Moorman, 1975.

D9640. *Baculites compressus* Zone, Pierre Shale, SE¼SW¼ sec. 35, T. 9 N., R. 78 W., North Park area, Jackson County, Colorado.

D9640. Pierre Shale, SE¼SW¼ sec. 35, T. 9 N., R. 78 W., Jackson County, Colorado. D.J. Madden and M.A. Moorman, 1975.

D9677. Pierre Shale, SW¼NW¼ sec. 2, T. 8 N., R. 78 W., Jackson County, Colorado. D.J. Madden and M.A. Moorman, 1975.

D9866. Transitonal beds from Horsethief Sandstone to Bearpaw Shale, southwest end of Pine Butte, Teton County, Montana. M.T. Goldman, 1916.

D11726. Marine shale below Twentymile Sandstone, *Baculites cuneatus–B. jenseni* zones, sec. 33 T. 5 N., R. 86 W., Routt County, Colorado.

D12201. *Didymoceras cheyennense* Zone (?), Bearpaw Shale, SW¼ sec. 26, T. 1 N., R. 35 E., Big Horn County, Montana. S.H. Patterson, 1948.

D12203. *Baculites compressus* Zone, Pierre Shale, SW¼ sec. 2, T. 1 N., R. 14 E., Cheyenne River, Pennington County, South Dakota.

D13507. Pierre Shale, near top, Oacoma Member, mouth of Crow Creek, SE¼SE¼ sec. 15, T. 106 N., R. 71 W., Buffalo County, South Dakota. G.A. Izett, 1993.

D13508. Pierre Shale, west of Highway 50, near center S½ sec. 13, T. 105 N., R. 71 W., Brule County, South Dakota. G.A. Izett and W.A. Cobban, 1993.

D13583. *Baculites compressus* Zone, uppermost 1 m, Oacoma Member, Pierre Shale, just west and east of highway near center of the E½E½ sec. 34 and W½W½ sec. 35, T. 107 N., R. 72 W., Lyman County, South Dakota.

D13686. *Baculites compressus* Zone, top, Oacoma Member, Pierre Shale, NW¼NW¼ sec. 19, T.108 N., R. 72 W., Buffalo County, South Dakota.

D13708. Pierre Shale, limestone concretions, Sage Creek, center SW¼ sec. 35, T. 1 S., R. 14 E., Pennington County, South Dakota. G.A. Izett and W.A. Cobban, 1996.

D13791. *Baculites compressus* Zone, DeGrey Member, Pierre Shale, SW¼NE¼ sec. 36, T. 110 N., R. 76 W., Hughes County, South Dakota. G.A. Izett and W.A. Cobban, 1997.

758. *Baculites reesidei* Zone, Larimer Sandstone Member, Pierre Shale, Fossil Creek south of Fort Collins, Larimer County, Colorado. T.W. Stanton, 1890.

4710. Bearpaw Shale, sec. 11, T. 7 N., R. 8 E., Meaghar County, Montana. R.W. Stone, 1907.

6037. Bearpaw Shale, upper part, sec. 5, T. 7 N., R. 9 E., Meaghar County, Montana. T.W. Stanton, M.R. Campbell, and W.R. Calvert, 1909.

7325. Bearpaw Shale, N½NE¼ sec. 4, T. 36 N., R. 8 W., along Coulee Slide Butte, Glacier County, Montana. E. Stebinger, 1911.

7892. Bearpaw Shale, sec. 3, T. 9 N., R. 29 E., 6.4 km north and 1.6 km east of Musselshell, Musselshell County, Montana. C.F. Bowen and H. Bassler, 1912.

9133. Pierre Shale, near Kremmling, Grand County, Colorado.

9154. Pierre Shale, near Kremmling, Grand County, Colorado.

9866. Horsethief Sandstone, southwest end of Pine Butte, Teton County, Montana. M.T. Goldman, 1916.

21224. Bearpaw Shale, calcareous concretions 154–156 m above base, S½ sec. 9, T. 1 S., R. 35 E., approximately 16 km east of Hardin, Big Horn County, Montana. W.A. Cobban, 1947.

21363. Bearpaw Shale, approximately 46 m below top, NE½ sec. 2, T. 1 N., R. 33 E., east bank of Big Horn River just above old Nine-Mile Bridge, 14.5 km north of Hardin, Big Horn County, Montana.

21405. Telegraph Creek Formation, limestone concretions 2 m above base, SE¼ sec. 5, T. 14 N., R. 31 E., Garfield County, Montana. W.A. Cobban, 1948.
21406. Gammon Shale, ironstone concretions 44–53 m above base, same locality as 21405. W.A. Cobban, 1948.
21407. Gammon Shale, ironstone concretions 54–59 m above base, same locality as 21405. W.A. Cobban, 1948.
21408. Gammon Shale, ironstone concretions 74–91 m above base, same locality as 21405. W.A. Cobban, 1948.
21409. Gammon Shale, limestone concretions 2 m below top, same locality as 21405. W.A. Cobban, 1948.
21410. Claggett Shale, calcareous septarian concretion 20–22 m above base, sec. 5, T. 14 N., R. 31 E., Garfield County, Montana. W. A. Cobban, 1948.
21411. Judith River Formation, lower 13 m, W½ sec. 4, T. 14 N., R. 31 E., Garfield County, Montana. W.A. Cobban, 1948.
21577. Bearpaw Shale, 232–240 m above base, northeast of Mosby, SE¼ sec. 4, T. 14 N., R. 31 E., Garfield County, Montana. W.A. Cobban, 1949.
22182. *Baculites compressus–B. reesidei* zones, Bearpaw Shale, 10 km north of Roy, secs. 12 and 13, T. 19 N., R. 21 E. and sec. 7, T. 19 N., R. 22 E., Fergus County, Montana.
23057. Pierre Shale, 52 m below top, head of Timber Creek in SE¾ sec. 10, T. 3 S., R. 56 E., Carter County, Montana. J.B. Reeside, Jr., 1950.
23070. Virgin Creek Shale Member, Pierre Shale, approximately 18–21 m below top, NE¼ sec. 4, T. 1 S., R. 14 E., near road, Wasta, Pennington County, South Dakota.
23072. Pierre Shale, Virgin Creek Shale, approximately 18–21 m below top, approximately in sec. 5, T. 1 S., R. 14 E., breaks of Cheyenne River, 1.6–2.4 km north of mouth of Sage Creek, Pennington County, South Dakota.
23072. Pierre Shale, bank of Cheyenne River approximately 3 km below mouth of Sage Creek, Pennington County, South Dakota. J.B. Reeside, W.A. Cobban, and H.R. Christner, 1950.
23349. *Baculites compressus* Zone, Pierre Shale, 18–23 m below top of Virgin Creek Member, SE¼ sec. 36, T. 2 N., R. 14 E., Pennington County, South Dakota.
23512. Upper part of Virgin Creek Member of Pierre Shale, SE¼ sec. 18, T. 1 N., R. 15 E., SW side Bull Creek, Wasta, Pennington County, South Dakota.
23537. *Didymoceras cheyennense* Zone, Pierre Shale, approximately 30 m above Monument Hill Member, head of Timber Creek, Carter County, Montana.
23650 *Didymoceras cheyennense* Zone, Monument Hill Shale Member, Pierre Shale, highly fossiliferous concretions in uppermost part, sec. 14, T. 3 S., R. 56 E., Carter County, Montana.W.A. Cobban, 1941.
23990. Bearpaw Shale, NE¼ sec. 25, T. 27 N., R. 14 E., Chouteau County, Montana. W.T. Pecora, 1952.
24178. Bearpaw Shale, NW¼NE¼ sec. 3, T. 25 N., R. 16 E., Chouteau County, Montana. R.M. Lindvall and R. Cholton, 1951.

Yale Peabody Museum (YPM) Localities

The names of collectors are indicated at the end of some entries.

A1461. Bearpaw Shale, Rosebud County, Montana.
A6520. Pierre Shale, Sage Creek, Pennington County, South Dakota. G.A. Clarke.
A6563. Pierre Shale, Badlands, South Dakota. G. Craven.
A6560. Pierre Shale, Box Elder Creek, Pennington County, South Dakota. O.C. Marsh Collection.
C3343. Pierre Shale, Cheyenne River, near Rapid Creek, Pennington County, South Dakota.
C3346. Pierre Shale, locality unknown.
C3347. Pierre Shale, Belle Fourche River, South Dakota. Princeton 1886 Expedition.

APPENDIX 2

Ontogenetic Measurements

Measurements through the ontogeny of *Hoploscaphites nodosus* (Owen, 1852) (figs. 74, 75) and *H. brevis* (Meek, 1876) (figs. 113, 114).

1. *Hoploscaphites nodosus* (Owen, 1852), slender macroconch, AMNH 9520/2, Pierre Shale, Pennington County, South Dakota

D (mm)	W (mm)	H (mm)	W/H	UD (mm)	UD/D
86.0 [a]	36.0	35.5	1.01	21.3	0.25
49.4 [b]	27.2	29.2	0.93	3.15	0.06
29.6	16.2	17.0	0.96	3.06	0.10
17.6	9.51	9.54	1.00	2.45	0.14
10.3	5.30	5.57	0.95	1.82	0.18
6.18	3.24	2.92	1.11	1.61	0.26
3.88	2.20	1.65	1.33	1.29	0.33
2.56	1.21	0.94	1.29	0.98	0.38
1.80	0.90	0.64	1.42	0.71	0.40
1.28	0.63	0.45	1.40	0.50	0.39
0.90	0.50	0.33	1.53	0.30	0.33
0.63	0.47	0.27	1.71	0.12	0.19
0.41	0.48	0.24	2.03	—	—

2. *Hoploscaphites nodosus* (Owen, 1852), robust macroconch, YPM 35593, YPM loc. C3346, Pierre Shale, locality unknown.

D (mm)	W (mm)	H (mm)	W/H	UD (mm)	UD/D
93.0 [a]	50.4	42.5	1.19	21.8	0.23
50.5 [b]	32.5	28.6	1.13	4.55	0.09
31.0	19.0	17.3	1.10	3.43	0.11
18.2	10.2	10.2	0.99	1.89	0.10
10.8	6.59	6.11	1.08	1.63	0.15
6.43	3.84	3.05	1.26	—	—

3. *Hoploscaphites nodosus* (Owen, 1852), depressed microconch, USNM 536246, USGS Mesozoic loc. D9133, Pierre Shale, Grand County, Colorado

D (mm)	W (mm)	H (mm)	W/H	UD (mm)	UD/D
85.0 [a]	38.7	31.0	1.25	28.0	0.33
46.1 [b]	30.2	26.1	1.16	4.23	0.09
28.7	18.1	15.8	1.14	3.58	0.12
17.3	11.7	9.24	1.27	2.73	0.16
10.5	7.13	5.34	1.34	2.20	0.21
6.49	4.02	2.98	1.35	1.86	0.29
4.12	2.31	1.65	1.40	1.45	0.35
2.76	1.38	1.02	1.35	1.07	0.39
1.96	0.94	0.67	1.40	—	—

4. *Hoploscaphites brevis* (Meek, 1876), macroconch, AMNH 45347, Pierre Shale, Meade County, South Dakota

D (mm)	W (mm)	H (mm)	W/H	UD (mm)	UD/D
79.0* [a]	29.9	33.0	0.91	19.5*	0.25*
46.0* [b]	19.6	26.5*	0.74	3.58*	0.08*
27.7	13.1	15.9	0.82	2.47	0.09
16.8	8.38	9.31	0.90	2.19	0.13
10.0	6.31	5.32	1.19	1.55	0.16
5.99	3.48	3.03	1.15	—	—

5. *Hoploscaphites brevis* (Meek, 1876), microconch, BHI 4248, Pierre Shale, Meade County, South Dakota

D (mm)	W (mm)	H (mm)	W/H	UD (mm)	UD/D
35.2 [a]	10.5	13.2	0.80	11.1	0.32
20.1 [b]	7.63	11.0	0.70	3.01	0.15
12.0	4.71	6.15	0.76	2.12	0.18
7.29	3.41	3.75	0.91	1.66	0.23
4.22	2.22	1.88	1.18	1.29	0.31
2.77	1.32	1.05	1.26	1.00	0.36
1.92	0.89	0.72	1.24	0.70	0.36
1.36	0.67	0.50	1.34	0.50	0.37
0.97	0.49	0.36	1.36	0.43	0.44
0.66	0.43	0.18	1.83	0.26	0.33
0.50	0.42	0.22	1.98	—	—

6. *Hoploscaphites brevis* (Meek, 1876), microconch, USNM 536254, USGS Mesozoic loc. D12203, Pierre Shale, Pennington County, South Dakota

D (mm)	W (mm)	H (mm)	W/H	UD (mm)	UD/D
43.2 [a]	14.7	16.4	0.90	12.1	0.28
25.0 [b]	9.90	13.6	0.72	3.47	0.14
14.9	6.89	8.49	0.81	1.94	0.13
8.46	4.18	4.48	0.93	1.82	0.22
4.89	2.87	2.16	1.33	1.51	0.31
3.13	1.57	1.22	1.29	1.14	0.36
2.09	1.07	0.77	1.39	0.80	0.38
1.46	0.70	0.52	1.35	0.58	0.40
1.01	0.50	0.36	1.39	0.36	0.36
0.70	0.47	0.30	1.57	—	—

7. *Hoploscaphites brevis* (Meek, 1876), microconch, AMNH 58555, Pierre Shale, Meade or Pennington County, South Dakota

D (mm)	W (mm)	H (mm)	W/H	UD (mm)	UD/D
54.7 [a]	18.4	26.9	0.68	10.4	0.19
31.0 [b]	12.9	17.4	0.74	3.84	0.12
17.8	7.58	9.76	0.78	2.30	0.13
10.8	5.26	5.78	0.91	1.77	0.16
6.59	3.57	3.22	1.10	1.60	0.24
4.00	2.23	1.77	1.26	1.22	0.30
2.55	1.29	1.01	1.28	0.89	0.35
1.72	0.79	0.65	1.23	0.63	0.36
1.22	0.59	0.45	1.32	0.46	0.37
0.86	0.46	0.32	1.44	0.25	0.30
0.61	0.46	0.29	1.61	0.62	0.10
0.42	0.50	0.26	—	—	—

D, shell diameter; W, whorl width; H, whorl height; W/H, ratio of whorl width to whorl height; UD, umbilical diameter; UD/D, ratio of umbilical diameter to shell diameter; [a], in mature body chamber. [b] = near base of mature body chamber; * = estimate. Values $\geq$ 10.0 mm are reported to one decimal, values $<$10.0 mm are reported to two decimals.